

Bone inside-out and outside-in signals: Control of body homeostasis

Edited by

Lilian Irene Plotkin, Uma Sankar, Arancha R. Gortazar,
Deborah Veis and Lucas R. Brun

Published in

Frontiers in Endocrinology



FRONTIERS EBOOK COPYRIGHT STATEMENT

The copyright in the text of individual articles in this ebook is the property of their respective authors or their respective institutions or funders. The copyright in graphics and images within each article may be subject to copyright of other parties. In both cases this is subject to a license granted to Frontiers.

The compilation of articles constituting this ebook is the property of Frontiers.

Each article within this ebook, and the ebook itself, are published under the most recent version of the Creative Commons CC-BY licence. The version current at the date of publication of this ebook is CC-BY 4.0. If the CC-BY licence is updated, the licence granted by Frontiers is automatically updated to the new version.

When exercising any right under the CC-BY licence, Frontiers must be attributed as the original publisher of the article or ebook, as applicable.

Authors have the responsibility of ensuring that any graphics or other materials which are the property of others may be included in the CC-BY licence, but this should be checked before relying on the CC-BY licence to reproduce those materials. Any copyright notices relating to those materials must be complied with.

Copyright and source acknowledgement notices may not be removed and must be displayed in any copy, derivative work or partial copy which includes the elements in question.

All copyright, and all rights therein, are protected by national and international copyright laws. The above represents a summary only. For further information please read Frontiers' Conditions for Website Use and Copyright Statement, and the applicable CC-BY licence.

ISSN 1664-8714
ISBN 978-2-83251-389-7
DOI 10.3389/978-2-83251-389-7

About Frontiers

Frontiers is more than just an open access publisher of scholarly articles: it is a pioneering approach to the world of academia, radically improving the way scholarly research is managed. The grand vision of Frontiers is a world where all people have an equal opportunity to seek, share and generate knowledge. Frontiers provides immediate and permanent online open access to all its publications, but this alone is not enough to realize our grand goals.

Frontiers journal series

The Frontiers journal series is a multi-tier and interdisciplinary set of open-access, online journals, promising a paradigm shift from the current review, selection and dissemination processes in academic publishing. All Frontiers journals are driven by researchers for researchers; therefore, they constitute a service to the scholarly community. At the same time, the *Frontiers journal series* operates on a revolutionary invention, the tiered publishing system, initially addressing specific communities of scholars, and gradually climbing up to broader public understanding, thus serving the interests of the lay society, too.

Dedication to quality

Each Frontiers article is a landmark of the highest quality, thanks to genuinely collaborative interactions between authors and review editors, who include some of the world's best academicians. Research must be certified by peers before entering a stream of knowledge that may eventually reach the public - and shape society; therefore, Frontiers only applies the most rigorous and unbiased reviews. Frontiers revolutionizes research publishing by freely delivering the most outstanding research, evaluated with no bias from both the academic and social point of view. By applying the most advanced information technologies, Frontiers is catapulting scholarly publishing into a new generation.

What are Frontiers Research Topics?

Frontiers Research Topics are very popular trademarks of the *Frontiers journals series*: they are collections of at least ten articles, all centered on a particular subject. With their unique mix of varied contributions from Original Research to Review Articles, Frontiers Research Topics unify the most influential researchers, the latest key findings and historical advances in a hot research area.

Find out more on how to host your own Frontiers Research Topic or contribute to one as an author by contacting the Frontiers editorial office: frontiersin.org/about/contact

Bone inside-out and outside-in signals: Control of body homeostasis

Topic editors

Lilian Irene Plotkin — Indiana University Bloomington, United States
Uma Sankar — Indiana University, Purdue University Indianapolis, United States
Arancha R. Gortazar — CEU San Pablo University, Spain
Deborah Veis — Washington University in St. Louis, United States
Lucas R. Brun — National University of Rosario, Argentina

Citation

Plotkin, L. I., Sankar, U., Gortazar, A. R., Veis, D., Brun, L. R., eds. (2023).
Bone inside-out and outside-in signals: Control of body homeostasis.
Lausanne: Frontiers Media SA. doi: 10.3389/978-2-83251-389-7

Table of contents

05	Editorial: Bone inside-out and outside-in signals: Control of body homeostasis Uma Sankar, Lucas R. Brun and Lilian I. Plotkin
09	Modulation of the Inflammatory Response and Bone Healing Masahiro Maruyama, Claire Rhee, Takeshi Utsunomiya, Ning Zhang, Masaya Ueno, Zhenyu Yao and Stuart B. Goodman
23	Osteoimmunology: The Regulatory Roles of T Lymphocytes in Osteoporosis Wenjuan Zhang, Kai Dang, Ying Huai and Airong Qian
31	Osteocytic FGF23 and Its Kidney Function Rafiou Agoro, Pu Ni, Megan L. Noonan and Kenneth E. White
48	Influence of HIV Infection and Antiretroviral Therapy on Bone Homeostasis María Victoria Delpino and Jorge Quarleri
57	Calcitonin Induces Bone Formation by Increasing Expression of Wnt10b in Osteoclasts in Ovariectomy-Induced Osteoporotic Rats Chen-Yuan Hsiao, Tien-Hua Chen, Tzu-Hui Chu, Yen-Nien Ting, Pei-Jiun Tsai and Jia-Fwu Shyu
69	Dual Effects of Lipid Metabolism on Osteoblast Function Nathalie S. Alekos, Megan C. Moorer and Ryan C. Riddle
84	The Role of Nerves in Skeletal Development, Adaptation, and Aging Ryan E. Tomlinson, Blaine A. Christiansen, Adrienne A. Giannone and Damian C. Genetos
96	Human Amniotic Mesenchymal Stem Cells Promote Endogenous Bone Regeneration Jin Li, Zhixuan Zhou, Jin Wen, Fei Jiang and Yang Xia
105	Intrinsic Restriction of TNF-Mediated Inflammatory Osteoclastogenesis and Bone Resorption Baohong Zhao
113	Osteocytes and Bone Metastasis Manuel A. Riquelme, Eduardo R. Cardenas and Jean X. Jiang
124	The Hyperglycemia and Hyperketonemia Impaired Bone Microstructures: A Pilot Study in Rats Qi Liu, Zhou Yang, Chuha Xie, Long Ling, Hailan Hu, Yanming Cao, Yan Huang, Qingan Zhu and Yue Hua
134	Control of Bone Matrix Properties by Osteocytes Amy Creecy, John G. Damrath and Joseph M. Wallace

- 144 **Interleukin-6 Knockout Inhibits Senescence of Bone Mesenchymal Stem Cells in High-Fat Diet-Induced Bone Loss**
Yujue Li, Lingyun Lu, Ying Xie, Xiang Chen, Li Tian, Yan Liang, Huifang Li, Jie Zhang, Yi Liu and Xijie Yu
- 156 **Muscle-Bone Crosstalk in the Masticatory System: From Biomechanical to Molecular Interactions**
Sonja Buvinic, Julián Balanta-Melo, Kornelius Kupczik, Walter Vásquez, Carolina Beato and Viviana Toro-Ibacache
- 175 **Sclerostin and Osteocalcin: Candidate Bone-Produced Hormones**
Jialiang S. Wang, Courtney M. Mazur and Marc N. Wein
- 190 **Circulating Carboxylated Osteocalcin Correlates With Skeletal Muscle Mass and Risk of Fall in Postmenopausal Osteoporotic Women**
Jacopo Antonino Vitale, Veronica Sansoni, Martina Faraldi, Carmelo Messina, Chiara Verdelli, Giovanni Lombardi and Sabrina Corbetta
- 201 **Hematopoietic Wnts Modulate Endochondral Ossification During Fracture Healing**
Kenon Chua, Victor K. Lee, Cheri Chan, Andy Yew, Eric Yeo and David M. Virshup
- 212 **Decreased Sclerostin Secretion in Humans and Mice With Nonalcoholic Fatty Liver Disease**
Fangli Zhou, Yan Wang, Yujue Li, Mengjia Tang, Shan Wan, Haoming Tian and Xiang Chen
- 221 **The Associations of Serum Osteocalcin and Cortisol Levels With the Psychological Performance in Primary Hyperparathyroidism Patients**
Shu-min Wang, Yang He, Min-ting Zhu, Bei Tao, Hong-yan Zhao, Li-hao Sun and Jian-min Liu
- 230 **NLRP3 Inflammasome: A New Target for Prevention and Control of Osteoporosis?**
Na Jiang, Jinyang An, Kuan Yang, Jinjin Liu, Conghui Guan, Chengxu Ma and Xulei Tang



OPEN ACCESS

EDITED AND REVIEWED BY
Jonathan H Tobias,
University of Bristol, United Kingdom

*CORRESPONDENCE

Uma Sankar
✉ usankar@iupui.edu
Lucas R. Brun
✉ lbrun@unr.edu.ar
Lilian I. Plotkin
✉ lplotkin@iu.edu

SPECIALTY SECTION

This article was submitted to
Bone Research,
a section of the journal
Frontiers in Endocrinology

RECEIVED 09 December 2022

ACCEPTED 19 December 2022

PUBLISHED 06 January 2023

CITATION

Sankar U, Brun LR and Plotkin LI
(2023) Editorial: Bone inside-out
and outside-in signals: Control of
body homeostasis.
Front. Endocrinol. 13:1120215.
doi: 10.3389/fendo.2022.1120215

COPYRIGHT

© 2023 Sankar, Brun and Plotkin. This is
an open-access article distributed under
the terms of the [Creative Commons
Attribution License \(CC BY\)](https://creativecommons.org/licenses/by/4.0/). The use,
distribution or reproduction in other
forums is permitted, provided the
original author(s) and the copyright
owner(s) are credited and that the
original publication in this journal is
cited, in accordance with accepted
academic practice. No use,
distribution or reproduction is
permitted which does not comply
with these terms.

Editorial: Bone inside-out and outside-in signals: Control of body homeostasis

Uma Sankar^{1,2*}, Lucas R. Brun^{3,4*} and Lilian I. Plotkin^{1,2,5*}

¹Department of Anatomy, Cell Biology & Physiology, Indiana University School of Medicine, Indianapolis, IN, United States, ²Indiana Center for Musculoskeletal Health, Indiana University School of Medicine, Indianapolis, IN, United States, ³Bone Biology Laboratory, School of Medicine, Rosario National University, Rosario, Argentina, ⁴Consejo Nacional de Investigaciones Científicas y Técnicas (CONICET), Rosario, Argentina, ⁵Roudebush Veterans Administration Medical Center, Indianapolis, IN, United States

KEYWORDS

bone, osteocyte, osteoclast, osteoblast, endocrine signals

Editorial on the Research Topic

Bone inside-out and outside-in signals: Control of body homeostasis

Summary

Bone mass is controlled by the coordinated actions of osteoblasts and osteoclasts, cells responsible for bone formation or bone resorption, respectively. It is now clear that the actions of these two cell types, as well as their differentiation from the corresponding precursor cells, is modulated by osteocytes, the cells embedded in the bone matrix. Recent findings indicate that in addition to their role in controlling bone mass, bone cells act as endocrine cells, and all cells produce factors able to regulate the function of distal organs, including muscle, pancreas, kidney and brain, among others. Conversely, hormones and growth factors produced by cells, other tissues modulate bone modeling and remodeling by altering osteoblast, osteoclast and osteocyte functions. Further, more recently studies provided evidence for a role of the gut microbiome on bone homeostasis. Understanding the molecular signature of bone cells, and how these cells are affected by circulating factors has provided new means to treat conditions with altered bone mass and strength.

The purpose of this Research Topic Issue was to discuss different aspects of bone interactions with other tissues, both inside-out (from bone cells to other organs) and outside-in (from other cells/tissues to bone cells). This Research Topic included 20 articles from which 7 are originals and 13 reviews. The following is a summary of the articles included in the Research Topic Issue.

Role of osteocytes as endocrine cells

Osteocytes, previously believed to be inert cells embedded in the bone matrix, are emerging as key regulators of bone homeostasis, as well as cells producing molecules that signal to other tissues and organs. **Fibroblast growth factor 23**, of osteocytic fibroblast growth factor 23 (FGF23) is produced and secreted primarily by osteocytes both as an active molecule and as truncated, inactive fragments that can be detected in the circulation. The authors describe the response of osteocytes to increased phosphate and 1,25(OH)₂ vitamin D, leading to the production of FGF23. In turn, FGF23 activate renal receptors to control circulating phosphate levels. The synthesis and secretion of FGF23 is regulated by positive and negative signals. Osteocytes can “sense” phosphate levels by a mechanism not completely understood, but that appears to involve the type III sodium phosphate co-transporter PiT2 (Slc20a2). In addition to high phosphate levels, FGF23 is positively regulated by pro-inflammatory molecules and iron deficiency, hypoxia and erythropoietin, TGFβ, calcineurin and NFAT, as well as transcriptional regulation by parathyroid hormone, and calcitriol. FGF23 can be also negatively regulated by PHEX, DMP1, insulin and IGF-1. In addition to these regulations, the level and activity of FGF23 is regulated by intracellular proteolytic enzymes. Upon enzymatic cleavage, FGF23 becomes inactive. Another important emerging function of osteocytes is the control of **bone matrix properties**. Thus, osteocytes have the ability to communicate and modulate the generation and function of osteoblasts and osteoclasts, which can in turn alter the properties of bone matrix through changes in bone formation and resorption. In addition, it has been proposed that osteocytes themselves have the ability to remodel the perilacunar space, changing the composition of the bone matrix. Studies *in vitro* described in this article used osteocytic cell lines, and their response to endocrine, paracrine, and mechanical stimuli has been studied using 2D and 3D systems. *In vivo* studies focused mainly on the perilacunar remodeling during lactation and hibernation, with emphasis in the consequences of these conditions on mineral composition and structure, as well as in the role of osteocytic genes on collagen degradation. More recent studies have shown the role of osteocytes in osteolytic metastasis. While reviewing the current understanding on how on how osteocytes regulate the growth of bone metastatic tumors **bone metastatic tumors**, the authors proposed both protective and enhancing effect of osteocytes on tumor growth and metastasis. For example, osteocytes can promote prostate cancer cell proliferation, migration, and invasion *via* the release of growth-derived factor 15 (GDF15), and osteocyte apoptosis within lytic multiple myeloma lesions leads to increased sclerostin and RANKL production, generating a negative bone remodeling balance. This is followed by

activation of Notch signaling and increased myeloma cell proliferation. Other studies have shown an inhibitory effect of osteocytic Cx43 on cancer cell growth, mediated at least in part but the release of ATP through Cx43 hemichannels.

Osteocalcin and its endocrine functions

Osteoblasts and osteocytes are proposed to be endocrine cells, producing and releasing **osteocalcin and sclerostin**, which in turn are able to act on cells and tissues outside the bone, fulfilling the definition of “hormones”. Osteocalcin (γ-carboxyglutamic acid, Gla, protein) is synthesized as pro-hormone by osteoblasts, it is later cleaved γ-carboxylated, which increases the affinity of the protein for the mineral component of the bone matrix. γ-carboxylated osteocalcin can be stored within the bone and later be released by bone resorbing osteoclasts. Full deletion of the osteocalcin gene has shown disparate effects on bone mass and strength. These differences could be due to different manners for gene deletion, differences in the mouse genetic background, sex, age in which the analyses were made. Discrepancies were also reported on the role of osteocalcin in energy metabolism, with disparate consequences on glucose levels, body weight, muscle weight, and male reproduction depending on the osteocalcin deficiency model used. Studies were also performed in mice lacking the *Bglap* (exon 4) and *Bglap2* genes to determine the role of osteocalcin in the central nervous system, prompted by observations during animal handling. Further studies showed that mice deficient in osteocalcin exhibit hippocampal atrophy and dramatic changes in neurotransmitter levels in the central nervous system. These effects are ascribed to the lack of circulating maternal uncarboxylated osteocalcin, which can cross the placenta and fetal blood-brain barrier. In another set of studies using the same mouse model, it was shown that osteocalcin regulates output of parasympathetic neurons under acute stress response, and that sympathetic input in this condition increases osteocalcin production by osteoblasts. These effects of osteocalcin have not been tested in the other osteocalcin deficiency models.

Osteocalcin secreted by osteoblasts and released from the bone matrix by osteoclasts has been shown to regulate muscle mass independently of its effects on systemic energy homeostasis. **Circulating osteocalcin** levels in older postmenopausal women with osteoporosis correlate with skeletal muscle mass and their OAK-score-related risk of falling. This study also found plasma carboxylated osteocalcin levels to positively correlate with lean body mass and muscle function. Thus, circulating osteocalcin could mediate bone-muscle crosstalk, and its levels could be predictive of muscle function and fall risk in older postmenopausal women. Further, bone-secreted factors such as lipocalin influence hypothalamic feeding behavior, suggesting

the existence of a bone-brain axis. Factors responsible for **neuropsychological symptoms** were evaluated in the serum of patients with primary hyperparathyroidism. The study found that serum osteocalcin levels positively correlate with parathyroid hormone (PTH) levels and negatively correlate with State-Trait Anxiety Inventory (STAI). Thus, serum osteocalcin was associated with psychological performance in patients with primary hyperparathyroidism and could mediate bone-brain crosstalk.

Outside-in signaling: hematopoietic and endocrine cells regulate bone cell function

Wnt signaling plays a critical role in skeletal homeostasis. The skeletal role for Wnt secreted by **hematopoietic cells** was examined by conditionally deleting Wnt modifying enzyme PORCN using *Vav-Cre* transgenic mice. Hematopoietic *Porcn* deletion did not affect normal skeletal development but delayed fracture healing. These mice possessed fewer osteoclasts at the fracture callus causing a delay in callus remodeling. Calcitonin is a small peptide hormone secreted by the thyroid gland in response to increases in serum calcium levels. It inhibits osteoclastic bone resorption and associated release of skeletal calcium. Calcitonin also enhances osteoblastic bone formation, but the underlying mechanism was not fully understood, especially because the calcitonin receptor is present only in osteoclasts and not osteoblasts. It is now reported that calcitonin induces bone formation by increasing the expression of the cytokine Wnt10b in osteoclasts in ovariectomized rat models of osteoporosis, indicating a thyroid-bone crosstalk.

Lipid regulation by bone-produced molecules

Sclerostin is a potent inhibitor of Wnt signaling that is mainly produced by mature osteocytes. Through its interaction with LRP4/5/6, sclerostin has been shown to stimulate adipogenesis by inhibiting Wnt signaling. Although no evidence of changes in adipose tissue in patients with absence of sclerostin has been reported, clinical studies showed positive correlations between serum sclerostin levels and fat mass and the incidence of **metabolic disorders**. Studies *in vitro* and in animal models support the role of sclerostin on adipogenesis and fat mass. Another set of studies showed that sclerostin has direct effects in the kidney, regulating calcium excretion and the synthesis of $1\alpha,25(\text{OH})_2\text{D}$, thereby contributing to the control of mineral homeostasis. Others have shown that sclerostin can affect the cardiovascular system *via* inhibition of vascular calcification, and that its inhibition can lead to elevated risk of

cardiovascular adverse events. **Serum sclerostin** was found to be significantly lower in patients with non-alcoholic fatty liver disease (NAFLD) patients compared to non-NAFLD patients. In NAFLD patients, serum sclerostin levels negatively correlated with metabolic parameters including fatty liver index and triglyceride levels. These findings indicate the existence of a bone-liver crosstalk playing a role in abnormal bone metabolism in NAFLD patients and suggest the utility of serum sclerostin as a biomarker for bone disease in NAFLD patients.

In addition of utilizing glucose as source of energy, osteoblasts are able to internalize and metabolize lipids. In a review by **Alekos et al.**, the mechanism by which disruption of lipid metabolism in osteoblasts affects the skeleton and whole body **lipid homeostasis** is discussed. In particular, the evidence supporting the requirement for fatty acid oxidation in osteoblasts and the detrimental consequences of its inhibition on the skeleton and bone repair following fractures. Further, fatty acid oxidation is regulated by bone anabolic treatments, and the review describes how Wnt and parathyroid hormone signaling. In particular, LRP5 deletion and expression of a gain of function mutant lead to opposite effects on lipids markers, with increase and decrease in fat mass and serum triglycerides and free fatty acid, respectively. These effects of Wnt signaling are dependent on β -catenin expression, suggesting that canonical Wnt signaling is involved in the regulation of lipid metabolism by osteoblasts. Evidence also suggests that parathyroid hormone and 1,25 dihydroxycholecalciferol influence fatty acid oxidation at least *in vitro/ex vivo*, and that intermittent PTH administration might induce the release of fatty acids from adipocyte to fuel osteoblast anabolic activity. The review further discusses the consequences of dyslipidemia in the skeleton, and how hyperlipidemia impacts the response of bone to anabolic signals. Thus, increase lipids induce the release of Wnt inhibitors, and accumulation of oxidized lipids inhibits PTH signaling. In addition, dyslipidemia leads to insulin resistance in osteoblasts, which might contribute to bone loss associated with this condition. PPAR γ , a transcription factor that regulates adipogenesis has been identified as a potential link between hyperlipidemia and bone loss. Metabolic diseases detrimentally affect the bone. Both **hyperglycemia** and ketogenic diet diminished bone mass, microstructure and strength due to enhanced osteoclast and diminished osteoblast activity.

Bone-muscle crosstalk in the masticatory system

Further evidence of the role of bone as an endocrine organ, and the crosstalk with skeletal muscle is described in the **masticatory system**. In addition of biomechanical interaction between bone and muscle, the authors describe the role of

myostatin, IGF-1 and IL-6 as mediators of the communication between the two tissues. The authors further discuss the clinical evidence supporting the biochemical interaction between muscle and bone at the masticatory system. For example, muscle-released IL-6 is proposed to mediate mandibular remodeling in tempomandibular disorders and potentially, the deleterious effects on mandibular bone following muscle paralysis by botulinum toxin. Conversely, bone-derived osteocalcin has been linked to masticatory muscle hypertrophy. Thus, osteocalcin can regulate IL-6 levels in skeletal muscle, which in turn upon release is able to modify bone remodeling, creating a feedback loop between bone and muscle. Other biochemical mediators of the bone-muscle interaction are sclerostin and RANKL, produce and released by osteocytes in bone, and with catabolic potential in skeletal muscle cells, can be further evaluated as complementary therapeutical targets for highly prevalent oral diseases such as periodontitis.

Osteoimmunology

Osteoimmunology is emerging as a new interdisciplinary field to explore the shared molecules and interactions between the skeletal and immune systems. Here, a review summarizes the **regulatory roles of T lymphocytes in osteoporosis** and the development of T cell therapy for osteoporosis from osteoimmunology perspective. The inflammatory response is related to **bone healing** due to chronic inflammation can lead to impaired fracture healing. This review summarizes the principles of inflammation and provide an update on cellular interactions and immunomodulation for optimal bone healing. Interleukin-6 (IL-6) is a pro-inflammatory mediator that plays a key role in obesity-induced loss of bone microarchitecture by inducing **senescence of mesenchymal stem cells**. Bone regeneration is promoted by **human amniotic mesenchymal stem cells** due to paracrine functions on immune-regulation, anti-inflammation and vascularized tissue regeneration. The review focus on the therapeutic effects and mechanisms of this cells in promoting bone regeneration in joint diseases and bone defects. Inflammasomes are multiprotein complex of the innate immune system responsible for secretion of pro-inflammatory cytokines. The chronic inflammatory microenvironment induced by aging or estrogen deficiency activates the NLRP3 inflammasome. The review about **NLRP3 Inflammasome** highlights the function of NLRP3 inflammasome in osteoporosis as a role in the pathogenesis of osteoporosis by affecting the differentiation of osteoblasts and osteoclasts. providing information on new strategies for managing osteoporosis. Further, the **TNF-mediated inflammatory osteoclastogenesis** is also considered providing potential therapeutic strategies to selectively treat inflammatory bone

resorption, without undesirable effects on normal bone remodeling or immune response in disease settings. **HIV infection** leads toward an inflammatory state associated with chronic and immune dysregulation activation and involve the OPG/RANKL/RANK system. It also provides antiretroviral therapy-related detrimental effects on bone metabolism.

Bone-nervous system interactions

Orthopaedic pain management remains a clinical and societal challenge. The skeleton is well-innervated, but its function remains under-appreciated. Understanding the **signaling between bone and nerve** during skeletal development, fracture healing and aging will lead to a better comprehension of skeletal pain and better therapeutic strategies to alleviate orthopaedic pain.

Author contributions

All authors listed have made a substantial, direct, and intellectual contribution to the work and approved it for publication.

Funding

This work was partially supported by the National Institute of Health (NIH) R01-AR053643 and the Veterans Research Administration Merit Award I01BX005154 to LP, by NIH R01AR076477 and U.S. ARMY MEDICAL RESEARCH ACQUISITION ACTIVITY Award W81XWH-20-1-0304 to US, and by Consejo Nacional de Investigaciones Científicas y Técnicas (CONICET), Argentina -PIP 11220200100085- to LB.

Conflict of interest

The authors declare that the research was conducted in the absence of any commercial or financial relationships that could be construed as a potential conflict of interest.

Publisher's note

All claims expressed in this article are solely those of the authors and do not necessarily represent those of their affiliated organizations, or those of the publisher, the editors and the reviewers. Any product that may be evaluated in this article, or claim that may be made by its manufacturer, is not guaranteed or endorsed by the publisher.



Modulation of the Inflammatory Response and Bone Healing

Masahiro Maruyama¹, Claire Rhee¹, Takeshi Utsunomiya¹, Ning Zhang¹, Masaya Ueno¹, Zhenyu Yao¹ and Stuart B. Goodman^{1,2*}

¹ Department of Orthopaedic Surgery, Stanford University, Stanford, CA, United States, ² Department of Bioengineering, Stanford University, Stanford, CA, United States

OPEN ACCESS

Edited by:

Deborah Veis,
Washington University School of
Medicine in St. Louis, United States

Reviewed by:

Michaela Tencerova,
Institute of Physiology
(ASCR), Czechia
Paula H. Stern,
Northwestern University, United States

*Correspondence:

Stuart B. Goodman
goodbone@stanford.edu

Specialty section:

This article was submitted to
Bone Research,
a section of the journal
Frontiers in Endocrinology

Received: 13 March 2020

Accepted: 14 May 2020

Published: 11 June 2020

Citation:

Maruyama M, Rhee C, Utsunomiya T,
Zhang N, Ueno M, Yao Z and
Goodman SB (2020) Modulation of
the Inflammatory Response and Bone
Healing. *Front. Endocrinol.* 11:386.
doi: 10.3389/fendo.2020.00386

The optimal treatment for complex fractures and large bone defects is an important unsolved issue in orthopedics and related specialties. Approximately 5–10% of fractures fail to heal and develop non-unions. Bone healing can be characterized by three partially overlapping phases: the inflammatory phase, the repair phase, and the remodeling phase. Eventual healing is highly dependent on the initial inflammatory phase, which is affected by both the local and systemic responses to the injurious stimulus. Furthermore, immune cells and mesenchymal stromal cells (MSCs) participate in critical inter-cellular communication or crosstalk to modulate bone healing. Deficiencies in this inter-cellular exchange, inhibition of the natural processes of acute inflammation, and its resolution, or chronic inflammation due to a persistent adverse stimulus can lead to impaired fracture healing. Thus, an initial and optimal transient stage of acute inflammation is one of the key factors for successful, robust bone healing. Recent studies demonstrated the therapeutic potential of immunomodulation for bone healing by the preconditioning of MSCs to empower their immunosuppressive properties. Preconditioned MSCs (also known as “primed/ licensed/ activated” MSCs) are cultured first with pro-inflammatory cytokines (e.g., TNF α and IL17A) or exposed to hypoxic conditions to mimic the inflammatory environment prior to their intended application. Another approach of immunomodulation for bone healing is the resolution of inflammation with anti-inflammatory cytokines such as IL4, IL10, and IL13. In this review, we summarize the principles of inflammation and bone healing and provide an update on cellular interactions and immunomodulation for optimal bone healing.

Keywords: bone healing, immunomodulation, inflammation, mesenchymal stromal cell, preconditioning, pro-inflammatory cytokines, anti-inflammatory cytokines

INTRODUCTION

The optimal treatment for complex fractures and large bone defects is an important unsolved issue in orthopedics and related specialties. In the United States alone, there are ~8 million bone fractures annually; 5–10% of fractures fail to heal and develop a non-union (1). The average cost for treatment of a bone non-union is estimated to be >US\$ 10,000 (2).

Bone healing after injury is a complex biological and biomechanical process. Bone healing can be characterized by three partially overlapping phases: the inflammatory phase, the repair phase, and the remodeling phase (3). Eventual healing is highly dependent on the initial inflammatory phase, which is affected by both the local and systemic responses to the injurious stimulus.

Furthermore, immune cells and mesenchymal stromal cells (MSCs) participate in critical inter-cellular communication or crosstalk to modulate bone healing. Thus, understanding and regulating inflammation is one of the key factors for successful, robust bone healing.

This review will summarize the principles of inflammation and bone healing, and provide an update on cellular interactions and immunomodulation for optimal bone healing.

WHAT IS INFLAMMATION?

Inflammation is the protective response of tissue to a noxious stimulus, leading to both the removal of harmful stimuli, and the initiation of the healing process (4, 5). Acute inflammation is marked by capillary dilatation and leukocytic migration and infiltration to the local area; this leads to the clinical symptoms of redness, heat, pain, and loss of function (6).

Acute Inflammation

Acute inflammation is initiated by endogenous or exogenous adverse stimuli (4, 6). The acute inflammatory response after injury peaks within the first 24–48 h and is generally complete after 7 days (7, 8). In acute inflammation, tissue-resident cells including tissue macrophages, dendritic cells, lymphocytes, endothelial cells, fibroblasts, and mast cells recognize invading pathogens, or tissue injury byproducts, and release a variety of pro-inflammatory mediators including cytokines, chemokines, and growth factors; this results in the infiltration of polymorphonuclear neutrophils (PMNs), monocytes/macrophages, and lymphocytes into the injured site. PMNs phagocytose and eliminate invading pathogens and tissue debris. Macrophages are polarized to the M1 phenotype by damage-associated molecular patterns (DAMPs, e.g., apoptotic cells and their byproducts), pathogen-associated molecular patterns (PAMPs, e.g., bacterial endotoxin, lipopolysaccharide [LPS]), and pro-inflammatory cytokines (e.g., interferon γ [IFN γ], tumor necrosis factor α [TNF α], interleukin 1 β [IL1 β]) (6, 9). During acute inflammation, M1 macrophages contribute to host defense as well as amplify the inflammatory reaction and recruit additional immune cells (10). M1 macrophages phagocytose and remove micro-organisms, necrotic tissue, and the provisional fibrin matrix (5, 6, 10). In addition, M1 macrophages secrete pro-inflammatory and chemotactic mediators, such as TNF α , IL1 β , IL6, and C-C motif chemokine 2 (CCL2) (known as monocyte chemoattractant protein 1 [MCP1]) (5, 6). These mediators initiate further recruitment of inflammatory cells and MSCs (5, 6).

The Resolution of Inflammation

The resolution of inflammation was traditionally characterized as a passive process (11, 12). However, more recently, the resolution of inflammation is thought to be an active process, regulated by various mediators and immune cells (13).

The resolution process begins a few hours after the acute inflammatory response is initiated. First, the initial inflammatory stimuli are eliminated; subsequently, pro-inflammatory

mediators are suspended, whereas anti-inflammatory (pro-resolving) mediators, such as IL4, IL10, and IL13, and CCL2, are promoted. PMNs cease to infiltrate the injury site and undergo apoptosis and subsequent efferocytosis by macrophages (14). Efferocytosis is the removal of apoptotic cells that are swiftly engulfed and digested by macrophages. Macrophages are polarized from a pro-inflammatory M1 phenotype to an anti-inflammatory tissue-repair M2 phenotype by anti-inflammatory cytokines, resulting in the advancement of the healing processes (9, 15).

Recently it has been proposed that the resolution of acute inflammation may not terminate the local immune response. Subsequent immunological activity after the resolution of the acute inflammatory stage is termed “the post-resolution stage,” to obtain a state of “adapted (or adaptive) homeostasis” at the injury site (13, 16). Adapted homeostasis alters the innate immune environment of tissues after the resolution of inflammation, including modifying the biochemical, phenotypic, and functional aspects of affected cells (13). This new adapted homeostatic environment may lead to new set-points and ranges of immune response, and is important for the maintenance of immune tolerance. This is an area of ongoing active research.

Chronic Inflammation

Chronic inflammation is a state in which acute inflammation, fibrosis, and repair occur simultaneously (17). In chronic inflammation, monocytes/macrophages, lymphocytes, fibroblasts, and other cells are present at the injury site (17, 18). Examples of chronic inflammation include periprosthetic osteolysis due to wear particles after total joint arthroplasty, and autoimmune diseases such as rheumatoid arthritis and systemic lupus erythematosus (SLE) (9, 17). The failure of the resolution stage may lead to chronic inflammation, which may persist for prolonged periods of several weeks, or in some cases, months to years (9, 17). In chronic inflammation, adaptive homeostasis is not achieved. Continued production of pro-inflammatory cytokines such as IFN γ and TNF α continues to polarize macrophages to a pro-inflammatory M1 phenotype rather than an anti-inflammatory tissue-repair M2 phenotype. Therefore, chronic inflammation fails to establish an adaptive homeostatic state (9).

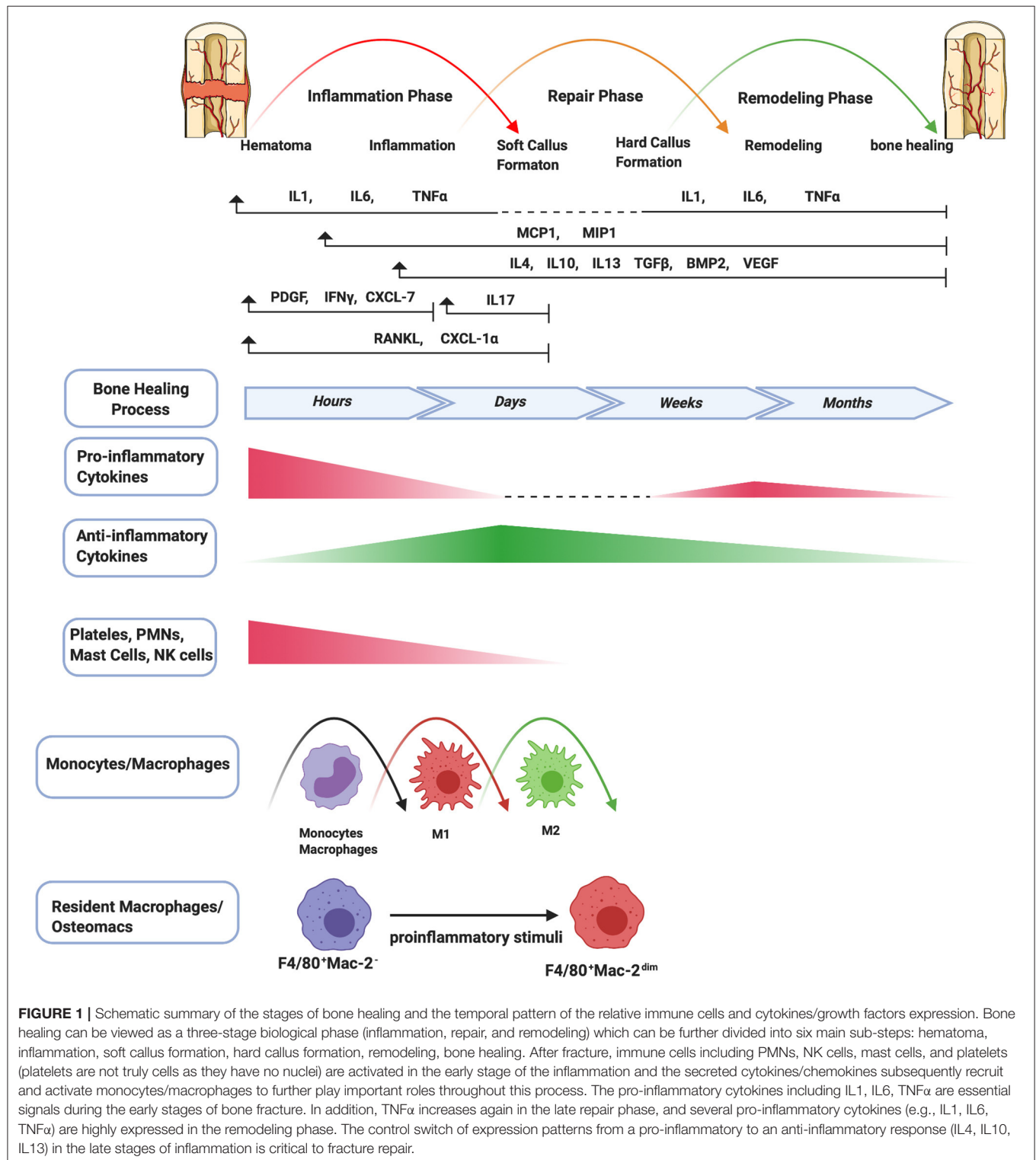
WHAT IS BONE HEALING?

Bone healing is an intricate regenerative process which can be classified into primary (direct) and secondary (indirect) bone healing (3, 19). Primary bone healing is uncommon in the process of fracture healing and occurs under extremely rigid fixation without any displacement of bony fragments. The fracture site is bridged by Haversian systems (or osteons), similar to the normal bone remodeling. Bone healing by Haversian systems has little or no inflammatory response and is a slow healing process that takes from a few months to a few years to achieve complete healing (3, 19). On the other hand, secondary bone healing is the most common form of fracture healing. Generally, the process of secondary bone healing is characterized by three partially overlapping phases:

the inflammatory phase, the repair phase, and the remodeling phase (3) (**Figure 1**). Eventual healing is highly dependent on the initial inflammatory phase. Furthermore, immune cells and bone marrow-derived MSCs (BM-MSCs) participate in critical inter-cellular communication or crosstalk to modulate bone healing.

Inflammatory Phase

An inflammatory response occurs immediately following bone fracture. The trauma leads to blood vessel rupture inside and surrounding the fracture site, resulting in a hematoma. The hematoma micro-environment is initially characterized by local hypoxia, acidity, and lower temperature, and is rich in



calcium and lactic acid (20). The hematoma works as a scaffold for recruited inflammatory cells and a variety of cytokines, including IL1, IL6, TNF α , CCL2, and others, to initiate the inflammatory cascade (20). First, PMNs are recruited and then monocytes/macrophages infiltrate into the fracture site (21). Macrophages are polarized to the M1 phenotype. After infiltration of macrophages, the immune response shifts toward adaptive immunity, reflected by the invasion of lymphocytes into the fracture zone. PMNs and macrophages clear the area of dead cells and debris, and the process transforms to the resolution of inflammation, which is a complex and well-regulated activity. In this process, the agents initiating the inflammatory response and the synthesis of pro-inflammatory mediators are reduced, and the immune cells are gradually cleared from the tissue (9). Osteomacs, a special subtype of macrophages residing in bone tissues, are distributed among bone lining cells within both endosteum and periosteum and contribute bone homeostasis. Osteomacs not only sense the original injurious stimulus and initiate the inflammatory cascade, but also provide a source of molecules that begins the essential cellular events for bone healing (22, 23).

During the resolution of acute inflammation, macrophages are polarized from an M1 phenotype to an M2 phenotype by anti-inflammatory cytokines such as IL4, IL10, and IL13. BM-MSCs are attracted locally by cytokines such as TNF α (24) and stromal cell-derived factor 1 (SDF1) (known as chemokine C-X-C motif chemokine ligand 12 [CXCL12]). Recruited inflammatory cells and BM-MSCs participate in critical inter-cellular communication or crosstalk via pro-inflammatory cytokines, anti-inflammatory cytokines, as well as transforming growth factor β (TGF β), bone morphogenetic proteins (BMPs), and growth factors (e.g., vascular endothelial growth factor [VEGF], platelet-derived growth factor [PDGF] and fibroblast growth factor-2 [FGF-2]) to initiate osteogenesis and angiogenesis (25). This process could also create a reparative granuloma forming a template for the following formation of callus (26). The acute inflammatory response peaks within 24–48 h and disappears at about 1-week post-fracture.

Repair Phase

During the repair phase, callus is formed as vascular buds grow into the area, and the collagen matrix is laid down. Callus formation has two types of processes: intramembranous ossification and endochondral ossification (27). Intramembranous ossification occurs at the periosteum and forms hard callus directly. Periosteal MSCs differentiate into osteoprogenitor cells, which subsequently proliferate and differentiate into osteoblasts that directly form woven bone. Endochondral ossification occurs at the endosteum and bone marrow, and forms soft callus and then hard callus. BM-MSCs differentiate into chondrocytes and secrete a cartilage matrix which forms a cartilaginous template. Chondrocytes subsequently undergo hypertrophic differentiation and mineralize the surrounding matrix to form cartilaginous callus. Finally, hypertrophic chondrocytes undergo apoptosis, resulting in vascular invasion and migration of osteoblasts.

Cartilage matrix subsequently converts to bone matrix (27). Pro-inflammatory cytokines including IL1 and IL6 are absent during this phase (19). TNF α is also diminished in the early repair phase but increases in the late repair phase (24). In the endochondral ossification process, TNF α facilitates chondrocyte apoptosis, resorption of mineralized cartilage, and vascularization (24, 28). Lower levels of TNF α also enhance osteoblast proliferation but high levels inhibit these processes (24). In addition, osteomacs are enriched at sites of bone formation, forming a canopy-like structure over sites of active cuboidal osteoblasts. Osteomacs are associated with maturing of bone tissues in the repair and remodeling phases (22, 23). Alternatively, osteoclasts are highly differentiated multinucleated cells that degrade bone.

Remodeling Phase

At the late stage of bone healing, bone is restored to its original structure, shape, and mechanical properties by remodeling. The balance between osteoblastic and osteoclastic activity which results in lamellar bone deposition and bone resorption plays an important role during the remodeling stage (19, 27). Several pro-inflammatory cytokines (e.g., IL1, IL6, and TNF α) are highly expressed (3, 19, 26).

IS INFLAMMATION NECESSARY TO OBTAIN BONE HEALING?

Inflammation is the crucial first step for bone healing as described above. However, deficiency and inhibition of acute inflammation can lead to impaired bone healing. For example, it is well-known that drugs such as non-steroidal anti-inflammatory drugs (NSAIDs), corticosteroids, chemotherapeutic agents and others increase the risk for non-union (29, 30). In addition, excess acute inflammation due to severe injuries such as polytrauma, and open fracture also increases the risk for impaired bone healing (31). Furthermore, chronic inflammation is detrimental to bone healing (31).

Deficiency and Inhibition of Acute Inflammation

NOD/SCID-IL2R γ ^{null} mice are innate and adaptive immunodeficient mice that lack functional monocytes, dendritic cells, natural killer cells, and lymphocytes (32). In addition, there is a defect in the common gamma-chain of the IL2 receptor (γ_c) such that signaling of IL-2, IL-4, IL-7, IL-9, IL-15, and IL-21 is defective (33). The fracture healing process in NOD/SCID-IL2R γ ^{null} mice demonstrates a callus whose bone content is unaffected during the early healing stage; however, the callus is reduced during the late healing phase and the amount of cartilage is significantly increased, indicating delayed endochondral ossification (34).

The pro-inflammatory cytokine TNF α has a complex role during bone healing, demonstrating biphasic peaks at 72 h and 3 weeks after injury (35). TNF α -receptor-deficient mice showed delayed endochondral and intramembranous bone formation (24, 36, 37). Furthermore, TNF α knockout mice demonstrated poor endochondral bone repair after

fracture, but had normal skeletogenesis, implicating TNF α signaling specifically in early fracture repair (38). IL6 has been shown to increase osteoclastogenesis (39). IL6 knockout mice demonstrated delayed fracture healing, with decreased osteoclastogenesis and impaired callus formation, but showed comparable bone healing and strength in the late stage of fracture healing (40, 41). The IL6 signal has two different pathways: the classic signaling pathway via the membrane-bound receptor (mIL6R) and the trans-signaling pathway via its soluble form (sIL6R) (42). Recent studies using a fracture model in rats demonstrated that the classic signaling pathway regulates the immune response and bone healing, whereas the trans-signaling pathway has a minor effect on the immune response and does not influence bone healing (43); rather it has negative effects on bone healing after severe trauma (44). IL17A, secreted mainly by $\gamma\delta$ T cells, has also been characterized as an inflammatory cytokine (45). IL17A expression is induced in the early phase of bone healing and stimulates the proliferation and osteoblastic differentiation of BM-MSCs (45–47). IL17A knockout mice exhibited delayed callus formation and lower bone mineral density due to a decrease in osteoblastic bone formation (45). CCL2 is an important chemokine expressed early in inflammatory conditions. CCL2 deficient mice showed diminished infiltration of macrophages and BM-MSCs, and impaired vascularization, resulting in delayed fracture healing, and less callus formation (48). Thus, pro-inflammatory cytokines and chemokines are critical to bone healing. Conversely, although IL1 β promotes the proliferation and differentiation of murine pre-osteoblasts *in vitro*, IL1 β receptor knockout mice had normal bone healing (49).

Prostaglandin E2 (PGE2) plays a key role in bone metabolism including homeostasis, inflammation, and healing (50, 51). Cyclooxygenase 2 (COX-2) is a key enzyme important to PGE2 synthesis. COX-2 knockout mice exhibited reduced osteoblastogenesis and impaired intramembranous and endochondral bone healing (52). NSAIDs have analgesic, antipyretic, and anti-inflammatory effects, and are frequently used to treat musculoskeletal conditions. Continuous use of NSAIDs is associated with delayed bone healing and non-union via inhibition of the COX2-PGE2 pathway (53, 54). In our previous study, co-culture of murine BM-MSCs with undifferentiated M0, pro-inflammatory M1, or anti-inflammatory M2 macrophages showed that celecoxib, a COX-2 selective NSAID, reduced bone mineralization in all co-cultures but most dramatically in the BM-MSC-M1 co-cultures (55). This study re-emphasized the importance of an initial transient acute inflammatory period during fracture healing.

Excess of Inflammation vs. Bone Healing

Excessive acute inflammation can be caused by several stimuli including microbial infection, surgical intervention, and injury due to mechanical, chemical, electrical, or thermal trauma (56), leading to the excessive production of pro-inflammatory cytokines (56, 57). TNF α stimulates osteoclastogenesis and inhibits osteoblast function (58). TNF α overexpression increases NF κ B and the mitogen-activated protein kinases (MAPKs), increasing the release of cytokines and chemokines and leading

to the activation of osteoclasts (58). In addition, TNF α inhibits BM-MSC differentiation into osteoblasts via the ubiquitin E3 ligase Wwp1 (59, 60). In polytrauma, excessive infiltration of activated neutrophils to the fracture site leads to poor fracture healing (21). Coculture of human BM-MSC with CD4+ T cells promoted increased expression of bone markers and mineralization, however, coculture of human BM-MSC with CD8+ T cells did not (61). Patients with impaired fracture healing had a lower CD4+/CD8+ ratio compared to patients with healed fractures (62). These data indicated that CD4+ T cells promoted osteogenic differentiation of human BM-MSCs. On the other hand, in patients with severe trauma, the CD4+/CD8+ ratio has been reported to be decreased (63). A rat model of tibial fracture with severe overlying muscle injury demonstrated not only excessive and prolonged infiltration of T cells but also a low CD4+/CD8+ ratio at 14 and 28 days, compared to a rat model of tibial fracture only. Furthermore, this rat model of tibial fracture with muscle injury showed persistence of M1 macrophages, resulting in impaired bone healing (64). Thus, excessive and/or prolonged acute inflammation alters the balance of inflammatory cells and inflammatory cytokines, which may lead to poor bone healing.

Chronic Inflammation vs. Bone Healing

Chronic inflammation can be highly detrimental to bone healing. In chronic inflammation, TNF α and the NF κ B signaling pathways are continuously upregulated, resulting in the differentiation and activation of osteoclasts (6, 65–68). High and persistent TNF α levels damage tissues and reduce bone volume (58). In the context of high TNF α levels, the eroded bone surface, which is a parameter of bone resorption, was significantly increased histomorphometrically in patients with inflammatory diseases, such as rheumatoid arthritis, Crohn's disease, and bronchial asthma (69). Chronically elevated NF κ B activity was associated with the impaired ability of BM-MSCs to form bone (70). Chronic inflammation due to polyethylene particles induced the activation of NF κ B pathways, leading to bone resorption in both the femoral intramedullary continuous polyethylene particle infusion model (71) and in the murine calvarial model (72). In addition, prolonged M1-macrophage activation continuously produced cytokines, resulting in bone resorption via increased osteoclast activity and suppression of bone formation by osteoblasts (5). Therefore, failed bone healing in chronic inflammation can be caused by the imbalance of M1/M2 macrophages (5).

WHAT HAPPENS IF BONE HEALING DOES NOT OCCUR?

According to the U.S. Food and Drug Administration (FDA), non-union is defined as a fractured bone that has not healed after a minimum of 9 months since the injury and shows no radiographic progressive bone healing for a minimum of 3 consecutive months (73). Although different definitions have been proposed, non-unions can be radiologically categorized as hypertrophic and atrophic non-unions (74).

Hypertrophic Non-union

On radiographs, a hypertrophic non-union is seen as a large broad callus facing the radiolucent fracture gap and is referred to as a horse-shoe or elephant-foot non-union (75). Hypertrophic non-union is believed to be caused by inadequate immobilization to maintain the necessary vascularity and biologic viability for complete bone healing to occur (76, 77). However, a previous *in vitro* study (78) demonstrated that cell viability and osteogenic ability of human osteoblasts isolated from hypertrophic non-unions were decreased. Iwakura et al. (79) showed that hypertrophic non-union tissue contained mesenchymal progenitor cells with multilineage capacity, but their proliferative capacity was decreased. Thus, the biological mechanisms and immunoregulatory controls in hypertrophic non-union remain largely unknown.

Atrophic Non-union

Atrophic non-union refers to an inadequate or poorly vascularized mesenchymal tissue with very limited potential for successful healing of the bone ends. Radiographically, there is little callus formation around a fibrous tissue-filled fracture gap (75). An *in vitro* study demonstrated that the fibroblast-like cells isolated from atrophic non-union tissues in humans had lower cell proliferation and osteogenic ability (80). El-Jawhari et al. (81) showed that BM-MSCs isolated from the iliac crest in patients with a non-union had low proliferative capacity and osteogenic ability compared with those with successful union. In addition, the passage-zero cultured BM-MSCs treated with a mixture of IFN γ , TNF α , IL1, and IL17 showed lower gene expression of indoleamine 2,3-dioxygenase (IDO), prostaglandin E synthetase 2 (PGES2), and TGF β 1, indicating reduced immunosuppressive potential. The immunoregulatory properties of cells in atrophic non-unions have not been fully clarified.

CAN WE MODULATE INFLAMMATION TO FACILITATE HEALING?

As stated previously, an initial and optimal transient stage of acute inflammation is a crucial event during fracture healing. One approach to facilitating bone healing by means of immunomodulation is the preconditioning of MSCs to empower their immunosuppressive properties (82). Preconditioned MSCs (also known as “primed/ licensed/ activated” MSCs) are cultured first with pro-inflammatory cytokines or exposed to hypoxic conditions for a few days to mimic the inflammatory microenvironment prior to their intended application in *in vitro* and *in vivo* studies in animals and humans (e.g., differentiation into special cell lineages, loading into scaffolds, and administration to animals and humans). Another approach involves the resolution of inflammation with anti-inflammatory cytokines.

Preconditioned MSC With Pro-Inflammatory Cytokines

Addition of different combinations of inflammatory cytokines to cell culture can dramatically affect the secretory profile

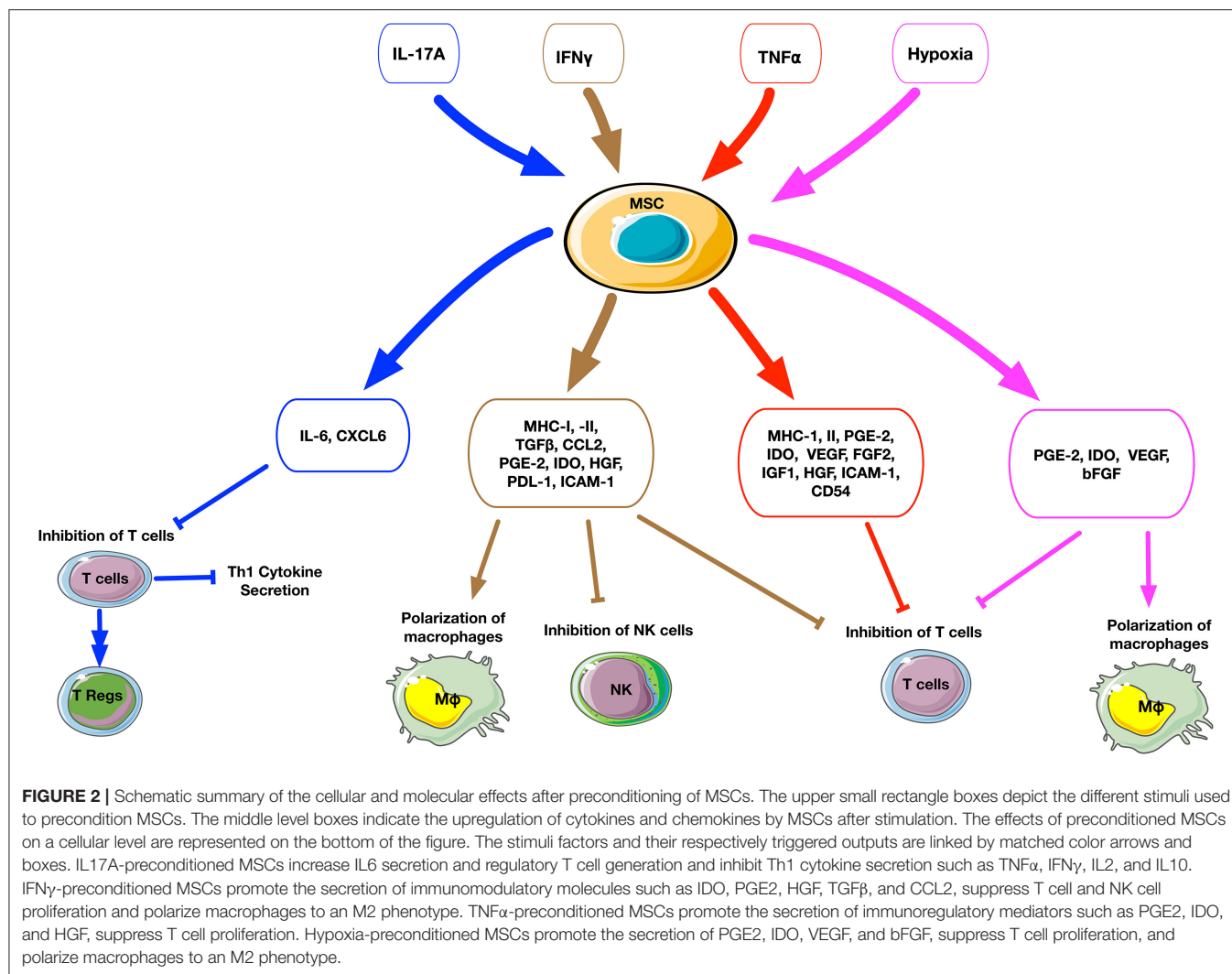
and osteogenic ability of MSCs (Figure 2, Table 1). IFN γ -preconditioned MSCs upregulated IDO and the secretion of immunomodulatory molecules, such as PGE2, hepatocyte growth factor (HGF), TGF β , and CCL2 (82, 89). IFN γ -preconditioned MSCs also suppressed CD4 $^{+}$ and CD 8 $^{+}$ T cell and NK cell proliferation and polarized macrophages to an M2 phenotype (87, 90). However, there are no studies concerning the osteogenic ability of IFN γ -preconditioned MSCs.

TNF α preconditioning also promotes immunoregulatory mediators such as PGE2, IDO, and HGF, but this is less pronounced compared to IFN γ preconditioning (82, 89). TNF α -preconditioned human adipose tissue-derived MSCs (AT-MSCs) (83) and their exosomes (84) promoted the proliferation and osteogenic differentiation of human primary osteoblastic cells. Another study demonstrated that TNF α -preconditioned human AT-MSCs reduced collagen type I gene expression but increased proliferation and ALP activity (85). Similarly, preconditioned human BM-MSCs exposed to TNF α enhanced their osteogenic capacity (86). However, our previous *in vitro* study demonstrated that preconditioning of murine BM-MSCs using TNF α alone or a combination TNF α and IFN γ did not promote osteogenesis; however, a combination of TNF α and LPS enhanced osteogenic differentiation including ALP activity and matrix mineralization (87).

IL17A-preconditioned MSCs increased IL6 and regulatory T cell generation and inhibited Th1 cytokine secretion (TNF α , IFN γ , IL2, and IL10) (91). In a rat calvarial defect model, the direct application of IL17A inhibited osteoblast precursor cells and bone regeneration (92). In other studies, IL17A promoted osteoblastic differentiation (46, 93, 94) and inhibited adipogenic differentiation (95) in human BM-MSCs. Ono et al. demonstrated that IL17A accelerated osteoblastogenesis *in vitro* and *in vivo* in mice (45). A recent study demonstrated that IL17 stimulated the osteogenic differentiation of the murine BM-MSC niche by using IL6 and IL1 β signaling to activate ERK1/2, STAT3, and AKT (47). When these BM-MSCs were exposed to IL17 in 3D coculture with osteocytes, the BM-MSCs showed enhanced osteogenesis. However, studies concerning the osteogenic ability of IL17A-preconditioned MSCs were not reported.

The effects of preconditioning of MSCs by other pro-inflammatory cytokines such as IL6, IL8, or IL17F have been reported. IL6-preconditioned human AT-MSCs demonstrated increased ALP activity and mineralization (85, 88). IL8-preconditioned human AT-MSCs did not show changes in proliferation or osteogenic gene expression, but had reduced bone nodule formation (85). IL17F-preconditioned human AT-MSCs had decreased proliferation but enhanced ALP activity (85).

These *in vitro* studies suggest that the osteogenic ability of preconditioned MSCs may be influenced not only by pro-inflammatory cytokines but also by the species selected and the tissue of origin. Interestingly, there are few *in vivo* studies concerning the efficacy of preconditioned MSCs using pro-inflammatory cytokines; further study is needed in this area.



Preconditioned MSC With Hypoxia

The effects of hypoxia-preconditioning on the immunomodulatory and osteogenic capacities of MSCs have become increasingly relevant, particularly as the potential therapeutic conditions of MSCs have an oxygen tension between 1 and 11%, compared to normal ambient oxygen tension (21% O₂) (82, 89). Downstream signaling of hypoxia-inducible factors (HIFs) modulates VEGF expression and activation of SDF1 and CXCR4, thus implicating hypoxia as a modifiable element to increase MSC migration and bone healing (96). The HIF1 α pathway is tightly linked to skeletal development and bone repair; mice exposed to hypoxic conditions had increased vascularity and bone healing via HIF1 α and VEGF mediated pathways (97). MSCs cultured under hypoxic conditions maintain or increase their proliferation rates with increased secretion of growth factors, including VEGF, basic FGF, and PDGF-BB (98–100). In addition, increased lactate production by MSCs under hypoxic conditions could contribute to the polarization of macrophages to an anti-inflammatory M2 phenotype (101).

A recent systematic review paper (102) described that MSCs cultured under severe hypoxic conditions (<2% O₂) with long-term exposure increased their proliferation rate and inhibited osteogenic differentiation, whereas MSCs cultured under moderate hypoxic conditions (2–5% O₂) with short-term or cyclic exposure had accelerated osteogenic differentiation and inhibited osteoclast function *in vitro*.

Although *in vivo* applications of hypoxia-preconditioned MSCs for bone healing are limited (Table 2), Lee et al. studied human BM-MSCs that were expanded under hypoxia with 1% O₂ and seeded on hydroxyapatite (HA)/tricalcium phosphate (TCP)-based scaffolds. These hypoxia-preconditioned BM-MSCs/HA/TCP-based scaffolds increased collagen tissue formation in a subcutaneous transplantation model in mice (103). A 21-months-old aged male rat model of hypoxia-preconditioned BM-MSCs with dimethylxalylglycine (DMOG), a prolyl hydroxylase inhibitor, under 1% O₂ conditions improved the repair of a critical-sized mandibular defect (106). The intramuscular injection of hypoxia-preconditioned human BM-MSCs under 1% O₂ for 48 h exhibited markedly increased cell

TABLE 1 | Immunomodulation for bone healing by the preconditioning of MSCs with pro-inflammatory cytokines *in vitro*.

Preconditioning of MSCs with pro-inflammatory cytokines				Results
Stimulus	Duration	Species	Type of MSCs	
TNF α	3 days	Human	AT-MSCs	TNF α -preconditioned human AT-MSCs (83) and their exosomes (84) promoted the proliferation and osteogenic differentiation of human primary osteoblastic cells.
TNF α	3 days	Human	AT-MSCs	TNF α -preconditioned human AT-MSCs reduced collagen type I gene expression but increased their proliferation and ALP activity (85).
TNF α	3 days	Human	BM-MSCs	TNF α -preconditioned human BM-MSCs increased their ALP activity and mineralization (86).
TNF α + LPS	3 days	Murine	BM-MSCs	A combination of TNF α and LPS enhanced osteogenic differentiation including ALP activity and matrix mineralization; however, TNF α alone or a combination (TNF α and IFN γ) did not promote osteogenesis (87).
IL6	3 days	Human	AT-MSCs	IL6-preconditioned human AT-MSCs stimulated ALP activity and mineralization (88).
IL8	3 days	Human	AT-MSCs	IL8-preconditioned human AT-MSCs did not affect proliferation or osteogenic gene expression but reduced bone nodule formation (85).
IL17F	3 days	Human	AT-MSCs	IL17F-preconditioned human AT-MSCs decreased their proliferation but enhanced ALP activity (85).

AT-MSCs, adipose tissue-derived mesenchymal stromal cells; BM-MSCs, bone marrow-derived mesenchymal stromal cells.

TABLE 2 | Immunomodulation for bone healing by hypoxia-reconditioned MSC *in vivo*.

Hypoxia-preconditioning				Study models	Carriers of cells	Results
Hypoxic condition	Duration	Species	Type of MSCs			
1% O ₂	-	Human	BM-MSCs	A subcutaneous transplantation model in immunocompromised mice	HA/TCP scaffolds	Hypoxia-preconditioned MSCs/HA/TCP scaffolds had increased bone tissue formation, as measured by histological analysis (103).
1% O ₂	96 h+	Rat	BM-MSCs	A critical-sized mandibular defect model in 21-months-old aged male SD rats	Gelatin sponges	Hypoxia-preconditioned BM-MSCs/gelatin sponges showed accelerated angiogenesis and osteogenesis and improved bone healing as measured by microCT and histological analyses (104).
1% O ₂	3 days	Human	BM-MSCs	A critical-sized femoral bone defect model in male athymic rats (10–12 weeks old)	Alginate hydrogels	Hypoxia-preconditioned MSC spheroids/alginate hydrogels accelerated angiogenesis at 2 weeks, and improved bone healing and mechanical strength at 12 weeks, as measured by microCT, mechanical testing, and histological analysis (105).

BM-MSC, bone marrow-derived mesenchymal stromal cells; HA, hydroxyapatite; TCP, tricalcium phosphate; DMOG, dimethylxalylglycine.

survival over 4 weeks in mice (107). A spheroid of hypoxia-preconditioned human BM-MSCs were cultured under 1% O₂ for 3 days (105). Hypoxia-preconditioned BM-MSC spheroids had high osteogenic differentiation and VEGF secretion *in vitro*, and an alginate hydrogel containing hypoxia-preconditioned BM-MSC spheroids improved bone healing of a critical-sized femoral bone defect in male athymic rats at the age of 10–12 weeks. Thus, although the molecular mechanisms of hypoxic conditioning on MSCs remain unclear, these results demonstrate the translatability of biochemical and *in vitro* studies of MSC hypoxia to *in vivo* therapies, even under challenging conditions such as critical-sized defects in aged models.

Immunomodulation by Accelerating the Resolution of Inflammation via Local Delivery of Anti-inflammatory Cytokines

Direct application of anti-inflammatory cytokines can modify the microenvironment and promote bone healing, particularly

when consideration is given to the timing and delivery method (Table 3). Anti-inflammatory cytokines IL4 and IL13 inhibit the proliferation of human osteoblasts (115) but increase collagen secretion, ALP expression, and mineralization (116). Alternatively, IL4 decreased osteogenic differentiation in monoculture of mouse BM-MSCs (108) and human AT-MSCs (88). However, IL4 and IL13 stimulate the polarization of macrophages from the inflammatory M1 phenotype to the anti-inflammatory M2 phenotype (117), and crosstalk between MSCs and macrophages is critical for successful bone healing (5). Therefore, monoculture models may not accurately reflect the full immunomodulatory and osteogenic potential of anti-inflammatory cytokines *in vivo*. An MSC-macrophage coculture model using either primary murine BM-MSCs (55) or pre-osteoblastic MC3T3 cells (109) with M1 macrophages showed enhanced bone mineralization and ALP activity. Moreover, the addition of IL4 at 72 h to polarize the M1 macrophages to an M2 phenotype further increased calcified matrix formation,

TABLE 3 | Immunomodulation for bone healing by the resolution of inflammation with anti-inflammatory cytokines.

Anti-inflammatory cytokines	Studies	Models	Delivery methods	Results
IL4	<i>In vitro</i>	Monoculture	-	IL4 decreased osteogenic differentiation in monoculture of mouse BM-MSCs (108), human AT-MSCs (88).
IL4	<i>In vitro</i>	MSC-macrophage coculture	-	IL4 enhanced bone mineralization and ALP activity of murine MSCs (55) or pre-osteoblastic MC3T3 cells (109) in coculture with M1 macrophages.
IL4	<i>In vitro</i>	MSC-macrophage coculture	-	The addition of IL4 at 72 h to polarize the M1 macrophages to an M2 phenotype further increased calcified matrix formation, compared to introducing IL4 earlier (110).
IL4, IL13	<i>In vivo</i>	A murine bone defect model	An IL4 and IL13 loaded collagen scaffolds	A collagen scaffold containing IL4 and IL13 increased callus formation in an <i>in vivo</i> murine bone defect model (111).
IL4	<i>In vivo</i>	A rat calvarial defect model	Daily injection of IL4 into the scaffold from day 3 to day 7	Low dose (10 ng) IL4 significantly increased bone formation and vascularization, with favorable M1/M2 polarization ratios, compared to higher doses (50 ng and 100 ng) of IL4 or none (112).
IL4	<i>In vivo</i>	A murine distal femoral bone marrow cavity model	Genetically modified IL4 secreting MSCs	Genetically modified IL4 secreting MSCs injected into the murine distal femoral bone marrow cavity increased bone mineralization (113).
IL4	<i>In vivo</i>	A mouse calvarial model with PE	Daily local IL4 injection	Bone loss was significantly decreased following IL4 administration to PE treated calvaria; increased M1/M2 ratio in the PE treated calvaria, which decreased with addition of IL4 (114).
IL4	<i>In vivo</i>	A mouse continuous PE femoral intramedullary infusion model	IL4 was infused into mouse distal femurs by osmotic pump	Continuous local IL4 delivery was an effective means to prevent particle-induced bone loss and enhance bone structural properties in the context of wear particle-induced inflammation (72).

AT-MSCs, adipose tissue-derived mesenchymal stromal cells; BM-MSCs, bone marrow-derived mesenchymal stromal cells; PE, polyethylene particle.

compared to introducing IL4 earlier (109, 110). Thus, acute inflammation is necessary to initiate bone healing; the specific timing of the resolution of inflammation is critical for optimal bone formation *in vitro*.

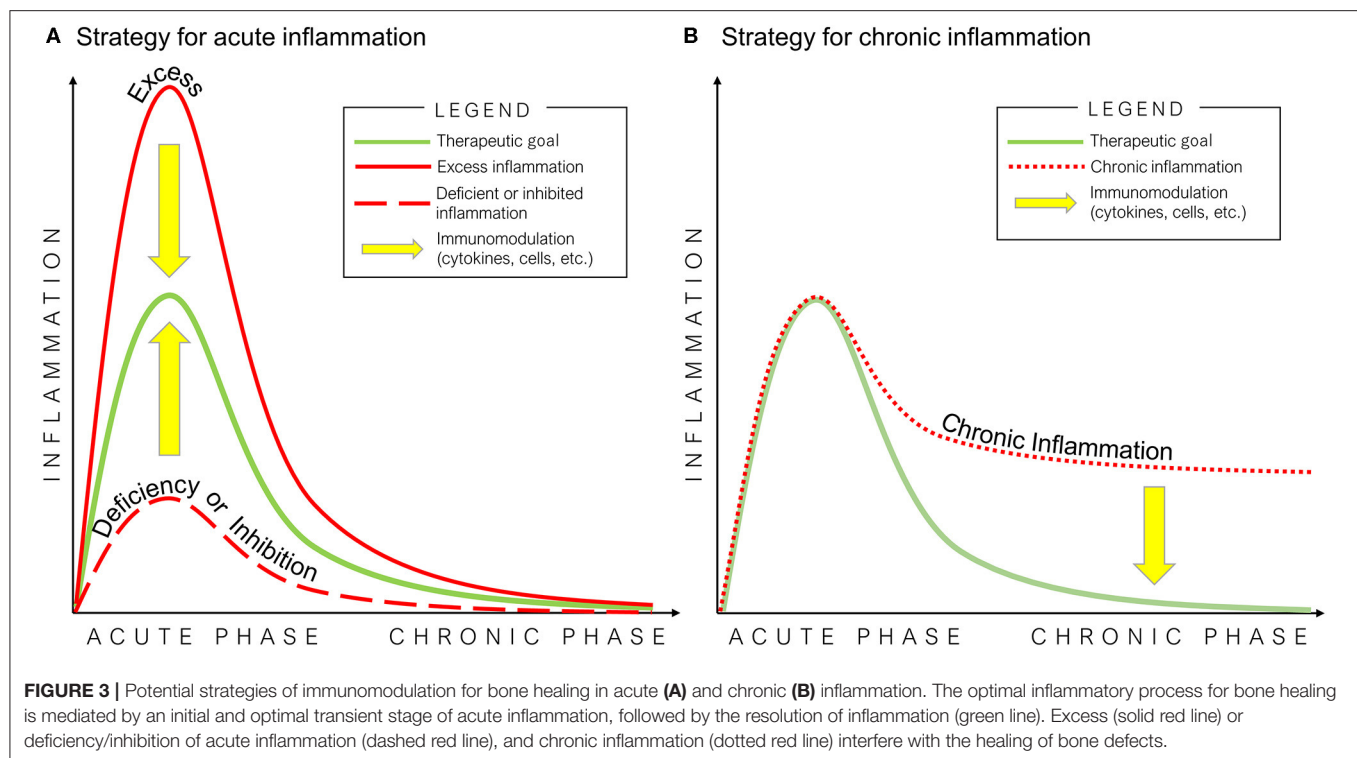
Others have demonstrated that a collagen scaffold containing IL4 and IL13 increased callus formation in an *in vivo* murine bone defect model (111). Zheng et al. (112) implanted a decellularized bone matrix (DBM) scaffold into a calvarial defect in rats and performed daily injection of different IL4 doses (0, 10, 50, and 100 ng) through the skin directly over the scaffold from day 3 to 7 after surgery. They found that a rat cranial bone defect model with low dose (10 ng) IL4 loaded into decellularized bone matrix significantly increased bone formation and vascularization, with favorable M1/M2 polarization ratios, compared to higher doses (50 and 100 ng) of IL4 or matrix alone. Indeed, as immunomodulation to improve bone healing becomes a therapeutic strategy, immunomodulatory scaffolds are becoming more complex. Other studies have fabricated a functional scaffold with differential release of immunomodulatory molecules, such as a decellularized bone scaffold with sustained release of IL4 via biotin-streptavidin binding (118) and a collagen scaffold with poly(lactic-co-glycolic acid)-multistage silicon particles composite microspheres releasing IL4 (119). A more recent method to provide controlled,

direct release of anti-inflammatory cytokines is through cell modification.

Our group (108) has established two types of genetically modified IL-4 secreting BM-MSCs using lentiviral vectors: one is a continuously-IL4-overexpressing BM-MSC driven by the cytomegalovirus (CMV) promoter, and the other is an NFκB-sensing-IL4-overexpressing BM-MSC driven by the NFκB promoter. NFκB-sensing-IL4-overexpressing BM-MSCs produce IL4 when NFκB is activated; thus, these cells secrete IL4 under the conditions of an inflammatory stimulus only. Transplantation of both types of genetically modified IL-4 secreting BM-MSCs into the murine distal femoral bone marrow cavity increased bone mineralization (113).

Although these *in vivo* studies demonstrated the therapeutic effect of IL4 and IL13 for bone healing, a comprehensive comparison of the optimal dose and delivery timing and methods (e.g., biomaterials and genetically modified MSCs, etc.) of pro-inflammatory cytokines for bone healing is still lacking; further *in vivo* studies are needed.

IL10 is another potent anti-inflammatory cytokine that can affect bone formation. Mechanistic studies in mice found that IL10 promotes chondrocyte proliferation and differentiation via the bone morphogenetic protein (BMP) pathway, thus influencing endochondral bone formation (120). IL10 deficient mice showed suppressed bone formation and osteoblastogenesis,



resulting in osteopenia and increased bone fragility (121, 122). However, various concentrations of IL10 exert different effects on the osteogenesis of human BM-MSCs. Low physiologic concentrations of IL10 (0.01–1.0 ng/ml) activate the p38/MAPK signaling pathway to promote osteogenesis, whereas higher doses of IL10 (10–100 ng/ml) inhibit p38/MAPK signaling by activating NF- κ B, inhibiting osteogenesis (123). An *in vitro* osteoblast-osteoclast coculture model demonstrated that genetically-modified IL10 and TGF β overexpressing osteoclasts inhibited osteoblast apoptosis and decreased osteoclast formation and bone absorption ability (124). Further translational studies using IL10 and other immunomodulatory molecules are needed.

Immunomodulatory strategies to resolve chronic inflammatory bone disease apply these same principles but require more advanced models and the ability to respond to inflammatory stimuli. For example, in wear particle-induced chronic inflammation, *in vivo* studies using a mouse calvarial model (114) and continuous polyethylene particle femoral intramedullary infusion model (125) showed that IL4 prevented bone loss and accelerated bone formation by modulating local macrophage polarization to an M2 phenotype. In a recent MSC-macrophage coculture study simulating wear particle-induced inflammation, we demonstrated that NF κ B-sensing-IL4-overexpressing BM-MSCs decreased ALP activity and osteocalcin expression (early osteogenic markers) but increased mineralization using Alizarin red staining (late osteogenic marker) (126). These results suggest that NF κ B-sensing-IL4-overexpressing BM-MSCs are useful to enhance osteogenesis at a later stage. In combination with preconditioned BM-MSCs, which increased early osteogenic markers, these immunomodulatory strategies may increase bone regeneration at different stages of chronic bone inflammatory disease.

DISCUSSION

This review summarizes current fundamental knowledge underlining the importance of acute inflammation for normal bone healing after injury. Numerous studies have now substantiated that deficiencies in critical cell crosstalk, inhibition of the natural processes of acute inflammation and its resolution, or chronic inflammation due to a persistent adverse stimulus can lead to impaired fracture healing. Thus, an initial and optimal transient stage of acute inflammation is one of the crucial events during fracture healing.

Once the basic principles associated with normal bone healing are clearly understood, then potential strategies for immunomodulation of critical biological events may be exploited (Figure 3). For example, *in vitro* studies demonstrated that preconditioning of MSCs by pro-inflammatory cytokines or hypoxic conditions enhances their osteogenic potential. However, a comprehensive comparison of the osteogenic ability of MSCs derived from different tissue sources is still limited. In addition, no study has directly and comprehensively compared preconditioning of MSCs using different pro-inflammatory cytokine combinations vs. hypoxic conditions. Furthermore, there are few *in vivo* studies concerning the efficacy of preconditioned MSCs. Thus, the clinical application of preconditioned MSCs and other novel technologies is not fully known. Further *in vivo* translational studies are needed in this regard. *In vitro* studies concerning immunomodulation for the resolution of inflammation using anti-inflammatory cytokines also demonstrated their therapeutic potential to improve bone healing. The clinical

application of immunomodulation for bone healing using anti-inflammatory cytokines would not be suitable before 3 days from the onset of acute inflammation. However, the optimal dose, timing, and methods of delivery of pro-inflammatory cytokines have not been fully clarified. Furthermore, similar to preconditioned MSCs, *in vivo* translational studies concerning the efficacy of immunomodulation for inflammatory resolution for bone healing are limited. Therefore, the therapeutic effects of immunomodulation for bone healing using preconditioned MSCs, anti-inflammatory cytokines to suppress inflammation, or a combination of these strategies should be further evaluated in future *in vivo* translational studies.

REFERENCES

- Holmes D. Non-union bone fracture: a quicker fix. *Nature*. (2017) 550:S193. doi: 10.1038/550S193a
- Hak DJ, Fitzpatrick D, Bishop JA, Marsh JL, Tilp S, Schnettler R, et al. Delayed union and nonunions: epidemiology, clinical issues, and financial aspects. *Injury*. (2014) 45(Suppl.2):S3–7. doi: 10.1016/j.injury.2014.04.002
- Claes L, Recknagel S, Ignatius A. Fracture healing under healthy and inflammatory conditions. *Nat Rev Rheumatol*. (2012) 8:133–43. doi: 10.1038/nrrheum.2012.1
- Pahwa R, Jialal I. *Chronic Inflammation*. Internet: StatPearls Publishing (2019).
- Pajarinen J, Lin T, Gibon E, Kohno Y, Maruyama M, Nathan K, et al. Mesenchymal stem cell-macrophage crosstalk and bone healing. *Biomaterials*. (2019) 196:80–9. doi: 10.1016/j.biomaterials.2017.12.025
- Loi F, Cordova LA, Pajarinen J, Lin TH, Yao Z, Goodman SB. Inflammation, fracture and bone repair. *Bone*. (2016a) 86:119–30. doi: 10.1016/j.bone.2016.02.020
- Cho TJ, Gerstenfeld LC, Einhorn TA. Differential temporal expression of members of the transforming growth factor beta superfamily during murine fracture healing. *J Bone Miner Res*. (2002) 17:513–20. doi: 10.1359/jbmr.2002.17.3.513
- Dimitriou R, Tsirodis E, Giannoudis PV. Current concepts of molecular aspects of bone healing. *Injury*. (2005) 36:1392–404. doi: 10.1016/j.injury.2005.07.019
- Fullerton JN, Gilroy DW. Resolution of inflammation: a new therapeutic frontier. *Nat Rev Drug Discov*. (2016) 15:551–67. doi: 10.1038/nrd.2016.39
- Mosser DM, Edwards JP. Exploring the full spectrum of macrophage activation. *Nat Rev Immunol*. (2008) 8:958–69. doi: 10.1038/nri2448
- Buckley CD, Gilroy DW, Serhan CN, Stockinger B, Tak PP. The resolution of inflammation. *Nat Rev Immunol*. (2012) 13:59–66. doi: 10.1038/nri3362
- Buckley CD, Gilroy DW, Serhan CN. Proresolving lipid mediators and mechanisms in the resolution of acute inflammation. *Immunity*. (2014) 40:315–27. doi: 10.1016/j.immuni.2014.02.009
- Feehan KT, Gilroy DW. Is resolution the end of inflammation? *Trends Mol Med*. (2019) 25:198–214. doi: 10.1016/j.molmed.2019.01.006
- Reville K, Crean JK, Vivers S, Dransfield I, Godson C. Lipoxin A4 redistributes myosin IIA and Cdc42 in macrophages: implications for phagocytosis of apoptotic leukocytes. *J Immunol*. (2006) 176:1878–88. doi: 10.4049/jimmunol.176.3.1878
- Serhan CN, Savill J. Resolution of inflammation: the beginning programs the end. *Nat Immunol*. (2005) 6:1191–7. doi: 10.1038/ni1276
- Newson J, Stables M, Karra E, Arce-Vargas F, Quezada S, Motwani M, et al. Resolution of acute inflammation bridges the gap between innate and adaptive immunity. *Blood*. (2014) 124:1748–64. doi: 10.1182/blood-2014-03-562710
- Lin TH, Tamaki Y, Pajarinen J, Waters HA, Woo DK, Yao Z, et al. Chronic inflammation in biomaterial-induced periprosthetic

AUTHOR CONTRIBUTIONS

All authors contributed to the initial concepts and writing of the present manuscript.

ACKNOWLEDGMENTS

The authors acknowledge the generous support of the National Institute of Arthritis and Musculoskeletal and Skin Diseases of the National Institute of Health (Grant Nos. R01AR055650, R01AR063717, R01AR073145, and R01AR72613), the Ellenburg Chair in Surgery, and the Stanford University Medical Scholars Research Grant.

- osteolysis: NF-kappaB as a therapeutic target. *Acta Biomater*. (2014) 10:1–10. doi: 10.1016/j.actbio.2013.09.034
- Chang MK, Raggatt LJ, Alexander KA, Kuliwaba JS, Fazzalari NL, Schroder K, et al. Osteal tissue macrophages are intercalated throughout human and mouse bone lining tissues and regulate osteoblast function *in vitro* and *in vivo*. *J Immunol*. (2008) 181:1232–44. doi: 10.4049/jimmunol.181.2.1232
- Marsell R, Einhorn TA. The biology of fracture healing. *Injury*. (2011) 42:551–5. doi: 10.1016/j.injury.2011.03.031
- Walters G, Pountos I, Giannoudis PV. The cytokines and micro-environment of fracture haematoma: current evidence. *J Tissue Eng Regen Med*. (2018) 12:e1662–77. doi: 10.1002/term.2593
- Bastian O, Pillay J, Alblas J, Leenen L, Koenderman L, Blokhuis T. Systemic inflammation and fracture healing. *J Leukoc Biol*. (2011) 89:669–73. doi: 10.1189/jlb.0810446
- Miron RJ, Bosshardt DD. OsteoMacs: key players around bone biomaterials. *Biomaterials*. (2016) 82:1–19. doi: 10.1016/j.biomaterials.2015.12.017
- Batoon L, Millard SM, Raggatt LJ, Pettit AR. Osteomacs and bone regeneration. *Curr Osteoporos Rep*. (2017) 15:385–95. doi: 10.1007/s11914-017-0384-x
- Karnes JM, Daffner SD, Watkins CM. Multiple roles of tumor necrosis factor-alpha in fracture healing. *Bone*. (2015) 78:87–93. doi: 10.1016/j.bone.2015.05.001
- Toosi S, Behravan J. Osteogenesis and bone remodeling: a focus on growth factors and bioactive peptides. *Biofactors*. (2019). doi: 10.1002/biof.1598. [Epub ahead of print].
- Gerstenfeld LC, Cullinane DM, Barnes GL, Graves DT, Einhorn TA. Fracture healing as a post-natal developmental process: molecular, spatial, and temporal aspects of its regulation. *J Cell Biochem*. (2003) 88:873–84. doi: 10.1002/jcb.10435
- Kenkre JS, Bassett J. The bone remodelling cycle. *Ann Clin Biochem*. (2018) 55:308–27. doi: 10.1177/0004563218759371
- Lim JC, Ko KI, Mattos M, Fang M, Zhang C, Feinberg D, et al. TNFalpha contributes to diabetes impaired angiogenesis in fracture healing. *Bone*. (2017) 99:26–38. doi: 10.1016/j.bone.2017.02.014
- Copuroglu C, Calori GM, Giannoudis PV. Fracture non-union: who is at risk? *Injury*. (2013) 44:1379–82. doi: 10.1016/j.injury.2013.08.003
- Foulke BA, Kendal AR, Murray DW, Pandit H. Fracture healing in the elderly: a review. *Maturitas*. (2016) 92:49–55. doi: 10.1016/j.maturitas.2016.07.014
- Andrzejowski P, Giannoudis PV. The 'diamond concept' for long bone non-union management. *J Orthop Traumatol*. (2019) 20:21. doi: 10.1186/s10195-019-0528-0
- Shultz LD, Lyons BL, Burzenski LM, Gott B, Chen X, Chaleff S, et al. Human lymphoid and myeloid cell development in NOD/LtSz-scid IL2R gamma null mice engrafted with mobilized human hemopoietic stem cells. *J Immunol*. (2005) 174:6477–89. doi: 10.4049/jimmunol.174.10.6477
- Kovanen PE, Leonard WJ. Cytokines and immunodeficiency diseases: critical roles of the gamma(c)-dependent cytokines interleukins 2, 4, 7, 9, 15, and

- 21, and their signaling pathways. *Immunol Rev.* (2004) 202:67–83. doi: 10.1111/j.0105-2896.2004.00203.x
34. Rapp AE, Bindl R, Recknagel S, Erbacher A, Muller I, Schrezenmeier H, et al. Fracture healing is delayed in immunodeficient NOD/scidIL2Rgammacnull mice. *PLoS ONE.* (2016) 11:e0147465. doi: 10.1371/journal.pone.0147465
35. Kon T, Cho TJ, Aizawa T, Yamazaki M, Nooh N, Graves D, et al. Expression of osteoprotegerin, receptor activator of NF-kappaB ligand (osteoprotegerin ligand) and related proinflammatory cytokines during fracture healing. *J Bone Miner Res.* (2001) 16:1004–14. doi: 10.1359/jbmr.2001.16.6.1004
36. Gerstenfeld LC, Cho TJ, Kon T, Aizawa T, Cruceta J, Graves BD, et al. Impaired intramembranous bone formation during bone repair in the absence of tumor necrosis factor-alpha signaling. *Cells Tissues Organs.* (2001) 169:285–94. doi: 10.1159/000047893
37. Gerstenfeld LC, Cho TJ, Kon T, Aizawa T, Tsay A, Fitch J, et al. Impaired fracture healing in the absence of TNF-alpha signaling: the role of TNF-alpha in endochondral cartilage resorption. *J Bone Miner Res.* (2003) 18:1584–92. doi: 10.1359/jbmr.2003.18.9.1584
38. Mountziaris PM, Mikos AG. Modulation of the inflammatory response for enhanced bone tissue regeneration. *Tissue Eng B Rev.* (2008) 14:179–86. doi: 10.1089/ten.teb.2008.0038
39. Tamura T, Udagawa N, Takahashi N, Miyaura C, Tanaka S, Yamada Y, et al. Soluble interleukin-6 receptor triggers osteoclast formation by interleukin-6. *Proc Natl Acad Sci USA.* (1993) 90:11924–8. doi: 10.1073/pnas.90.24.11924
40. Yang X, Ricciardi BF, Hernandez-Soria A, Shi Y, Pleshko Camacho N, Bostrom MP. Callus mineralization and maturation are delayed during fracture healing in interleukin-6 knockout mice. *Bone.* (2007) 41:928–36. doi: 10.1016/j.bone.2007.07.022
41. Wallace A, Cooney TE, Englund R, Lubahn JD. Effects of interleukin-6 ablation on fracture healing in mice. *J Orthop Res.* (2011) 29:1437–42. doi: 10.1002/jor.21367
42. Schaper F, Rose-John S. Interleukin-6: biology, signaling and strategies of blockade. *Cytokine Growth Factor Rev.* (2015) 26:475–87. doi: 10.1016/j.cytogfr.2015.07.004
43. Prystaz K, Kaiser K, Kovtun A, Haffner-Luntzer M, Fischer V, Rapp AE, et al. Distinct effects of IL-6 classic and trans-signaling in bone fracture healing. *Am J Pathol.* (2018) 188:474–90. doi: 10.1016/j.ajpath.2017.10.011
44. Kaiser K, Prystaz K, Vikman A, Haffner-Luntzer M, Bergdolt S, Strauss G, et al. Pharmacological inhibition of IL-6 trans-signaling improves compromised fracture healing after severe trauma. *Naunyn Schmiedeberg Arch Pharmacol.* (2018) 391:523–36. doi: 10.1007/s00210-018-1483-7
45. Ono T, Okamoto K, Nakashima T, Nitta T, Hori S, Iwakura Y, et al. IL-17-producing gamma delta T cells enhance bone regeneration. *Nat Commun.* (2016) 7:10928. doi: 10.1038/ncomms10928
46. Croes M, Oner FC, van Neerven D, Sabir E, Kruyt MC, Blokhuis TJ, et al. Proinflammatory T cells and IL-17 stimulate osteoblast differentiation. *Bone.* (2016) 84:262–70. doi: 10.1016/j.bone.2016.01.010
47. Liao C, Zhang C, Jin L, Yang Y. IL-17 alters the mesenchymal stem cell niche towards osteogenesis in cooperation with osteocytes. *J Cell Physiol.* (2020) 235:4466–80. doi: 10.1002/jcp.29323
48. Ishikawa M, Ito H, Kitaori T, Murata K, Shibuya H, Furu M, et al. MCP/CCR2 signaling is essential for recruitment of mesenchymal progenitor cells during the early phase of fracture healing. *PLoS ONE.* (2014) 9:e104954. doi: 10.1371/journal.pone.0104954
49. Lange J, Sapozhnikova A, Lu C, Hu D, Li X, Miclau T 3rd, et al. Action of IL-1beta during fracture healing. *J Orthop Res.* (2010) 28:778–84. doi: 10.1002/jor.21061
50. Raisz LG. Prostaglandins and bone: physiology and pathophysiology. *Osteoarthritis Cartil.* (1999) 7:419–21. doi: 10.1053/joca.1998.0230
51. Lisowska B, Kosson D, Domaracka K. Lights and shadows of NSAIDs in bone healing: the role of prostaglandins in bone metabolism. *Drug Des Devel Ther.* (2018) 12:1753–8. doi: 10.2147/DDDT.S164562
52. Zhang X, Schwarz EM, Young DA, Puzas JE, Rosier RN, O'Keefe RJ. Cyclooxygenase-2 regulates mesenchymal cell differentiation into the osteoblast lineage and is critically involved in bone repair. *J Clin Invest.* (2002) 109:1405–15. doi: 10.1172/jci0215681
53. Marquez-Lara A, Hutchinson ID, Nunez FJr, Smith TL, Miller AN. Nonsteroidal anti-inflammatory drugs and bone-healing: a systematic review of research quality. *JBJS Rev.* (2016) 4:55. doi: 10.2106/JBJS.RVW.O.00055
54. Lisowska B, Kosson D, Domaracka K. Positives and negatives of nonsteroidal anti-inflammatory drugs in bone healing: the effects of these drugs on bone repair. *Drug Des Devel Ther.* (2018) 12:1809–14. doi: 10.2147/DDDT.S164565
55. Lu LY, Loi F, Nathan K, Lin TH, Pajarinen J, Gibon E, et al. Pro-inflammatory M1 macrophages promote Osteogenesis by mesenchymal stem cells via the COX-2-prostaglandin E2 pathway. *J Orthop Res.* (2017) 35:2378–85. doi: 10.1002/jor.23553
56. Valparaíso AP, Vicente DA, Bograd BA, Elster EA, Davis TA. Modeling acute traumatic injury. *J Surg Res.* (2015) 194:220–32. doi: 10.1016/j.jss.2014.10.025
57. Lenz A, Franklin GA, Cheadle WG. Systemic inflammation after trauma. *Injury.* (2007) 38:1336–45. doi: 10.1016/j.injury.2007.10.003
58. Osta B, Benedetti G, Miossec P. Classical and paradoxical effects of TNF-alpha on bone homeostasis. *Front Immunol.* (2014) 5:48. doi: 10.3389/fimmu.2014.00048
59. Zhao L, Huang J, Zhang H, Wang Y, Matesic LE, Takahata M, et al. Tumor necrosis factor inhibits mesenchymal stem cell differentiation into osteoblasts via the ubiquitin E3 ligase Wwp1. *Stem Cells.* (2011) 29:1601–10. doi: 10.1002/stem.703
60. Adamopoulos IE. Inflammation in bone physiology and pathology. *Curr Opin Rheumatol.* (2018) 30:59–64. doi: 10.1097/BOR.0000000000000449
61. Grassi F, Cattini L, Gambari L, Manferdini C, Piacentini A, Gabusi E, et al. T cell subsets differently regulate osteogenic differentiation of human mesenchymal stromal cells *in vitro*. *J Tissue Eng Regen Med.* (2016) 10:305–14. doi: 10.1002/term.1727
62. Wendler S, Schlundt C, Bucher CH, Birkigt J, Schipp CJ, Volk HD, et al. Immune modulation to enhance bone healing-a new concept to induce bone using prostacyclin to locally modulate immunity. *Front Immunol.* (2019) 10:713. doi: 10.3389/fimmu.2019.00713
63. Menges T, Engel J, Welters J, Wagner RM, Little S, Ruwoldt R, et al. Changes in blood lymphocyte populations after multiple trauma: association with posttraumatic complications. *Crit Care Med.* (1999) 27:733–40. doi: 10.1097/00003246-199904000-00026
64. Hurtgen BJ, Ward CL, Garg K, Pollot BE, Goldman SM, McKinley TO, et al. Severe muscle trauma triggers heightened and prolonged local musculoskeletal inflammation and impairs adjacent tibia fracture healing. *J Musculoskelet Neuronal Interact.* (2016) 16:122–34.
65. Chiu R, Ma T, Smith RL, Goodman SB. Polymethylmethacrylate particles inhibit osteoblastic differentiation of bone marrow osteoprogenitor cells. *J Biomed Mater Res A.* (2006) 77:850–6. doi: 10.1002/jbm.a.30697
66. Chiu R, Ma T, Smith RL, Goodman SB. Ultrahigh molecular weight polyethylene wear debris inhibits osteoprogenitor proliferation and differentiation *in vitro*. *J Biomed Mater Res A.* (2009) 89:242–7. doi: 10.1002/jbm.a.32001
67. Kodaya YRP, Al-Saffar N, Kobayashi A, Scott G, Freeman AR. Bone formation and bone resorption in failed total joint arthroplasties: histomorphometric analysis with histochemical and immunohistochemical technique. *J Orthop Res.* (1996) 14:473–82.
68. Martinez FOSA, Mantovani A, Locati M. Macrophage activation and polarization. *Front Biosci.* (2008) 13:453–61. doi: 10.2741/2692
69. Shi C, Pamer EG. Monocyte recruitment during infection and inflammation. *Nat Rev Immunol.* (2011) 11:762–74. doi: 10.1038/nri3070
70. Lin TH, Gibon E, Loi F, Pajarinen J, Cordova LA, Nabeshima A, et al. Decreased osteogenesis in mesenchymal stem cells derived from the aged mouse is associated with enhanced NF-kappaB activity. *J Orthop Res.* (2017) 35:281–8. doi: 10.1002/jor.23270
71. Lin TH, Pajarinen J, Sato T, Loi F, Fan C, Cordova LA, et al. NF-kappaB decoy oligodeoxynucleotide mitigates wear particle-associated bone loss in the murine continuous infusion model. *Acta Biomater.* (2016) 41:273–81. doi: 10.1016/j.actbio.2016.05.038
72. Sato T, Pajarinen J, Lin TH, Tamaki Y, Loi F, Egashira K, et al. NF-kappaB decoy oligodeoxynucleotide inhibits wear particle-induced inflammation in a murine calvarial model. *J Biomed Mater Res A.* (2015) 103:3872–8. doi: 10.1002/jbm.a.35532

73. Bishop JA, Palanca AA, Bellino MJ, Lowenberg DW. Assessment of compromised fracture healing. *J Am Acad Orthop Surg* (2012) 20:273–82. doi: 10.5435/JAAOS-20-05-273
74. Toosi S, Behravan N, Behravan J. Nonunion fractures, mesenchymal stem cells and bone tissue engineering. *J Biomed Mater Res A*. (2018) 106:2552–62. doi: 10.1002/jbm.a.36433
75. Megas P. Classification of non-union. *Injury*. (2005) 36(Suppl.4):S30–7. doi: 10.1016/j.injury.2005.10.008
76. Gomez-Barrena E, Rosset P, Lozano D, Stanovici J, Ermthaller C, Gerbhard F. Bone fracture healing: cell therapy in delayed unions and nonunions. *Bone*. (2015) 70:93–101. doi: 10.1016/j.bone.2014.07.033
77. Schlundt C, Bucher CH, Tsitsilonis S, Schell H, Duda GN, Schmidt-Bleek K. Clinical and research approaches to treat non-union fracture. *Curr Osteoporos Rep*. (2018) 16:155–68. doi: 10.1007/s11914-018-0432-1
78. Hofmann A, Ritz U, Hessmann MH, Schmid C, Tresch A, Rompe JD, et al. Cell viability, osteoblast differentiation, and gene expression are altered in human osteoblasts from hypertrophic fracture non-unions. *Bone*. (2008) 42:894–906. doi: 10.1016/j.bone.2008.01.013
79. Iwakura T, Miwa M, Sakai Y, Niikura T, Lee SY, Oe K, et al. Human hypertrophic nonunion tissue contains mesenchymal progenitor cells with multilineage capacity *in vitro*. *J Orthop Res*. (2009) 27:208–15. doi: 10.1002/jor.20739
80. Bajada S, Marshall MJ, Wright KT, Richardson JB, Johnson WE. Decreased osteogenesis, increased cell senescence and elevated Dickkopf-1 secretion in human fracture non union stromal cells. *Bone*. (2009) 45:726–35. doi: 10.1016/j.bone.2009.06.015
81. El-Jawhari JJ, Klefthouris G, El-Sherbiny Y, Saleeb H, West RM, Jones E, et al. Defective proliferation and osteogenic potential with altered immunoregulatory phenotype of native bone marrow-multipotential stromal cells in atrophic fracture non-union. *Sci Rep*. (2019) 9:17340. doi: 10.1038/s41598-019-53927-3
82. Noronha Nc NC, Mizukami A, Caliar-Oliveira C, Cominal JG, Rocha JLM, Covas DT, et al. Priming approaches to improve the efficacy of mesenchymal stromal cell-based therapies. *Stem Cell Res Ther*. (2019) 10:131. doi: 10.1186/s13287-019-1224-y
83. Lu Z, Wang G, Dunstan CR, Chen Y, Lu WY, Davies B, et al. Activation and promotion of adipose stem cells by tumour necrosis factor- α preconditioning for bone regeneration. *J Cell Physiol*. (2013) 228:1737–44. doi: 10.1002/jcp.24330
84. Lu Z, Chen Y, Dunstan C, Roohani-Esfahani S, Zreiqat H. Priming adipose stem cells with tumor necrosis factor- α preconditioning potentiates their exosome efficacy for bone regeneration. *Tissue Eng A*. (2017) 23:1212–20. doi: 10.1089/ten.tea.2016.0548
85. Bastidas-Coral AP, Bakker AD, Zandieh-Doulabi B, Kleverlaan CJ, Bravenboer N, Forouzanfar T, et al. Cytokines TNF- α , IL-6, IL-17F, and IL-4 differentially affect osteogenic differentiation of human adipose stem cells. *Stem Cells Int* (2016) 2016:1318256. doi: 10.1155/2016/1318256
86. Croes M, Oner FC, Kruyt MC, Blokhuis TJ, Bastian O, Dhert WJ, et al. Proinflammatory mediators enhance the osteogenesis of human mesenchymal stem cells after lineage commitment. *PLoS ONE*. (2015) 10:e0132781. doi: 10.1371/journal.pone.0132781
87. Lin T, Pajarinen J, Nabeshima A, Lu L, Nathan K, Jansen E, et al. Preconditioning of murine mesenchymal stem cells synergistically enhanced immunomodulation and osteogenesis. *Stem Cell Res Ther*. (2017) 8:277. doi: 10.1186/s13287-017-0730-z
88. Bastidas-Coral AP, Hogervorst JMA, Forouzanfar T, Kleverlaan CJ, Koolwijk P, Klein-Nulend J, et al. IL-6 counteracts the inhibitory effect of IL-4 on osteogenic differentiation of human adipose stem cells. *J Cell Physiol*. (2019) 234:20520–32. doi: 10.1002/jcp.28652
89. de Witte SF, Franquesa M, Baan CC, Hoogduijn MJ. Toward development of iMesenchymal stem cells for immunomodulatory therapy. *Front Immunol*. (2015) 6:648. doi: 10.3389/fimmu.2015.00648
90. Philipp D, Suhr L, Wahlers T, Choi YH, Paunel-Gorgulu A. Preconditioning of bone marrow-derived mesenchymal stem cells highly strengthens their potential to promote IL-6-dependent M2b polarization. *Stem Cell Res Ther*. (2018) 9:286. doi: 10.1186/s13287-018-1039-2
91. Sivanathan KN, Rojas-Canales DM, Hope CM, Krishnan R, Carroll RP, Gronthos S, et al. Interleukin-17A-induced human mesenchymal stem cells are superior modulators of immunological function. *Stem Cells*. (2015) 33:2850–63. doi: 10.1002/stem.2075
92. Kim Y-G, Park J-W, Lee J-M, Suh J-Y, Lee J-K, Chang B-S, et al. IL-17 inhibits osteoblast differentiation and bone regeneration in rat. *Arch Oral Biol*. (2014) 59:897–905. doi: 10.1016/j.archoralbio.2014.05.009
93. Huang H, Kim HJ, Chang EJ, Lee ZH, Hwang SJ, Kim HM, et al. IL-17 stimulates the proliferation and differentiation of human mesenchymal stem cells: implications for bone remodeling. *Cell Death Differ*. (2009) 16:1332–43. doi: 10.1038/cdd.2009.74
94. Noh M. Interleukin-17A increases leptin production in human bone marrow mesenchymal stem cells. *Biochem Pharmacol*. (2012) 83:661–70. doi: 10.1016/j.bcp.2011.12.010
95. Shin JH, Shin DW, Noh M. Interleukin-17A inhibits adipocyte differentiation in human mesenchymal stem cells and regulates pro-inflammatory responses in adipocytes. *Biochem Pharmacol*. (2009) 77:1835–44. doi: 10.1016/j.bcp.2009.03.008
96. Lin W, Xu L, Zwillingenberger S, Gibon E, Goodman SB, Li G. Mesenchymal stem cells homing to improve bone healing. *J Orthop Translat*. (2017) 9:19–27. doi: 10.1016/j.jot.2017.03.002
97. Wan C, Gilbert SR, Wang Y, Cao X, Shen X, Ramaswamy G, et al. Activation of the hypoxia-inducible factor-1 α pathway accelerates bone regeneration. *Proc Natl Acad Sci USA*. (2008) 105:686–91. doi: 10.1073/pnas.0708474105
98. Crisostomo PR, Wang Y, Markel TA, Wang M, Lahm T, Meldrum DR. Human mesenchymal stem cells stimulated by TNF- α , LPS, or hypoxia produce growth factors by an NF kappa B- but not JNK-dependent mechanism. *Am J Physiol, Cell Physiol*. (2008) 294:C675–82. doi: 10.1152/ajpcell.00437.2007
99. Liu L, Gao J, Yuan Y, Chang Q, Liao Y, Lu F. Hypoxia preconditioned human adipose derived mesenchymal stem cells enhance angiogenic potential via secretion of increased VEGF and bFGF. *Cell Biol Int*. (2013) 37:551–60. doi: 10.1002/cbin.10097
100. Fotia C, Massa A, Boriani F, Baldini N, Granchi D. Prolonged exposure to hypoxic milieu improves the osteogenic potential of adipose derived stem cells. *J Cell Biochem*. (2015) 116:1442–53. doi: 10.1002/jcb.25106
101. Colegio OR, Chu NQ, Szabo AL, Chu T, Rhebergen AM, Jairam V, et al. Functional polarization of tumour-associated macrophages by tumour-derived lactic acid. *Nature*. (2014) 513:559–63. doi: 10.1038/nature13490
102. Camacho-Cardenosa M, Camacho-Cardenosa A, Timon R, Olcina G, Tomas-Carus P, Brazo-Sayavera J. Can hypoxic conditioning improve bone metabolism? A systematic review. *Int J Environ Res Public Health*. (2019) 16:1799. doi: 10.3390/ijerph16101799
103. Lee JS, Park JC, Kim TW, Jung BJ, Lee Y, Shim EK, et al. Human bone marrow stem cells cultured under hypoxic conditions present altered characteristics and enhanced *in vivo* tissue regeneration. *Bone*. (2015) 78:34–45. doi: 10.1016/j.bone.2015.04.044
104. Zhang J, Feng Z, Wei J, Yu Y, Luo J, Zhou J, et al. Repair of critical-sized mandible defects in aged rat using hypoxia preconditioned BMSCs with up-regulation of Hif-1 α . *Int J Biol Sci*. (2018) 14:449–60. doi: 10.7150/ijbs.24158
105. Ho SS, Hung BP, Heyrani N, Lee MA, Leach JK. Hypoxic preconditioning of mesenchymal stem cells with subsequent spheroid formation accelerates repair of segmental bone defects. *Stem Cells*. (2018) 36:1393–403. doi: 10.1002/stem.2853
106. Zhang J, Feng Z, Wei J, Yu Y, Luo J, Zhou J, et al. Repair of critical-sized mandible defects in aged rat using hypoxia preconditioned BMSCs with up-regulation of Hif-1 α . *Int J Biol Sci*. (2018) 14:449–60. doi: 10.7150/ijbs.24158
107. Beegle J, Lakatos K, Kalomoiris S, Stewart H, Isseroff RR, Nolte JA, et al. Hypoxic preconditioning of mesenchymal stromal cells induces metabolic changes, enhances survival, and promotes cell retention *in vivo*. *Stem Cells*. (2015) 33:1818–28. doi: 10.1002/stem.1976
108. Lin T, Pajarinen J, Nabeshima A, Lu L, Nathan K, Yao Z, et al. Establishment of NF- κ B sensing and interleukin-4 secreting mesenchymal stromal cells as an “on-demand” drug delivery system to modulate inflammation. *Cytotherapy*. (2017) 19:1025–34. doi: 10.1016/j.jcyt.2017.06.008

109. Loi F, Cordova LA, Zhang R, Pajarinen J, Lin TH, Goodman SB, et al. The effects of immunomodulation by macrophage subsets on osteogenesis *in vitro*. *Stem Cell Res Ther.* (2016) 7:15. doi: 10.1186/s13287-016-0276-5
110. Nathan K, Lu LY, Lin T, Pajarinen J, Jansen E, Huang JF, et al. Precise immunomodulation of the M1 to M2 macrophage transition enhances mesenchymal stem cell osteogenesis and differs by sex. *Bone Joint Res.* (2019) 8:481–8. doi: 10.1302/2046-3758.810.BJR-2018-0231.R2
111. Schlundt C, El Khassawna T, Serra A, Dienelt A, Wendler S, Schell H, et al. Macrophages in bone fracture healing: their essential role in endochondral ossification. *Bone.* (2018) 106:78–89. doi: 10.1016/j.bone.2015.10.019
112. Zheng ZW, Chen YH, Wu DY, Wang JB, Lv MM, Wang XS, et al. Development of an accurate and proactive immunomodulatory strategy to improve bone substitute material-mediated osteogenesis and angiogenesis. *Theranostics.* (2018) 8:5482–500. doi: 10.7150/thno.28315
113. Lin T, Pajarinen J, Kohno Y, Maruyama M, Romero-Lopez M, Huang JF, et al. Transplanted interleukin-4-secreting mesenchymal stromal cells show extended survival and increased bone mineral density in the murine femur. *Cytotherapy.* (2018) 20:1028–36. doi: 10.1016/j.jcyt.2018.06.009
114. Rao AJ, Nich C, Dhulipala LS, Gibon E, Valladares R, Zwillingenberger S, et al. Local effect of IL-4 delivery on polyethylene particle induced osteolysis in the murine calvarium. *J Biomed Mater Res A.* (2013) 101:1926–34. doi: 10.1002/jbm.a.34486
115. Frost A, Jonsson KB, Brändström H, Ljunghall S, Nilsson O, Ljunggren Ö. Interleukin (IL)-13 and IL-4 inhibit proliferation and stimulate IL-6 formation in human osteoblasts: evidence for involvement of receptor subunits IL-13R, IL-13R α , and IL-4R α . *Bone.* (2001) 28:268–74. doi: 10.1016/s8756-328200449-x
116. Silfversward CJ, Penno H, Frost A, Nilsson O, Ljunggren O. Expression of markers of activity in cultured human osteoblasts: effects of interleukin-4 and interleukin-13. *Scand J Clin Lab Invest.* (2010) 70:338–42. doi: 10.3109/00365513.2010.488698
117. Shapouri-Moghaddam A, Mohammadian S, Vazini H, Taghadosi M, Esmaili SA, Mardani F, et al. Macrophage plasticity, polarization, and function in health and disease. *J Cell Physiol.* (2018) 233:6425–40. doi: 10.1002/jcp.26429
118. Spiller KL, Nassiri S, Witherell CE, Anfang RR, Ng J, Nakazawa KR, et al. Sequential delivery of immunomodulatory cytokines to facilitate the M1-to-M2 transition of macrophages and enhance vascularization of bone scaffolds. *Biomaterials.* (2015) 37:194–207. doi: 10.1016/j.biomaterials.2014.10.017
119. Minardi S, Corradetti B, Taraballi F, Byun JH, Cabrera F, Liu X, et al. IL-4 release from a biomimetic scaffold for the temporally controlled modulation of macrophage response. *Ann Biomed Eng.* (2016) 44:2008–19. doi: 10.1007/s10439-016-1580-z
120. Jung YK, Kim GW, Park HR, Lee EJ, Choi JY, Beier F, et al. Role of interleukin-10 in endochondral bone formation in mice: anabolic effect via the bone morphogenetic protein/Smad pathway. *Arthritis Rheum.* (2013) 65:3153–64. doi: 10.1002/art.38181
121. Dresner-Pollak R, Gelb N, Rachmilewitz D, Karmeli F, Weinreb M. Interleukin 10-deficient mice develop osteopenia, decreased bone formation, and mechanical fragility of long bones. *Gastroenterology.* (2004) 127:792–801. doi: 10.1053/j.gastro.2004.06.013
122. Holgersen K, Dobie R, Farquharson C, van't Hof R, Ahmed SF, Hansen AK, et al. Piroxicam treatment augments bone abnormalities in interleukin-10 knockout mice. *Inflamm. Bowel Dis.* (2015) 21:257–66. doi: 10.1097/MIB.0000000000000269
123. Chen E, Liu G, Zhou X, Zhang W, Wang C, Hu D, et al. Concentration-dependent, dual roles of IL-10 in the osteogenesis of human BMSCs via P38/MAPK and NF-kappaB signaling pathways. *FASEB J.* (2018) 32:4917–29. doi: 10.1096/fj.201701256RRR
124. Yi L, Li Z, Jiang H, Cao Z, Liu J, Zhang X. Gene modification of transforming growth factor beta (TGF-beta) and interleukin 10 (IL-10) in suppressing Mt sonicate induced osteoclast formation and bone absorption. *Med Sci Monit.* (2018) 24:5200–7. doi: 10.12659/MSM.909720
125. Sato T, Pajarinen J, Behn A, Jiang X, Lin TH, Loi F, et al. The effect of local IL-4 delivery or CCL2 blockade on implant fixation and bone structural properties in a mouse model of wear particle induced osteolysis. *J Biomed Mater Res A.* (2016) 104:2255–62. doi: 10.1002/jbm.a.35759
126. Lin T, Kohno Y, Huang JF, Romero-Lopez M, Maruyama M, Ueno M, et al. Preconditioned or IL4-secreting mesenchymal stem cells enhanced osteogenesis at different stages. *Tissue Eng A.* (2019) 25:1096–103. doi: 10.1089/ten.TEA.2018.0292

Conflict of Interest: The authors declare that the research was conducted in the absence of any commercial or financial relationships that could be construed as a potential conflict of interest.

Copyright © 2020 Maruyama, Rhee, Utsunomiya, Zhang, Ueno, Yao and Goodman. This is an open-access article distributed under the terms of the Creative Commons Attribution License (CC BY). The use, distribution or reproduction in other forums is permitted, provided the original author(s) and the copyright owner(s) are credited and that the original publication in this journal is cited, in accordance with accepted academic practice. No use, distribution or reproduction is permitted which does not comply with these terms.



Osteoimmunology: The Regulatory Roles of T Lymphocytes in Osteoporosis

Wenjuan Zhang[†], Kai Dang[†], Ying Huai[†] and Airong Qian^{*}

Lab for Bone Metabolism, Xi'an Key Laboratory of Special Medicine and Health Engineering, Key Lab for Space Biosciences and Biotechnology, Research Center for Special Medicine and Health Systems Engineering, NPU-UAB Joint Laboratory for Bone Metabolism, School of Life Sciences, Northwestern Polytechnical University, Xi'an, China

OPEN ACCESS

Edited by:

Lilian Irene Plotkin,
Indiana University Bloomington,
United States

Reviewed by:

Rajeev Aurora,
Saint Louis University, United States
Anna Teti,
University of L'Aquila, Italy

*Correspondence:

Airong Qian
qianair@nwpu.edu.cn

[†]These authors have contributed
equally to this work and share first
authorship

Specialty section:

This article was submitted to
Bone Research,
a section of the journal
Frontiers in Endocrinology

Received: 31 December 2019

Accepted: 15 June 2020

Published: 11 August 2020

Citation:

Zhang W, Dang K, Huai Y and Qian A
(2020) Osteoimmunology: The
Regulatory Roles of T Lymphocytes in
Osteoporosis.
Front. Endocrinol. 11:465.
doi: 10.3389/fendo.2020.00465

Immune imbalance caused bone loss. Osteoimmunology is emerging as a new interdisciplinary field to explore the shared molecules and interactions between the skeletal and immune systems. In particular, T lymphocytes (T cells) play pivotal roles in the regulation of bone health. However, the roles and mechanisms of T cells in the treatment of osteoporosis are not fully understood. The present review aims to summarize the essential regulatory roles of T cells in the pathophysiology of various cases of osteoporosis and the development of T cell therapy for osteoporosis from osteoimmunology perspective. As T cell-mediated immunomodulation inhibition reduced bone loss, there is an increasing interest in T cell therapy in an attempt to treat osteoporosis. In summary, the T cell therapy may be further pursued as an immunomodulatory strategy for the treatment of osteoporosis, which can provide a novel perspective for drug development in the future.

Keywords: osteoimmunology, T lymphocytes, osteoporosis, bone formation, bone resorption

INTRODUCTION

Osteoporosis is a prevailing metabolic bone disease in both men > 50 years and postmenopausal women, which increases bone fragility and may further result in bone fractures, thus significantly leading to serious health problems for patients (1). Worldwide, nearly 200 million people are diagnosed with osteoporosis annually, even leading to almost 9 million osteoporotic fractures (2). In the US, it was approximately 53.6 million of the adult population of years > 50 who suffered from osteoporosis and low bone mass (54% of the population) (3). In fact, osteoporosis patients not only suffer from the enormous pain and disability but also bring a huge economic burden for patients and their families. In the US, it has been estimated that the financial costs associated with bone fractures will reach \$25.3 billion by the end of 2025 (4).

In traditional view, osteoporosis was considered as the imbalance of bone remodeling between osteoclasts and osteoblasts (5). Recently, the immune system was reported to regulate the bone system, which promoted the emergence of interdisciplinary field of osteoimmunology (6–9). The immune and bone systems share the same microenvironment. The immune system regulates osteocytes by the secretion of inflammatory factors and related ligand, which further affects bone formation and bone resorption (8, 10). T cells, B cells, and cytokines are important regulatory factors in the bone resorption. Among them, T cells play pivotal roles in the regulation of bone remodeling (11, 12). The osteoclast differentiation was enhanced, and the bone mineral density was decreased in the nude mice (T cell deficient), which was due to the immune imbalance of T cells

promoting osteoclast differentiation and bone resorption (13, 14). In pathophysiological condition, activated T cells secreted multiple inflammatory factors and related ligands such as TNF- α , IL-1, IL-6, IL-17, and CD40L, which enhanced bone resorption and disrupted bone balance, resulting in bone loss (15, 16). Th17 cells are mainly involved in inducing bone resorption (osteoclastogenesis) (17), while Treg cells are major suppressors of bone loss (18, 19) by inhibiting differentiation of monocytes into osteoclasts (17, 20, 21). These reports indicated that immune imbalance promoted osteoclast differentiation, further leading to bone loss. However, the roles of T cells in osteoporosis and the underlying mechanism of T cells in the regulation of bone system are still unclear.

Recently, there is an increasing interest in immune therapies especially T cell therapies for the treatment of osteoporosis (22). For example, antiretroviral therapy worsens HIV-induced bone loss (23), which may be an important future approach to treat osteoporosis in human. That is because T cell reconstitution induces RANKL and TNF α production by B-cells and/or T-cells, which further enhancing bone resorption and bone loss. T cell therapy became the effective strategy for the treatment of osteoporosis. For example, RANKL/RANK inhibition may be an attractive approach for the treatment of postmenopausal osteoporosis (24). Sclareol is a natural product (initially isolated from the leaves and flowers of *Salvia sclarea*) with immune regulation and anti-inflammatory effects, and it prevents ovariectomy-induced bone loss *in vivo* and inhibits osteoclastogenesis *in vitro* via suppressing NF- κ B and MAPK/ERK signaling pathways (25). Thus, it will be essential to develop T cell therapy that may be a huge potential for the treatment of osteoporosis in future clinical applications.

Herein, we briefly highlight the roles of T cells in various types of osteoporosis and uncover novel mechanisms of osteoimmunology, which provides new insight for clinical implications in the treatment of osteoporosis. Nonetheless, the underlying mechanisms of bone-immune interactions need to be further dissected, and an accumulative evidence continues to be made in favor of regulation roles of immune cells in osteoporosis. Most importantly, the T cell therapy may represent a suitable and potential approach to reinstate aberrant bone remodeling in the bone metabolism diseases.

OSTEOIMMUNOLOGY AND THE REGULATION OF T CELL CYTOKINES IN OSTEOPOROSIS

Osteoimmunology is the intricate interaction between the immune system and the bone system (6–9). The

RANKL/RANK/OPG pathway is essential for the differentiation of bone-resorbing osteoclasts and immune regulation (26, 27). Activated T cells directly produce RANKL, which further stimulates osteoclast formation (28, 29). RANKL and RANK were identified as key factors in the mediation of bone remodeling, especially in the osteoclast formation (29, 30). Furthermore, the activated RANK facilitated the expression of tumor necrosis factor (TNF) receptor-associated factors (TRAFs), such as TRAF6, which leads to osteoclast differentiation (31, 32). In OVX mice, the low-dose RANKL of CD8⁺ Treg cells decreased the expression of inflammatory and osteoclastogenic cytokines, thus suppressing bone resorption (33). Multiple cytokines produced by T cell including interleukin (IL)-12, IL-17, IL-18, and TNF- α were involved in RANK signaling, and thus play essential roles in regulating osteoclastogenesis and osteoclast differentiation (34). In addition, activated T cells suppress osteoclast differentiation by the antiviral cytokine IFN- γ (35). Various inflammatory cytokines were necessary and sufficient for bone metabolism (11). IL-17A also upregulates the expression of RANK, thus promoting the osteoclastogenic activity of RANKL (36). All these studies indicated that T cell cytokines play essential roles in osteoporosis, which may be the potential targets for the treatment of osteoporosis. Various T cell cytokines are listed in Table 1.

THE T CELLS IN THE REGULATION OF VARIOUS OSTEOPOROSIS

T cells perform a dual role in the regulation of bone remodeling: resting T cells protect osteoclasts from bone resorption, and activated T cells actively regulate the osteoclasts generation. This review aims to summarize the regulatory roles of T cells in various types of osteoporosis such as chronic inflammation-induced osteoporosis, senile osteoporosis, estrogen deficiency-induced osteoporosis, parathyroid hormone (PTH)-induced osteoporosis, and glucocorticoid-induced osteoporosis (GIO).

The Regulatory Roles of T Cells in Chronic Inflammation-Induced Osteoporosis

Osteoporosis commonly occurred in various chronic inflammatory diseases, such as rheumatic arthritis (RA), gout, psoriatic disease, osteoarthritis, and axial spondylarthritis and even leads to functional disability and increased mortality (49–52). It is interesting to note that Tregs play pivotal roles in inflammation-induced bone loss by inhibiting the functions of Th17 cells (19, 53). In particular, Foxp3⁺ Treg cells play an indispensable role in bone and hematopoietic homeostasis acting on osteoclast development and function (54). In addition, in inflammation condition, the expression of nuclear factor of activated T cells cytoplasmic 1 (NFATc1), as well as by inflammatory cytokines such as TNF α , IL-1 β , and IL-6 was induced and produced to promote osteoclast differentiation mediated by the RANKL-RANK and calcium signaling (8). INF γ , the main Th1 cytokine, can strongly inhibit osteoclast differentiation *in vitro* through the proteasomal degradation of TRAF6, indicating that T cells regulate osteoclastogenesis (28). The T cell subset, Tregs, also suppresses osteoclast

Abbreviations: BMMs, Bone marrow macrophages; BMSCs, bone marrow stromal cells; Cbfa1, core-binding factor subunit alpha-1; DC, dendritic cell; GCs, glucocorticoids; GIO, glucocorticoid-induced osteoporosis; GSK-3 β , glycogen synthase kinase 3 β ; IGF, insulin-like growth factor; IFN, interferon; M-CSF, macrophage-colony stimulating factor; MSCs, mesenchymal stem cells; NFATc1, nuclear factor of activated T cells cytoplasmic 1; NKT, natural killer T cells; iNOS, inducible NOS; RANKL, nuclear factor-kappa-B ligand; OVX, ovariectomized; OPG, osteoprotegerin; PTH, parathyroid hormone; T cells, T lymphocytes; TRAF6, TNF receptor associated factor 6; Runx2, Transcription Factor 2; RANK, receptor activator of NF- κ B ligand; RA, rheumatoid arthritis.

TABLE 1 | Roles of various T cell cytokines in the regulation of osteoclastogenesis.

Cytokine	Source	Modulation of immunology	Osteoclastogenic function	References
RANKL	Th17 cells	Osteoclast differentiation dendritic cells (DCs) maturation	Osteoclast activation via RANK	(37)
RANK	Osteoclasts, DCs	DCs activation	Osteoclast differentiation and activation	(38)
OPG	Osteoclasts	Decoy receptor for RANKL	Inhibits osteoclastogenesis	(39)
TNF α	Th17, macrophage DCs	Pro-inflammatory cytokine	Indirect osteoclastic activation through RANKL	(37)
M-CSF	Th1	Pro-inflammatory	Inhibits osteoclastogenesis	(38)
IL-4	Th2	Humoral immunity	Inhibits osteoclastogenesis	(40)
IL-6	Macrophage, DCs	Pro-inflammation, Th17 induction	Activation of osteoclastogenesis	(41)
IL-7	T cells	Pro-inflammatory cytokine	Inhibits osteoclast formation	(42)
IL-8				
IL-10	Regulatory T (Treg)	Anti-inflammatory	Suppress bone resorption	(43)
IL-17	T cells	Pro-inflammatory cytokine	RANKL expression and vigorous pro-inflammatory potency	(44)
IL-27	Macrophage and DCs	Th1 and Treg Th17 induction	Inhibits osteoclast formation, blocking receptor activator of NF- κ B (RANK)-dependent osteoclastogenesis	(45)
IL-12	Antigen-presenting cells	Pro-inflammatory cytokine	Inhibits RANKL-stimulated Osteoclastogenesis	(46)
IL-15	NK cells	Pro-inflammatory cytokine	Enhances RANK ligand (RANKL) and macrophage colony-stimulating factor expression	(47)
IL-23	Macrophage and DCs	Th17 induction	Indirect osteoclast activation	(48)
IFN- γ	Th1, NK cells	Cellular immunity	Inhibits osteoclastogenesis	(41)

formation and bone resorbing *in vitro* (53). CTLA-4 is the most essential regulator in the Treg-mediated inhibition of osteoclast differentiation, whereas the major cytokines of Tregs-TGF β and IL-10 do not possess any essential roles (53). All these studies suggest that T cells and their related cytokine play pivotal roles in the regulation of osteoporosis, and they may be the potential therapeutic targets for bone loss.

Generally, chronic inflammatory diseases are associated with bone resorption. HIV-infected men had low CD4 T cells, which is inversely associated with bone loss (55). Some studies suggest that T cells are not associated with bone mineral density in HIV-infected patients treated with combination antiretroviral therapy (cART) (56). However, cART seems to influence bone mineral density (BMD) with the protective effect. Therefore, the regulatory roles for activated T cells in the pathogenesis of osteoporosis warrant further investigation. In RA patients, the enhanced osteoclast differentiation and activation lead to bone erosion and systematic osteoporosis (57). Indeed, inflammatory cytokines including RANKL, TNF α , IL-6, and IL-1 were elevated in RA patients, which promoted the osteoclast differentiation (58). Taken together, these studies suggest that the T cells may determine the osteoclast differentiation in the chronic inflammatory diseases, and the T cell regulatory therapy could potentially have significant impact on the drug development for osteoporosis. However, whether the T cell therapy is efficient for osteoporosis in clinical studies needs further investigation.

The Regulation Roles of T Cells in Senile Osteoporosis

Aging is always accompanied with the imbalance between bone formation and resorption, causing skeletal microarchitecture damage and bone loss (59). The production of naïve T cells is severely impaired due to a decreased output of lymphoid cells from the bone marrow and the deterioration of the thymus (60). Incidence and severity of osteoporosis are increased in the older population (61). The prevalence of low BMD is associated with immune activation and senescence induced by HIV infection (62). Total T cells were increased in the bone marrow (BM) with age, especially the highly differentiated CD8⁺ T cells without the expression of the co-stimulatory molecule CD28, while natural killer T (NKT) cells, monocytes, and naïve CD8⁺ T cells were decreased in the BM with age (63). It seems that the immune system abnormality plays important roles in the regulation of senile osteoporosis.

Recent discoveries suggest that T cell dysfunction induced the accumulation of cytokines, immunological mediators, and transcription factors, which affect osteoclast and osteoblast in the elderly (64). Cytokines such as IL-6, TNF- α , and IL-1 increased with age (65, 66). IL-1 and TNF- α activate the inducible NOS (iNOS) pathway, which inhibited osteoblast differentiation and enhanced osteoblast apoptosis *in vitro* (67). IL-12 derived from T cells, alone or combined with IL-18, was identified to inhibit osteoclast formation *in vitro* (68). IL-4 regulated osteoclast

differentiation through the antagonism between STAT6 and NF- κ B signaling (69). In addition, T cell mediated the bone balance by the inhibition of osteoclastogenesis through the crucial immunoregulatory control, mainly OPG expression and simultaneous production of cytokines (64). IFN- γ , IL-12, and IL-18 inhibited the RANKL-induced maturation and activation of osteoclasts (64). Furthermore, senescent T cells impaired the production of IFN- γ , OPG, and osteoclast-inhibiting cytokines, which increased the incidence of aged osteoporosis. In addition, cytokines such as TGF β and RANKL secreted by activated T cells can activate p38 MAPKs and further regulate bone development and remodeling. P38 α MAPK mediates osteoclast proliferation and bone remodeling in an aging-dependent manner (70). Overall, T cells and their cytokines play important roles in the regulation of aged osteoporosis, which may be the novel targets for the treatment of osteoporosis, suggesting that T cell therapy could be used as immunotherapy and may be beneficial in counteracting immunosenescence in old population. Meanwhile, in females, osteoporosis occurrence is generally attributed to the decrease in estrogen, thus leading to estrogen deficiency-induced osteoporosis. The underlying mechanisms of T cells involved in the mediation of the postmenopausal osteoporosis were dissected in the next section, The Regulatory Roles of T Cells in Estrogen Deficiency-Induced Osteoporosis.

The Regulatory Roles of T Cells in Estrogen Deficiency-Induced Osteoporosis

The loss of estrogen initiates the inflammatory changes of bone-microenvironment state, inducing a rapid phase of bone loss leading to osteoporosis in half of postmenopausal women. In postmenopausal women, estrogen deficiency stimulates CD4⁺ T cell dysregulation and induces elevated circulating levels of inflammatory cytokines, especially TNF α , IFN- γ , IL-17, RANKL, and CD40L (71–74). These cytokines exert impressive regulatory effects on bone resorption. For example, TNF- α was overexpressed in the BM in postmenopausal osteoporosis, which promotes RANKL-induced osteoclast formation through the activation of NF- κ B and PI3K/Akt signaling (74). Besides, TNF- α was identified to induce both autophagy and apoptosis in osteoblasts to enhance bone loss in postmenopausal women (75). Besides, estrogen deficiency increased the number of the costimulatory factors, CD40L, expressed on activated T cells, inducing the expressions of M-CSF and RANKL on stromal cells and downregulating the production of OPG, ultimately resulting in a remarkable increase in osteoclast numbers (76, 77). The pro-osteoclastic cytokines, such as IL-6, TNF- α , and IL-1, were increased significantly in estrogen deficiency-induced osteoporosis (78). All these studies indicated that the inflammatory cytokines and costimulatory factors of T cells changed significantly in estrogen deficiency-induced osteoporosis, which may provide the novel perspective for the treatment of bone loss in postmenopausal women.

Moreover, estrogen deficiency stimulates the IL-17 differentiation of Th17 cells (79) and augments the expression levels of pro-osteoclastogenic cytokines, such as TNF- α , IL-6, and RANKL, ultimately leading to bone loss. Nevertheless, IL-17

receptor deficiency induced more serious bone loss in OVX mice than that in control groups, implying that IL-17 may possess the bone protective effects (80). The pro-osteoclastogenic cytokine changes were reversed with the supplementary oral estrogen, indicating that estrogen may suppress Th17 differentiation and IL-17 production to protect bone health (81). In summary, in postmenopausal women, both aging and hormonal deficiency stimulate the deregulation of T cells contributing to the inflammatory, which increased bone resorption, resulting in a bone loss or osteoporosis. We believe that focusing on the potential biological mechanisms of T cells is of paramount importance for developing novel therapy strategies for the treatment of postmenopausal osteoporosis. However, further confirmation in phase I/II trials is needed to validate these strategies in a broader clinical evaluation.

The Regulatory Roles of T Cells in PTH-Induced Osteoporosis

PTH is a key calciotropic hormone and a critical regulator for postnatal skeletal development (82). The secretion of inflammatory or osteoclastogenic cytokines of T cells and bone cells was facilitated under long-term PTH administration, such as RANKL, TNF- α , and IL-17, which promoted the bone resorption (83). PTH induced bone loss via the expansion of intestinal TNF⁺ T and Th17 cells, and the increase in their S1P-receptor-1 mediated egress from the intestine and recruitment to the BM (84). So targeting the gut microbiota or T cell migration may represent novel therapeutic strategies for PTH-induced osteoporosis. In addition, PTH exploited CD4⁺ T cells to induce TNF α production that enhances the formation of IL-17A secreting Th17 T cells. Both TNF α and IL-17 further facilitated the development of an increased RANKL/OPG ratio favorable to osteoclastic bone resorption (85). Moreover, PTH boosted the production of TNF- α and RANKL in CD4⁺ T cells, which triggered osteoclastogenic generation and bone resorption activity (86). Clinical studies also showed that PTH treatment increased Th17 cell numbers and the IL-17 production in humans with primary hyperparathyroidism (34). IL-17 intensified PTH-induced bone loss through the stimulation of the RANKL production in osteoblast-lineage cells, which is parallel to the roles of IL-17 in estrogen deficiency-induced osteoporosis.

Notably, T cells also secreted PTH receptors involved in the regulation of trabecular bone development (87). For example, T cells promoted the signals of BMSC proliferation through the combination of CD40L on T cells and its receptor on BMSC, weakening the bone catabolic activity of cPTH, leading to a reduction of the RANKL to OPG ratio and osteoclastogenic activity (88). Several studies found that the intermittent PTH administration at low dosage increased bone formation and bone mass, thus attenuating bone loss (89, 90). The deletion of PTH receptor in BM mesenchymal progenitors results in a rapid increase in BM adipocyte accompanied with the reduction of bone mass. Given the essential regulatory roles of T cells for the PTH-induced bone loss, particular attention will be paid toward the combinations of intermittent PTH (iPTH) and T cell therapy for PTH-induced osteoporosis.

The Regulatory Roles of T Cells in GIO

Glucocorticoids (GCs) are extensively used for the treatment of immune and inflammatory disorders due to their powerful immunosuppressive and anti-inflammatory actions (91, 92). However, long-term exogenous GC therapy might cause rapid and pronounced bone loss and subsequently osteoporosis (93, 94). The pathogenesis of GIO was predominantly attributed to the fact that GCs impaired bone formation by reduction of osteoblast differentiation and activity via the expression of the osteoblast-specific transcription factor runt-related Runx2 (95–97). In addition, the long-term GC administration affects bone remodeling by whittling the insulin-like growth factor (IGF) in ossification (98). GCs enhanced the expression levels of RANKL in both osteoblasts and stromal cells, which triggered osteoclastogenesis and activated osteoclastic bone resorption by binding to the RANKL receptor RANK (99), thus resulting in the primary phase of rapid bone loss. On the other hand, GCs contributed to the apoptosis of certain T cell subsets, further augmented the secretion of RANKL, and directly induced osteoclast differentiation (100). Interestingly, different T cell subsets exhibit distinct sensitivity to GC-induced apoptosis. For example, Th17 cells, as an osteoclastogenesis-promoting factor, are resistant to GC-induced apoptosis and cytokine suppression mostly through the high production of IL-17 and RANKL (79). Therefore, GC therapy fails to inhibit the Th17 cell activation and the IL-17 and RANKL production. Excessive GCs could reduce the production of OPG, further promoting osteoclast differentiation and resulting in bone resorption. Given above, we assert that T cell therapy may be effective for the GC-induced osteoporosis.

T CELL THERAPY FOR OSTEOPOROSIS

T cells and their secreted cytokines are responsible for bone resorption in various osteoporosis. T cell therapy may be a potentially therapeutic approach to osteoporosis. For example, anti-inflammatory therapies have shown good potential in an animal model, although they have not been widely used clinically to treat osteoporosis (101). Immune modulation therapy such as probiotics was considered as a novel strategy for bone loss (102–104). RANKL was considered as an activator of dendritic cell (DC) expression in T cells. Anti-RANKL therapeutic antibody drug, denosumab, has been successfully applied in the treatment of osteoporosis in clinics (105–107). In addition, a novel vaccine targeting RANKL by introducing a p-nitrophenylalanine at a single site in mRANKL immunization could prevent OVX-induced bone loss in mice (108). Notably, anti-RANKL antibody inhibited osteoporosis and bone destruction, but possesses no therapeutic effect on RA disease. Therefore, it is

necessary to rethink about the underlying mechanisms of bone-related diseases.

Recently, extracts and natural products derived from traditional Chinese medicine (TCM) have great potential as well as advantages in the prevention and treatment of osteoporosis in terms of good therapeutic effect, low toxicity, and side effects (109, 110), and they have gained increasing attention from the medical community. For example, polysaccharides derived from persimmon leaves down-regulated RANKL-induced activation of mitogen-activated protein kinases (MAPKs) to suppress the nuclear factor of NFATc1 expression, thus possessing anti-osteoporotic effects in OVX-induced bone loss. The natural product cyperenoic acid is a terpenoid isolated from the medicinal plant *Croton crassifolius*, and it suppressed osteoclast differentiation by inhibiting the NF- κ B pathway and suppressed RANKL expression (111). Baohuoside I is an active component of *Herba Epimedii* with the immune regulation functions of T cells and antioxidant activity, which serves as a candidate for treating postmenopausal osteoporosis (112). All these results indicated that drugs from TCM possess anti-osteoporosis effects by the regulation of T cells, and they may show great potential as therapeutic agents for osteoporosis. However, further experimental and clinical research remains to be specifically conducted to explore the cellular and molecular mechanisms of the drugs from TCM.

CONCLUSION AND PERSPECTIVE

The pathogen clearance of various types of osteoporosis would be impaired or would delay bone resorption due to the dysfunction of the T cells. Therefore, understanding the roles of T cells in the pathogenesis of osteoporosis and the mechanisms underlying these pathologies between the immune system and the bone system may lead to the development of new treatments for osteoporosis. However, further studies, especially clinical studies, are required to explore the safety of T cell therapy for bone loss.

AUTHOR CONTRIBUTIONS

WZ designed, wrote and revised the whole manuscript. YH wrote the manuscript. AQ and KD helped to revise the manuscript. All authors contributed to the article and approved the submitted version.

FUNDING

This work was funded by the National Natural Science Foundation of China (No. 81901917), China's Postdoctoral Science Fund (No. 2017M623249), and the Key Research and Development Project of Shaanxi Province (No. 2018SF-363).

REFERENCES

- Dai Z, Zhang Y, Lu N, Felson DT, Kiel DP, Sahni S. Association between dietary fiber intake and bone loss in the Framingham Offspring Study. *J Bone Miner Res.* (2018) 33:241–9. doi: 10.1002/jbmr.3308
- Yaacobi E, Sanchez D, Maniar H, Horwitz DS. Surgical treatment of osteoporotic fractures: an update on the principles of management. *Injury.* (2017) 48:S34–40. doi: 10.1016/j.injury.2017.08.036
- Wright NC, Looker AC, Saag KG, Curtis JR, Delzell ES, Randall S, et al. The recent prevalence of osteoporosis and low bone mass in the United States

- based on bone mineral density at the femoral neck or lumbar spine. *J Bone Miner Res.* (2016) 29:2520–6. doi: 10.1002/jbmr.2269
4. Yu B, Wang C-Y. Osteoporosis: the result of an 'aged' bone microenvironment. *Trends Mol Med.* (2016) 22:641–4. doi: 10.1016/j.molmed.2016.06.002
 5. Raisz LG, Seeman E. Causes of age-related bone loss and bone fragility: an alternative view. *Eur J Bone Miner. Res.* (2002) 16:1948–52. doi: 10.1359/jbmr.2001.16.11.1948
 6. Okamoto K, Nakashima T, Shinohara M, Negishi-Koga T, Komatsu N, Terashima A, et al. Osteoimmunology: the conceptual framework unifying the immune and skeletal systems. *Physiol Rev.* (2017) 97:1295–349. doi: 10.1152/physrev.00036.2016
 7. Srivastava RK. Osteoimmunology: the nexus between bone and immune system. *Front Biosci.* (2018) 23:464–92. doi: 10.2741/4600
 8. Takayanagi H. Osteoimmunology and the effects of the immune system on bone. *Nat Rev Rheumatol.* (2009) 5:667–76. doi: 10.1038/nrrheum.2009.217
 9. Takayanagi H. Osteoimmunology in 2014: two-faced immunology-from osteogenesis to bone resorption. *Nat Rev Rheumatol.* (2015) 11:74–6. doi: 10.1038/nrrheum.2014.219
 10. Okamoto K, Takayanagi H. Osteoimmunology. *Cold Spring Harb Perspect Med.* (2018) 9:a031245. doi: 10.1101/cshperspect.a031245
 11. Srivastava RK, Dar HY, Mishra PK. Immunoporosis: immunology of osteoporosis-role of t cells. *Front. Immunol.* (2018) 9:657. doi: 10.3389/fimmu.2018.00657
 12. Kalyan S. It may seem inflammatory, but some T cells are innately healing to the bone. *J Bone Miner Res.* (2016) 31:1997–2000. doi: 10.1002/jbmr.2875
 13. Harmer D, Falank C, Reagan MR. Interleukin-6 interweaves the bone marrow microenvironment, bone loss, and multiple myeloma. *Front Endocrinol.* (2019) 9:788. doi: 10.3389/fendo.2018.00788
 14. Li Y, Toraldo G, Li A, Yang X, Weitzmann MN. B cells and T cells are critical for the preservation of bone homeostasis and attainment of peak bone mass *in vivo*. *Blood.* (2007) 109:3839–48. doi: 10.1182/blood-2006-07-037994
 15. Weitzmann MN, Ofotokun I. Physiological and pathophysiological bone turnover-role of the immune system. *Nat Rev Endocrinol.* (2016) 12:518–32. doi: 10.1038/nrendo.2016.91
 16. Fuller K, Murphy C, Kirstein B, Fox SW, Chambers TJ. TNF α potentially activates osteoclasts, through a direct action independent of and strongly synergistic with RANKL. *Endocrinol.* (2002) 143:1108–18. doi: 10.1210/endo.143.3.8701
 17. Dar HY, Shukla P, Mishra PK, Anupam R, Mondal RK, Tomar GB, et al. *Lactobacillus acidophilus* inhibits bone loss and increases bone heterogeneity in osteoporotic mice via modulating Treg-Th17 cell balance. *Bone Rep.* (2018) 8:46–56. doi: 10.1016/j.bonr.2018.02.001
 18. Buchwald ZS, Kiesel JR, Yang C, DiPaolo R, Novack DV, Aurora R. Osteoclast-induced Foxp3+ CD8 T-cells limit bone loss in mice. *Bone.* (2013) 56:163–73. doi: 10.1016/j.bone.2013.05.024
 19. Glowacki AJ, Yoshizawa S, Jhunjhunwala S, Vieira AE, Garlet GP, Sfeir C, et al. Prevention of inflammation-mediated bone loss in murine and canine periodontal disease via recruitment of regulatory lymphocytes. *Proc Natl Acad Sci USA.* (2013) 110:18525–30. doi: 10.1073/pnas.1302829110
 20. Luo C, Wang L, Sun C, Li D. Estrogen enhances the functions of CD4+CD25+Foxp3+ regulatory T cells that suppress osteoclast differentiation and bone resorption *in vitro*. *Cell Mol Immunol.* (2011) 8:50–8. doi: 10.1038/cmi.2010.54
 21. Yuan FL, Li X, Lu W-G, Xu R-S, Zhao Y-Q, Li C-W, et al. Regulatory T cells as a potent target for controlling bone loss. *Biochem Biophys Res Commun.* (2010) 402:173–6. doi: 10.1016/j.bbrc.2010.09.120
 22. Tanaka Y. Clinical immunity in bone and joints. *J Bone Miner Metab.* (2018) 37:2–8. doi: 10.1007/s00774-018-0965-5
 23. Ofotokun I, Titanji K, Vikulina T, Roser-Page S, Yamaguchi M, Zayzafoon M, et al. Role of T-cell reconstitution in HIV-1 antiretroviral therapy-induced bone loss. *Nat Commun.* (2016) 6:8282. doi: 10.1038/ncomms9282
 24. Santana-Davila R, Show LQ. The use of combination immunotherapies as frontline therapy for non-small cell lung cancer. *Future Oncol.* (2018) 14:191–4. doi: 10.2217/fon-2017-0124
 25. Jin HM, Shao ZX, Wang QQ, Miao JS, Bai XQ, Liu Q, et al. Sclerol prevents ovariectomy-induced bone loss *in vivo* and inhibits osteoclastogenesis *in vitro* via suppressing NF- κ B and MAPK/ERK signaling pathways. *Food Funct.* (2019) 10:6556. doi: 10.1039/C9FO00206E
 26. Bozec A, Zaiss MM. T regulatory cells in bone remodelling. *Curr Osteoporos Rep.* (2017) 15:121–5. doi: 10.1007/s11914-017-0356-1
 27. Walsh MC, Choi Y. Biology of the RANKL-RANK-OPG system in immunity, bone, and beyond. *Front Immunol.* (2014) 5:511. doi: 10.3389/fimmu.2014.00511
 28. Takayanagi H, Ogasawara K, Hida S, Chiba T, Taniguchi T. T-cell-mediated regulation of osteoclastogenesis by signalling cross-talk between RANKL and IFN- γ . *Nature.* (2000) 408:600–5. doi: 10.1038/35046102
 29. Theill LE, Boyle WJ, Penninger JM. RANK-L and RANK: T cells, bone loss, and mammalian evolution. *Annu Rev Immunol.* (2002) 20:795–823. doi: 10.1146/annurev.immunol.20.100301.064753
 30. Ginaldi L, Benedetto MCD, Martinis MD. Osteoporosis, inflammation and ageing. *Immun Ageing.* (2005) 2:1–5. doi: 10.1186/1742-4933-2-14
 31. Schett G, David JP. The multiple faces of autoimmune-mediated bone loss. *Nat Rev Endocrinol.* (2010) 6:698–706. doi: 10.1038/nrendo.2010.190
 32. Nagy V, Penninger JM. The RANKL-RANK story. *Gerontol.* (2015) 61:534–42. doi: 10.1159/000371845
 33. Pacifici R. T cells, osteoblasts, and osteocytes: interacting lineages key for the bone anabolic and catabolic activities of parathyroid hormone. *Ann N Y Acad Sci.* (2016) 1364:11–24. doi: 10.1111/nyas.12969
 34. Li JY, D'Amelio P, Robinson J, Walker LD, Vaccaro C, Luo T, et al. IL-17A is increased in humans with primary hyperparathyroidism and mediates PTH-induced bone loss in mice. *Cell Metab.* (2015) 22:799–810. doi: 10.1016/j.cmet.2015.09.012
 35. Kotake S, Nanke Y, Mogi M, Kawamoto M, Furuya T, Yago T, et al. IFN- γ -producing human T cells directly induce osteoclastogenesis from human monocytes via the expression of RANKL. *Eur J Immunol.* (2005) 35:3353–63. doi: 10.1002/eji.200526141
 36. Adamopoulos IE, Chao CC, Geissler R, Laface D, Bowman EP. Interleukin17A upregulates receptor activator of NF- κ B on osteoclast precursors. *Arthritis Res Ther.* (2010) 12:1–11. doi: 10.1186/ar2936
 37. Boyce BF, Xing L. Functions of RANKL/RANK/OPG in bone modeling and remodeling. *Arch Biochem Biophys.* (2008) 473:139–46. doi: 10.1016/j.abb.2008.03.018
 38. Adamopoulos IE, Bowman EP. Immune regulation of bone loss by Th17 cells in oestrogen-deficient osteoporosis. *Eur J Clin Invest.* (2013) 43:1195–203. doi: 10.1111/eci.12158
 39. Harrington L. Expanding the effector CD4 T-cell repertoire: the Th17 lineage. *Curr Opin Immunol.* (2006) 18:349–56. doi: 10.1016/j.coi.2006.03.017
 40. Mangashetti LS, Khapli SM, Wani MR. IL-4 inhibits bone-resorbing activity of mature osteoclasts by affecting NF-KB and Ca²⁺ Signaling. *J Immunol.* (2005) 175:917–25. doi: 10.4049/jimmunol.175.2.917
 41. Yun TJ, Chaudhary PM, Shu GL, Frazer JK, Ewings MK, Schwartz SM, et al. OPG/FDCR-1, a TNF receptor family member, is expressed in lymphoid cells and is up-regulated by ligating CD40. *J Immunol.* (1998) 161:6113–21.
 42. Sun-Kyeong L, Kalinowski JF, Jastrzebski SL, Lynn P, Lorenzo JA. Interleukin-7 is a direct inhibitor of *in vitro* osteoclastogenesis. *Endocrinology.* (2003) 144:3524–31. doi: 10.1210/en.2002-221057
 43. Wing K, Yamaguchi T, Sakaguchi S. Cell-autonomous and -non-autonomous roles of CTLA-4 in immune regulation. *Trends Immunol.* (2011) 32:428–33. doi: 10.1016/j.it.2011.06.002
 44. Arboleya L, Castañeda S. Osteoimmunology: the study of the relationship between the immune system and bone tissue. *Reumatol Clin.* (2013) 9:303–15. doi: 10.1016/j.reuma.2013.02.004
 45. Woodward J. Regulation of haematopoietic progenitor cell proliferation and survival The involvement of the osteoblast. *Cell Adh Migr.* (2010) 4:4–6. doi: 10.4161/cam.4.1.10106
 46. Nagata N. Inhibition of RANKL-induced osteoclast formation in mouse bone marrow cells IL-12 : involvement of IFN- γ possibly induced from non-T cell population. *Bone.* (2003) 33:721–32. doi: 10.1016/S8756-3282(03)00213-8
 47. Hayday AC. $\gamma\delta$ T Cells and the lymphoid stress-surveillance response. *Immunity.* (2009) 31:184–96. doi: 10.1016/j.immuni.2009.08.006
 48. Sato K, Suematsu A, Okamoto K, Yamaguchi A, Morishita Y, Kadono Y, et al. Th17 functions as an osteoclastogenic helper T cell subset that links

- T cell activation and bone destruction. *J Exp Med.* (2006) 203:2673–82. doi: 10.1084/jem.20061775
49. Clayton ES, Hochberg MC. Osteoporosis and osteoarthritis, rheumatoid arthritis and spondylarthropathies. *Curr Osteoporos Rep.* (2013) 11:257–62. doi: 10.1007/s11914-013-0172-1
 50. Gulati AM, Michelsen B, Diamantopoulos A, Grandaunet B, Salvesen Ø, Kavanaugh A, et al. Osteoporosis in psoriatic arthritis: a cross-sectional study of an outpatient clinic population. *RMD Open.* (2018) 4:e000631. doi: 10.1136/rmdopen-2017-000631
 51. Schett G, Gravallese E. Bone erosion in rheumatoid arthritis: mechanisms, diagnosis and treatment. *Nat Rev Rheumatol.* (2012) 8:656–64. doi: 10.1038/nrrheum.2012.153
 52. Ødegård S, Landewé R, van der Heijde D, Kvien TK, Mowinckel P, Uhlig T. Association of early radiographic damage with impaired physical function in rheumatoid arthritis: a ten-year, longitudinal observational study in 238 patients. *Arthritis Rheum.* (2006) 54:68–75. doi: 10.1002/art.21548
 53. Zaiss MM, Axmann R, Zwerina J, Polzer K, Gückel E, Skapenko A, et al. Treg cells suppress osteoclast formation: a new link between the immune system and bone. *Arthritis Rheum.* (2007) 56:4104–12. doi: 10.1002/art.23138
 54. Fischer L, Herkner C, Kite R, Dohnke S, Riewaldt J, Kretschmer K, et al. Foxp3⁺ regulatory T cells in bone and hematopoietic homeostasis. *Front Endocrinol.* (2019) 10:578. doi: 10.3389/fendo.2019.00578
 55. Kwak MK, Lee EJ, Park JW, Park SY, Kim BJ, Kim TH, et al. CD4 cell count is inversely associated with lumbar spine bone mass in HIV-infected men under the age of 50 years. *Osteoporosis Int.* (2019) 30:1501–30. doi: 10.1007/s00198-019-05115-2
 56. Krikke M, Klomberg RCW, Veer EVD, Tesselaaar K, Verhaar HJJ, Hoepelman AIM, et al. Osteoporosis and osteopenia are not associated with T-cell activation in older cART-treated HIV-infected patients. *Neth J Med.* (2017) 75:138–44.
 57. Jung YK, Kang YM, Han S. Osteoclasts in the inflammatory arthritis: implications for pathologic osteolysis. *Immune Netw.* (2019) 19:1–13. doi: 10.4110/in.2019.19.e2
 58. Braun T, Zwerina J. Positive regulators of osteoclastogenesis and bone resorption in rheumatoid arthritis. *Arthritis Res Ther.* (2011) 13:1–11. doi: 10.1186/ar3380
 59. Fei D, Zhang Y, Wu J, Zhang H, Liu A, He X, et al. Cav 1.2 regulates osteogenesis of bone marrow-derived mesenchymal stem cells via canonical Wnt pathway in age-related osteoporosis. *Aging Cell.* (2019) 18:e12967. doi: 10.1111/ace1.12967
 60. Pangrazzi L, Weinberger B. T cells, aging and senescence. *Exp Gerontol.* (2020) 22:110887. doi: 10.1016/j.exger.2020.110887
 61. Borrelli J, Anglen JO (editors). Arthroplasty for the treatment of fractures in the older patient (indications and current techniques) || The relationship of peak bone mass, aging, and bone loss to osteoporosis and fragility fractures. In: *Arthroplasty for the Treatment of Fractures in the Older Patient Chapter*. New York, NY: Springer (2018). p. 3–17.
 62. Jiménez B, Sainz T, Díaz L, Mellado MJ, Navarro ML, Rojo P. Low bone mineral density in vertically HIV-infected children and adolescents: risk factors and the role of T-cell activation and senescence. *Pediatr Infect Dis J.* (2017) 36:578–83. doi: 10.1097/INF.0000000000001506
 63. Naismith E, Pangrazzi L, Grasse M, Keller M, Miggitsch C, Weinberger B, et al. Peripheral antibody concentrations are associated with highly differentiated T cells and inflammatory processes in the human bone marrow. *Immun Ageing.* (2019) 16:21. doi: 10.1186/s12979-019-0161-z
 64. Martinis MD, Benedetto MCD, Mengoli LP, Ginaldi L. Senile osteoporosis: is it an immune-mediated disease? *Inflamm Res.* (2006) 55:399–404. doi: 10.1007/s00011-006-6034-x
 65. Mundy GR. Osteoporosis and inflammation. *Nutr Rev.* (2007) 65:S147–51. doi: 10.1111/j.1753-4887.2007.tb00353.x
 66. Deng L, Hu G, Jin L, Wang C, Niu H. Involvement of microRNA-23b in TNF- α -reduced BMSC osteogenic differentiation via targeting runx2. *J Bone Miner Metab.* (2018) 36:648–60. doi: 10.1007/s00774-017-0886-8
 67. Wei S, Kitaura H, Zhou P, Ross FP, Teitelbaum SL. IL-1 mediates TNF-induced osteoclastogenesis. *J Clin Invest.* (2005) 115:282–90. doi: 10.1172/JCI200523394
 68. Horwood NJ, Elliott J, Martin TJ, Gillespie MT. IL-12 alone and in synergy with IL-18 inhibits osteoclast formation *in vitro*. *J Immunol.* (2001) 166:4915–21. doi: 10.4049/jimmunol.166.8.4915
 69. Abu-Amer Y. IL-4 abrogates osteoclastogenesis through STAT6-dependent inhibition of NF- κ B. *J Clin Invest.* (2001) 107:1375–85. doi: 10.1172/JCI10530
 70. Cong Q, Jia H, Li P, Qiu S, Yeh J, Wang Y, et al. p38 α MAPK regulates proliferation and differentiation of osteoclast progenitors and bone remodeling in an aging-dependent manner. *Sci Rep.* (2017) 7:45964. doi: 10.1038/srep45964
 71. Zhang J, Fu Q, Ren Z, Wang Y, Wang C, Shen T, et al. Changes of serum cytokines-related Th1/Th2/Th17 concentration in patients with postmenopausal osteoporosis. *Gynecol Endocrinol.* (2015) 31:183–90. doi: 10.3109/09513590.2014.975683
 72. Giorgio M, Patrizia DA, Roberta F, Giacomina B. Bone-immune cell crosstalk: bone diseases. *J Immunol Res.* (2015) 2015:1–11. doi: 10.1155/2015/108451
 73. Sang C, Zhang J, Zhang Y, Chen F, Cao X, Guo L. TNF- α promotes osteoclastogenesis through JNK signaling-dependent induction of Semaphorin3D expression in estrogen-deficiency induced osteoporosis. *J Cell Physiol.* (2017) 232:3396–408. doi: 10.1002/jcp.25784
 74. Zha L, He L, Liang Y, Qin H, Yu B, Chang L, et al. TNF- α contributes to postmenopausal osteoporosis by synergistically promoting RANKL-induced osteoclast formation. *Biomed Pharmacother.* (2018) 102:369–74. doi: 10.1016/j.biopha.2018.03.080
 75. Du D, Zhou Z, Zhu L, Hu X, Lu J, Shi C, et al. TNF- α suppresses osteogenic differentiation of MSCs by accelerating P2Y2 receptor in estrogen-deficiency induced osteoporosis. *Bone.* (2018) 117:161–70. doi: 10.1016/j.bone.2018.09.012
 76. Douin-Echinard V, Laffont S, Seillet C, Delpy L, Krust A, Chambon P, et al. Estrogen receptor alpha, but not beta, is required for optimal dendritic cell differentiation and CD40-induced cytokine production. *J Immunol.* (2008) 180:3661–9. doi: 10.4049/jimmunol.180.6.3661
 77. Zheng L, Wang W, Ni J, Mao X, Song D, Liu T, et al. Role of autophagy in tumor necrosis factor- α -induced apoptosis of osteoblast cells. *J Invest Med.* (2017) 65:1014–20. doi: 10.1136/jim-2017-000426
 78. Moffett SP, Zmuda JM, Oakley JL, Beck TJ, Cauley JA, Stone KL, et al. Tumor necrosis factor- α polymorphism, bone strength phenotypes, and the risk of fracture in older women. *J Clin Endocrinol Metab.* (2005) 90:3491–7. doi: 10.1210/jc.2004-2235
 79. Tyagi AM, Srivastava K, Mansoori MN, Trivedi R, Chattopadhyay N, Singh D, et al. Estrogen deficiency induces the differentiation of IL-17 secreting Th17 cells: a new candidate in the pathogenesis of osteoporosis. *PLoS ONE.* (2012) 7:e44552. doi: 10.1371/journal.pone.0044552
 80. Xu F, Dong Y, Huang X, Chen P, Huang S. Pioglitazone affects the OPG/RANKL/RANK system and increase osteoclastogenesis. *Mol Med Rep.* (2016) 14:2289–96. doi: 10.3892/mmr.2016.5515
 81. Pacifici R. (2007). T cells and post menopausal osteoporosis in murine models. *Arthritis Res Ther.* 9:1–4. doi: 10.1186/ar2126
 82. Wein MN, Kronenberg HM. Regulation of bone remodeling by parathyroid hormone. *Cold Spring Harb Perspect Med.* (2018) 8:a031237. doi: 10.1101/cshperspect.a031237
 83. Roberto P. The Role of IL-17 and Th17 cells in the bone catabolic activity of PTH. *Front Immunol.* (2016) 7:57. doi: 10.3389/fimmu.2016.00057
 84. Yu M, Tyagi AM, Li JY, Adams J, Denning TL, Weitzmann MN, et al. PTH induces bone loss via microbial-dependent expansion of intestinal TNF + T Cells and Th17 cells. *Nat Commun.* (2020) 11:468. doi: 10.1038/s41467-019-14148-4
 85. Neale Weitzmann M, Pacifici R. Parathyroid diseases and T cells. *Curr Osteoporosis Rep.* (2017) 15:135–41. doi: 10.1007/s11914-017-0359-y
 86. Pacifici R. T cells: critical bone regulators in health and disease. *Bone.* (2010) 47:461–71. doi: 10.1016/j.bone.2010.04.611
 87. Li JY, Walker LD, Tyagi AM, Adams J, Weitzmann MN, Pacifici R. The sclerostin-independent bone anabolic activity of intermittent PTH treatment is mediated by T-Cell-produced Wnt10b. *J Bone Miner Res.* (2014) 29:43–54. doi: 10.1002/jbmr.2044

88. Hesham T, Brahmachetna B, Jau-Yi L, Jonathan A, Tatsuya K, Neale WM, et al. Disruption of PTH receptor 1 in t cells protects against pth-induced bone loss. *PLoS ONE*. (2010) 5:e12290. doi: 10.1371/journal.pone.0012290
89. Fan Y, Hanai J-I, Le PT, Bi R, Maridas D, DeMambro V, et al. Parathyroid hormone directs bone marrow mesenchymal cell fate. *Cell Metab*. (2017) 25:661–72. doi: 10.1016/j.cmet.2017.01.001
90. Sang WK, Pajevic PD, Selig M, Barry KJ, Yang JY, Chan SS, et al. Intermittent parathyroid hormone administration converts quiescent lining cells to active osteoblasts. *J Bone Miner Res*. (2012) 27:2075–84. doi: 10.1002/jbmr.1665
91. Geurtzen K, Vernet A, Freidin A, Rauner M, Hofbauer LC, Schneider JE, et al. Immune suppressive and bone inhibitory effects of prednisolone in growing and regenerating zebrafish tissues. *J Bone Miner Res*. (2017) 32:2476–88. doi: 10.1002/jbmr.3231
92. Sato AY, Peacock M, Bellido T. Glucocorticoid excess in bone and muscle. *Clin Rev Bone Miner Metab*. (2018) 16:1–15. doi: 10.1007/s12018-018-9242-3
93. Compston J. Glucocorticoid-induced osteoporosis: an update. *Endocrine*. (2018) 61:7–16. doi: 10.1007/s12020-018-1588-2
94. Wang N, Zhang J, Yang JX. Growth factor progranulin blocks tumor necrosis factor- α -mediated inhibition of osteoblast differentiation. *Genet Mol Res*. (2016) 15. doi: 10.4238/gmr.15038126
95. Rauch A, Seitz S, Baschant U, Schilling AF, Illing A, Stride B, et al. Glucocorticoids suppress bone formation by attenuating osteoblast differentiation via the monomeric glucocorticoid receptor. *Cell Metab*. (2010) 11:517–31. doi: 10.1016/j.cmet.2010.05.005
96. Reid IR. Glucocorticoid-induced osteoporosis. *New Engl J Med*. (2010) 14:279–98. doi: 10.1053/beem.2000.0074
97. Weinstein RS. Glucocorticoid-induced bone disease. *N Engl J Med*. (2011) 365:62–70. doi: 10.1056/NEJMcp1012926
98. Beattie J, Al-Khafaji H, Noer PR, Alkharobi HE, Alhodhodi A, Meade J, et al. (2018). Insulin-like growth factor-binding protein action in bone tissue: a key role for pregnancy-associated plasma protein-A. *Front Endocrinol*. 9:31. doi: 10.3389/fendo.2018.00510
99. Wehmeyer C, Pap T, Buckley CD, Naylor AJ. The role of stromal cells in inflammatory bone loss. *Clin Exp Immunol*. (2017) 189:1–11. doi: 10.1111/cei.12979
100. Banuelos J, Lu NZ. A gradient of glucocorticoid sensitivity among helper T cell cytokines. *Cytokine Growth Factor Rev*. (2016) 31:27–35. doi: 10.1016/j.cytogfr.2016.05.002
101. Xie Y, Zhang LC, Xiong Q, Gao YP, Ge W, Tang PF. Bench-to-bedside strategies for osteoporotic fracture: from osteoimmunology to mechanosensation. *Bone Res*. (2019) 7:259–71. doi: 10.1038/s41413-019-0066-7
102. Dar HY, Singh A, Shukla P, Anupam R, Mondal RK, Mishra PK, et al. High dietary salt intake correlates with modulated Th17-Treg cell balance resulting in enhanced bone loss and impaired bone-microarchitecture in male mice. *Sci Rep*. (2018) 8:2503. doi: 10.1038/s41598-018-20896-y
103. Kennel KA, Drake MT. Adverse effects of bisphosphonates: implications for osteoporosis management. *Mayo Clin Proc*. (2009) 84:632–8. doi: 10.1016/S0025-6196(11)60752-0
104. Sharma D, Singh J. Synthesis and characterization of fatty acid grafted chitosan polymer and their nanomicelles for non-viral gene delivery applications. *Bioconj Chem*. (2017) 28:2772–83. doi: 10.1021/acs.bioconjchem.7b00505
105. Bone H, Brandi M, Brown J, Chapurlat R, Cummings S, Czerwinski E, et al. 10 years of denosumab treatment in postmenopausal women with osteoporosis: results from the phase 3 randomised FREEDOM trial and open-label extension. *Lancet Diabetes Endocrinol*. (2017) 5:513–23. doi: 10.1016/S2213-8587(17)30138-9
106. Juji T, Hertz M, Aoki K, Horie D, Ohya K, Gautam A, et al. A novel therapeutic vaccine approach, targeting RANKL, prevents bone destruction in bone related disorders. *J Bone Miner Metabol*. (2002) 20:266–8. doi: 10.1007/s007740200038
107. Zaheer S, LeBoff M, Lewiecki EM. Denosumab for the treatment of osteoporosis. *Expert Opin Drug Metab Toxicol*. (2015) 11:461–70. doi: 10.1517/17425255.2015.1000860
108. Li F, Li H, Zhai Q, Li FY, Wu TL, Sha X, et al. A new vaccine targeting RANKL, prepared by incorporation of an unnatural amino acid into RANKL, prevents OVX-induced bone loss in mice. *Biochem Biophys Res Commun*. (2018) 499:648–54. doi: 10.1016/j.bbrc.2018.03.205
109. Curate F. Osteoporosis and paleopathology: a review. *J Anthropol Sci*. (2014) 92:119–46.
110. Yang YH, Li B, Zheng XF, Chen JW, Chen K, Jiang SD, et al. Oxidative damage to osteoblasts can be alleviated by early autophagy through the endoplasmic reticulum stress pathway-implications for the treatment of osteoporosis. *Free Radic Biol Med*. (2014) 77:10–20. doi: 10.1016/j.freeradbiomed.2014.08.028
111. Chawalitpong S, Chokchaisiri R, Suksamrarn A, Katayama S, Mitani T, Nakamura T. Cyperenoic acid suppresses osteoclast differentiation and delays bone loss in a senile osteoporosis mouse model by inhibiting non-canonical NF- κ B pathway. *Sci Rep*. (2018) 8:5625. doi: 10.1038/s41598-018-23912-3
112. Xi YH, Jiang TW, Yu JM, Xue MT, Xu N, Wen JK, et al. Preliminary studies on the anti-osteoporosis activity of Baohuoside I. *Biomed Pharmacother*. (2019) 115:108850. doi: 10.1016/j.biopha.2019.108850

Conflict of Interest: The authors declare that the research was conducted in the absence of any commercial or financial relationships that could be construed as a potential conflict of interest.

Copyright © 2020 Zhang, Dang, Huai and Qian. This is an open-access article distributed under the terms of the Creative Commons Attribution License (CC BY). The use, distribution or reproduction in other forums is permitted, provided the original author(s) and the copyright owner(s) are credited and that the original publication in this journal is cited, in accordance with accepted academic practice. No use, distribution or reproduction is permitted which does not comply with these terms.



Osteocytic FGF23 and Its Kidney Function

Rafiou Agoro¹, Pu Ni¹, Megan L. Noonan¹ and Kenneth E. White^{1,2*}

¹ Department of Medical and Molecular Genetics, Indiana University School of Medicine, Indianapolis, IN, United States,

² Medicine/Division of Nephrology, Indiana University School of Medicine, Indianapolis, IN, United States

Osteocytes, which represent up to 95% of adult skeletal cells, are deeply embedded in bone. These cells exhibit important interactive abilities with other bone cells such as osteoblasts and osteoclasts to control skeletal formation and resorption. Beyond this local role, osteocytes can also influence the function of distant organs due to the presence of their sophisticated lacunocanalicular system, which connects osteocyte dendrites directly to the vasculature. Through these networks, osteocytes sense changes in circulating metabolites and respond by producing endocrine factors to control homeostasis. One critical function of osteocytes is to respond to increased blood phosphate and 1,25(OH)₂ vitamin D (1,25D) by producing fibroblast growth factor-23 (FGF23). FGF23 acts on the kidneys through partner fibroblast growth factor receptors (FGFRs) and the co-receptor Klotho to promote phosphaturia *via* a downregulation of phosphate transporters, as well as the control of vitamin D metabolizing enzymes to reduce blood 1,25D. In the first part of this review, we will explore the signals involved in the positive and negative regulation of FGF23 in osteocytes. In the second portion, we will bridge bone responses with the review of current knowledge on FGF23 endocrine functions in the kidneys.

OPEN ACCESS

Edited by:

Lilian Irene Plotkin,
School of Medicine, Indiana University
Bloomington, United States

Reviewed by:

Paola Divieti Pajevic,
Boston University, United States
Jan Josef Stepan,
Charles University, Czechia

*Correspondence:

Kenneth E. White
kenewhit@iu.edu

Specialty section:

This article was submitted to
Bone Research,
a section of the journal
Frontiers in Endocrinology

Received: 15 June 2020

Accepted: 20 July 2020

Published: 28 August 2020

Citation:

Agoro R, Ni P, Noonan ML and
White KE (2020) Osteocytic FGF23
and Its Kidney Function.
Front. Endocrinol. 11:592.
doi: 10.3389/fendo.2020.00592

Keywords: osteocyte, FGF23, FGF23 signaling, Klotho, kidney

INTRODUCTION

The mammalian skeleton is formed by several types of bone which interconnect to provide structural support for the body. In adult humans, the reference value for the skeleton weight is 10.5 kg (1, 2) representing up to 15% of the average body weight. Bone mass is dynamically regulated during a lifetime, and subjected to changes with uncontrollable parameters such as age, gender, genetics, and ethnicity; as well as controllable factors such as lifestyle behaviors including physical activity levels, smoking and alcohol consumption patterns, and diet (3, 4). Beyond its important role to enable mobility and provide needed support and structure to the body, bone represents an important reservoir of several minerals including phosphate and calcium, both of which are required for proper mineral metabolism and cellular functions (5).

Bone is a mineralized connective tissue formed with three primary cell types that direct intrinsic skeletal properties: osteoclasts, which resorb mineralized bone; osteoblasts, which form the bone matrix; and osteocytes, which are considered terminally differentiated osteoblasts (6, 7). Although morphologically and functionally distinct in the bone, osteoclasts, osteoblasts, and osteocytes are interdependent and produce growth factors to support each other's functions as well as responding in a coordinated manner to metabolic demands, physical stimuli, and structural duties (8). The three main bone cells are derived from two distinct lineages; osteoblasts and osteocytes derive from

pluripotent mesenchymal stem cells and share the same progenitors as fibroblasts and adipocytes (9, 10), whereas osteoclasts are derived from hematopoietic progenitors in the monocyte and macrophage lineage (11–13).

The osteocytes, which represent the majority of adult skeletal cells, are deeply embedded with abilities to communicate locally with osteoblasts and osteoclasts. This function is necessary to control skeletal formation as orchestrated by osteoblasts, and bone resorption dictated by osteoclasts, as well as controlling the physiological function of distant organs such as the kidney. Taking advantage of its dendrites, which connect to the vasculature and give these atypical cells direct access to the circulation, the osteocyte can send and receive signals with the vascularized organs. Among the important osteocyte-secreted factors is fibroblast growth factor-23 (FGF23). Once produced and secreted by osteocytes, this hormone preferentially acts on kidney and parathyroid glands to regulate phosphate and vitamin D homeostasis. FGF23 activity mainly occurs through the binding of FGF23 to FGF receptor (likely FGFR1), which requires the presence of its membrane and/or soluble co-receptor Klotho for a potent FGF23-induced downstream signaling cascade (14). In this review, the stimulative and repressive regulatory mechanisms involved in FGF23 production and processing in osteocytes will be discussed. We will also bridge the control of FGF23 in osteocytes with highlighting the key signaling pathways involved in phosphate, 1,25D, calcium, and sodium metabolism induced by FGF23 in the kidneys.

THE OSTEOCYTE: A CRITICAL BONE AND ENDOCRINE CELL

As the most prevalent cell in bone, osteocytes have important roles both within, and outside the skeleton. The osteocytes are considered as major orchestrators of skeletal activity; these cells can sense and integrate mechanical and chemical stimuli from the microenvironment with the goal to properly regulate bone formation and resorption. Osteocytes derive from mature and matrix-producing terminally differentiated osteoblasts (6). During their last phase of differentiation, mature osteoblasts become embedded in the matrix and generate cellular extensions, which are future osteocyte dendrites. To establish a sophisticated and complex network called the lacunocanalicular system, the dendrites of the newly formed osteocytes are fastened with the dendrites of existing osteocytes through a multitude of canaliculi (15). Even after the terminal differentiation of mature osteoblasts to generate osteocytes, the latter remain active in contributing to bone remodeling. For instance, osteocytes produce sclerostin (SOST), which binds to low-density lipoprotein receptor-related protein (Lrp)5/6, and neutralizes the anabolic Wnt/beta-catenin pathway (16, 17), thus negatively regulating bone formation. Osteocytes also produce the receptor activator of nuclear factor- κ B ligand (RANKL) which stimulates osteoclastogenesis, thus promoting bone resorption (18, 19).

In bone, osteocytes are bathed in canalicular fluid that delivers and exchanges nutrients, circulating factors, mechanical signals, and oxygen between the circulation and the “fixed and

embedded” osteocytes (20). During the last decade, the osteocyte lacunocanalicular network has gained tremendous attention because of accumulating and convincing evidence describing osteocytes as a major endocrine cell, and its role in the production of critical hormones targeting several organs. One of the most important osteocyte-secreted factors is FGF23. This hormone was first characterized as a mammalian “phosphatonin” by identifying stabilizing mutations in the *FGF23* gene in patients with autosomal dominant hypophosphatemic rickets (ADHR), a renal phosphate wasting disorder (21).

FGF23 PRODUCTION AND CLEAVAGE IN OSTEOCYTES

FGF23 is a phosphaturic hormone derived and secreted primarily by bone osteocytes. Mature, bioactive FGF23 is physiologically designed to target the kidney to regulate phosphate and vitamin D homeostasis; and, in a feedback mechanism to control bone mineralization and FGF23 production (22, 23). The mechanisms of FGF23 regulation in osteocytes are not fully understood. Several breakthroughs have been made that greatly improved our knowledge on the mechanisms of osteocytic FGF23 upregulation or downregulation through differential signaling pathways, as well as the pathophysiological response to multiple stimuli. In addition to several mechanisms involved in the transcriptional regulation of FGF23, another layer of FGF23 regulation in bone is the ability of the mature protein to be proteolytically cleaved within osteocytes to generate inactive FGF23 fragments before its secretion into the bloodstream (24).

Regulation of Osteocytic FGF23 by Phosphate, FGF23, FGFR Activation, and Klotho

Circulating levels of phosphate control FGF23 production in mammals (25, 26). Although the mechanisms of FGF23 regulation by phosphate are not fully understood, recent studies have implicated the type III sodium phosphate co-transporter PiT2 (Slc20a2) as being required for mediating phosphate-dependent FGF23 production (27). Indeed, *in vivo* studies using dietary protocols in PiT2 knock out mice showed that the deletion of PiT2 results in “inappropriately” normal intact, bioactive FGF23 in the circulation in response to high or low phosphate diet, which should normally increase or decrease FGF23, respectively (27). Using an *ex vivo* system of cultured long bone shafts, parallel studies showed that the PiT2 KO bone shafts failed to undergo Pi-induced FGF23 production, illustrating that PiT2 could be required for FGF23 induction in mouse bone (27). These new findings provided interesting insight underlying the phosphate-dependent regulation of FGF23 secretion, perhaps *via* PiT2 regulating phosphate uptake in osteocytes (27) (**Figure 1**).

In another study, using proteomic analysis to identify potential upstream sensors in response to elevated phosphate through dietary intervention, the FGFR1 isoform FGFR1c was shown to be activated through the phosphorylation of FGFR substrate 2 α (FRS2 α , on tyrosine 196) under high phosphate conditions, but in the absence of an FGF ligand. These

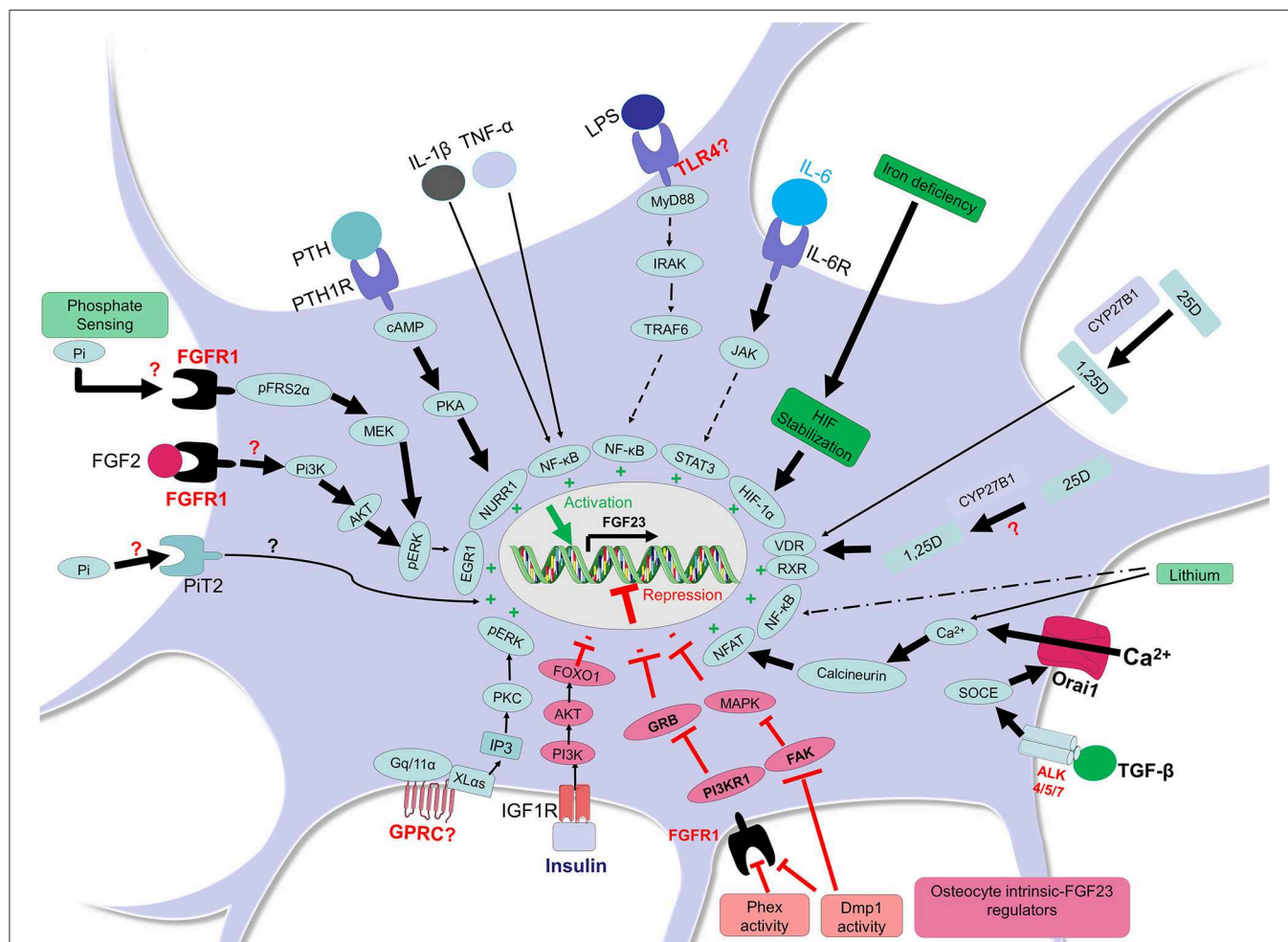


FIGURE 1 | FGF23 regulation in osteocytes. In osteocytes, FGF23 is positively regulated by different factors and pathways (shown in green). In presence of high phosphate, the receptor FGFR1 may sense this condition and the adaptor FRS2 α is phosphorylated thus activating FGFR1 and the MEK/pERK/EGR1 pathway leading to FGF23 transcription. It is also possible that the transporter Pit2 senses phosphate increases in osteocyte and responds by inducing FGF23. The activation of FGFR1 by other FGFs such as FGF2 may induce PI3K/AKT/pERK/EGR1 leading to FGF23 upregulation. The activation of PTH1R by PTH induces cAMP/PKA and the transcription factor NURR1 leading to FGF23 induction. Inflammatory conditions are potent FGF23 inducers; lipopolysaccharide (LPS) may bind to osteocyte toll like receptor 4 (TLR4) and induce MyD88/IRAK/TRAF6/NF- κ B to trigger FGF23 transcription (or may act through anemia/hypoxia). The binding of IL-6 to IL-6R in osteocytes may induce JAK/STAT3 and subsequent FGF23 expression. The cytokines IL-1 β and TNF- α can induce NF- κ B in osteocytes leading to FGF23 transcription. In the condition of iron deficiency, HIF protein is stabilized, an important mechanism involved in FGF23 upregulation. The active form of vitamin D (1,25-dihydroxyvitamin D; 1,25D), which results from the conversion of 25-hydroxyvitamin D (25D) inside or outside the osteocyte, could promote the formation of the complex 1,25D-VDR-RXR which binds the vitamin D receptor element (VDRE, not shown here) and induces FGF23 transcription. The signaling through the TGF- β -Activin Receptors ALK4/5/7 promotes calcium entry in cell through Orai1 and this process activates calcineurin and NFAT and their binding, which induces FGF23. Lithium-induced increased intracellular calcium could also increase FGF23 in osteocytes through calcineurin and NFAT activity. An activation of a yet unknown GPCR could trigger FGF23 transcription through XL α s or Gq/11 α and inositol 1,4,5-trisphosphate (IP3) which may activate PKC and stimulate the MAPK pathway. FGF23 can be negatively regulated by other elements and pathways (shown in red). For instance, insulin can bind to IGF1R and induce PI3K/AKT/FOXO1 pathway which represses FGF23. Phex and Dmp1 activities in osteocytes may control FGFR1/PI3KR1/GRB and cell differentiation to restrain FGF23 production. Dmp1 activity may also neutralize the FAK/MAPK pathway restricting FGF23 expression.

studies were consistent with the idea that phosphate-sensing mechanisms could control FGF23 production in osteocytes through ligand-independent FGFR1 activation (28, 29). These data suggested that high Pi diet-induced serum FGF23 increases in mice may be mediated by the phosphorylation of FGFR1, a potential “phosphate receptor” upstream of FGF23, which induced the mitogen activated protein kinase (MAPK) and extracellular signal-regulated kinase (ERK) pathways to control

FGF23 synthesis (28). Structural and crystallographic studies may be required to understand how an ion can activate an FGFR, as well as whether Pit2 is involved in this regulation (Figure 1).

Additionally, *in vivo* studies have reported that conditional deletion of FGFR1 specifically from the osteocytes of *Hyp* mice, a mouse model of X-linked hypophosphatemia (XLH) that exhibits elevated FGF23 production, improves the rickets and osteomalacia phenotype of these mice in association

with a decrease in both FGF23 bone mRNA and circulating protein. These mice also undergo an alleviation of their hypophosphatemic status, as well as an increase of plasma 1,25D levels (30). Furthermore, promoter studies identified that the activation of FGFR1 signaling through FGF2 is dependent on the PI3K-AKT pathway in the MC3T3-E1 osteoblastic cell line, providing evidence that *Fgf23* gene promoter activity is induced by FGFR1 activation (30). In addition to genetic interventions, pharmacologic-based studies have shown that activation of FGFR1 induces FGF23 production and leads to hypophosphatemia, whereas the inhibition of FGFR signaling attenuates FGF23 production (31) (**Figure 1**).

Another study by Hori et al. investigated whether phosphate could induce reactive oxygen species (ROS) *in vitro*, leading to increased FGF23 expression. Using the osteoblastic cell line UMR-106, these investigators showed that elevated phosphate in the culture media enhances the production of ROS, and that hydrogen peroxide further boosts FGF23 production in a dose-dependent manner, an effect which can be neutralized by an inhibitor of NADPH oxidase (32). These discoveries suggested that *in vitro* phosphate directly enhanced *FGF23* transcription by stimulating NADPH-induced ROS production and the MEK-ERK pathway. How this translates to the signaling in the osteocyte *in vivo* will be an interesting facet to this potential regulatory network.

Circulating FGF23 is markedly elevated during chronic kidney disease (CKD), and this is associated with poor long-term outcomes. By investigating the regulation of FGF23 through FGFR1, Hassan et al. demonstrated that the activation of FGFR1 is essential for the high levels of FGF23 observed during both acute and chronic uremia in mice and rats (33). In addition, in mice treated with the receptor FGFR1 inhibitor PD173074 by oral gavage followed with an acute kidney injury induction using folic acid, the prevailing increased FGF23 was reduced by 50% in calvaria and led to a complete prevention of the circulating intact FGF23 rises (33). In a more prolonged uremic condition using a diet with adenine plus high-phosphorus for 14 days to induce CKD, which resulted in high levels of *Fgf23* mRNA and serum FGF23 in rats, an oral gavage intervention with PD173074 given during the last 2 days of treatment reduced FGF23 induction by 75% in calvaria and completely normalized circulating FGF23 (33). Therefore, the FGFRs may play an important role in osteocyte-bloodstream communication to control FGF23 production.

As mentioned above, FGF23 signals *via* the interaction with its receptor FGFR1c and its specific co-receptor Klotho (14, 34). A recent investigation has shown that Klotho could be detected in osteocytes (35) suggesting that FGF23 may be one of the ligands that activates FGFR1 in osteocytes, thereby regulating the *FGF23* gene transcription in a positive feedback loop. The expression of Klotho in osteocytes has been suggested to contribute to bone formation and bone volume increases coupled with enhanced osteoblast activity (35). Although Klotho has been detected in bone (35), the kidney, parathyroid glands and brain remain the primary organs with abundant expression of Klotho to the best of our current knowledge (36–38). However, it is possible that in response to pathological circumstances, bone cells

could enhance Klotho expression, thus modulating bone FGFR1 signaling via FGF23.

Through proteolytic cleavage of the membrane-bound klotho (mKL) (39–42), a soluble form of Klotho (sKL) can be liberated into the circulation (43, 44). Soluble Klotho has been described to have a direct role to regulate Wnt and MAPK pathways in osteoblastic UMR-106 cells in concert with the presence of FGF23 (45). Indeed, *in vitro* studies showed that a co-treatment of UMR-106 cells with FGF23 and soluble Klotho activated MAPK signaling, leading to an increase of Dickkopf-1 (DKK1) protein, a soluble inhibitor of Wnt/beta-catenin signaling (45). The induction of Dkk1 through FGF23/FGFR/sKL was shown to be dependent upon the MAPK pathway since the inhibition of this pathway using the MEK inhibitor U0126 completely abrogated p-ERK/ERK induction and abolished downstream Dkk1 expression (45). The binding of the secreted Dkk1 to the receptors Frizzled (Fz) and Lrp5/6 thus promoted the phosphorylation of β -catenin and inactivated the Wnt pathway in osteoblasts (45). Other studies have shown that a treatment of UMR-106 cells with soluble Klotho and FGF23 dose-dependently increased MAPK and *Egr1* mRNA responses, an effect which was FGFR- and MEK-dependent, and led to FGF23 upregulation (46). Future studies are needed to confirm potential expression of Klotho in osteocytes and under some circumstances whether FGF23 binding to FGFR1-Klotho complex in osteocytes could induce FGF23 expression.

Signals Involved in the Positive Regulation of FGF23 by Inflammation and Iron

Inflammation is a complex phenomenon involving multiple immune and non-immune cells which cooperate to respond to endogenous and exogenous events by secreting specific pro-inflammatory and/or anti-inflammatory factors. Pro-inflammatory stimuli such as the cytokines tumor necrosis factor alpha (TNF α), interleukin 1 β (IL-1 β), the tumor necrosis factor-like weak inducer of apoptosis (TWEAK), and the bacterial component lipopolysaccharide (LPS) have all been shown to dose-dependently upregulate FGF23 in the osteocyte-like cell line IDG-SW3 (47). Particularly, TNF and IL-1 β induce FGF23 expression *via* nuclear factor kappa-light-chain-enhancer of activated B cells (NF- κ B) (47), a major transcription factor complex involved in the control of cytokines and in the mediation of multiple pro-inflammatory cellular responses. The serine/threonine kinase p38 mitogen-activated protein kinase (p38MAPK), which is activated by several cellular stress stimuli and involved in the transcriptional activity of NF- κ B, is another positive regulator of FGF23 in bone cells (48). Other investigations have shown that the serine/threonine kinase protein kinase C (PKC), which drives FGF23 expression in response to phorbol ester 12-O-tetradecanoylphorbol-13-acetate (PMA), can be suppressed by 75% in the presence of the PKC α / β inhibitor Go6976. These studies suggested that PKC is a positive regulator of FGF23 synthesis in IDG-SW3 osteocytic cells *via* NF- κ B (49). Furthermore, Notch signaling, which can be mediated by pro-inflammatory cytokines such as TNF- α (50), has been described by Tamamura et al., to positively regulate

FGF23 expression which colocalizes with Notch signaling downstream targets, Notch, and Hes1 in mouse osteocytes and UMR-106 osteoblastic cells (51). A study also identified a potential new pathway mediated by G protein-IP3/PKC events to control FGF23 production (52). It was shown that the ablation of the extra-large G α subunit (XL α s) or Gq/11 α in osteocyte-like Ocy454 cells activated IP3/PKC and stimulated the MAPK/ERK1/2 pathway leading to FGF23 induction (52). It is assumed that the trigger of the IP3/PKC/MAPK pathway is controlled by a G protein-coupled receptor which remains to be identified (**Figure 1**).

More recently, the use of CRISPR/Cas9 technology has helped to identify control regions for the *Fgf23* gene in response to various inflammatory stimuli in mice. An enhancer site – 16kb from the transcription start site of the murine *Fgf23* gene was deleted via CRISPR, and this study demonstrated that FGF23 expression in bone, bone marrow, spleen, liver, thymus, and intestine was attenuated in response to LPS injection. This deletion was also associated with decreased intact FGF23 compared to normal mice treated with LPS. Similar effects were observed in response to direct TNF- α and IL-1 β injections, highlighting the importance of this genomic region in mediating inflammation-induced FGF23 expression (53). Further studies showed that an additional proximal enhancer region in *Fgf23* mediates LPS-induced FGF23 expression *in vivo* through binding motifs to several known transcription factors that mediate inflammation, including NF- κ B (54).

Persistent iron deficiency in mice has been shown to induce a pro-inflammatory state (55) that induces a heightened inflammatory response to stimuli such as LPS (55, 56). Both iron deficiency and inflammation increase *FGF23* transcription by activating among other signaling pathways, Hif1 α , and associated MAPK signaling, in osteocytes (57, 58). Wild type mice fed an iron deficient diet for 8 and 12 weeks showed 5- and 10-fold increases of *Fgf23* transcripts, respectively, in femur/tibia samples (57). *In vitro*, treatment of UMR-106 cells with the iron chelator, deferroxamine (DFO) resulted in marked increases in *Fgf23* mRNA, partially dependent on MAPK activity in association with Hif1 α stabilization (57, 58) (**Figure 1**). These discoveries suggest that absolute iron deficiency, characterized by a depletion of both iron stores and circulating iron, promotes *FGF23* transcription through Hif1 α . Similarly, a functional iron deficiency *via* a treatment of mice with hepcidin also increased bone *Fgf23* mRNA expression (58).

The cytokine IL-6, a known marker of inflammatory states has also been shown to contribute to FGF23 production. In a mouse model of folic acid-induced acute kidney injury, bone *Fgf23* mRNA expression increased together with serum FGF23 as well as several circulating cytokines including IL-6 (33). When fed with an adenine diet to induce CKD, IL-6 knock-out mice failed to increase bone *Fgf23* mRNA, resulting in an attenuation of circulating FGF23 levels in comparison to wild-type mice with CKD; these data suggest a direct contribution of IL-6 to the increased FGF23 observed during CKD (59). Further, *ex vivo* and *in vitro* studies have shown that a treatment of calvaria organ cultures and UMR-106 cells with the IL-6/soluble IL-6 receptor fusion protein induced STAT3 phosphorylation, and increased

Fgf23 promoter activity, suggesting a direct effect of IL-6 on the positive regulation of FGF23 expression (59).

Hypoxia and Erythropoietin as Positive Regulators of FGF23

Hypoxia inducible factors (HIFs) are constitutively expressed transcription factors that are critical for sensing oxygen and iron levels in the body. Oxygen and iron are important co-factors for the function of HIF-prolyl hydroxylase domain enzymes (HIF-PHDs), which help maintain the constant turnover of HIFs by marking them for degradation. As stated above, it was shown that iron deficiency can drive FGF23 expression in a mouse model of autosomal dominant hypophosphatemic rickets (ADHR) (57). Wild type and ADHR mice (harboring the FGF23-R176Q stabilizing ADHR mutation) fed an iron-deficient diet had elevations in “total” serum FGF23 (intact bioactive FGF23 + proteolytic fragments), however only iron-deficient ADHR mice had increases in intact FGF23 due to their inability to cleave and inactivate the bioactive form of FGF23. This and subsequent studies helped tie together iron handling and phosphate homeostasis, a link that can likely be explained through HIF activity. An iron-deficient state leads to HIF stabilization due to the lack of iron as a co-factor for the HIF-PHDs to tag HIF for degradation. *In vitro* studies have shown HIF-mediated induction of FGF23 mRNA expression in two different osteoblast cell lines, as well as evidence of HIF binding to the FGF23 promoter (60). More recently, a prospective study in ADHR patients that co-presented with an iron deficiency phenotype demonstrated that iron repletion in these patients reduced their circulating levels of FGF23 and normalized serum phosphate levels. Thus, providing oral iron is a novel therapeutic approach to this disease (61). This finding was supported by studies in iron-deficient women showing that rescue of iron deficiency using iron dextran lowered the prevailing elevated FGF23 (62). It is important to note the type of intravenous iron used, as it has been well-documented that certain types of iron formulations, especially those with carboxymaltose backbones can cause hypophosphatemia due to elevating intact FGF23 (63), potentially through altering FGF23 intracellular proteolysis (see below).

Erythropoietin (EPO) is a hormone made in the kidney that induces new red blood cell production in the bone marrow in response to anemia or blood loss. Recombinant human EPO (rhEPO) is currently used as a therapy to treat anemia related to CKD. Recently, several studies revealed that this hormone can induce FGF23 expression (64–66). WT mice given acute rhEPO treatment after 6 h or after 3–4 days of consecutive injections resulted in elevated total and intact FGF23 and bone marrow *Fgf23* mRNA expression (64). To understand the effects of chronically elevated EPO, reports using the transgenic Tg6 mouse model of EPO overexpression showed that these mice have basal elevations in total and intact FGF23 (65, 67). Chronic overexpression of EPO can lead to iron deficiency, so to determine whether the iron deficiency was causing the elevated FGF23, mice were given iron dextran. This only modestly decreased intact FGF23, showing that EPO was primarily driving

FGF23 expression (65). In healthy human subjects, total FGF23 was elevated 24 h after a single rhEPO dose with no changes in intact FGF23 (66). In another study, a small population of anemic patients with normal kidney function were given a single dose of rhEPO. This increased total and intact FGF23 over the span of 12–18 h after the injection (64). Few *in vivo* studies have examined the effect of curing anemia of CKD on mineral metabolism. Most recently, a single rhEPO injection in CKD mice did increase total serum FGF23 after 6 and 24 h but had no effect on intact FGF23 (65).

To mitigate potential adverse effects of high rhEPO treatment, new strategies are leveraging the HIF system by creating inhibitors of the HIF prolyl hydroxylases (HIF-PHDs) called HIF-PHDs inhibitors (HIF-PHI). These therapeutics have become increasingly important for anemic patients with CKD, where they promote endogenous EPO production by stabilizing HIFs. This class of drug also reduce hepcidin levels to increase iron utilization in tissues thereby creating a synergistic effect in providing iron availability to newly forming red blood cells (68). Recent studies have shown in normal mice that several HIF-PHIs can regulate *Fgf23* expression. For instance, FG-4592 (Roxadustat) was shown to increase bone *Fgf23* mRNA and circulating intact FGF23 (58, 66). Elevations in total and intact FGF23 were observed in WT mice treated with the HIF-PHI BAY 85-3934 (Molidustat) after 6 h that returned to baseline by 24 h. This study showed that elevated EPO precedes increases in FGF23 in response to HIF-PHI BAY85-3934, suggesting that the cause for elevated FGF23 in response to this treatment was due to elevated EPO. This was confirmed by treating HIF-PHI mice with an EPO-neutralizing antibody, which completely attenuated the increased serum total FGF23 (69). A recent paper, however, showed that EPO and HIF-PHI treatment of anemic mice with CKD resulted in suppressed FGF23. This study suggested that under conditions of anemia, as opposed to mice with normal iron homeostasis, rescuing iron utilization during CKD may be a more potent suppressor of FGF23 than EPO and HIF-PHIs are stimulators (70). Although EPO and HIF-PHI can induce FGF23, further studies are required to delineate the mechanisms directing these components on osteocytic FGF23 production.

Signals Involved in the Transcriptional Regulation of FGF23 by PTH

Parathyroid hormone (PTH) is a hormone secreted by the parathyroid glands that regulates calcium utilization through its effects on bone, kidney, and intestine (71–73). During CKD, a secondary hyperparathyroidism occurs in which PTH is excessively secreted, in response to factors such as hyperphosphatemia, hypocalcemia, and low 1,25D levels, to potentially promote elevated FGF23 (74). Using bioinformatics and chromatin immunoprecipitation assays, studies have reported that *Nurr1* is an essential transcription factor involved in FGF23 upregulation in response to PTH in UMR-106 cells. Furthermore, in a mouse model of CKD, the administration of a calcimimetic, which is known to activate the calcium-sensing receptor in different tissues (75) with the goal to attenuate PTH levels and actions, reduced FGF23 concentrations as well as bone

Nurr1 mRNA and protein levels (76). To test the relationships between PTH and FGF23, a mouse model with constitutive activation of PTH receptor (PTHr) signaling in osteocytes was used by Rhee et al. in a report that showed that PTHr activation increased FGF23 expression *in vivo* and *in vitro* through cAMP and Wnt-dependent mechanisms (77). In addition, Knab et al. showed that PTH-induced increases in FGF23 expression were PKA-dependent in osteocyte-like cells, suggesting that FGF23 production is regulated by the cAMP/PKA/*Nurr1* pathway in response to PTH (78) (Figure 1).

Signals Involved in the Positive Regulation of FGF23 by TGF- β , Calcineurin, and NFAT

TGF- β has been reported to regulate the extracellular matrix by activating ROS, which increases calcium influx and activates calcineurin (79–81). Using UMR-106 cells, TGF- β 2 has been described to enhance store-operated Ca^{2+} entry (SOCE) and induce the stimulation of FGF23, an effect significantly attenuated by both the inhibitor of TGF- β type I receptor activin receptor-like kinases (ALK5, ALK4, and ALK7) SB431542 and SOCE inhibitor 2-APB (82). Recent investigation has shown that the synthesis of FGF23 in UMR-106 cells can be induced by SOCE through *Orai1* (83). In addition, the Ca^{2+} entry activates the phosphatase calcineurin, which dephosphorylates nuclear factor of activated T cells (NFAT) thereby stimulating its transcriptional activity and targeting the *Fgf23* gene. This suggested that FGF23 may be positively regulated by calcineurin-NFAT signaling (84). Further analyses confirmed that either the inhibition of calcineurin using cyclosporin A (CsA) and tacrolimus (FK-506) or the blocking of the interaction between calcineurin and NFAT using the inhibitor INCA-6 reduced the abundance of *Fgf23* transcripts as well as FGF23 protein (84). Additionally, lithium, a widely used drug for the treatment of mood disorders and known to modify Ca^{2+} signaling, stimulated the release of FGF23, partially through NF- κ B dependent up-regulation of *Orai1* transcription and SOCE in UMR-106 cells (85) (Figure 1).

Signals Involved in the Positive Transcriptional Regulation of FGF23 by Calcitriol

Early FGF23 physiological studies demonstrated that the administration of 1,25D dose-dependently increased both serum FGF23 as well as serum inorganic phosphorus in normal rats (25). In wild type mice with normal renal function, injection of calcitriol increased serum FGF23 levels 1-week post treatment by 15-fold. Calcidiol (25-hydroxyvitamin D), although with a lesser effect could also induce FGF23 in normal mice (86). In a mouse model of adenine diet-induced CKD, a 5 weeks-regimen induced a 40-fold increase of circulating FGF23. However, in the background of a global deletion of *Cyp27b1*, the gene encoding the enzyme vitamin D 1- α -hydroxylase involved in the formation of calcitriol (1(OH)ase^{-/-} mice), only a 2-fold circulating FGF23 was observed with this treatment, suggesting a contribution of calcitriol to the increased FGF23. At the bone compartment level, a specific deletion of *Cyp27b1* in osteoblasts reduced FGF23

induction in long bones from 58-fold in normal mice treated with a 5-weeks adenine diet to a 10-fold induction, suggesting a potential role of a local osteoblastic vitamin D conversion process in the induction of bone FGF23. This attenuation of increased FGF23 was independent of a potential reduction in PTH levels since plasma PTH remained elevated in response to the adenine diet-induced CKD in the mice with global deletion of *Cyp27b1*, as well as those with osteoblast-specific deletion of *Cyp27b1* (86) (Figure 1).

NEGATIVE REGULATORS OF FGF23

Dentin Matrix Acidic Phosphoprotein 1 and Phosphate-Regulating Gene With Homologies to Endopeptidases on the X Chromosome

The disease XLH is characterized by hypophosphatemia and impaired mineralization caused by mutations of the *phosphate-regulating gene with homologies to endopeptidases on the X chromosome* (PHEX). Loss of PHEX leads to the overproduction of FGF23 in osteocytes, causing hypophosphatemia with bone mineralization impairment, and thus bone fragility. Similar to XLH, recessive loss-of-function mutations in the dentin matrix protein-1 (DMP1) gene, a member of small integrin-binding ligand N-linked glycoprotein (SIBLING) proteins, is responsible for a human phosphate wasting and impaired bone mineralization disease termed autosomal recessive hypophosphatemic rickets type 1 (ARHR1). It was shown that a lack of DMP1 in both humans and mice markedly increased FGF23 expression in bone (87).

To gain insight into the mechanisms by which PHEX mutations upregulate FGF23 expression, studies have been designed to investigate the local effects in bone from a mouse model of XLH (Hyp mice) in a normal hormonal environment in comparison to the function of wild type bone in the abnormal metabolic environment of Hyp mice. Using a surgical procedure to perform intramuscular bone cross-transplantations between wild-type and Hyp mice, a study found that increased FGF23 expression in Hyp bone results from intrinsic PHEX deficiency from bone, since FGF23 was increased in Hyp osteocytes before and after explantation into WT mice but was not increased in WT osteocytes after explantation into Hyp mice. This evidence suggested that the mechanisms whereby PHEX mutations lead to increased FGF23 expression in osteocytes is intrinsic to bone (88).

Similar to the phenotype resulting from PHEX inactivation, the inactivation of *Dmp1* in mice resulted in equivalent intrinsic bone mineralization defects associated with increased FGF23 expression in osteocytes (89–91). Using cortical bone isolated from 12-days old WT, Hyp, *Dmp1*^{−/−}, and Hyp/*Dmp1*^{−/−} mice to perform a genome-wide microarray analysis, the phosphatidylinositol 3-kinase regulatory α subunit (PIK3R1) and growth factor receptor-bound protein 2 (GRB2) pathways were identified as potential common signaling controlled by PHEX and DMP1 to regulate *FGF23* promoter activity through FGFs/FGFR in osteocytes (91, 92) (Figure 1). These findings

highlight that the activation of FGFRs which contribute to FGF23 production in osteocytes may be independent from the phosphate sensing pathways described above. Additionally, recent *in vivo* and *in vitro* studies suggested a direct negative regulation of DMP1 in FGF23 expression in osteocytes by activating FAK-mediated MAPK signaling, thus coordinating the extracellular environment of osteocytic lacunae as well as bone metabolism (93) (Figure 1). The creation of the floxed-Fgf23 mouse has recently emerged as a critical tool to understand FGF23 function *in vivo* (94). To this end, flox-Fgf23 mice were mated to the global eIIa-cre which mimicked the phenotype of the Fgf23-KO mouse. Fgf23 was also specifically deleted from either the osteoblast lineage using the Col2.3 promoter to drive Cre expression, or from late osteoblasts/osteocytes using the *Dmp1*-Cre. This resulted in ~50% reduction of iFGF23, with compromised ability to respond to changes in phosphate (94), demonstrating the specificity of osteoblast/osteocyte FGF23 production in response to metabolic changes.

Negative Regulation of FGF23 by Insulin and Insulin-Like Growth Factor 1

Recent studies reported insulin and insulin-like growth factor 1 (IGF1) as negative regulators of FGF23 production *in vitro* as well as in mice and humans (95). *In vitro*, insulin and IGF1 down-regulated FGF23 production by inhibiting the transcription factor forkhead box protein O1 (FOXO1) through phosphoinositide 3-kinase (PI3K)/protein kinase B (PKB)/Akt signaling in UMR-106 cells (95). *In vivo*, insulin deficiency resulted in an increase of serum FGF23 concentrations in mice, which was reversed by insulin administration. Interestingly, in women subjects, an increase in plasma insulin levels following an oral glucose administration correlated negatively with plasma FGF23 concentrations (95) (Figure 1).

FGF23 CLEAVAGE: A PHYSIOLOGICAL AND ENDOGENOUS MECHANISM TO ATTENUATE FGF23 BIOACTIVITY

FGF23 is synthesized as a 251-amino acid protein, primarily in osteocytes. The FGF23 signal peptide is represented by the first N-terminal 24 aa. The cleavage of the signal peptide results in a release of a mature peptide that can be secreted as the bioactive hormone, referred to as “intact” FGF23 (“iFGF23”). To control the bioactivity of iFGF23, the protein can be cleaved at the subtilisin-like proprotein convertase (SPC) site R₁₇₆HTR₁₇₉/S₁₈₀AE (RXXR/SAE motif) generating at least two fragments identified as an N-terminal fragment which is structurally similar to other FGF family members and a more unique C-terminal tail (21, 96). The proteolytic cleavage of excess iFGF23 represents a critical secondary regulatory mechanism to maintain stable serum iFGF23 and normal serum phosphate. The absence of this proteolytic activity in humans through the *FGF23* gene mutations R176Q, R176W, R179Q, and R179W are causative for autosomal dominant hypophosphatemic rickets (ADHR), characterized by elevated intact FGF23 and hypophosphatemia (21) (Figure 2). In mice

carrying the ADHR point mutation R176Q-Fgf23, in response to absolute iron deficiency using dietary intervention, the iFGF23 levels were elevated due to the stabilization of the bioactive FGF23 (57). This elevated iFGF23 condition in response to iron-deficient diet in ADHR mice caused similar phenotypes as observed in ADHR/XLH patients, such as alterations in genes controlling phosphate reabsorption and 1,25D production, and a hypophosphatemic bone disease (57). These findings suggested that iron status is a synergistic factor of the ADHR phenotype, and that ADHR is a disease of gene-environment interactions (57).

The cleavage of FGF23 is controlled by the serine endoprotease furin, a subtilisin-like convertase, at the site R₁₇₉/S₁₈₀ in response to several stimuli including PTH (78). Previous investigations have shown that an iron deficient state also promotes iFGF23 cleavage leading to increased secretion of FGF23 fragments but normal iFGF23 in WT mice (57, 58). In HeLa Cells, it was described that an iron deficient state induces furin upregulation *via* the stabilization of Hif1 α (97), a similar mechanism which occurs in osteocytes. Posttranslational modifications of iFGF23 can occur via the O-glycosylation of Thr₁₇₈ in the furin proprotein processing motif RHT₁₇₈R₁₇₉, which stabilized FGF23 (98) (**Figure 2**). This glycosylation process at Thr₁₇₈ is controlled by the enzymatic actions of N-acetylgalactosaminyltransferase 3 (GALNT3) which can be upregulated under high phosphate conditions potentially *via* the control of FGFR1c activation and the induction of the transcriptional activators early growth response 1 (EGR1) and ETS variant 5 (ETV5) (28).

In a recent study, Thr₁₇₈ was identified as a poor substrate site with limited glycosylation acceptance, likely a protective mechanism to prevent cellular resistances to FGF23 cleavage. Interestingly, Thr₁₇₈ glycosylation was shown to require a previous glycosylation at Thr₁₇₁ before generating a furin-resistant and secreted stable iFGF23 (99) (**Figure 2**). These new discoveries suggest that GALNT3 specificity for FGF23 and its ability to control circulating levels of bioactive FGF23 is a control point achieved by FGF23 being a rather poor substrate for this enzyme (99). In contrast to the O-glycosylation induced by GALNT3 which stabilizes FGF23, the phosphorylation at position S₁₈₀ by the kinase FAM20C inhibited O-glycosylation of FGF23, thus promoting FGF23 cleavage (98) (**Figure 2**). Indeed, recessive inactivating mutations in human FAM20C cause ARHR type 3 (ARHR3; Raines syndrome), consistent with its role as an FGF23 de-stabilizer (100, 101).

Besides furin which is thought to cleave FGF23 mainly intracellularly, the extracellular proteases of the plasminogen activation system, tissue-type PA (tPA), and urokinase-type PA (uPA), as well as plasmin may also display proteolytic activity on FGF23 protein at the RXXR motif (R₁₇₆), with potential additional cleavages at arginine residues R₁₁₄, R₁₄₀, R₁₄₃, R₁₆₀, R₁₉₆, and R₂₂₈ (102). Of note, Klotho knock out mice as well as mice with acute kidney injury, which both exhibit elevated levels of intact FGF23, also display elevated plasminogen activator inhibitor-1 (103, 104). Thus, the proteolysis of FGF23

by tPA, uPA, and plasmin may potentially regulate the levels of active FGF23 thus in part, controlling phosphate and mineral homeostasis.

These collective studies demonstrated that FGF23 protein cleavage is a dynamic process which can be adjusted after production at the cell level with phosphorylation and glycosylation dictating the levels of bioactive FGF23 depending upon the osteocyte cell state. Certainly, future studies are needed to understand the regulation of GALNT3, furin, FAM20C, and potentially the enzymes of the plasminogen activation system in the coordinated control of FGF23 production and bioactivity.

FGF23 RENAL SIGNAL TRANSDUCTION

In contrast to paracrine FGFs, such as FGF1 and FGF2, endocrine FGFs such as FGF23 lack the heparin-binding domain in their C-terminus, which enables escape from the osteocyte cell matrix after secretion and their actions on distant target organs including kidney (14, 105). FGF23 acts primarily on kidney to promote phosphaturia and parallel reductions in 1,25D (14, 34). The phosphaturic activity of FGF23 is critical in CKD, preventing and delaying hyperphosphatemia and vascular calcifications as FGF23 progressively rises with the loss of renal function (106). In a study among patients undergoing hemodialysis, high serum phosphate levels across a quartile of patients (>5.5 mg/dl) was associated with a 20% increase in the multivariable adjusted risk of death, as compared with normal levels (3.5–4.5 mg/dl) (107). These findings underscore the importance of controlling circulating phosphate in kidney disease patients. During CKD, as kidney function decreases with a progressive decrease of glomerular filtration rate (GFR), the kidney loses functioning nephrons decreasing the overall excretion capability of the kidney. The dramatic rise of FGF23 during CKD is likely to attempt to boost the excretory capacity of the existing nephrons to maintain normal serum phosphate levels. This is likely the primary reason why early stage CKD patients exhibit normal serum phosphate over much of the disease course [for review (108)].

FGF23 actions are likely mediated by FGF receptors FGFR1c, FGFR3c, and FGFR4 and the co-receptor Klotho, a single-pass transmembrane protein highly expressed in kidney (109–113). FGF23 binds to FGFR1c and the interaction between these two proteins with the co-receptor Klotho (which dramatically increases the binding affinity of the complex FGF23-FGFR-Klotho) triggers potent FGF23 signaling and activity (114). In kidney, FGF23 signaling on the basolateral side of proximal nephron cells causes the internalization of the sodium-dependent phosphate co-transporters NPT2A and NPT2C from the apical surface. These actions decrease phosphate reabsorption processes from the kidney (115) (**Figure 3**). A global genetic deletion of FGF23 in mice resulted in severe hyperphosphatemia, due to the absence of the FGF23-mediated phosphaturia mechanism (116). In addition, FGF23 signaling regulates vitamin D metabolism *via* the modulation of the vitamin D metabolic enzymes expression as well as regulating calcium and sodium reabsorption processes (**Figure 3**).

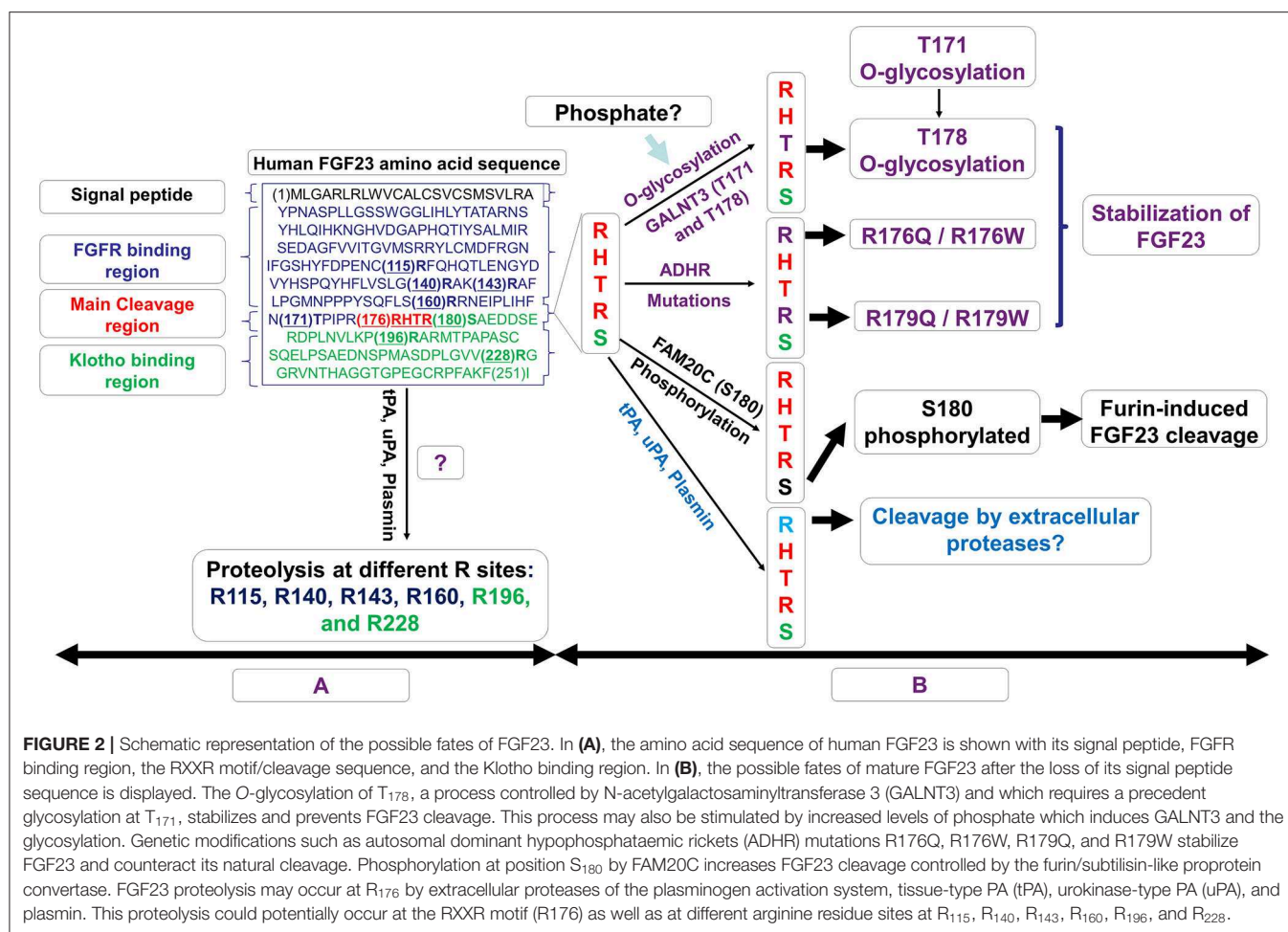


FIGURE 2 | Schematic representation of the possible fates of FGF23. In (A), the amino acid sequence of human FGF23 is shown with its signal peptide, FGFR binding region, the RXXR motif/cleavage sequence, and the Klotho binding region. In (B), the possible fates of mature FGF23 after the loss of its signal peptide sequence is displayed. The O-glycosylation of T178, a process controlled by N-acetylgalactosaminyltransferase 3 (GALNT3) and which requires a precedent glycosylation at T171, stabilizes and prevents FGF23 cleavage. This process may also be stimulated by increased levels of phosphate which induces GALNT3 and the glycosylation. Genetic modifications such as autosomal dominant hypophosphataemic rickets (ADHR) mutations R176Q, R176W, R179Q, and R179W stabilize FGF23 and counteract its natural cleavage. Phosphorylation at position S180 by FAM20C increases FGF23 cleavage controlled by the furin/subtilisin-like proprotein convertase. FGF23 proteolysis may occur at R176 by extracellular proteases of the plasminogen activation system, tissue-type PA (tPA), urokinase-type PA (uPA), and plasmin. This proteolysis could potentially occur at the RXXR motif (R176) as well as at different arginine residue sites at R115, R140, R143, R160, R196, and R228.

Unbiased Approaches to Understanding FGF23 Function in Kidney

Unbiased studies using large-scale microarray and gene expression approaches from FGF23 transgenic (FGF23 Tg) mice and WT littermates have identified several renal genes associated with increased FGF23. Particularly, genes involved in the phosphate reabsorption process such as Npt2a, Pdzk1 (a scaffolding protein known to interact with Npt2a) and Klotho, the co-receptor for FGF23 were among the genes which showed significantly decreased expression (117). The angiotensin I converting enzyme 2 (Ace2), known to decrease Angiotensin II with potential disruption of the renin-angiotensin system balance (118) was also decreased in FGF23 Tg kidney (117). It was later hypothesized that FGF23 induced the activation of FGFR1, leading to Ace2 reduction, causing hypertension (119). Other genes such as Atp1a2, which has been described to interact with Klotho and regulate calcium metabolism (120), was 2.5-fold-upregulated (117) and lipocalin 2, a neutrophil-derived marker previously described to be involved in CKD progression in mice and humans (121), was also modestly induced (117).

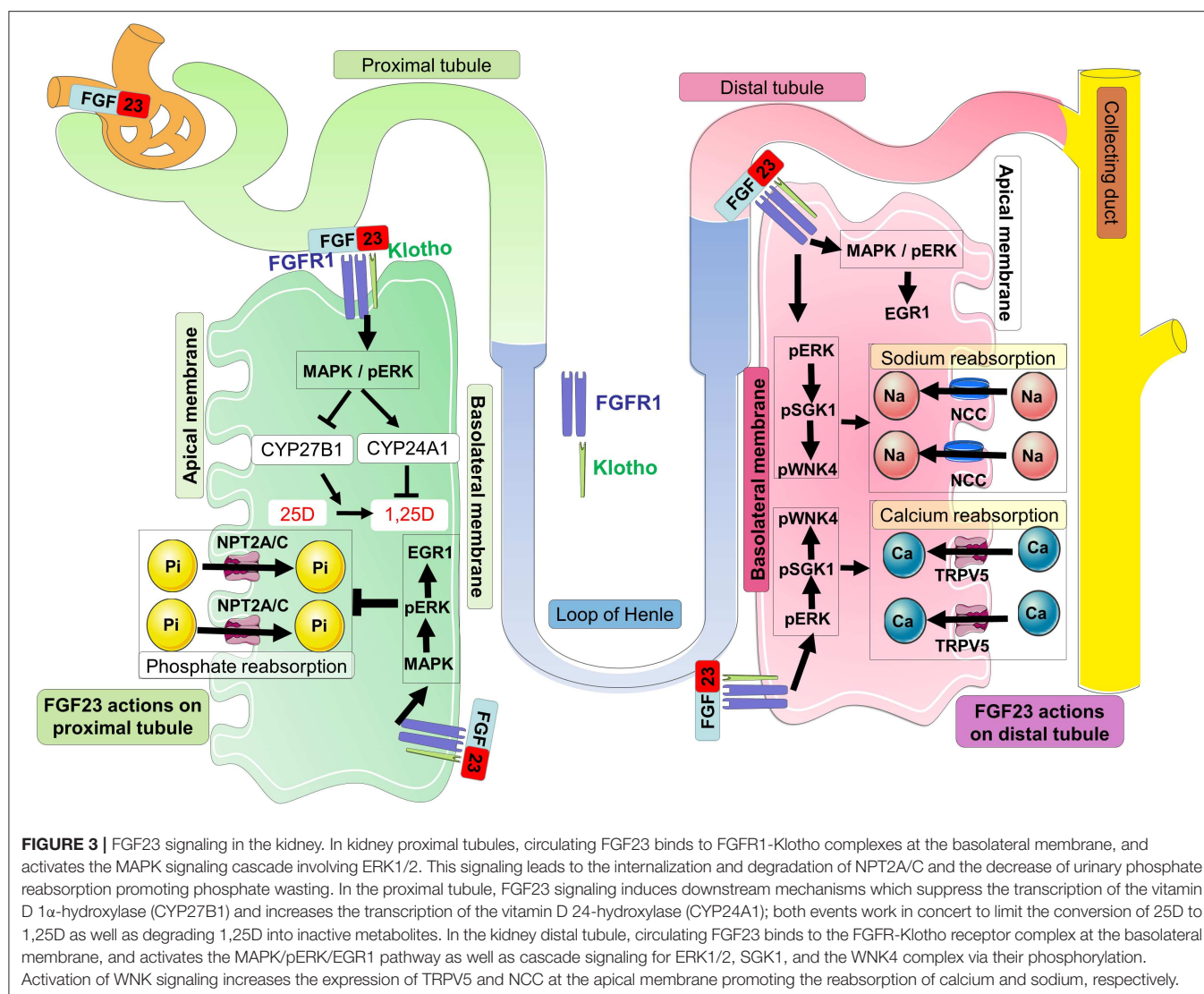
Other approaches using an acute 1-h FGF23 injection revealed that the MAPK related transcription factor Egr1 is typically the most up-regulated gene in microarray datasets testing FGF23

bioactivity. It was also determined that EGR1 binding near genes encoding Npt2a, Npt2c, as well as scaffold proteins (NHERF1-3, EZR and GABARAP), and trafficking proteins (megalin and vacuolar ATPase), known to putatively mediate NPT2A protein internalization and degradation, were increased after FGF23 injection. Collectively, these results suggested a coordinated regulation of renal Pi transport genes through EGR1 (122).

EGR1: An FGF23 Biomarker and Beyond

As mentioned above, it has been well-studied that FGF23 delivery induces EGR1, a transcription factor and downstream marker of MAPK signaling, in mice and cells (112, 123). It was shown in the Hyp mouse that MAPK/ERK1/2 signaling is activated in the kidney and this pathway induction drives EGR1 (112, 123). Other studies revealed that an inhibition of ERK1/2 signaling using a selective MEK inhibitor, PD0325901, was associated with a reduction of renal Egr1 upregulation induced by a Phex deletion. This led to improvement in the hypophosphatemia associated with decreased NPT2a protein expression, correction of 1,25D and calcium deficiency, with a reduction of cortical porosity (124, 125).

To further understand the contribution of Egr1 on FGF23-dependent regulation of renal Pi and vitamin D metabolism,



the *Egr1* knockout mouse (*Egr1*^{-/-}) has been studied with interesting findings. Reports showed that the effect of FGF23-induced decreases in renal *Npt2a* and *Npt2c* proteins is completely abrogated in *Egr1*^{-/-} mice (122). To potentially attenuate *Egr1* activity, FGF23 also upregulates two isoforms of *Nab2* which are known to be corepressors of *Egr1* (126); however whether this is a direct or an indirect mechanism through *Egr1*, which is known to induce *Nab2* thus establishing a negative feedback loop (127), remains to be investigated.

Physiological Role of Renal FGF23 Receptors

Four FGFR isoforms (FGFR 1-4) have been described in mammals and an alternative splicing of these isoforms can generate seven major FGFR proteins (FGFRs 1b, 1c, 2b, 2c, 3b, 3c, and 4) (105). FGFR1, FGFR3, and FGFR4 are the most expressed FGFRs in the mouse kidney with potential functional

roles in mineral homeostasis (128–130). In mice, a deletion of *Fgfr1*, *Fgfr2*, *Fgfr3*, and *Fgfr4* from renal proximal tubules induces hyperphosphatemia, hypercalcemia, hypervitaminosis with elevated FGF23 (128). Other studies using mice with a specific deletion of FGFR1 in distal tubule segments have suggested that FGF23 activates FGFR1/ α -Klotho complexes in the distal tubule leading to an increase of sodium-chloride symporter (NCC)-dependent sodium (Na) reabsorption, a decrease of *Ace2* and renal Klotho, leading to increased blood pressure and hypertension (119). Further, activation of FGFR1 using pharmacologic intervention normalized blood pressure in Hyp mice, a mouse model of elevated FGF23 (119). Although the roles of FGFR3 and FGFR4 in kidney are not completely understood, *in vivo* studies proposed that FGFR3 and FGFR4 may contribute by acting in concert with FGFR1 to mediate FGF23 effects in kidney. Although their roles may be less substantial at the physiological level, under conditions of high circulating FGF23 in Hyp mice, the deletion of FGFR3 leads

to a feedback stimulation of *Fgf23* mRNA expression in bone (129, 131), suggesting complex kidney-bone crosstalk.

The co-receptor KL is required for high-affinity FGF23 activity in the kidney. Whole-nephron deletion of *Klotho* in mice results in renal FGF23 resistance, characterized by hypervitaminosis D, hyperphosphatemia, and other phenotypes that may resemble premature aging (39, 132). However, provision of a low phosphate diet to KL-null mice reversed the severe phenotypes, showing that the majority of KL-null phenotypes are due to extreme phosphate imbalances (133, 134). *Klotho* is highly expressed in the distal tubule segments of the nephron in comparison to its relatively modest expression in proximal tubules (123) although the phosphate reabsorption occurs primarily in the proximal tubules due to an abundant expression of the sodium phosphate transporters *Npt2a* and *Npt2c* (135–137). To delineate and identify the main effector sites of FGF23 actions in kidney, recent elegant studies have been performed using mouse models with nephron segment-specific deletion of *Klotho* in concert with a full characterization of mineral metabolism of these mice (138, 139). Olauson et al. generated a mouse model with deletion of *Klotho* in distal tubular segments (*Ksp-KL2/2*) which was characterized as fertile with a normal gross phenotype despite a disrupted mineral metabolism. These phenotypes were in contrast to *Klotho*-null mice which are not fertile in addition to undergoing premature death and severe vascular calcifications (138). By using immunohistochemistry analysis, investigators showed that partial deletion of *Klotho* in distal tubule resulted in hyperphosphatemia with elevated plasma FGF23 and increased *Npt2a* protein expression in the proximal tubule apical membrane (138). In other studies where *Klotho* was conditionally deleted from renal proximal tubule, the mineral metabolism phenotype was variable depending upon the strategies used to perform specific *Klotho* deletion. Indeed, in the studies of Ide et al., only a mild phenotype on mineral metabolism with a decrease of urinary phosphate was observed when *Klotho* was deleted from proximal tubules using three different proximal tubule specific *Cre* transgenic mice: *Kap-Cre* (kidney androgen-regulated protein), *Slc34a1-Cre* (sodium phosphate cotransporter-2a1) or *Pepck-Cre* (phosphoenolpyruvate carboxykinase) (139). The latter, harbors elevated serum iFGF23 and a slight increase in *Npt2a* protein (139). In contrast, other studies using an inducible promoter-*Cre*, *Ndr1-Cre*, to delete *Klotho* from proximal tubules revealed a more pronounced effect on mineral metabolism with markedly elevated iFGF23 and hyperphosphatemia (128). The phenotypic differences across these mouse models could be explained by the variability in *Cre*-mediated recombination efficiency, which can be factored by the cell-type specificity of *Cre* expression, the *Cre* expression efficiency in specific cell types, and the recombination feasibility from different genetic modification strategies.

It was later shown that FGF23 signaling can cross-talk with PTH signaling to control mineral metabolism. A deletion of both *PTH1R* and *Klotho* from the kidney proximal tubule (PT-*PTH1R/KL*^{-/-} mice) led to a severe disturbance of mineral metabolism including hyperphosphatemia at baseline and increased circulating phosphate in response to high

phosphate diet (140). The hyperphosphatemia observed in PT-*PTH1R/KL*^{-/-} mice was associated with elevated circulating FGF23, PTH, decreased circulating 1,25D and increased *Npt2a* (140). These new data underscore that FGF23 and PTH signaling pathways can interact in kidney thus coordinating renal phosphate handling in the proximal tubule (140, 141).

Using animal models, studies confirmed over recent years that FGF23 is a negative regulator of 1,25D production. Indeed, FGF23 potentially inhibits the expression of the 25(OH)D-1 α -hydroxylase *CYP27B1* in the renal proximal tubule while stimulating *in contrario* the expression of the vitamin D catabolic enzyme *CYP24A1* at the mRNA level (23, 142–144). Mice with global deletion of the *Fgf23* gene displayed elevations in serum 1,25D by 2–4 fold (144). Since FGF23 acts as a requisite partner with its co-receptor *Klotho* to control mineral metabolism, *Klotho* ablation in mice resulted in a strikingly similar phenotype to the *Fgf23*-null mice, including increased serum levels of 1,25D associated with increased renal *Cyp27b1* expression (39, 145). Interestingly, the premature aging-like phenotype of *Fgf23*^{-/-} and *Klotho*^{-/-} mice can be completely rescued using a genetic approach to ablate 1,25D synthesis through the generation of double mutant *Fgf23*^{-/-}/*1 α (OH)ase*^{-/-} and *Klotho*^{-/-}/*1 α (OH)ase*^{-/-} mice (146, 147). These data suggested that increased vitamin D played a major role in the abnormal mineral ion metabolism and soft-tissue anomalies observed in *Fgf23*^{-/-} and *Klotho*^{-/-} mice. Although *Klotho* deletion results in hypervitaminosis, and the kidney is the predominant organ expressing *Klotho*, studies using targeted deletion of *Klotho* in the proximal or distal tubule segment of the nephron have shown an overall modest effects on circulating vitamin D levels (138, 139), likely due to endocrine compensation.

It has also been described that the deletion of vitamin D receptor (VDR) in *Fgf23*^{-/-} and *Klotho*^{-/-} mice rescued these mice from an early lethality phenotype due to the absence of vitamin D signaling causing reduced phosphate absorption (148, 149). Therefore, *Fgf23*^{-/-}/*VDR* ^{Δ/Δ} and *KL*^{-/-}/*VDR* ^{Δ/Δ} double mutant mice can be used to examine the roles of FGF23 and *Klotho* at older ages by keeping these mice on a rescue diet rich in calcium, phosphorus, and lactose (150, 151) with the goal of preventing hypocalcemia and severe hyperparathyroidism due to the non-functioning VDR status.

Study of the *Fgf23*^{-/-}/*VDR* ^{Δ/Δ} and *KL*^{-/-}/*VDR* ^{Δ/Δ} mice showed that the deletion of *Fgf23* or *Klotho* leads to a decrease in the membrane abundance of NCC (the sodium chloride cotransporter) in the kidney distal tubule and subsequently to decreased Na⁺ reabsorption (152). In contrast, treatment of WT mice with FGF23 over 5 days upregulated distal tubular NCC resulting in increased Na⁺ reabsorption and increased blood Na⁺ concentrations (152). Using Hyp mice with elevated FGF23, studies have also shown that these mice have increased distal tubular Na⁺ uptake and membrane abundance of NCC (152). It was explored whether the effects of FGF23 on NCC expression in kidney may potentially drive physiological changes including hypertension and heart hypertrophy in a α *Klotho*-dependent manner. The inhibition of NCC using chlorothiazide abrogated FGF23-induced heart hypertrophy suggesting that

FGF23 may act as a potential regulator of renal Na^+ reabsorption with downstream consequences, although patients with FGF23-related gain or loss of function mutations primarily show more severe defects in phosphate metabolism. Another mineral that may be regulated by FGF23 in distal tubule is calcium (153). In this regard, studies have shown that renal calcium reabsorption and renal membrane abundance of TRPV5 are reduced in *Fgf23*^{-/-}/*VDR*^{Δ/Δ} and *Kl*^{-/-}/*VDR*^{Δ/Δ} double mutant mice (153).

Renal FGF23 Signal Transduction

Although FGFR1c, 3c, and 4 are ubiquitously expressed, Klotho expression is predominantly expressed in specific tissues such as kidney renal tubules, parathyroid gland, and choroid plexus of brain, suggesting that these organs are the physiological targets for FGF23-mediated endocrine actions (39, 154, 155). FGF23 preferentially binds to FGFR1c and Klotho, and this complex initiates FGFR1c signal transduction via the cytoplasmic adaptor FRS2α (156), which activates the FRS2α/Ras/MAPK pathway (157) (**Figure 3**). *In vitro* studies using human embryonic kidney cells (HEK293), which endogenously express FGFRs but not Klotho (158), showed that the presence of soluble Klotho (sKL) or membrane-bound Klotho (mKL) is required for FGF23-induced MAPK activity, which was assessed by pERK1/2 induction and EGR1 mRNA expression (157, 159). Although initial studies suggested that mKL and sKL share a common function of mediating FGF23-induced FRS2α/Ras/MAPK signaling, recent findings suggested that FGF23 responses were quantitatively different depending on mKL or sKL availability (159). *In vivo* studies, potentially using genetic targeting to isolate the biological effects of mKL from sKL will be required to deepen our understanding of these interactions.

In the absence of Klotho, in HEK293 cells, FGF23 alone can activate pPLCγ and pAKT, and these activities are completely neutralized by the presence of Klotho (159, 160). These studies further suggested that FGF23 preferentially induced FGFR1c signaling *via* Klotho. However, in the absence of Klotho, high concentrations of FGF23 can activate FGFR4 (157). The activation of FGFR4 was shown to induce PLCγ-catalyzed production of diacylglycerol and inositol 1,4,5-triphosphate that increased cytoplasmic calcium levels, thereby activating several calcium-sensing signal mediators, including the protein phosphatase calcineurin (157). The activation of calcineurin dephosphorylates the transcription factor NFAT, which permits its translocation into the nucleus to modulate the expression of specific target genes (161). This FGFR4-mediated effect may play a key role in cardiac hypertrophy through FGFR4 during highly elevated FGF23 in CKD (157, 162).

The phosphaturic action of FGF23 in kidney proximal tubule and actions in the distal tubule may occur primarily through FGFR1c, the main “phosphaturic” FGFR expressed in both segments and colocalized with Klotho (123, 129). A C-terminal FGF23 peptide antagonist has been developed recently to block FGF23 signaling by inhibiting tyrosine phosphorylation of FRS2α and downstream activation of the MAPK cascades (34). Studies in Hyp mice using this novel peptide confirmed that the inhibition of FGF23 signaling in kidney upregulates

the expression of the sodium-phosphate cotransporters Npt2a and Npt2c, coupled with the alleviation of the observed hypophosphatemia (34). In a mouse model of CKD, this FGF23 antagonist peptide has been shown to rescue the prevailing anemia (163).

Beside the effects of FGF23 on phosphate homeostasis, FGF23 signaling has been described to promote renal calcium reabsorption through the TRPV5 channel. Indeed, the apical membrane abundance of TRPV5 in renal distal tubules could be regulated by the binding of FGF23 to FGFR-Klotho complexes which activated a signaling pathway implicating ERK1/2, SGK1, and WNK4. This signaling pathway led to the increase of intracellular transport of fully glycosylated TRPV5 from the Golgi apparatus to the apical plasma membrane, thus decreasing the renal loss of calcium (153). In distal convoluted tubule, the ERK1/2-SGK1-WNK4 signaling pathway leads to WNK4 serine phosphorylation at residue 71 and kinase activation. FGF23 promoted the physical interaction between NCC and WNK4, increasing NCC membrane abundance, and would promote sodium reabsorption (152). Additional studies of the actions of FGF23 and Klotho specifically within the kidney distal tubule are required to determine the full extent of kidney FGF23 bioactivity.

CONCLUSION

The hormone FGF23 is mainly produced by osteocytes with the ability to target distant organs such as kidney. In late osteoblasts and osteocytes, FGF23 can be upregulated by elevated phosphate, anemia, inflammation, PTH and 1,25D; and downregulated by hypophosphatemia, insulin, and insulin-like growth factor 1. Although not covered here, studies have shown that FGF23 can be produced at lower levels by other cells such as immune cells, bone marrow erythroid cells and other tissues such as liver in response to diverse stimuli (106, 164). The posttranslational modifications of FGF23 protein *via* O-glycosylation and phosphorylation controls the proteolytic cleavage of mature FGF23 protein which dictates biologically active FGF23 concentrations.

The binding of FGF23 to FGFR1-Klotho complexes in the kidney has been shown to induce a signaling cascade through MAPK which controls mineral metabolism. The signals induced by FGF23 in kidney downregulate the expression of Npt2a/c leading to decreased phosphate reabsorption in proximal tubules, and upregulation of TRPV5 and NCC, potentially promoting calcium and sodium reabsorption, respectively, in the distal tubule. Alterations of FGF23 expression in osteocytes, FGF23 processing, and FGF23 activity cause severe endocrine pathologies resulting in rare and common diseases. Thus, further understanding the mechanisms controlling FGF23 production in osteocytes and bioactivity in kidney will lead to improved patient outcomes.

In summary, although much is known regarding FGF23 regulation and actions, gaps in our knowledge exist. These include the potential contributions of bone cells such as

osteoblasts and osteoclasts in the regulation of osteocytic FGF23, and it remains unclear whether aged osteocytes (mature cells and deeply embedded in the mineralized bone matrix) are more effective in terms of upregulating FGF23 in response to physiological and pathological changes vs. early osteocytes. Finally, whether FGF23 can target other cell-types in the kidney beyond its defined actions on proximal and distal tubules remains unknown, thus future investigation could examine the effects of FGF23 on renal immune cells such as macrophages and regulatory T cells, critical for the control of renal inflammation and kidney remodeling during acute kidney injury and CKD.

REFERENCES

- ICRP. *Basic Anatomical and Physiological Data for use in Radiological Protection—The Skeleton*. Kidlington; Oxford: Elsevier Science (1995).
- Avtandilashvili M, Tolmachev SY. Modeling the skeleton weight of an adult caucasian man. *Health Phys.* (2019) 117:149–55. doi: 10.1097/HP.0000000000000881
- Mosekilde L. Age-related changes in bone mass, structure, and strength—effects of loading. *Z Rheumatol.* (2000) 59(Suppl.1):1–9. doi: 10.1007/s003930070031
- Cahman KDG. *Age-Related Changes in Bone Mass. Encyclopedia of Food Sciences and Nutrition*. 2nd ed. Cambridge, MA: Academic Press (2003). p. 6,000.
- Bonjour JP. Calcium and phosphate: a duet of ions playing for bone health. *J Am Coll Nutr.* (2011) 30(5Suppl.1):438S–48S. doi: 10.1080/07315724.2011.10719988
- Dallas SL, Bonewald LF. Dynamics of the transition from osteoblast to osteocyte. *Ann N Y Acad Sci.* (2010) 1192:437–43. doi: 10.1111/j.1749-6632.2009.05246.x
- Downey PA, Siegel MI. Bone biology and the clinical implications for osteoporosis. *Phys Ther.* (2006) 86:77–91. doi: 10.1093/ptj/86.1.77
- Lerner UH. Osteoblasts, osteoclasts, and osteocytes: unveiling their intimate-associated responses to applied orthodontic forces. *Semin Orthodontics.* (2012) 18:237–48. doi: 10.1053/j.sodo.2012.06.002
- Aubin JE. Bone stem cells. *J Cell Biochem Suppl.* (1998) 30–1:73–82. doi: 10.1002/(SICI)1097-4644(200003/04)30:1<73::AID-JCB11>3.0.CO;2-L
- Pittenger MF, Mackay AM, Beck SC, Jaiswal RK, Douglas R, Mosca JD, et al. Multilineage potential of adult human mesenchymal stem cells. *Science.* (1999) 284:143–7. doi: 10.1126/science.284.5411.143
- Ash P, Loutit JF, Townsend KM. Osteoclasts derived from haematopoietic stem cells. *Nature.* (1980) 283:669–70. doi: 10.1038/283669a0
- Scheven BA, Visser JW, Nijweide PJ. *In vitro* osteoclast generation from different bone marrow fractions, including a highly enriched haematopoietic stem cell population. *Nature.* (1986) 321:79–81. doi: 10.1038/321079a0
- Tondravi MM, McKercher SR, Anderson K, Erdmann JM, Quiroz M, Maki R, et al. Osteopetrosis in mice lacking haematopoietic transcription factor PU.1. *Nature.* (1997) 386:81–4. doi: 10.1038/386081a0
- Goetz R, Mohammadi M. Exploring mechanisms of FGF signalling through the lens of structural biology. *Nat Rev Mol Cell Biol.* (2013) 14:166–80. doi: 10.1038/nrm3528
- Dallas SL, Veno PA, Tiede-Lewis LM. Live cell imaging of bone cell and organ cultures. *Methods Mol Biol.* (2019) 1914:467–506. doi: 10.1007/978-1-4939-8997-3_27
- Balemans W, Ebeling M, Patel N, Van Hul E, Olson P, Dioszegi M, et al. Increased bone density in sclerosteosis is due to the deficiency of a novel secreted protein (SOST). *Hum Mol Genet.* (2001) 10:537–43. doi: 10.1093/hmg/10.5.537
- Brunkow ME, Gardner JC, Van Ness J, Paepers BW, Kovacevich BR, Proll S, et al. Bone dysplasia sclerosteosis results from loss of the SOST gene product, a novel cystine knot-containing protein. *Am J Hum Genet.* (2001) 68:577–89. doi: 10.1086/318811
- Nakashima T, Hayashi M, Fukunaga T, Kurata K, Oh-Hora M, Feng JQ, et al. Evidence for osteocyte regulation of bone homeostasis through RANKL expression. *Nat Med.* (2011) 17:1231–4. doi: 10.1038/nm.2452
- Xiong J, Piemontese M, Thostenson JD, Weinstein RS, Manolagas SC, O'Brien CA. Osteocyte-derived RANKL is a critical mediator of the increased bone resorption caused by dietary calcium deficiency. *Bone.* (2014) 66:146–54. doi: 10.1016/j.bone.2014.06.006
- Knothe Tate ML, Niederer P, Knothe U. *In vivo* tracer transport through the lacunocanalicular system of rat bone in an environment devoid of mechanical loading. *Bone.* (1998) 22:107–17. doi: 10.1016/S8756-3282(97)00234-2
- Consortium A. Autosomal dominant hypophosphataemic rickets is associated with mutations in FGF23. *Nat Genet.* (2000) 26:345–8. doi: 10.1038/81664
- Perwad F, Zhang MY, Tenenhouse HS, Portale AA. Fibroblast growth factor 23 impairs phosphorus and vitamin D metabolism *in vivo* and suppresses 25-hydroxyvitamin D-1 α -hydroxylase expression *in vitro*. *Am J Physiol Renal Physiol.* (2007) 293:F1577–83. doi: 10.1152/ajprenal.00463.2006
- Shimada T, Hasegawa H, Yamazaki Y, Muto T, Hino R, Takeuchi Y, et al. FGF-23 is a potent regulator of vitamin D metabolism and phosphate homeostasis. *J Bone Miner Res.* (2004) 19:429–35. doi: 10.1359/JBMR.0301264
- Wolf M, White KE. Coupling fibroblast growth factor 23 production and cleavage: iron deficiency, rickets, and kidney disease. *Curr Opin Nephrol Hypertens.* (2014) 23:411–9. doi: 10.1097/01.mnh.0000447020.74593.6f
- Saito H, Maeda A, Ohtomo S, Hirata M, Kusano K, Kato S, et al. Circulating FGF-23 is regulated by 1 α ,25-dihydroxyvitamin D3 and phosphorus *in vivo*. *J Biol Chem.* (2005) 280:2543–9. doi: 10.1074/jbc.M408903200
- Perwad F, Azam N, Zhang MY, Yamashita T, Tenenhouse HS, Portale AA. Dietary and serum phosphorus regulate fibroblast growth factor 23 expression and 1,25-dihydroxyvitamin D metabolism in mice. *Endocrinology.* (2005) 146:5358–64. doi: 10.1210/en.2005-0777
- Bon N, Frangi G, Sourice S, Guicheux J, Beck-Cormier S, Beck L. Phosphate-dependent FGF23 secretion is modulated by PiT2/Slc20a2. *Mol Metab.* (2018) 11:197–204. doi: 10.1016/j.molmet.2018.02.007
- Takashi Y, Kosako H, Sawatsubashi S, Kinoshita Y, Ito N, Tsoumpra MK, et al. Activation of unliganded FGF receptor by extracellular phosphate potentiates proteolytic protection of FGF23 by its O-glycosylation. *Proc Natl Acad Sci USA.* (2019) 116:11418–27. doi: 10.1073/pnas.1815166116
- Takashi Y, Fukumoto S. Phosphate-sensing and regulatory mechanism of FGF23 production. *J Endocrinol Invest.* (2020) 43:877–83. doi: 10.1007/s40618-020-01205-9
- Xiao Z, Huang J, Cao L, Liang Y, Han X, Quarles LD. Osteocyte-specific deletion of Fgfr1 suppresses FGF23. *PLoS ONE.* (2014) 9:e104154. doi: 10.1371/journal.pone.0104154
- Wu AL, Feng B, Chen MZ, Kolumam G, Zavala-Solorio J, Wyatt SK, et al. Antibody-mediated activation of FGFR1 induces FGF23 production and hypophosphatemia. *PLoS ONE.* (2013) 8:e57322. doi: 10.1371/journal.pone.0057322

AUTHOR CONTRIBUTIONS

RA, PN, MN, and KW wrote and edited the manuscript and figures. All authors contributed to the article and approved the submitted version.

FUNDING

The authors would like to acknowledge NIH grants R21-AR059278, R01-DK112958, and R01-HL145528 (KW); T32-HL007910 and F31-DK122679 (MN); and The David Weaver Professorship (KW).

32. Hori M, Kinoshita Y, Taguchi M, Fukumoto S. Phosphate enhances Fgf23 expression through reactive oxygen species in UMR-106 cells. *J Bone Miner Metab.* (2016) 34:132–9. doi: 10.1007/s00774-015-0651-9
33. Hassan A, Durlacher K, Silver J, Naveh-Many T, Levi R. The fibroblast growth factor receptor mediates the increased FGF23 expression in acute and chronic uremia. *Am J Physiol Renal Physiol.* (2016) 310:F217–21. doi: 10.1152/ajprenal.00332.2015
34. Goetz R, Nakada Y, Hu MC, Kurosu H, Wang L, Nakatani T, et al. Isolated C-terminal tail of FGF23 alleviates hypophosphatemia by inhibiting FGF23-FGFR-Klotho complex formation. *Proc Natl Acad Sci USA.* (2010) 107:407–12. doi: 10.1073/pnas.0902006107
35. Komaba H, Kaludjerovic J, Hu DZ, Nagano K, Amano K, Ide N, et al. Klotho expression in osteocytes regulates bone metabolism and controls bone formation. *Kidney Int.* (2017) 92:599–611. doi: 10.1016/j.kint.2017.02.014
36. Avin KG, Coen PM, Huang W, Stolz DB, Sowa GA, Dube JJ, et al. Skeletal muscle as a regulator of the longevity protein, Klotho. *Front Physiol.* (2014) 5:189. doi: 10.3389/fphys.2014.00189
37. Drueke TB, Massy ZA. Circulating Klotho levels: clinical relevance and relationship with tissue Klotho expression. *Kidney Int.* (2013) 83:13–5. doi: 10.1038/ki.2012.370
38. Lim K, Groen A, Molostvov G, Lu T, Lilley KS, Snead D, et al. α -klotho expression in human tissues. *J Clin Endocrinol Metab.* (2015) 100:E1308–18. doi: 10.1210/jc.2015-1800
39. Kuro-o M, Matsumura Y, Aizawa H, Kawaguchi H, Suga T, Utsugi T, et al. Mutation of the mouse klotho gene leads to a syndrome resembling ageing. *Nature.* (1997) 390:45–51. doi: 10.1038/36285
40. Matsumura Y, Aizawa H, Shiraki-Iida T, Nagai R, Kuro-o M, Nabeshima Y. Identification of the human klotho gene and its two transcripts encoding membrane and secreted klotho protein. *Biochem Biophys Res Commun.* (1998) 242:626–30.
41. Bloch L, Sineshchekova O, Reichenbach D, Reiss K, Saftig P, Kuro-o M, et al. Klotho is a substrate for α -, β - and γ -secretase. *FEBS Lett.* (2009) 583:3221–4. doi: 10.1016/j.febslet.2009.09.009
42. Chen CD, Podvin S, Gillespie E, Leeman SE, Abraham CR. Insulin stimulates the cleavage and release of the extracellular domain of Klotho by ADAM10 and ADAM17. *Proc Natl Acad Sci USA.* (2007) 104:19796–801. doi: 10.1073/pnas.0709805104
43. Lindberg K, Amin R, Moe OW, Hu MC, Erben RG, Ostman Wernerson A, et al. The kidney is the principal organ mediating klotho effects. *J Am Soc Nephrol.* (2014) 25:2169–75. doi: 10.1681/ASN.2013111209
44. Hu MC, Shi M, Zhang J, Addo T, Cho HJ, Barker SL, et al. Renal production, uptake, and handling of circulating α Klotho. *J Am Soc Nephrol.* (2016) 27:79–90. doi: 10.1681/ASN.2014101030
45. Carrillo-Lopez N, Panizo S, Alonso-Montes C, Roman-Garcia P, Rodriguez I, Martinez-Salgado C, et al. Direct inhibition of osteoblastic Wnt pathway by fibroblast growth factor 23 contributes to bone loss in chronic kidney disease. *Kidney Int.* (2016) 90:77–89. doi: 10.1016/j.kint.2016.01.024
46. Hum JM, O'Bryan LM, Tatiparthi AK, Cass TA, Clinkenbeard EL, Cramer MS, et al. Chronic hyperphosphatemia and vascular calcification are reduced by stable delivery of soluble klotho. *J Am Soc Nephrol.* (2017) 28:1162–74. doi: 10.1681/ASN.2015111266
47. Ito N, Wijanayaka AR, Pridaux M, Kogawa M, Ormsby RT, Evdokiou A, et al. Regulation of FGF23 expression in IDG-SW3 osteocytes and human bone by pro-inflammatory stimuli. *Mol Cell Endocrinol.* (2015) 399:208–18. doi: 10.1016/j.mce.2014.10.007
48. Ewendt F, Foller M. p38MAPK controls fibroblast growth factor 23 (FGF23) synthesis in UMR106-osteoblast-like cells and in IDG-SW3 osteocytes. *J Endocrinol Invest.* (2019) 42:1477–83. doi: 10.1007/s40618-019-01073-y
49. Bar L, Hase P, Foller M. PKC regulates the production of fibroblast growth factor 23 (FGF23). *PLoS ONE.* (2019) 14:e0211309. doi: 10.1371/journal.pone.0211309
50. Maniati E, Bossard M, Cook N, Candido JB, Emami-Shahri N, Nedospasov SA, et al. Crosstalk between the canonical NF- κ B and Notch signaling pathways inhibits Ppar γ expression and promotes pancreatic cancer progression in mice. *J Clin Invest.* (2011) 121:4685–99. doi: 10.1172/JCI45797
51. Tamamura Y, Sakamoto K, Katsube KI, Yamaguchi A. Notch signaling is involved in Fgf23 upregulation in osteocytes. *Biochem Biophys Res Commun.* (2019) 518:233–8. doi: 10.1016/j.bbrc.2019.08.038
52. He Q, Shumate LT, Matthias J, Aydin C, Wein MN, Spatz JM, et al. A G protein-coupled, IP3/protein kinase C pathway controlling the synthesis of phosphaturic hormone FGF23. *JCI Insight.* (2019) 4:125007. doi: 10.1172/jci.insight.125007
53. Onal M, Carlson AH, Thostenson JD, Benkusky NA, Meyer MB, Lee SM, et al. A novel distal enhancer mediates inflammation-, PTH-, and early onset murine kidney disease-induced expression of the mouse Fgf23 gene. *JBM R Plus.* (2018) 2:32–47. doi: 10.1002/jbm4.10023
54. Lee SM, Carlson AH, Onal M, Benkusky NA, Meyer MB, Pike JW. A control region near the fibroblast growth factor 23 gene mediates response to phosphate, 1,25(OH) $_2$ D $_3$, and LPS *in vivo*. *Endocrinology.* (2019) 160:2877–91. doi: 10.1210/en.2019-00622
55. Pagani A, Nai A, Corna G, Bosurgi L, Rovere-Querini P, Camaschella C, et al. Low hepcidin accounts for the pro-inflammatory status associated with iron deficiency. *Blood.* (2011) 118:736–46. doi: 10.1182/blood-2011-02-337212
56. Agoro R, Taleb M, Quesniaux VFJ, Mura C. Cell iron status influences macrophage polarization. *PLoS ONE.* (2018) 13:e0196921. doi: 10.1371/journal.pone.0196921
57. Farrow EG, Yu X, Summers LJ, Davis SI, Fleet JC, Allen MR, et al. Iron deficiency drives an autosomal dominant hypophosphatemic rickets (ADHR) phenotype in fibroblast growth factor-23 (Fgf23) knock-in mice. *Proc Natl Acad Sci USA.* (2011) 108:E1146–55. doi: 10.1073/pnas.1110905108
58. David V, Martin A, Isakova T, Spaulding C, Qi L, Ramirez V, et al. Inflammation and functional iron deficiency regulate fibroblast growth factor 23 production. *Kidney Int.* (2016) 89:135–46. doi: 10.1038/ki.2015.290
59. Durlacher-Betzer K, Hassan A, Levi R, Axelrod J, Silver J, Naveh-Many T. Interleukin-6 contributes to the increase in fibroblast growth factor 23 expression in acute and chronic kidney disease. *Kidney Int.* (2018) 94:315–25. doi: 10.1016/j.kint.2018.02.026
60. Zhang Q, Doucet M, Tomlinson RE, Han X, Quarles LD, Collins MT, et al. The hypoxia-inducible factor-1 α activates ectopic production of fibroblast growth factor 23 in tumor-induced osteomalacia. *Bone Res.* (2016) 4:16011. doi: 10.1038/boneres.2016.11
61. Imel EA, Liu Z, Coffman M, Acton D, Mehta R, Econs MJ. Oral iron replacement normalizes fibroblast growth factor 23 in iron-deficient patients with autosomal dominant hypophosphatemic rickets. *J Bone Miner Res.* (2019) 35:231–8. doi: 10.1002/jbmr.3878
62. Wolf M, Koch TA, Bregman DB. Effects of iron deficiency anemia and its treatment on fibroblast growth factor 23 and phosphate homeostasis in women. *J Bone Miner Res.* (2013) 28:1793–803. doi: 10.1002/jbmr.1923
63. Klein K, Asaad S, Econs M, Rubin JE. Severe FGF23-based hypophosphatemic osteomalacia due to ferric carboxymaltose administration. *BMJ Case Rep.* (2018) 2018:222851. doi: 10.1136/bcr-2017-222851
64. Clinkenbeard EL, Hanudel MR, Stayrook KR, Appaiah HN, Farrow EG, Cass TA, et al. Erythropoietin stimulates murine and human fibroblast growth factor-23, revealing novel roles for bone and bone marrow. *Haematologica.* (2017) 102:e427–30. doi: 10.3324/haematol.2017.167882
65. Hanudel MR, Eisenga MF, Rappaport M, Chua K, Qiao B, Jung G, et al. Effects of erythropoietin on fibroblast growth factor 23 in mice and humans. *Nephrol Dial Transplant.* (2018) 34:2057–65. doi: 10.1093/ndt/gfy189
66. Daryadel A, Bettoni C, Haider T, Imenez Silva PH, Schnitzbauer U, Pastor-Arroyo EM, et al. Erythropoietin stimulates fibroblast growth factor 23 (FGF23) in mice and men. *Pflugers Arch.* (2018) 470:1569–82. doi: 10.1007/s00424-018-2171-7
67. Daryadel A, Natale L, Seebeck P, Bettoni C, Schnitzbauer U, Gassmann M, et al. Elevated FGF23 and disordered renal mineral handling with reduced bone mineralization in chronically erythropoietin over-expressing transgenic mice. *Sci Rep.* (2019) 9:14989. doi: 10.1038/s41598-019-51577-z
68. Haase VH. HIF-prolyl hydroxylases as therapeutic targets in erythropoiesis and iron metabolism. *Hemodial Int.* (2017) 21(Suppl.1):S110–24. doi: 10.1111/hdi.12567
69. Flamme I, Ellinghaus P, Urrego D, Kruger T. FGF23 expression in rodents is directly induced via erythropoietin after inhibition of

- hypoxia inducible factor proline hydroxylase. *PLoS ONE*. (2017) 12:e0186979. doi: 10.1371/journal.pone.0186979
70. Noonan ML, Clinkenbeard EL, Ni P, Swallow EA, Tippen SP, Agoro R, et al. Erythropoietin and a hypoxia-inducible factor prolyl hydroxylase inhibitor (HIF-PHDi) lowers FGF23 in a model of chronic kidney disease (CKD). *Physiol Rep*. (2020) 8:e14434. doi: 10.14814/phy2.14434
 71. Qin L, Raggatt LJ, Partridge NC. Parathyroid hormone: a double-edged sword for bone metabolism. *Trends Endocrinol Metab*. (2004) 15:60–5. doi: 10.1016/j.tem.2004.01.006
 72. Hou YC, Lu CL, Lu KC. Mineral bone disorders in chronic kidney disease. *Nephrology*. (2018) 23(Suppl.4):88–94. doi: 10.1111/nep.13457
 73. Murray TM, Rao LG, Divieti P, Bringham FR. Parathyroid hormone secretion and action: evidence for discrete receptors for the carboxyl-terminal region and related biological actions of carboxyl-terminal ligands. *Endocr Rev*. (2005) 26:78–113. doi: 10.1210/er.2003-0024
 74. Hruska KA, Seifert M. Pathophysiology of chronic kidney disease mineral bone disorder (CKD-MBD). In: Rosen JC, editor. *Primer on the Metabolic Bone Diseases and Disorders of Mineral Metabolism*. Hoboken, NJ: Wiley-Blackwell (2013). p. 632–9.
 75. Goodman WG. Calcimimetic agents and secondary hyperparathyroidism: treatment and prevention. *Nephrol Dial Transplant*. (2002) 17:204–7. doi: 10.1093/ndt/17.2.204
 76. Meir T, Durlacher K, Pan Z, Amir G, Richards WG, Silver J, et al. Parathyroid hormone activates the orphan nuclear receptor Nurr1 to induce FGF23 transcription. *Kidney Int*. (2014) 86:1106–15. doi: 10.1038/ki.2014.215
 77. Rhee Y, Bivi N, Farrow E, Lezcano V, Plotkin LI, White KE, et al. Parathyroid hormone receptor signaling in osteocytes increases the expression of fibroblast growth factor-23 *in vitro* and *in vivo*. *Bone*. (2011) 49:636–43. doi: 10.1016/j.bone.2011.06.025
 78. Knab VM, Corbin B, Andrukhova O, Hum JM, Ni P, Rabadi S, et al. Acute parathyroid hormone injection increases C-terminal but not intact fibroblast growth factor 23 levels. *Endocrinology*. (2017) 158:1130–9. doi: 10.1016/en.2016-1451
 79. Ishiyama N, Shibata H, Kanzaki M, Shiozaki S, Miyazaki J, Kobayashi I, et al. Calcium as a second messenger of the action of transforming growth factor- β on insulin secretion. *Mol Cell Endocrinol*. (1996) 117:1–6. doi: 10.1016/0303-7207(95)03726-8
 80. McGowan TA, Madesh M, Zhu Y, Wang L, Russo M, Deelman L, et al. TGF- β -induced Ca(2+) influx involves the type III IP(3) receptor and regulates actin cytoskeleton. *Am J Physiol Renal Physiol*. (2002) 282:F910–20. doi: 10.1152/ajprenal.00252.2001
 81. Gooch JL, Gorin Y, Zhang BX, Abboud HE. Involvement of calcineurin in transforming growth factor- β -mediated regulation of extracellular matrix accumulation. *J Biol Chem*. (2004) 279:15561–70. doi: 10.1074/jbc.M308759200
 82. Feger M, Hase P, Zhang B, Hirche F, Glosse P, Lang F, et al. The production of fibroblast growth factor 23 is controlled by TGF- β 2. *Sci Rep*. (2017) 7:4982. doi: 10.1038/s41598-017-05226-y
 83. Zhang B, Yan J, Umbach AT, Fakhri H, Fajol A, Schmidt S, et al. NF- κ B-sensitive Orail expression in the regulation of FGF23 release. *J Mol Med*. (2016) 94:557–66. doi: 10.1007/s00109-015-1370-3
 84. Bar L, Grossmann C, Gekle M, Foller M. Calcineurin inhibitors regulate fibroblast growth factor 23 (FGF23) synthesis. *Naunyn Schmiedeberg Arch Pharmacol*. (2017) 390:1117–23. doi: 10.1007/s00210-017-1411-2
 85. Zhang B, Yan J, Schmidt S, Salker MS, Alexander D, Foller M, et al. Lithium-sensitive store-operated Ca²⁺ entry in the regulation of FGF23 release. *Neurosignals*. (2015) 23:34–48. doi: 10.1159/000442602
 86. Nguyen-Yamamoto L, Karaplis AC, St-Arnaud R, Goltzman D. Fibroblast growth factor 23 regulation by systemic and local osteoblast-synthesized 1,25-dihydroxyvitamin D. *J Am Soc Nephrol*. (2017) 28:586–97. doi: 10.1681/ASN.2016010066
 87. Feng JQ, Ward LM, Liu S, Lu Y, Xie Y, Yuan B, et al. Loss of DMP1 causes rickets and osteomalacia and identifies a role for osteocytes in mineral metabolism. *Nat Genet*. (2006) 38:1310–5. doi: 10.1038/ng1905
 88. Liu S, Tang W, Zhou J, Vierthaler L, Quarles LD. Distinct roles for intrinsic osteocyte abnormalities and systemic factors in regulation of FGF23 and bone mineralization in Hyp mice. *Am J Physiol Endocrinol Metab*. (2007) 293:E1636–44. doi: 10.1152/ajpendo.00396.2007
 89. Liu S, Zhou J, Tang W, Jiang X, Rowe DW, Quarles LD. Pathogenic role of Fgf23 in Hyp mice. *Am J Physiol Endocrinol Metab*. (2006) 291:E38–49. doi: 10.1152/ajpendo.00008.2006
 90. Liu S, Zhou J, Tang W, Menard R, Feng JQ, Quarles LD. Pathogenic role of Fgf23 in Dmp1-null mice. *Am J Physiol Endocrinol Metab*. (2008) 295:E254–61. doi: 10.1152/ajpendo.90201.2008
 91. Martin A, Liu S, David V, Li H, Karydis A, Feng JQ, et al. Bone proteins PHEX and DMP1 regulate fibroblastic growth factor Fgf23 expression in osteocytes through a common pathway involving FGF receptor (FGFR) signaling. *FASEB J*. (2011) 25:2551–62. doi: 10.1096/fj.10-177816
 92. Liu S, Tang W, Fang J, Ren J, Li H, Xiao Z, et al. Novel regulators of Fgf23 expression and mineralization in Hyp bone. *Mol Endocrinol*. (2009) 23:1505–18. doi: 10.1210/me.2009-0085
 93. Lee JW, Yamaguchi A, Iimura T. Functional heterogeneity of osteocytes in FGF23 production: the possible involvement of DMP1 as a direct negative regulator. *Bonekey Rep*. (2014) 3:543. doi: 10.1038/bonekey.2014.38
 94. Clinkenbeard EL, Cass TA, Ni P, Hum JM, Bellido T, Allen MR, et al. Conditional deletion of murine Fgf23: interruption of the normal skeletal responses to phosphate challenge and rescue of genetic hypophosphatemia. *J Bone Miner Res*. (2016) 31:1247–57. doi: 10.1002/jbmr.2792
 95. Bar L, Feger M, Fajol A, Klotz LO, Zeng S, Lang F, et al. Insulin suppresses the production of fibroblast growth factor 23 (FGF23). *Proc Natl Acad Sci USA*. (2018) 115:5804–9. doi: 10.1073/pnas.1800160115
 96. Gribaa M, Younes M, Bouyacoub Y, Korbaa W, Ben Charfeddine I, Touzi M, et al. An autosomal dominant hypophosphatemic rickets phenotype in a Tunisian family caused by a new FGF23 missense mutation. *J Bone Miner Metab*. (2010) 28:111–5. doi: 10.1007/s00774-009-0111-5
 97. Silvestri L, Pagani A, Camaschella C. Furin-mediated release of soluble hemojuvelin: a new link between hypoxia and iron homeostasis. *Blood*. (2008) 111:924–31. doi: 10.1182/blood-2007-07-100677
 98. Tagliabracci VS, Engel JL, Wiley SE, Xiao J, Gonzalez DJ, Nidumanda Appaiah H, et al. Dynamic regulation of FGF23 by Fam20c phosphorylation, GalNAc-T3 glycosylation, and furin proteolysis. *Proc Natl Acad Sci USA*. (2014) 111:5520–5. doi: 10.1073/pnas.1402218111
 99. de Las Rivas M, Paul Daniel EJ, Narimatsu Y, Companon I, Kato K, Hermosilla P, et al. Molecular basis for fibroblast growth factor 23 O-glycosylation by GalNAc-T3. *Nat Chem Biol*. (2020) 16:351–60. doi: 10.1038/s41589-019-0444-x
 100. Rafaelsen SH, Raeder H, Fagerheim AK, Knappskog P, Carpenter TO, Johansson S, et al. Exome sequencing reveals FAM20c mutations associated with fibroblast growth factor 23-related hypophosphatemia, dental anomalies, and ectopic calcification. *J Bone Miner Res*. (2013) 28:1378–85. doi: 10.1002/jbmr.1850
 101. Liu P, Ma S, Zhang H, Liu C, Lu Y, Chen L, et al. Specific ablation of mouse Fam20C in cells expressing type I collagen leads to skeletal defects and hypophosphatemia. *Sci Rep*. (2017) 7:3590. doi: 10.1038/s41598-017-03960-x
 102. Eren M, Place AT, Thomas PM, Flevaris P, Miyata T, Vaughan DE. PAI-1 is a critical regulator of FGF23 homeostasis. *Sci Adv*. (2017) 3:e1603259. doi: 10.1126/sciadv.1603259
 103. Takeshita K, Yamamoto K, Ito M, Kondo T, Matsushita T, Hirai M, et al. Increased expression of plasminogen activator inhibitor-1 with fibrin deposition in a murine model of aging, “Klotho” mouse. *Semin Thromb Hemost*. (2002) 28:545–54. doi: 10.1055/s-2002-36699
 104. Eren M, Boe AE, Murphy SB, Place AT, Nagpal V, Morales-Nebreda L, et al. PAI-1-regulated extracellular proteolysis governs senescence and survival in Klotho mice. *Proc Natl Acad Sci USA*. (2014) 111:7090–5. doi: 10.1073/pnas.1321942111
 105. Itoh N, Nakayama Y, Konishi M. Roles of FGFs as paracrine or endocrine signals in liver development, health, and disease. *Front Cell Dev Biol*. (2016) 4:30. doi: 10.3389/fcell.2016.00030
 106. Clinkenbeard EL, Noonan ML, Thomas JC, Ni P, Hum JM, Aref M, et al. Increased FGF23 protects against detrimental cardio-renal consequences during elevated blood phosphate in CKD. *JCI Insight*. (2019) 4:123817. doi: 10.1172/jci.insight.123817
 107. Gutierrez OM, Mannstadt M, Isakova T, Rauh-Hain JA, Tamez H, Shah A, et al. Fibroblast growth factor 23 and mortality among

- patients undergoing hemodialysis. *N Engl J Med.* (2008) 359:584–92. doi: 10.1056/NEJMoa0706130
108. John GB, Cheng CY, Kuro-o M. Role of Klotho in aging, phosphate metabolism, and CKD. *Am J Kidney Dis.* (2011) 58:127–34. doi: 10.1053/j.ajkd.2010.12.027
 109. Gattineni J, Twombly K, Goetz R, Mohammadi M, Baum M. Regulation of serum 1,25(OH)₂ vitamin D₃ levels by fibroblast growth factor 23 is mediated by FGF receptors 3 and 4. *Am J Physiol Renal Physiol.* (2011) 301:F371–7. doi: 10.1152/ajprenal.00740.2010
 110. Gattineni J, Alphonse P, Zhang Q, Mathews N, Bates CM, Baum M. Regulation of renal phosphate transport by FGF23 is mediated by FGFR1 and FGFR4. *Am J Physiol Renal Physiol.* (2014) 306:F351–8. doi: 10.1152/ajprenal.00232.2013
 111. Kurosu H, Ogawa Y, Miyoshi M, Yamamoto M, Nandi A, Rosenblatt KP, et al. Regulation of fibroblast growth factor-23 signaling by klotho. *J Biol Chem.* (2006) 281:6120–3. doi: 10.1074/jbc.C500457200
 112. Urakawa I, Yamazaki Y, Shimada T, Iijima K, Hasegawa H, Okawa K, et al. Klotho converts canonical FGF receptor into a specific receptor for FGF23. *Nature.* (2006) 444:770–4. doi: 10.1038/nature05315
 113. Nabeshima Y. [Discovery of alpha-Klotho and FGF23 unveiled new insight into calcium and phosphate homeostasis]. *Clin Calcium.* (2008) 18:923–34.
 114. Chen G, Liu Y, Goetz R, Fu L, Jayaraman S, Hu MC, et al. α -Klotho is a non-enzymatic molecular scaffold for FGF23 hormone signalling. *Nature.* (2018) 553:461–6. doi: 10.1038/nature25451
 115. Larsson T, Marsell R, Schipani E, Ohlsson C, Ljunggren O, Tenenhouse HS, et al. Transgenic mice expressing fibroblast growth factor 23 under the control of the α 1(I) collagen promoter exhibit growth retardation, osteomalacia, and disturbed phosphate homeostasis. *Endocrinology.* (2004) 145:3087–94. doi: 10.1210/en.2003-1768
 116. Sitara D, Razzaque MS, Hesse M, Yoganathan S, Taguchi T, Erben RG, et al. Homozygous ablation of fibroblast growth factor-23 results in hyperphosphatemia and impaired skeletogenesis, and reverses hypophosphatemia in PheX-deficient mice. *Matrix Biol.* (2004) 23:421–32. doi: 10.1016/j.matbio.2004.09.007
 117. Marsell R, Krajisnik T, Goransson H, Ohlsson C, Ljunggren O, Larsson TE, et al. Gene expression analysis of kidneys from transgenic mice expressing fibroblast growth factor-23. *Nephrol Dial Transplant.* (2008) 23:827–33. doi: 10.1093/ndt/gfm672
 118. Wysocki J, Gonzalez-Pacheco FR, Batlle D. Angiotensin-converting enzyme 2: possible role in hypertension and kidney disease. *Curr Hypertens Rep.* (2008) 10:70–7. doi: 10.1007/s11906-008-0014-1
 119. Han X, Ross J, Kolumam G, Pi M, Sonoda J, King G, et al. Cardiovascular effects of renal distal tubule deletion of the FGF receptor 1 gene. *J Am Soc Nephrol.* (2018) 29:69–80. doi: 10.1681/ASN.2017040412
 120. Imura A, Tsuji Y, Murata M, Maeda R, Kubota K, Iwano A, et al. α -Klotho as a regulator of calcium homeostasis. *Science.* (2007) 316:1615–8. doi: 10.1126/science.1135901
 121. Viau A, El Karoui K, Laouari D, Burtin M, Nguyen C, Mori K, et al. Lipocalin 2 is essential for chronic kidney disease progression in mice and humans. *J Clin Invest.* (2010) 120:4065–76. doi: 10.1172/JCI42004
 122. Portale AA, Zhang MY, David V, Martin A, Jiao Y, Gu W, et al. Characterization of FGF23-dependent Egr-1 cistrome in the mouse renal proximal tubule. *PLoS ONE.* (2015) 10:e0142924. doi: 10.1371/journal.pone.0142924
 123. Farrow EG, Davis SI, Summers LJ, White KE. Initial FGF23-mediated signaling occurs in the distal convoluted tubule. *J Am Soc Nephrol.* (2009) 20:955–60. doi: 10.1681/ASN.2008070783
 124. Zhang MY, Ranch D, Pereira RC, Armbricht HJ, Portale AA, Perwad F. Chronic inhibition of ERK1/2 signaling improves disordered bone and mineral metabolism in hypophosphatemic (Hyp) mice. *Endocrinology.* (2012) 153:1806–16. doi: 10.1210/en.2011-1831
 125. Ranch D, Zhang MY, Portale AA, Perwad F. Fibroblast growth factor 23 regulates renal 1,25-dihydroxyvitamin D and phosphate metabolism via the MAP kinase signaling pathway in Hyp mice. *J Bone Miner Res.* (2011) 26:1883–90. doi: 10.1002/jbmr.401
 126. Fukuda T, Kanomata K, Nojima J, Urakawa I, Suzawa T, Imada M, et al. FGF23 induces expression of two isoforms of NAB2, which are corepressors of Egr-1. *Biochem Biophys Res Commun.* (2007) 353:147–51. doi: 10.1016/j.bbrc.2006.12.011
 127. Kumbink J, Gerlinger M, Johnson JP. Egr-1 induces the expression of its corepressor nab2 by activation of the nab2 promoter thereby establishing a negative feedback loop. *J Biol Chem.* (2005) 280:42785–93. doi: 10.1074/jbc.M511079200
 128. Takeshita A, Kawakami K, Furushima K, Miyajima M, Sakaguchi K. Central role of the proximal tubular α Klotho/FGF receptor complex in FGF23-regulated phosphate and vitamin D metabolism. *Sci Rep.* (2018) 8:6917. doi: 10.1038/s41598-018-25087-3
 129. Liu S, Vierthaler L, Tang W, Zhou J, Quarles LD. FGFR3 and FGFR4 do not mediate renal effects of FGF23. *J Am Soc Nephrol.* (2008) 19:2342–50. doi: 10.1681/ASN.2007121301
 130. Gattineni J, Bates C, Twombly K, Dwarakanath V, Robinson ML, Goetz R, et al. FGF23 decreases renal NaPi-2a and NaPi-2c expression and induces hypophosphatemia *in vivo* predominantly via FGF receptor 1. *Am J Physiol Renal Physiol.* (2009) 297:F282–91. doi: 10.1152/ajprenal.90742.2008
 131. Li H, Martin A, David V, Quarles LD. Compound deletion of Fgfr3 and Fgfr4 partially rescues the Hyp mouse phenotype. *Am J Physiol Endocrinol Metab.* (2011) 300:E508–17. doi: 10.1152/ajpendo.00499.2010
 132. Nakatani T, Ohnishi M, Razzaque MS. Inactivation of klotho function induces hyperphosphatemia even in presence of high serum fibroblast growth factor 23 levels in a genetically engineered hypophosphatemic (Hyp) mouse model. *FASEB J.* (2009) 23:3702–11. doi: 10.1096/fj.08-123992
 133. Morishita K, Shirai A, Kubota M, Katakura Y, Nabeshima Y, Takeshige K, et al. The progression of aging in klotho mutant mice can be modified by dietary phosphorus and zinc. *J Nutr.* (2001) 131:3182–8. doi: 10.1093/jn/131.12.3182
 134. Ohnishi M, Razzaque MS. Dietary and genetic evidence for phosphate toxicity accelerating mammalian aging. *FASEB J.* (2010) 24:3562–71. doi: 10.1096/fj.09-152488
 135. Murer H, Hernando N, Forster I, Biber J. Proximal tubular phosphate reabsorption: molecular mechanisms. *Physiol Rev.* (2000) 80:1373–409. doi: 10.1152/physrev.2000.80.4.1373
 136. Ohkido I, Segawa H, Yanagida R, Nakamura M, Miyamoto K. Cloning, gene structure and dietary regulation of the type-IIc Na/Pi cotransporter in the mouse kidney. *Pflugers Arch.* (2003) 446:106–15. doi: 10.1007/s00424-003-1010-6
 137. Prie D, Urena Torres P, Friedlander G. Latest findings in phosphate homeostasis. *Kidney Int.* (2009) 75:882–9. doi: 10.1038/ki.2008.643
 138. Olausson H, Lindberg K, Amin R, Jia T, Wernerson A, Andersson G, et al. Targeted deletion of Klotho in kidney distal tubule disrupts mineral metabolism. *J Am Soc Nephrol.* (2012) 23:1641–51. doi: 10.1681/ASN.2012010048
 139. Ide N, Olausson H, Sato T, Densmore MJ, Wang H, Hanai JI, et al. *In vivo* evidence for a limited role of proximal tubular Klotho in renal phosphate handling. *Kidney Int.* (2016) 90:348–62. doi: 10.1016/j.kint.2016.04.009
 140. Ide N, Ye R, Courbebaisse M, Olausson H, Densmore MJ, Larsson TE, et al. *In vivo* evidence for an interplay of FGF23/Klotho/PTH axis on the phosphate handling in renal proximal tubules. *Am J Physiol Renal Physiol.* (2018) 315:F1261–70. doi: 10.1152/ajprenal.00650.2017
 141. Andrukhova O, Streicher C, Zeitz U, Erben RG. Fgf23 and parathyroid hormone signaling interact in kidney and bone. *Mol Cell Endocrinol.* (2016) 436:224–39. doi: 10.1016/j.mce.2016.07.035
 142. Shimada T, Mizutani S, Muto T, Yoneya T, Hino R, Takeda S, et al. Cloning and characterization of FGF23 as a causative factor of tumor-induced osteomalacia. *Proc Natl Acad Sci USA.* (2001) 98:6500–5. doi: 10.1073/pnas.101545198
 143. Saito H, Kusano K, Kinoshita M, Ito H, Hirata M, Segawa H, et al. Human fibroblast growth factor-23 mutants suppress Na⁺-dependent phosphate co-transport activity and 1 α ,25-dihydroxyvitamin D₃ production. *J Biol Chem.* (2003) 278:2206–11. doi: 10.1074/jbc.M207872200
 144. Shimada T, Kakitani M, Yamazaki Y, Hasegawa H, Takeuchi Y, Fujita T, et al. Targeted ablation of Fgf23 demonstrates an essential physiological role of FGF23 in phosphate and vitamin D metabolism. *J Clin Invest.* (2004) 113:561–8. doi: 10.1172/JCI200419081

145. Nakatani T, Sarraj B, Ohnishi M, Densmore MJ, Taguchi T, Goetz R, et al. *In vivo* genetic evidence for klotho-dependent, fibroblast growth factor 23 (Fgf23) -mediated regulation of systemic phosphate homeostasis. *FASEB J.* (2009) 23:433–41. doi: 10.1096/fj.08-114397
146. Razzaque MS, Sitara D, Taguchi T, St-Arnaud R, Lanske B. Premature aging-like phenotype in fibroblast growth factor 23 null mice is a vitamin D-mediated process. *FASEB J.* (2006) 20:720–2. doi: 10.1096/fj.05-5432fje
147. Ohnishi M, Nakatani T, Lanske B, Razzaque MS. Reversal of mineral ion homeostasis and soft-tissue calcification of klotho knockout mice by deletion of vitamin D 1 α -hydroxylase. *Kidney Int.* (2009) 75:1166–72. doi: 10.1038/ki.2009.24
148. Hesse M, Frohlich LF, Zeitz U, Lanske B, Erben RG. Ablation of vitamin D signaling rescues bone, mineral, and glucose homeostasis in Fgf-23 deficient mice. *Matrix Biol.* (2007) 26:75–84. doi: 10.1016/j.matbio.2006.10.003
149. Anour R, Andrukhova O, Ritter E, Zeitz U, Erben RG. Klotho lacks a vitamin D independent physiological role in glucose homeostasis, bone turnover, and steady-state PTH secretion *in vivo*. *PLoS ONE.* (2012) 7:e31376. doi: 10.1371/journal.pone.0031376
150. Li YC, Amling M, Pirro AE, Priemel M, Meuse J, Baron R, et al. Normalization of mineral ion homeostasis by dietary means prevents hyperparathyroidism, rickets, and osteomalacia, but not alopecia in vitamin D receptor-ablated mice. *Endocrinology.* (1998) 139:4391–6. doi: 10.1210/endo.139.10.6262
151. Erben RG, Soegiarto DW, Weber K, Zeitz U, Lieberherr M, Gniadecki R, et al. Deletion of deoxyribonucleic acid binding domain of the vitamin D receptor abrogates genomic and non-genomic functions of vitamin D. *Mol Endocrinol.* (2002) 16:1524–37. doi: 10.1210/mend.16.7.0866
152. Andrukhova O, Slavic S, Smorodchenko A, Zeitz U, Shalhoub V, Lanske B, et al. FGF23 regulates renal sodium handling and blood pressure. *EMBO Mol Med.* (2014) 6:744–59. doi: 10.1002/emmm.201303716
153. Andrukhova O, Smorodchenko A, Egerbacher M, Streicher C, Zeitz U, Goetz R, et al. FGF23 promotes renal calcium reabsorption through the TRPV5 channel. *EMBO J.* (2014) 33:229–46. doi: 10.1002/embj.201284188
154. Ben-Dov IZ, Galitzer H, Lavi-Moshayoff V, Goetz R, Kuro-o M, Mohammadi M, et al. The parathyroid is a target organ for FGF23 in rats. *J Clin Invest.* (2007) 117:4003–8. doi: 10.1172/JCI32409
155. Olauson H, Mencke R, Hillebrands JL, Larsson TE. Tissue expression and source of circulating α Klotho. *Bone.* (2017) 100:19–35. doi: 10.1016/j.bone.2017.03.043
156. Xu Y, Sun Z. Regulation of S-formylglutathione hydrolase by the anti-aging gene klotho. *Oncotarget.* (2017) 8:88259–75. doi: 10.18632/oncotarget.19111
157. Grabner A, Amaral AP, Schramm K, Singh S, Sloan A, Yanucil C, et al. Activation of cardiac fibroblast growth factor receptor 4 causes left ventricular hypertrophy. *Cell Metab.* (2015) 22:1020–32. doi: 10.1016/j.cmet.2015.09.002
158. Xiao Z, Riccardi D, Velazquez HA, Chin AL, Yates CR, Carrick JD, et al. A computationally identified compound antagonizes excess FGF-23 signaling in renal tubules and a mouse model of hypophosphatemia. *Sci Signal.* (2016) 9:ra113. doi: 10.1126/scisignal.aaf5034
159. Xiao Z, King G, Mancarella S, Munkhsaikh U, Cao L, Cai C, et al. FGF23 expression is stimulated in transgenic α -Klotho longevity mouse model. *JCI Insight.* (2019) 4:132820. doi: 10.1172/jci.insight.132820
160. Han X, Cai C, Xiao Z, Quarles LD. FGF23 induced left ventricular hypertrophy mediated by FGFR4 signaling in the myocardium is attenuated by soluble Klotho in mice. *J Mol Cell Cardiol.* (2020) 138:66–74. doi: 10.1016/j.yjmcc.2019.11.149
161. Crabtree GR, Olson EN. NFAT signaling: choreographing the social lives of cells. *Cell.* (2002) 109(Suppl.):S67–79. doi: 10.1016/S0092-8674(02)00699-2
162. Faul C, Amaral AP, Oskoue B, Hu MC, Sloan A, Isakova T, et al. FGF23 induces left ventricular hypertrophy. *J Clin Invest.* (2011) 121:4393–408. doi: 10.1172/JCI46122
163. Agoro R, Montagna A, Goetz R, Aligbe O, Singh G, Coe LM, et al. Inhibition of fibroblast growth factor 23 (FGF23) signaling rescues renal anemia. *FASEB J.* (2018) 32:3752–64. doi: 10.1096/fj.201700667R
164. Agoro R, Park MY, Le Henaff C, Jankauskas S, Gaia A, Chen G, et al. C-FGF23 peptide alleviates hypoferrremia during acute inflammation. *Haematologica.* (2020). doi: 10.3324/haematol.2019.237040. [Epub ahead of print].

Conflict of Interest: KW receives royalties from Kyowa-Hakko-Kirin Pharmaceuticals, Inc., and research funding from Akebia-Keryx, both of which had no part in the study design, data collection and analysis, decision to publish, or preparation of this manuscript.

The remaining authors declare that the research was conducted in the absence of any commercial or financial relationships that could be construed as a potential conflict of interest.

Copyright © 2020 Agoro, Ni, Noonan and White. This is an open-access article distributed under the terms of the Creative Commons Attribution License (CC BY). The use, distribution or reproduction in other forums is permitted, provided the original author(s) and the copyright owner(s) are credited and that the original publication in this journal is cited, in accordance with accepted academic practice. No use, distribution or reproduction is permitted which does not comply with these terms.



Influence of HIV Infection and Antiretroviral Therapy on Bone Homeostasis

María Victoria Delpino^{1*} and Jorge Quarleri^{2*}

¹ Instituto de Inmunología, Genética y Metabolismo (INIGEM), Universidad de Buenos Aires, CONICET, Buenos Aires, Argentina, ² Instituto de Investigaciones Biomédicas en Retrovirus y Sida (INBIRS), Universidad de Buenos Aires, CONICET, Buenos Aires, Argentina

OPEN ACCESS

Edited by:

Lilian Irene Plotkin,
Indiana University Bloomington,
United States

Reviewed by:

Marlena Cathorina Kruger,
Massey University, New Zealand
Mohamed El Sayed Abdel Wanis,
Sohag University, Egypt

*Correspondence:

María Victoria Delpino
mdelpino@ffyb.uba.ar
Jorge Quarleri
quarleri@fmed.uba.ar

Specialty section:

This article was submitted to
Bone Research,
a section of the journal
Frontiers in Endocrinology

Received: 07 April 2020

Accepted: 23 June 2020

Published: 02 September 2020

Citation:

Delpino MV and Quarleri J (2020)
Influence of HIV Infection and
Antiretroviral Therapy on Bone
Homeostasis.
Front. Endocrinol. 11:502.
doi: 10.3389/fendo.2020.00502

The human immunodeficiency virus type 1 (HIV)/AIDS pandemic represents the most significant global health challenge in modern history. This infection leads toward an inflammatory state associated with chronic immune dysregulation activation that tilts the immune-skeletal interface and its deep integration between cell types and cytokines with a strong influence on skeletal renewal and exacerbated bone loss. Hence, reduced bone mineral density is a complication among HIV-infected individuals that may progress to osteoporosis, thus increasing their prevalence of fractures. Highly active antiretroviral therapy (HAART) can effectively control HIV replication but the regimens, that include tenofovir disoproxil fumarate (TDF), may accelerate bone mass density loss. Molecular mechanisms of HIV-associated bone disease include the OPG/RANKL/RANK system dysregulation. Thereby, osteoclastogenesis and osteolytic activity are promoted after the osteoclast precursor infection, accompanied by a deleterious effect on osteoblast and its precursor cells, with exacerbated senescence of mesenchymal stem cells (MSCs). This review summarizes recent basic research data on HIV pathogenesis and its relation to bone quality. It also sheds light on HAART-related detrimental effects on bone metabolism, providing a better understanding of the molecular mechanisms involved in bone dysfunction and damage as well as how the HIV-associated imbalance on the gut microbiome may contribute to bone disease.

Keywords: HIV, HAART, bone, osteoblast, osteoclast

INTRODUCTION

According to UNAIDS, 37.9 million people worldwide are currently living with HIV/AIDS and about 22 million are on highly active antiretroviral therapy (HAART). The life expectancy of HIV-infected individuals treated with HAART is nearly normal, with a decreased incidence in AIDS-related morbidity and mortality (1).

Low bone mineral density (BMD) has frequently been observed among HIV-infected individuals, likely leading to osteopenia and osteoporosis with a high prevalence of fractures compared with the general population (2).

In HIV-infected patients, bone loss is primarily enhanced by two pivotal factors: HIV infection and its direct consequences, and HAART, mainly during the first years of treatment (3–8). The contribution of each one is still controversial. The evidence of reduced bone mass in treatment-naïve patients indicates that the virus alone directly affects bone homeostasis (9–14). Moreover,

some reports indicate that low BMD is not completely attributable to HIV infection alone or HIV infection plus treatments with HAART (15–23).

The bone as part of the skeletal system interacts with immune cells in the bone marrow, interacting with each other in a significant mutual influence (24). Recently, the molecular mechanisms involved in the homeostatic interactions between bone and immune cells has been elucidated (25–27), which HIV appears to be able to disturb.

MICROBIOTA CONTRIBUTION IN HIV INTERACTION WITH BONE

HIV Proteins

HIV genes encode regulatory, auxiliary, and structural proteins. The regulatory proteins include the HIV trans-activator (Tat) involved in the regulation of the reverse transcription of the viral genome, and the regulator of expression of virion proteins (Rev) responsible for the synthesis of major viral proteins. The auxiliary HIV proteins comprise the negative factor (Nef), which is implicated in multiple functions during the viral replication cycle, including, among other functions, the lentivirus protein R (Vpr) responsible for nuclear import of the pre-integration complex. It is also comprised of the viral infectivity factor (Vif) required to synthesize infectious viruses in several human cells and the virus protein U (Vpu) the main role of which is the successful release of virions from infected cells. The structural proteins included the group-specific antigen (p55 gag polyprotein), a polyprotein which is processed by viral proteases during maturation to matrix protein (p17), capsid protein (p24), spacer peptide 1 (p2), nucleocapsid protein (p7), spacer peptide 2 (p1), and P6 protein. Other structural proteins involve the polymerase (Pol) and the envelope protein (gp160) that is post-translationally processed to produce the surface glycoprotein (gp120) and gp41 that mediate binding to the CD4 receptor, and envelope fusion to target cells, respectively (28).

Interaction of HIV and Its Proteins With Bone Cells

Among many of the viral pathogenic mechanisms, HIV regulatory, auxiliary, and structural proteins play critical roles during cell-host interaction and thus have shown significant impacts on bone in experimental studies, promoting changes in the balance of bone formation and resorption. It is important to highlight that the HIV-induced detrimental effects on cells are not only a consequence of the active viral replication and the role of infectious virions but are also caused by several HIV proteins that are released to extracellular media which could induce bystander harmful effects, such as apoptosis, oxidative stress, mitochondrial dysfunctions, or autophagy alterations, on surrounding cells (29, 30).

Mesenchymal stem cells (MSCs) are multipotent precursors able to differentiate toward multiple tissue lineages such as adipocytes, chondroblasts, and osteoblasts (31, 32). As MSCs express CD4 receptors and CCR5 and CXCR4 coreceptors, these cells are likely susceptible to HIV infection, although integrated

proviruses are rarely found and productive infection has not yet been documented (33). Nonetheless, hematopoietic progenitor cells (HPCs) in the bone marrow of HIV-infected individuals have been regarded as a persistent HIV reservoir (34).

Differentiation of MSCs *ex vivo* into both osteoblasts and adipocytes depicted a dichotomy upon exposure to the serum source, since those in contact with a high HIV viral load preferentially acquired a proadipogenic phenotype whereas those in contact with low viral load serum were induced toward an osteogenic condition. This phenomenon may involve Tat protein, which inhibits the transcription factor COUP TF-I (chicken ovalbumin upstream promoter transcription factor), thus favoring adipocyte differentiation while preventing osteoblast development.

To command the balance of bone resorption and formation, osteoblasts produce a receptor activator factor of nuclear factor- κ B ligand (RANKL) that controls the differentiation of osteoclasts (35). Osteocytes -the terminally differentiated form of osteoblast- also produce RANKL to regulate osteoclast activity (36). Under physiological conditions, osteoclastogenesis involves RANKL and macrophage colony-stimulating factor (M-CSF) produced by osteoblast and bone marrow stromal cells (37). M-CSF prompts the expression of RANKL receptor (RANK), on osteoclast precursor which then interacts with RANKL to initiate osteoclasts' differentiation (38). As a counterpart, osteoprotegerin (OPG) is a neutralizing soluble trap receptor expressed by bone marrow stromal cells and osteoblasts able to inhibit the RANKL-RANK interaction (39).

The Tat protein enhances peripheral blood monocyte-derived osteoclast differentiation and activity by RANKL plus M-CSF treatment, which increases both the mRNA transcription of specific osteoclast differentiation markers, such as cathepsin K and calcitonin receptor, and the tartrate-resistant acidic phosphatase (TRAP) expression and activity. Together, these results show that Tat may be considered a viral factor that stimulates osteoclastogenesis and bone resorption activity (11, 40–42). *In vitro*, Tat and Nef proteins reduce -in a cumulative manner- the number of bone marrow MSCs available to differentiate into osteoblasts by inducing early senescence, associated with increased oxidative stress and mitochondrial dysfunction of these cells. Moreover, Tat, but not Nef, induced an early increase in NF- κ B activity and cytokine/chemokine secretion, and reciprocally, Nef- but no Tat-treated cells -have shown early autophagy inhibition (43).

The HIV accessory protein Vpr upregulates the RANKL expression in peripheral mononuclear cells from healthy donors, enhancing osteoclastic activity. This action is synergized by both exogenous and endogenous glucocorticoids as a potent cofactor in bone mineral loss (44). Moreover, Tat and Rev proteins increase monocyte differentiation into osteoclasts, as well as boost osteoclast resorption function by increasing reactive oxygen species and TNF- α production in osteoclast precursors (45, 46).

In an *in vivo* humanized mice and *ex vivo* human joint tissue study, Raynaud-Messina et al. have contributed to our current understanding of the HIV-induced bone loss mechanisms. For the first time, the authors demonstrated that

HIV infects osteoclast precursors even at different stages of osteoclastogenesis, either via cell-free viruses or, more efficiently, through transfer from infected T cells. These infected precursor cells have been proposed as HIV reservoirs that display a greater migratory capacity and exhibit the enhanced ability to recruit and concentrate in the bones where the viral infection alters the bone resorption machinery. HIV can enlarge podosomes and enhance the osteolytic activity of the bone resorption apparatus, also known as the “sealing zone” (SZ). The virus is also able to increase the TRAP secretion by osteoclasts, leading to demineralization and degradation of larger bone extensions. These viral-directed actions are Nef-mediated and are abundantly produced and secreted during the early phase of viral replication. Such Nef-mediated actions occur through the activation of Src, which regulates podosomes into the SZ (47).

Soluble HIV-structural proteins are also mediators of cytopathogenic effects. These proteins may act as part of the viral particle or as bystander effect mediators after their release from productively infected cells (48). Both, p55-gag and gp120 were found to reduce calcium deposition, alkaline-phosphatase activity, levels of secreted BMP-2, -7, and RANKL, as well as the expression and activity of the pro-osteogenic transcription factor runt-related transcription factor 2 (RUNX2) in human osteoblasts. The levels of osteocalcin were also significantly reduced by p55-gag treatment, while gp120 also increased the pro-adipogenic transcription factor and peroxisome proliferator-activated receptor γ (PPAR γ) activity. The ability of MSCs to develop into functioning osteoblasts was also affected by the presence of HIV proteins, with p55-gag inducing a decrease in osteogenesis, while rev induced an increase (49). A positive feedback loop exists between RANKL production and HIV replication, which may be relevant to both the pathophysiology of HIV-linked osteopenia and the control of HIV replication (50).

Furthermore, HIV gp120 can trigger *in vitro* osteoblast apoptosis induction mediated by the up-regulation of TNF- α (51). In these cells, gp120 enhances the expression of Dickkopf-1 (Dkk1), the antagonist of the Wnt, significantly reducing the intracytosolic and intranuclear β -catenin expression, the alkaline phosphatase activity, and the cell proliferation (52).

In HIV-infected individuals, B and T lymphocytes have exhibited several signs of dysfunction with an impact on bone homeostasis. They are sources of OPG and, consequently, their dysfunction contributes to viral-induced bone loss. Hence, there is a higher frequency of RANKL-expressing B cells (resting memory and exhausted tissue-like memory B cells) expanded as a consequence of inflammation and a lower frequency of OPG-expressing B cells (resting memory B cells) in HIV-infected compared to HIV-uninfected individuals, thus resulting in a lower RANKL/OPG ratio that correlates with total hip BMD, T-, and Z-scores in the HIV-infected participants (14).

Similarly, T-cell OPG production was also significantly lower in CD4 T-cell-sufficient HIV-infected individuals (>200 cells/ μ l) but not in those with lower cell counts. It was coupled with moderately higher T-cell RANKL production, resulting in a significantly higher T-cell RANKL/OPG ratio. Such a T-cell RANKL/OPG lowered ratio correlated significantly with BMD-derived z-scores at the hip, lumbar

spine, and femur neck (53). Moreover, as a bystander effect, such an abnormal RANKL expression by T cells is mimicked when these cells are exposed to soluble gp120 (Figure 1) (54).

HIV-Related Gut Microbiome Alterations and Its Relationship With Bone Loss

Recently, the gut microbiota has been reported to have an influence on bone metabolism, attracting attention as a prospective new target to balance BMD. The basis of this evidence is mainly concentrated on its involvement in modulating the interface between the immune system and bone cells (55, 56).

As an early event, the gut microbiome in HIV-infected individuals exhibits different compositions compared to uninfected individuals (57, 58). Among them, the bacterial composition is altered on its diversity, genes, and functional capabilities, that are either pro-inflammatory or potentially pathogenic and whose abundance correlated with immune status (59, 60). T-cell depletion is pronounced at the gut-associated lymphoid tissue (GALT) promptly after HIV infection, followed by an increase in the barrier permeability and microbial translocation with increased LPS levels (61). This context induces an innate immune activation leading to a shift toward a pro-inflammatory cytokine environment with osteoclastogenesis and bone resorption enhancement (62, 63).

Since chronic immune activation with progressive immune suppression impacts on the gut microbiome, a differential contribution of gut bacteria and their molecular agents (metabolites and proteins) is desirable to promote immune recovery in HIV-infected individuals. Hence, after characterizing the interplay between the active gut microbiota and the host, it is plausible to reduce inflammation and recover the immune-skeletal interface (64–66).

The HAART treatment effect on gut microbiota in HIV patients is uncertain (67). One hypothesis is that HIV treatment stimulates the restoration of normal microbial flora (68). However, some studies show a minimal effect of HAART on the restoration of normal microbial flora (68–70) while others reveal a negative impact (71).

ROLE OF ANTIRETROVIRAL THERAPY ON BONE TISSUE METABOLISM

The widespread accessibility of HAART has changed HIV from a life-limiting condition to one with a near-normal life expectancy. Unexpectedly, throughout such a therapy, the bone loss promoted by HIV-infection may continue unabated. However, among HIV-infected individuals on HAART, the presence of osteoporosis appears to be about three times higher than those uninfected (3–8). Although, far from consensus, other reports have estimated up to a 6% decrease in BMD upon HAART treatment initiation for a 2-year period, but then the BMD remains unchanged despite continuing therapy (72–74).

As mentioned above, in naïve immunosuppressed HIV-infected individuals a decrease in BMD is observed.

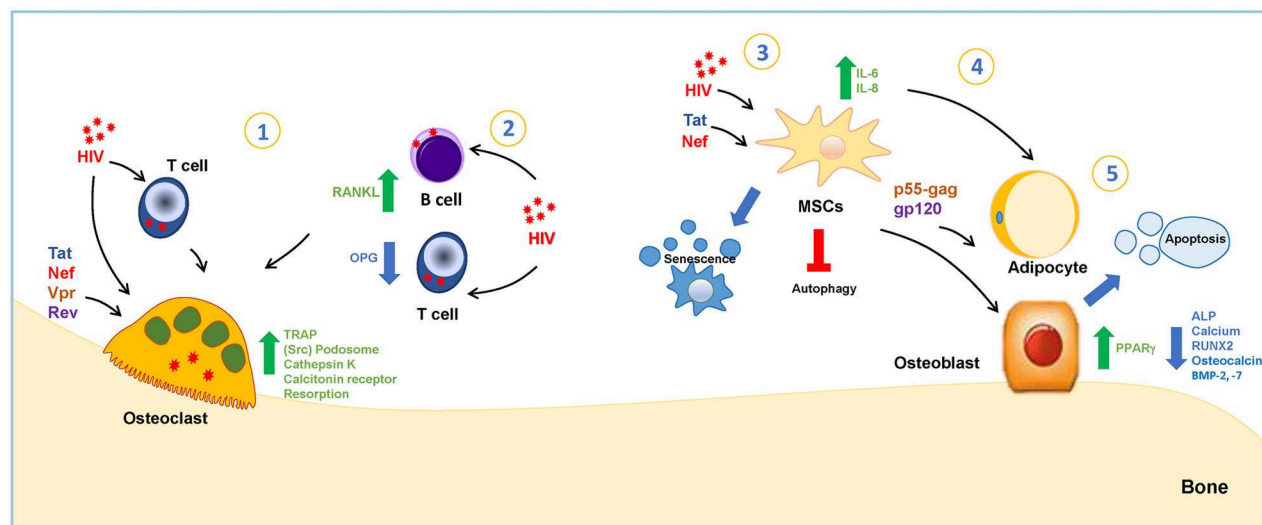


FIGURE 1 | HIV and viral proteins' interaction with bone cells. **1-**HIV infects osteoclasts via cell-free viruses or by cell-to-cell transfer from infected T cells. The infection increases the tartrate-resistant acidic phosphatase (TRAP) secretion by osteoclasts. The viral protein Tat increases mRNA transcription of cathepsin K, calcitonin receptor, TRAP, and Nef-regulate podosomes through activation of Src. Vpr upregulates RANKL expression, stimulating osteoclastogenesis. Tat and Rev increase osteoclastogenesis. **2-**HIV infection induces an increase in RANKL-expression and the reduction of OPG-expression in B and T cells. **3-**HIV proteins Tat and Nef reduce the number of bone marrow MSCs by inducing early senescence. Tat stimulates MSC to secrete IL-6 and IL-8, and Nef induces the inhibition of autophagy. **4-**Human serum with a high HIV viral load preferentially acquired a proadipogenic phenotype in a mechanism dependent on Tat protein, while those in contact with a low viral load serum were induced toward osteogenic conditions. **5-**p55-gag and gp120 stimulate osteoblast apoptosis and reduce alkaline-phosphatase activity (ALP), calcium deposition, the runt-related transcription factor 2 (RUNX-2), and Bone morphogenic protein-2 and -7 (BMP-2–7), and p55-gag also reduces osteocalcin levels, and gp120 induces the increase in peroxisome proliferator-activated receptor γ (PPAR γ).

Paradoxically, when these individuals are on HAART they achieve their immune reconstitution by CD4⁺ T cell repopulation (75, 76). These reports offer evidence of stable or increasing BMD with plausible early, but small and not sustained, loss of BMD that accompanies the initiation of HAART, and without accelerated bone loss in the medium term (77–82).

The gender of the HIV-infected individual also influences the BMD reduction grade. Among HAART-treated patients, it appears to be more accentuated in women than in men (83, 84), but is at a level similar to that observed initially during menopause (85).

Several studies have directly emphasized HIV factors associated with low BMD: duration of infection, HIV viral burden, and a more advanced HIV disease (86–88). In this regard, data presented in a sub-study of the Strategy for Management of Antiretroviral Therapy (SMART) study demonstrated a low level of bone turnover markers but higher BMD when HAART is interrupted, thus inferring a higher HIV RNA level and lower CD4⁺ T cell counts (89). In contrast, Grund et al. have reported that continuous HAART was associated with significant reductions in BMD with no changes or increases in BMD observed in those on intermittent ART (90). Similarly, longitudinal data collected from randomized control trials have insinuated that the initiation of HAART at higher viral RNA and lower CD4⁺ T cell counts at baseline were associated with more pronounced reductions in BMD (88). Such low pre-treatment CD4 counts were reported

as a strong and independent risk factor for loss of BMD during treatment. However, loss of bone continues for up to 2 years after HAART initiation and the extent of immune reconstitution was not related to BMD improvement (88). In conjunction, these data suggest that important roles are played directly by HIV and/or indirectly by the immune response in BMD loss.

The effect of HAART on BMD seems to be influenced by the specific type of treatment. Low BMD has been associated with regimens such as nucleoside analog reverse-transcriptase inhibitors (NRTIs) (74, 91, 92). Individuals exposed to tenofovir disoproxil fumarate (TDF)-based treatment in particular exhibited a more accentuated BMD loss compared to individuals on other regimens, such as lamivudine (3TC) and emtricitabine (FTC), or those who have been switched to two-drug regimens (74, 91–97). However, others have reported contradictory findings regarding TDF-therapy duration and BMD loss, even after long-term exposure to the drug (98).

The underlying mechanisms by which antiretroviral drugs promote BMD loss are still controversial. The mechanism to NRTIs-mediated BMD loss may be promoted by elevated lactic acid concentration in the blood leading to calcium hydroxyapatite loss, especially in the trabecular bone, due to the labile of calcium storage (99). Regarding the underlying mechanisms that may be related to TDF-associated lower BMD, mitochondrial toxicity, hyperphosphaturia secondary to tubular dysfunction, and renal osteodystrophy have been considered

(92, 100–102). Despite the bone loss, there are contradictory findings about phosphate metabolism abnormalities observed among HAART-treated individuals who can present higher phosphate blood levels and lower bone density (86). These data offer supportive information to avoid the use of TDF and its replacement with bone-friendly regimens among the HIV-infected population with fracture risks (103).

Besides the BMD reduction related to NRTIs, available data regarding protease inhibitors (PIs) remain contradictory (104). On the one hand, increased bone turnover, accelerated bone loss, and a higher prevalence of reduced BMD have been reported (3, 72, 92, 105–107), whereas other studies showed opposed results (9, 10, 73, 108). Detrimental effects on BMD are in line with *in vitro* observations evaluating the effect of different PIs on osteoblast activity (109). For example, pharmacologic levels of two PIs that are clinically linked to osteopenia, ritonavir (RTV) and saquinavir (SQV) but not indinavir (IDV) and nelfinavir (NFV), abolish the interferon- γ -mediated degradation of the RANKL signaling adapter protein TRAF6 (tumor necrosis factor receptor-associated protein 6) in proteasomes. Moreover, under inflammatory conditions, interferon- γ promotes bone loss mainly by up-regulating the activity of macrophages, leading to T cell activation and osteoclastogenic cytokine production (110).

RTV appears as an osteoclast-activating agent that promotes the proliferation and activation of osteoclasts *in vitro* (111, 112) and *ex vivo* studies (113), causing increased bone absorption.

Importantly, most of these *in vitro* direct effects of PIs on bone cells did not resemble the *in vivo* observations collected from patients on HAART. RTV, SQV, and fosamprenavir (FPV) appear to improve the BMD *in vitro* rather than the loss observed *in vivo*, by decreasing RANKL and increasing OPG secretion (54, 109). The impact on BMD loss was also reported in several *in vivo* studies which also observed a strong difference in bone loss according to PI discontinued and continued schemes between patients (72, 92, 107). RTV -but not IDV- at a greater than normal concentration was able to inhibit osteoclast function and suppress osteoclastogenesis *in vitro* and *in vivo* by impairing RANKL-induced signaling (114). However, RTV at plasma concentration, as a PI-boosting drug, favors the differentiation of blood monocytes into osteoclasts by up-regulating the production of transcripts for osteoclast growth factors using the non-canonical Wnt proteins 5B and 7B as well as activated promoters of nuclear factor-kappaB signaling, but suppressing genes involved in canonical Wnt signaling. Additionally, RTV blocks the cytoplasmic-to-nuclear translocation of β -catenin, the molecular node of the Wnt signaling pathway, in association with enhanced β -catenin ubiquitination (111, 112). *In vivo*, among RTV-treated patients, its discontinuation resulted in a slower decrease in BMD (107), and the bone mineral loss appeared in a time-dependent manner irrespective of dosage (107). Other PIs, such as IDV and NFV, have been shown to have a negative impact on osteoblasts by impairing its alkaline phosphatase activity and calcium

deposition. Lastly, *in vivo* and *in vitro* studies demonstrate that PIs atazanavir (ATV) and lopinavir (LPV) also decrease BMD by impairing the MSCs differentiation to osteoblasts (72, 92, 115).

Finally, in addition to immune cells, the HIV-coreceptor CCR5 has been involved in the regulation of the function of bone cells by directly modulating osteoclastogenesis and the communication between osteoclasts and osteoblasts (116–118). In this regard, epidemiological evidence suggests that the functional loss of CCR5 is correlated with a lower incidence of bone-destructive diseases as well as of HIV transmission. Using a CCR5-deficient murine model, the osteoclasts appeared dysfunctional in their cellular locomotion and bone-resorption activity, which is associated with the disarrangement of podosomes and adhesion complex molecules including Pyk2. Such an experimental model exhibited an osteoporosis-resistance induced by RANKL (119). These data are in line with a previous study showing the CCR5-antagonist Maraviroc associated with a lower degree of bone loss in the hip and lumbar spine of HIV-infected individuals, as an example of a CCR5-antagonist treatment that might help to improve bone health among HIV-infected patients (120).

In conclusion, important progress has been made in our understanding of the effect of antiretroviral drugs on bone health in HIV-infected people. Such advances have enriched our ability to apply treatment to diminish aging-associated complications, such as osteoporosis and fractures.

CONCLUDING REMARKS

During HIV infection and its progression to AIDS, bone loss occurs and HAART likely contributes -at least in part- to this comorbidity, involving both factors associated with disease reversal and direct skeletal effects. Although the clinical and imaging characterization of HIV bone pathology has been well-documented, the pathogenic mechanisms of bone loss have only been partially elucidated at present.

Irrespective of the mechanisms involved, diagnostic and therapeutic measures are necessary to delay the onset of bone disease in HIV patients to prevent a significant new threat to the health of the HIV/AIDS population.

AUTHOR CONTRIBUTIONS

MD and JQ conceived the idea and drafted the manuscript. All authors contributed to the article and approved the submitted version.

FUNDING

This work was supported by grant from Agencia Nacional de Promoción Científica y Tecnológica (ANPCYT, Argentina) PICT 2015-0316.

REFERENCES

- Back D, Marzolini C. The challenge of HIV treatment in an era of polypharmacy. *J Int AIDS Soc.* (2020) 23:e25449. doi: 10.1002/jia2.25449
- Cotter AG, Mallon PW. The effects of untreated and treated HIV infection on bone disease. *Curr Opin HIV AIDS.* (2014) 9:17–26. doi: 10.1097/COH.0000000000000028
- Brown TT, Qaqish RB. Antiretroviral therapy and the prevalence of osteopenia and osteoporosis: a meta-analytic review. *Aids.* (2006) 20:2165–74. doi: 10.1097/QAD.0b013e32801022eb
- Powderly WG. Osteoporosis and bone health in HIV. *Current HIV/AIDS Reports.* (2012) 9:218–22. doi: 10.1007/s11904-012-0119-7
- Maffezzoni F, Porcelli T, Karamouzian I, Quiros-Roldan E, Castelli F, Mazziotti G, et al. Osteoporosis in human immunodeficiency virus patients - an emerging clinical concern. *Eur Endocrinol.* (2014) 10:79–83. doi: 10.17925/EE.2014.10.1.79
- Cervero M, Torres R, Agud JL, Alcazar V, Jurdado JJ, Garcia-Lacalle C, et al. Prevalence of and risk factors for low bone mineral density in Spanish treated HIV-infected patients. *PLoS ONE.* (2018) 13:e0196201. doi: 10.1371/journal.pone.0196201
- Calmy A, Chevalley T, Delhumeau C, Toutous-Trellu L, Spycher-Elbes R, Ratib O, et al. Long-term HIV infection and antiretroviral therapy are associated with bone microstructure alterations in premenopausal women. *Osteoporos Int.* (2013) 24:1843–52. doi: 10.1007/s00198-012-2189-1
- Dalla Grana E, Rigo F, Lanzafame M, Lattuada E, Suardi S, Mottes M, et al. Relationship between vertebral fractures, bone mineral density, and osteometabolic profile in HIV and hepatitis B and C-infected patients treated with ART. *Front Endocrinol.* (2019) 10:302. doi: 10.3389/fendo.2019.00302
- Arnst JH, Freeman R, Howard AA, Floris-Moore M, Santoro N, Schoenbaum EE. HIV infection and bone mineral density in middle-aged women. *Clin Infect Diseases.* (2006) 42:1014–20. doi: 10.1086/501015
- Bruera D, Luna N, David DO, Bergoglio LM, Zamudio J. Decreased bone mineral density in HIV-infected patients is independent of antiretroviral therapy. *Aids.* (2003) 17:1917–23. doi: 10.1097/00002030-200309050-00010
- Gibellini D, Borderi M, De Crignis E, Cicola R, Vescini F, Caudarella R, et al. RANKL/OPG/TRAIL plasma levels and bone mass loss evaluation in antiretroviral naive HIV-1-positive men. *J Med Virol.* (2007) 79:1446–54. doi: 10.1002/jmv.20938
- Teichmann J, Stephan E, Lange U, Discher T, Friese G, Lohmeyer J, et al. Osteopenia in HIV-infected women prior to highly active antiretroviral therapy. *J Infect.* (2003) 46:221–7. doi: 10.1053/jinf.2002.1109
- Wattanachanya L, Jantrapakde J, Avihingsanon A, Ramautarsing R, Kerr S, Trachunthong D, et al. Antiretroviral-naive HIV-infected patients had lower bone formation markers than HIV-uninfected adults. *AIDS Care.* (2020) 32:984–93. doi: 10.1080/09540121.2019.1622631
- Titanji K, Vunnavu A, Sheth AN, Delille C, Lennox JL, Sanford SE, et al. Dysregulated B cell expression of RANKL and OPG correlates with loss of bone mineral density in HIV infection. *PLoS Pathog.* (2014) 10:e1004497. doi: 10.1371/journal.ppat.1004497
- Grijns ML, Vrouwenraets SM, Steingrover R, Lips P, Reiss P, Wit FW, et al. High prevalence of reduced bone mineral density in primary HIV-1-infected men. *Aids.* (2010) 24:2233–8. doi: 10.1097/QAD.0b013e3283c393fe
- Grijns ML, Vrouwenraets SM, Wit FW, Stolte IG, Prins M, Lips P, et al. Low bone mineral density, regardless of HIV status, in men who have sex with men. *J Infect Dis.* (2013) 207:386–91. doi: 10.1093/infdis/jis687
- Bolland MJ, Grey A, Reid IR. Skeletal health in adults with HIV infection. *Lancet Diabetes Endocrinol.* (2015) 3:63–74. doi: 10.1016/S2213-8587(13)70181-5
- Jimenez B, Sainz T, Diaz L, Mellado MJ, Navarro ML, Rojo P, et al. Low bone mineral density in vertically HIV-infected children and adolescents: risk factors and the role of t-cell activation and senescence. *Pediatric Infect Disease J.* (2017) 36:578–83. doi: 10.1097/INF.0000000000001506
- Jones S, Restrepo D, Kasowitz A, Korenstein D, Wallenstein S, Schneider A, et al. Risk factors for decreased bone density and effects of HIV on bone in the elderly. *Osteoporos Int.* (2008) 19:913–8. doi: 10.1007/s00198-007-0524-8
- Knobel H, Guelar A, Vallecillo G, Nogues X, Diez A. Osteopenia in HIV-infected patients: is it the disease or is it the treatment? *Aids.* (2001) 15:807–8. doi: 10.1097/00002030-200104130-00022
- Starup-Linde J, Rosendahl SB, Storgaard M, Langdahl B. Management of osteoporosis in patients living with HIV-A systematic review and meta-analysis. *J Acquired Immune Deficiency Syndromes.* (2020) 83:1–8. doi: 10.1097/QAI.0000000000002207
- Yin M, Dobkin J, Brudney K, Becker C, Zadel JL, Manandhar M, et al. Bone mass and mineral metabolism in HIV+ postmenopausal women. *Osteoporos Int.* (2005) 16:1345–52. doi: 10.1007/s00198-005-1845-0
- Tebas P, Powderly WG, Claxton S, Marin D, Tantisiriwat W, Teitelbaum SL, et al. Accelerated bone mineral loss in HIV-infected patients receiving potent antiretroviral therapy. *Aids.* (2000) 14:F63–7. doi: 10.1097/00002030-200003100-00005
- Tsukasaki M, Takayanagi H. Osteoimmunology: evolving concepts in bone-immune interactions in health and disease. *Nat Rev Immunol.* (2019) 19:626–42. doi: 10.1038/s41577-019-0178-8
- Takayanagi H. Osteoimmunology - bidirectional dialogue and inevitable union of the fields of bone and immunity. *Proc Jpn Acad Ser B Phys Biol Sci.* (2020) 96:159–69. doi: 10.2183/pjab.96.013
- Arron JR, Choi Y. Bone versus immune system. *Nature.* (2000) 408:535–6. doi: 10.1038/35046196
- Takayanagi H, Ogasawara K, Hida S, Chiba T, Murata S, Sato K, et al. T-cell-mediated regulation of osteoclastogenesis by signalling cross-talk between RANKL and IFN-gamma. *Nature.* (2000) 408:600–5. doi: 10.1038/35046102
- German Advisory Committee Blood SAoPTbB. Human immunodeficiency virus (HIV). *Transfus Med Hemother.* (2016) 43:203–22. doi: 10.1159/000445852
- Liu Z, Xiao Y, Torresilla C, Rassart E, Barbeau B. Implication of different HIV-1 genes in the modulation of autophagy. *Viruses.* (2017) 9:389. doi: 10.3390/v9120389
- Welch JL, Stapleton JT, Okeoma CM. Vehicles of intercellular communication: exosomes and HIV-1. *J Gen Virol.* (2019) 100:350–66. doi: 10.1099/jgv.0.001193
- Verma S, Rajaratnam JH, Denton J, Hoyland JA, Byers RJ. Adipocytic proportion of bone marrow is inversely related to bone formation in osteoporosis. *J Clin Pathol.* (2002) 55:693–8. doi: 10.1136/jcp.55.9.693
- Kim BS, Kim JS, Sung HM, You HK, Lee J. Cellular attachment and osteoblast differentiation of mesenchymal stem cells on natural cuttlefish bone. *J Biomed Mater Res A.* (2012) 100:1673–9. doi: 10.1002/jbm.a.34113
- Nazari-Shafti TZ, Freisinger E, Roy U, Bulot CT, Sensi C, Dupin CL, et al. Mesenchymal stem cell derived hematopoietic cells are permissive to HIV-1 infection. *Retrovirology.* (2011) 8:3. doi: 10.1186/1742-4690-8-3
- McNamara LA, Onafuwa-Nuga A, Sebastian NT, Riddell Jt, Bixby D, Collins KL. CD133+ hematopoietic progenitor cells harbor HIV genomes in a subset of optimally treated people with long-term viral suppression. *J Infect Dis.* (2013) 207:1807–16. doi: 10.1093/infdis/jit118
- Karner CM, Long F. Wnt signaling and cellular metabolism in osteoblasts. *Clin Mol Life Sci.* (2017) 74:1649–57. doi: 10.1007/s00018-016-2425-5
- Chen H, Senda T, Kubo KY. The osteocyte plays multiple roles in bone remodeling and mineral homeostasis. *Med Mol Morphol.* (2015) 48:61–8. doi: 10.1007/s00795-015-0099-y
- Lampiasi N, Russo R, Zito F. The Alternative Faces of Macrophage Generate Osteoclasts. *Biomed Res Int.* (2016) 2016:9089610. doi: 10.1155/2016/9089610
- Yasuda H, Shima N, Nakagawa N, Yamaguchi K, Kinoshita M, Mochizuki S, et al. Osteoclast differentiation factor is a ligand for osteoprotegerin/osteoclastogenesis-inhibitory factor and is identical to TRANCE/RANKL. *Proc Natl Acad Sci USA.* (1998) 95:3597–602. doi: 10.1073/pnas.95.7.3597
- Grundt A, Grafe IA, Liegibel U, Sommer U, Nawroth P, Kasperk C. Direct effects of osteoprotegerin on human bone cell metabolism. *Biochem Biophys Res Commun.* (2009) 389:550–5. doi: 10.1016/j.bbrc.2009.09.026
- Cotter EJ, Chew N, Powderly WG, Doran PP. HIV type 1 alters mesenchymal stem cell differentiation potential and cell phenotype *ex vivo*. *AIDS Res Hum Retroviruses.* (2011) 27:187–99. doi: 10.1089/aid.2010.0114
- Gibellini D, De Crignis E, Ponti C, Borderi M, Clo A, Misserocchi A, et al. HIV-1 Tat protein enhances RANKL/M-CSF-mediated osteoclast differentiation. *Biochem Biophys Res Commun.* (2010) 401:429–34. doi: 10.1016/j.bbrc.2010.09.071

42. Caldwell RL, Gadipatti R, Lane KB, Shepherd VL. HIV-1 TAT represses transcription of the bone morphogenic protein receptor-2 in U937 monocytic cells. *J Leukoc Biol.* (2006) 79:192–201. doi: 10.1189/jlb.0405194
43. Beaupere C, Garcia M, Larghero J, Feve B, Capeau J, Lagathu C. The HIV proteins Tat and Nef promote human bone marrow mesenchymal stem cell senescence and alter osteoblastic differentiation. *Aging Cell.* (2015) 14:534–46. doi: 10.1111/ace.12308
44. Fakruddin JM, Laurence J. HIV-1 Vpr enhances production of receptor of activated NF-kappaB ligand (RANKL) via potentiation of glucocorticoid receptor activity. *Arch Virol.* (2005) 150:67–78. doi: 10.1007/s00705-004-0395-7
45. Chew N, Tan E, Li L, Lim R. HIV-1 tat and rev upregulates osteoclast bone resorption. *J Int AIDS Soc.* (2014) 17(4 Suppl. 3):19724. doi: 10.7448/IAS.17.4.19724
46. Agidighi TS, Kim C. Reactive oxygen species in osteoclast differentiation and possible pharmaceutical targets of ROS-mediated osteoclast diseases. *Int J Mol Sci.* (2019) 20:3576. doi: 10.3390/ijms20143576
47. Raynaud-Messina B, Bracq L, Dupont M, Souriant S, Usmani SM, Proag A, et al. Bone degradation machinery of osteoclasts: an HIV-1 target that contributes to bone loss. *Proc Natl Acad Sci USA.* (2018) 115:E2556–65. doi: 10.1073/pnas.1713701115
48. Ran X, Ao Z, Trajtmann A, Xu W, Kobinger G, Keynan Y, et al. HIV-1 envelope glycoprotein stimulates viral transcription and increases the infectivity of the progeny virus through the manipulation of cellular machinery. *Sci Rep.* (2017) 7:9487. doi: 10.1038/s41598-017-10272-7
49. Cotter EJ, Malizia AP, Chew N, Powderly WG, Doran PP. HIV proteins regulate bone marker secretion and transcription factor activity in cultured human osteoblasts with consequent potential implications for osteoblast function and development. *AIDS Res Hum Retroviruses.* (2007) 23:1521–30. doi: 10.1089/aid.2007.0112
50. Fakruddin JM, Laurence J. Interactions among human immunodeficiency virus (HIV)-1, interferon-gamma and receptor of activated NF-kappa B ligand (RANKL): implications for HIV pathogenesis. *Clin Exp Immunol.* (2004) 137:538–45. doi: 10.1111/j.1365-2249.2004.02568.x
51. Gibellini D, De Crignis E, Ponti C, Cimatti L, Borderi M, Tschon M, et al. HIV-1 triggers apoptosis in primary osteoblasts and HOBIT cells through TNFalpha activation. *J Med Virol.* (2008) 80:1507–14. doi: 10.1002/jmv.21266
52. Butler JS, Dunning EC, Murray DW, Doran PP, O'Byrne JM. HIV-1 protein induced modulation of primary human osteoblast differentiation and function via a Wnt/beta-catenin-dependent mechanism. *J Orthop Res.* (2013) 31:218–26. doi: 10.1002/jor.22196
53. Titanji K, Vunnavu A, Foster A, Sheth AN, Lennox JL, Knezevic A, et al. T-cell receptor activator of nuclear factor-kappaB ligand/osteoprotegerin imbalance is associated with HIV-induced bone loss in patients with higher CD4+ T-cell counts. *Aids.* (2018) 32:885–94. doi: 10.1097/QAD.0000000000001764
54. Fakruddin JM, Laurence J. HIV envelope gp120-mediated regulation of osteoclastogenesis via receptor activator of nuclear factor kappa B ligand (RANKL) secretion and its modulation by certain HIV protease inhibitors through interferon-gamma/RANKL cross-talk. *J Biol Chem.* (2003) 278:48251–8. doi: 10.1074/jbc.M304676200
55. Yan J, Charles JF. Gut microbiome and bone: to build, destroy, or both? *Curr Osteoporosis Rep.* (2017) 15:376–84. doi: 10.1007/s11914-017-0382-z
56. Locantore P, Del Gatto V, Gelli S, Paragliola RM, Pontecorvi A. The interplay between immune system and microbiota in osteoporosis. *Mediators Inflamm.* (2020) 2020:3686749. doi: 10.1155/2020/3686749
57. Mudd JC, Brenchley JM. Gut mucosal barrier dysfunction, microbial dysbiosis, and their role in HIV-1 disease progression. *J Infect Dis.* (2016) 214 (Suppl. 2):S58–66. doi: 10.1093/infdis/jiw258
58. Tuddenham SA, Koay WLA, Zhao N, White JR, Ghanem KG, Sears CL, et al. The impact of human immunodeficiency virus infection on gut microbiota alpha-diversity: an individual-level meta-analysis. *Clin Infect Diseases.* (2020) 70:615–27. doi: 10.1093/cid/ciz258
59. Vazquez-Castellanos JF, Serrano-Villar S, Latorre A, Artacho A, Ferrus ML, Madrid N, et al. Altered metabolism of gut microbiota contributes to chronic immune activation in HIV-infected individuals. *Mucosal Immunol.* (2015) 8:760–72. doi: 10.1038/mi.2014.107
60. Alzahrani J, Hussain T, Simar D, Palchaudhuri R, Abdel-Mohsen M, Crowe SM, et al. Inflammatory and immunometabolic consequences of gut dysfunction in HIV: parallels with IBD and implications for reservoir persistence and non-AIDS comorbidities. *EBioMedicine.* (2019) 46:522–31. doi: 10.1016/j.ebiom.2019.07.027
61. Storm-Larsen C, Stiksrud B, Eriksen C, Nowak P, Holm K, Thalme A, et al. Microbial translocation revisited: targeting the endotoxin potential of gut microbes in HIV-infected individuals. *Aids.* (2019) 33:645–53. doi: 10.1097/QAD.0000000000002087
62. McGinty T, Mirmonef P, Mallon PW, Landay AL. Does systemic inflammation and immune activation contribute to fracture risk in HIV? *Current Opinion HIV AIDS.* (2016) 11:253–60. doi: 10.1097/COH.0000000000000275
63. Gootenberg DB, Paer JM, Luevano JM, Kwon DS. HIV-associated changes in the enteric microbial community: potential role in loss of homeostasis and development of systemic inflammation. *Curr Opin Infect Dis.* (2017) 30:31–43. doi: 10.1097/QCO.0000000000000341
64. Serrano-Villar S, Rojo D, Martinez-Martinez M, Deusch S, Vazquez-Castellanos JF, Bargiela R, et al. Gut bacteria metabolism impacts immune recovery in HIV-infected individuals. *EBioMedicine.* (2016) 8:203–16. doi: 10.1016/j.ebiom.2016.04.033
65. Wang Z, Usyk M, Sollecito CC, Qiu Y, Williams-Nguyen J, Hua S, et al. Altered gut microbiota and host metabolite profiles in HIV-infected women. *Clin Infect Diseases.* (2019). doi: 10.1093/cid/ciz1117. [Epub ahead of print].
66. Lu W, Feng Y, Jing F, Han Y, Lyu N, Liu F, et al. Association between gut microbiota and CD4 recovery in HIV-1 infected patients. *Front Microbiol.* (2018) 9:1451. doi: 10.3389/fmicb.2018.01451
67. Nowak RG, Bentzen SM, Ravel J, Crowell TA, Dauda W, Ma B, et al. Rectal microbiota among HIV-uninfected, untreated HIV, and treated HIV-infected in Nigeria. *Aids.* (2017) 31:857–62. doi: 10.1097/QAD.0000000000001409
68. Nowak P, Trosheid M, Avershina E, Barqasho B, Neogi U, Holm K, et al. Gut microbiota diversity predicts immune status in HIV-1 infection. *Aids.* (2015) 29:2409–18. doi: 10.1097/QAD.0000000000000869
69. Lozupone CA, Rhodes ME, Neff CP, Fontenot AP, Campbell TB, Palmer BE. HIV-induced alteration in gut microbiota: driving factors, consequences, and effects of antiretroviral therapy. *Gut Microbes.* (2014) 5:562–70. doi: 10.4161/gmic.32132
70. Lozupone CA, Li M, Campbell TB, Flores SC, Linderman D, Gebert MJ, et al. Alterations in the gut microbiota associated with HIV-1 infection. *Cell Host Microbe.* (2013) 14:329–39. doi: 10.1016/j.chom.2013.08.006
71. Zilberman-Schapiro G, Zmora N, Itav S, Bashardes S, Elinav H, Elinav E. The gut microbiome in human immunodeficiency virus infection. *BMC Med.* (2016) 14:83. doi: 10.1186/s12916-016-0625-3
72. Duvivier C, Kolta S, Assoumou L, Ghosn J, Rozenberg S, Murphy RL, et al. Greater decrease in bone mineral density with protease inhibitor regimens compared with nonnucleoside reverse transcriptase inhibitor regimens in HIV-1 infected naive patients. *Aids.* (2009) 23:817–24. doi: 10.1097/QAD.0b013e328328f789
73. Brown TT, McComsey GA, King MS, Qaqish RB, Bernstein BM, da Silva BA. Loss of bone mineral density after antiretroviral therapy initiation, independent of antiretroviral regimen. *J Acquired Immune Deficiency Syndromes.* (2009) 51:554–61. doi: 10.1097/QAI.0b013e3281adce44
74. Gallant JE, Staszewski S, Pozniak AL, DeJesus E, Suleiman JM, Miller MD, et al. Efficacy and safety of tenofovir DF vs stavudine in combination therapy in antiretroviral-naïve patients: a 3-year randomized trial. *JAMA.* (2004) 292:191–201. doi: 10.1001/jama.292.2.191
75. Ofotokun I, Titanji K, Vikulina T, Roser-Page S, Yamaguchi M, Zayzafoon M, et al. Role of T-cell reconstitution in HIV-1 antiretroviral therapy-induced bone loss. *Nat Commun.* (2015) 6:8282. doi: 10.1038/ncomms9282
76. Ofotokun I, Titanji K, Vunnavu A, Roser-Page S, Vikulina T, Villinger F, et al. Antiretroviral therapy induces a rapid increase in bone resorption that is positively associated with the magnitude of immune reconstitution in HIV infection. *Aids.* (2016) 30:405–14. doi: 10.1097/QAD.0000000000000918
77. Nolan D, Upton R, McKinnon E, John M, James I, Adler B, et al. Stable or increasing bone mineral density in HIV-infected patients treated with nelfinavir or indinavir. *Aids.* (2001) 15:1275–80. doi: 10.1097/00002030-200107060-00009

78. Mondy K, Yarasheski K, Powderly WG, Whyte M, Claxton S, DeMarco D, et al. Longitudinal evolution of bone mineral density and bone markers in human immunodeficiency virus-infected individuals. *Clin Infect Diseases*. (2003) 36:482–90. doi: 10.1086/367569
79. Dolan SE, Kanter JR, Grinspoon S. Longitudinal analysis of bone density in human immunodeficiency virus-infected women. *J Clin Endocrinol Metabolism*. (2006) 91:2938–45. doi: 10.1210/jc.2006-0127
80. Bolland MJ, Grey AB, Horne AM, Briggs SE, Thomas MG, Ellis-Pegler RB, et al. Bone mineral density remains stable in HAART-treated HIV-infected men over 2 years. *Clin Endocrinol*. (2007) 67:270–5. doi: 10.1111/j.1365-2265.2007.02875.x
81. Sharma A, Flom PL, Weedon J, Klein RS. Prospective study of bone mineral density changes in aging men with or at risk for HIV infection. *Aids*. (2010) 24:2337–45. doi: 10.1097/QAD.0b013e32833d7da7
82. Bolland MJ, Grey A, Horne AM, Briggs SE, Thomas MG, Ellis-Pegler RB, et al. Stable bone mineral density over 6 years in HIV-infected men treated with highly active antiretroviral therapy (HAART). *Clin Endocrinol*. (2012) 76:643–8. doi: 10.1111/j.1365-2265.2011.04274.x
83. Kalayjian RC, Albert JM, Cremers S, Gupta SK, McComsey GA, Klingman KL, et al. Women have enhanced bone loss associated with phosphaturia and CD4+ cell restoration during initial antiretroviral therapy. *Aids*. (2018) 32:2517–24. doi: 10.1097/QAD.0000000000001995
84. Erlandson KM, Lake JE, Sim M, Falutz J, Prado CM, Domingues da Silva AR, et al. Bone mineral density declines twice as quickly among HIV-infected women compared with men. *J Acquired Immune Deficiency Syndromes*. (2018) 77:288–94. doi: 10.1097/QAI.0000000000001591
85. Finnerty F, Walker-Bone K, Tariq S. Osteoporosis in postmenopausal women living with HIV. *Maturitas*. (2017) 95:50–4. doi: 10.1016/j.maturitas.2016.10.015
86. Cotter AG, Powderly WG. Endocrine complications of human immunodeficiency virus infection: hypogonadism, bone disease and tenofovir-related toxicity. *Best Pract Res Clin Endocrinol Metab*. (2011) 25:501–15. doi: 10.1016/j.beem.2010.11.003
87. Young B, Dao CN, Buchacz K, Baker R, Brooks JT, Investigators HIVOS. Increased rates of bone fracture among HIV-infected persons in the HIV Outpatient Study (HOPS) compared with the US general population, 2000–2006. *Clin Infect Diseases*. (2011) 52:1061–8. doi: 10.1093/cid/ciq242
88. Grant PM, Kitch D, McComsey GA, Dube MP, Haubrich R, Huang J, et al. Low baseline CD4+ count is associated with greater bone mineral density loss after antiretroviral therapy initiation. *Clin Infect Diseases*. (2013) 57:1483–8. doi: 10.1093/cid/cit538
89. Hoy J, Grund B, Roediger M, Ensrud KE, Brar I, Colebunders R, et al. Interruption or deferral of antiretroviral therapy reduces markers of bone turnover compared with continuous therapy: the SMART body composition substudy. *J Bone Mineral Res*. (2013) 28:1264–74. doi: 10.1002/jbmr.1861
90. Grund B, Peng G, Gibert CL, Hoy JF, Isaksson RL, Shlay JC, et al. Continuous antiretroviral therapy decreases bone mineral density. *Aids*. (2009) 23:1519–29. doi: 10.1097/QAD.0b013e32832c1792
91. Stellbrink HJ, Orkin C, Arribas JR, Compston J, Gerstoft J, Van Wijngaerden E, et al. Comparison of changes in bone density and turnover with abacavir-lamivudine versus tenofovir-emtricitabine in HIV-infected adults: 48-week results from the ASSERT study. *Clin Infect Diseases*. (2010) 51:963–72. doi: 10.1086/656417
92. McComsey GA, Kitch D, Daar ES, Tierney C, Jahed NC, Tebas P, et al. Bone mineral density and fractures in antiretroviral-naïve persons randomized to receive abacavir-lamivudine or tenofovir disoproxil fumarate-emtricitabine along with efavirenz or atazanavir-ritonavir: Aids Clinical Trials Group A5224s, a substudy of ACTG A5202. *J Infect Dis*. (2011) 203:1791–801. doi: 10.1093/infdis/jir188
93. McComsey GA, Lupo S, Parks D, Poggio MC, De Wet J, Kahl LP, et al. Switch from tenofovir disoproxil fumarate combination to dolutegravir with rilpivirine improves parameters of bone health. *Aids*. (2018) 32:477–85. doi: 10.1097/QAD.0000000000001725
94. Aupibul L, Puthanakit T. Review of tenofovir use in HIV-infected children. *Pediatric Infect Disease J*. (2015) 34:383–91. doi: 10.1097/INF.0000000000000571
95. Negredo E, Domingo P, Perez-Alvarez N, Gutierrez M, Mateo G, Puig J, et al. Improvement in bone mineral density after switching from tenofovir to abacavir in HIV-1-infected patients with low bone mineral density: two-centre randomized pilot study (OsteoTDF study). *J Antimicrob Chemotherapy*. (2014) 69:3368–71. doi: 10.1093/jac/dku300
96. Bloch M, Tong WW, Hoy J, Baker D, Lee FJ, Richardson R, et al. Switch from tenofovir to raltegravir increases low bone mineral density and decreases markers of bone turnover over 48 weeks. *HIV Med*. (2014) 15:373–80. doi: 10.1111/hiv.12123
97. Maggiolo F, Rizzardini G, Raffi F, Pulido F, Mateo-Garcia MG, Molina JM, et al. Bone mineral density in virologically suppressed people aged 60 years or older with HIV-1 switching from a regimen containing tenofovir disoproxil fumarate to an elvitegravir, cobicistat, emtricitabine, and tenofovir alafenamide single-tablet regimen: a multicentre, open-label, phase 3b, randomised trial. *Lancet HIV*. (2019) 6:e655–66. doi: 10.1016/S2352-3018(19)30195-X
98. Cotter AG, Vrouenraets SM, Brady JJ, Wit FW, Fux CA, Furrer H, et al. Impact of switching from zidovudine to tenofovir disoproxil fumarate on bone mineral density and markers of bone metabolism in virologically suppressed HIV-1 infected patients; a substudy of the PREPARE study. *J Clin Endocrinol Metab*. (2013) 98:1659–66. doi: 10.1210/jc.2012-3686
99. Carr A, Miller J, Eisman JA, Cooper DA. Osteopenia in HIV-infected men: association with asymptomatic lactic acidemia and lower weight pre-antiretroviral therapy. *Aids*. (2001) 15:703–9. doi: 10.1097/00002030-200104130-00005
100. Woodward CL, Hall AM, Williams IG, Madge S, Copas A, Nair D, et al. Tenofovir-associated renal and bone toxicity. *HIV Med*. (2009) 10:482–7. doi: 10.1111/j.1468-1293.2009.00716.x
101. Moyle GJ, Stellbrink HJ, Compston J, Orkin C, Arribas JR, Domingo P, et al. 96-Week results of abacavir/lamivudine versus tenofovir/emtricitabine, plus efavirenz, in antiretroviral-naïve, HIV-1-infected adults: ASSERT study. *Antiviral Therapy*. (2013) 18:905–13. doi: 10.3851/IMP2667
102. Grigsby IF, Pham L, Mansky LM, Gopalakrishnan R, Carlson AE, Mansky KC. Tenofovir treatment of primary osteoblasts alters gene expression profiles: implications for bone mineral density loss. *Biochem Biophys Res Commun*. (2010) 394:48–53. doi: 10.1016/j.bbrc.2010.02.080
103. Shiao S, Arpad SM, Yin MT. Bone update: is it still an issue without tenofovir disoproxil fumarate? *Current HIV/AIDS Reports*. (2020) 1:1–5. doi: 10.1007/s11904-019-00474-1
104. Moran CA, Weitzmann MN, Oforokun I. The protease inhibitors and HIV-associated bone loss. *Curr Opin HIV AIDS*. (2016) 11:333–42. doi: 10.1097/COH.0000000000000260
105. Hirakawa H, Gatanaga H, Ochi H, Fukuda T, Sunamura S, Oka S, et al. Antiretroviral therapy containing HIV protease inhibitors enhances fracture risk by impairing osteoblast differentiation and bone quality. *J Infect Dis*. (2017) 215:1893–7. doi: 10.1093/infdis/jix246
106. Calmy A, Fux CA, Norris R, Vallier N, Delhumeau C, Samaras K, et al. Low bone mineral density, renal dysfunction, and fracture risk in HIV infection: a cross-sectional study. *J Infect Dis*. (2009) 200:1746–54. doi: 10.1086/644785
107. Kinai E, Nishijima T, Mizushima D, Watanabe K, Aoki T, Honda H, et al. Long-term use of protease inhibitors is associated with bone mineral density loss. *AIDS Res Hum Retroviruses*. (2014) 30:553–9. doi: 10.1089/aid.2013.0252
108. Amiel C, Ostertag A, Slama L, Baudoin C, N'Guyen T, Lajeunie E, et al. BMD is reduced in HIV-infected men irrespective of treatment. *J Bone Mineral Res*. (2004) 19:402–9. doi: 10.1359/JBMR.0301246
109. Gibellini D, Borderi M, de Crignis E, Clo A, Miserocchi A, Viale P, et al. Analysis of the effects of specific protease inhibitors on OPG/RANKL regulation in an osteoblast-like cell line. *New Microbiol*. (2010) 33:109–15.
110. Gao Y, Grassi F, Ryan MR, Terauchi M, Page K, Yang X, et al. IFN-gamma stimulates osteoclast formation and bone loss *in vivo* via antigen-driven T cell activation. *J Clin Invest*. (2007) 117:122–32. doi: 10.1172/JCI30074
111. Modarresi R, Xiang Z, Yin M, Laurence J. WNT/beta-catenin signaling is involved in regulation of osteoclast differentiation by human immunodeficiency virus protease inhibitor ritonavir: relationship to human immunodeficiency virus-linked bone mineral loss. *Am J Pathol*. (2009) 174:123–35. doi: 10.2353/ajpath.2009.080484
112. Santiago F, Oguma J, Brown AM, Laurence J. Noncanonical Wnt signaling promotes osteoclast differentiation and is facilitated by the human

- immunodeficiency virus protease inhibitor ritonavir. *Biochem Biophys Res Commun.* (2012) 417:223–30. doi: 10.1016/j.bbrc.2011.11.089
113. Yin MT, Modarresi R, Shane E, Santiago F, Ferris DC, McMahon DJ, et al. Effects of HIV infection and antiretroviral therapy with ritonavir on induction of osteoclast-like cells in postmenopausal women. *Osteoporos Int.* (2011) 22:1459–68. doi: 10.1007/s00198-010-1363-6
 114. Wang MW, Wei S, Faccio R, Takeshita S, Tebas P, Powderly WG, et al. The HIV protease inhibitor ritonavir blocks osteoclastogenesis and function by impairing RANKL-induced signaling. *J Clin Invest.* (2004) 114:206–13. doi: 10.1172/JCI15797
 115. Hernandez-Vallejo SJ, Beaupere C, Larghero J, Capeau J, Lagathu C. HIV protease inhibitors induce senescence and alter osteoblastic potential of human bone marrow mesenchymal stem cells: beneficial effect of pravastatin. *Aging Cell.* (2013) 12:955–65. doi: 10.1111/acer.12119
 116. Yano S, Mentaverri R, Kanuparthi D, Bandyopadhyay S, Rivera A, Brown EM, et al. Functional expression of beta-chemokine receptors in osteoblasts: role of regulated upon activation, normal T cell expressed and secreted (RANTES) in osteoblasts and regulation of its secretion by osteoblasts and osteoclasts. *Endocrinology.* (2005) 146:2324–35. doi: 10.1210/en.2005-0065
 117. Han JH, Choi SJ, Kurihara N, Koide M, Oba Y, Roodman GD. Macrophage inflammatory protein-1alpha is an osteoclastogenic factor in myeloma that is independent of receptor activator of nuclear factor kappaB ligand. *Blood.* (2001) 97:3349–53. doi: 10.1182/blood.V97.11.3349
 118. Oba Y, Lee JW, Ehrlich LA, Chung HY, Jelinek DF, Callander NS, et al. MIP-1alpha utilizes both CCR1 and CCR5 to induce osteoclast formation and increase adhesion of myeloma cells to marrow stromal cells. *Exp Hematol.* (2005) 33:272–8. doi: 10.1016/j.exphem.2004.11.015
 119. Lee JW, Hoshino A, Inoue K, Saitou T, Uehara S, Kobayashi Y, et al. The HIV co-receptor CCR5 regulates osteoclast function. *Nat Commun.* (2017) 8:2226. doi: 10.1038/s41467-017-02368-5
 120. Taiwo BO, Chan ES, Fichtenbaum CJ, Ribaud H, Tsibris A, Klingman KL, et al. Less bone loss with maraviroc- versus tenofovir-containing antiretroviral therapy in the AIDS clinical trials group A5303 study. *Clin Infect Diseases.* (2015) 61:1179–88. doi: 10.1093/cid/civ455

Conflict of Interest: The authors declare that the research was conducted in the absence of any commercial or financial relationships that could be construed as a potential conflict of interest.

Copyright © 2020 Delpino and Quarleri. This is an open-access article distributed under the terms of the Creative Commons Attribution License (CC BY). The use, distribution or reproduction in other forums is permitted, provided the original author(s) and the copyright owner(s) are credited and that the original publication in this journal is cited, in accordance with accepted academic practice. No use, distribution or reproduction is permitted which does not comply with these terms.



Calcitonin Induces Bone Formation by Increasing Expression of Wnt10b in Osteoclasts in Ovariectomy-Induced Osteoporotic Rats

Chen-Yuan Hsiao^{1,2}, Tien-Hua Chen^{3,4,5}, Tzu-Hui Chu⁶, Yen-Nien Ting⁶, Pei-Jiun Tsai^{3,4,7*} and Jia-Fwu Shyu^{6,8*}

¹ National Defense Medical Center, Graduate Institute of Medical Sciences, Taipei, Taiwan, ² Department of Surgery, Landseed International Hospital, Taoyuan, Taiwan, ³ School of Medicine, Institute of Anatomy and Cell Biology, National Yang Ming University, Taipei, Taiwan, ⁴ Department of Surgery, Trauma Center, Veterans General Hospital, Taipei, Taiwan, ⁵ Division of General Surgery, Department of Surgery, Veterans General Hospital, Taipei, Taiwan, ⁶ Department of Biology and Anatomy, National Defense Medical Center, Taipei, Taiwan, ⁷ Department of Critical Care Medicine, Veterans General Hospital, Taipei, Taiwan, ⁸ Department of Psychiatry, National Defense Medical Center, Tri-Service General Hospital, Taipei, Taiwan

OPEN ACCESS

Edited by:

Arancha R. Gortazar,
CEU San Pablo University, Spain

Reviewed by:

Jesus Delgado-Calle,
University of Arkansas for Medical
Sciences, United States

Marta Martin,
Marqués de Valdecilla University
Hospital, Spain

*Correspondence:

Pei-Jiun Tsai
pjtsai@vghtpe.gov.tw
Jia-Fwu Shyu
shyujeff@ndmctsgh.edu.tw

Specialty section:

This article was submitted to
Bone Research,
a section of the journal
Frontiers in Endocrinology

Received: 02 May 2020

Accepted: 27 July 2020

Published: 08 September 2020

Citation:

Hsiao C-Y, Chen T-H, Chu T-H,
Ting Y-N, Tsai P-J and Shyu J-F
(2020) Calcitonin Induces Bone
Formation by Increasing Expression of
Wnt10b in Osteoclasts in
Ovariectomy-Induced Osteoporotic
Rats. *Front. Endocrinol.* 11:613.
doi: 10.3389/fendo.2020.00613

Calcitonin is a small peptide hormone secreted from the parafollicular cells of the thyroid gland in response to an increase in serum calcium. The inhibition of osteoclastic resorption is the main mechanism by which calcitonin quickly decreases circulating calcium levels. Although calcitonin pharmacologically acts on osteoclasts to prevent bone resorption, the results of studies on genetically modified animals have shown that the physiological effect of calcitonin is in the inhibition of osteoblastic bone formation. Because the calcitonin receptor is only expressed in osteoclasts, the effect of calcitonin on osteoblasts maybe indirect and mediated via osteoclasts. Wnt ligands are involved in various aspects of skeletal biology, including bone remodeling and endochondral bone formation. Wnt10b has recently been recognized as a clastokine, and is potentially a therapeutic target for treating bone disorders. However, the extent to which Wnt signaling is involved in bone physiology and disease is not yet fully understood. We hypothesize that calcitonin indirectly increases osteoblastic bone formation by inducing Wnt10b expression in osteoclasts. Micro-CT analysis revealed reduced bone loss in calcitonin-treated ovariectomized rats. The serum of animals treated with calcitonin had decreased TRAP5b and CTX-1 but increased osteocalcin, P1NP, and Wnt10b. Immunohistochemistry staining showed that the level of Wnt10b in the femur was increased in calcitonin-treated groups as compared with control groups. Hematopoietic mononuclear cells were separated from rat femur and tibia bone marrow, and were induced into osteoclasts following treatment with M-CSF and RANKL. In these cells, immunoconfocal microscopy and Western blot analysis showed that calcitonin induced an increase in Wnt10b expression. In a culture of osteoblasts isolated from neonatal rat calvariae, the calcitonin-treated osteoclast supernatant showed an increase in mineralization, as indicated by ALP and alizarin red staining. Taken together, these

results indicate that calcitonin induces bone formation by increasing the expression of Wnt10b in osteoclasts in ovariectomy-induced osteoporotic rats. The present study provides in-depth information about the effects of calcitonin on bone remodeling and will thus help in the development of future potential therapeutic strategies for postmenopausal osteoporosis.

Keywords: calcitonin, Wnt10b, osteoporosis, osteoclasts, ovariectomy

INTRODUCTION

The secretion of calcitonin, a 32 aa peptide hormone, from the parafollicular cells of the thyroid gland is induced by increased serum calcium (1) leading to rapid reduction in circulating calcium levels, mainly through the inhibition of bone resorption. The binding of calcitonin to its receptors on osteoclasts causes a series of major reactions within minutes, including loss of the ruffled border, cell retraction, and the suppression of cell motility and bone resorption (2). It is evident that the pharmacological function of calcitonin is to inhibit bone resorption through lowered levels of circulating calcium; nevertheless, the physiological role of calcitonin remains unclear. Previous studies have found that bone mineral density and calcium metabolism were not influenced in patients either with excess endogenous calcitonin (e.g., those with medullary thyroid carcinoma) or with undetectable circulating calcitonin (e.g., those who had undergone thyroidectomy) (3, 4). Because the fluctuation in serum calcitonin levels does not have any obvious pathological outcomes, it has been suggested that calcitonin should have no physiological role in mammals. This theory is, however, not widely accepted, and the existing consensus is that calcitonin plays a significant role in protecting the skeleton under circumstances of calcium stress (5, 6).

In addition, research on genetically modified animals has demonstrated that the physiological role of calcitonin in bone cells could be in the inhibition of bone formation, in contrast to its pharmacological function of inhibiting bone resorption. The high bone mass attributed to increased bone formation has been found in both Calca KO and Calcr KO mice (7, 8), even though Calcr did not manifest in osteoblasts. Naot and colleagues suggested that the skeletal phenotype of an osteoclast-specific Calcr KO could enhance bone formation (6), similar to that of the global Calcr KO; thus, such findings have solved the previously mentioned contradiction. In short, calcitonin probably has indirect effects on osteoblasts that are mediated via osteoclasts.

Osteoporosis, characterized by remarkable losses of bone mineral density and strength, results in fragility fractures and subsequent high morbidity and mortality (9). During

bone remodeling, the bone resorption exerted by osteoclasts in the bone matrix has the capacity to activate osteoblastic bone formation through a coupling reaction. This coupling process ensures the succession of bone formation to bone resorption in the remodeling cycle. Recent studies of the regulatory mechanisms for the cross-talk between osteoclasts and osteoblasts have identified several bone formation-stimulating osteoclast-derived factors (i.e., clastokines) and matrix-derived growth factors, and the authors have asserted that these factors may contribute to the future design of novel osteoanabolic compounds (10). Uncoupling anti-resorptive (e.g., calcitonin, odanacatib, and saracatinib) would be better drugs because they could inhibit osteoclastic bone-resorbing activity while maintaining the bone formation attributed to sustained communication between osteoclasts and osteoblasts (9). A recent study revealed that calcitonin only inhibited bisphosphonate-induced osteoclast apoptosis, and the combined usage of calcitonin and bisphosphonate increased the efficacy of bisphosphonate on bone formation in a rat model of osteoporosis (11). This result implies that different kinds of anti-resorptive agents may induce distinct clastokines. Wnt proteins are usually involved in various aspects of bone biology, including osteoblastic, and osteoclastic functions as well as endochondral bone formation (12, 13). For example, Wnt10b was recently identified as a clastokine, and a potential novel therapeutic target of postmenopausal osteoporosis. However, the role of Wnt ligands in skeletal physiology and disease is not fully comprehended. Therefore, we hypothesize that calcitonin increases bone formation by inducing Wnt10b expression in osteoclasts.

To acquire appropriate data and verify our hypotheses, a number of valid techniques were employed in this study. In ovariectomized rats, the effects of calcitonin on the protection of bone loss and Wnt10b expression were determined by micro-CT, bone histomorphometry, and immunohistochemistry analysis. In osteoclasts obtained from M-CSF- and RANKL-treated hematopoietic mononuclear cells isolated from rat femur and tibia bone marrow, the expression of Wnt10b was determined by ELISA, Western blot, and confocal microscopy analysis. Bone formation analysis was performed in osteoblasts isolated from neonatal rat calvariae and cultured with the calcitonin-treated osteoclast-conditioned medium.

The present study provides evidence that calcitonin induces bone formation by increasing the expression of Wnt10b in osteoclasts and offers further information

Abbreviations: ALP, alkaline phosphate; CKD, chronic kidney disease; CTX-1, type 1 carboxyterminal collagen fragments; Calca, calcitonin; Calcr, calcitonin receptor; CT, computer tomography; M-CSF, macrophage colony-stimulating factor; OVX, ovariectomy; PINP, amino-terminal propeptide of type 1 procollagen; RANKL, receptor activator of nuclear factor kappa B ligand; S1P, sphingosine-1-phosphate; TGF- β 1, transforming growth factor-beta 1; TRAP5b, tartrate-resistant acid phosphatase 5b.

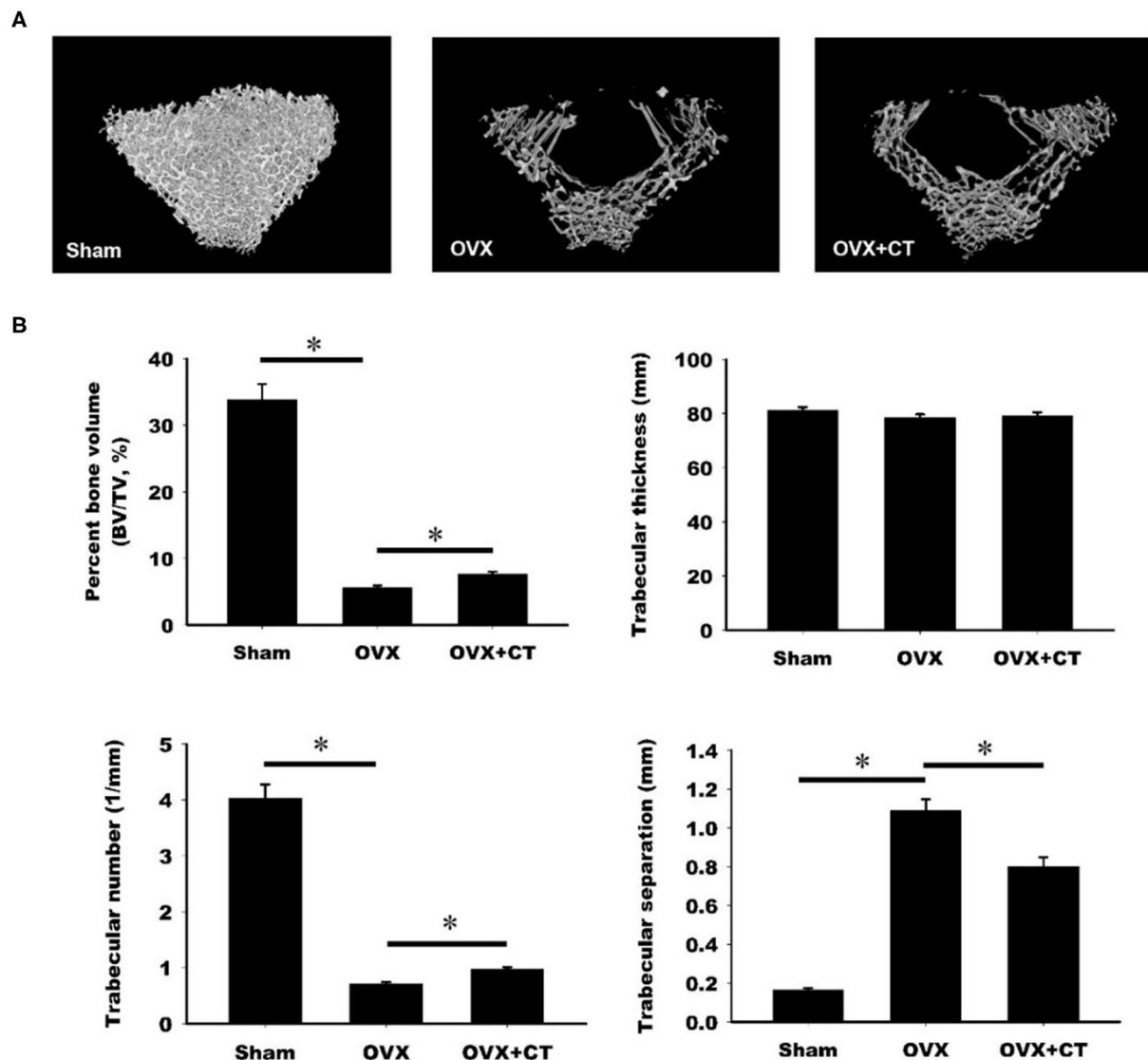


FIGURE 1 | Calcitonin increases femoral trabecular bone in ovariectomized osteoporotic rats. **(A)** Upper panel: micro-computed tomography analysis of the femoral bones in sham-operated rats and ovariectomized (OVX) rats treated with saline or calcitonin (CT, 5 IU/kg/day) five times per week for 4 weeks. Figures are representative reconstructed 3D images from each treatment group. **(B)** Lower panel: quantitative results of the experiment shown in **(A)**. *Indicates a significant difference ($p < 0.05$). $N = 6$ in each group.

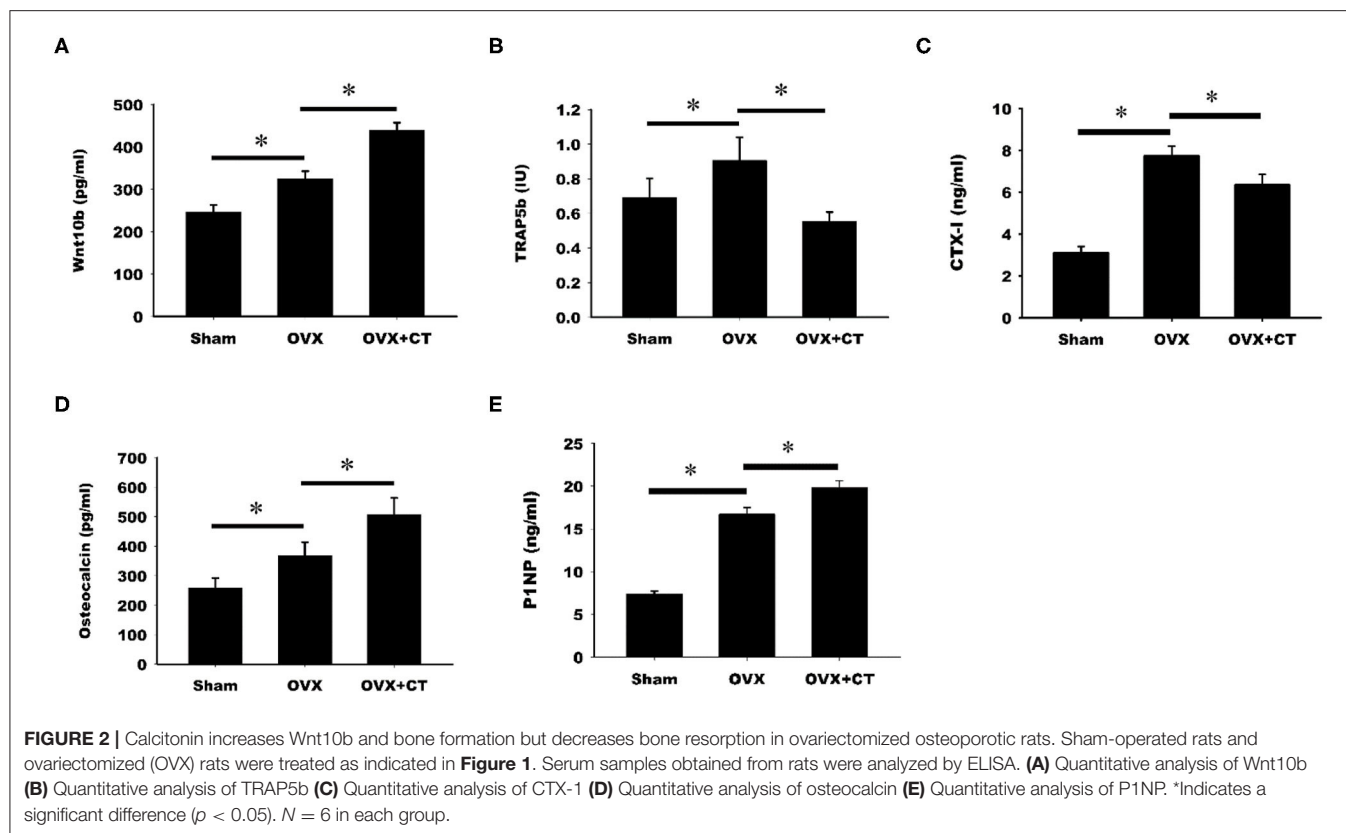
about the involvement of calcitonin in bone remodeling at the molecular level. These findings will help in future potential therapeutic studies of postmenopausal osteoporosis.

RESULTS

Calcitonin Alleviates Bone Loss in Ovariectomy-Induced Osteoporotic Rats

The effect of calcitonin on bone deposition was determined in osteoporotic rats 4 weeks after ovariectomy (OVX; **Figure 1**).

OVX or a sham operation was performed in 4-month-old female Sprague-Dawley rats. After 4 weeks, OVX rats received a normal saline or calcitonin treatment for four additional weeks, after which the 6-month-old rats were sacrificed and underwent micro-CT analysis of the femoral bone (**Figure 1**). Although the 2D images also included cortical bone, the regions of interest containing trabecular bone in metaphysis were selected for subsequent quantification (**Figure 1A**). Quantitation of these results (**Figure 1B**) indicated that OVX led to significant bone loss, increased trabecular separation, and decreased trabecular number compared



with the control sham operation. Compared with saline, calcitonin treatment significantly increased the percent bone volume and trabecular number in OVX rats. A significant decrease in trabecular separation was found in the calcitonin treatment group.

Calcitonin Decreases TRAP5b and CTX-1 but Increases Osteocalcin, P1NP, and Wnt10b Serum Levels in Ovariectomy-Induced Osteoporotic Rats

The serum levels of Wnt10b and bone formation and resorption markers were analyzed by ELISA. As shown in **Figure 2A**, a significant increase in Wnt10b was found in OVX rats compared with sham rats. Calcitonin treatment caused a further increase in Wnt10b in OVX rats. Analysis of serum bone resorption markers, TRAP5b and CTX-1, revealed increased bone resorption in OVX rats compared with sham rats (**Figures 2B,C**). TRAP5b and CTX-1 were significantly lower in the calcitonin treatment group compared with the untreated group. Increases in the serum bone formation markers, osteocalcin, and P1NP, were observed in OVX rats compared with sham rats (**Figures 2D,E**). Calcitonin treatment caused a further increase in osteocalcin and P1NP in OVX rats.

Calcitonin Treatment Increases the Expression in Metaphysis of Femoral Bone in Ovariectomy-Induced Osteoporotic Rats

Immunohistochemistry labeling of Wnt10b was performed in femoral bone (**Figure 3**). Positive Wnt10b labeling was noted as green near resorption zone of growth plate in femoral bone of sham rats. Decreased Wnt10b and increased TRAP expressions were found in OVX rats as compared with sham rats. In the CT treatment group, increase of Wnt10b and decrease of TRAP expressions were also found near resorption zone of growth plate in femoral bone.

Calcitonin Increases Wnt10b Expression in Osteoclasts

Immunofluorescent labeling of Wnt10b was performed in osteoclasts isolated from rat bone marrow. Confocal analysis of immunofluorescently labeled Wnt10b showed that it was greater in osteoclasts treated with calcitonin compared with controls (**Figure 4**). Pretreatment with C59, a Wnt secretion inhibitor, further increased the calcitonin effect of Wnt10b expression within the osteoclasts and demonstrated that calcitonin increased Wnt10b release from osteoclasts.

Western blot analysis revealed a significant time-dependent increase in Wnt10b expression in calcitonin-treated osteoclasts

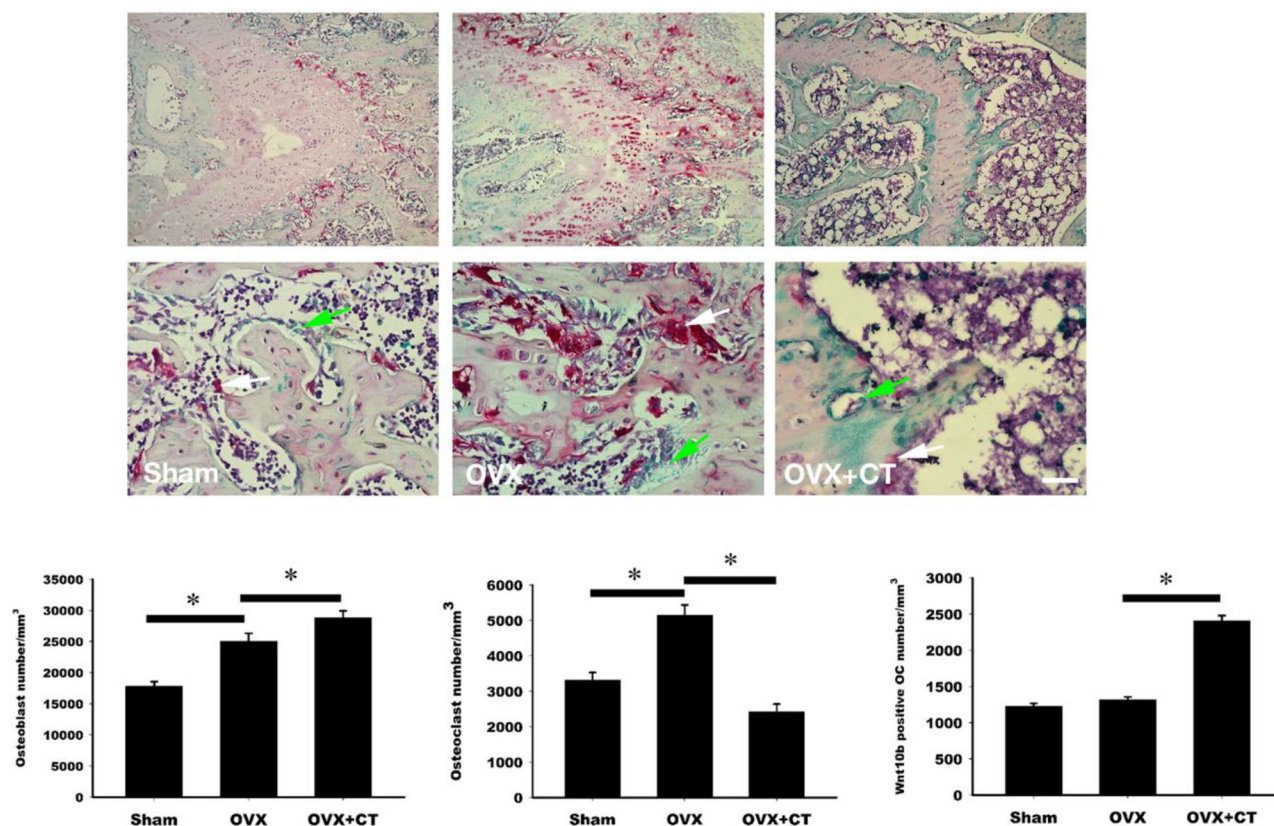


FIGURE 3 | Calcitonin treatment increases the osteoclastic Wnt10b expression in metaphysis of femoral bone in ovariectomy-induced osteoporotic rats.

Sham-operated rats and ovariectomized (OVX) rats were treated as indicated in **Figure 1**. Immunohistochemistry labeling of Wnt10b (green) and TRAP stain (red) were performed near resorption zone of growth plate in femoral bone. Decreased Wnt10b expression was found in OVX rats. CT treatment increased Wnt10b expression. The number of the osteoblast, osteoclast, and osteoclast with Wnt10b were counted. Green arrow showed osteoclasts to secrete Wnt10b; White arrow showed osteoclasts that did not secrete Wnt10b. Scale bar = 50 μ m. *Indicates a significant difference ($p < 0.05$). $N = 6$ in each group.

(**Figure 5**). Pretreatment with C59, a Wnt secretion inhibitor, further enhanced the effect of calcitonin in increasing Wnt10b expression within the osteoclasts.

Calcitonin-Induced Osteoclastic Wnt10b Secretion Improves Osteoblastic Mineralization

Osteoblastic mineralization was analyzed by alkaline phosphate (ALP, **Figure 6A**) and alizarin red (**Figure 6B**) staining. As a negative control, osteoblasts isolated from the calvariae of 1-day-old rats were cultured in α -MEM with or without C59 (a and b in **Figure 6**). Significant increase of ALP and alizarin red staining (c and d in **Figure 6**) were found in osteoblasts cultured in conditioned medium with or without C59. Further increase of ALP and alizarin red staining (e in **Figure 6**) were found in calcitonin-treated conditioned medium. The calcitonin-induced increase of ALP and alizarin red staining was reduced by C59 cotreatment (f in **Figure 6**). Similar finding of change of Wnt10b concentration was noted in these groups.

DISCUSSION

The present study used micro-CT analysis to show that calcitonin alleviated bone loss in ovariectomy-induced osteoporotic rats (**Figure 1**). Though calcitonin is no longer considered an appropriate treatment option for osteoporosis, the effects of calcitonin on the coupling process between osteoclasts and osteoblasts remain uncertain. Thus, it is fundamentally important to uncover the mechanism by which calcitonin affects osteoblastic bone formation through its actions on osteoclasts (**Figure 7**).

Consistent with previous studies, we found that calcitonin treatment not only decreased the levels of serum bone resorption markers (i.e., TRAP5b and CTX-1) in OVX rats (**Figure 2**) (14, 15) but also led to increased levels of bone formation markers (i.e., osteocalcin and P1NP) in OVX rats (11, 15). Because Wnt10b has recently been identified as a clastokine able to increase osteoblast activity, the finding that increased Wnt10b serum levels are correlated with osteocalcin and Wnt10b expression in bone marrow in calcitonin-treated OVX rats (**Figure 3**) implies that Wnt10b may be involved

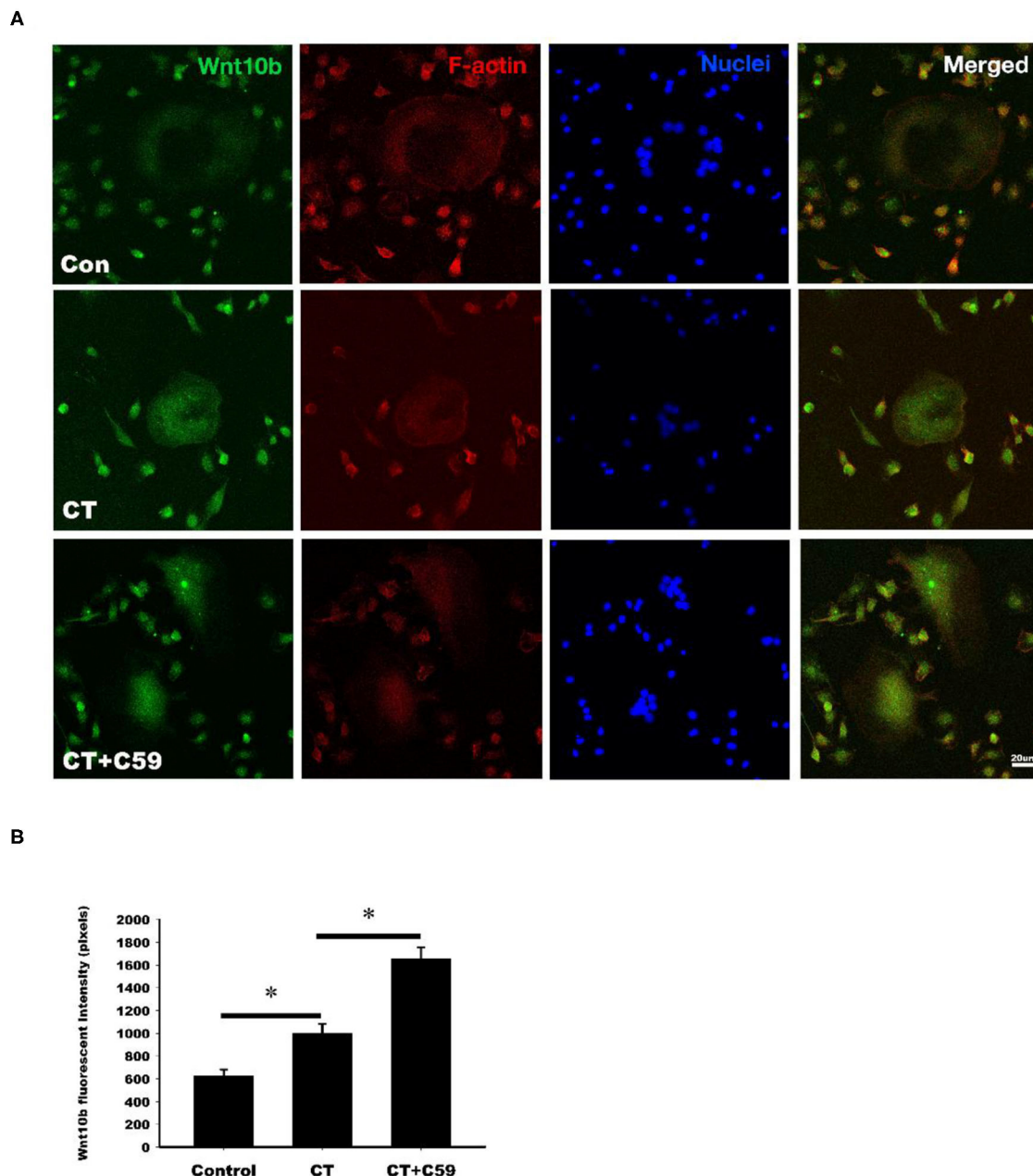


FIGURE 4 | Calcitonin increases intracellular Wnt10b expression in osteoclasts. Bone marrow monocytes were isolated from femoral and tibial bones of 8-week-old SD rats. They were induced into osteoclasts by M-CSF and RANKL stimulation. **(A)** Confocal analysis was performed in osteoclasts treated with 3 nM calcitonin alone or with C59 for 16 h. Osteoclasts were labeled with rhodamine phalloidin (red) to visualize F-actin and Nuclear Red (blue) to visualize nuclei. Scale bar = 20 μ m. **(B)** The statistics of Wnt10b fluorescent intensity was showed in each group. *Indicates a significant difference ($p < 0.05$).

in the effects of osteoclasts coupling to osteoblasts. Confocal microscopy of immunofluorescently labeled Wnt10b (**Figure 4**) and Western blot analysis of Wnt10b expression (**Figure 5**) in osteoclasts provided additional evidence to support this hypothesis. Moreover, osteoblastic mineralization was enhanced in conditioned medium derived from calcitonin-treated osteoclasts (**Figure 6**). Taken together, these results demonstrate

that calcitonin induces bone formation by increasing the expression of Wnt10b in osteoclasts in ovariectomy-induced osteoporotic rats (**Figure 7**).

It is well-documented that Wnt signaling plays a crucial role in many biological processes (e.g., cellular proliferation, tissue regeneration, and other systemic effects) (16). This is because the Wnt family is characterized by at least 19 different

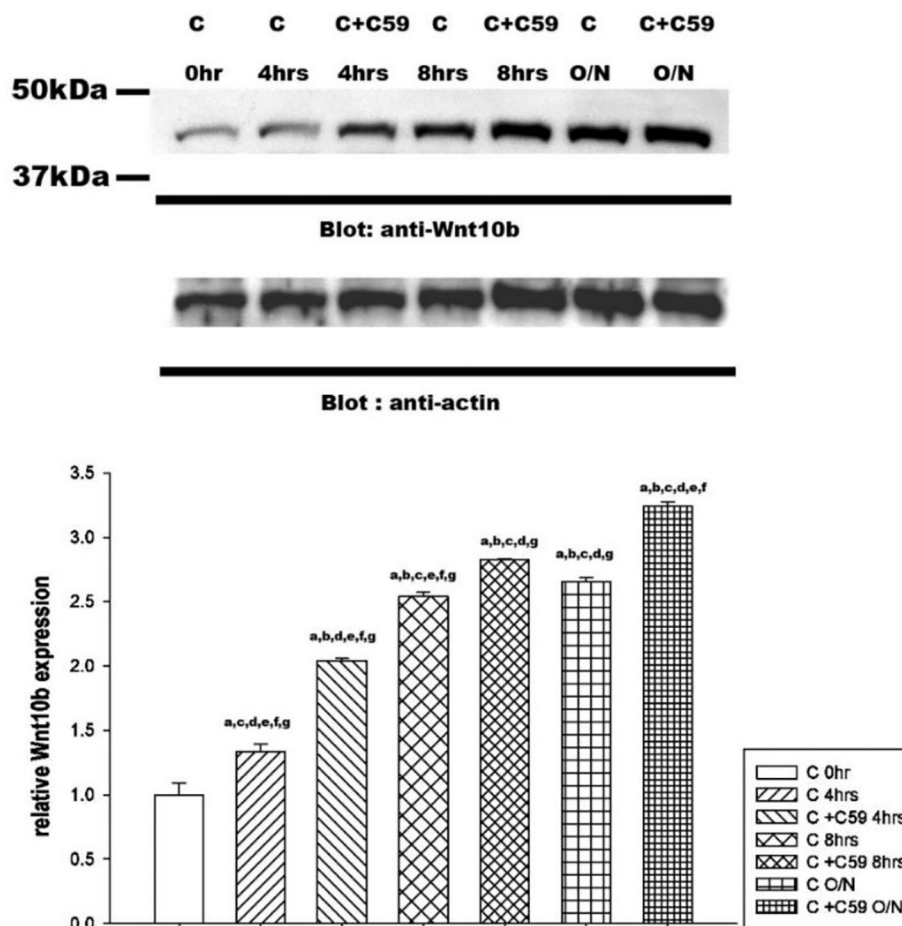


FIGURE 5 | Calcitonin increases Wnt10b levels in osteoclasts. Osteoclasts were prepared and treated as indicated in **Figure 4**. Western blot analysis was performed on osteoclasts treated with 3 nM calcitonin alone or with C59 for the various times indicated. Protein levels were quantified by densitometry, corrected for sample loading on the basis of actin levels, and expressed as the fold change relative to the control lane. Each blot is representative of at least three replicate experiments.

glycoproteins, each of which is responsible for triggering multiple signaling cascades. Accordingly, Wnt proteins are likely to be involved in various aspects of bone biology, including osteoblastic and osteoclastic functions and endochondral bone formation. A study indicated that Wnt signaling plays a vital role in osteoblast differentiation from both mesenchymal precursors and osteochondro progenitors as well as the proliferation and survival of osteoblasts (17). Wnt ligands have been widely studied by means of various osteoblastic models and, later, animal models. Currently, existing murine models suggest that Wnt3a, Wnt5a, and Wnt10b are critical for osteoblast regulation, whereas Wnt14 is important for endochondral bone formation (18–20). Further investigations in this research area are necessary to comprehend the scope of Wnt effects on bone metabolism and the effectiveness of Wnt-based therapeutics on bone structure and functions.

In contrast to the numerous findings regarding Wnt signaling in osteoblast lineage cells, little is known about the influence of Wnt proteins on osteoclasts in the context of cell autonomy. It

has been proposed that matrix-bound TGF- β 1 could function as an effective coupling agent for actively recruiting osteoblast-lineage cells to bone-resorption positions following its osteoclast-mediated release. A study indicated that TGF- β 1 improves the coupling to osteoblasts by inducing Wnt10b expression in osteoclasts (21). Moreover, researchers have suggested that cinacalcet, probably via increased bone mineralization related to osteoclastic Wnt10b secretion, might improve bone quantity, and quality in chronic kidney disease (CKD) mice (22). Moreover, in a study involving calcitriol treatment of secondary hyperparathyroidism in CKD patients, it was demonstrated that the increased secretion of osteoclast-derived Wnt10b was critical for the improvement of bone anabolism through its inhibition of osteoclastogenesis and promotion osteoblastogenesis (23). Hence, Wnt10b is a cytokine and a potential novel therapeutic target of postmenopausal osteoporosis and CKD-related bone disorder. On the other hand, runx2 directly induces Wnt10b expression in osteoblasts (24). PTH is a bone anabolic agent and effective treatment for postmenopausal osteoporosis, maybe

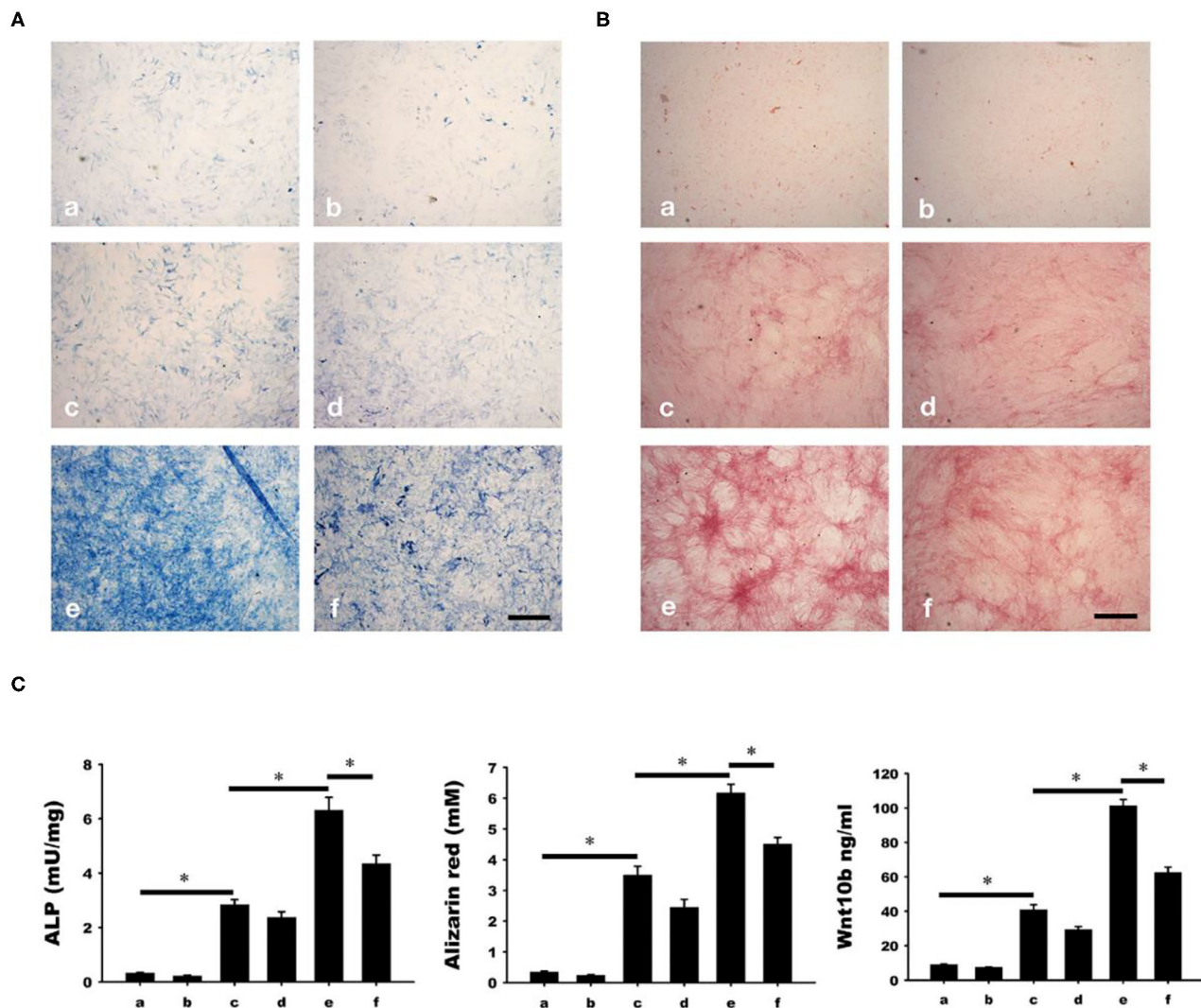


FIGURE 6 | Calcitonin indirectly increases osteoblast mineralization. Osteoblasts were isolated from the calvariae of 1-day-old newborn SD rats and cultured in groups a-f medium as indicated in Materials and Methods. Analysis of osteoblast mineralization was performed by ALP (A) and alizarin red staining (B). (C) Quantitative results of the experiment shown in (A,B), and Wnt10b concentration in mediums of each group before cultured with osteoblasts. *Indicates a significant difference ($p < 0.05$). Bar = 500 μ m.

by its effect of increase Wnt10b production in osteoblasts (25). Therefore, the role of osteoblast-derived Wnt10b could not be underestimated.

The elemental mechanisms of calcitonin receptor (CTR) bone activity were discovered by Keller et al. (8) through experiments on a new strain of viable global *CalcR* KO mice, which were generated by applying a specific technique to knockout the expression of CTR. Briefly, the study asserted that losing CTR in osteoclasts would increase the levels of sphingolipid transporter 2 (spinster 2, SPNS2), an exporter protein required for the secretion of sphingosine-1-phosphate (S1P), which can effectively induce bone formation. Thus, on the basis of the above mechanisms, calcitonin binding to CTR on osteoclasts will inhibit SPNS2 expression, causing the decreased secretion

of S1P and subsequent inhibition of osteoblast activity. Because calcitonin-stimulated osteoclasts could inhibit or stimulate osteoblast functions through the modulation of different cytokines, the roles that these cytokines may play in various stages of bone resorption remain unknown. Consequently, further studies are needed to dissect the underlying mechanisms and corresponding physiological relevance during bone remodeling.

However, C59 is a Wnt inhibitor, not specific for Wnt10b. This is a limitation in our experiment. In addition, osteoblasts may also secrete Wnt10b which is interesting issue worth of more study. The current clinical application of calcitonin is gradually decreasing because the other long-acting drugs for inhibition of bone resorption are effective and convenient. Many studies still have a great interest in calcitonin and the effect of the bone

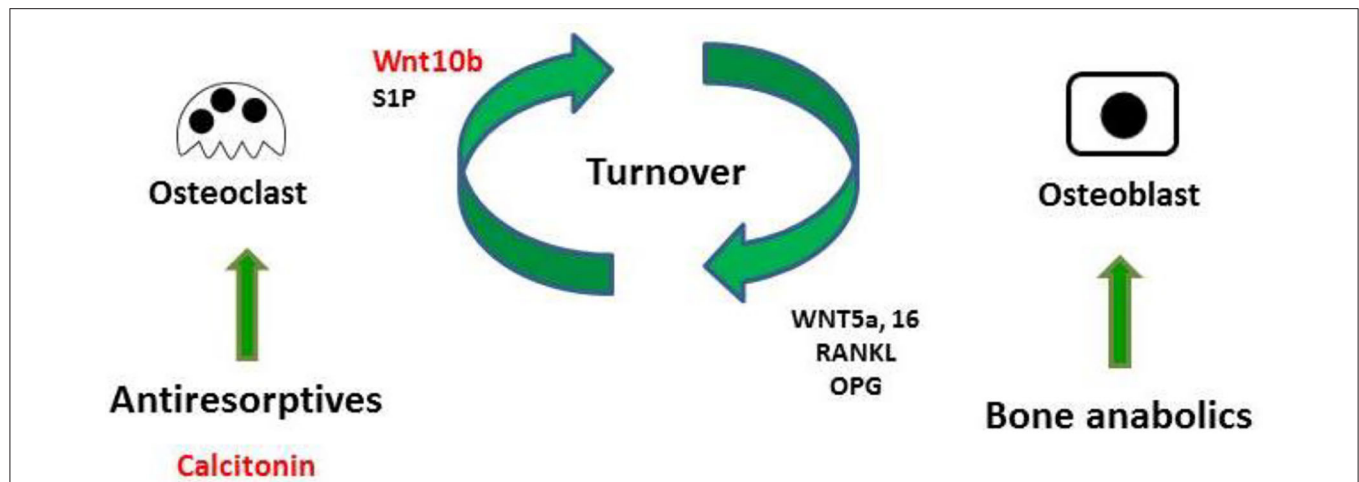


FIGURE 7 | Model of calcitonin-induced bone formation through action on osteoclasts. Bones undergo constant remodeling throughout the lifetime of the organism, and this involves the continuous activity of osteoblasts and osteoclasts. Osteoblastic bone formation is communicated to osteoclastic bone resorption by positive and negative modulators (RANKL/OPG or WNT). Osteoclasts also communicate to osteoblasts by cytokines (Wnt10b and S1P). Bone anabolic such as PTH also increase osteoclastic bone resorption through their control of RANKL/OPG and WNT signaling. Anti-resorptive inhibit osteoclast resorption, which usually causes the inhibition of bone formation. Uncoupling anti-resorptive, such as calcitonin, may modulate osteoblast mineralization through the controlled secretion of Wnt10b and S1P.

metabolism, physiological roles, and the activities. This is an intricate and fantastic peptide.

MATERIALS AND METHODS

Ovariectomy-Induced Osteoporosis RAT Model

All rat experiments were reviewed and approved by the Institutional Animal Care and Use Committee (IACUC) of the Laboratory Animal Center of the National Defense Medical Center; the identification number is IACUC-14-104. Briefly, 18 4-month-old female Sprague–Dawley (SD) rats were purchased from a specific pathogen-free laboratory animal company (BioLASCO, Taipei, Taiwan) and separated randomly into three groups. All rats were acclimatized under accepted laboratory conditions (temperature was $22 \pm 2^\circ\text{C}$, and humidity was $50 \pm 10\%$). Food and water were provided ad libitum. Rats were anesthetized by the administration of isoflurane (Forane® AbbVie Inc., Queenborough, UK), and bilateral ovariectomy (OVX) was performed to build an osteoporosis model in OVX and OVX calcitonin-treated groups. The sham control group comprised rats whose ovaries were exposed but not removed. Twenty-eight days after surgery, the following three groups (6 rats per group) were set up: (a) sham control group: rats underwent a sham operation and were subcutaneously injected with the same volume of normal saline; (b) OVX group: rats underwent the OVX operation and were subcutaneously injected with the same volume of normal saline; (c) OVX-calcitonin group: rats underwent the OVX operation and were subcutaneously injected with calcitonin (5 IU/kg/day, Miacalcin, NovartisPharma). All groups were treated five times per week for 4 weeks. At the endpoint of the experiment, blood and femurs

were obtained from the rats, which were first fasted overnight and euthanized, coded, and prepared for blinded distribution. Collected sera were frozen at -80°C , and femurs were kept in alcohol at 4°C .

Micro-Computed Tomography

The micro architecture of the 18 femoral trabecular bones was investigated using micro-computed tomography (Skyscan 2211 Nanotomograph Micro-CT; Skyscan, Aartselaar, Belgium) at a resolution of $8.5\ \mu\text{m}$. The scan was performed with 180° scanning at a voltage of 80 kVp and a current of $500\ \mu\text{A}$ (7.9 W output). Image reconstruction was performed using GPU-based reconstruction software, GPU-Nrecon. Ring artifacts and beam-hardening corrections were also performed using this software. Reconstructed cross-sections were reorientated, and the region of interest (ROI) was further selected. We performed the analysis of the secondary trabecular bone area using 2 mm (236 slices) images. The volume of interest was 1.5–3.5 mm below the growth plate. Thresholding, region of interest selection, and bone morphometric analysis were performed using CTAn software. The volume of interest was selected as 1.5–3.5 mm below the growth plate. In addition, the region of interest (ROI) of the trabecular bone area was selected and then analyzed by using CTAn software.

Biochemical Analyses

The concentrations in sera of Wnt10b and the bone resorption marker TRAP5b (tartrate-resistant acid phosphatase from 5b) were measured by ELISA (Wnt 10b (MBS2533600, MyBioSource, San Diego, CA, USA), TRAP5b (SB-TR102, Immunodiagnostic Systems, East Boldon, UK), and resorption marker CTX-1 (C-telopeptide of type I collagen) and formation

markers osteocalcin and P1NP (type 1 procollagen amino-terminal—propeptide) were measured EIA (AC-06F1, AC-12F1, and AC-33F1 Immunodiagnostic Systems, UK).

Immunohistochemistry and TRAP Double Stain of the Femur

Femurs were taken from experimental rats, then washed several times in PBS and fixed overnight in formalin substitute solution (FX1075, Cancer Diagnostics, Durham, NC, USA). The femurs were decalcified in Decalcifying Solution (REF. No.3840, Thermo Scientific, Waltham, MA, USA) for 24 h, then transferred to 0.5 M EDTA, pH 8, for several days until a biopsy needle could be inserted into the femur. After decalcification, tissues were dehydrated, embedded in paraffin, and cut into 10 μ m thickness per slices. After deparaffinization, rehydration, and antigen retrieval and blocking, anti-Wnt10b Ab (NBP2-49165, Novus Biologicals, Centennial, CO, USA) was applied to the slides followed by incubation overnight. The prepared slides were then developed with the substrate chromogen of HRP-green (TA01HG-15, BioTnA, Kaohsiung, Taiwan). After chromogen properly developing the TRAP staining (AK04F-COS, COSMO BIO, Tokyo, Japan) was applied. Briefly, the chromogen was mixed with buffer immediately. Finally, hematoxylin was applied to show the nuclei.

Osteoclast Differentiation From Bone Marrow-Derived Monocytes

After 8-week-old Sprague-Dawley (SD) rats were sacrificed, bone marrow from the tibiae and femurs were collected in 0.05% citric acid normal saline. Harvested cells (contained monocytes) from bone marrow were extracted by centrifugation in an equal volume of Ficoll-Paque PLUS (17144002, GE Healthcare, Chicago, IL, USA). A total of 10^6 harvested cells were cultured in a 10 cm dish with osteoclast differentiation medium (α -MEM medium containing 10% fetal bovine serum (FBS, SH30088.03, GE Healthcare, USA), 50 ng/mL macrophage colony-stimulating factor (M-CSF, 400-28, PEPROTECH, Rocky Hill, NJ, USA), 50 ng/mL RANKL (315-11, PEPROTECH, USA), and 1% Antibiotic-Antimycotic Solution (30-004-CI, CORNING, Corning, NY, USA). The medium was changed every 3 days.

Analysis of the Distribution of Wnt10b in Osteoclasts by Confocal Microscopy

Osteoclasts induced from bone marrow-derived monocytes were cultured on 22 \times 22 mm glass coverslips in the medium described above. After the osteoclasts formed, they were separated into three groups: the control group, the group treated with 3 nM calcitonin (05-23-2401, Sigma-Aldrich, St. Louis, MO, USA), and the group treated with 3 nM calcitonin combined with a Wnt inhibitor, C59 (sc-475634, SANTA CRUZ BIOTECHNOLOGY); all the groups were cultured with α -MEM medium containing 10% FBS and 1% Antibiotic-Antimycotic Solution for 24 h. C59 was added in the medium in control group. After the osteoclasts were washed with PBS, fixed with formalin substitute, and permeabilized with 0.1% Triton X-100 in PBS for 10 min,

the cells were blocked in PBS containing 10% normal rabbit serum (AR1010, BOSTER, Pleasanton, CA, USA) for 1 h at room temperature. Then, anti-Wnt10b Ab was applied overnight at 4°C. On the second day, after washing in 0.05% Triton X-100 PBS three times, anti-rabbit Ab conjugated FITC was applied at room temperature for 2 h. F-actin was labeled with F-Actin Labeling Kit (22663, AAT Bioquest, Sunnyvale, CA, USA), and nuclei were stained with Nuclear Red DCS1 (157199-63-8, AAT Bioquest, USA). The distribution and intensity of Wnt10b was analyzed using a confocal microscope (LSM 510, Zeiss, Oberkochen, Germany).

Quantitation of Wnt10b in Osteoclasts by Western Blot

The total protein was extracted from lysed osteoclasts treated with or without calcitonin and C59 in a lysis buffer (100 mM Tris-HCl, pH7.4, 1% NP-40) containing protease inhibitor cocktail (F1PICo25, Bio Future, New York, NY, USA). The proteins were separated by 10% SDS-PAGE and transferred to a PVDF membrane. After blocking, the membrane was incubated with primary Ab overnight at 4°C. The next day, after washing, the secondary Ab was applied at room temperature for 2 h. Finally, the membrane was treated with electrogenerated chemiluminescence reagent (RPN2235, GE Healthcare, USA) and detected using UVP ChemStudio PLUS (849-97-0851-03, Analytik Jena, Jena, Germany).

Rat Calvariae Osteoblast Separation

The calvariae of newborn rats were cut into chips and digested in a digestive solution of α -MEM medium containing 1% type 2 collagenase (LS004174, Worthington, OH, USA) and 0.05% trypsin for 30 min. After removing the solution, fresh digestive solution was added to digest the calvariae chips; this process was repeated three times. Finally, after the fourth time, centrifuged osteoblasts, and calvariae chips were cultured in α -MEM medium containing 10% FBS and 1% Antibiotic-Antimycotic Solution.

Conditioned Medium Culture of Osteoblasts

Osteoblasts separated from rat calvariae were cultured in group a: osteoblast culture medium alone as mentioned in 4.8; group b: osteoblast culture medium with C59; group c: half of osteoclast culture medium as mentioned in 4.5 (conditioned medium) and half of osteoblast culture medium with 50 mg/mL ascorbic acid (A1968, Sigma Aldrich, USA) and 2 mM β -glycerophosphate (G9422, Sigma Aldrich, USA) (bone formation medium); group d: half of conditioned medium with C59 and half of bone formation medium; group e: half of 3 nM calcitonin-treated conditioned medium and half of bone formation medium; group f: half of 3 nM calcitonin-treated conditioned medium with C59 and half of bone formation medium. For the ALP stain and ALP activity assay, each group was cultured for 7 days. For the alizarin red stain, each group was cultured for 18 days. Before osteoblast were cultured, the concentration of Wnt10b in each group of medium were detected by ELISA (MBS2533600, MyBioSource, San Diego, USA).

ALP Staining and ALP Activity Assay of Osteoblasts

Osteoblasts were stained with an ALP staining kit (AK20-COS, COSMO BIO, Tokyo, Japan). Briefly, for staining, osteoblasts were fixed by formalin substitute solution. The buffer and the substrate were mixed, and the solution was then applied to coverslips containing osteoblasts at room temperature for 20 min, followed by washing with deionized water to stop the reaction. The images were captured by microscopy (Axio Imager A2, Zeiss, Germany). Quantified ALP activity in osteoblasts was measured using an Alkaline Phosphatase Assay Kit (ab83369, Abcam, Cambridge, UK). Briefly, cells were lysed in lysis buffer and combined with p-nitrophenyl phosphate (pNPP) as a phosphatase substrate, then incubated at room temperature for 1 h. Finally, the reaction was stopped by the addition of 0.1 M NaOH solution, and the ALP activity was estimated by the optical absorbance measured at 405 nm.

Alizarin Red S Staining and Quantification

Osteoblasts were cultured for 18 days and stained with Alizarin Red S (0223, ScienCell, Carlsbad, CA, USA) at room temperature for 20 min, and images were captured after washing. To quantify calcium mineralization in cells, the stained material in cells was dissolved in 10% cetylpyridinium chloride (C0732, Sigma-Aldrich, USA) at room temperature for 1 h, and the quantification was estimated by the optical absorbance measured at 405 nm.

Statistical Analysis

Each series of experiments was repeated at least three times. The results obtained from a typical experiment were expressed as the means \pm S.D. Significant differences were determined using factorial analysis of variance. Group comparisons were made by one-way ANOVA followed by the Dunnett's test using SPSS software, version 15.0 (Armonk, NY, USA).

CONCLUSIONS

Using *in vivo* OVX rats and *in vitro* osteoclast and osteoblast cultures, we show that calcitonin induces bone formation by increasing the expression of Wnt10b in osteoclasts in ovariectomy-induced osteoporotic rats. The present study provides further information about calcitonin at the molecular

level of bone remodeling, and will thus help in future potential therapeutic studies on postmenopausal osteoporosis.

DATA AVAILABILITY STATEMENT

The raw data supporting the conclusions of this article will be made available by the authors, without undue reservation.

ETHICS STATEMENT

The animal study was reviewed and approved by the Institutional Animal Care and Use Committee (IACUC) of the Laboratory Animal Center of the National Defense Medical Center; the identification number is IACUC-14-104.

AUTHOR CONTRIBUTIONS

J-FS, C-YH, T-HChe, and P-JT: study conception and design. T-HChe, C-YH, J-FS, Y-NT, and T-HChu: methodology and investigation. C-YH: formal analysis. J-FS and T-HChe: resources. T-HChu, J-FS, and P-JT: writing—original draft preparation. C-YH, P-JT, T-HChe, and J-FS: writing—review and editing. C-YH, J-FS, and T-HChe: supervision. C-YH, P-JT, T-HChe, and J-FS: project administration. All authors have read and agreed to the published version of the manuscript.

FUNDING

This research was supported by research grants from the Ministry of Science and Technology (MOST 108-2320-B-016-013), Ministry of National Defense-Medical Affairs Bureau (MAB-108-0088), Tri-Service General Hospital (TSGH-D109137), and Chi Mei Medical Center (CMNDMC10713) to J-FS.

ACKNOWLEDGMENTS

The authors acknowledge the technical support provided by the Instrument Center of the National Defense Medical Center; micro-CT scans, bone morphometric analysis, volumetric bone mineral density, and 3D image visualization were performed by Tzu-Hung Lin and Shen-Chuan Lo, Material and Chemical Research Laboratories, Industrial Technology Research Institute.

REFERENCES

- Copp DH, Cheney B. Calcitonin—a hormone from the parathyroid which lowers the calcium-level of the blood. *Nature*. (1962) 193:381–2. doi: 10.1038/193381a0
- Chambers TJ, Athanasou NA, Fuller K. Effect of parathyroid hormone and calcitonin on the cytoplasmic spreading of isolated osteoclasts. *J Endocrinol*. (1984) 102:281–6. doi: 10.1677/joe.0.1020281
- Hurley DL, Tiegs RD, Wahner HW, Heath H III. Axial and appendicular bone mineral density in patients with long-term deficiency or excess of calcitonin. *N Engl J Med*. (1987) 317:537–41. doi: 10.1056/NEJM198708273170904
- Wuster C, Raue F, Meyer C, Bergmann M, Ziegler R. Long-term excess of endogenous calcitonin in patients with medullary thyroid carcinoma does not affect bone mineral density. *J Endocrinol*. (1992) 134:141–7. doi: 10.1677/joe.0.1340141
- Davey RA, Findlay DM. Calcitonin: physiology or fantasy? *J Bone Miner Res*. (2013) 28:973–9. doi: 10.1002/jbmr.1869
- Naot D, Musson DS, Cornish J. The activity of peptides of the calcitonin family in bone. *Physiol Rev*. (2019) 99:781–805. doi: 10.1152/physrev.00066.2017
- Hoff AO, Catala-Lehnen P, Thomas PM, Priemel M, Rueger JM, Nasonkin I, et al. Increased bone mass is an unexpected phenotype associated with deletion of the calcitonin gene. *J Clin Invest*. (2002) 110:1849–57. doi: 10.1172/JCI200214218

8. Keller J, Catala-Lehnen P, Huebner AK, Jeschke A, Heckt T, Lueth A, et al. Calcitonin controls bone formation by inhibiting the release of sphingosine 1-phosphate from osteoclasts. *Nat Commun.* (2014) 5:5215. doi: 10.1038/ncomms6215
9. Khosla S, Hofbauer LC. Osteoporosis treatment: recent developments and ongoing challenges. *Lancet Diabetes Endocrinol.* (2017) 5:898–907. doi: 10.1016/S2213-8587(17)30188-2
10. Baron R, Hesse E. Update on bone anabolics in osteoporosis treatment: rationale, current status, and perspectives. *J Clin Endocrinol Metab.* (2012) 97:311–25. doi: 10.1210/jc.2011-2332
11. Kuo YJ, Tsuang FY, Sun JS, Lin CH, Chen CH, Li Y, et al. Calcitonin inhibits SDCP-induced osteoclast apoptosis and increases its efficacy in a rat model of osteoporosis. *PLoS ONE.* (2012) 7:e40272. doi: 10.1371/journal.pone.0040272
12. Baron R, Kneissel M. WNT signaling in bone homeostasis and disease: from human mutations to treatments. *Nat. Med.* (2013) 19:179–92. doi: 10.1038/nm.3074
13. Baron R, Gori F. Targeting WNT signaling in the treatment of osteoporosis. *Curr Opin Pharmacol.* (2018) 40:134–41. doi: 10.1016/j.coph.2018.04.011
14. Shyu JF, Shih C, Tseng CY, Lin CH, Sun DT, Liu T, et al. Calcitonin induces podosome disassembly and detachment of osteoclasts by modulating Pyk2 and Src activities. *Bone.* (2007) 40:1329–42. doi: 10.1016/j.bone.2007.01.014
15. Wang JW, Yeh CB, Chou SJ, Lu KC, Chu TH, Chen Y, et al. YC-1 alleviates bone loss in ovariectomized rats by inhibiting bone resorption and inducing extrinsic apoptosis in osteoclasts. *J Bone Miner Metab.* (2018) 36:508–18. doi: 10.1007/s00774-017-0866-z
16. Shi J, Chi S, Xue J, Yang J, Li F, Liu X. Emerging role and therapeutic implication of Wnt signaling pathways in autoimmune diseases. *J Immunol Res.* (2016) 2016:9392132. doi: 10.1155/2016/9392132
17. Maruotti N, Corrado A, Neve A, Cantatore FP. Systemic effects of Wnt signaling. *J Cell Physiol.* (2013) 228:1428–32. doi: 10.1002/jcp.24326
18. Boland GM, Perkins G, Hall DJ, Tuan RS. Wnt 3a promotes proliferation and suppresses osteogenic differentiation of adult human mesenchymal stem cells. *J Cell Biochem.* (2004) 93:1210–30. doi: 10.1002/jcb.20284
19. Day TE, Guo X, Garrett-Beal L, Yang Y. Wnt/beta-catenin signaling in mesenchymal progenitors controls osteoblast and chondrocyte differentiation during vertebrate skeletogenesis. *Dev Cell.* (2005) 8:739–50. doi: 10.1016/j.devcel.2005.03.016
20. Baksh D, Boland GM, Tuan RS. Cross-talk between Wnt signaling pathways in human mesenchymal stem cells leads to functional antagonism during osteogenic differentiation. *J Cell Biochem.* (2007) 101:1109–24. doi: 10.1002/jcb.21097
21. Ota K, Quint P, Ruan M, Pederson L, Westendorf JJ, Khosla S, et al. TGF-beta induces Wnt10b in osteoclasts from female mice to enhance coupling to osteoblasts. *Endocrinology.* (2013) 154:3745–52. doi: 10.1210/en.2013-1272
22. Zheng CM, Hsu YH, Wu CC, Lu CL, Liu WC, Zheng Q, et al. Osteoclast-released Wnt-10b underlies cinacalcet related bone improvement in chronic kidney disease. *Int J Mol Sci.* (2019) 20:2800. doi: 10.3390/ijms20112800
23. Lu CL, Shyu JF, Wu CC, Hung CF, Liao MT, Liu C, et al. Association of anabolic effect of calcitriol with osteoclast-derived Wnt 10b secretion. *Nutrients.* (2018) 10:1164. doi: 10.3390/nu10091164
24. Komori T. Regulation of proliferation, differentiation and functions of osteoblasts by runx2. *Int J Mol Sci.* (2019) 20:1694. doi: 10.3390/ijms20071694
25. Liu H, Zhang N, Liu Y, Liu L, Yin G, En L. Effect of human Wnt10b transgene overexpression on peri-implant osteogenesis in ovariectomized rats. *Hum Gene Ther.* (2018) 29:1416–27. doi: 10.1089/hum.2018.003

Conflict of Interest: The authors declare that the research was conducted in the absence of any commercial or financial relationships that could be construed as a potential conflict of interest.

Copyright © 2020 Hsiao, Chen, Chu, Ting, Tsai and Shyu. This is an open-access article distributed under the terms of the Creative Commons Attribution License (CC BY). The use, distribution or reproduction in other forums is permitted, provided the original author(s) and the copyright owner(s) are credited and that the original publication in this journal is cited, in accordance with accepted academic practice. No use, distribution or reproduction is permitted which does not comply with these terms.



Dual Effects of Lipid Metabolism on Osteoblast Function

Nathalie S. Alekos¹, Megan C. Moorer^{1,2} and Ryan C. Riddle^{1,2*}

¹ Department of Orthopaedic Surgery, Johns Hopkins University School of Medicine, Baltimore, MD, United States,

² Baltimore Veterans Administration Medical Center, Baltimore, MD, United States

The skeleton is a dynamic and metabolically active organ with the capacity to influence whole body metabolism. This newly recognized function has propagated interest in the connection between bone health and metabolic dysfunction. Osteoblasts, the specialized mesenchymal cells responsible for the production of bone matrix and mineralization, rely on multiple fuel sources. The utilization of glucose by osteoblasts has long been a focus of research, however, lipids and their derivatives, are increasingly recognized as a vital energy source. Osteoblasts possess the necessary receptors and catabolic enzymes for internalization and utilization of circulating lipids. Disruption of these processes can impair osteoblast function, resulting in skeletal deficits while simultaneously altering whole body lipid homeostasis. This article provides an overview of the metabolism of postprandial and stored lipids and the osteoblast's ability to acquire and utilize these molecules. We focus on the requirement for fatty acid oxidation and the pathways regulating this function as well as the negative impact of dyslipidemia on the osteoblast and skeletal health. These findings provide key insights into the nuances of lipid metabolism in influencing skeletal homeostasis which are critical to appreciate the extent of the osteoblast's role in metabolic homeostasis.

Keywords: osteoblast, fatty acid metabolism, dyslipidemia, bone mass, lipoproteins

OPEN ACCESS

Edited by:

Lilian Irene Plotkin,
Indiana University Bloomington,
United States

Reviewed by:

Ahmed Al Saedi,
The University of Melbourne, Australia
Mathieu Ferron,
Institute of Clinical Research De
Montreal (IRCM), Canada

*Correspondence:

Ryan C. Riddle
riddle1@jhmi.edu

Specialty section:

This article was submitted to
Bone Research,
a section of the journal
Frontiers in Endocrinology

Received: 30 June 2020

Accepted: 25 August 2020

Published: 23 September 2020

Citation:

Alekos NS, Moorer MC and Riddle RC
(2020) Dual Effects of Lipid
Metabolism on Osteoblast Function.
Front. Endocrinol. 11:578194.
doi: 10.3389/fendo.2020.578194

INTRODUCTION

Development of the mammalian skeleton and maintenance of its structure for the life of the organism requires the coordinated actions of two specialized cells. Osteoclasts, large multinucleated cells that are derived from the monocyte/macrophage lineage of hematopoietic cells, are responsible for bone resorption. After attaching to an exposed bone surface, osteoclasts acidify a resorption lacuna to dissolve the mineral fraction of bone and then secrete proteolytic enzymes that degrade the organic matrix component (1). During the resorption process, growth factors trapped within bone matrix are released and trigger the recruitment of osteoblasts responsible for new bone formation (2, 3). Derived from mesenchymal stem cells present in the bone marrow stroma, these cells are characterized by their cuboidal shape and abundance of rough endoplasmic reticulum necessary for the production of the collagen-rich bone matrix (4). After building a packet of bone most osteoblasts will die by apoptosis, but small fractions will either become encapsulated within the bone matrix and fulfill regulatory functions as osteocytes or dedifferentiate and line bone surfaces. Known as bone remodeling, this process prevents the accumulation of old or damaged bone that may lead to fracture. In humans, peak bone mass is reached during the second decade of life as a result of net bone accrual during childhood, when bone formation exceeds resorption and osteoblasts and osteoclasts act on different bone surfaces to maintain the overall shape of bones during longitudinal growth (known as modeling). A balance between formation and resorption

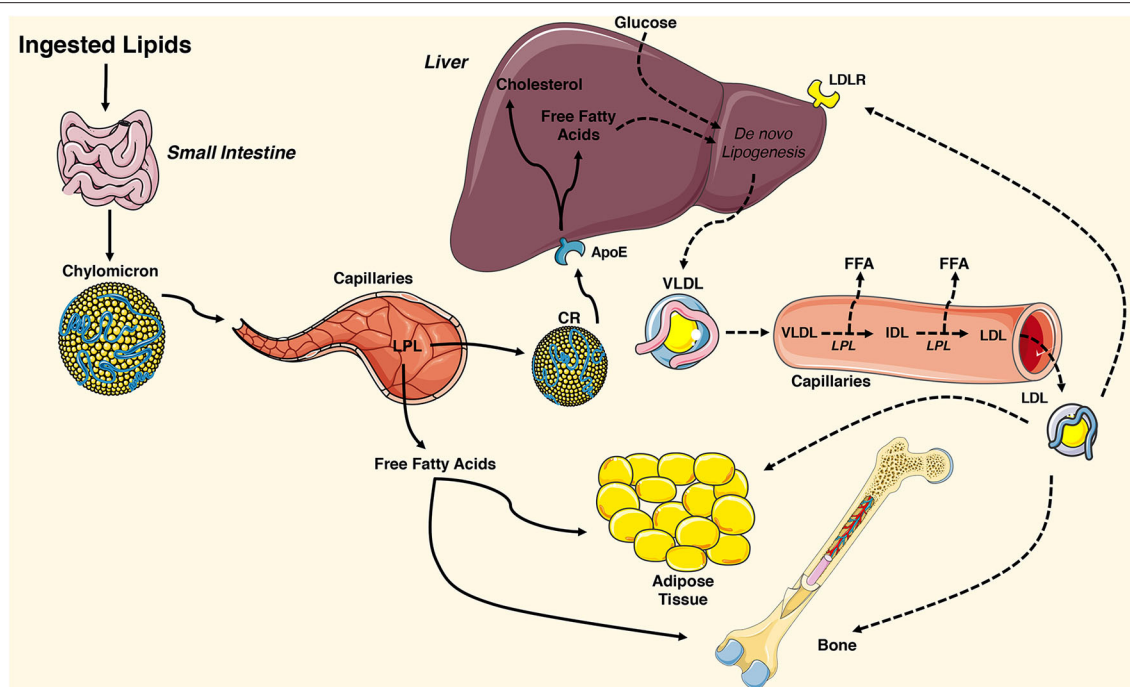


FIGURE 1 | Overview of tissue-targeted lipid metabolism. Ingested lipids are broken down in the intestinal lumen and internalized by enterocytes of the small intestine. The water insoluble triglycerides and cholesterol are repackaged into chylomicrons and travel through the lymphatic system and into the circulatory system where they engage lipoprotein lipase (LPL) on the surface of capillary endothelial cells. The hydrolyzed triglycerides result in release of free fatty acids that are taken up by adipose tissue and the skeleton. The remaining chylomicron remnants (CR) are cleared by the liver via the apolipoprotein E (ApoE) receptor. CR-derived cholesterol and free fatty acids and circulating glucose are used for *de novo* lipogenesis, generating ATP for the liver, or repackaged into very low-density lipoproteins (VLDL). VLDL particles are released into the circulation where they engage LPL and release free fatty acids, which are also available for uptake. The remaining low-density lipoprotein (LDL) are internalized by cells expressing the low-density lipoprotein receptor (LDLR) including adipocytes and osteoblasts. This figure was created using Servier Medical Art image templates under a Creative Commons Attribution 3.0 Unported License.

then occurs in early adulthood. However, with advancing age or as a result of numerous endocrine pathologies, an acceleration of osteoclastic activity leads to bone loss as osteoblastic activity is unable to keep pace. As bone mass decreases and structure integrity deteriorates, the risk of fracture increases (5, 6).

The tremendous economic impact of osteoporotic fractures (7–9) and development of comorbidities after fracture (10–12) highlight the need to understand the genetic, cellular, and endocrine mechanisms that influence bone mass. With the renewed interest in intermediary metabolism in cancer (13–15) and the recognition that bone is not merely a structural organ acting as a reserve of minerals but also an endocrine organ that can influence systemic metabolism (16–21), research in the field of skeletal biology has coalesced over the last few years on the contributions of cellular metabolism to osteoblast function and bone formation. The field reasoned that if bone contributes to the regulation of metabolic homeostasis through the release of osteocalcin and other hormones (16, 21), then the availability of nutrients must be critical to osteoblast function. Indeed, hierarchical analysis of energy requirements of cellular function (22) suggest that the bone remodeling process is energy intensive due to the synthesis of large extracellular matrix proteins and the necessity of concentrating mineral ions for hydroxyapatite crystal formation. Evidence from both the laboratory and the clinic

supports this hypothesis as caloric restriction during gestation or during postnatal life strongly influences the trajectory of both the accrual and the maintenance of bone mass (23–25). Additionally, an increase in oxidative phosphorylation and the abundance of mitochondria appears to be a requirement for the differentiation of osteoblasts from marrow stem cells (26–29).

Osteoblasts harvest energy from a number of fuel molecules. Studies performed more than 50 years ago first highlighted the avidity of osteoblasts for glucose. Isolated osteoblasts or bone tissue explants from mice, rats, rabbits, and humans all used glucose to produce lactate even under aerobic conditions (30–34). More contemporary studies indicated that glucose acquisition is mediated by glucose transporter-1 (35) and that metabolic programming of glucose utilization is adjusted according to the stage of differentiation (28, 36). Cells of the osteoblast lineage also consume a significant amount of glutamine which is required for skeletal stem cell specification, can be catabolized by the tricarboxylic acid cycle to generate ATP, and serves as a regulatory signal to maintain endoplasmic reticulum health during stages of heightened protein synthesis (37, 38).

While lipid metabolism yields significantly more ATP than glucose or glutamine catabolism, its role in osteoblast function remains more controversial. Recent studies have highlighted

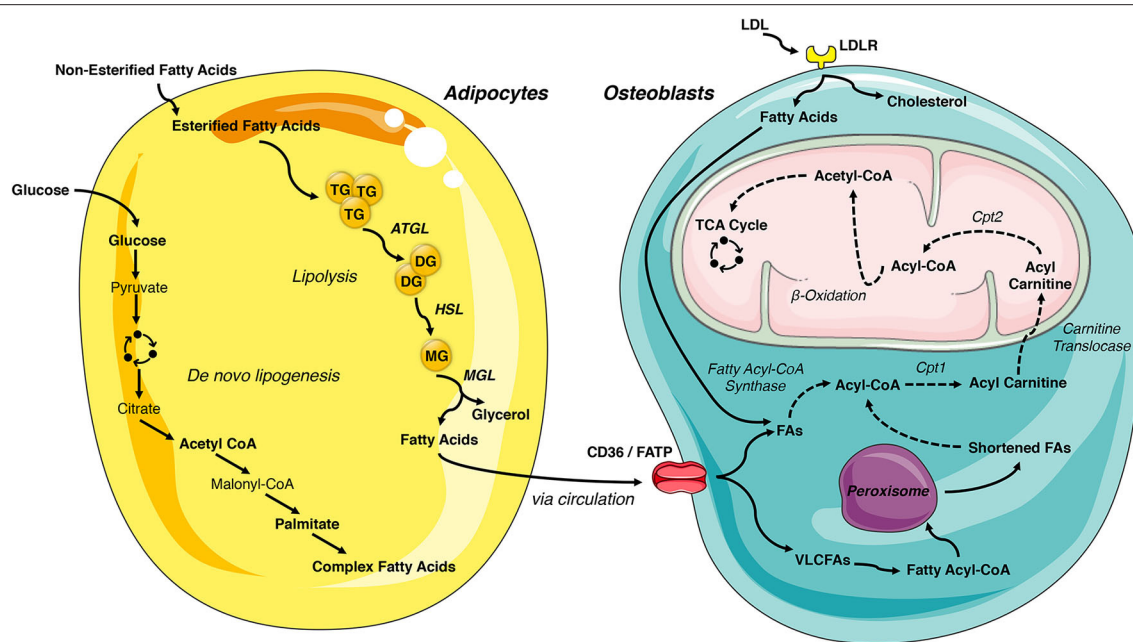


FIGURE 2 | Lipid- flux between the adipocyte and osteoblast. White adipose tissue is the primary storage depot of lipids during excess consumption, which are subsequently released when energy expenditure exceeds caloric intake. Esterified fatty acids are stored in the adipocytes as triglycerides and are hydrolyzed by the rate limiting enzyme, adipose triglyceride lipase (ATGL), into diglycerides. Diglycerides are hydrolyzed into monoglycerides by hormone sensitive lipase (HSL) and further into fatty acids by monoacylglycerol lipase (MGL), which are then released into circulation. Adipocyte uptake of glucose is metabolized to acetyl-CoA and used for *de novo* fatty acid synthesis. These newly synthesized fatty acids are another lipid source for the osteoblast. LDL-derived fatty acids and uptake of circulating free fatty acids via CD36/FATPs are vital energy sources for the osteoblast. These internalized free fatty acids are converted into acyl-CoA by fatty acyl-CoA synthase. Very long chain fatty acids (VLCFAs) (more than 22 carbons) are first shortened by the peroxisome. Acyl-CoA is transported to the mitochondrial matrix by a carnitine exchange system in order to undergo β -oxidation. The product, acetyl-CoA is transferred to the TCA cycle and electron transport chain for generation of ATP. This figure was created using Servier Medical Art image templates under a Creative Commons Attribution 3.0 Unported License.

the importance of fatty acid catabolism for normal bone formation (39, 40), but detrimental effects of lipids on osteoblast performance are also well-known (41, 42). In this review, we discuss the dual effects of lipids on osteoblast function and the maintenance of bone mass and strength. We provide a brief overview of the trafficking and metabolism of lipids in target tissues like bone. We then describe studies which highlight the importance of fatty acids metabolism for the accrual of bone mass and the mechanisms that regulate fatty acid utilization. Finally, we discuss the effects of dyslipidemia on osteoblast function and the potential for this condition to desensitize osteoblasts to anabolic signals.

OVERVIEW OF LIPID METABOLISM

The lipid molecules that support cellular metabolism are primarily derived from three sources: ingested fat, lipoproteins produced by the liver, and non-esterified fatty acids released by white adipose tissue (Figure 1). Postprandial triglycerides and cholesterol esters are broken down in the intestinal lumen by cholesterol esterases, pancreatic lipases, and bile salts. These molecules are then taken up by the enterocyte of the small intestine, re-esterified, and packaged with lipid-soluble vitamins, and apolipoproteins into chylomicrons. Chylomicrons enable

water-insoluble fats and cholesterol to move through the lymphatic system and into the circulatory system. Engagement of the chylomicron by lipoprotein lipase (LPL) on capillary endothelium results in the hydrolysis of triglycerides and the delivery of fatty acids to target tissues (43, 44). The chylomicron remnants containing cholesterol and apolipoproteins are then cleared by the liver (45).

In healthy individuals, the liver exhibits a nearly constant lipid flux. Chylomicron remnants and free fatty acids are taken up by the liver, while a portion of the circulating glucose taken up by the organ is used for *de novo* lipogenesis. Lipid molecules from each of these sources can be used to generate ATP in the liver or they can be packaged along with apolipoprotein (Apo) B-100, ApoC, and ApoE into very low-density lipoproteins (VLDL) on the endoplasmic reticulum. VLDL are released into the circulation and metabolized by target tissues in a manner similar to that of chylomicrons, with LPL hydrolyzing triglycerides to fatty acids that can be imported by cells. In this case, the remaining lipoprotein particle is further metabolized to low density lipoprotein (LDL), which can be taken up by many tissues via the LDL receptor (44).

White adipose tissue is the primary storage depot for excess calories. Non-esterified fatty acids are taken up by adipocytes, esterified and stored as triglycerides, while glucose is metabolized to acetyl-CoA and then used as a substrate for *de novo* fatty

acid synthesis. When energy expenditure exceeds caloric intake or in response to a number of lipolytic hormones, the stored triglycerides can be hydrolyzed to glycerol and free fatty acids that are released into the circulation to be used for β -oxidation in other organs, including the skeleton. Lipolysis is mediated by the stepwise action of three lipases (illustrated in **Figure 2**). The rate limiting enzyme, adipose triglyceride lipase (ATGL), catalyzes the first reaction by hydrolyzing triacylglycerols at the sn-2 position to diacylglycerol and one fatty acid. Diacylglycerides are then preferentially hydrolyzed by hormone sensitive lipase (HSL) at the sn-3 position to yield a second free fatty acid (46). Monoacylglycerol lipase (MGL) catalyzes the final reaction generating glycerol and a third fatty acid (47). Most free fatty acids released into circulation are bound by albumin (48).

The intracellular metabolism of fatty acids taken up by cells depends on chain length. Short-chain (1-6 carbons) and medium-chain (7-12 carbons) fatty acids are produced by the bacterial fermentation of dietary fiber or the ingestion of dairy products. These lipids are primarily metabolized by enterocytes or by hepatocytes and are beyond the scope of this review (47). Long-chain fatty acids (13-21 carbons) are transported into cells by specific transporters (discussed below) but have limited solubility in the cytosol. To increase solubility, trap fatty acids in the cell, and produce a high energy thioester necessary for the next steps of catabolism, long-chain fatty acyl-CoA ligases catalyze the formation of fatty acyl-CoA in a reaction that requires the hydrolysis of 1 ATP to AMP. Acyl-CoA must then be transferred to the mitochondria by a carnitine exchange system to undergo β -oxidation. Carnitine palmitoyltransferase 1 (CPT1), the first and rate-limiting step in this process, is located on the outer mitochondrial membrane and catalyzes the replacement of CoA with carnitine. Acyl-carnitines are recognized and transferred by carnitine-acylcarnitine translocase into the mitochondria matrix where carnitine palmitoyltransferase 2 (CPT2) reverses the reaction of CPT1 and regenerates Acyl-CoA. The four reaction β -oxidation process removes 2 carbons from the carboxy end of the acyl-CoA to generate acetyl-CoA, 1 NADH and 1 FADH₂ that are transferred to the TCA cycle and electron transport chain for the generation of ATP (**Figure 2**). Successive rounds of β -oxidation are necessary to fully metabolize long-chain fatty acids (49).

Very long chain fatty acids (more than 22 carbons) can also be used to generate ATP but must be chain-shortened in peroxisomes before they can enter the mitochondria (50). Multi-functional peroxisomes encase more than 50 enzymes, with more than half involved in fat metabolism, in a single lipid bilayer. As in long chain fatty acid metabolism, very long chain fatty acids are first converted to acyl-CoAs in the cytosol. The fatty acyl-CoA is then transported into the peroxisome by members of the ATP binding cassette transporter D subfamily. Peroxisomal oxidation also involves four reactions but utilizes a separate set of enzymes to shorten the fatty acid chain and is not as efficient at ATP generation as there is no respiratory chain. Indeed, while the FADH₂ produced by one round of mitochondrial β -oxidation yields 2 ATP, the electrons from FADH₂ produced by peroxisomal oxidation are donated to oxygen to form H₂O₂. For this reason, chain shortened fatty

acids can be shuttled to the mitochondria for further metabolism via β -oxidation.

MECHANISMS OF LIPID UPTAKE BY OSTEOBLASTS

Although they are smaller than those evident in adipocytes, most cells contain a lipid droplet that can presumably be used to generate ATP via β -oxidation. Histological studies indicate that both mature osteoblasts and differentiating osteoblast progenitors contain stored lipid (51, 52), but these stored lipids do not appear to be a major energy source for mature osteoblast function. Kim et al. (39) ablated the expression of ATGL in cultures of calvarial osteoblasts and mature osteoblasts and osteocytes *in vivo* (Atgl^{flox/flox}; Osteocalcin-Cre), which should eliminate intracellular lipolysis, but did not find a defect in either *in vitro* osteoblast performance or bone structure *in vivo*. Therefore, osteoblasts appear to require extracellular lipid sources.

A combination of *in vivo* and *in vitro* studies have examined the uptake of circulating lipoproteins and free fatty acids by the osteoblast and the skeleton. In perhaps the most comprehensive study, Neimeier and colleagues (53) modeled postprandial lipoprotein uptake by intravenously injecting fluorescent- or ¹²⁵I-labeled chylomicron remnants into mice. Skeletal uptake was 17% that of liver but was greater than other catabolic organs including muscle and heart. Importantly, chylomicron remnant uptake by the osteoblast/osteocyte-enriched femoral diaphysis was greater than that of bone marrow, indicating the skeletal acquisition was not simply carried out by marrow adipocytes. Osteoblasts also appear to take up of LDL and VLDL and acquisition can be enhanced by co-administration with ApoE, but these studies have primarily been performed in cultured osteoblasts (54–56). Skeletal uptake of fatty acids was assessed *in vivo* by Bartelt et al. (57) and Kim et al. (39) after delivering ³H-linoleic acid and ¹⁴C-palmitic acid or ³H-bromo-palmitate, respectively, via oral gavage. Similar to the uptake of chylomicron remnants, these studies revealed that skeletal acquisition of fatty acids is comparable to tissues that are more classically associated with fatty acid metabolism. Together, these studies highlight a potential role of bone in fatty acid metabolism and postprandial clearance of fat from the circulation.

The identity and requirements for specific receptors and transporters that allow osteoblasts to take up fatty acids and lipoproteins (**Figure 2**) need additional study, but experimental data exists for a number of possible mechanisms. Consistent with osteoblastic uptake of chylomicron remnants and lipoproteins, osteoblasts express the low-density lipoprotein receptor (LDLR) and low-density lipoprotein receptor-related protein-1 (LRP1) (58, 59). Interpretation of the skeletal phenotypes of mice engineered to be deficient for LDLR (LDLR^{-/-}) requires care as studies have reported both reduced (60) and elevated bone volume (61) relative to wildtype mice. Both *in vivo* (60) and *in vitro* (62) analyses indicate that the actions of the LDLR are important for osteoblast function as its ablation results in reductions in the expression of gene markers of osteoblastic

differentiation. These data accord with the ability of LDL to stimulate cell growth and sustain responsivity to anabolic stimuli in osteoblasts cultured under serum-free conditions (63). The discrepancies in bone volume observed *in vivo* are likely be related to the requirement for LDLR during osteoclast differentiation (60, 61).

LRP1 can facilitate the endocytosis of triglyceride and cholesterol containing chylomicron remnants in cultures of osteoblastic cell models (58) and polymorphisms in the gene encoding this receptor are associated with bone mineral density (64). However, analysis of an osteoblast-specific knockout mouse (*Lrp1*^{flox/flox}; Runx2-Cre) revealed an osteopenic phenotype but there was no effect on systemic lipoprotein clearance or osteoblasts' ability to sequester fatty acids (65). While the bone phenotype has been attributed to marked increases in osteoclastogenesis (65), the sustained ability to take up lipoproteins could be due to the engagement of other LDLR family members. LRP5 and LRP6 are most typically associated with the propagation of signaling in response to Wnt ligands (66), but these receptors also have the capacity to bind and mediate the endocytosis of lipoproteins and chylomicron remnants (67, 68). Cultured osteoblasts rendered deficient for LRP5 also retained the ability to take up LDL (56), indicating that combinatorial genetic studies wherein the expression of multiple LRP receptors are simultaneously ablated may be necessary to discern receptor function in lipid particle uptake.

Osteoblasts also take up high density lipoproteins (HDL) and express Scarb1 (also referred to as SR-B1) (55), the major receptor for high-density lipoproteins (69). Some epidemiological studies suggest a positive correlation between BMD and HDL levels, but others have reported contradictory results [see (70) for a comprehensive review]. Interpretation of an association between HDL and bone mass in animal models has been equally challenging. Martineau and colleagues (71) reported that Scarb1 null mice display increases in HDL-associated cholesterol and increases in femoral bone volume and mineralization at 2 and 4 months in association with increases in osteoblast surface and bone formation rate, which suggests a detrimental effect of HDL on skeletal homeostasis. However, it remains possible that the high bone mass phenotype in these mice is due to an increase in serum adrenocorticotropin (ACTH), which has anabolic effects on osteoblasts (72, 73). Furthermore, control and Scarb1 deficient osteoblasts exhibited similar levels of HDL-cholesterol uptake *in vitro* (71). A follow-up study by this same group reported that Scarb1 deletion in MSCs increased osteoblastogenesis but decreased terminal osteocyte differentiation as vertebral osteocyte density was modestly decreased in the mutant mice (74). However, a more recent study contradicted these findings and reported Scarb1 null animals to be osteopenic in the vertebrae at 16 weeks with decreases in resorption and formation markers, and diminished osteoblast differentiation markers both *in vitro* and *in vivo* (73). Here too, alterations in bone volume were attributed to dose dependent effects of ACTH on bone. Similarly, mice with impaired HDL synthesis displayed reduced bone mass and impaired differentiation (75) suggesting a necessity for HDL in osteoblast function. Further *in vivo* studies using genetic models with osteoblast specific deletions

are required to further delineate Scarb1 function and a role for reverse cholesterol transport will need to be considered.

Osteoblasts also express the receptors necessary to take up and metabolize free fatty acids. CD36 is a two-transmembrane glycoprotein receptor that binds long-chain fatty acids as well as oxidized low-density lipoprotein (oxLDL) and facilitates their transport into the cell (55, 76). While direct studies of its effect on fatty acid uptake have not yet been completed, CD36 null mice exhibit a low bone mass phenotype secondary to impaired bone formation (77) that implies fatty acid uptake is essential for osteoblast function. The SLC27 family of fatty acid transport proteins (also referred to as FATP1-6), may also contribute to osteoblasts acquisition of long-chain fatty acids for oxidation (76, 78), as multiple family members are expressed by primary osteoblasts (40).

REQUIREMENT FOR FATTY ACID OXIDATION IN OSTEOSTASTS

The effects of specific fatty acids on the functions of the major bone cells has recently been reviewed elsewhere (79). Direct examination of the requirement for fatty acid oxidation during postnatal bone acquisition and bone repair has been examined in two studies. In the first, Kim and colleagues disrupted the expression of CPT2 in mature osteoblasts and osteocytes (*Cpt2*^{flox/flox}; Osteocalcin-Cre) (39). As noted above, CPT2 catalyzes an obligate step in fatty acid β -oxidation and was selected for ablation in this model because it is encoded by a single gene (three isoforms of *CPT1* are present in mammalian genomes). The skeletal phenotype of the mutant mice was sexually dimorphic, with male mice fed a normal chow diet exhibiting only a transient decrease in trabecular bone volume in the distal femur and L5 vertebrae at 6 weeks of age. By contrast, female mutants exhibited defects in trabecular bone volume in the distal femur and L5 vertebrae and an expansion of cortical bone tissue area at both 6 and 12 weeks. This discrepancy between sexes appears to be related to a greater ability to adjust fuel utilization in males, as male mutants exhibited an increase in femoral glucose uptake that was not evident in female mutants. The greater inhibition of osteoblast performance and inhibition of glucose uptake in CPT2 mutant osteoblasts treated with estrogen may explain the sex differences in metabolic flexibility. Interestingly, both male and female CPT2 mutants exhibited an increase in serum free fatty acid levels, which suggests that disrupting fatty acid utilization by osteoblasts and osteocytes is sufficient to alter lipid homeostasis (39).

In the second study, van Gastel et. al. (40) identified a role for fatty acid utilization during fracture healing and the specification of skeletal cell fate. During the bone healing process, endochondral ossification is initiated by periosteal progenitor cells that differentiate to chondrocytes and form an avascular, cartilaginous callus. The callus is subsequently invaded by the vasculature (80) and replaced by bone (81, 82). Blood vessels are expected to deliver the oxygen, nutrients, and growth factors necessary to drive bone formation. Through biochemical assays and the reanalysis of an existing single cell RNAseq study

of skeletal progenitors (83), Van Gastel et al. (40) reported that chondrocytes express low levels of CPT1a and high Glut1 levels as well as elevated lactate production, which suggests that glycolysis meets the chondrocyte's energy needs. On the other hand, osteoblasts expressed high levels of Glut1 and CPT1a, exhibited higher levels of oxygen consumption, and an increased ability to metabolize palmitate, indicating a reliance on fatty acid oxidation. Importantly, knocking down the expression of CPT1a prevented the differentiation of skeletal stem cells to osteoblasts while local injection of free fatty acids during fracture repair increased the amount of bone formed in the callus and reduced the amount of cartilage. Mechanistic studies demonstrated that reduced fatty acid availability increased the activation of FOXO3, which in turn activated SOX9 and chondrogenic specification. Taken together, these studies highlight the requirement for fatty acid β -oxidation for bone-forming osteoblasts in bone repair and skeletal development.

Evidence for a role of peroxisomal lipid oxidation in bone is largely based on the phenotypes evident in patients affected by peroxisomal disorders and global knockout models. Human and mouse genetic studies have identified 14 peroxin genes (*PEX1-PEX26*) that encode proteins necessary for either the formation of peroxisomes or the transport of cargo into the organelle. Loss of function mutations in peroxin genes, which occur at a rate of ~ 1 in 50,000 births, result in autosomal recessive peroxisomal biogenesis disorders (PBD) that affect a number of organ systems. Individuals with more severe PBD subtypes often exhibit craniofacial anomalies, short stature, and limb length discrepancies. Less severe subtypes have been associated with reductions in bone mineral density and an increased susceptibility for non-traumatic fractures (84–86). In the mouse, hypomorphic alleles for *Pex7* leads to a reduction in longitudinal growth and impaired ossification of the digits (87), while a global knockout resulted in delayed ossification at multiple skeletal sites (88). Additional mouse genetic studies will be necessary to fully delineate the role of peroxisomes in skeletal tissue maintenance and function.

PATHWAYS REGULATING FATTY ACID OXIDATION

If fatty acid metabolism is used to generate the ATP necessary for osteoblast function, then metabolic flux in this pathway should be regulated by the signals that drive bone formation. Indeed, two of the most potently anabolic pathways, Wnt signaling and parathyroid hormone signaling, appear to drive fatty acid oxidation.

Wnt Signaling

The anabolic effects of Wnt signaling on skeletal development, repair, and homeostasis have been well-studied (89, 90), and a number of studies have now demonstrated that the pathway coordinates the intermediary metabolism of the osteoblast with the energetic demands of bone formation (38, 91–93). LRP5 and LRP6 act as co-receptors for the Frizzled receptors that propagate Wnt signals and lead to the stabilization and activation

of β -catenin (66). While the osteoblast-specific ablation of either receptor (*Lrp5*^{flox/flox}; Osteocalcin-Cre and *Lrp6*^{flox/flox}; Osteocalcin-Cre) results in decreases in bone mineral density and vertebral trabecular bone volume (94), Frey et al. (56) found that the LRP5 mutants also exhibited increases in fat mass and serum triglycerides and free fatty acids, suggestive of a disruption in fatty acid utilization. Indeed, analysis of gene expression in cultured osteoblasts by microarray revealed that LRP5-deficient osteoblasts exhibited a downregulation of multiple genes involved in mitochondrial long-chain fatty acid β -oxidation. The effects of these changes in gene expression on β -oxidation were confirmed by examining the oxidation of oleate, which was reduced in LRP5 deficient osteoblasts when compared to control. Expression of LRP5 with a gain of function mutation (*Lrp5*^{G171V}) in osteoblasts produced the opposite phenotype, as the transgenic mice exhibited increases in bone volume and oxidative gene expression as well as decreases in fat mass, serum triglycerides, and fatty acids.

Subsequent genetic studies revealed that Wnt-mediated regulation of fatty acid oxidation proceeds via a β -catenin-dependent mechanism. Frey et al. (95) found that only Wnt ligands that increase the abundance of β -catenin in cultured osteoblasts, increase the capacity to fully oxidize oleate to carbon dioxide. Since constitutive ablation of β -catenin in osteoblasts results in early lethality (96) *in vivo*, the generation of an inducible β -catenin knockout mouse (*Ctnnb*^{flox/flox}; Osteocalcin-CreER^{T2}) was necessary to examine the transcription factor's effects on fatty acid oxidation. In this model, the temporal ablation of β -catenin resulted in high-turnover bone loss as well as increased fat mass and the development of insulin resistance. Additionally, the expression of genes involved in long-chain fatty acid oxidation and the ability to oxidize oleate were reduced in β -catenin deficient osteoblasts *in vitro*, while serum fatty acid levels were increased in the mutants *in vivo*. These studies have expanded the role of canonical Wnt-signaling to influencing fatty acid utilization and coordinating whole-body energy homeostasis.

As indicated above, a number of contemporary studies suggest that Wnt signaling also regulates glucose and glutamine utilization by the osteoblast. Wnt signaling through LRP5 increased aerobic glycolysis in the ST2 bone marrow stromal cell line (93) and mice engineered to overexpress Wnt7b in osteoblasts exhibit dramatic increases in bone volume, but simultaneously ablating the expression of Glut1 completely inhibited the increase in bone accrual (92). Similarly, Wnt signaling induced glutamine catabolism via the TCA cycle (38) which in turn stimulated the expression of genes involved in protein synthesis. Interestingly, these effects were mediated by the activation of mTOR and not β -catenin (92, 93, 97). Thus, the metabolic actions of Wnt signaling appear to depend on the specific downstream pathways that are activated.

Parathyroid Hormone Signaling

Parathyroid hormone (PTH) is a master regulator of serum calcium that signals in the bone, kidney, and intestine to increase calcium levels. Intermittent administration of human recombinant PTH (1–34) is now used to reduce the occurrence

of vertebral and non-vertebral fractures and increased bone mineral density in postmenopausal osteoporotic women (98). This therapeutic effect is mediated by PTH's ability to decrease apoptosis of mature osteoblasts (99), activate preexisting bone lining cells (100, 101), and stimulate osteoprogenitor recruitment (102).

The first indication that PTH might influence fatty acid oxidation were completed by Adamek et al. (103). In this study, PTH increased palmitate oxidation in specific cell populations isolated from bone by enzymatic digestion, while 1,25-Dihydroxycholecalciferol administration produced a more dramatic effect in multiple cell fractions. A greater reliance of lipids was suggested by Catherwood et al. (63) who demonstrated that the inclusion of LDL or VLDL in a basic medium was sufficient to support the proliferative response of rat ROS17/2.8 to PTH. In a more recent work, Esen et al. (104) used Seahorse technology, radiolabeled metabolites, and MC3T3-E1 cells to examine the effect of PTH on osteoblast metabolism. These studies demonstrated that PTH stimulates glucose uptake and increases lactate production but reduces the shuttling of glucose-derived carbon to the TCA cycle. These findings suggest that the increased rate of oxygen consumption after PTH administration is due to the oxidation of another fuel source, perhaps fatty acids imported from serum. While additional studies will be necessary, this paradigm is congruent with findings from Maridas et al. (105) that tracked the transfer of fatty acids from adipocytes to bone marrow stromal cells as well as the established ability of PTH to induce lipolysis in adipocytes (106). Likewise, the reduction in marrow adipose tissue volume after intermittent PTH treatment suggests that marrow adipocytes represent an energy reserve that provides fatty acids to fuel the anabolic activity of osteoblasts (105, 107). The finding that PTH can increase bone mass even under conditions of caloric restriction suggests that the relationship between PTH activity and metabolism is more complex and worthy of further study (105).

SKELETAL CONSEQUENCES OF DYSLIPIDEMIA

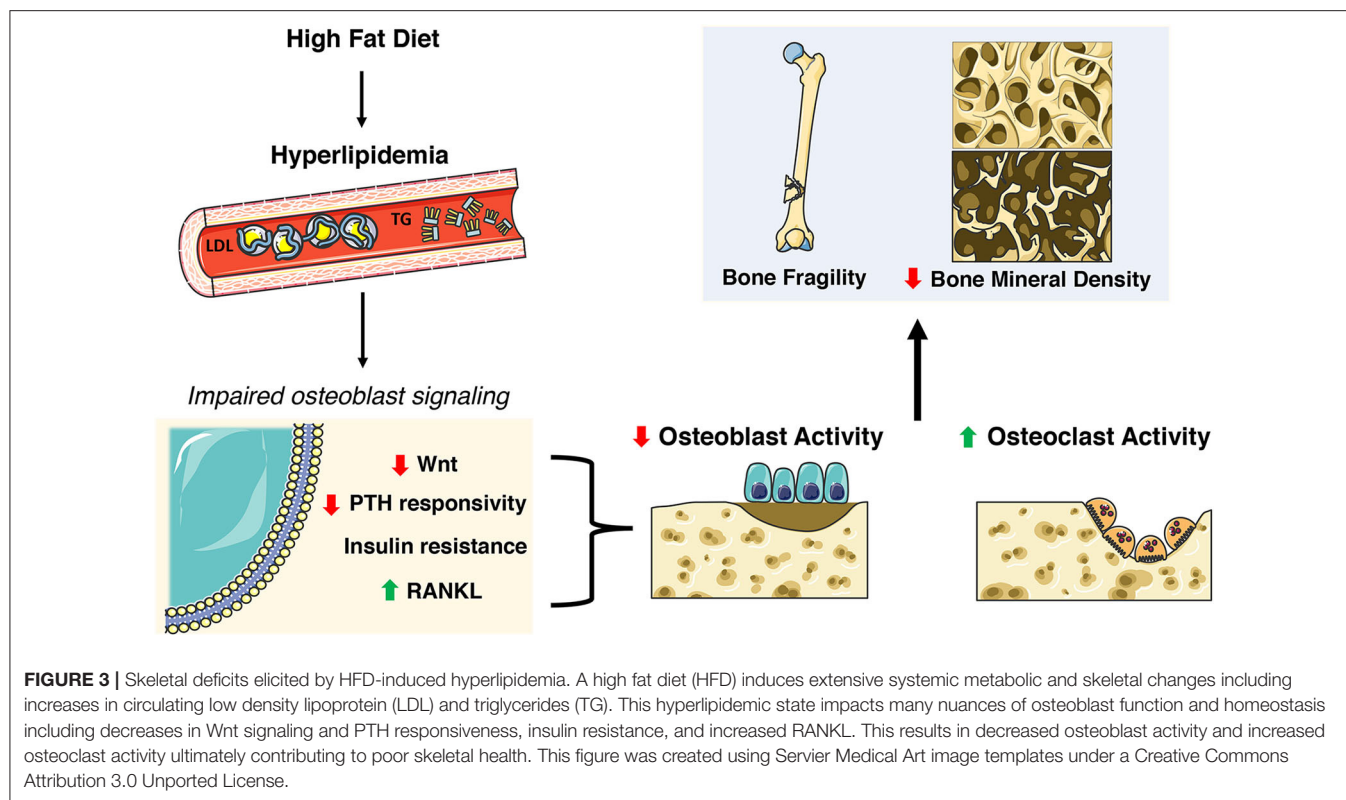
The Centers for Disease Control (CDC) reports that 95 million adults age 20 and older have high cholesterol (>200 ng/dL) while about 25% have elevated triglyceride levels (108). The aforementioned preclinical studies suggest a requirement for fatty acid oxidation for normal skeletal development and homeostasis, but epidemiological studies suggest that dyslipidemia has detrimental effects on bone (109–114). Elevated triglycerides, hypercholesterolemia and increased LDL are associated with higher risk of osteoporosis (111, 114) while increased LDL has been associated with non-vertebral fractures (115). Likewise, the National Health and Nutrition Examination Survey (NHANES III) reports that 63% of osteoporotic patients have hyperlipidemia (116). Studies from elite endurance athletes suggest that even short term exposure to a diet rich in fat can elicit a catabolic state in bone with an increase in markers of bone resorption and decreases in bone formation markers at rest and

following high-intensity exercise (117). The inverse relationship between hyperlipidemia and osteoporosis is further noted by the use of statins, a class of drugs used to lower cholesterol by blocking 3-hydroxy-3-methyl-glutaryl-CoA reductase, which was associated with an increase in BMD but no improvement in fracture risk (118–120). The sections below describe effects of dyslipidemia on osteoblast function and skeletal homeostasis in rodent models (Figure 3).

Effect of Dyslipidemia on Bone Structure and Remodeling

Over the last decade a combination of high fat diet (HFD) feeding models and hyperlipidemic mouse models have been used to investigate the effects of dyslipidemia on skeletal homeostasis. In addition to the development of hypertriglyceridemia, these models exhibit a host of metabolic defects, including but not limited to adipose hyperplasia, hyperinsulinemia, insulin resistance, central leptin resistance, and hepatic steatosis [reviewed in (121)], that can alter the balance of bone remodeling and influence bone strength. The consensus from the majority of these studies is that HFD feeding leads to a deterioration of trabecular bone mass at multiple skeletal sites in the axial and appendicular skeleton (60, 116, 122–126). A hypercholesteremic diet produces a similar effect on trabecular bone parameters (127). Reports on the effects of HFD on cortical bone parameters are more variable. Tencerova and colleagues (125) reported that 12 weeks of HFD increased cortical porosity and decreased cortical thickness in the tibia of male C57Bl/6J mice. These phenotypes would be expected to reduce bone strength and indeed a reduction in maximum force and energy to failure were noted in the femur by Picke et al. (128) when a similar HFD feeding paradigm was employed. By contrast, Silva et al. (129) found that HFD had minimal effects on cortical bone material properties and modestly increased cortical bone area and strength in mice derived from a Large-by-Small advanced intercross, wherein inbred mouse strains with extreme body sizes were crossed. However, this study did note a discrepancy in the relationship between the expansion of femoral tissue area with increasing body mass in HFD fed mice. This finding would appear to be in agreement with the minimal effects of a HFD on cortical bone geometry in female C57Bl/6J until data were normalized to body mass (130). In all likelihood, the differences observed in the cortical bone envelope are due to the balancing of detrimental effects of metabolic dysfunction with increased mechanical loading secondary to weight gain.

Histomorphometric analyses and serum measurements of bone turnover markers consistently demonstrated that trabecular bone loss in HFD and hyperlipidemic mice is secondary to a reduction in osteoblast numbers and function as well as an increase in the abundance of osteoclasts (122, 124, 127, 131, 132). Consistent with this finding, a HFD induces a decrease in the expression of the key osteogenic transcription factors RUNX2 and OSTERIX in the bone (60, 124, 132, 133) and impairments in proliferation and colony forming capacity in bone marrow-derived mesenchymal stem cells (BM-MSCs) (125). Additionally, osteoclast precursors isolated from HFD fed mice exhibit



an increased ability to form TRAP-positive osteoclasts after treatment with M-CSF and RANKL (134). The extensive effects of high fat intake were further revealed in gene expression profiling experiments performed by You et al. (135). In this study, 3 months of a high fat/high cholesterol diet led to the down-regulation of 2,200 genes and the up-regulation of 992 genes in RNA samples isolated from whole femur. Downregulated genes were implicated in a number of pathway associated with bone formation including the TGF- β /BMP2 pathway and the Wnt pathway, while up-regulated genes were associated with the control of bone resorption. Strikingly, comparative cluster analysis of these data with changes in gene expression in ovariectomized rats, a model of osteoporosis, revealed the co-regulation of more than 1,300 genes, suggestive of a convergence of pathogenic pathways.

To dissect the effects of altered lipid metabolism from other metabolic derangements in these models, *in vitro* culture systems wherein cultures of primary osteoblasts or osteoblast-like cell lines are treated with exogenous lipids have proven helpful (124, 135–139). The common finding in these studies is that the exposure to sufficient quantities of cholesterol, palmitate or oxidized LDL [a product of LDL interaction with reactive oxygen species (140)] reduces the proliferation of osteoblastic cells, induces cell death, and impairs osteoblast differentiation. These same stimuli induce an increase in the expression of RANKL by osteoblasts and enhance osteoclastic differentiation (127). Together these studies suggest that elevated lipid levels or the presence of oxidized lipids alone are sufficient to diminish osteoblast function and in turn lead to an imbalance in anabolic and catabolic processes in the skeleton.

HYPERLIPIDEMIA'S IMPACT ON ANABOLIC PATHWAYS OF THE OSTEOBLAST

The precise mechanisms by which exogenous or oxidized lipids impair osteoblast function are not completely understood. One potential explanation is the development of an inflammatory state that is thought to contribute to metabolic dysfunction in other tissues. In support of this idea, genetic ablation of the inflammatory cytokine TNF α inhibits bone loss associated with a HFD and the detrimental effects of palmitate on osteoblast differentiation (124). Additionally, a dual impact of lipids on inflammation has been noted. While polyunsaturated omega-3 fatty acids are thought to be beneficial to bone health (79, 141–144), and have anti-inflammatory effects (145), omega-6 fatty acids have been reported to be pro-inflammatory (146), leading to pathological bone remodeling and contributing to bone fracture and osteoporosis (79). In addition to inflammatory effects, a combination of *in vitro* and *in vivo* evidence suggests that dyslipidemia desensitizes osteoblasts to anabolic stimuli, including those that regulate lipid utilization.

Wnt Signaling

In addition to regulating the utilization of fatty acids by osteoblasts, Wnt/ β -catenin signaling is vulnerable to the detrimental effects of HFD feeding. At the most proximal end of the signaling pathway, dyslipidemia appears to result in an increase in the expression of several secreted antagonists of Wnt signaling. Increases in the abundance of both Dkk1 and

Sclerostin in serum have been reported in mice fed a HFD, while the latter was also found to be increased in the serum of *ob/ob* and *db/db* mice (128, 147–149). Similar increases have also been noted in obese humans and were accompanied by increases in Dkk-2 and secreted Frizzled-related proteins (150). At the distal end of the pathway, obesity and high fat diet feeding were associated with a reduction in β -catenin protein levels in the femur (151, 152). In a more extreme example, HFD feeding of the ApoE^{-/-} atherosclerosis mouse model, which induces marked decreases in osteoblast numbers and an inhibition of bone formation, resulted in widespread reductions in the expression of Wnt ligands and target genes at multiple skeletal sites (131). The mechanisms underlying these changes in transcription are not yet known.

Aside from changes in gene expression, Wang et al. (153) documented an interaction between the Wnt co-receptor LRP6 and oxidized phospholipids and oxidized LDL, produced as a result of an increase in reactive oxygen species. In this study, HFD fed mice exhibited consistent decreases in the numbers of osteoblast progenitors and the abundance of LRP6 at the cell surface in this cell population. Additional studies revealed that oxidized phospholipids and oxidized LDL induced the endocytosis of LRP6 and rendered cells resistant to the propagation of Wnt signaling. Considering the requirement for LRP6 function for the maintenance of normal bone mass (94), this mechanism may partially explain the ability of antibodies that neutralize oxidized phospholipids to attenuate bone loss due to a HFD (154).

Parathyroid Hormone Signaling

As indicated earlier, supplementation of basal, serum-free medium with LDL is sufficient to rescue responsivity to PTH (63). However, an overabundance of serum lipid can attenuate intermittent PTH-induced bone formation as evidenced by studies in the hyperlipidemic *Ldlr*^{-/-} and *ApoE*^{-/-} mouse lines. Intermittent PTH did not increase total bone mineral density or bone mineral content in the femur of these models, and PTH-induced increases in multiple parameters of trabecular bone structure were diminished or abolished in *Ldlr*^{-/-} mice (155). Later studies suggested that PTH resistance is likely to be due to the accumulation of oxidized lipids as administration of the D-4F peptide, which reduced lipid oxidation products, restored the anabolic effect of PTH (156–158). Given the requirement for LRP6 for normal PTH signaling (157, 159), resistance to PTH may also be mediated by oxidized LDL-induced internalization of LRP6 (157).

Insulin

The importance of insulin signaling in the osteoblast is revealed by the increased risk of fracture and decreased BMD in type 1 diabetes [reviewed in (160–162)], increased fracture risk despite an increase in BMD in type 2 diabetes (163, 164), and studies utilizing genetic mouse models in which insulin receptor expression is manipulated. The latter demonstrates that insulin receptor signaling is required for proliferation, survival, and osteoblast differentiation, as well as the ability of the osteoblast to contribute to the regulation of whole-body metabolism (165–167). As in skeletal muscle and adipose, dyslipidemia

appears to lead to insulin resistance in the osteoblast. Wei and colleagues (168) demonstrated that mice fed a HFD exhibited reduced IRS1/2 phosphorylation in osteoblasts after insulin stimulation *in vivo* and that stearate treatment *in vitro* led to SMURF-mediated ubiquitination of the insulin receptor. HFD did not reduce trabecular bone volume in this study (perhaps due to a reduced number of osteoclasts), but multiple markers of bone formation were reduced which suggests that skeletal insulin resistance may contribute to bone loss associated with dyslipidemia.

PEROXISOME PROLIFERATOR-ACTIVATED RECEPTOR γ (PPAR γ)

A final mechanism by which hyperlipidemia could impact osteoblast performance and skeletal homeostasis is through the activation of PPAR γ , a transcriptional regulator of adipogenesis that can be activated by elevated lipid levels. In bone, the nuclear receptor influences bone remodeling by stimulating adipogenic differentiation of mesenchymal stem cell at the expense of osteoblastogenesis and by stimulating osteoclastogenesis (169–171). HFD-fed rodents exhibit increased PPAR γ gene expression likely leading to defects in osteoblastogenesis (124, 151). Additionally, HFD caused an increase in callus adiposity attributed to increased PPAR γ expression and was associated with decreased osteoblast surface during late stages of healing post-fracture (172). One potential explanation for these finds is the ability of PPAR γ to interfere with anabolic Wnt/ β -catenin signaling (173–175). These effects are critically important for the targeting of PPAR γ function in the treatment of type 2 diabetes. Thiazolidinediones (TZDs), synthetic PPAR γ ligands, are used to increase insulin sensitivity (176–178) but do so at the expense of skeletal health. Long term use of these agonists increased risk of fractures in women (179, 180) and decreased bone formation markers (181) while short term use was sufficient to decrease bone formation markers, total hip bone density, and lumbar spine bone density (182).

It is important to note that genetic ablation of PPAR γ has beneficial effects on bone and body composition. Akune and colleagues (169) reported that PPAR^{+/-} exhibit an increase in trabecular bone volume secondary to a doubling of the osteoblast surface. When PPAR γ expression was ablated in mature osteoblasts and osteocytes (PPAR^{lox/lox} DMP1-Cre), the mutant mice exhibited increases in femoral bone mineral density and trabecular bone volume as well as reduced fat mass and increased energy expenditure (183). Crosstalk between osteoblasts and adipocytes in this model was indicated by *in vitro* studies wherein the 3T3-L1 adipocyte cell line was treated with medium conditioned by PPAR γ deficient osteoblasts culture media and exhibited reduced Oil Red O staining than those exposed to medium conditioned by wildtype osteoblasts (183). Furthermore, PPAR γ ablation in mature osteoblast/osteocytes protected against HFD-induced metabolic affects by improving liver steatosis, increasing lean mass, preventing fat mass increases, maintaining wild-type glycemic control, and improved

biomechanical strength (183). Therefore, modulating PPAR γ 's function in the osteoblast could be a potential target for combating bone loss associated with hyperlipidemia.

CONCLUDING REMARKS

In this review, we have attempted to convey the necessity of lipid utilization by the osteoblast for normal skeletal homeostasis as well as the potential for dyslipidemia to impair osteoblast function and lead to an imbalance in bone remodeling. Mitochondrial long chain fatty acid oxidation is of sufficient importance for osteoblast function that [1] genetic impairments in this metabolic pathway lead to alterations in whole body lipid homeostasis and [2] signaling pathways essential to bone mass accrual influence fatty acid metabolism. Future studies should be directed toward more fully delineating the mechanisms of fatty acquisition by osteoblasts. These studies will require the development of new genetic mouse models in which transporters are disrupted specifically in the osteoblasts as global knockout models exhibit disturbances in metabolism that may indirectly influence bone remodeling. Determining the mechanisms by which osteoblasts convey their need for sufficient fatty acid supply to other tissues is equally vital. In this regard, the emergence of bone as a hormone-producing tissue is likely to provide key insights into the responsible endocrine networks. As we noted above, the detrimental effects of dyslipidemia,

particularly in response to a high fat feeding in rodent models, on bone mass and the balance of bone formation and resorption are well-known, but the underlying mechanisms are still poorly understood. The increased recognition of bone as a lipid-utilizing tissue is likely to lead to a renewed interest in this area. Together these studies will provide a deeper understanding of the intimate interaction between the skeleton and metabolism and hopefully lead to treatment strategies that simultaneously reduce the burden of obesity and metabolic disease and preserve skeletal homeostasis.

AUTHOR CONTRIBUTIONS

All authors contributed to the drafting of this manuscript and approved the final version.

FUNDING

This work was supported by National Institutes of Health grant DK099134 and Biomedical Laboratory Research and Development Service of the Veterans Affairs Office of Research and Development grant BX003724.

ACKNOWLEDGMENTS

The authors are grateful to the many other investigators whose work has not been cited here due to space limitations.

REFERENCES

- Teitelbaum SL. Bone resorption by osteoclasts. *Science*. (2000) 289:1504–8. doi: 10.1126/science.289.5484.1504
- Tang Y, Wu X, Lei W, Pang L, Wan C, Shi Z, et al. TGF- β 1-induced migration of bone mesenchymal stem cells couples bone resorption with formation. *Nat Med*. (2009) 15:757–65. doi: 10.1038/nm.2793
- Xian L, Wu X, Pang L, Lou M, Rosen CJ, Qiu T, et al. Matrix IGF-1 maintains bone mass by activation of mTOR in mesenchymal stem cells. *Nat Med*. (2012) 18:1095–101. doi: 10.1038/nm.2793
- Dudley HR, Spiro D. The fine structure of bone cells. *J Biophys Biochem Cytol*. (1961) 11:627–49. doi: 10.1083/jcb.11.3.627
- Khosla S, Amin S, Orwoll E. Osteoporosis in men. *Endocr Rev*. (2008) 29:441–64. doi: 10.1210/er.2008-0002
- Syed FA, Ng AC. The pathophysiology of the aging skeleton. *Curr Osteoporos Rep*. (2010) 8:235–40. doi: 10.1007/s11914-010-0035-y
- Borgström F, Karlsson L, Orsäter G, Norton N, Halbout P, Cooper C, et al. Fragility fractures in Europe: burden, management and opportunities. *Arch Osteoporos*. (2020) 15:59. doi: 10.1007/s11657-020-0706-y
- Lewiecki EM, Ortendahl JD, Vanderpuye-Orgle J, Grauer A, Arellano J, Lemay J, et al. Healthcare policy changes in osteoporosis can improve outcomes and reduce costs in the United States. *JBM Plus*. (2019) 3:e10192. doi: 10.1002/jbm4.10192
- Tatangelo G, Watts J, Lim K, Connaughton C, Abimanyi-Ochom J, Borgström F, et al. The cost of osteoporosis, osteopenia, and associated fractures in Australia in 2017. *J Bone Miner Res*. (2019) 34:616–25. doi: 10.1002/jbmr.3640
- Edelmuth SVCL, Sorio GN, Sprovieri FAA, Gali JC, Peron SF. Comorbidities, clinical interurrences, and factors associated with mortality in elderly patients admitted for a hip fracture. *Rev Bras Ortop*. (2018) 53:543–51. doi: 10.1016/j.rboe.2018.07.014
- Pedersen AB, Ehrenstein V, Szépligeti SK, Sørensen HT. Hip fracture, comorbidity, and the risk of myocardial infarction and stroke: a danish nationwide cohort study, 1995–2015. *J Bone Miner Res*. (2017) 32:2339–46. doi: 10.1002/jbmr.3242
- Roche JJW, Wenn RT, Sahota O, Moran CG. Effect of comorbidities and postoperative complications on mortality after hip fracture in elderly people: Prospective observational cohort study. *Br Med J*. (2005) 331:1374–6. doi: 10.1136/bmj.38643.663843.55
- Pavlova NN, Thompson CB. The emerging hallmarks of cancer metabolism. *Cell Metab*. (2016) 23:27–47. doi: 10.1016/j.cmet.2015.12.006
- Yi M, Li J, Chen S, Cai J, Ban Y, Peng Q, et al. Emerging role of lipid metabolism alterations in Cancer stem cells. *J Exp Clin Cancer Res*. (2018) 37:1–18. doi: 10.1186/s13046-018-0784-5
- Currie E, Schulze A, Zechner R, Walther TC, Farese R V. Cellular fatty acid metabolism and cancer. *Cell Metab*. (2013) 18:153–61. doi: 10.1016/j.cmet.2013.05.017
- Lee NK, Sowa H, Hinoi E, Ferron M, Ahn JD, Confavreux C, et al. Endocrine regulation of energy metabolism by the skeleton. *Cell*. (2007) 130:456–69. doi: 10.1016/j.cell.2007.05.047
- Oury F, Sumara G, Sumara O, Ferron M, Chang H, Smith CE, et al. Endocrine regulation of male fertility by the skeleton. *Cell*. (2011) 144:796–809. doi: 10.1016/j.cell.2011.02.004
- Wei J, Karsenty G. An overview of the metabolic functions of osteocalcin. *Rev Endocr Metab Disord*. (2015) 16:93–8. doi: 10.1007/s11154-014-9307-7
- Guntur AR, Rosen CJ. Bone as an endocrine organ. *Endocr Pract*. (2012) 18:758–62. doi: 10.4158/EP12141.RA
- Lee W-C, Guntur AR, Long F, Rosen CJ. Energy metabolism of the osteoblast: implications for osteoporosis. *Endocr Rev*. (2017) 38:255–66. doi: 10.1210/er.2017-00064
- Dirckx N, Moorer MC, Clemens TL, Riddle RC. The role of osteoblasts in energy homeostasis. *Nat Rev Endocrinol*. (2019) 15:651–65. doi: 10.1038/s41574-019-0246-y
- Buttgereit F, Brand MD. A hierarchy of ATP-consuming processes in mammalian cells. *Biochem J*. (1995) 312(Pt 1):163–7. doi: 10.1042/bj3120163

23. Knight BS, Pennell CE, Adamson SL, Lye SJ. The impact of murine strain and sex on postnatal development after maternal dietary restriction during pregnancy. *J Physiol.* (2007) 581:873–81. doi: 10.1113/jphysiol.2006.126573
24. Devlin MJ, Cloutier AM, Thomas NA, Panus DA, Lotinun S, Pinz I, et al. Caloric restriction leads to high marrow adiposity and low bone mass in growing mice. *J Bone Miner Res.* (2010) 25:2078–88. doi: 10.1002/jbmr.82
25. Miller KK, Lee EE, Lawson EA, Misra M, Minihan J, Grinspoon SK, et al. Determinants of skeletal loss and recovery in anorexia nervosa. *J Clin Endocrinol Metab.* (2006) 91:2931–7. doi: 10.1210/jc.2005.2818
26. Shum LC, White NS, Mills BN, Bentley KL de M, Eliseev RA. Energy metabolism in mesenchymal stem cells during osteogenic differentiation. *Stem Cells Dev.* (2016) 25:114–22. doi: 10.1089/scd.2015.0193
27. Shares BH, Busch M, White N, Shum L, Eliseev RA. Active mitochondria support osteogenic differentiation by stimulating β -catenin acetylation. *J Biol Chem.* (2018) 293:16019–27. doi: 10.1074/jbc.RA118.004102
28. Guntur AR, Le PT, Farber CR, Rosen CJ. Bioenergetics during calvarial osteoblast differentiation reflect strain differences in bone mass. *Endocrinology.* (2014) 155:1589–95. doi: 10.1210/en.2013-1974
29. Chen C-T, Shih Y-RV, Kuo TK, Lee OK, Wei YH. Coordinated changes of mitochondrial biogenesis and antioxidant enzymes during osteogenic differentiation of human mesenchymal stem cells. *Stem Cells.* (2008) 26:960–8. doi: 10.1634/stemcells.2007-0509
30. Nichols FC, Neuman WF. Lactic acid production in mouse calvaria *in vitro* with and without parathyroid hormone stimulation: lack of acetazolamide effects. *Bone.* (1987) 8:105–9. doi: 10.1016/8756-3282(87)90078-0
31. Neuman WF, Neuman MW, Brommage R. Aerobic glycolysis in bone: lactate production and gradients in calvaria. *Am J Physiol.* (1978) 234:C41–50. doi: 10.1152/ajpcell.1978.234.1.C41
32. Borle AB, Nichols N, Nichols G. Metabolic studies of bone *in vitro*. *J Biol Chem.* (1960) 235:1206–10.
33. Cohn DV, Forscher BK. Aerobic metabolism of glucose by bone. *J Biol Chem.* (1962) 237:615–8.
34. Felix R, Neuman WF, Fleisch H. Aerobic glycolysis in bone: lactic acid production by rat calvaria cells in culture. *Am J Physiol.* (1978) 234:C51–5. doi: 10.1152/ajpcell.1978.234.1.C51
35. Wei J, Shimazu J, Makinistoglu MP, Maurizi A, Kajimura D, Zong H, et al. Glucose uptake and Runx2 synergize to orchestrate osteoblast differentiation and bone formation. *Cell.* (2015) 161:1576–91. doi: 10.1016/j.cell.2015.05.029
36. Komarova SV, Ataullakhanov FI, Globus RK. Bioenergetics and mitochondrial transmembrane potential during differentiation of cultured osteoblasts. *Am J Physiol Cell Physiol.* (2000) 279:C1220–9. doi: 10.1152/ajpcell.2000.279.4.C1220
37. Yu Y, Newman H, Shen L, Sharma D, Hu G, Mirando AJ, et al. Glutamine metabolism regulates proliferation and lineage allocation in skeletal stem cells. *Cell Metab.* (2019) 29:966–78.e4. doi: 10.1016/j.cmet.2019.01.016
38. Karner CM, Esen E, Okunade AL, Patterson BW, Long F. Increased glutamine catabolism mediates bone anabolism in response to WNT signaling. *J Clin Invest.* (2015) 125:551–62. doi: 10.1172/JCI78470
39. Kim SP, Li Z, Zoch ML, Frey JL, Bowman CE, Kushwaha P, et al. Fatty acid oxidation by the osteoblast is required for normal bone acquisition in a sex- and diet-dependent manner. *JCI insight.* (2017) 2:e92704. doi: 10.1172/jci.insight.92704
40. van Gestel N, Stegen S, Eelen G, Schoors S, Carlier A, Daniëls VW, et al. Lipid availability determines fate of skeletal progenitor cells via SOX9. *Nature.* (2020) 579:111–7. doi: 10.1038/s41586-020-2050-1
41. Singh L, Tyagi S, Myers D, Duque GG. Bad or Ugly: the biological roles of bone marrow fat. *Curr Osteoporos Rep.* (2018) 16:130–7. doi: 10.1007/s11914-018-0427-y
42. Tintut Y, Demer LL. Effects of bioactive lipids and lipoproteins on bone. *Trends Endocrinol Metab.* (2014) 25:53–9. doi: 10.1016/j.tem.2013.10.001
43. Tso P, Balint JA. Formation and transport of chylomicrons by enterocytes to the lymphatics. *Am J Physiol.* (1986) 250:G715–26. doi: 10.1152/ajpgi.1986.250.6.G715
44. Kersten S. Physiological regulation of lipoprotein lipase. *Biochim Biophys Acta.* (2014) 1841:919–33. doi: 10.1016/j.bbalip.2014.03.013
45. Wandler E, Chao Y, Havel RJ. Determinants of hepatic uptake of triglyceride-rich lipoproteins and their remnants in the rat. *J Biol Chem.* (1980) 255:5475–80.
46. Eichmann TO, Kumari M, Haas JT, Farese RV, Zimmermann R, Lass A, et al. Studies on the substrate and stereo/regioselectivity of adipose triglyceride lipase, hormone-sensitive lipase, and diacylglycerol-O-acyltransferases. *J Biol Chem.* (2012) 287:41446–57. doi: 10.1074/jbc.M112.400416
47. Schönfeld P, Wojtczak L. Short- and medium-chain fatty acids in energy metabolism: the cellular perspective. *J Lipid Res.* (2016) 57:943–54. doi: 10.1194/jlr.R067629
48. Richieri G V, Anel A, Kleinfeld AM. Interactions of long-chain fatty acids and albumin: determination of free fatty acid levels using the fluorescent probe ADIFAB. *Biochemistry.* (1993) 32:7574–80. doi: 10.1021/bi00080a032
49. Adeva-Andany MM, Carneiro-Freire N, Seco-Filgueira M, Fernández-Fernández C, Mourinho-Bayolo D. Mitochondrial β -oxidation of saturated fatty acids in humans. *Mitochondrion.* (2019) 46:73–90. doi: 10.1016/j.mito.2018.02.009
50. Reddy JK, Hashimoto T. Peroxisomal beta-oxidation and peroxisome proliferator-activated receptor alpha: an adaptive metabolic system. *Annu Rev Nutr.* (2001) 21:193–230. doi: 10.1146/annurev.nutr.21.1.193
51. Enlow DH, Conklin JL, Bang S. Observations on the occurrence and the distribution of lipids in compact bone. *Clin Orthop Relat Res.* (1965) 38:157–69. doi: 10.1097/00003086-196500380-00022
52. Rendina-Ruedy E, Guntur AR, Rosen CJ. Intracellular lipid droplets support osteoblast function. *Adipocyte.* (2017) 6:250–8. doi: 10.1080/21623945.2017.1356505
53. Niemeier A, Niedzielska D, Secer R, Schilling A, Merkel M, Enrich C, et al. Uptake of postprandial lipoproteins into bone *in vivo*: impact on osteoblast function. *Bone.* (2008) 43:230–7. doi: 10.1016/j.bone.2008.03.022
54. Newman P, Bonello F, Wierzbicki AS, Lumb P, Savidge GF, Shearer MJ. The uptake of lipoprotein-borne phyloquinone. (vitamin K1) by osteoblasts and osteoblast-like cells: role of heparan sulfate proteoglycans and apolipoprotein E. *J Bone Miner Res.* (2002) 17:426–33. doi: 10.1359/jbmr.2002.17.3.426
55. Brodeur MR, Brissette L, Falstra L, Luangrath V, Moreau R. Scavenger receptor of class B expressed by osteoblastic cells are implicated in the uptake of cholesteryl ester and estradiol from LDL and HDL3. *J Bone Miner Res.* (2008) 23:326–37. doi: 10.1359/jbmr.071022
56. Frey JL, Li Z, Ellis JM, Zhang Q, Farber CR, Aja S, et al. Wnt-Lrp5 signaling regulates fatty acid metabolism in the osteoblast. *Mol Cell Biol.* (2015) 35:1979–91. doi: 10.1128/MCB.01343-14
57. Bartelt A, Koehne T, Tödter K, Reimer R, Müller B, Behler-Janbeck F, et al. Quantification of bone fatty acid metabolism and its regulation by adipocyte lipoprotein lipase. *Int J Mol Sci.* (2017) 18:1264. doi: 10.3390/ijms18061264
58. Niemeier A, Kassem M, Toedter K, Wendt D, Ruether W, Beisiegel U, et al. Expression of LRP1 by human osteoblasts: a mechanism for the delivery of lipoproteins and vitamin K1 to bone. *J Bone Miner Res.* (2005) 20:283–93. doi: 10.1359/JBMR.041102
59. Grey A, Banovic T, Zhu Q, Watson M, Callon K, Palmano K, et al. The low-density lipoprotein receptor-related protein 1 is a mitogenic receptor for lactoferrin in osteoblastic cells. *Mol Endocrinol.* (2004) 18:2268–78. doi: 10.1210/me.2003-0456
60. Chen X, Wang C, Zhang K, Xie Y, Ji X, Huang H, et al. Reduced femoral bone mass in both diet-induced and genetic hyperlipidemia mice. *Bone.* (2016) 93:104–12. doi: 10.1016/j.bone.2016.09.016
61. Okayasu M, Nakayachi M, Hayashida C, Ito J, Kaneda T, Masuhara M, et al. Low-density lipoprotein receptor deficiency causes impaired osteoclastogenesis and increased bone mass in mice because of defect in osteoclastic cell-cell fusion. *J Biol Chem.* (2012) 287:19229–41. doi: 10.1074/jbc.M111.323600
62. Zhang N, Zhang Y, Lin J, Qiu X, Chen L, Pan X, et al. Low-density lipoprotein receptor deficiency impaired mice osteoblastogenesis *in vitro*. *Biosci Trends.* (2018) 11:658–66. doi: 10.5582/bst.2017.01267
63. Catherwood BD, Addison J, Chapman G, Contreras S, Lorang M. Growth of rat osteoblast-like cells in a lipid-enriched culture medium and regulation of function by parathyroid hormone and 1,25-dihydroxyvitamin D. *J Bone Miner Res.* (1988) 3:431–8. doi: 10.1002/jbmr.5650030410
64. Sims A-M, Shephard N, Carter K, Doan T, Dowling A, Duncan EL, et al. Genetic analyses in a sample of individuals with high or low BMD shows association with multiple Wnt pathway genes. *J Bone Miner Res.* (2008) 23:499–506. doi: 10.1359/jbmr.071113

65. Bartelt A, Behler-Janbeck F, Beil FT, Koehne T, Müller B, Schmidt T, et al. Lrp1 in osteoblasts controls osteoclast activity and protects against osteoporosis by limiting PDGF-RANKL signaling. *Bone Res.* (2018) 6:4. doi: 10.1038/s41413-017-0006-3
66. Teufel S, Hartmann C. Wnt-signaling in skeletal development. *Curr Top Dev Biol.* (2019) 133:235–79. doi: 10.1016/bs.ctdb.2018.11.010
67. Kim DH, Inagaki Y, Suzuki T, Ioka RX, Yoshioka SZ, Magoori K, et al. A new low density lipoprotein receptor related protein, LRP5, is expressed in hepatocytes and adrenal cortex, and recognizes apolipoprotein E. *J Biochem.* (1998) 124:1072–6. doi: 10.1093/oxfordjournals.jbchem.a022223
68. Fujino T, Asaba H, Kang M-J, Ikeda Y, Sone H, Takada S, et al. Low-density lipoprotein receptor-related protein 5. (LRP5) is essential for normal cholesterol metabolism and glucose-induced insulin secretion. *Proc Natl Acad Sci USA.* (2003) 100:229–34. doi: 10.1073/pnas.0133792100
69. Shen W-J, Hu J, Hu Z, Kraemer FB, Azhar S. Scavenger receptor class B type I. (SR-BI): a versatile receptor with multiple functions and actions. *Metabolism.* (2014) 63:875–86. doi: 10.1016/j.metabol.2014.03.011
70. Ackert-Bicknell CL. HDL cholesterol and bone mineral density: is there a genetic link? *Bone.* (2012) 50:525–33. doi: 10.1016/j.bone.2011.07.002
71. Martineau C, Martin-Falstra L, Brissette L, Moreau R. The atherogenic Scarb1 null mouse model shows a high bone mass phenotype. *Am J Physiol Endocrinol Metab.* (2014) 306:E48–57. doi: 10.1152/ajpendo.00421.2013
72. Isaacs CM, Zaidi M, Blair HC. ACTH is a novel regulator of bone mass. *Ann N Y Acad Sci.* (2010) 1192:110–6. doi: 10.1111/j.1749-6632.2009.05231.x
73. Tourkova IL, Dobrowolski SF, Secunda C, Zaidi M, Papadimitriou-Oliveri I, Papachristou DJ, et al. The high-density lipoprotein receptor Scarb1 is required for normal bone differentiation *in vivo* and *in vitro*. *Lab Invest.* (2019) 99:1850–60. doi: 10.1038/s41374-019-0311-0
74. Martineau C, Kevorkova O, Brissette L, Moreau R. Scavenger receptor class B, type I. (Scarb1) deficiency promotes osteoblastogenesis but stunts terminal osteocyte differentiation. *Physiol Rep.* (2014) 2:1–12. doi: 10.14814/phy2.12117
75. Blair HC, Kalyvoti E, Papachristou NI, Tourkova IL, Syggelos SA, Deligianni D, et al. Apolipoprotein A-1 regulates osteoblast and lipoblast precursor cells in mice. *Lab Invest.* (2016) 96:763–72. doi: 10.1038/labinvest.2016.51
76. Glatz JFC, Luiken JJFP, Bonen A. Membrane fatty acid transporters as regulators of lipid metabolism: implications for metabolic disease. *Physiol Rev.* (2010) 90:367–417. doi: 10.1152/physrev.00003.2009
77. Kevorkova O, Martineau C, Martin-Falstra L, Sanchez-Dardon J, Brissette L, Moreau R. Low-bone-mass phenotype of deficient mice for the cluster of differentiation 36. (CD36). *PLoS ONE.* (2013) 8:e77701. doi: 10.1371/journal.pone.0077701
78. Anderson CM, Stahl A. SLC27 fatty acid transport proteins. *Mol Aspects Med.* (2013) 34:516–28. doi: 10.1016/j.mam.2012.07.010
79. Bao M, Zhang K, Wei Y, Hua W, Gao Y, Li X, Ye L. Therapeutic potentials and modulatory mechanisms of fatty acids in bone. *Cell Prolif.* (2020) 53:e12735. doi: 10.1111/cpr.12735
80. Mark H, Penington A, Nannmark U, Morrison W, Messina A. Microvascular invasion during endochondral ossification in experimental fractures in rats. *Bone.* (2004) 35:535–42. doi: 10.1016/j.bone.2004.04.010
81. Thompson Z, Miclau T, Hu D, Helms JA. A model for intramembranous ossification during fracture healing. *J Orthop Res.* (2002) 20:1091–8. doi: 10.1016/S0736-0266(02)00017-7
82. Kronenberg HM. Developmental regulation of the growth plate. *Nature.* (2003) 423:332–6. doi: 10.1038/nature01657
83. Baryawno N, Przybylski D, Kowalczyk MS, Kfoury Y, Severe N, Gustafsson K, et al. A cellular taxonomy of the bone marrow stroma in homeostasis and leukemia. *Cell.* (2019) 177:1915–32.e16. doi: 10.1016/j.cell.2019.04.040
84. Steinberg SJ, Raymond G V, Braverman NE, Moser AB. *Zellweger Spectrum Disorder.* (1993). Available at: <https://www.ncbi.nlm.nih.gov/books/NBK1448/>
85. Brosius U, Gärtner J. Cellular and molecular aspects of Zellweger syndrome and other peroxisome biogenesis disorders. *Cell Mol Life Sci.* (2002) 59:1058–69. doi: 10.1007/s00018-002-8486-7
86. Heymans HS, Oorthuys JW, Nelck G, Wanders RJA, Schutgens RBH. Rhizomelic chondrodysplasia punctata: another peroxisomal disorder. *N Engl J Med.* (1985) 313:187–8. doi: 10.1056/NEJM198507183130322
87. Braverman N, Zhang R, Chen L, Nimmo G, Scheper S, Tran T, et al. A Pex7 hypomorphic mouse model for plasmalogen deficiency affecting the lens and skeleton. *Mol Genet Metab.* (2010) 99:408–16. doi: 10.1016/j.ymgme.2009.12.005
88. Brites P, Motley AM, Gressens P, Mooyer PAW, Ploegaert I, Everts V, et al. Impaired neuronal migration and endochondral ossification in Pex7 knockout mice: a model for rhizomelic chondrodysplasia punctata. *Hum Mol Genet.* (2003) 12:2255–67. doi: 10.1093/hmg/ddg236
89. Huybrechts Y, Mortier G, Boudin E, Van Hul W. WNT signaling and bone: lessons from skeletal dysplasias and disorders. *Front Endocrinol.* (2020) 11:165. doi: 10.3389/fendo.2020.00165
90. Zhong Z, Ethen NJ, Williams BO. WNT signaling in bone development and homeostasis. *Wiley Interdiscip Rev Dev Biol.* (2014) 3:489–500. doi: 10.1002/wdev.159
91. Moorer MC, Riddle RC. Regulation of Osteoblast Metabolism by Wnt Signaling. *Endocrinol Metab.* (2018) 33:318–30. doi: 10.3803/EnM.2018.33.3.318
92. Chen H, Ji X, Lee W-C, Shi Y, Li B, Abel ED, et al. Increased glycolysis mediates Wnt7b-induced bone formation. *FASEB J.* (2019) 33:7810–21. doi: 10.1096/fj.201900201RR
93. Esen E, Chen J, Karner CM, Okunade AL, Patterson BW, Long F. WNT-LRP5 signaling induces Warburg effect through mTORC2 activation during osteoblast differentiation. *Cell Metab.* (2013) 17:745–55. doi: 10.1016/j.cmet.2013.03.017
94. Riddle RC, Diegel CR, Leslie JM, Van Koeveing KK, Faugere M-C, Clemens TL, et al. Lrp5 and Lrp6 exert overlapping functions in osteoblasts during postnatal bone acquisition. *PLoS ONE.* (2013) 8:e63323. doi: 10.1371/journal.pone.0063323
95. Frey JL, Kim SP, Li Z, Wolfgang MJ, Riddle RC. β -catenin directs long-chain fatty acid catabolism in the osteoblasts of male mice. *Endocrinology.* (2018) 159:272–84. doi: 10.1210/en.2017-00850
96. Holmen SL, Zylstra CR, Mukherjee A, Sigler RE, Faugere M-C, Bouxsein ML, et al. Essential role of beta-catenin in postnatal bone acquisition. *J Biol Chem.* (2005) 280:21162–8. doi: 10.1074/jbc.M501900200
97. Chen J, Tu X, Esen E, Joeng KS, Lin C, Arbeit JM, Rüegg MA, et al. WNT7B promotes bone formation in part through mTORC1. *PLoS Genet.* (2014) 10:e1004145. doi: 10.1371/journal.pgen.1004145
98. Neer RM, Arnau CD, Zanchetta JR, Prince R, Gaich GA, Reginster JY, et al. Effect of parathyroid hormone. (1-34) on fractures and bone mineral density in postmenopausal women with osteoporosis. *N Engl J Med.* (2001) 344:1434–41. doi: 10.1097/00006254-200110000-00018
99. Jilka RL, Weinstein RS, Bellido T, Roberson P, Parfitt AM, Manolagas SC. Increased bone formation by prevention of osteoblast apoptosis with parathyroid hormone. *J Clin Invest.* (1999) 104:439–46. doi: 10.1172/JCI6610
100. Dobnig H, Turner RT. Evidence that intermittent treatment with parathyroid hormone increases bone formation in adult rats by activation of bone lining cells. *Endocrinology.* (1995) 136:3632–8. doi: 10.1210/endo.136.8.7628403
101. Kim SW, Pajevic PD, Selig M, Barry KJ, Yang J-Y, Shin CS, et al. Intermittent parathyroid hormone administration converts quiescent lining cells to active osteoblasts. *J Bone Miner Res.* (2012) 27:2075–84. doi: 10.1002/jbmr.1665
102. Wu X, Pang L, Lei W, Lu W, Li J, Li Z, et al. Inhibition of Sca-1-positive skeletal stem cell recruitment by alendronate blunts the anabolic effects of parathyroid hormone on bone remodeling. *Cell Stem Cell.* (2010) 7:571–80. doi: 10.1016/j.stem.2010.09.012
103. Adamek G, Felix R, Guenther HL, Fleisch H. Fatty acid oxidation in bone tissue and bone cells in culture. Characterization and hormonal influences. *Biochem J.* (1987) 248:129–37. doi: 10.1042/bj2480129
104. Esen E, Lee S-Y, Wice BM, Long F. PTH promotes bone anabolism by stimulating aerobic glycolysis via IGF signaling. *J Bone Miner Res.* (2015) 30:2137. doi: 10.1002/jbmr.2714
105. Maridas DE, Rendina-Ruedy E, Helderman RC, DeMambro VE, Brooks D, Guntur AR, et al. Progenitor recruitment and adipogenic lipolysis contribute to the anabolic actions of parathyroid hormone on the skeleton. *FASEB J.* (2019) 33:2885–98. doi: 10.1096/fj.201800948RR
106. Larsson S, Jones HA, Göransson O, Degerman E, Holm C. Parathyroid hormone induces adipocyte lipolysis via PKA-mediated phosphorylation of hormone-sensitive lipase. *Cell Signal.* (2016) 28:204–13. doi: 10.1016/j.cellsig.2015.12.012

107. Fan Y, Hanai J-I, Le PT, Bi R, Maridas D, DeMambro V, et al. Parathyroid hormone directs bone marrow mesenchymal cell fate. *Cell Metab.* (2017) 25:661–72. doi: 10.1016/j.cmet.2017.01.001
108. Carroll M, Kit B, Lacher D. Trends in elevated triglyceride in adults: United States, 2001–2012. *NCHS Data Brief.* (2015) 198.
109. Saoji R, Das RS, Desai M, Pasi A, Sachdeva G, Das TK, et al. Association of high-density lipoprotein, triglycerides, and homocysteine with bone mineral density in young Indian tribal women. *Arch Osteoporos.* (2018) 13:108. doi: 10.1007/s11657-018-0525-6
110. Chi JH, Shin MS, Lee BJ. Identification of hypertriglyceridemia based on bone density, body fat mass, and anthropometry in a Korean population. *BMC Cardiovasc Disord.* (2019) 19:66. doi: 10.1186/s12872-019-1050-2
111. Hsu Y-H, Venners SA, Terwedow HA, Feng Y, Niu T, Li Z, et al. Relation of body composition, fat mass, and serum lipids to osteoporotic fractures and bone mineral density in Chinese men and women. *Am J Clin Nutr.* (2006) 83:146–54. doi: 10.1093/ajcn/83.1.146
112. Cui L-H, Shin M-H, Chung E-K, Lee Y-H, Kweon S-S, Park K-S, et al. Association between bone mineral densities and serum lipid profiles of pre- and post-menopausal rural women in South Korea. *Osteoporos Int.* (2005) 16:1975–81. doi: 10.1007/s00198-005-1977-2
113. Nuzzo V, de Milita AM, Ferraro T, Monaco A, Florio E, Miano P, et al. Analysis of skeletal status by quantitative ultrasonometry in a cohort of postmenopausal women with high blood cholesterol without documented osteoporosis. *Ultrasound Med Biol.* (2009) 35:717–22. doi: 10.1016/j.ultrasmedbio.2008.11.003
114. Bijelic R, Balaban J, Milicevic S. Correlation of the lipid profile, BMI and bone mineral density in postmenopausal women. *Mater Sociomed.* (2016) 28:412–5. doi: 10.5455/msm.2016.28.412-415
115. Yamauchi M, Yamaguchi T, Nawata K, Tanaka K, Takaoka S, Sugimoto T. Increased low-density lipoprotein cholesterol level is associated with non-vertebral fractures in postmenopausal women. *Endocrine.* (2015) 48:279–86. doi: 10.1007/s12020-014-0292-0
116. Pirih F, Lu J, Ye F, Bezouglaia O, Atti E, Ascenzi M-G, et al. Adverse effects of hyperlipidemia on bone regeneration and strength. *J Bone Miner Res.* (2012) 27:309–18. doi: 10.1002/jbmr.541
117. Heikura IA, Burke LM, Hawley JA, Ross ML, Garvican-Lewis L, Sharma AP, et al. A Short-term ketogenic diet impairs markers of bone health in response to exercise. *Front Endocrinol.* (2019) 10:880. doi: 10.3389/fendo.2019.00880
118. Edwards CJ, Hart DJ, Spector TD. Oral statins and increased bone-mineral density in postmenopausal women. *Lancet.* (2000) 355:2218–9. doi: 10.1016/S0140-6736(00)02408-9
119. Wang Z, Li Y, Zhou F, Piao Z, Hao J. Effects of statins on bone mineral density and fracture risk: a PRISMA-compliant systematic review and meta-analysis. *Medicine.* (2016) 95:e3042. doi: 10.1097/MD.0000000000003042
120. Zheng J, Brion M-J, Kemp JP, Warrington NM, Borges M-C, Hemani G, et al. The effect of plasma lipids and lipid-lowering interventions on bone mineral density: a mendelian randomization study. *J Bone Miner Res.* (2020) 35:1224–35. doi: 10.1002/jbmr.3989
121. Wali JA, Jarzebska N, Raubenheimer D, Simpson SJ, Rodionov RN, O'Sullivan JF. Cardio-metabolic effects of high-fat diets and their underlying mechanisms: a narrative review. *Nutrients.* (2020) 12:1–18. doi: 10.3390/nut12051505
122. Montalvany-Antonucci CC, Zicker MC, Ferreira AVM, Macari S, Ramos-Junior ES, Gomez RS, et al. High-fat diet disrupts bone remodeling by inducing local and systemic alterations. *J Nutr Biochem.* (2018) 59:93–103. doi: 10.1016/j.jnutbio.2018.06.006
123. Shu L, Beier E, Sheu T, Zhang H, Zuscik MJ, Puzas EJ, et al. High-fat diet causes bone loss in young mice by promoting osteoclastogenesis through alteration of the bone marrow environment. *Calcif Tissue Int.* (2015) 96:313–23. doi: 10.1007/s00223-015-9954-z
124. Zhang K, Wang C, Chen Y, Ji X, Chen X, Tian L, et al. Preservation of high-fat diet-induced femoral trabecular bone loss through genetic target of TNF- α . *Endocrine.* (2015) 50:239–49. doi: 10.1007/s12020-015-0554-5
125. Tencerova M, Figeac F, Ditzel N, Taipaleenmäki H, Nielsen TK, Kassem M. High-fat diet-induced obesity promotes expansion of bone marrow adipose tissue and impairs skeletal stem cell functions in mice. *J Bone Miner Res.* (2018) 33:1154–65. doi: 10.1002/jbmr.3408
126. McCabe LR, Irwin R, Tekalur A, Evans C, Schepper JD, Parameswaran N, et al. Exercise prevents high fat diet-induced bone loss, marrow adiposity and dysbiosis in male mice. *Bone.* (2019) 118:20–31. doi: 10.1016/j.bone.2018.03.024
127. Sul O-J, Kim J-E, Ke K, Suh J-H, Choi H-S. Atherogenic diet-induced bone loss is primarily due to increased osteoclastogenesis in mice. *J Nutr Biochem.* (2020) 79:108337. doi: 10.1016/j.jnutbio.2019.108337
128. Picke A-K, Sylow L, Møller LLV, Kjøbsted R, Schmidt FN, Steejn MW, et al. Differential effects of high-fat diet and exercise training on bone and energy metabolism. *Bone.* (2018) 116:120–34. doi: 10.1016/j.bone.2018.07.015
129. Silva MJ, Eekhoff JD, Patel T, Kenney-Hunt JP, Brodt MD, Steger-May K, et al. Effects of high-fat diet and body mass on bone morphology and mechanical properties in 1100 advanced intercross mice. *J Bone Miner Res.* (2019) 34:711–25. doi: 10.1002/jbmr.3648
130. Devlin MJ, Robbins A, Cosman MN, Moursi CA, Cloutier AM, Louis L, et al. Differential effects of high fat diet and diet-induced obesity on skeletal acquisition in female C57BL/6J vs. FVB/NJ Mice. *Bone Rep.* (2018) 8:204–14. doi: 10.1016/j.bonr.2018.04.003
131. Liu Y, Almeida M, Weinstein RS, O'Brien CA, Manolagas SC, Jilka RL. Skeletal inflammation and attenuation of Wnt signaling, Wnt ligand expression, and bone formation in atherosclerotic ApoE-null mice. *Am J Physiol Endocrinol Metab.* (2016) 310:E762–73. doi: 10.1152/ajpendo.00501.2015
132. Colditz J, Picke A, Hofbauer LC, Rauner M. Contributions of Dickkopf-1 to obesity-induced bone loss and marrow adiposity. *JBM plus.* (2020) 4:e10364. doi: 10.1002/jbm4.10364
133. Xiao Y, Cui J, Li YX, Shi YH, Le GW. Expression of genes associated with bone resorption is increased and bone formation is decreased in mice fed a high-fat diet. *Lipids.* (2010) 45:345–55. doi: 10.1007/s11745-010-3397-0
134. Cao JJ, Sun L, Gao H. Diet-induced obesity alters bone remodeling leading to decreased femoral trabecular bone mass in mice. *Ann N Y Acad Sci.* (2010) 1192:292–7. doi: 10.1111/j.1749-6632.2009.05252.x
135. You L, Sheng Z, Tang C, Chen L, Pan L, Chen J. High cholesterol diet increases osteoporosis risk via inhibiting bone formation in rats. *Acta Pharmacol Sin.* (2011) 32:1498–504. doi: 10.1038/aps.2011.135
136. Brodeur MR, Brissette L, Falstraull L, Ouellet P, Moreau R. Influence of oxidized low-density lipoproteins (LDL) on the viability of osteoblastic cells. *Free Radic Biol Med.* (2008) 44:506–17. doi: 10.1016/j.freeradbiomed.2007.08.030
137. Parhami F, Morrow AD, Balucan J, Leitinger N, Watson AD, Tintut Y, et al. Lipid oxidation products have opposite effects on calcifying vascular cell and bone cell differentiation. A possible explanation for the paradox of arterial calcification in osteoporotic patients. *Arterioscler Thromb Vasc Biol.* (1997) 17:680–7. doi: 10.1161/01.ATV.17.4.680
138. Kim J-E, Ahn M-W, Baek S-H, Lee IK, Kim Y-W, Kim J-Y, et al. AMPK activator, AICAR, inhibits palmitate-induced apoptosis in osteoblast. *Bone.* (2008) 43:394–404. doi: 10.1016/j.bone.2008.03.021
139. Yang L, Guan G, Lei L, Lv Q, Liu S, Zhan X, et al. Palmitic acid induces human osteoblast-like Saos-2 cell apoptosis via endoplasmic reticulum stress and autophagy. *Cell Stress Chaperones.* (2018) 23:1283–94. doi: 10.1007/s12192-018-0936-8
140. Kita T, Kume N, Yokode M, Ishii K, Arai H, Horiuchi H, et al. Oxidized-LDL and atherosclerosis. Role of LOX-1. *Ann N Y Acad Sci.* (2000) 902:95–100; discussion 100–2. doi: 10.1111/j.1749-6632.2000.tb06304.x
141. Li Y, Greiner RS, Salem N, Watkins BA. Impact of dietary n-3 FA deficiency on rat bone tissue FA composition. *Lipids.* (2003) 38:683–6. doi: 10.1007/s11745-003-1115-8
142. Watkins BA, Li Y, Lippman HE, Feng S. Modulatory effect of omega-3 polyunsaturated fatty acids on osteoblast function and bone metabolism. *Prostaglandins Leukot Essent Fatty Acids.* (2003) 68:387–98. doi: 10.1016/S0952-3278(03)00063-2
143. Reinwald S, Li Y, Moriguchi T, Salem N, Watkins BA. Repletion with (n-3) fatty acids reverses bone structural deficits in (n-3)-deficient rats. *J Nutr.* (2004) 134:388–94. doi: 10.1093/jn/134.2.388
144. Kuroda T, Ohta H, Onoe Y, Tsugawa N, Shiraki M. Intake of omega-3 fatty acids contributes to bone mineral density at the hip in a younger Japanese female population. *Osteoporos Int.* (2017) 28:2887–91. doi: 10.1007/s00198-017-4128-7

145. Saini RK, Keum Y-S. Omega-3 and omega-6 polyunsaturated fatty acids: Dietary sources, metabolism, and significance - A review. *Life Sci.* (2018) 203:255–67. doi: 10.1016/j.lfs.2018.04.049
146. Innes JK, Calder PC. Omega-6 fatty acids and inflammation. *Prostaglandins Leukot Essent Fatty Acids.* (2018) 132:41–8. doi: 10.1016/j.plefa.2018.03.004
147. Kim SP, Frey JL, Li Z, Kushwaha P, Zoch ML, Tomlinson RE, et al. Sclerostin influences body composition by regulating catabolic and anabolic metabolism in adipocytes. *Proc Natl Acad Sci USA.* (2017) 114:E11238–47. doi: 10.1073/pnas.1707876115
148. Mabileau G, Perrot R, Flatt PR, Irwin N, Chappard D. High fat-fed diabetic mice present with profound alterations of the osteocyte network. *Bone.* (2016) 90:99–106. doi: 10.1016/j.bone.2016.06.008
149. Baek K, Hwang HR, Park H-J, Kwon A, Qadir AS, Ko S-H, et al. TNF- α upregulates sclerostin expression in obese mice fed a high-fat diet. *J Cell Physiol.* (2014) 229:640–50. doi: 10.1002/jcp.24487
150. Razny U, Polus A, Goralska J, Zdzienicka A, Gruca A, Kapusta M, et al. Effect of insulin resistance on whole blood mRNA and microRNA expression affecting bone turnover. *Eur J Endocrinol.* (2019) 181:525–37. doi: 10.1530/EJE-19-0542
151. Chen J-R, Lazarenko OP, Wu X, Tong Y, Blackburn ML, Shankar K, et al. Obesity reduces bone density associated with activation of PPAR γ and suppression of Wnt/ β -catenin in rapidly growing male rats. *PLoS ONE.* (2010) 5:e13704. doi: 10.1371/journal.pone.0013704
152. Zahoor M, Cha P-H, Choi K-Y. Indirubin-3'-oxime, an activator of Wnt/ β -catenin signaling, enhances osteogenic commitment of ST2 cells and restores bone loss in high-fat diet-induced obese male mice. *Bone.* (2014) 65:60–8. doi: 10.1016/j.bone.2014.05.003
153. Wang L, Chai Y, Li C, Liu H, Su W, Liu X, et al. Oxidized phospholipids are ligands for LRP6. *Bone Res.* (2018) 6:22. doi: 10.1038/s41413-018-0023-x
154. Ambrogini E, Que X, Wang S, Yamaguchi F, Weinstein RS, Tsimikas S, et al. Oxidation-specific epitopes restrain bone formation. *Nat Commun.* (2018) 9:2193. doi: 10.1038/s41467-018-04047-5
155. Huang MS, Lu J, Ivanov Y, Sage AP, Tseng W, Demer LL, et al. Hyperlipidemia impairs osteoanabolic effects of PTH. *J Bone Miner Res.* (2008) 23:1672–9. doi: 10.1359/jbmr.080513
156. Sage AP, Lu J, Atti E, Tetradis S, Ascenzi M-G, Adams DJ, et al. Hyperlipidemia induces resistance to PTH bone anabolism in mice via oxidized lipids. *J Bone Miner Res.* (2011) 26:1197–206. doi: 10.1002/jbmr.312
157. Li C, Xing Q, Yu B, Xie H, Wang W, Shi C, et al. Disruption of LRP6 in osteoblasts blunts the bone anabolic activity of PTH. *J Bone Miner Res.* (2013) 28:2094–108. doi: 10.1002/jbmr.1962
158. Huang MS, Morony S, Lu J, Zhang Z, Bezouglaia O, Tseng W, et al. Atherogenic phospholipids attenuate osteogenic signaling by BMP-2 and parathyroid hormone in osteoblasts. *J Biol Chem.* (2007) 282:21237–43. doi: 10.1074/jbc.M701341200
159. Wan M, Yang C, Li J, Wu X, Yuan H, Ma H, et al. Parathyroid hormone signaling through low-density lipoprotein-related protein 6. *Genes Dev.* (2008) 22:2968–79. doi: 10.1101/gad.1702708
160. Palermo A, D'Onofrio L, Buzzetti R, Manfrini S, Napoli N. Pathophysiology of bone fragility in patients with diabetes. *Calcif Tissue Int.* (2017) 100:122–32. doi: 10.1007/s00223-016-0226-3
161. Shah VN, Carpenter RD, Ferguson VL, Schwartz AV. Bone health in type 1 diabetes. *Curr Opin Endocrinol Diabetes Obes.* (2018) 25:231–6. doi: 10.1097/MED.0000000000000421
162. Keenan HA, Maddaloni E. Bone microarchitecture in type 1 diabetes: it is complicated. *Curr Osteoporos Rep.* (2016) 14:351–8. doi: 10.1007/s11914-016-0338-8
163. Strotmeyer ES, Cauley JA, Schwartz AV, Nevitt MC, Resnick HE, Zmuda JM, et al. Diabetes is associated independently of body composition with BMD and bone volume in older white and black men and women: the health, aging, and body composition study. *J Bone Miner Res.* (2004) 19:1084–91. doi: 10.1359/JBMR.040311
164. Vestergaard P. Discrepancies in bone mineral density and fracture risk in patients with type 1 and type 2 diabetes—a meta-analysis. *Osteoporos Int.* (2007) 18:427–44. doi: 10.1007/s00198-006-0253-4
165. Fulzele K, Riddle RC, DiGirolamo DJ, Cao X, Wan C, Chen D, et al. Insulin receptor signaling in osteoblasts regulates postnatal bone acquisition and body composition. *Cell.* (2010) 142:309–19. doi: 10.1016/j.cell.2010.06.002
166. Ferron M, Wei J, Yoshizawa T, Del Fattore A, DePinho RA, Teti A, et al. Insulin signaling in osteoblasts integrates bone remodeling and energy metabolism. *Cell.* (2010) 142:296–308. doi: 10.1016/j.cell.2010.06.003
167. Thrailkill K, Bunn RC, Lumpkin C, Wahl E, Cockrell G, Morris L, et al. Loss of insulin receptor in osteoprogenitor cells impairs structural strength of bone. *J Diabetes Res.* (2014) 2014:703589. doi: 10.1155/2014/703589
168. Wei J, Ferron M, Clarke CJ, Hannun YA, Jiang H, Blazer WS, et al. Bone-specific insulin resistance disrupts whole-body glucose homeostasis via decreased osteocalcin activation. *J Clin Invest.* (2014) 124:1–13. doi: 10.1172/JCI72323
169. Akune T, Ohba S, Kamekura S, Yamaguchi M, Chung U-I, Kubota N, et al. PPAR γ insufficiency enhances osteogenesis through osteoblast formation from bone marrow progenitors. *J Clin Invest.* (2004) 113:846–55. doi: 10.1172/JCI200419900
170. Sun H, Kim JK, Mortensen R, Mutyaba LP, Hankenson KD, Krebsbach PH. Osteoblast-targeted suppression of PPAR γ increases osteogenesis through activation of mTOR signaling. *Stem Cells.* (2013) 31:2183–92. doi: 10.1002/stem.1455
171. Muruganandan S, Ionescu AM, Sinal CJ. At the crossroads of the adipocyte and osteoclast differentiation programs: future therapeutic perspectives. *Int J Mol Sci.* (2020) 21:2277. doi: 10.3390/ijms21072277
172. Brown ML, Yukata K, Farnsworth CW, Chen D-G, Awad H, Hilton MJ, et al. Delayed fracture healing and increased callus adiposity in a C57BL/6J murine model of obesity-associated type 2 diabetes mellitus. *PLoS ONE.* (2014) 9:e99656. doi: 10.1371/journal.pone.0099656
173. Rahman S, Czernik PJ, Lu Y, Lecka-Czernik B. β -catenin directly sequesters adipocytic and insulin sensitizing activities but not osteoblastic activity of PPAR γ 2 in marrow mesenchymal stem cells. *PLoS ONE.* (2012) 7:e51746. doi: 10.1371/journal.pone.0051746
174. Almeida M, Ambrogini E, Han L, Manolagas SC, Jilka RL. Increased lipid oxidation causes oxidative stress, increased peroxisome proliferator-activated receptor- γ expression, and diminished pro-osteogenic Wnt signaling in the skeleton. *J Biol Chem.* (2009) 284:27438–48. doi: 10.1074/jbc.M109.023572
175. Shockley KR, Lazarenko OP, Czernik PJ, Rosen CJ, Churchill GA, Lecka-Czernik B. PPAR γ 2 nuclear receptor controls multiple regulatory pathways of osteoblast differentiation from marrow mesenchymal stem cells. *J Cell Biochem.* (2009) 106:232–46. doi: 10.1002/jcb.21994
176. Nolan JJ, Ludvik B, Beersden P, Joyce M, Olefsky J. Improvement in glucose tolerance and insulin resistance in obese subjects treated with troglitazone. *N Engl J Med.* (1994) 331:1188–93. doi: 10.1056/NEJM199411033311803
177. Lehmann JM, Moore LB, Smith-Oliver TA, Wilkison WO, Willson TM, Kliewer SA. An antidiabetic thiazolidinedione is a high affinity ligand for peroxisome proliferator-activated receptor γ . (PPAR γ). *J Biol Chem.* (1995) 270:12953–6. doi: 10.1074/jbc.270.22.12953
178. Tontonoz P, Spiegelman BM. Fat and beyond: the diverse biology of PPAR γ . *Annu Rev Biochem.* (2008) 77:289–312. doi: 10.1146/annurev.biochem.77.061307.091829
179. Kahn SE, Haffner SM, Heise MA, Herman WH, Holman RR, Jones NP, et al. Glycemic durability of rosiglitazone, metformin, or glyburide monotherapy. *N Engl J Med.* (2006) 355:2427–43. doi: 10.1056/NEJMoa066224
180. Home PD, Pocock SJ, Beck-Nielsen H, Curtis PS, Gomis R, Hanefeld M, et al. RECORD Study Team. Rosiglitazone evaluated for cardiovascular outcomes in oral agent combination therapy for type 2 diabetes. (RECORD): a multicentre, randomised, open-label trial. *Lancet.* (2009) 373:2125–35. doi: 10.1016/S0140-6736(09)60953-3
181. Zinman B, Haffner SM, Herman WH, Holman RR, Lachin JM, Kravitz BG, et al. Effect of rosiglitazone, metformin, and glyburide on bone biomarkers in patients with type 2 diabetes. *J Clin Endocrinol Metab.* (2010) 95:134–42. doi: 10.1210/jc.2009-0572

182. Grey A, Bolland M, Gamble G, Wattie D, Horne A, Davidson J, et al. The peroxisome proliferator-activated receptor-gamma agonist rosiglitazone decreases bone formation and bone mineral density in healthy postmenopausal women: a randomized, controlled trial. *J Clin Endocrinol Metab.* (2007) 92:1305–10. doi: 10.1210/jc.2006-2646
183. Brun J, Berthou F, Trajkovski M, Maechler P, Foti M, Bonnet N. Bone regulates browning and energy metabolism through mature osteoblast/osteocyte PPAR γ expression. *Diabetes.* (2017) 66:2541–54. doi: 10.2337/db17-0116

Conflict of Interest: The authors declare that the research was conducted in the absence of any commercial or financial relationships that could be construed as a potential conflict of interest.

Copyright © 2020 Alekos, Moorer and Riddle. This is an open-access article distributed under the terms of the Creative Commons Attribution License (CC BY). The use, distribution or reproduction in other forums is permitted, provided the original author(s) and the copyright owner(s) are credited and that the original publication in this journal is cited, in accordance with accepted academic practice. No use, distribution or reproduction is permitted which does not comply with these terms.



The Role of Nerves in Skeletal Development, Adaptation, and Aging

Ryan E. Tomlinson^{1†}, Blaine A. Christiansen^{2†}, Adrienne A. Giannone³ and Damian C. Genetos³

¹ Department of Orthopaedic Surgery, Thomas Jefferson University, Philadelphia, PA, United States, ² Department of Orthopaedic Surgery, School of Medicine, University of California, Davis, Sacramento, CA, United States, ³ Department of Anatomy, Physiology, and Cell Biology, School of Veterinary Medicine, University of California, Davis, Davis, CA, United States

OPEN ACCESS

Edited by:

Lilian Irene Plotkin,
Indiana University Bloomington,
United States

Reviewed by:

Giovanni Lombardi,
Galeazzi Orthopedic Institute
(IRCCS), Italy
Michaël R. Laurent,
University Hospitals Leuven, Belgium

*Correspondence:

Ryan E. Tomlinson
ryan.tomlinson@jefferson.edu

[†]These authors have contributed
equally to this work

Specialty section:

This article was submitted to
Bone Research,
a section of the journal
Frontiers in Endocrinology

Received: 27 May 2020

Accepted: 07 August 2020

Published: 23 September 2020

Citation:

Tomlinson RE, Christiansen BA,
Giannone AA and Genetos DC (2020)
The Role of Nerves in Skeletal
Development, Adaptation, and Aging.
Front. Endocrinol. 11:646.
doi: 10.3389/fendo.2020.00646

The skeleton is well-innervated, but only recently have the functions of this complex network in bone started to become known. Although our knowledge of skeletal sensory and sympathetic innervation is incomplete, including the specific locations and subtypes of nerves in bone, we are now able to reconcile early studies utilizing denervation models with recent work dissecting the molecular signaling between bone and nerve. In total, sensory innervation functions in bone much as it does elsewhere in the body—to sense and respond to stimuli, including mechanical loading. Similarly, sympathetic nerves regulate autonomic functions related to bone, including homeostatic remodeling and vascular tone. However, more study is required to translate our current knowledge of bone-nerve crosstalk to novel therapeutic strategies that can be effectively utilized to combat skeletal diseases, disorders of low bone mass, and age-related decreases in bone quality.

Keywords: mechanotransduction, nervous system, bone, skeleton, aging, disuse

INTRODUCTION

The presence and purpose of nerves in bones has been under investigation for many decades, beginning in earnest with the use of routine histological preparations and electron microscopy in the 1960s, 1970s, and 1980s (1–3). These studies were motivated by the desire for greater understanding of skeletal pain, such as that induced by surgical operations to resect tumors or stabilize broken bones. Many early studies using denervation models to abruptly sever the nerve supply of bones reported minimal effects of diminished nerve activity on bone mass or accrual in a variety of animal species. Nonetheless, recent immunohistochemical studies have revealed abundant sensory, sympathetic, and parasympathetic axons of the peripheral nervous system that terminate in bone (4–10). As a result, research into each of these nerve populations has revealed the unique functions of each subtype within the skeletal microenvironment. However, much remains to be uncovered. In this review, we will discuss the sensory, sympathetic, and parasympathetic actions on bone, as well as the current understanding of nerve roles during skeletal development, adaptation to mechanical load, and aging.

SKELETAL INNERVATION

Sensory Nerves in Bone

The somatic nervous system (SNS) includes the sensory nerves distributed throughout the body after their extension from the dorsal root ganglia during development. Skin is well-innervated

by sensory nerves, along with the underlying bone, joints, tendon, and muscle. These nerves serve a variety of important roles in the body, including the production of signals that provide spatial orientation (proprioception), interpret pain and noxious stimuli (nociception), recognize temperature changes, and allow the perception of non-painful tactile stimuli (11–14). Most sensory nerves can be categorized by their expression of channels and receptors (15); these include toll-like receptors (TLRs), transient receptor potential (TRP) ion channels, and receptor tyrosine kinases (RTKs) as well as the recently identified mechanosensitive Piezo channels (15, 16). These receptors are utilized to initiate the appropriate intracellular signaling as well as the neuropeptide or neurotransmitter release. In bone, nearly all of the thinly myelinated and unmyelinated sensory nerves express neurotrophic receptor tyrosine kinase type 1 (TrkA), the high affinity receptor for nerve growth factor (NGF) (10, 17). This specialization is likely due to the NGF expression that occurs during the initiation of primary and secondary ossification in endochondral bone formation (18, 19). Nonetheless, innervation of bone is most dense in the periosteum and marrow spaces, with relatively few nerves present in the mineralized bone (9, 10). Furthermore, innervation density is increased at sites nearest to active bone remodeling surfaces (20).

Function of Sensory Nerves in Skeletal Pain

One of the original motivations for studying sensory nerves in bone was to determine the mechanisms of osseous pain. This objective has been bolstered by the prevalence of musculoskeletal pain, including lower back pain, joint pain, and fracture pain, which collectively are the leading cause of disability in the world (21). Much of this work has been centered on NGF, which is expressed by osteoblasts and acts directly on sensory nerve axons present in bone through TrkA receptors to induce skeletal pain; furthermore, NGF also functions to enhance the activation of other nociceptive pathways in skeletal sensory nerves (22). As a result, the blockade of NGF activity has been explored extensively in a variety of animal models of skeletal pain. For example, anti-NGF antibodies profoundly reduce osteosarcoma-related bone pain in mice as well as tumor-induced nerve sprouting in a preclinical model of metastatic prostate cancer (23, 24). Furthermore, consistent with the wide-spread expression of NGF observed in fracture (25, 26), anti-NGF antibodies decrease fracture-related pain behavior in mice (27, 28). Subsequent research suggested that analgesia using anti-NGF antibodies can be achieved without affecting fracture healing outcomes (29), although others have shown that silencing the activation of TrkA diminishes innervation and stress fracture healing in mice (30). This concept of NGF acting as an osteoanabolic agent is consistent with earlier work, which reported that topical application of NGF to rib fractures decreased healing time in rats (27) and improved healing outcomes in distraction osteogenesis in rabbits (28). Nonetheless, a complete understanding of the role of NGF-TrkA signaling in bone healing should be a research priority, since the humanized monoclonal anti-NGF antibody Tanezumab (Pfizer and Lilly) received FDA Fast Track approval

in 2017 as the first in a new class of non-opioid pain relievers. This approval followed a halt in Phase III clinical trials in 2010 due to an increased incidence of adverse skeletal events, which remains incompletely understood (31).

Release of Neuropeptides by Skeletal Sensory Nerves

Stimulation of sensory nerves in bone may result in the release of neuropeptides, particularly calcitonin gene-related peptide (CGRP) and substance P (SP), but may also include glutamate and pituitary adenylate cyclase-activating polypeptide (PACAP) (32). A potential role for neuropeptides to act as bone therapeutics has been investigated extensively, since both osteoblasts and osteoclasts express the necessary receptors to for direct cell-autonomous activation (33, 34). In general, CGRP increases osteoblast bone formation through stimulation of Wnt signaling and inhibition of apoptosis (35, 36). Furthermore, CGRP appears to inhibit osteoclast differentiation and function (37, 38). Consistent with these findings, mice lacking α CGRP have low bone mass as a result of decreased bone formation (39). SP appears to increase bone resorption as well as bone formation, although its contribution toward formation outweighs its role in bone resorption and lead to impaired material and structural bone strength (40, 41). These findings are consistent with results from previous *in vitro* experimentation that have demonstrated both mechanisms (42–44). Neuropeptide release within the skeleton is potentiated by osteoblast-derived NGF, which increases both basal and stimulus-evoked release of SP and CGRP from spinal cord slices *in vitro* (33). Nonetheless, the therapeutic application of these osteoanabolic neuropeptides toward diseases of low bone mass may be limited by drug delivery, since neuropeptides are widely active outside of bone.

Autonomic Nervous System (ANS) in Bone

The peripheral nervous system also includes the autonomic nervous system (ANS), which is further divided into the sympathetic and parasympathetic nervous systems. In general, the action of these two systems oppose each other and serve to coordinate unconscious activities of the body, such as breathing and blood pressure regulation. Coordinated action of these opposing systems involves unique signaling mechanisms: sympathetic nerves release of norepinephrine to activate α - and β -adrenergic receptors, whereas parasympathetic nerves release acetylcholine to activate muscarinic acetylcholine receptors (mAChR) and nicotinic acetylcholine receptors (nAChR). Both sympathetic and parasympathetic nerves have been identified in the bone, and are typically observed in close contact with large vascular structures in the long bones (5, 7, 34). Tyrosine hydroxylase (TH), the rate limiting enzyme in the synthesis of catecholamines, is typically used as an immunohistochemical marker for sympathetic nerves. TH⁺ axons are typically observed with a spiral morphology in the bone marrow, essentially wrapping around blood vessels (10, 45). Conversely, axons expressing vesicular acetylcholine transporter (VACHT) and choline acetyltransferase (ChAT), two markers for parasympathetic nerves, can also be readily observed in the marrow space of long bones (46). The innervation density of

these nerve axons is less well-described than sensory nerves, but is presumed to follow a similar pattern.

Function of ANS in Bone

The major function of the ANS on the skeleton is restraint of bone remodeling (37). Specifically, activation of the sympathetic nervous system acts to stimulate bone resorption as well as negatively affect bone formation (37, 38). Conversely, the parasympathetic nervous system activity inhibits bone resorption, which results in bone mass accrual (46). These activities may also be related to the general circadian rhythm of the autonomic nervous system. Sympathetic nervous activity is generally dominant during the day, which is the peak time for bone resorption, while parasympathetic nervous activity is generally dominant at night, when bone formation peaks (47–49). Osteoblasts and osteoclasts express a wide variety of adrenergic receptors that could be activated in response to norepinephrine released from sympathetic nerve terminals (50, 51). Similarly, osteoblast and osteoclasts may be able to respond to the release of acetylcholine from parasympathetic nerve terminals due to their expression of the $\alpha 2$ and $\beta 2$ subunits of the nAChRs; mAChRs expression is absent in these cell types (46). Due to the expression of these receptors on bone cells, it has been presumed that the ANS exerts its effect on the skeleton through the release of neurotransmitters in close proximity to bone cells, which subsequently bind to their cognate receptors to initiate a biological response. However, recent work reporting relatively limited direct interaction of ANS nerve fibers with skeletal cells suggests that an alternative diffusion-based mechanism may be plausible (32, 52). Nonetheless, mice lacking $\beta 2$ adrenergic receptor in the osteoblast lineage have increased bone mass in adulthood, due to increased bone formation and decreased bone resorption (50). This encouraging result, along with the known safety profile of “ β blockers” (β adrenergic antagonists), suggested that pharmacological blockade of sympathetic nervous signaling would increase bone mass and decrease fracture risk in humans. Surprisingly, subsequent preclinical research utilizing β adrenergic receptor agonist (salbutamol) or antagonist (isoprenaline) failed to recapitulate the previous findings in mice; instead, these drugs were both associated with bone loss, mostly due to increased bone resorption (53, 54). Similarly, a randomized clinical trial observed no significant effects of either $\beta 2$ adrenergic agonists or antagonists on bone turnover in adults (55). A meta-analysis of 16 studies published in 2014 reported that the use of β blockers decreased overall fracture risk by 15%, with $\beta 1$ -specific blockers most strongly associated with the reduction in risk (56). Consistent with this report, a recent randomized controlled trial utilized the relative selectivity of β -blockers to show that patients treated with $\beta 1$ -selective drugs had improved parameters of bone density and turnover (57). In total, much of the direct and specific effects of the autonomic nervous system, as well as the potential therapeutic opportunities in modulating this signaling pathway, remains to be determined.

Release of Neuropeptides by ANS in Bone

Similar to sensory nerve axons of the SNS, sympathetic nerves of the ANS can also release neuropeptides, particularly in response

to stress. One such neurotransmitter released by sympathetic nerves is neuropeptide Y (NPY), which can signal through one of five NPY receptors that are expressed in both the central and peripheral nervous systems (58, 59). A role for NPY in bone homeostasis was first recognized in 2002, when Y2 receptor null mice were found to have significant increased trabecular bone volume due to increased osteoblastic activity without an alteration in osteoclast resorptive area (60). Similarly, in the setting of ovariectomy, mice lacking hypothalamic Y2 receptors were found to be protected from bone loss through an increase in osteoblastic activity (61). More recently, mice in which NPY was expressed exclusively in noradrenergic nerves of mice otherwise lacking NPY were used to demonstrate that NPY acts both centrally and peripherally through Y2 receptors to protect against stress-induced loss of bone mass (62). Consistent with these studies, *in vitro* work utilizing primary osteoblasts has revealed a direct inhibitory effect of NPY on osteoblast differentiation, indicating NPY exerts its effects both directly and indirectly on bone (63–65). Similarly, nerve axons expressing vasoactive intestinal peptide (VIP) have been observed in bone for some time (4, 66). Recent interest in this neuropeptide secreted from the ANS has shown that it promotes osteogenic differentiation *in vitro* and stimulates bone repair when delivered *in vivo* (67). Alternately, VIP appears to be implicated in the progression of osteoarthritis through actions on subchondral bone sclerosis and vascularity (68).

Modifiers of Sympathetic Signaling in Bone

Restraint of sympathetic signaling on bone is achieved *via* antagonistic sympathetic projections and degradation or sequestration of sympathetic neurotransmitters; each are implicated in an aging skeletal phenotype. Endocannabinoids, such as 2-arachidonylglycerol (2-AG), are generated by bone cells and act on CB1 receptors on skeletal sympathetic nerve endings. In support of endocannabinoid restraining the inhibitory effect of sympathetic transmission of skeletal mass and microarchitecture, global deletion of the CB1 receptor (*Cnr1*) produces a skeletal phenotype characterized by decreased trabecular microarchitecture, low bone mass, and increased osteoclast activation (69). However, functional impact of cannabinoid receptor signaling on restraint of SNS outflow and resultant skeletal effects are clouded by contrasting results from different groups, related to choice of mouse models, sex, and animal age. For example, enhanced bone mass and resistance to ovariectomy-induced bone loss was recently reported in congenic Swiss albino ABH and CD1 congenic *Cnr1*-deficient mice (70). However, divergent skeletal phenotypes were observed in C57BL/6J vs. CD1 *Cnr1*-deficient mice producing both loss and gain, respectively, of bone mass in the absence of *Cnr1*. Furthermore, the divergent skeletal phenotype was sexually-dimorphic in CD1 *Cnr1*^{-/-} mice, affecting males but not females, whereas the effect was independent of sex in C57BL/6J strain of mice (69).

Neurotransmitter clearance from the synaptic cleft presents as another mechanism to influence magnitude or duration of sympathetic signaling on the skeleton. Clearance of NE from the synaptic cleft by the norepinephrine transport NET (*SLC6A2*),

a sodium- and chloride-dependent monoamine transporter. Provided that sympathetic signaling exerts negative skeletal effects *via* RANKL-mediated osteoclast activation and inhibition of osteoblast function (71), pharmacologic inhibition or genetic deletion of NET would be expected to produce a high bone mass phenotype. Whereas, mature osteoblasts express high levels of NET, its inhibition with reboxetine elicited sexually-dimorphic reductions in osteoblast number and bone mineralization in male, but not female, mice, findings which were also recapitulated in global *Slc6a2*^{-/-} mice. Clearance of NE may contribute to aging-associated skeletal wasting, as NE uptake is greater in young (3 months) than aged (18 months) mice, reflective from decreased *Slc6a2* expression increased tibial NE content with age (71). These results demonstrate that NE clearance and catabolism is a fundamental aspect of skeletal homeostasis with a potential function in involutional bone loss, yet the unexpected results from pharmacologic inhibition or genetic deletion of *Slc6a2*^{-/-} reveal the need for inducible murine knockout models to more clearly detail where and when loss of *Slc6a2* or *Cnr1* most potently influence bone mass.

NERVES IN THE DEVELOPING SKELETON

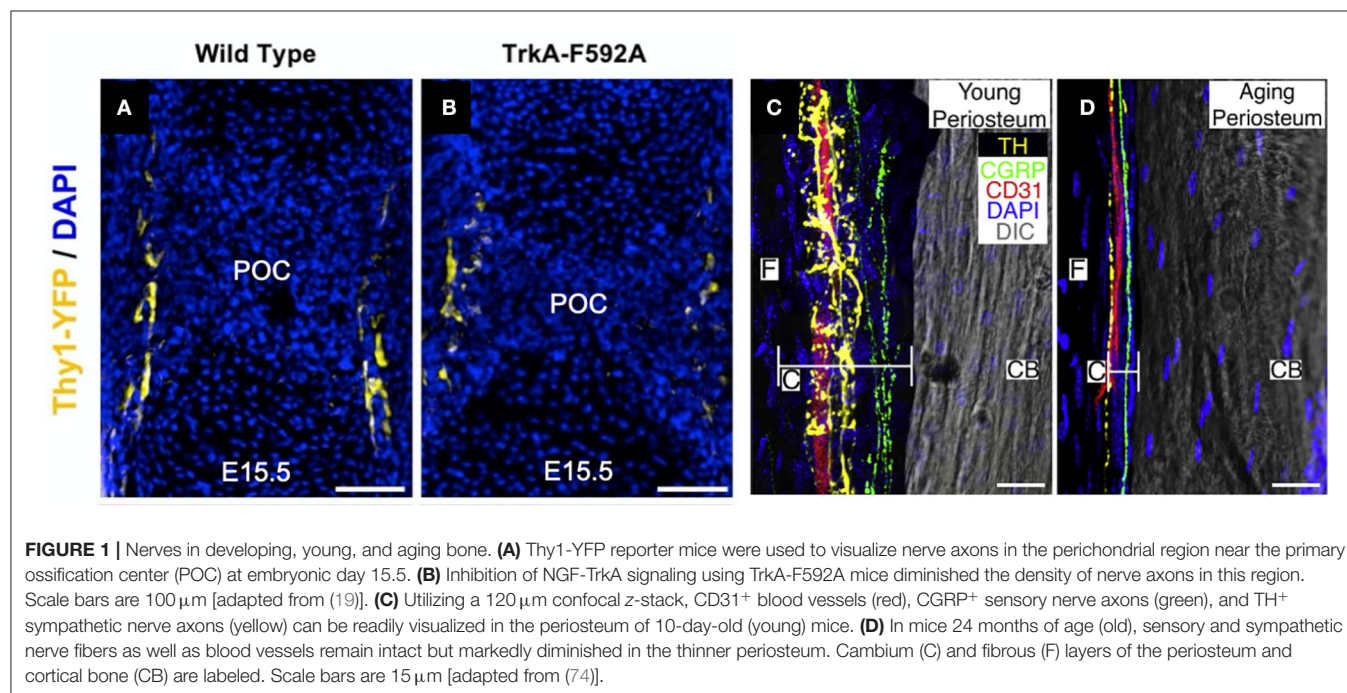
Timing of Skeletal Innervation During Endochondral Ossification

The exact location, timing, and subtype of nerves entering developing bone has been a topic of research interest for some time. Early work established that the innervation of bone occurs approximately simultaneously with endochondral ossification during embryonic development, including studies in mice illustrating a functional nerve supply in areas of high osteogenic activity by embryonic day 15 as well as the presence

of CGRP immunoreactive nerves by embryonic day 16.5 (72, 73). Consistent with these studies, we have recently demonstrated that TrkA expressing sensory nerves arrive at the perichondrial surface of developing bone at embryonic day 14.5 in mice (Figure 1A), in response to the expression of the neurotrophin NGF by osteoprogenitors and coincident with the initiation of primary ossification (75). After birth, nerve density in bone continues to increase, coinciding with the bone modeling and remodeling necessary for shaping long bones. Sensory nerve axons expressing CGRP and Substance P are present at postnatal day 1 in the epiphysis and endosteum of the distal femur and proximal tibia, and by postnatal day 6, these sensory nerves appear in the cartilage canal and 2 days later in the secondary ossification centers (76). Similar to the invasion of the primary ossification center by sensory nerves, the sensory nerve axons entering the secondary ossification center through cartilage canals is in response to the expression of NGF at the epiphysis and the majority of these nerves express TrkA (75). Unlike sensory nerves, autonomic fibers staining for NPY do not appear in bone until postnatal day 4 (72). The autonomic fibers first appear as single, non-vascular, branching fibers in the tibial and femoral periosteum. NPY fibers next appear in the medullary cavity accompanying blood vessels until postnatal day 14, when the occurrence of the fibers decreases in all bone compartments.

Effects of Diminished Skeletal Innervation on Developing Bone

Although the presence of nerves during primary and secondary ossification is well-documented, their function during skeletal development remains poorly understood. Denervation and associated models of nerve inactivation provide some insights



into the role of peripheral nerves during bone development. For example, sectioning the sciatic nerve in 1-month-old rats reduced metatarsal length 3–5%, while femora and tibiae, containing femoral and obturator nerves which could potentially compensate for sciatic neurectomy, were unaffected (77). Notably in this study, early reductions in bone length were maintained, and were not exacerbated, up to the end of the 12-week study. Similarly, sciatic neurectomy prevented gains in bone mass and improvements in microarchitecture, instead inducing considerable trabecular bone loss in growing rats, due to decreased bone formation and increased bone resorption, though it is unclear how much of these bone changes were due to disuse (78). In mice either globally- or neuronally-deficient in semaphorin 3A, an axonal chemorepellant important to axon guidance, decreases in sensory innervation of trabecular bone reduced bone mass *via* decreased bone formation in 8-week old mice (79). Mice lacking TRPV1 (capsaicin receptor/vanilloid receptor1), a cation channel involved in nociception found on sensory nerves, displayed a similar phenotype to wildtype mice, with similar size and bodyweight. However, TRPV1 knockout mice exhibited a reduction in the basal levels of the osteoclast activation biomarker TRAP in the femur (80) and ovariectomy of these knockout mice did not cause the elevation in TRAP levels or bone loss as normally occurs in wildtype mice. α CGRP knockout mice displayed osteopenia associated with low bone formation rate without changes in osteoblast number or surface (39). In our previous study (81), we investigated bone development in mice treated with capsaicin as neonates to destroy unmyelinated and small diameter myelinated sensory neurons (82, 83). We found that neonatal capsaicin treatment in mice modestly decreased femur length, femur cross-sectional area, and trabecular bone thickness, but did not reduce mechanical properties or bone remodeling rates. In another study, we showed that nerve

growth factor (NGF) signaling through neurotrophic tyrosine kinase receptor type 1 (TrkA) directs sensory innervation during long bone development to promote vascularization and osteoprogenitor differentiation (75). Inactivation of NGF or TrkA signaling during embryogenesis in mice impaired sensory innervation (**Figure 1B**), delayed vascularization of ossification centers, decreased numbers of osteoprogenitors, and decreased femoral length and volume. In total, these studies indicate that sensory innervation is required for attaining normal bone mass and length, as well as vascularization, during skeletal development. Future work should determine if any specific osteogenic factors are delivered by sensory nerves to bone.

NERVES AND SKELETAL ADAPTATION

Bone tissue contains a dense network of sensory and sympathetic nerve fibers, which appears to play important roles in bone modeling, remodeling, metabolism, and adaptation (84). For example, in a study of bone remodeling induced by maxillary molar removal in rats, investigators found that normal tibial growth was not impaired by neonatal sympathectomy (guanethidine treatment) or sensory denervation (capsaicin treatment), but that osteoclast surface was increased 45% in sympathectomized animals and decreased 21% in sensory denervated animals (85). These data indicate that both sympathetic and sensory nerves play a role in bone adaptation, and that these unique fiber types may play opposing roles on skeletal adaptation. We have provided a concise summary of the previous work that studied the roles of sensory and sympathetic nerves in scenarios of increased (**Table 1**) and decreased (**Table 2**) mechanical loading.

TABLE 1 | Increased mechanical loading and altered nerve function.

	Model of altered nerve function	Loading method	Effect on bone	References
Sensory nerves	↓ Sensory function—perineural anesthesia of brachial plexus with bupivacaine in rats	Ulnar compression	↓ Labeled bone area	(80)
	↓ Sensory function—perineural anesthesia of brachial plexus with bupivacaine in rats	Ulnar compression	↓ Labeled bone area	(82)
	↓ Sensory function—inhibition of TrkA signaling by 1NMPP1 in mice	Ulnar compression	↓ Bone formation rate ↓ Wnt/ β -catenin activity in osteocytes ↓ Periosteal nerve sprouting	(19)
	↑ Sensory function—exogenous NGF administration in mice	Ulnar compression	↑ Bone formation rate ↑ Wnt/ β -catenin activity in osteocytes	(19)
	↓ Sensory function—neonatal capsaicin treatment in mice	Tibial compression	↑ Bone mineral content ↑ Mineral apposition rate	(84)
Sympathetic nerves	↓ Sympathetic function—guanethidine sulfate or propranolol treatment in mice	Tibial compression	No effect	(83)
	↓ Sympathetic function—propranolol treatment in mice	Tibial compression	No effect	(85)
	↓ Sympathetic function—propranolol treatment in ovariectomized rats	Treadmill exercise	↓ Trabecular BV/TV and Tb.Th	(86)
	↑ Sympathetic function—salbutamol treatment in rats	Treadmill exercise	↓ MAR, Tb.Th, ultimate force, stiffness, Young's modulus	(53)
	↑ Sympathetic function—salbutamol treatment in ovariectomized rats	Treadmill exercise	↓ Trabecular BV/TV and Tb.Th	(87)
	↓ Sympathetic function—genetic deletion of β 1-adrenergic receptors and/or β 2-adrenergic receptors in mice	Tibial compression	↓ BMD, Tb.Th, MAR, BFR/BS in <i>Adrb1</i> ^{-/-} and <i>Adrb1b2</i> ^{-/-} mice	(88)

TABLE 2 | Decreased mechanical loading and altered nerve function.

	Model of altered nerve function	Loading method	Effect on bone	References
Sensory nerves	↓ Sensory function—neonatal capsaicin treatment in rats	Molar extraction	↓ Osteoclast surface	(78)
	↓ Sensory function—capsaicin treatment in adult rats	Hindlimb unloading	↑ Energy to failure	(92)
Sympathetic nerves	↓ Sympathetic function—guanethidine treatment in rats	Molar extraction	↑ Osteoclast surface	(78)
	↓ Sympathetic function—guanethidine or propranolol treatment in mice	Hindlimb unloading	↑ Trabecular BV/TV ↑ MAR, MS/BS, BFR/BS ↓ Oc.N and Oc.S	(93)
	↑ Sympathetic function—isoproterenol treatment in mice	Hindlimb unloading	No effect	(93)
	↓ Sympathetic function—guanethidine sulfate or propranolol treatment in mice	Sciatic neurectomy	No effect	(85)
	↓ Sympathetic function—propranolol treatment in rats	Hindlimb unloading	↑ Trabecular Bone Volume ↑ MAR, BFR/BS ↓ Resorbing surface	(94)
	↑ Sympathetic function—dobutamine treatment in rats	Hindlimb unloading	↑ BMD, BMC, Bone Area ↑ MAR, MS/BS, BFR/BS	(95)
	↑ Sympathetic function—dobutamine treatment in rats	Hindlimb unloading	↑ BV/TV, Tb.Th, Tb.N ↑ OS/BS, Ob.S/BS ↑ MAR, MS/BS, BFR/BS ↓ Osteocyte apoptosis	(96)

Peripheral Nerves Support Load-Induced Bone Formation

The role of peripheral nerves in sensing and responding to mechanical stimuli is an area of equal parts interest and contradiction. Early studies reported that denervation had essentially no effect on the bone formation response to mechanical loading. For example, intermittent loading (bending) initiated similar magnitudes of cortical bone formation in the denervated rabbit tibia as in intact tibias (86). This led the authors to conclude that the nervous system has no significant effect on the functional adaptation of bone. However, recent studies have established a notable role of peripheral nerves in bone mechanosensing and adaptation to mechanical stimuli. A pivotal study used bupivacaine to induce perineural anesthesia of the brachial plexus of rats to achieve temporary neuronal blocking prior to ulnar compression (87). They found that temporarily blocking neuronal signaling reduced bone formation (total labeled bone area) by 81% in the compressed ulna relative to sensory intact ulnae. Further studies by this group revealed that mechanical loading increased bone formation in the contralateral limb and at other non-loaded skeletal sites, which was modulated through sensory nerves (88, 89); however, load-induced increases in contralateral bone formation have been directly contradicted by others (90) and indirectly by the large number of related studies that utilize contralateral limbs as an internal control.

Our study investigating bone adaptation to increased mechanical loading in mice treated with capsaicin to induce destruction of TRPV1-expression peripheral nerves found that tibial compression increased cortical bone area in the loaded tibia, accompanied by changes in bone formation, which was generally greater in capsaicin-treated mice than in vehicle-treated mice (91). In contrast, our study of NGF-TrkA signaling in sensory nerves in bone showed that elimination of TrkA signaling attenuated bone formation and reduced Wnt/ β -catenin activity in osteocytes in bones loaded by axial forelimb compression.

Furthermore, administration of exogenous NGF to wild-type mice significantly increased load-induced bone formation and Wnt/ β -catenin activity in osteocytes (75). The contrasting results from these two studies of decreased sensory nerve signaling in bone suggest a heterogeneous population of sensory nerves in bone with non-overlapping functions in strain adaptive bone remodeling.

The role of the sympathetic nervous system in the anabolic bone response to mechanical loading is unclear. One study in mice reported that sciatic neurectomy enhanced tibial compression-induced cortical bone formation, but pharmacological blockade of the SNS with guanethidine sulfate or propranolol did not affect the bone formation response (90). The same group found that load-induced bone formation and unloading-induced bone resorption were unaffected by propranolol or guanethidine sulfate treatment (92). Another study found that either propranolol treatment or exercise in ovariectomized rats was able to partially preserve trabecular bone volume, but these treatments did not have a synergistic effect, and in fact exhibited an antagonist effect on trabecular bone (93). Similarly, treatment of rats with a selective β 2-adrenergic receptor agonist (salbutamol) decreased bone mineral density and increased bone resorption, and salbutamol treatment mitigated the beneficial effects of treadmill exercise on bone structure in these rats (53, 94). In genetic mouse models of β 1-adrenergic receptor and/or β 2-adrenergic receptor deficiency, tibial compression induced increases in bone density, trabecular and cortical microarchitecture, and bone formation in *Adrb2*^{-/-} and wild-type mice, but not in *Adrb1*^{-/-} or *Adrb1b2*^{-/-} mice, suggesting that β 1, but not β 2, has a role in mechanoadaptation to mechanical stimulation (95).

Peripheral Nerve Impact in Disuse

The initial rapid loss of bone following spinal cord injury suggests that factors other than disuse osteoporosis may drive the

catabolic skeletal response (96). Indeed, electrical stimulation of muscle does not restore bone mass *post* trauma (97). Similarly, unilateral sciatic nerve transection causes bone loss not only in the denervated limb, but in the contralateral limb as well—even when use remains unchanged (98). Altogether, these data suggest that peripheral nerve activity may modulate the bone resorption response during disuse. A study of hindlimb unloading-induced bone loss in capsaicin-treated rats showed that both capsaicin treatment and 4 weeks of hindlimb unloading resulted in considerable loss of trabecular bone at the proximal tibia, but that hindlimb unloading of capsaicin-treated rats did not promote further bone loss (99). Altogether, these data suggest that diminished sensory nerve function diminishes bone volume but may make the bone less sensitive to the mechanical environment. Together, these data suggest that diminished sensory nerve function diminishes bone volume and may make the bone less sensitive to the mechanical environment. Moreover, results from a model of disuse-induced remodeling in the mandible is consistent with this view. Here, significantly decreased osteoclast surface was observed in rats with decreased sensory nerve function due to neonatal capsaicin treatment (85).

Sympathetic nerves have a notable effect modulating unloading-induced bone loss. One study reported that inhibiting sympathetic nerves in mice using propranolol or guanethidine suppressed bone loss associated with hindlimb unloading by diminishing the reduction in osteoblast activity and the increase in osteoclast activity associated with unloading (100). Conversely, activating sympathetic nerves using isoproterenol reduced bone mass in normally loaded mice, but did not cause additional bone loss in hindlimb unloaded mice. Similarly, others found that treatment of rats with propranolol or a leptin analog during 28 days of hindlimb unloading reduced unloading-associated bone loss; propranolol treatment effectively preserved bone formation and prevented increased bone resorption, while leptin analog treatment was only able to prevent changes in osteoclastic bone resorption (101). Conversely, treatment of rats with a β 1-adrenergic receptor agonist (dobutamine) attenuated hindlimb unloading-induced bone loss, prevented the decline in bone formation induced by unloading, and diminished unloading-induced osteocyte apoptosis (102, 103).

Load-Induced Neurotransmitter Expression in Bone

The first evidence of mechanical regulation of neurotransmitters was the observation that ulnar loading in rats decreased expression of GLAST, a glutamate/aspartate transporter previously thought to be present only in mammalian CNS (104). Quantification of CGRP, VIP, and SP in the rat ulna after mechanical loading (ulnar compression) using ELISA revealed that CGRP concentrations in both the loaded and contralateral limbs were reduced 1 h after loading, and that this reduction was sustained for at least 10 days (87). Bilateral decreases in SP concentrations were also observed, although the effect was less persistent. Ulnar VIP concentrations were increased bilaterally 10 days after mechanical loading at medium or high strain magnitudes. In contrast, both CGRP and SP levels were increased in the sciatic nerve after 4 weeks of cast immobilization (105). Our results partially agreed with

these data, as mechanically loading tibias in mice resulted in significantly decreased SP concentrations, but increased CGRP concentrations relative to controls, while unloaded tibias exhibited trends toward increased concentrations of both CGRP and SP (91).

NERVES AND THE AGING SKELETON

Chronological aging causes cell and tissue dysfunction, which compromises individual capacity to maintain homeostasis. In the context of the skeleton, uncoupled remodeling promotes net bone loss, characterized by reductions in bone mineral density and bone strength and increased fracture risk. Suggestive links between autonomic tone and bone strength with aging are evident in associations such as increased sympathetic tone in post-menopausal women (106) who are at risk of osteoporotic fractures, and hereditary neuropathies with skeletal manifestations [reviewed in (32)]. Provided the distribution and patterning of sympathetic and sensory nerves in bone, changes in fiber presentation, function, or restraint have each been presented as correlative—if not causative—for bone loss with age.

Fiber Number and Density

Aging reduces nerve fiber frequency and their organization. A recent study evaluated sensory and sympathetic innervation of the periosteum, cortical bone, and bone marrow in femora of C57BL/6 mice at 10 days, 3 months, or 24 months of age (74). They observed highest density of sensory (CGRP⁺) and sympathetic (TH⁺) neurons in the inner cambial layer of the periosteum; CGRP⁺ sensory fibers displayed a linear pattern along the long axis of the femur, whereas TH⁺ sympathetic fibers were highly branched and closely associated with CD31⁺ blood vessels (**Figure 1C**). Despite substantial periosteal thinning with age—~75% reduction in total thickness, with greatest reduction in the cambium (~90% decrease)—which reduced total fiber number, fiber density was greatest in aged animals, likely owing to the dramatic reductions in periosteal thickness in which fibers were located (**Figure 1D**). Within cortical bone, CGRP⁺ and TH⁺ fibers were observed exclusively in Haversian canals, and fiber morphology was similar as observed in the periosteum. TH⁺ fibers decreased in aged animals (~48–14%), whereas a similar fraction (26%) of fibers were CGRP⁺ in adult and aged animals, and there was a modest reduction in CD31⁺ blood vessels (89% in 3 months vs. 62% in 24 months). There were no statistically distinct differences in fiber density in bone marrow as a function of chronological age. However, other studies do not fully corroborate these findings. Using a similar approach in a rat model, reductions in cambium thickness with age were observed without change in fibrous periosteum thickness or periosteal innervation (107); in a human study of femora and tibiae of aged individuals (68–99 years), significant intraindividual differences in periosteal thickness of tibia and femur were reported, yet there was no correlation of periosteal thickness of either bone as a function of age or weight (108). Thus, whereas supportive evidence for decreased periosteal thickness as a consequence of aging suggests a relationship to decreased nerve fiber number and/or density, more detailed

investigation across a number of species is necessary to faithfully support such conclusions.

Alterations in fiber density with aging may drive reduced tissue function, specifically aging of the hematopoietic stem cell niche within the skeleton. By comparing young (8–10 weeks) and old (20–24-month-old) mice on a Nestin-GFP reporter background, aging associated with remodeling of bone marrow vascular architecture: total vascular density (CD31⁺ CD144⁺) increased in aged mice which was driven by reductions in arteriolar segment length despite cellular expansion away from the endosteum and which converged on the central vein (109). Concomitant with arteriolar remodeling were reductions in TH⁺ fiber density, total nerve density (β -III tubulin), and neural dysfunction (reduced synaptophysin density as a marker of synaptic contacts between blood vessels and nerves). Surgical transection of femoral and sciatic nerves in young mice fully recapitulated the effect of age, indicated by absence of TH⁺ fibers, expanded myeloid-biased CD41⁺ HSCs with reduced competitive engraftment potential, and vascular remodeling. Niche-derived noradrenaline maintains HSC function, as β 2- or β 3-selective sympathomimetics reduced both absolute numbers and frequencies of MSCs and ECs in aged mice, comparable to young mice; further, β 3 agonists increased donor HSC engraftment following transplantation in aged mice and rescued the premature aging phenotype in denervated mice. Conversely, constitutive deletion of *Adrb3* accelerated HSC niche aging in young mice. Thus, age-associated alterations in bone marrow innervation and vasculature drive hallmarks of immune dysfunction, although the direct impact on skeletal involution requires elaboration.

Sympathetic Outflow, Aging, and Skeletal Disease

Restraint of sympathetic outflow in the skeleton presents as another potential mechanism whereby age-associated impairment of cell function produces organ-level dysfunction. For example, sustained presentation of NE within the skeleton—given its established catabolic effect on the skeleton—may drive imbalanced remodeling as observed in older animals and humans. Indeed, differential clearance of NE by the norepinephrine transporter NET (*Slc6a2*) was observed to be a function of age: specific NE uptake from flushed femoral cortical bone was greater in young (3 months) than aged (18 months) mice (71). Correspondingly, basal NE content was greater in aged compared to young mice, although this did not associate with increased sympathetic outflow in older animals. Thus, inadequate clearance of NE in aged bone may contribute to skeletal wasting due to sustained β 2 adrenergic stimulation. Similarly, the cannabinoid receptors Cb1 (*Cnr1*) and CB2 (*Cnr2*), which restrain sympathetic signaling, are implicated in age-related bone loss and joint disease. Dual deletion of both Cb1 and CB2 (*Cnr1*^{-/-}/*Cnr2*^{-/-}) mice reveal attenuated bone loss as a function of age or estrogen status resulting from deficits in osteoclast formation (110). Further, CB receptor agonists protect against both collagen- (111, 112) and destabilization-induced arthritis (113), and loss of *Cnr2* delays osteoarthritis progression (113). Whilst illuminating, such studies do not identify which

cells mediate the observed influence: they do not reveal if cell-autonomous defects in osteoclastogenesis *in vivo* mitigate bone loss, nor do they establish sympathetic involvement.

Neurotrophin Presentation With Aging

Despite a name suggesting neural-specific expression and function, neurotrophins and their receptors are highly expressed in osteochondrogenic cells during development and repair [reviewed in (114)] Thus, changes in neurotrophin ligand or receptor expression in the skeleton can alter the ingrowth or maintenance of neural fibers in the skeleton. Whether aging influences presentation of NGF or other neurotrophins, is unresolved: serum NGF levels appear unaffected by aging (115, 116) or modestly decrease (117), as does serum BDNF levels (118). While *Ngf* expression in bone is mechanically regulated, and is induced less in aged mice compared to younger mice (119), if attenuated load-induced expression with increasing age impacts sympathetic or sensory signaling in the skeleton requires greater elaboration. Further, detailed studies defining the contribution of NGF to post-menopausal vs. sex-independent involutional bone loss are lacking.

CONCLUSIONS

Extensive and sustained efforts reveal that the skeleton is richly innervated by sensory and sympathetic nerves which appear during and participate in skeletal development; further investigations have implicated these same nerve fibers in skeletal homeostasis and adaptation, as well as contributions toward bone loss with age. Yet, with each discovery, the relationships become more complex, demanding more precise interrogation and articulation in order to weave together a precise narrative. Indeed, the development of this narrative is hampered by a variety of questions. To what extent conclusions about the impact of sympathetic or sensory fiber number, density, etc. on the skeleton limited by an experimental approach that may not be as robust as assumed. For example, the decalcification of bone that is necessary for its immunohistological evaluation can prevent retention of neurologic markers, as demonstrated in (74), wherein labeling of TrkA, p75, and NGF in the periosteum and bone marrow was diminished in specimens that had undergone decalcification. Observations such as these motivate the opportunity to utilize or develop models whose results are less ambiguous and with greater fidelity, such as cell-specific fluorescent reporter mice. Furthermore, despite the mandate from the National Institutes of Health to include sex as a biological variable, many of the studies reviewed here used animals of a single sex. Provided the overwhelming fact of skeletal sexual dimorphism and evidence supporting sexual dimorphism in neurotrophin and receptor expression (120–122), the opportunity to establish correlation, if not causation, is missed. Indeed, a novel role for kisspeptin-expressing cells within the arcuate nucleus—wherein estrogen receptor alpha drives central and peripheral energy metabolism to exert inhibitory effects on bone mass—was discovered recently in female, but not male, mice (123). Studies like these, and other reports whose seeming contradictions with previous reports may originate in sexual dimorphism, reveal the obligation to evaluate both

sexes. Furthermore, this study also illuminates another area of nerve-bone interaction outside scope of the present review—signaling in the central nervous system. In total, more research to resolve outstanding issues and improve our knowledge of nerve-bone interaction may permit the use of these signaling mechanisms to combat skeletal diseases, effectively treat skeletal pain, increase bone mass in healthy individuals, and address age-related declines in skeletal health.

AUTHOR CONTRIBUTIONS

All authors contributed to development of this article, reviewed pertinent literature, wrote, and edited the manuscript.

REFERENCES

- Milgram JW, Robinson RA. An electron microscopic demonstration of unmyelinated nerves in the Haversian canals of the adult dog. *Bull Johns Hopkins Hosp.* (1965) 117:163–73.
- Linder JE. A simple and reliable method for the silver impregnation of nerves in paraffin sections of soft and mineralized tissues. *J Anat.* (1978) 127:543–51.
- Thurston TJ. Distribution of nerves in long bones as shown by silver impregnation. *J Anat.* (1982) 134:719.
- Hohmann EL, Elde RP, Rysavy JA, Einzig S, Gebhard RL. Innervation of periosteum and bone by sympathetic vasoactive intestinal peptide-containing nerve fibers. *Science.* (1986) 232:868–71. doi: 10.1126/science.3518059
- Bjurholm A, Kreicbergs A, Brodin E, Schultzberg M. Substance P- and CGRP-immunoreactive nerves in bone. *Peptides.* (1988) 9:165–71. doi: 10.1016/0196-9781(88)90023-x
- Wojtyś EM, Beaman DN, Glover RA, Janda D. Innervation of the human knee joint by substance-P fibers. *Arthroscopy.* (1990) 6:254–63. doi: 10.1016/0749-8063(90)90054-h
- Hill EL, Elde R. Distribution of CGRP-, VIP-, D beta H-, SP-, and NPY-immunoreactive nerves in the periosteum of the rat. *Cell Tissue Res.* (1991) 264:469–80. doi: 10.1007/BF00319037
- Hukkanen M, Konttinen YT, Rees RG, Gibson SJ, Santavirta S, Polak JM. Innervation of bone from healthy and arthritic rats by substance P and calcitonin gene related peptide containing sensory fibers. *J Rheumatol.* (1992) 19:1252–9.
- Mach DB, Rogers SD, Sabino MC, Luger NM, Schwei MJ, Pomonis JD, et al. Origins of skeletal pain: sensory and sympathetic innervation of the mouse femur. *Neuroscience.* (2002) 113:155–66. doi: 10.1016/S0306-4522(02)00165-3
- Castañeda-Corral G, Jimenez-Andrade JM, Bloom AP, Taylor RN, Mantyh WG, Kaczmarek MJ, et al. The majority of myelinated and unmyelinated sensory nerve fibers that innervate bone express the tropomyosin receptor kinase A. *Neuroscience.* (2011) 178:196–207. doi: 10.1016/j.neuroscience.2011.01.039
- Julius D, Basbaum AI. Molecular mechanisms of nociception. *Nature.* (2001) 413:203–10. doi: 10.1038/35093019
- Proske U, Gandevia SC. The proprioceptive senses: their roles in signaling body shape, body position and movement, and muscle force. *Physiol Rev.* (2012) 92:1651–97. doi: 10.1152/physrev.00048.2011
- Jones LA, Smith AM. Tactile sensory system: encoding from the periphery to the cortex. *Wiley Interdiscip Rev Syst Biol Med.* (2014) 6:279–87. doi: 10.1002/wsbm.1267
- McKemy DD, Neuhauser WM, Julius D. Identification of a cold receptor reveals a general role for TRP channels in thermosensation. *Nature.* (2002) 416:52–8. doi: 10.1038/nature719
- Pongratz G, Straub RH. Role of peripheral nerve fibres in acute and chronic inflammation in arthritis. *Nat Rev Rheumatol.* (2013) 9:117–26. doi: 10.1038/nrrheum.2012.181
- Coste B, Mathur J, Schmidt M, Earley TJ, Ranade S, Petrus MJ, et al. Piezo1 and Piezo2 are essential components of distinct mechanically activated cation channels. *Science.* (2010) 330:55–60. doi: 10.1126/science.1193270
- Nencini S, Ringuet M, Kim D-H, Chen Y-J, Greenhill C, Ivanusic JJ. Mechanisms of nerve growth factor signaling in bone nociceptors and in an animal model of inflammatory bone pain. *Mol Pain.* (2017) 13:1744806917697011. doi: 10.1177/1744806917697011
- Jimenez-Andrade JM, Mantyh WG, Bloom AP, Xu H, Ferng AS, Dussor G, et al. A phenotypically restricted set of primary afferent nerve fibers innervate the bone versus skin: therapeutic opportunity for treating skeletal pain. *Bone.* (2010) 46:306–13. doi: 10.1016/j.bone.2009.09.013
- Tomlinson RE, Li Z, Zhang Q, Goh BC, Li Z, Thorek DLJ, et al. NGF-TrkA signaling by sensory nerves coordinates the vascularization and ossification of developing endochondral bone. *Cell Rep.* (2016) 16:2723–35. doi: 10.1016/j.celrep.2016.08.002
- Sayilekshmy M, Hansen RB, Delaissé J-M, Rolighed L, Andersen TL, Heegaard A-M. Innervation is higher above bone remodeling surfaces and in cortical pores in human bone: lessons from patients with primary hyperparathyroidism. *Sci Rep.* (2019) 9:5361–14. doi: 10.1038/s41598-019-41779-w
- Blyth FM, Briggs AM, Schneider CH, Hoy DG, March LM. The global burden of musculoskeletal pain—where to from here? *Am J Public Health.* (2019) 109:35–40. doi: 10.2105/AJPH.2018.304747
- Mantyh PW. The neurobiology of skeletal pain. *Eur J Neurosci.* (2014) 39:508–19. doi: 10.1111/ejn.12462
- Sevcik MA, Ghilardi JR, Peters CM, Lindsay TH, Halvorson KG, Jonas BM, et al. Anti-NGF therapy profoundly reduces bone cancer pain and the accompanying increase in markers of peripheral and central sensitization. *Pain.* (2005) 115:128–41. doi: 10.1016/j.pain.2005.02.022
- Jimenez-Andrade JM, Ghilardi JR, Castañeda-Corral G, Kuskowski MA, Mantyh PW. Preventive or late administration of anti-NGF therapy attenuates tumor-induced nerve sprouting, neuroma formation, and cancer pain. *Pain.* (2011) 152:2564–74. doi: 10.1016/j.pain.2011.07.020
- Grills BL, Schuijers JA. Immunohistochemical localization of nerve growth factor in fractured and unfractured rat bone. *Acta Orthop Scand.* (1998) 69:415–9. doi: 10.3109/17453679808999059
- Jimenez-Andrade JM, Martin CD, Koewler NJ, Freeman KT, Sullivan LJ, Halvorson KG, et al. Nerve growth factor sequestering therapy attenuates non-malignant skeletal pain following fracture. *Pain.* (2007) 133:183–96. doi: 10.1016/j.pain.2007.06.016
- Grills BL, Schuijers JA, Ward AR. Topical application of nerve growth factor improves fracture healing in rats. *J Orthop Res.* (1997) 15:235–42. doi: 10.1002/jor.1100150212
- Wang L, Zhou S, Liu B, Lei D, Zhao Y, Lu C, et al. Locally applied nerve growth factor enhances bone consolidation in a rabbit model of mandibular distraction osteogenesis. *J Orthop Res.* (2006) 24:2238–45. doi: 10.1002/jor.20269
- Rapp AE, Kroner J, Baur S, Schmid F, Walmsley A, Mottl H, et al. Analgesia via blockade of NGF/TrkA signaling does not influence fracture

FUNDING

This publication was supported by the National Institute of Arthritis and Musculoskeletal and Skin Diseases and the National Institute of Dental and Craniofacial Research of the National Institutes of Health under award numbers AR073772 to DG, AR074953 and DE028397 to RT, AR071459 to BC, and AR075013 to BC, and by the Department of Defense—Congressional Directed Medical Research Programs under award number PR180268P1 to BC. The content is solely the responsibility of the authors and does not necessarily represent the official views of the funding bodies.

- healing in mice. *J Orthop Res.* (2015) 33:1235–41. doi: 10.1002/jor.22892
30. Li Z, Meyers CA, Chang L, Lee S, Li Z, Tomlinson R, et al. Fracture repair requires TrkA signaling by skeletal sensory nerves. *J Clin Invest.* (2019) 129:5137–50. doi: 10.1172/JCI128428
 31. Hochberg MC. Serious joint-related adverse events in randomized controlled trials of anti-nerve growth factor monoclonal antibodies. *Osteoarthritis Cartil.* (2015) 23(Suppl. 1):S18–21. doi: 10.1016/j.joca.2014.10.005
 32. Eleftheriou F. Impact of the autonomic nervous system on the skeleton. *Physiol Rev.* (2018) 98:1083–112. doi: 10.1152/physrev.00014.2017
 33. Malcangio M, Garrett NE, Tomlinson DR. Nerve growth factor treatment increases stimulus-evoked release of sensory neuropeptides in the rat spinal cord. *Eur J Neurosci.* (1997) 9:1101–4. doi: 10.1111/j.1460-9568.1997.tb01462.x
 34. Tabarowski Z, Gibson-Berry K, Felten SY. Noradrenergic and peptidergic innervation of the mouse femur bone marrow. *Acta Histochem.* (1996) 98:453–7. doi: 10.1016/S0065-1281(96)80013-4
 35. Mrak E, Guidobono F, Moro G, Frascini G, Rubinacci A, Villa I. Calcitonin gene-related peptide (CGRP) inhibits apoptosis in human osteoblasts by β -catenin stabilization. *J Cell Physiol.* (2010) 225:701–8. doi: 10.1002/jcp.22266
 36. Villa I, Dal Fiume C, Maestroni A, Rubinacci A, Ravasi F, Guidobono F. Human osteoblast-like cell proliferation induced by calcitonin-related peptides involves PKC activity. *Am J Physiol Endocrinol Metab.* (2003) 284:E627–33. doi: 10.1152/ajpendo.00307.2002
 37. Eleftheriou F, Ahn JD, Takeda S, Starbuck M, Yang X, Liu X, et al. Leptin regulation of bone resorption by the sympathetic nervous system and CART. *Nature.* (2005) 434:514–20. doi: 10.1038/nature03398
 38. Katayama Y, Battista M, Kao W-M, Hidalgo A, Peired AJ, Thomas SA, et al. Signals from the sympathetic nervous system regulate hematopoietic stem cell egress from bone marrow. *Cell.* (2006) 124:407–21. doi: 10.1016/j.cell.2005.10.041
 39. Schinke T, Liese S, Priemel M, Haberland M, Schilling AF, Catala-Lehnen P, et al. Decreased bone formation and osteopenia in mice lacking alpha-calcitonin gene-related peptide. *J Bone Miner Res.* (2004) 19:2049–56. doi: 10.1359/JBMR.040915
 40. Niedermair T, Kuhn V, Doranegard F, Stange R, Wieskötter B, Beckmann J, et al. Absence of substance P and the sympathetic nervous system impact on bone structure and chondrocyte differentiation in an adult model of endochondral ossification. *Matrix Biol.* (2014) 38:22–35. doi: 10.1016/j.matbio.2014.06.007
 41. Niedermair T, Schirner S, Seebrocker R, Straub RH, Grassel S. Substance P modulates bone remodeling properties of murine osteoblasts and osteoclasts. *Sci Rep.* (2018) 8:9199–15. doi: 10.1038/s41598-018-27432-y
 42. Goto T, Nakao K, Gunjigake KK, Kido MA, Kobayashi S, Tanaka T. Substance P stimulates late-stage rat osteoblastic bone formation through neurokinin-1 receptors. *Neuropeptides.* (2007) 41:25–31. doi: 10.1016/j.npep.2006.11.002
 43. Wang L, Zhao R, Shi X, Wei T, Halloran BP, Clark DJ, et al. Substance P stimulates bone marrow stromal cell osteogenic activity, osteoclast differentiation, and resorption activity *in vitro*. *Bone.* (2009) 45:309–20. doi: 10.1016/j.bone.2009.04.203
 44. Mori T, Ogata T, Okumura H, Shibata T, Nakamura Y, Kataoka K. Substance P regulates the function of rabbit cultured osteoclast; increase of intracellular free calcium concentration and enhancement of bone resorption. *Biochem Biophys Res Commun.* (1999) 262:418–22. doi: 10.1006/bbrc.1999.1220
 45. Mach DB, Rogers SD, Sabino MC, Luger NM, Schwei MJ, Pomonis JD, et al. Origins of skeletal pain: sensory and sympathetic innervation of the mouse femur. *Neuroscience.* (2002) 113:155–66. doi: 10.1016/S0306-4522(02)00165-3
 46. Bajayo A, Bar A, Denes A, Bachar M, Kram V, Attar-Namdar M, et al. Skeletal parasympathetic innervation communicates central IL-1 signals regulating bone mass accrual. *Proc Natl Acad Sci USA.* (2012) 109:15455. doi: 10.1073/pnas.1206061109
 47. Shao P, Ohtsuka-Isoya M, Shinoda H. Circadian rhythms in serum bone markers and their relation to the effect of etidronate in rats. *Chronobiol Int.* (2003) 20:325–36. doi: 10.1081/cbi-120019343
 48. Komoto S, Kondo H, Fukuta O, Togari A. Comparison of β -adrenergic and glucocorticoid signaling on clock gene and osteoblast-related gene expressions in human osteoblast. *Chronobiol Int.* (2012) 29:66–74. doi: 10.3109/07420528.2011.636496
 49. Dudek M, Meng Q-J. Running on time: the role of circadian clocks in the musculoskeletal system. *Biochem J.* (2014) 463:1–8. doi: 10.1042/BJ20140700
 50. Kajimura D, Hinoi E, Ferron M, Kode A, Riley KJ, Zhou B, et al. Genetic determination of the cellular basis of the sympathetic regulation of bone mass accrual. *J Exp Med.* (2011) 208:841–51. doi: 10.1084/jem.20102608
 51. Togari A. Adrenergic regulation of bone metabolism: possible involvement of sympathetic innervation of osteoblastic and osteoclastic cells. *Microsc Res Tech.* (2002) 58:77–84. doi: 10.1002/jemt.10121
 52. Dénes A, Boldogkoi Z, Uherezky G, Hornyák A, Rusvai M, Palkovits M, et al. Central autonomic control of the bone marrow: multisynaptic tract tracing by recombinant pseudorabies virus. *Neuroscience.* (2005) 134:947–63. doi: 10.1016/j.neuroscience.2005.03.060
 53. Bonnet N, Benhamou CL, Beaupied H, Laroche N, Vico L, Dolleans E, et al. Doping dose of salbutamol and exercise: deleterious effect on cancellous and cortical bones in adult rats. *J Appl Physiol.* (2007) 102:1502–9. doi: 10.1152/jappphysiol.00815.2006
 54. Kondo H, Togari A. Continuous treatment with a low-dose β -agonist reduces bone mass by increasing bone resorption without suppressing bone formation. *Calcif Tissue Int.* (2011) 88:23–32. doi: 10.1007/s00223-010-9421-9
 55. Veldhuis-Vlug AG, Tanck MW, Limonard EJ, Endert E, Heijboer AC, Lips P, et al. The effects of beta-2 adrenergic agonist and antagonist on human bone metabolism: a randomized controlled trial. *Bone.* (2015) 71:196–200. doi: 10.1016/j.bone.2014.10.024
 56. Toulis KA, Hemming K, Stergianos S, Nirantharakumar K, Bilezikian JP. β -Adrenergic receptor antagonists and fracture risk: a meta-analysis of selectivity, gender, and site-specific effects. *Osteoporos Int.* (2014) 25:121–9. doi: 10.1007/s00198-013-2498-z
 57. Khosla S, Drake MT, Volkman TL, Thicke BS, Achenbach SJ, Atkinson EJ, et al. Sympathetic β 1-adrenergic signaling contributes to regulation of human bone metabolism. *J Clin Invest.* (2018) 128:4832–42. doi: 10.1172/JCI122151
 58. Heilig M. The NPY system in stress, anxiety and depression. *Neuropeptides.* (2004) 38:213–24. doi: 10.1016/j.npep.2004.05.002
 59. Zhou Z, Zhu G, Hariri AR, Enoch M-A, Scott D, Sinha R, et al. Genetic variation in human NPY expression affects stress response and emotion. *Nature.* (2008) 452:997–1001. doi: 10.1038/nature06858
 60. Baldock PA, Sainsbury A, Couzens M, Enriquez RF, Thomas GP, Gardiner EM, et al. Hypothalamic Y2 receptors regulate bone formation. *J Clin Invest.* (2002) 109:915–21. doi: 10.1172/JCI14588
 61. Allison SJ, Baldock P, Sainsbury A, Enriquez R, Lee NJ, Lin E-JD, et al. Conditional deletion of hypothalamic Y2 receptors reverts gonadectomy-induced bone loss in adult mice. *J Biol Chem.* (2006) 281:23436–44. doi: 10.1074/jbc.M604839200
 62. Baldock PA, Lin S, Zhang L, Karl T, Shi Y, Driessler F, et al. Neuropeptide Y attenuates stress-induced bone loss through suppression of noradrenaline circuits. *J Bone Miner Res.* (2014) 29:2238–49. doi: 10.1002/jbmr.2205
 63. Igwe JC, Jiang X, Paic F, Ma L, Adams DJ, Baldock PA, et al. Neuropeptide Y is expressed by osteocytes and can inhibit osteoblastic activity. *J Cell Biochem.* (2009) 108:621–30. doi: 10.1002/jcb.22294
 64. Matic I, Matthews BG, Kizivat T, Igwe JC, Marijanovic I, Ruohonen ST, et al. Bone-specific overexpression of NPY modulates osteogenesis. *J Musculoskelet Neuronal Interact.* (2012) 12:209–18.
 65. Sousa DM, Baldock PA, Enriquez RF, Zhang L, Sainsbury A, Lamghari M, et al. Neuropeptide Y Y1 receptor antagonism increases bone mass in mice. *Bone.* (2012) 51:8–16. doi: 10.1016/j.bone.2012.03.020
 66. Cherruau M, Morvan FO, Schirar A, Saffar JL. Chemical sympathectomy-induced changes in TH-, VIP-, and CGRP-immunoreactive fibers in the rat mandible periosteum: influence on bone resorption. *J Cell Physiol.* (2003) 194:341–8. doi: 10.1002/jcp.10209
 67. Shi L, Feng L, Zhu M-L, Yang Z-M, Wu T-Y, Xu J, et al. Vasoactive intestinal peptide stimulates bone marrow-mesenchymal stem cells osteogenesis differentiation by activating Wnt/ β -catenin signaling

- pathway and promotes rat skull defect repair. *Stem Cells Dev.* (2020) 29:655–66. doi: 10.1089/scd.2019.0148
68. Kanemitsu M, Nakasa T, Shirakawa Y, Ishikawa M, Miyaki S, Adachi N. Role of vasoactive intestinal peptide in the progression of osteoarthritis through bone sclerosis and angiogenesis in subchondral bone. *J Orthop Sci.* (2020) doi: 10.1016/j.jos.2019.11.010. [Epub ahead of print].
 69. Tam J, Ofek O, Fride E, Ledent C, Gabet Y, Müller R, et al. Involvement of neuronal cannabinoid receptor CB1 in regulation of bone mass and bone remodeling. *Mol Pharmacol.* (2006) 70:786–92. doi: 10.1124/mol.106.026435
 70. Idris AI, van 't Hof RJ, Greig IR, Ridge SA, Baker D, Ross RA, et al. Regulation of bone mass, bone loss and osteoclast activity by cannabinoid receptors. *Nat Med.* (2005) 11:774–9. doi: 10.1038/nm1255
 71. Zhu Y, Ma Y, Eleftheriou F. Cortical bone is an extraneuronal site of norepinephrine uptake in adult mice. *Bone Rep.* (2018) 9:188–98. doi: 10.1016/j.bonr.2018.11.002
 72. Sisask G, Silfverswärd C-J, Bjurholm A, Nilsson O. Ontogeny of sensory and autonomic nerves in the developing mouse skeleton. *Auton Neurosci.* (2013) 177:237–43. doi: 10.1016/j.autneu.2013.05.005
 73. Bidegain M, Roos BA, Hill EL, Howard GA, Balkan W. Calcitonin gene-related peptide (CGRP) in the developing mouse limb. *Endocr Res.* (1995) 21:743–55. doi: 10.1080/07435809509030488
 74. Chartier SR, Mitchell SAT, Majuta LA, Mantyh PW. The changing sensory and sympathetic innervation of the young, adult and aging mouse femur. *Neuroscience.* (2018) 387:178–90. doi: 10.1016/j.neuroscience.2018.01.047
 75. Tomlinson RE, Li Z, Li Z, Minichiello L, Riddle RC, Venkatesan A, et al. NGF-TrkA signaling in sensory nerves is required for skeletal adaptation to mechanical loads in mice. *Proc Natl Acad Sci USA.* (2017) 114:E3632–41. doi: 10.1073/pnas.1701054114
 76. Sisask G, Bjurholm A, Ahmed M, Kreicbergs A. Ontogeny of sensory nerves in the developing skeleton. *Anat Rec.* (1995) 243:234–40. doi: 10.1002/ar.1092430210
 77. Garcés GL, Santandreu ME. Longitudinal bone growth after sciatic denervation in rats. *J Bone Joint Surg Br.* (1988) 70:315–8.
 78. Zeng QQ, Jee WS, Bigornia AE, King JG, D'Souza SM, Li XJ, et al. Time responses of cancellous and cortical bones to sciatic neurectomy in growing female rats. *Bone.* (1996) 19:13–21. doi: 10.1016/8756-3282(96)00112-3
 79. Fukuda T, Takeda S, Xu R, Ochi H, Sunamura S, Sato T, et al. Sema3A regulates bone-mass accrual through sensory innervations. *Nature.* (2013) 497:490–3. doi: 10.1038/nature12115
 80. Rossi F, Bellini G, Torella M, Tortora C, Manzo I, Giordano C, et al. The genetic ablation or pharmacological inhibition of TRPV1 signalling is beneficial for the restoration of quiescent osteoclast activity in ovariectomized mice. *Br J Pharmacol.* (2014) 171:2621–30. doi: 10.1111/bph.12542
 81. Heffner MA, Anderson MJ, Yeh GC, Genetos DC, Christiansen BA. Altered bone development in a mouse model of peripheral sensory nerve inactivation. *J Musculoskelet Neuronal Interact.* (2014) 14:1–9.
 82. Nagy JI, Iversen LL, Goedert M, Chapman D, Hunt SP. Dose-dependent effects of capsaicin on primary sensory neurons in the neonatal rat. *J Neurosci.* (1983) 3:399–406. doi: 10.1523/JNEUROSCI.03-02-00399.1983
 83. Scadding JW. The permanent anatomical effects of neonatal capsaicin on somatosensory nerves. *J Anat.* (1980) 131:471–82.
 84. García-Castellano JM, Díaz-Herrera P, Morcuende JA. Is bone a target-tissue for the nervous system? New advances on the understanding of their interactions. *Iowa Orthop J.* (2000) 20:49–58.
 85. Hill EL, Turner R, Elde R. Effects of neonatal sympathectomy and capsaicin treatment on bone remodeling in rats. *Neuroscience.* (1991) 44:747–55. doi: 10.1016/0306-4522(91)90094-5
 86. Hert J, Sklenská A, Lisková M. Reaction of bone to mechanical stimuli. 5. Effect of intermittent stress on the rabbit tibia after resection of the peripheral nerves. *Folia Morphol.* (1971) 19:378–87.
 87. Sample SJ, Behan M, Smith L, Oldenhoff WE, Markel MD, Kalschauer VL, et al. Functional adaptation to loading of a single bone is neuronally regulated and involves multiple bones. *J Bone Miner Res.* (2008) 23:1372–81. doi: 10.1359/jbmr.080407
 88. Wu Q, Sample SJ, Baker TA, Thomas CF, Behan M, Muir P. Mechanical loading of a long bone induces plasticity in sensory input to the central nervous system. *Neurosci Lett.* (2009) 463:254–57. doi: 10.1016/j.neulet.2009.07.078
 89. Sample SJ, Collins RJ, Wilson AP, Racette MA, Behan M, Markel MD, et al. Systemic effects of ulna loading in male rats during functional adaptation. *J Bone Miner Res.* (2010) 25:2016–28. doi: 10.1002/jbmr.101
 90. De Souza RL, Pitsillides AA, Lanyon LE, Skerry TM, Chenu C. Sympathetic nervous system does not mediate the load-induced cortical new bone formation. *J Bone Miner Res.* (2005) 20:2159–68. doi: 10.1359/JBMR.050812
 91. Heffner MA, Genetos DC, Christiansen BA. Bone adaptation to mechanical loading in a mouse model of reduced peripheral sensory nerve function. *PLoS ONE.* (2017) 12:e0187354. doi: 10.1371/journal.pone.0187354
 92. Marenzana M, De Souza RL, Chenu C. Blockade of beta-adrenergic signaling does not influence the bone mechano-adaptive response in mice. *Bone.* (2007) 41:206–15. doi: 10.1016/j.bone.2007.04.184
 93. Bonnet N, Beaupied H, Vico L, Dolleans E, Laroche N, Courteix D, et al. Combined effects of exercise and propranolol on bone tissue in ovariectomized rats. *J Bone Miner Res.* (2007) 22:578–88. doi: 10.1359/jbmr.070117
 94. Bonnet N, Laroche N, Beaupied H, Vico L, Dolleans E, Benhamou CL, et al. Doping dose of salbutamol and exercise training: impact on the skeleton of ovariectomized rats. *J Appl Physiol.* (2007) 103:524–33. doi: 10.1152/japplphysiol.01319.2006
 95. Pierroz DD, Bonnet N, Bianchi EN, Boussein ML, Baldock PA, Rizzoli R, et al. Deletion of β -adrenergic receptor 1, 2, or both leads to different bone phenotypes and response to mechanical stimulation. *J Bone Miner Res.* (2012) 27:1252–62. doi: 10.1002/jbmr.1594
 96. Jones KB, Mollano AV, Morcuende JA, Cooper RR, Saltzman CL. Bone and brain: a review of neural, hormonal, and musculoskeletal connections. *Iowa Orthop J.* (2004) 24:123–32.
 97. Bickel CS, Slade JM, Haddad F, Adams GR, Dudley GA. Acute molecular responses of skeletal muscle to resistance exercise in able-bodied and spinal cord-injured subjects. *J Appl Physiol.* (2003) 94:2255–62. doi: 10.1152/japplphysiol.00014.2003
 98. Kingery WS, Offley SC, Guo T-Z, Davies MF, Clark JD, Jacobs CR. A substance P receptor (NK1) antagonist enhances the widespread osteoporotic effects of sciatic nerve section. *Bone.* (2003) 33:927–36. doi: 10.1016/j.bone.2003.07.003
 99. Zhang Z-K, Guo X, Lao J, Qin Y-X. Effect of capsaicin-sensitive sensory neurons on bone architecture and mechanical properties in the rat hindlimb suspension model. *J Orthop Translat.* (2017) 10:12–7. doi: 10.1016/j.jot.2017.03.001
 100. Kondo H, Nifuji A, Takeda S, Ezura Y, Rittling SR, Denhardt DT, et al. Unloading induces osteoblastic cell suppression and osteoclastic cell activation to lead to bone loss via sympathetic nervous system. *J Biol Chem.* (2005) 280:30192–200. doi: 10.1074/jbc.M504179200
 101. Baek K, Bloomfield SA. Beta-adrenergic blockade and leptin replacement effectively mitigate disuse bone loss. *J Bone Miner Res.* (2009) 24:792–9. doi: 10.1359/jbmr.081241
 102. Swift JM, Hogan HA, Bloomfield SA. β -1 adrenergic agonist mitigates unloading-induced bone loss by maintaining formation. *Med Sci Sports Exerc.* (2013) 45:1665–73. doi: 10.1249/MSS.0b013e31828d39bc
 103. Swift JM, Swift SN, Allen MR, Bloomfield SA. Beta-1 adrenergic agonist treatment mitigates negative changes in cancellous bone microarchitecture and inhibits osteocyte apoptosis during disuse. *PLoS ONE.* (2014) 9:e106904. doi: 10.1371/journal.pone.0106904
 104. Mason DJ, Suva LJ, Genever PG, Patton AJ, Steuckle S, Hillam RA, et al. Mechanically regulated expression of a neural glutamate transporter in bone: a role for excitatory amino acids as osteotropic agents? *Bone.* (1997) 20:199–205. doi: 10.1016/s8756-3282(96)00386-9
 105. Guo T-Z, Wei T, Li W-W, Li X-Q, Clark JD, Kingery WS. Immobilization contributes to exaggerated neuropeptide signaling, inflammatory changes, and nociceptive sensitization after fracture in rats. *J Pain.* (2014) 15:1033–45. doi: 10.1016/j.jpain.2014.07.004
 106. Hart ECJ, Charkoudian N. Sympathetic neural regulation of blood pressure: influences of sex and aging. *Physiology.* (2014) 29:8–15. doi: 10.1152/physiol.00031.2013
 107. Jimenez-Andrade JM, Mantyh WG, Bloom AP, Freeman KT, Ghilardi JR, Kuskowski MA, et al. The effect of aging on the density of the sensory nerve

- fiber innervation of bone and acute skeletal pain. *Neurobiol Aging*. (2012) 33:921–32. doi: 10.1016/j.neurobiolaging.2010.08.008
108. Moore SR, Milz S, Knothe Tate ML. Periosteal thickness and cellularity in mid-diaphyseal cross-sections from human femora and tibiae of aged donors. *J Anat.* (2014) 224:142–9. doi: 10.1111/joa.12133
 109. Maryanovich M, Zahalka AH, Pierce H, Pinho S, Nakahara F, Asada N, et al. Adrenergic nerve degeneration in bone marrow drives aging of the hematopoietic stem cell niche. *Nat Med.* (2018) 24:782–91. doi: 10.1038/s41591-018-0030-x
 110. Sophocleous A, Marino S, Kabir D, Ralston SH, Idris AI. Combined deficiency of the Cnr1 and Cnr2 receptors protects against age-related bone loss by osteoclast inhibition. *Aging Cell.* (2017) 16:1051–61. doi: 10.1111/ace.12638
 111. Malfait AM, Gallily R, Sumariwalla PF, Malik AS, Andreaskos E, Mechoulam R, et al. The nonpsychoactive cannabis constituent cannabidiol is an oral anti-arthritis therapeutic in murine collagen-induced arthritis. *Proc Natl Acad Sci USA.* (2000) 97:9561–6. doi: 10.1073/pnas.160105897
 112. Sumariwalla PF, Gallily R, Tchilibon S, Fride E, Mechoulam R, Feldmann M. A novel synthetic, nonpsychoactive cannabinoid acid (HU-320) with antiinflammatory properties in murine collagen-induced arthritis. *Arthritis Rheum.* (2004) 50:985–98. doi: 10.1002/art.20050
 113. Sophocleous A, Börjesson AE, Salter DM, Ralston SH. The type 2 cannabinoid receptor regulates susceptibility to osteoarthritis in mice. *Osteoarthritis Cartil.* (2015) 23:1586–94. doi: 10.1016/j.joca.2015.04.020
 114. Su Y-W, Zhou X-F, Foster BK, Grills BL, Xu J, Xian CJ. Roles of neurotrophins in skeletal tissue formation and healing. *J Cell Physiol.* (2018) 233:2133–45. doi: 10.1002/jcp.25936
 115. Serrano T, Lorigados LC, Armenteros S. Nerve growth factor levels in normal human sera. *Neuroreport.* (1996) 8:179–81. doi: 10.1097/00001756-199612200-00036
 116. Dicou E, Vermersch P, Penisson-Besnier I, Dubas F, Nerrière V. Anti-NGF autoantibodies and NGF in sera of Alzheimer patients and in normal subjects in relation to age. *Autoimmunity.* (1997) 26:189–94. doi: 10.3109/08916939708994740
 117. Lang UE, Gallinat J, Danker-Hopfe H, Bajbouj M, Hellweg R. Nerve growth factor serum concentrations in healthy human volunteers: physiological variance and stability. *Neurosci Lett.* (2003) 344:13–6. doi: 10.1016/s0304-3940(03)00403-8
 118. Ziegenhorn AA, Schulte-Herbrüggen O, Danker-Hopfe H, Malbranc M, Hartung H-D, Anders D, et al. Serum neurotrophins—a study on the time course and influencing factors in a large old age sample. *Neurobiol Aging.* (2007) 28:1436–45. doi: 10.1016/j.neurobiolaging.2006.06.011
 119. Chermide-Scabbo CJ, Harris TL, Brodt MD, Braenne I, Zhang B, Farber CR, et al. Old mice have less transcriptional activation but similar periosteal cell proliferation compared to young-adult mice in response to *in vivo* mechanical loading. *J Bone Miner Res.* (2020). doi: 10.1002/jbmr.4031
 120. Hill RA, van den Buuse M. Sex-dependent and region-specific changes in TrkB signaling in BDNF heterozygous mice. *Brain Res.* (2011) 1384:51–60. doi: 10.1016/j.brainres.2011.01.060
 121. Chavez-Valdez R, Martin LJ, Razdan S, Gauda EB, Northington FJ. Sexual dimorphism in BDNF signaling after neonatal hypoxia-ischemia and treatment with necrostatin-1. *Neuroscience.* (2014) 260:106–19. doi: 10.1016/j.neuroscience.2013.12.023
 122. Brague JC, Swann JM. Sexual dimorphic expression of TrkB, TrkB-T1, and BDNF in the medial preoptic area of the Syrian hamster. *Brain Res.* (2017) 1669:122–5. doi: 10.1016/j.brainres.2017.06.008
 123. Herber CB, Krause WC, Wang L, Bayrer JR, Li A, Schmitz M, et al. Estrogen signaling in arcuate Kiss1 neurons suppresses a sex-dependent female circuit promoting dense strong bones. *Nat Commun.* (2019) 10:163. doi: 10.1038/s41467-018-08046-4

Conflict of Interest: The authors declare the absence of any commercial or financial relationships that could be construed as a potential conflict of interest.

Copyright © 2020 Tomlinson, Christiansen, Giannone and Genetos. This is an open-access article distributed under the terms of the Creative Commons Attribution License (CC BY). The use, distribution or reproduction in other forums is permitted, provided the original author(s) and the copyright owner(s) are credited and that the original publication in this journal is cited, in accordance with accepted academic practice. No use, distribution or reproduction is permitted which does not comply with these terms.



Human Amniotic Mesenchymal Stem Cells Promote Endogenous Bone Regeneration

Jin Li^{1†}, Zhixuan Zhou^{1,2†}, Jin Wen³, Fei Jiang^{1,2*} and Yang Xia^{1,4*}

¹ Jiangsu Key Laboratory of Oral Diseases, Nanjing Medical University, Nanjing, China, ² Department of General Dentistry, Affiliated Hospital of Stomatology, Nanjing Medical University, Nanjing, China, ³ Department of Prosthodontics, School of Medicine, College of Stomatology, Shanghai Ninth People's Hospital, Shanghai Jiao Tong University, Shanghai, China, ⁴ Department of Prosthodontics, Affiliated Hospital of Stomatology, Nanjing Medical University, Nanjing, China

OPEN ACCESS

Edited by:

Lilian Irene Plotkin,
Indiana University Bloomington,
United States

Reviewed by:

Johannes Jung,
Sanofi, Germany
Paulus Wohlfart,
Sanofi, Germany

*Correspondence:

Fei Jiang
nykqjf@njmu.edu.cn
Yang Xia
xiayang@njmu.edu.cn

[†]These authors have contributed
equally to this work

Specialty section:

This article was submitted to
Bone Research,
a section of the journal
Frontiers in Endocrinology

Received: 17 March 2020

Accepted: 27 August 2020

Published: 02 October 2020

Citation:

Li J, Zhou Z, Wen J, Jiang F and Xia Y
(2020) Human Amniotic Mesenchymal
Stem Cells Promote Endogenous
Bone Regeneration.
Front. Endocrinol. 11:543623.
doi: 10.3389/fendo.2020.543623

Bone regeneration has become a research hotspot and therapeutic target in the field of bone and joint medicine. Stem cell-based therapy aims to promote endogenous regeneration and improves therapeutic effects and side-effects of traditional reconstruction of significant bone defects and disorders. Human amniotic mesenchymal stem cells (hAMSCs) are seed cells with superior paracrine functions on immune-regulation, anti-inflammation, and vascularized tissue regeneration. The present review summarized the source and characteristics of hAMSCs and analyzed their roles in tissue regeneration. Next, the therapeutic effects and mechanisms of hAMSCs in promoting bone regeneration of joint diseases and bone defects. Finally, the clinical application of hAMSCs from current clinical trials was analyzed. Although more studies are needed to confirm that hAMSC-based therapy to treat bone diseases, the clinical application prospect of the approach is worth investigating.

Keywords: hAMSCs, paracrine functions, endogenous bone regeneration, arthritis, bone defects, clinical trials

INTRODUCTION

Large bone defects and disorders, either congenital or acquired, severely affect the patients' appearance and function (1). Moreover, the incidence of these bone diseases is high and has been on the rise in the past decade. In terms of bone defects, approximately more than 350 million people suffer from fractures, about 46 million people have head injuries, and 20 million people are subject to spinal injuries. Meanwhile, more than 300 million people have been diagnosed with osteoarthritis while about 20 million people have got rheumatoid arthritis around the world. Periodontal disease, which tends to cause severe alveolar bone loss and tooth loss, also has a high prevalence rate of about 800 million (2). Currently, the reconstruction of the bone defects mainly depends on autologous tissue transplantation due to various factors, such as biocompatibility and histocompatibility (3). However, this strategy has limited applications due to a shortage of harvest sites, incomplete integration into the defects, and risk of disease transfer (4). In addition to various defects, bone disorders also include joint diseases associated with an autoimmune disorder, such as rheumatoid arthritis (RA) (5), osteoarthritis (OA) (6), and ankylosing spondylitis (AS) (7). Typically, these joint diseases are treated by drugs (for example, glucocorticoid, immunosuppressive agents, non-steroidal anti-inflammatory drugs, and disease modifying antirheumatic drug) to reduce the symptoms and improve the joint function; however, therapeutic interventions are essential in the advanced stage characterized by loss of articular cartilage, subchondral sclerosis, osteophyte

formation, and joint capsule thickening (8). Nowadays, tissue engineering is gaining increasing attention and is expected to resolve these clinical issues.

Different types of scaffold, bioactive factors, and seed cells are the three major elements of tissue engineering. Thus, finding an ideal scaffold to replace the autologous bone translation in the treatment of bone disorder is under intensive research. Nowadays, the scaffold matrix used for bone tissue engineering includes inorganic material, polymers, and their composites (9). In addition, bioactive factors, such as bone morphogenetic protein-2 (BMP-2), fibroblast growth factor-2 (FGF-2), vascular endothelial growth factor (VEGF), and epidermal growth factor (EGF), also play a vital role in bone rebuilding (10). Among those growth factors, BMP-2 and FGF-2 have been utilized to promote bone regeneration and angiogenesis in clinical practice (11, 12). Currently, stem cell-based tissue regeneration has some curative effects (13), but the effect of seed cells in repairing the bone disorders is yet controversial.

Endogenous regeneration, proposed in recent years, focuses on the stimulation and regulation of endogenous factors to achieve *in situ* tissue regeneration by applying bioactive factors locally (14). Stem cells possess robust biological potential with respect to self-renewal, multidirectional differentiation, and paracrine functions (15, 16). These might act as bioactive factors to activate the endogenous regeneration by local or systematic applications (14, 17). The homeostasis of tissues and organs relies on the coordination and regulation of the nervous, endocrine, and immune systems (18). The endocrine system is a complex network of hormone-producing cells and tissues, which secrete a variety of hormones to act on distant and/or adjacent target cells through endocrine, paracrine, autocrine, or intracrine mechanisms to exert biological activities (19). In addition to enteroendocrine cells, other tissues and cells, such as retinal ganglion cells (RGCs) (20), bone (21), and muscle (22), have paracrine and endocrine functions to maintain homeostasis. Growth hormone (GH) can be expressed in RGCs, and retinal GH has a paracrine role in ocular development and vision (20). It has been widely accepted that stem cells could secrete a variety of bioactive factors which regulate immune state of the body and local microenvironment of tissue regeneration (23). These mechanisms of stem cell-based therapy are to some extent similar to those of some hormones, such as GH. Based on these similarities, stem cell-based therapy might exert a positive effect on promoting endogenous bone regeneration.

Stem cells are divided into embryonic stem cells and adult stem cells (16). The embryonic stem cells for stem cell therapy shows high tumorigenicity and ethical problems in the application process (24). Adult stem cells, including mesenchymal stem cells (MSCs), are undifferentiated cells found in various tissues and organs (25). Nowadays, researchers can isolate MSCs from bone marrow (bone-marrow mesenchymal stem cells, BMSCs) (26), fat (adipose-derived stem cells, AdSCs) (27), peripheral blood (peripheral blood-derived mesenchymal stem cells, PMSCs) (28), umbilical cord blood (umbilical cord blood-derived mesenchymal stem cells, CB-MSCs) (29), and other tissues (30–32) for tissue engineering, immune-regulation, and anti-inflammation. However, it is also unknown which

source of stem cells is better for promoting tissue regeneration after transplantation.

Currently, we are focusing on promoting bone regeneration in the oral and maxillofacial regions using human amniotic mesenchymal stem cells (hAMSCs). In this study, we reviewed the source, characteristics, and roles of hAMSCs in bone regeneration, not only in the reconstruction of bone defects but also in the treatment of arthritis. Thus, hAMSCs might be used as an innovative treatment option to promote endogenous bone regeneration.

SOURCE AND CHARACTERISTICS OF HAMSCS

MSCs are specialized cells with multi-differentiation potentials, which can be activated to differentiate into tissue cells under specific inducing conditions (33, 34). Previous studies have demonstrated that MSCs have abilities of regeneration and immunoregulation (35). The hAMSCs, isolated from the amniotic membrane (AM) of the human term placenta that plays a key role in maintaining maternal-neonatal tolerance, not only share phenotypes similar to typical MSCs, including fibroblast-like morphology, specific surface molecules, and multi-differentiation potential but also have superior immunomodulatory (36–39) and paracrine properties (40, 41). Compared to hAMSCs, most MSCs have inevitable disadvantages on clinical use, including invasive access procedure, host immune response after transplantation, age-related heterogeneity in the quality of MSCs, and extremely low acquisition rate of MSCs (33).

The AM is the innermost layer of the placenta consisting of two sets of cells; one is the amnion epithelial cells that are in direct contact with the amniotic fluid, and the other is the amnion MSCs dispersed in the matrix (42, 43). Since AM is an avascular structure and its epithelial layer can be easily removed by Dispase II, the hAMSCs can be obtained without contamination of endothelial cells and hematopoietic cells (42, 44). Each gram of wet amnion tissue can provide $1.7 \pm 0.3 \times 10^6$ hAMSCs (45), which are positive for CD44 and CD90 (46, 47). Moreover, the placental tissue becomes a medical waste after childbirth, and hAMSCs can be harvested non-invasively and without ethical controversy (48). In addition, parturients are usually young women, and hence, age-related heterogeneity of hAMSCs might be relatively better than that of stem cells from other sources. The hAMSCs lack the expression of human major histocompatibility complex (MHC) antigens (human leukocyte antigens, HLA), including HLA class I antigens (HLA-DP, HLA-DA, HLA-DR) and HLA class II antigens (HLA-A, HLA-B, HLA-C), showing low immunogenicity (49, 50), while they also exhibit low tumorigenicity due to lack of expression of telomerase (48, 51, 52). Low immunogenicity and low tumorigenicity of hAMSCs render them conducive for allotransplantation to promote tissue regeneration. Also, their paracrine properties have multiple regulatory functions (40). Furthermore, several bioactive factors could be produced by hAMSCs, including immunomodulatory factors that are crucial for the resolution of inflammation (44, 53).

TABLE 1 | The mechanisms of hAMSCs in regulating joint diseases.

References	Disease Model	Method	Conclusion
Shu et al. (55)	RA	Intraperitoneal injection	hAMSCs inhibited the production of proinflammatory cytokines and the response of T-cell, and restored CD4+/CD8+ T cell ratio in CIA rats.
Parolini et al. (56)	RA	Subcutaneous injection	hAMSCs decreased the production of inflammatory cytokines, stimulated the generation of human CD4+CD25+FoxP3+ Treg cells, and suppressed the antigen-specific Th1/Th17 activation in CIA mice.
Huss et al. (57)	OA	Culture <i>in vitro</i>	NK cells were a principal infiltrating immune cells in synovial tissue of patients with osteoarthritis.
Pianta et al. (58)	Inflammation	Co-culture	hAMSC-CM regulated T-cell polarization toward Th1, Th2, Th17, and T-regulatory (Treg) subsets.
Topoluk et al. (59)	OA	Co-culture	hAMSCs were better than AdSCs in shifting OA synovial macrophage M1:M2 ratio.
Cargnoni et al. (60)	Lung fibrosis	Intrathoracic injection	hAMSC-CM reduced the levels of pro-inflammatory and pro-fibrotic cytokines, and reduced lung macrophage levels.
Borem et al. (61)	IVDD	Co-culture	hAMSCs produced more anti-inflammatory cytokines than AdSCs under identical inflammatory conditions.
Miceli et al. (62)	Inflammation	Culture <i>in vitro</i>	hAMSCs in 3D culture system produced more angiogenic and immunosuppressive factors than in 2D cultures.
Banerjee et al. (63)	Inflammation	Culture <i>in vitro</i>	hAMSCs changed mitochondrial function and increased IL-6, and maintained the low levels of ROS at 20% oxygen.

RA, rheumatoid arthritis; hAMSCs, human amniotic mesenchymal stem cells; CIA, collagen-induced arthritis; OA, osteoarthritis; hAMSC-CM, hAMSCs conditioned medium; AdSCs, human adipose stem cells; IVDD, intervertebral disc degeneration; 3D, three-dimensional; 2D, two-dimensional; ROS, reactive oxygen species.

and growth and angiogenic factors that are critical for tissue remodeling (41). These exogenous molecules have been shown to be important in inducing endogenous regeneration.

EFFICACY OF HAMSCS IN JOINT DISEASES

Arthritis is a characteristic of rheumatic diseases, which are chronic, intractable, and musculoskeletal system diseases, such as RA, OA, AS, and juvenile idiopathic arthritis (JIA) (54). Although the pathological characteristics of these joint disorders are different, the joint symptoms are associated with abnormal autoimmune function, inflammatory cell infiltration, and joint structural lesions (5). Stem cells, including hAMSCs, have been introduced to arthritis models, such as rat, to improve the treatment by inhibiting inflammation, regulating the status of autoimmunity, and promoting tissue regeneration (Table 1) (55, 64, 65).

RA is a chronic, autoimmune, inflammatory joint disease characterized by hyperplasia of the synovial membrane and infiltration of immune and inflammatory cells. The synovial cell

fibrosis, excessive production of inflammatory cytokines, and osteoclast appearance led to joint destruction and disability (5). The immunomodulatory and anti-inflammatory properties of hAMSCs indicated the therapeutic potential for the treatment of RA. In the classic rat arthritis model for human RA, hAMSCs significantly ameliorated the severity of arthritis and decreased the histopathological changes due to dramatic inhibition of the production of proinflammatory cytokines, such as interferon- γ (IFN- γ) and tumor necrosis factor- α (TNF- α) (55). For a T cell-mediated disease, such as RA, the therapeutic effects of hAMSCs are crucial because they could remarkably restore the CD4+/CD8+ T-cell ratio and inhibit the response of T-cells (55). In addition, hAMSCs suppressed the antigen-specific Th1/Th17 activation and stimulated the generation of CD4+CD25+FoxP3+ Treg cells (56). In mice with collagen-induced arthritis (CIA), systemic infusion of hAMSCs markedly reduces Th1-driven autoimmunity and inflammation, as shown by decreased production of TNF- α , IFN- γ , and some interleukins (IL-2 and IL-17) and increased production of IL-10 and activation of cyclooxygenase 1/2 (COX1/2) (56).

OA is another chronic joint disease with an incidence as high as 40% (66). It is a degenerative disease characterized by progressive cartilage degradation, subchondral bone remodeling, osteophyte formation, and synovitis (67). Synovial NK cells and macrophages secrete abnormally large amounts of perforins, granzymes, and pro-inflammatory cytokines (TNF- α , IL-1 β) to induce and aggravate the synovial inflammation and bone/cartilage resorption (57), while activation of CD4+Th1 cells contributes to the development of inflammation (68). The hAMSCs might be beneficial for OA as they inhibit the proliferation of T-cells *in vitro* (58), polarize M2 macrophages in the condition with the hallmarks of RA *in vitro* (59), and promote bone/cartilage regeneration in rabbits (69, 70). The conditioned medium of hAMSCs (hAMSC-CM) was reported to remedy tissue fibrosis by lowering the levels of T-cells and macrophages, leading to a decline in pro-inflammatory cytokines (60). When hAMSCs were introduced to the OA model established by coculturing the OA patients' cartilage and synovium, the M1:M2 percentage ratio of synovial macrophages was decreased significantly; also, the concentrations of IL-1 β and matrix metalloproteinase-13 (MMP-13) was declined, and macrophage-mediated cartilage destruction was effectively abrogated (59).

In addition, hAMSCs not only secreted active factors with therapeutic effects routinely but also produced abundant cytokines in specific environments. Under identical inflammatory conditions, hAMSCs produce more anti-inflammatory cytokines than AdSCs, such as IL-10 (61). Under three-dimensional (3D) culture conditions, hAMSCs spheroids could secrete considerable amounts of angiogenic and immunosuppressive factors while remaining viable and multipotent (62). The production of some cytokines by hAMSCs vary under different conditions of different oxygen tension. Consequent to exposure to 20% oxygen culture condition, hAMSCs secrete abundant IL-6 as a response to changes in the mitochondrial function, but the content of intracellular reactive oxygen species (ROS) remained unaltered (63). These properties

of hAMSCs rendered the stem cell-based therapy applicable and also provided valuable guidance for bone regeneration.

EFFICACY OF HAMSCS IN BONE DEFECTS

The hAMSCs, as a kind of stem cells, can be induced to osteogenic differentiation to form refracted crystal-like nodules which could be indicated by alkaline phosphatase staining or/and alizarin red S staining (71–73). The expression of osteogenesis-related genes and proteins, such as alkaline phosphatase (ALP), runt-related transcription factor 2 (Runx2), osteopontin (OPN), and osteocalcin (OCN), was significantly enhanced in osteo-induced hAMSCs (74–76); also, their osteogenic differentiation capacity is superior to other MSCs derived from chorionic membrane and decidua (77, 78). However, the comparison of the osteogenic capacity of hAMSCs and BMSCs revealed that BMSCs are more likely to differentiate into osteoblasts *in vitro* and seem to be appropriate for bone regeneration (79). Nevertheless, the capacity of hAMSCs might not be inferior to that of BMSCs in improving bone regeneration *in vivo*. Several studies have reported that transplanted MSCs might play therapeutic roles by paracrine signaling rather than becoming target tissue cells directly (80–82). In recent years, several studies have focused on hAMSCs promoting tissue regeneration, based on their functions of anti-inflammation, pro-angiogenesis, and chemotaxis (Table 2) (38, 83, 96). To the best of our knowledge, hAMSCs secrete more cytokines than BMSCs, including interleukins (IL-6 and IL-8), C-X-C motif chemokine ligand-1/5 (CXCL1 and CXCL5), Angiogenin (ANG), hepatocyte growth factor (HGF), and fibroblast growth factor-7 (FGF-7) (83). These paracrine properties of hAMSCs make them suitable for the restoration of bone defects (40, 83).

Fracture healing is a complex, well-orchestrated, regenerative process that is coordinated by a variety of cell types, including inflammatory cells, vascular endothelial cells, MSCs, and fibroblasts (97). In the various stages of the bone healing process, inflammation and angiogenesis precede osteogenesis, thereby indicating that controlling inflammation and promoting angiogenesis in an early stage might speed up the subsequent bone formation and ultimately bone remodeling (97). Therefore, we proposed to introduce hAMSCs to bone defects' microenvironment and stimulate and accelerate the endogenous vascularized bone regeneration. Several studies have shown that hAMSCs enhance the osteogenic differentiation of AdSCs, BMSCs, and promote the tube-formation of human umbilical vein endothelial cells (HUVECs) (84–89). When hAMSCs are co-cultured with BMSCs in a transwell system, ALP activity of BMSCs and the expression of osteogenic markers, including OCN and Runx2, were upregulated (90). Conversely, in the co-culture, hAMSCs reverse the inhibition of oxidative stress-induced osteogenic differentiation of caused by hydrogen peroxide, which in turn, inhibits the inflammatory response *in vivo* (91). When hAMSCs are co-cultured with HUVECs, high levels of Collagen-1 (COL1), ANG, and VEGF were detected in the co-culture medium, and capillary-like tube structures were observed in HUVEC tube-formation assay (92). Interestingly,

a correlation was established between the high expression of lncRNA H19 and the pro-angiogenic functions of hAMSCs (93).

Based on the *in vitro* data, the researchers applied hAMSCs to animal bone defect models. Ranzoni et al. injected hAMSCs intraperitoneally into mice that suffered from osteogenesis imperfecta (OI). The transplanted mice had improved bone structural quality, high mineral density, and better mineralization, while the genes related to osteogenesis were upregulated and those associated with inflammation, TGF- β , and osteoclast differentiation were downregulated (94). The β -tricalcium phosphate (TCP) scaffolds containing xenograft hAMSCs have been reported to improve regeneration of Wistar rats' skull defects. The xenograft cells did not cause obvious immune response in the transplanted rats (95). In our recent studies, we comprehensively analyzed the survival of hAMSCs after transplantation in nude mice and the specific mechanism of hAMSCs in promoting bone tissue regeneration. It had been confirmed that hAMSCs could be survival in bone defects for at least 2 weeks after transplantation. Although hAMSCs survived *in vivo*, they did not seem to transform into osteoblasts. In specimens from early bone defect healing, hAMSCs polarized macrophages to M2 that could secrete pro-angiogenic and osteogenic cytokines, such as BMP-2 and VEGF (83). Moreover, we also found that hAMSCs promote extracellular matrix remodeling (98). Combined with these functions, we believed hAMSCs could start endogenous vascularized bone regeneration. And in terms of the ultimate osteogenic effect, our findings showed that hAMSCs accelerated new bone formation not only in bone defects but promoted rapid osseointegration of dental implants (69, 83).

CLINICAL TRIALS

Stem cell therapies exert their effects on a wide range of diseases and injuries, including immune disorders (99), various neural disorders or injuries (100), myocardial injury (101), pulmonary diseases (102), diabetes (103), cancer treatments (104), and bone/cartilage degenerative disorders or injuries (105). Several types of stem cells have been subjected to clinical trials (106). Stem cells derived from the human placenta have been reported to be in clinical trials for a variety of therapeutic applications (107). In a single-center, non-randomized, intravenous dose-escalation phase Ib trial, patients with idiopathic pulmonary fibrosis received intravenous administration of placental MSCs from unrelated donors. Previous data demonstrated that placental MSC therapy is feasible and has a satisfactory short-term safety profile in idiopathic pulmonary fibrosis (108). Clinical trials using placental MSCs to treat OA, Crohn's disease, and multiple sclerosis (MS) have shown that the cells were well-tolerated, and cell therapy was dose-related (109–111). Amnion is a part of the placenta that has been used in clinical trials to treat skin and corneal burns (112, 113). These clinical trials suggested that the amniotic membrane accelerates recovery via inhibiting inflammation and releasing growth factors. These therapeutic effects could also be found in hAMSC-CM. In the subsequent clinical trials using this conditioned media,

TABLE 2 | The role of hAMSCs in bone regeneration.

References	Disease model	Method	Conclusion
Yin et al. (69)	MSFE	Intravenous injection	hAMSCs accelerated mineralized deposition rates and enhanced bone regeneration after MSFE.
Topoluk et al. (71)	Bone defects	Culture <i>in vitro</i>	hAMSCs had a greater differentiation potential toward bone and cartilage compared with AdSCs.
Li et al. (72)	Bone defects	Implantation with PLGA	The BMP9-induced osteogenic differentiation and angiogenesis of hAMSCs could be inhibited by Schnurri-3.
Li et al. (73)	Bone defects	Implantation with scaffolds	The osteogenic differentiation and angiogenesis of hAMSCs could be enhanced by 3D silk fibroin scaffolds.
Leyva-Leyva et al. (75)	Bone defects	Culture <i>in vitro</i>	Different hAMSCs subpopulations had dissimilar osteoblastic differentiation potential, and CD105 ⁺ cells were better than CD105 ⁺ cells.
Fan et al. (76)	Bone defects	culture <i>in vitro</i>	<1.0 mM sodium butyrate enhanced the expression of osteogenesis-related genes and proteins of hAMSCs.
Shen et al. (77)	Bone defects	Culture <i>in vitro</i>	hAMSCs and UC-MSC had a higher osteogenic differentiation potential than the MSCs from chorionic membrane and decidua.
Ma et al. (78)	Bone defects	Culture <i>in vitro</i>	hAMSCs had a greater osteogenic differentiation than the MSCs from umbilical cord and chorionic plate.
Liu et al. (80)	Osteopenia	Hypodermic implantation	MSCs secreted exosomes to regulate the miR-29b/Dnmt1/Notch epigenetic cascade.
Jiang et al. (83)	Bone defects	Subcutaneous injection	hAMSCs stimulated endogenous regeneration of bone via paracrine function.
Zhang et al. (84)	Osteoporosis	Co-culture	hAMSCs enhanced the cell proliferation, antioxidant properties, osteogenic, and angiogenic differentiation of BMSCs and HUVECs.
Wang et al. (85)	Periodontitis	Culture <i>in vitro</i>	hAMSCs promoted the osteoblastic differentiation of BMSCs and influenced p38 MAPK signaling to reducing bone loss.
Wang et al. (86)	Bone defects	Co-culture	hAMSCs regulated the differentiation processes in BMSCs by influencing the differentiation antagonizing non-protein coding RNA.
Zhang et al. (87)	Bone defects	Co-culture	hAMSCs increased the proliferation and osteoblastic differentiation of AdSCs and enhanced angiogenic potential of AdSCs via secretion of VEGF.
Wang et al. (88)	Bone defects	Culture <i>in vitro</i>	hAMSCs enhanced the osteogenesis of AdSCs by promoting APN excretion through APPL1-ERK1/2 activation.
Ma et al. (89)	Bone volume inadequacy	Hypodermic implantation	hAMSCs promoted osteogenic differentiation of BMSCs via H19/miR-675/APC pathway.
Wang et al. (90)	Bone defects	Co-culture	hAMSCs promoted BMSCs proliferation and osteogenic differentiation <i>in vitro</i> .
Wang et al. (91)	Bone deficiency	Culture <i>in vitro</i>	hAMSCs promoted the proliferation and osteoblastic differentiation of BMSCs via ERK1/2 MAPK signaling, and down-regulated ROS level.
Bian et al. (92)	Bone deficiency	Co-culture	hAMSCs/BMSCs cultured in transwell coculture system had better performance in bone regeneration than those in mixed coculture systems.
Yuan et al. (93)	Bone defects	Co-culture	hAMSCs promoted angiogenesis regulating by the expression of lncRNA H19.
Ranzoni et al. (94)	OI	Intraperitoneal injection	hAMSCs accelerated the bone formation via differentiating into osteoblasts and promoting endogenous osteogenesis and the maturation of resident osteoblasts.
Tsuno et al. (95)	Bone defects	Implantation with scaffolds	hAMSCs promoted bone regeneration via increasing ALP activity, calcium deposition, and the expression of osteocalcin mRNA.

MSFE, maxillary sinus floor elevation; hAMSCs, human amniotic mesenchymal stem cells; AdSCs, adipose-derived stem cells; BMP9, bone morphogenetic protein 9; PLGA, poly(lactic-co-glycolic acid); 3D, three-dimensional; UC-MSC, umbilical cord mesenchymal stem cells; MSCs, mesenchymal stem cells; BMSCs, bone marrow mesenchymal stem cell; HUVECs, human umbilical vein endothelial cells; MAPK, mitogen-activated protein kinase; VEGF, vascular endothelial growth factor; APN, adiponectin; APPL1, adaptor protein; PH, phosphotyrosine interaction, domain and leucine zipper containing 1; ERK1/2, extracellular signaling-regulated kinase 1/2; APC, adenomatous polyposis coli; ROS, reactive oxygen species; OI, osteogenesis imperfecta; ALP, alkaline phosphatase.

the bioactive cytokines, such as VEGF, FGFs, and keratinocyte growth factor (KGF) were identified and were found to promote ulcer healing (114) and improved photoaging (115) when the medium was locally injected into the lesions. Currently, there are no reports on the clinical trials using hAMSCs on bone regeneration; however, BMSCs (116, 117), AdSCs (118), and dental pulp stem cells (DPSCs) (119) had shown to be safe, feasible, and effective (120). Based on the data of the clinical trials, we speculated that hAMSCs could be studied in the clinical trials of bone regeneration for future applications.

CONCLUSION AND PERSPECTIVES

Although hAMSCs have become an alternative source of stem cells in regenerative medicine and tissue engineering due to their advantages such as easy gain, sufficient quantity, and superior properties, the application from laboratory research to clinical practice in the future needs further exploration. We still need to carry out further studies on hAMSCs acquisition, storage, and transportation to form standardized standards to maintain and improve the therapeutic potential of hAMSCs, so as to ensure the clinical application effects. It has been well-known that autologous MSCs represent the primary sources considered safe for transplantation and minimization of immunological risk. Preclinical studies should confirm the safety and immunological risk of allogenic hAMSCs for transplantation by comparing with autologous MSCs, and then the mechanisms of hAMSCs in promoting skeletal system diseases *in vivo* are also needed

to further elucidate, which are important to determine the indications, timing, dosage, and accurate administration of hAMSC-based therapy. For the treatment of bone regeneration and other bone disorders, more efforts should be made to optimize the therapeutic effects of hAMSC-based therapy by combining with other biomaterials and bioactive factors. Despite these challenges, it is no doubt that MSC-based therapy has a promising clinical application prospect. Since previous studies have demonstrated the hAMSCs with excellent MSC properties, hAMSC-based therapy is worthy to be further studied in depth and finally put into clinical practice.

AUTHOR CONTRIBUTIONS

JL and ZZ helped to draft the manuscript. FJ and YX contributed to the conception and supervision of the study. JW contributed to the consultation and revision of the manuscript. All authors contributed to the article and approved the submitted version.

FUNDING

This study was jointly supported by the National Natural Science Foundation of China (81670966, 81900960), Young Elite Scientists Sponsorship Program by CAST, 2018QNRC001, the Natural Science Foundation of Jiangsu Province (SBK2018042855), Qing Lan Project and the Priority Academic Program Development of Jiangsu Higher Education Institutions (PAPD, 2018-87).

REFERENCES

- Chen FM, Liu X. Advancing biomaterials of human origin for tissue engineering. *Prog Polym Sci.* (2016) 53:86–168. doi: 10.1016/j.progpolymsci.2015.02.004
- Disease GBD, Injury I, Prevalence C. Global, regional, and national incidence, prevalence, and years lived with disability for 354 diseases and injuries for 195 countries and territories, 1990–2017: a systematic analysis for the global burden of disease study 2017. *Lancet.* (2018) 392:1789–858. doi: 10.1016/S0140-6736(18)32279-7
- Atala A, Kasper FK, Mikos AG. Engineering complex tissues. *Sci Transl Med.* (2012) 4:160rv12. doi: 10.1126/scitranslmed.3004890
- Kolk A, Handschel J, Drescher W, Rothamel D, Kloss F, Blessmann M, et al. Current trends and future perspectives of bone substitute materials - from space holders to innovative biomaterials. *J Craniomaxillofac Surg.* (2012) 40:706–18. doi: 10.1016/j.jcms.2012.01.002
- McInnes IB, Schett G. The pathogenesis of rheumatoid arthritis. *N Engl J Med.* (2011) 365:2205–19. doi: 10.1056/NEJMra1004965
- Berenbaum F. Osteoarthritis as an inflammatory disease (osteoarthritis is not osteoarthritis!). *Osteoarthritis Cartilage.* (2013) 21:16–21. doi: 10.1016/j.joca.2012.11.012
- Braun J, Sieper J. Ankylosing spondylitis. *Lancet.* (2007) 369:1379–90. doi: 10.1016/S0140-6736(07)60635-7
- Lin YJ, Anzaghe M, Schulke S. Update on the pathomechanism, diagnosis, and treatment options for rheumatoid arthritis. *Cells.* (2020) 9:880. doi: 10.3390/cells9040880
- Qu HW, Fu HY, Han ZY, Sun, Y. Biomaterials for bone tissue engineering scaffolds: a review. *RSC Adv.* (2019) 26252–62. doi: 10.1039/c9ra05214c
- Kowalczewski CJ, Saul JM. Biomaterials for the delivery of growth factors and other therapeutic agents in tissue engineering approaches to bone regeneration. *Front Pharmacol.* (2018) 9:513. doi: 10.3389/fphar.2018.00513
- Caballe-Serrano J, Abdeslam-Mohamed Y, Munar-Frau A, Fujioka-Kobayashi M, Hernandez-Alfaro F, Miron R. Adsorption and release kinetics of growth factors on barrier membranes for guided tissue/bone regeneration: a systematic review. *Arch Oral Biol.* (2019) 100:57–68. doi: 10.1016/j.archoralbio.2019.02.006
- Kuroda Y, Kawai T, Goto K, Matsuda S. Clinical application of injectable growth factor for bone regeneration: a systematic review. *Inflamm Regen.* (2019) 39:20. doi: 10.1186/s41232-019-0109-x
- Badyrak SE, Nerem RM. Progress in tissue engineering and regenerative medicine. *Proc Natl Acad Sci USA.* (2010) 107:3285–6. doi: 10.1073/pnas.1000256107
- Chen FM, Wu LA, Zhang M, Zhang R, Sun HH. Homing of endogenous stem/progenitor cells for in situ tissue regeneration: promises, strategies, and translational perspectives. *Biomaterials.* (2011) 32:3189–209. doi: 10.1016/j.biomaterials.2010.12.032
- Weissman IL. Stem cells: units of development, units of regeneration, and units in evolution. *Cell.* (2000) 100:157–68. doi: 10.1016/S0092-8674(00)81692-X
- Zakrzewski W, Dobrzynski M, Szymonowicz M, Rybak Z. Stem cells: past, present, and future. *Stem Cell Res Ther.* (2019) 10:68. doi: 10.1186/s13287-019-1165-5
- Ebrahimi M, Botelho M. Adult stem cells of orofacial origin: current knowledge and limitation and future trend in regenerative medicine. *Tissue Eng Regen Med.* (2017) 14:719–733. doi: 10.1007/s13770-017-0078-6
- Kotas ME, Medzhitov R. Homeostasis, inflammation, and disease susceptibility. *Cell.* (2015) 160:816–27. doi: 10.1016/j.cell.2015.02.010
- Gribble FM, Reimann F. Enteroendocrine cells: chemosensors in the intestinal epithelium. *Annu Rev Physiol.* (2016) 78:277–99. doi: 10.1146/annurev-physiol-021115-105439
- Harvey S, Martinez-Moreno CG. Growth hormone and ocular dysfunction: endocrine, paracrine or autocrine etiologies? *Growth Horm IGF Res.* (2016) 29:28–32. doi: 10.1016/j.ghir.2016.03.004

21. Han Y, You X, Xing W, Zhang Z, Zou W. Paracrine and endocrine actions of bone-the functions of secretory proteins from osteoblasts, osteocytes, and osteoclasts. *Bone Res.* (2018) 6:16. doi: 10.1038/s41413-018-0019-6
22. Giudice J, Taylor JM. Muscle as a paracrine and endocrine organ. *Curr Opin Pharmacol.* (2017) 34:49–55. doi: 10.1016/j.coph.2017.05.005
23. Murphy MB, Moncivais K, Caplan AI. Mesenchymal stem cells: environmentally responsive therapeutics for regenerative medicine. *Exp Mol Med.* (2013) 45:e54. doi: 10.1038/emmm.2013.94
24. Deb KD, Sarda K. Human embryonic stem cells: preclinical perspectives. *J Transl Med.* (2008) 6:7. doi: 10.1186/1479-5876-6-7
25. Clevers H. What is an adult stem cell? *Science.* (2015) 350:1319–20. doi: 10.1126/science.aad7016
26. Bianco P, Riminucci M, Gronthos S, Robey PG. Bone marrow stromal stem cells: nature, biology, and potential applications. *Stem Cells.* (2001) 19:180–92. doi: 10.1634/stemcells.19-3-180
27. Gimble JM, Katz AJ, Bunnell BA. Adipose-derived stem cells for regenerative medicine. *Circ Res.* (2007) 100:1249–60. doi: 10.1161/01.RES.0000265074.83288.09
28. Kang HJ, Kim HS, Zhang SY, Park KW, Cho HJ, Koo BK, et al. Effects of intracoronary infusion of peripheral blood stem-cells mobilised with granulocyte-colony stimulating factor on left ventricular systolic function and restenosis after coronary stenting in myocardial infarction: the MAGIC cell randomised clinical trial. *Lancet.* (2004) 363:751–6. doi: 10.1016/s0140-6736(04)15689-4
29. Wagner W, Wein F, Seckinger A, Frankhauser M, Wirkner U, Krause U, et al. Comparative characteristics of mesenchymal stem cells from human bone marrow, adipose tissue, and umbilical cord blood. *Exp Hematol.* (2005) 33:1402–16. doi: 10.1016/j.exphem.2005.07.003
30. Carlotti F, Zaldumbide A, Loomans CJ, van Rossenberg E, Engelse M, de Koning EJ, et al. Isolated human islets contain a distinct population of mesenchymal stem cells. *Islets.* (2010) 2:164–73. doi: 10.4161/isl.2.3.11449
31. Huang F, Chen M, Chen W, Gu J, Yuan J, Xue Y, et al. Human gingiva-derived mesenchymal stem cells inhibit xeno-graft-versus-host disease via CD39-CD73-Adenosine and IDO Signals. *Front Immunol.* (2017) 8:68. doi: 10.3389/fimmu.2017.00068
32. De Bari C, Dell'Accio F, Tylzanowski P, Luyten FP. Multipotent mesenchymal stem cells from adult human synovial membrane. *Arthritis Rheum.* (2001) 44:1928–42. doi: 10.1002/1529-0131(200108)44:8<1928::AID-ART331>3.0.CO;2-P
33. Pittenger MF, Mackay AM, Beck SC, Jaiswal RK, Douglas R, Mosca JD, et al. Multilineage potential of adult human mesenchymal stem cells. *Science.* (1999) 284:143–7. doi: 10.1126/science.284.5411.143
34. Berebichez-Fridman R, Montero-Olvera PR. Sources and clinical applications of mesenchymal stem cells: state-of-the-art review. *Sultan Qaboos Univ Med J.* (2018) 18:e264–e77. doi: 10.18295/squmj.2018.18.03.002
35. Dimarino AM, Caplan AI, Bonfield TL. Mesenchymal stem cells in tissue repair. *Front Immunol.* (2013) 4:201. doi: 10.3389/fimmu.2013.00201
36. Magatti M, Caruso M, De Munari S, Vertua E, De D, Manuelpillai U, et al. Human amniotic membrane-derived mesenchymal and epithelial cells exert different effects on monocyte-derived dendritic cell differentiation and function. *Cell Transplant.* (2015) 24:1733–52. doi: 10.3727/096368914X684033
37. Magatti M, Vertua E, Cargnoni A, Silini A, Parolini O. The immunomodulatory properties of amniotic cells: the two sides of the coin. *Cell Transplant.* (2018) 27:31–44. doi: 10.1177/0963689717742819
38. Silini AR, Magatti M, Cargnoni A, Parolini O. Is immune modulation the mechanism underlying the beneficial effects of amniotic cells and their derivatives in regenerative medicine? *Cell Transplant.* (2017) 26:531–9. doi: 10.3727/096368916X693699
39. Insausti CL, Blanquer M, Garcia-Hernandez AM, Castellanos G, Moraleda JM. Amniotic membrane-derived stem cells: immunomodulatory properties and potential clinical application. *Stem Cells Cloning.* (2014) 7:53–63. doi: 10.2147/SCCAA.S58696
40. Ling L, Feng X, Wei T, Wang Y, Wang Y, Wang Z, et al. Human amnion-derived mesenchymal stem cell (hAD-MSC) transplantation improves ovarian function in rats with premature ovarian insufficiency (POI) at least partly through a paracrine mechanism. *Stem Cell Res Ther.* (2019) 10:46. doi: 10.1186/s13287-019-1136-x
41. Li JY, Ren KK, Zhang WJ, Xiao L, Wu HY, Liu QY, et al. Human amniotic mesenchymal stem cells and their paracrine factors promote wound healing by inhibiting heat stress-induced skin cell apoptosis and enhancing their proliferation through activating PI3K/AKT signaling pathway. *Stem Cell Res Ther.* (2019) 10:247. doi: 10.1186/s13287-019-1366-y
42. Parolini O, Alviano F, Bagnara GP, Bilic G, Buhning HJ, Evangelista M, et al. Concise review: isolation and characterization of cells from human term placenta: outcome of the first international workshop on placenta derived stem cells. *Stem Cells.* (2008) 26:300–11. doi: 10.1634/stemcells.2007-0594
43. Antoniadou E, David AL. Placental stem cells. *Best Pract Res Clin Obstet Gynaecol.* (2016) 31:13–29. doi: 10.1016/j.bpobgyn.2015.08.014
44. Lindenmair A, Hatlapatka T, Kollwig G, Hennerbichler S, Gabriel C, Wolbank S, et al. Mesenchymal stem or stromal cells from amnion and umbilical cord tissue and their potential for clinical applications. *Cells.* (2012) 1:1061–88. doi: 10.3390/cells1041061
45. Bilic G, Zeisberger SM, Mallik AS, Zimmermann R, Zisch AH. Comparative characterization of cultured human term amnion epithelial and mesenchymal stromal cells for application in cell therapy. *Cell Transplant.* (2008) 17:955–68. doi: 10.3727/096368908786576507
46. Wei X, Sun G, Zhao X, Wu Q, Chen L, Xu Y, et al. Human amnion mesenchymal stem cells attenuate atherosclerosis by modulating macrophage function to reduce immune response. *Int J Mol Med.* (2019) 44:1425–35. doi: 10.3892/ijmm.2019.4286
47. Koike C, Zhou K, Takeda Y, Fathy M, Okabe M, Yoshida T, et al. Characterization of amniotic stem cells. *Cell Reprogram.* (2014) 16:298–305. doi: 10.1089/cell.2013.0090
48. Parolini O, Soncini M, Evangelista M, Schmidt D. Amniotic membrane and amniotic fluid-derived cells: potential tools for regenerative medicine? *Regen Med.* (2009) 4:275–91. doi: 10.2217/17460751.4.2.275
49. Bailo M, Soncini M, Vertua E, Signoroni PB, Sanzone S, Lombardi G, et al. Engraftment potential of human amnion and chorion cells derived from term placenta. *Transplantation.* (2004) 78:1439–48. doi: 10.1097/01.TP.0000144606.84234.49
50. Evangelista M, Soncini M, Parolini O. Placenta-derived stem cells: new hope for cell therapy? *Cytotechnology.* (2008) 58:33–42. doi: 10.1007/s10616-008-9162-z
51. Miki T, Lehmann T, Cai H, Stolz DB, Strom SC. Stem cell characteristics of amniotic epithelial cells. *Stem Cells.* (2005) 23:1549–59. doi: 10.1634/stemcells.2004-0357
52. Meng MY, Li L, Wang WJ, Liu FF, Song J, Yang SL, et al. Assessment of tumor promoting effects of amniotic and umbilical cord mesenchymal stem cells *in vitro* and *in vivo*. *J Cancer Res Clin Oncol.* (2019) 145:1133–46. doi: 10.1007/s00432-019-02859-6
53. Farhadihosseinabadi B, Farahani M, Tayebi T, Jafari A, Biniiazan F, Modaresifar K, et al. Amniotic membrane and its epithelial and mesenchymal stem cells as an appropriate source for skin tissue engineering and regenerative medicine. *Artif Cells Nanomed Biotechnol.* (2018) 46:431–40. doi: 10.1080/21691401.2018.1458730
54. Narazaki M, Tanaka T, Kishimoto T. The role and therapeutic targeting of IL-6 in rheumatoid arthritis. *Expert Rev Clin Immunol.* (2017) 13:535–51. doi: 10.1080/1744666X.2017.1295850
55. Shu J, He XJ, Li H, Liu X, Qiu XM, Zhou TL, et al. The beneficial effect of human amnion mesenchymal cells in inhibition of inflammation and induction of neuronal repair in EAE mice. *J Immunol Res.* (2018) 2018:5083797. doi: 10.1155/2018/5083797
56. Parolini O, Souza-Moreira L, O'Valle F, Magatti M, Hernandez-Cortes P, Gonzalez-Rey E, et al. Therapeutic effect of human amniotic membrane-derived cells on experimental arthritis and other inflammatory disorders. *Arthritis Rheumatol.* (2014) 66:327–39. doi: 10.1002/art.38206
57. Huss RS, Huddleston JI, Goodman SB, Butcher EC, Zabel BA. Synovial tissue-infiltrating natural killer cells in osteoarthritis and periprosthetic inflammation. *Arthritis Rheum.* (2010) 62:3799–805. doi: 10.1002/art.27751
58. Pianta S, Bonassi Signoroni P, Muradore I, Rodrigues MF, Rossi D, Silini A, et al. Amniotic membrane mesenchymal cells-derived factors skew T cell polarization toward Treg and downregulate Th1 and Th17 cells subsets. *Stem Cell Rev Rep.* (2015) 11:394–407. doi: 10.1007/s12015-014-9558-4

59. Topoluk N, Steckbeck K, Siatkowski S, Burnikel B, Tokish J, Mercuri J. Amniotic mesenchymal stem cells mitigate osteoarthritis progression in a synovial macrophage-mediated *in vitro* explant coculture model. *J Tissue Eng Regen Med.* (2018) 12:1097–110. doi: 10.1002/term.2610
60. Cargnoni A, Piccinelli EC, Ressel L, Rossi D, Magatti M, Toschi I, et al. Conditioned medium from amniotic membrane-derived cells prevents lung fibrosis and preserves blood gas exchanges in bleomycin-injured mice—specificity of the effects and insights into possible mechanisms. *Cytotherapy.* (2014) 16:17–32. doi: 10.1016/j.jcyt.2013.07.002
61. Borem R, Madeline A, Bowman M, Gill S, Tokish J, Mercuri J. Differential effector response of amnion- and adipose-derived mesenchymal stem cells to inflammation; implications for intradiscal therapy. *J Orthop Res.* (2019) 37:2445–56. doi: 10.1002/jor.24412
62. Miceli V, Pampaloni M, Vella S, Carreca AP, Amico G, Conaldi PG. Comparison of immunosuppressive and angiogenic properties of human amnion-derived mesenchymal stem cells between 2d and 3d culture systems. *Stem Cells Int.* (2019) 2019:7486279. doi: 10.1155/2019/7486279
63. Banerjee A, Lindenmair A, Steinborn R, Dumitrescu SD, Hennerbichler S, Kozlov AV, et al. Oxygen tension strongly influences metabolic parameters and the release of interleukin-6 of human amniotic mesenchymal stromal cells *in vitro*. *Stem Cells Int.* (2018) 2018:9502451. doi: 10.1155/2018/9502451
64. Chahal J, Gomez-Aristizabal A, Shestopaloff K, Bhatt S, Chaboureaux A, Fazio A, et al. Bone marrow mesenchymal stromal cell treatment in patients with osteoarthritis results in overall improvement in pain and symptoms and reduces synovial inflammation. *Stem Cells Transl Med.* (2019) 8:746–57. doi: 10.1002/sctm.18-0183
65. Park KH, Mun CH, Kang MI, Lee SW, Lee SK, Park YB. Treatment of collagen-induced arthritis using immune modulatory properties of human mesenchymal stem cells. *Cell Transplant.* (2016) 25:1057–72. doi: 10.3727/096368915X687949
66. Safiri S, Kolahi AA, Smith E, Hill C, Bettampadi D, Mansournia MA, et al. Global, regional and national burden of osteoarthritis 1990–2017: a systematic analysis of the global burden of disease study 2017. *Ann Rheum Dis.* (2020) 79:819–28. doi: 10.1136/annrheumdis-2019-216515
67. Glyn-Jones S, Palmer AJ, Agricola R, Price AJ, Vincent TL, Weinans H, et al. Osteoarthritis. *Lancet.* (2015) 386:376–87. doi: 10.1016/S0140-6736(14)60802-3
68. Li YS, Luo W, Zhu SA, Lei GH. T cells in osteoarthritis: alterations and beyond. *Front Immunol.* (2017) 8:356. doi: 10.3389/fimmu.2017.00356
69. Yin L, Zhou ZX, Shen M, Chen N, Jiang F, Wang SL. The human amniotic mesenchymal stem cells (hamsCs) improve the implant osseointegration and bone regeneration in maxillary sinus floor elevation in rabbits. *Stem Cells Int.* (2019) 2019:9845497. doi: 10.1155/2019/9845497
70. You Q, Liu Z, Zhang J, Shen M, Li Y, Jin Y, et al. Human amniotic mesenchymal stem cell sheets encapsulating cartilage particles facilitate repair of rabbit osteochondral defects. *Am J Sports Med.* (2020) 48:599–611. doi: 10.1177/0363546519897912
71. Topoluk N, Hawkins R, Tokish J, Mercuri J. Amniotic mesenchymal stromal cells exhibit preferential osteogenic and chondrogenic differentiation and enhanced matrix production compared with adipose mesenchymal stromal cells. *Am J Sports Med.* (2017) 45:2637–46. doi: 10.1177/0363546517706138
72. Li Y, Liu Z, Tang Y, Feng W, Zhao C, Liao J, et al. Schnurri-3 regulates BMP9-induced osteogenic differentiation and angiogenesis of human amniotic mesenchymal stem cells through Runx2 and VEGF. *Cell Death Dis.* (2020) 11:72. doi: 10.1038/s41419-020-2279-5
73. Li Y, Liu Z, Tang Y, Fan Q, Feng W, Luo C, et al. Three-dimensional silk fibroin scaffolds enhance the bone formation and angiogenic differentiation of human amniotic mesenchymal stem cells: a biocompatibility analysis. *Acta Biochim Biophys Sin.* (2020) 52:590–602. doi: 10.1093/abbs/gmaa042
74. Meesuk L, Tantrawatpan C, Kheolamai P, Manochantr S. The immunosuppressive capacity of human mesenchymal stromal cells derived from amnion and bone marrow. *Biochem Biophys Res.* (2016) 8:34–40. doi: 10.1016/j.bbrep.2016.07.019
75. Leyva-Leyva M, Barrera L, Lopez-Camarillo C, Arriaga-Pizano L, Orozco-Hoyuela G, Carrillo-Casas EM, et al. Characterization of mesenchymal stem cell subpopulations from human amniotic membrane with dissimilar osteoblastic potential. *Stem Cells Dev.* (2013) 22:1275–87. doi: 10.1089/scd.2012.0359
76. Fan X, Li L, Ye Z, Zhou Y, Tan WS. Regulation of osteogenesis of human amniotic mesenchymal stem cells by sodium butyrate. *Cell Biol Int.* (2018) 42:457–69. doi: 10.1002/cbin.10919
77. Shen C, Yang C, Xu S, Zhao H. Comparison of osteogenic differentiation capacity in mesenchymal stem cells derived from human amniotic membrane (AM), umbilical cord (UC), chorionic membrane (CM), and decidua (DC). *Cell Biosci.* (2019) 9:17. doi: 10.1186/s13578-019-0281-3
78. Ma J, Wu J, Han L, Jiang X, Yan L, Hao J, et al. Comparative analysis of mesenchymal stem cells derived from amniotic membrane, umbilical cord, and chorionic plate under serum-free condition. *Stem Cell Res Ther.* (2019) 10:19. doi: 10.1186/s13287-018-1104-x
79. Schmelzer E, McKeel DT, Gerlach JC. Characterization of human mesenchymal stem cells from different tissues and their membrane encasement for prospective transplantation therapies. *Biomed Res Int.* (2019) 2019:6376271. doi: 10.1155/2019/6376271
80. Liu S, Liu D, Chen C, Hamamura K, Moshaverinia A, Yang R, et al. MSC transplantation improves osteopenia via epigenetic regulation of notch signaling in lupus. *Cell Metab.* (2015) 22:606–18. doi: 10.1016/j.cmet.2015.08.018
81. Li H, Shen S, Fu H, Wang Z, Li X, Sui X, et al. Immunomodulatory functions of mesenchymal stem cells in tissue engineering. *Stem Cells Int.* (2019) 2019:9671206. doi: 10.1155/2019/9671206
82. Gnecci M, Danieli P, Malpasso G, Ciuffreda MC. Paracrine mechanisms of mesenchymal stem cells in tissue repair. *Methods Mol Biol.* (2016) 1416:123–46. doi: 10.1007/978-1-4939-3584-0_7
83. Jiang F, Zhang W, Zhou M, Zhou Z, Shen M, Chen N, et al. Human amniotic mesenchymal stromal cells promote bone regeneration via activating endogenous regeneration. *Theranostics.* (2020) 10:6216–30. doi: 10.7150/thno.45249
84. Zhang C, Du Y, Yuan H, Jiang F, Shen M, Wang Y, et al. HAMSCs/HBMSCs coculture system ameliorates osteogenesis and angiogenesis against glucolipotoxicity. *Biochimie.* (2018) 152:121–33. doi: 10.1016/j.biochi.2018.06.028
85. Wang Y, Wu H, Shen M, Ding S, Miao J, Chen N. Role of human amnion-derived mesenchymal stem cells in promoting osteogenic differentiation by influencing p38 MAPK signaling in lipopolysaccharide-induced human bone marrow mesenchymal stem cells. *Exp Cell Res.* (2017) 350:41–9. doi: 10.1016/j.yexcr.2016.11.003
86. Wang J, Miao J, Meng X, Chen N, Wang Y. Expression of long noncoding RNAs in human bone marrow mesenchymal stem cells cocultured with human amnion-derived mesenchymal stem cells. *Mol Med Rep.* (2017) 16:6683–9. doi: 10.3892/mmr.2017.7465
87. Zhang C, Yu L, Liu S, Wang Y. Human amnion-derived mesenchymal stem cells promote osteogenic and angiogenic differentiation of human adipose-derived stem cells. *PLoS ONE.* (2017) 12:e0186253. doi: 10.1371/journal.pone.0186253
88. Wang Y, Du Y, Yuan H, Pan Y, Wu J, Du X, et al. Human amnion-derived mesenchymal stem cells enhance the osteogenic differentiation of human adipose-derived stem cells by promoting adiponectin excretion via the APPL1-ERK1/2 signaling pathway. *IUBMB Life.* (2020) 72:296–304. doi: 10.1002/iub.2165
89. Ma X, Bian Y, Yuan H, Chen N, Pan Y, Zhou W, et al. Human amnion-derived mesenchymal stem cells promote osteogenic differentiation of human bone marrow mesenchymal stem cells via H19/miR-675/APC axis. *Aging.* (2020) 12:103277. doi: 10.18632/aging.103277
90. Wang Y, Yin Y, Jiang F, Chen N. Human amnion mesenchymal stem cells promote proliferation and osteogenic differentiation in human bone marrow mesenchymal stem cells. *J Mol Histol.* (2015) 46:13–20. doi: 10.1007/s10735-014-9600-5
91. Wang Y, Ma J, Du Y, Miao J, Chen N. Human amnion-derived mesenchymal stem cells protect human bone marrow mesenchymal stem cells against oxidative stress-mediated dysfunction via erk1/2 mapk signaling. *Mol Cells.* (2016) 39:186–94. doi: 10.14348/molcells.2016.2159
92. Bian Y, Du Y, Wang R, Chen N, Du X, Wang Y, et al. A comparative study of HAMSCs/HBMSCs transwell and mixed coculture systems. *IUBMB Life.* (2019) 71:1048–55. doi: 10.1002/iub.2074
93. Yuan Z, Bian Y, Ma X, Tang Z, Chen N, Shen M. LncRNA H19 knockdown in human amniotic mesenchymal stem cells suppresses angiogenesis by

- associating with EZH2 and Activating Vasohibin-1. *Stem Cells Dev.* (2019) 28:781–90. doi: 10.1089/scd.2019.0014
94. Ranzoni AM, Corcelli M, Hau KL, Kerns JG, Vanleene M, Shefelbine S, et al. Counteracting bone fragility with human amniotic mesenchymal stem cells. *Sci Rep.* (2016) 6:39656. doi: 10.1038/srep39656
 95. Tsuno H, Yoshida T, Nogami M, Koike C, Okabe M, Noto Z, et al. Application of human amniotic mesenchymal cells as an allogeneic transplantation cell source in bone regenerative therapy. *Mater Sci Eng C.* (2012) 32:2452–8. doi: 10.1016/j.msec.2012.07.021
 96. Manuelpillai U, Moodley Y, Borlongan CV, Parolini O. Amniotic membrane and amniotic cells: potential therapeutic tools to combat tissue inflammation and fibrosis? *Placenta.* (2011) 32(Suppl. 4):S320–5. doi: 10.1016/j.placenta.2011.04.010
 97. Bahney CS, Zondervan RL, Allison P, Theologis A, Ashley JW, Ahn J, et al. Cellular biology of fracture healing. *J Orthop Res.* (2019) 37:35–50. doi: 10.1002/jor.24170
 98. Jiang F, Ma J, Liang Y, Niu Y, Chen N, Shen M. Amniotic mesenchymal stem cells can enhance angiogenic capacity via MMPs *in vitro* and *in vivo*. *Biomed Res Int.* (2015) 2015:324014. doi: 10.1155/2015/324014
 99. Prasad VK, Lucas KG, Kleiner GI, Talano JA, Jacobsohn D, Broadwater G, et al. Efficacy and safety of *ex vivo* cultured adult human mesenchymal stem cells (Prochymal) in pediatric patients with severe refractory acute graft-versus-host disease in a compassionate use study. *Biol Blood Marrow Transplant.* (2011) 17:534–41. doi: 10.1016/j.bbmt.2010.04.014
 100. Gupta N, Henry RG, Strober J, Kang SM, Lim DA, Buccini M, et al. Neural stem cell engraftment and myelination in the human brain. *Sci Transl Med.* (2012) 4:155ra137. doi: 10.1126/scitranslmed.3004373
 101. Hare JM, Fishman JE, Gerstenblith G, DiFede Velazquez DL, Zambrano JP, Suncion VY, et al. Comparison of allogeneic vs autologous bone marrow-derived mesenchymal stem cells delivered by transendocardial injection in patients with ischemic cardiomyopathy: the POSEIDON randomized trial. *JAMA.* (2012) 308:2369–79. doi: 10.1001/jama.2012.25321
 102. Chang YS, Ahn SY, Yoo HS, Sung SI, Choi SJ, Oh WI, et al. Mesenchymal stem cells for bronchopulmonary dysplasia: phase 1 dose-escalation clinical trial. *J Pediatr.* (2014) 164:966–72.e6. doi: 10.1016/j.jpeds.2013.12.011
 103. Liu X, Zheng P, Wang X, Dai G, Cheng H, Zhang Z, et al. A preliminary evaluation of efficacy and safety of Wharton's jelly mesenchymal stem cell transplantation in patients with type 2 diabetes mellitus. *Stem Cell Res Ther.* (2014) 5:57. doi: 10.1186/scrt446
 104. Aboody KS, Najbauer J, Metz MZ, D'Apuzzo M, Gutova M, Annala AJ, et al. Neural stem cell-mediated enzyme/prodrug therapy for glioma: preclinical studies. *Sci Transl Med.* (2013) 5:184ra59. doi: 10.1126/scitranslmed.3005365
 105. Orozco L, Munar A, Soler R, Alberca M, Soler F, Huguet M, et al. Treatment of knee osteoarthritis with autologous mesenchymal stem cells: a pilot study. *Transplantation.* (2013) 95:1535–41. doi: 10.1097/TP.0b013e318291a2da
 106. Trounson A, McDonald C. Stem cell therapies in clinical trials: progress and challenges. *Cell Stem Cell.* (2015) 17:11–22. doi: 10.1016/j.stem.2015.06.007
 107. Abbaspanah B, Momeni M, Ebrahimi M, Mousavi SH. Advances in perinatal stem cells research: a precious cell source for clinical applications. *Regen Med.* (2018) 13:595–610. doi: 10.2217/rme-2018-0019
 108. Chambers DC, Ennever D, Ilic N, Sparks L, Whitelaw K, Ayres J, et al. A phase 1b study of placenta-derived mesenchymal stromal cells in patients with idiopathic pulmonary fibrosis. *Respirology.* (2014) 19:1013–8. doi: 10.1111/resp.12343
 109. Mayer L, Pandak WM, Melmed GY, Hanauer SB, Johnson K, Payne D, et al. Safety and tolerability of human placenta-derived cells (PDA001) in treatment-resistant crohn's disease: a phase 1 study. *Inflamm Bowel Dis.* (2013) 19:754–60. doi: 10.1097/MIB.0b013e31827f27df
 110. Lublin FD, Bowen JD, Huddleston J, Kremenutzky M, Carpenter A, Corboy JR, et al. Human placenta-derived cells (PDA-001) for the treatment of adults with multiple sclerosis: a randomized, placebo-controlled, multiple-dose study. *Mult Scler Relat Disord.* (2014) 3:696–704. doi: 10.1016/j.msard.2014.08.002
 111. Khalifeh Soltani S, Forogh B, Ahmadbeigi N, Hadizadeh Kharazi H, Fallahzadeh K, Kashani L, et al. Safety and efficacy of allogeneic placental mesenchymal stem cells for treating knee osteoarthritis: a pilot study. *Cytotherapy.* (2019) 21:54–63. doi: 10.1016/j.jcyt.2018.11.003
 112. Meller D, Pires RT, Mack RJ, Figueiredo F, Heiligenhaus A, Park WC, et al. Amniotic membrane transplantation for acute chemical or thermal burns. *Ophthalmology.* (2000) 107:980–9. doi: 10.1016/S0161-6420(00)00024-5
 113. Momeni M, Fallah N, Bajouri A, Bagheri T, Orouji Z, Pahlevanpour P, et al. A randomized, double-blind, phase I clinical trial of fetal cell-based skin substitutes on healing of donor sites in burn patients. *Burns.* (2019) 45:914–22. doi: 10.1016/j.burns.2018.10.016
 114. Prakoeswa CRS, Natallya FR, Harnindya D, Thohiroh A, Oktaviyanti RN, Pratiwi KD, et al. The efficacy of topical human amniotic membrane-mesenchymal stem cell-conditioned medium (hAMMSC-CM) and a mixture of topical hAMMSC-CM + vitamin C and hAMMSC-CM + vitamin E on chronic plantar ulcers in leprosy: a randomized control trial. *J Dermatolog Treat.* (2018) 29:835–840. doi: 10.1080/09546634.2018.1467541
 115. Prakoeswa CRS, Pratiwi FD, Herwanto N, Citrashanty I, Indramaya DM, Murtiastutik D, et al. The effects of amniotic membrane stem cell-conditioned medium on photoaging. *J Dermatolog Treat.* (2019) 30:478–82. doi: 10.1080/09546634.2018.1530438
 116. Bajestan MN, Rajan A, Edwards SP, Aronovich S, Cevindanes LHS, Polymeri A, et al. Stem cell therapy for reconstruction of alveolar cleft and trauma defects in adults: a randomized controlled, clinical trial. *Clin Implant Dent Relat Res.* (2017) 19:793–801. doi: 10.1111/cid.12506
 117. Gjerde C, Mustafa K, Hellem S, Rojewski M, Gjengedal H, Yassin MA, et al. Cell therapy induced regeneration of severely atrophied mandibular bone in a clinical trial. *Stem Cell Res Ther.* (2018) 9:213. doi: 10.1186/s13287-018-0951-9
 118. Khojasteh A, Kheiri L, Behnia H, Tehranchi A, Nazeman P, Nadjmi N, et al. Lateral ramus cortical bone plate in alveolar cleft osteoplasty with concomitant use of buccal fat pad derived cells and autogenous bone: phase I clinical trial. *Biomed Res Int.* (2017) 2017:6560234. doi: 10.1155/2017/6560234
 119. Ferrarotti F, Romano F, Gamba MN, Quirico A, Giraudi M, Audagna M, et al. Human intrabony defect regeneration with micrografts containing dental pulp stem cells: a randomized controlled clinical trial. *J Clin Periodontol.* (2018) 45:841–50. doi: 10.1111/jcpe.12931
 120. Iaquina MR, Mazzoni E, Bononi I, Rotondo JC, Mazziotto C, Montesi M, et al. Adult stem cells for bone regeneration and repair. *Front Cell Dev Biol.* (2019) 7:268. doi: 10.3389/fcell.2019.00268

Conflict of Interest: The authors declare that the research was conducted in the absence of any commercial or financial relationships that could be construed as a potential conflict of interest.

Copyright © 2020 Li, Zhou, Wen, Jiang and Xia. This is an open-access article distributed under the terms of the Creative Commons Attribution License (CC BY). The use, distribution or reproduction in other forums is permitted, provided the original author(s) and the copyright owner(s) are credited and that the original publication in this journal is cited, in accordance with accepted academic practice. No use, distribution or reproduction is permitted which does not comply with these terms.



Intrinsic Restriction of TNF-Mediated Inflammatory Osteoclastogenesis and Bone Resorption

Baohong Zhao^{1,2,3*}

¹ Arthritis and Tissue Degeneration Program and David Z. Rosensweig Genomics Research Center, Hospital for Special Surgery, New York, NY, United States, ² Graduate Program in Biochemistry, Cell and Molecular Biology, Weill Cornell Graduate School of Medical Sciences, New York, NY, United States, ³ Department of Medicine, Weill Cornell Medical College, New York, NY, United States

OPEN ACCESS

Edited by:

Deborah Veis,
Washington University School of
Medicine in St. Louis, United States

Reviewed by:

Aline Bozec,
University of Erlangen Nuremberg,
Germany
Sudip Sen,
All India Institute of Medical Sciences,
India

*Correspondence:

Baohong Zhao
zhaob@hss.edu

Specialty section:

This article was submitted to
Bone Research,
a section of the journal
Frontiers in Endocrinology

Received: 15 July 2020

Accepted: 24 September 2020

Published: 08 October 2020

Citation:

Zhao B (2020) Intrinsic Restriction of
TNF-Mediated Inflammatory
Osteoclastogenesis
and Bone Resorption.
Front. Endocrinol. 11:583561.
doi: 10.3389/fendo.2020.583561

TNF (Tumor necrosis factor) is a pleiotropic cytokine that plays an important role in immunity and inflammatory bone destruction. Homeostatic osteoclastogenesis is effectively induced by RANKL (Receptor activator of nuclear factor kappa-B ligand). In contrast, TNF often acts on cell types other than osteoclasts, or synergically with RANKL to indirectly promote osteoclastogenesis and bone resorption. TNF and RANKL are members of the TNF superfamily. However, the direct osteoclastogenic capacity of TNF is much weaker than that of RANKL. Recent studies have uncovered key intrinsic mechanisms by which TNF acts on osteoclast precursors to restrain osteoclastogenesis, including the mechanisms mediated by RBP-J signaling, RBP-J and ITAM (Immunoreceptor tyrosine-based activation motif) crosstalk, RBP-J mediated regulatory network, NF- κ B p100, IRF8, and Def6. Some of these mechanisms, such as RBP-J and its mediated regulatory network, uniquely and predominantly limit osteoclastogenesis mediated by TNF but not by RANKL. As a consequence, targeting RBP-J activities suppresses inflammatory bone destruction but does not significantly impact normal bone remodeling or inflammation. Hence, discovery of these intrinsic inhibitory mechanisms addresses why TNF has a weak osteoclastogenic potential, explains a significant difference between RANKL and TNF signaling, and provides potentially new or complementary therapeutic strategies to selectively treat inflammatory bone resorption, without undesirable effects on normal bone remodeling or immune response in disease settings.

Keywords: tumor necrosis factor, osteoclasts, bone resorption, rheumatoid arthritis, RBP-J, IRF8, Def6

INTRODUCTION

Adult skeleton undergoes constant remodeling throughout life to maintain bone homeostasis. Normal bone remodeling requires a delicate balance between the activities of major bone cell types: bone-resorbing osteoclasts and bone-forming osteoblasts, as well as osteocytes. Osteoclasts are bone cells derived from monocyte/macrophage lineage and are exclusively responsible for bone

resorption, which contributes to skeletal development, bone homeostasis, and remodeling. Osteoclast differentiation is induced by the master osteoclastogenic factor, RANKL, which acts in concert with M-CSF and ITAM-mediated co-stimulatory signaling. These stimulations activate a broad range of signaling cascades, such as canonical and non-canonical NF- κ B pathways, mitogen-activated kinase (MAPK) pathways and calcium signaling, which in turn activate downstream transcriptional regulators to drive osteoclastogenesis. Under inflammatory conditions, abnormal osteoclast differentiation and function often results in excessive bone resorption, which is a common characteristic of many diseases, such as osteoporosis, rheumatoid arthritis (RA), psoriatic arthritis and periodontitis (1–5).

Inflammatory conditions have complex impacts on osteoclastogenesis and bone remodeling (1, 5, 6). Current treatments for excessive bone resorption utilize RANK receptor blockers or neutralizing antibodies, which are able to inhibit osteoclast formation. However, inhibition of osteoclast formation *via* blocking RANK signaling can result in long-term bone remodeling defects. The approved TNF blockade therapy (TNFi) has been a medical breakthrough that successfully ameliorates the quality of life of patients suffering from TNF-mediated diseases. TNFi includes monoclonal antibodies to TNF, such as Infliximab, Adalimumab, Certolizumab Pegol, and Golimumab, as well as soluble TNF receptor(s), such as Enbrel. Using TNFi has shown to help treat inflammation and joint erosion that occur in RA. However, immunosuppression from long-term utilization of TNFi is a side effect that can result in patients being susceptible to opportunistic infections. Understanding the mechanistic difference between RANKL-mediated physiological and TNF-mediated inflammatory osteoclastogenesis, and especially TNF-induced intrinsic inhibitory mechanisms, will strengthen the development of therapeutic approaches to treat pathological bone destruction in disease settings and prevent negative side effects on bone remodeling and immunity.

Tumor necrosis factor (TNF) is a pleiotropic inflammatory cytokine that is important for inflammation, immunity, and disease pathogenesis. TNF is known to play a key role in driving chronic inflammation as well as in pathological bone erosion associated with multiple inflammatory bone diseases, such as RA, periodontitis and periprosthetic osteolysis (1, 2, 7, 8). TNF particularly promotes osteoclastogenesis in these common pathological bone diseases *via* multiple mechanisms, such as increasing osteoclast precursor cells, acting on other cell types and in synergy with additional cytokines, mostly with RANKL (Figure 1). However, its direct osteoclastogenic capacity on its own is dramatically weaker than that of RANKL. Both TNF and RANKL belong to the TNF superfamily; however, there is a longstanding enigma in the field as to why TNF alone is unable to efficiently induce osteoclastogenesis, and the mechanisms that restrain TNF-induced osteoclastogenesis are poorly understood (6, 8). Since bone remodeling plays a key role in skeletal health, it is of particular clinical interest to develop therapeutic strategies specifically targeting pathological bone destruction, meanwhile without or minimizing undesirable effects on physiological bone remodeling. Therefore, in contrast to the traditional approaches

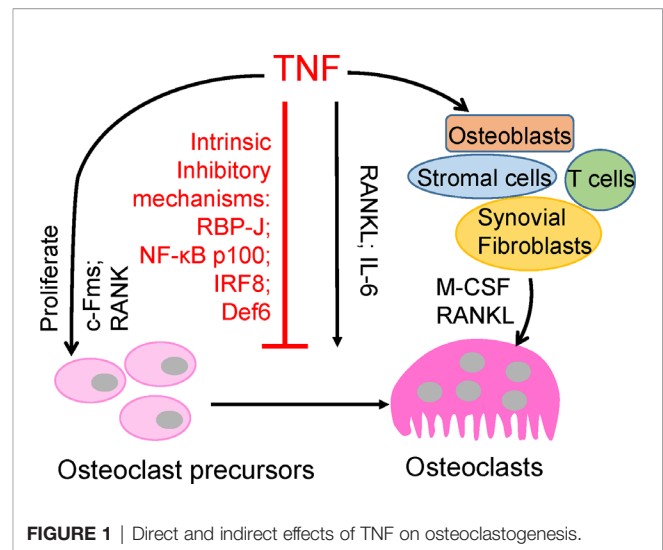


FIGURE 1 | Direct and indirect effects of TNF on osteoclastogenesis.

by blocking physiological RANK signaling or global TNF inhibition, elucidation and augmentation of these TNF-induced intrinsic inhibitory mechanisms will have high potential to provide novel treatments that are selective for inflammatory bone resorption, which will have long-term benefits for bone healing and maintenance of healthy skeleton.

Recent studies have provided evidence that uncover TNF-mediated intrinsic inhibitory mechanisms during osteoclastogenesis. In this review, we will highlight these discoveries and discuss their potential clinical relevance in treating inflammatory bone destruction.

DOES TNF PROMOTE OR RESTRAIN OSTEOCLASTOGENESIS AND INFLAMMATORY BONE RESORPTION?

TNF plays a key role in chronic inflammation and, notably, in bone destruction observed in diseases such as RA, periodontitis, and periprosthetic osteolysis. Clinical evidence from TNFi therapy further supports the role of TNF in promoting pathological bone resorption. However, genetic evidence and osteoclast differentiation of human CD14-positive cells demonstrate that TNF cannot effectively induce osteoclast differentiation directly as RANKL does (9–11). TNF acts, mainly in synergy with RANKL and/or together with other inflammatory cytokines, such as IL6, on osteoclast precursors to promote osteoclastogenesis and bone resorption under inflammatory conditions (3, 7, 12–17). Evidence indicates that TNF promotes the increase of osteoclast precursors *in vivo* (18–21). TNF can also indirectly promote osteoclastogenesis *via* augmentation of c-Fms and RANK expression in osteoclast precursors, and M-CSF and RANKL expression in osteoblasts, stromal cells, T cells and synovial fibroblasts (7, 22, 23). Therefore, TNF generally indirectly promotes osteoclastogenesis and bone resorption through other cell populations or cytokines (Figure 1). The direct osteoclastogenic capacity of TNF is weak. Recent

studies have revealed key mechanisms by which TNF restrains its osteoclastogenic potential, such as through osteoclastic inhibitors RBP-J, NF- κ B p100, IRF8, and Def6, which will be discussed below (**Figure 1**).

RBP-J PREDOMINANTLY SUPPRESSES TNF-INDUCED OSTEOCLASTOGENESIS COMPARED TO THAT INDUCED BY RANKL

Recombinant recognition sequence binding protein at the J κ site (RBP-J) is a nuclear DNA-binding protein that is expressed in a wide range of cell types and was originally identified as a key transcription factor in the canonical Notch signaling (24). Upon activation *via* Notch ligands, Notch intracellular cytoplasmic domains (NICDs) translocate to the nucleus and bind to RBP-J, which induces Notch target gene transcription. RBP-J has also been shown to function as a transcriptional activator or repressor for other signaling pathways, such as TNF (25), TLR (26, 27), Wnt- β -catenin (28), NF- κ B (29, 30), TAK1 (31), and ITAM-signaling pathways (32). RBP-J is also targeted by viral proteins (30, 33) and cellular proteins of unknown function (34, 35). Through its involvement of a multitude of signaling pathways, RBP-J is an important regulator of cell differentiation and proliferation, cell cycle, and survival, and diverse cellular functions including stem cell maintenance, neurogenesis, and lymphocyte development (24, 36). RBP-J has been identified in inflammatory macrophage activation and function (26, 27, 37), dendritic cell (DC) differentiation and maintenance of CD8-negative DC populations (38, 39). Many of these functions are associated with Notch signaling; however, the function of RBP-J is context-dependent and found to be significant in inflammatory disease conditions that are not related to canonical Notch signaling (27).

RBP-J function is also implicated in osteoclastogenesis. We demonstrated that RBP-J is activated by TNF in bone marrow-derived macrophages (BMMs), which are osteoclast precursors, and dramatically suppresses TNF-induced osteoclastogenesis and bone resorption *in vitro* and *in vivo* (25, 32), while modestly suppressing RANKL-induced osteoclastogenesis (25, 32, 40). Genetic evidence showed that Notch-RBP-J signaling plays a minor role in homeostatic bone resorption. Myeloid-specific deletion of RBP-J (RBP-J^{fl/fl}; LysM-Cre), deletion of Notch 1/2/3, or constitutively-active NICD1 expression in the myeloid compartment (NICD1^M) in mice did not exhibit significant bone defects under physiological conditions (25, 41). However, TNF-induced osteoclastogenesis was dramatically increased in RBP-J^{fl/fl}; LysM-Cre mice, comparable to RANKL-induced osteoclastogenesis and in a TNF-induced inflammatory bone resorption model. Osteoclast differentiation and bone resorption can be effectively induced by TNF in osteoclast precursor cells lacking RBP-J and even in the absence of RANK signaling (25). Thus, RBP-J restrains the full osteoclastogenic potential of TNF.

The mechanism by which RBP-J restrains TNF-induced osteoclastogenesis is by suppressing induction of NFATc1

through attenuation of c-Fos activation and suppression of Blimp1 induction (25). These events maintain the expression of osteoclastogenic repressor, IRF-8, which prevents cell differentiation (25). RBP-J deficiency allows for the drastic increase of NFATc1 transcription by TNF stimulation. These studies identified the role of RBP-J in transcriptional repression of osteoclastogenic factors to specifically suppress and restrain TNF-mediated inflammatory osteoclastogenesis and bone resorption (**Figure 2**). This selective role of RBP-J presents clinical potential in developing therapeutic strategies in suppressing inflammatory bone destruction.

CROSSTALK BETWEEN RBP-J AND ITAM SIGNALING

The immunoreceptor tyrosine-based activation motif (ITAM) is a highly conserved signaling motif contained in the cytoplasmic domain of transmembrane receptors and adaptors that are crucial mediators of various cellular activities, particularly immune response and cancer activation. ITAM-mediating signaling regulates hematopoietic cells including myeloid osteoclast precursor cells. The main ITAM-containing adaptors expressed by myeloid osteoclast precursors that play crucial roles in the osteoclast program include DNAX-activating protein 12 (DAP12) and Fc receptor common γ subunit (FcR γ). These adaptors associate with various receptors in myeloid cells to mediate signaling, including DAP12-associated triggering receptor expressed in myeloid cells 2 (TREM2), signal-regulatory protein β 1 (SIRP β 1), FcR γ -associated osteoclast-associated receptor (OSCAR), paired immunoglobulin-like

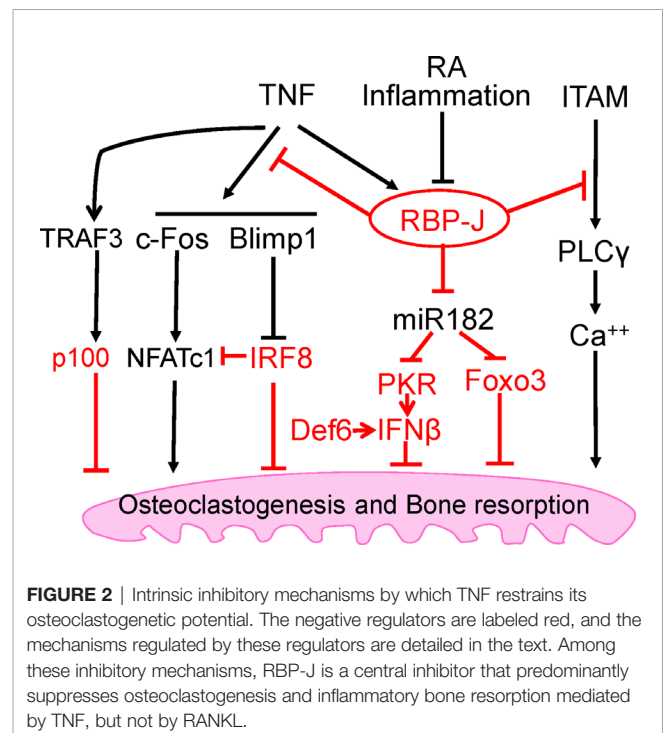


FIGURE 2 | Intrinsic inhibitory mechanisms by which TNF restrains its osteoclastogenic potential. The negative regulators are labeled red, and the mechanisms regulated by these regulators are detailed in the text. Among these inhibitory mechanisms, RBP-J is a central inhibitor that predominantly suppresses osteoclastogenesis and inflammatory bone resorption mediated by TNF, but not by RANKL.

receptor-A (PIR-A) and FcRs. Osteoclasts require co-stimulation of RANK *via* ITAM-mediated signaling pathways to drive osteoclastogenesis (42). Deficiency of both DAP12 and FcR γ in mice results in significant osteopetrosis and defects in osteoclast differentiation. Our previous study has demonstrated that myeloid-specific RBP-J deficiency in *Dap12*^{-/-} or *Dap12*^{-/-}*Fcrg*^{-/-} mice significantly rescued the bone defects (32). This indicated that the lack of RBP-J allowed for osteoclastogenesis in homeostatic bone remodeling to occur by bypassing the requirement of ITAM-mediated co-stimulation. Under inflammatory conditions, RBP-J restrains ITAM signaling and suppresses the basal expression and activity of PLC γ 2, limiting calcium signaling that is needed to induce osteoclast differentiation (42) (**Figure 2**). Consistently, RBP-J deficiency reversed this effect and enabled TNF stimulation to induce osteoclastogenesis in *Dap12*^{-/-}*Fcrg*^{-/-} mice. RBP-J deficiency allows for osteoclastogenesis to occur independently of ITAM-mediated co-stimulation, indicating that RBP-J functions to enforce ITAM-mediated co-stimulatory calcium signaling to induce osteoclast differentiation and function in both homeostatic and inflammatory settings. This balance between ITAM-mediated co-stimulation and RBP-J-mediated suppression settles the basal level of PLC γ 2/calcium signaling, and presents a mechanistic model whereby the regulation of this basal level of PLC γ 2/calcium signaling determines whether osteoclastogenic factors, such as RANKL or TNF, are able to effectively induce sufficient calcium signaling required for NFATc1 induction and downstream osteoclastogenesis. These studies demonstrate the inhibitory effect of RBP-J on ITAM-signaling and shed insight into the mechanisms mediated by the RBP-J and ITAM crosstalk, which can partially explain why TNF alone is unable to effectively induce osteoclastogenesis as RANKL can.

In addition to canonical Notch-dependent RBP-J signaling, modern genomic studies provide important evidence of Notch-independent RBP-J signaling pathways (43–45). Therefore, it would be of interest to elucidate whether RBP-J functions are dependent on canonical Notch signaling in TNF-mediated osteoclast differentiation and what upstream pathways would regulate RBP-J activities in this setting.

RBP-J TARGETS AND THE REGULATORY NETWORK MEDIATED BY RBP-J/NFATC1-MIR182 IN TNF-MEDIATED OSTEOCLASTOGENESIS

Despite its selective regulation in inflammatory conditions associated with bone destruction, RBP-J is a widely expressed transcription factor involved in many diverse cellular functions and therefore, unideal for direct targeting for therapeutic approaches. It is important to uncover and focus on its downstream targets in specific cell types of interest. Through genome-wide miRNA expression profiling, our group identified miR-182 as a TNF-induced miRNA that is directly targeted and suppressed by RBP-J in bone marrow macrophages and

osteoclast precursors (46, 47). RBP-J inhibits the expression and function of NFATc1 (25), which in turn acts as an upstream regulator activating miR-182, pointing to a novel regulatory network (48). Both *in vitro* and *in vivo* evidence supports the role of miR-182 as a positive regulator of TNF-mediated osteoclastogenesis. Myeloid-specific double knockout of miR-182 and RBP-J showed abolishment of the enhanced TNF-induced osteoclast differentiation and activity that occurs in the absence of only RBP-J in myeloid cells. Furthermore, inflammatory bone erosion *in vivo* mouse models demonstrated that miR-182 deletion reversed RBP-J deficiency enhanced osteoclast formation and bone erosion. Collectively with previous studies, these data reveal a crucial regulatory mechanism whereby RBP-J inhibits TNF-induced osteoclastogenesis through suppression of its downstream target, miR-182 (**Figure 2**).

Studies on inflammatory bone diseases, such as RA, present a disrupted balance of osteoclastogenic regulatory mechanisms. Monocytes isolated from RA patients show elevated levels of positive osteoclastic regulators miR-182 and NFATc1, and repressed levels of anti-osteoclastic regulators including RBP-J, Forkhead box class O 3 (FOXO3) and protein kinase double-stranded RNA-dependent (PKR) compared to healthy donors (46, 47). The administration of Enbrel, a TNFi therapy, to RA patients reverses these levels of regulators towards healthy levels, further supporting the RBP-J/NFATc1-miR-182 regulatory network in controlling TNF-mediated osteoclastogenesis. This data further supports the notion that disruption of the RBP-J/NFATc1-miR-182 regulatory network is responsible for pathological osteoclastogenesis and bone destruction in inflammatory bone diseases, and targeting this network holds potential for the development of novel treatment (**Figure 2**).

NF- κ B p100 and TRAF3

The nuclear factor NF- κ B family is involved in a number of cellular functions and plays a key role in immunity and proinflammatory signaling pathway. This family includes the transcription factors p65/RelA, RelB, c-Rel, NF- κ B1 (p105/p50), and NF- κ B2 (p100/p52). NF- κ B activation can be induced *via* canonical or classical signaling pathway involving TNFR activation or TLR ligand binding and dependent on IKK β -induced I κ B α degradation, which leads to RelA/p50 activation and downstream gene transcription. The non-canonical or alternative pathway involves NIK-induced phosphorylation of NF- κ B2/p100, which is crucial for p100 processing to p52 and RelB/p52 activation for downstream gene transcription. RelB was found to be essential for RANKL-induced osteoclast maturation and TNF-induced bone resorption (49). Activation of IKK β has been implicated in RANKL-induced osteoclastogenesis; however, it was also found to be sufficient for osteoclast differentiation and osteolysis independent of RANK (50). There is crosstalk between canonical and non-canonical NF- κ B pathways, and NF- κ B activation in these two pathways plays important positive regulatory roles in osteoclastogenesis (49, 51–53). In contrast, NF- κ B p100 has been shown to function as a negative regulator of osteoclastogenesis by binding to NF- κ B complexes and preventing their nuclear translocation. This consequently leads

to cytosolic accumulation of p100 and impairment of osteoclast differentiation. Deficiency of p100 reverses this inhibition and results in enhanced osteoclastogenesis that contributes to an osteopenic phenotype *in vivo* (49, 52–55). TNF cannot efficiently activate the alternative pathway which requires processing of p100 to p52. Therefore, unlike RANKL, TNF induces p100 accumulation in osteoclast precursors *via* induction of TNF receptor-associated factor 3 (TRAF3), limiting TNF-induced osteoclastogenesis (54) (**Figure 2**). *In vivo* evidence showed that TNF induced robust osteoclast differentiation in mice lacking RANK/RANKL and NF- κ B p100, and enhanced bone erosion in TNF-Tg mice lacking NF- κ B p100 compared to TNF-Tg littermates (54). These data suggest that promoting TRAF3 or targeting NF- κ B p100 processing to prevent TNF-induced NF- κ B p100 accumulation may represent novel therapeutic strategies to treat inflammatory bone resorption associated with RA, periodontitis, or periprosthetic osteolysis.

IRF-8

Within osteoclast differentiation program, transcriptional repressors contribute to the 'braking system', which is necessary to be overridden during differentiation process by master osteoclastogenic factor RANKL. These repressors include inhibitors of differentiation/DNA binding (Ids) (56, 57), Eos (58), v-maf musculoaponeurotic fibrosarcoma oncogene family protein B (MafB) (59), IFN regulatory factor-8 (IRF-8) (60) and B cell lymphoma 6 (Bcl6) (61). Among these transcriptional repressors, IRF-8 is of particular interest due to the dramatic augmentation of TNF-induced osteoclast differentiation in the absence of IRF8, resulting in increased NFATc1 expression. This indicates that IRF-8 plays a suppressive role in TNF-induced osteoclastogenesis (**Figure 2**). Additionally, IRF-8 deficiency significantly attenuates TLR-induced inhibition of osteoclastogenesis, suggesting that IRF-8 also plays a crucial role in the inhibitory mechanisms of TLR stimulation. In an LPS-induced inflammatory bone resorption model, IRF-8 deficient mice exhibited enhanced osteoclast formation and more severe bone destruction than WT littermates (60). These data suggest that IRF-8 is a negative regulator of osteoclastogenesis and may be important in limiting bone destruction during acute infections as well as in chronic inflammatory conditions such as rheumatoid arthritis.

Recently, inspiring studies highlight novel epigenetic regulatory mechanisms that control IRF8 downregulation, which present translational implications towards developing promising therapeutic strategies (62, 63). Epigenetic mechanisms of gene expression regulation are involved in virtually all biological processes in the human body and include transcriptional activation and repression *via* interplay of DNA methylation and histone post-translational modifications. DNA methylations *via de novo* DNA methyltransferases (DNMTs), such as DNMT3a and DNMT3b, and histone post-translational modifications (histone tail modifications), such as acetylation, methylation, phosphorylation, ubiquitylation, and sumoylation of histones, are common types of epigenetic modifications. Epigenetic repressors generally include DNMTs, histone deacetylases (HDACs), and polycomb group proteins (PcG). It has been shown that epigenetic repression of *Irf8* by Dnmt3a-mediated DNA hypermethylation leads to decreased IRF-

8 expression and enhanced osteoclastogenesis and bone resorption (62). Previous study by our group has found that polycomb repressive complex 2 (PRC2) component, EZH2, is recruited to the IRF8 promoter after RANKL stimulation, inducing transcriptional repressor mark H3K27me3 and subsequently downregulating *Irf8* expression (63). There are functional links between DNMTs, PRC2, and HDACs (64), and thus it is likely that IRF8 expression can be regulated through both DNA methylation and histone modification in a synergistic manner. It would be of great interest to investigate whether inflammatory conditions would impact the interplay of these epigenetic mechanisms and whether these regulatory mechanisms also regulate TNF-mediated osteoclastogenesis and bone resorption.

Def6

Differentially expressed in FDCP 6 homolog (Def6), also known as IRF4-binding protein (IBP) or SWAP-70-like adaptor protein of T cells (SLAT), is a type of guanine nucleotide exchange factor (GEF) expressed predominantly in T cells and regulates T cell development, activation, and function (65, 66). Expression of Def6 was also identified in myeloid cells and is functionally essential for regulating innate immunity (67). Previous study found that TCR-Tg (DO11.10) mice with Def6 deficiency developed RA-like joint disease (68). Our group further explored the role of Def6 in osteoclast formation and provided *in vitro* and *in vivo* evidence of the inhibitory role of Def6 in osteoclastogenesis (69). Def6 deficiency enhanced the sensitivity of osteoclast precursors to RANKL stimulation. Importantly, Def6 deficiency enabled TNF alone to induce osteoclastogenesis in the absence of RANKL, and markedly enhanced TNF-induced osteoclast formation and bone resorption. In human macrophages, TNF downregulated Def6 expression. Furthermore, we observed a close correlation between Def6 expression levels in osteoclast precursors, serum TNF levels from RA patients and the osteoclastogenic capacity of these precursors, indicating that Def6 inhibits excessive osteoclast formation and bone destruction in RA. Anti-TNF treatment resulted in significantly increased Def6 levels in peripheral blood mononuclear cells (PBMCs) from RA patients, further confirming that TNF downregulates Def6 expression and supporting a role for Def6 in modulating the effects of TNF on osteoclastogenesis. It was shown that Def6 suppresses NFATc1, Blimp1 and c-Fos by regulating an autocrine feedback loop mediated by endogenous IFN- β (69), leading to inhibition of osteoclastogenesis. Collectively, these findings identify Def6 as a negative regulator in TNF-mediated osteoclastogenesis and inflammatory bone resorption (**Figure 2**).

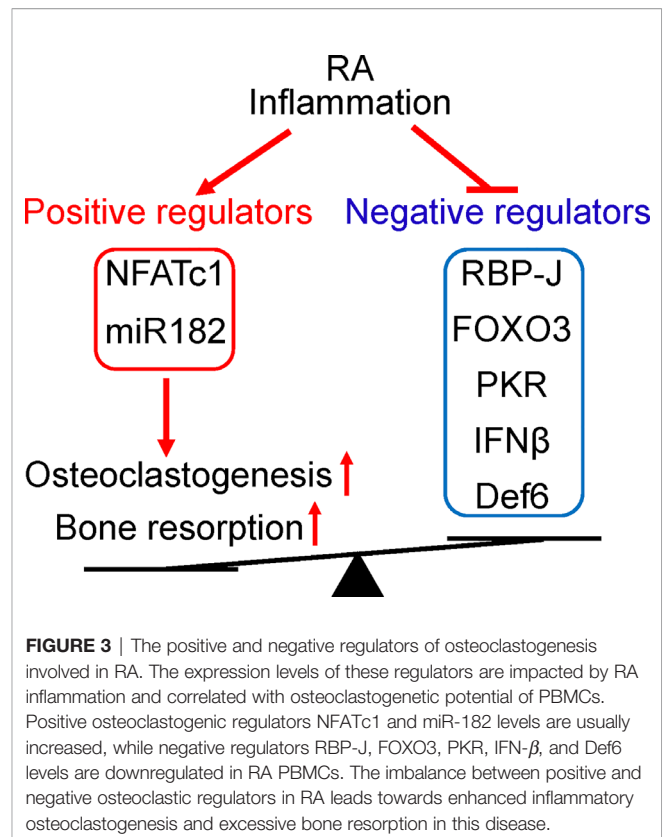
CLINICAL RELEVANCE OF TNF-INDUCED INHIBITORY MECHANISMS IN INFLAMMATORY BONE RESORPTION

An extensive and complex regulatory network exists to delicately control and maintain formation and activity of osteoclasts throughout lifetime. Many players are involved in contributing to the opposing osteoclastogenic and anti-osteoclastogenic mechanisms required for physiological bone remodeling. These

mechanisms are often dysregulated in pathological conditions. Potential long-term side effects on physiological bone remodeling by targeting these mechanisms should especially be given attention. Recent studies identified novel TNF-induced intrinsic inhibitory mechanisms of osteoclastogenesis, which are unique from RANKL-mediated mechanisms (25, 32, 48). Exploring these mechanisms would shed insight into developing selective therapeutic approaches to prevent TNF-mediated bone resorption associated with inflammatory diseases, without undesirably impacting physiological bone remodeling. A good example is targeting the RBP-J signaling pathway in osteoclasts as discussed above. Notably, *RBP-J* was validated as an RA risk allele in a genome-wide association study (GWAS) meta-analysis (70). Mounting evidence shows that the expression and function of RBP-J can be altered by various environmental cues, such as those involved in pathological settings. For example, we observed that RBP-J expression level was significantly suppressed in RA synovial fluid macrophages (32). However, it is clear that TNF activates and maintains RBP-J activity to suppress TNF-induced osteoclastogenesis. Thus, an interesting question arises as to why RBP-J expression level is decreased in RA, in which TNF activity is generally high and supposed to increase RBP-J expression/activity. Literature suggests that cytokines that activate Jak-STAT signaling are implicated in RA pathogenesis and may suppress Notch/RBP-J signaling and activity (27, 71, 72). Therefore, although TNF stimulation maintains RBP-J expression level and promotes its activity in macrophages/osteoclast precursors, the complex chronic inflammatory states in RA, such as involving the cytokines that activate Jak-STAT rather than TNF, lead to overall decreased RBP-J expression level/activity in this disease condition.

The identification of miR-182 as a key downstream target of RBP-J lead to the finding of a novel RBP-J/NFATc1-miR182 regulatory network (47, 48). Positive osteoclastogenic regulators NFATc1 and miR-182 levels were elevated, while negative regulators RBP-J, FOXO3, PKR and IFN- β levels were repressed in PBMCs isolated from RA patients compared to healthy donors (**Figure 3**). Serum TNF levels are correlated with these gene expression levels, and Enbrel treatment is able to reverse the expression profile of this regulatory network towards the level of health donors. Moreover, the osteoclastogenic capacity of RA PBMCs is strongly correlated with the expression levels of these regulators, through positive correlation with upregulated NFATc1 and miR-182, and negative correlation with downregulated RBP-J, FOXO3, PKR and IFN- β .

Evidence from both murine and human data indicate that the regulatory pattern and the function of the RBP-J/NFATc1-miR182 network are well conserved, and therefore strengthen the translational implications of this regulatory network in treating diseases associated with bone destruction, such as RA. Through this exploration, the negative impact of TNFi treatment on immune response may be preventable. Indeed, manipulation of RBP-J activity or the downstream target miR182 expression levels in inflammatory arthritis mouse models has significant impact on bone while discernable implications on TNF-mediated inflammation (25, 73). These findings therefore suggest a possibility of exploring selective control of RBP-J activity to



attenuate inflammatory bone destruction without significantly affecting the immune response mediated by TNF and physiological bone remodeling.

CONCLUDING REMARKS

The process of osteoclast differentiation is regulated by both osteoclastogenic and anti-osteoclastogenic mechanisms. Recent discovery of the intrinsic inhibitory mechanisms involved in TNF-mediated osteoclastogenesis and inflammatory bone resorption shifts the paradigm of inflammatory osteoclastogenesis. Some of these intrinsic mechanisms, such as those mediated by RBP-J, mostly selectively restrain TNF-mediated osteoclast differentiation and bone resorption, without significantly affecting RANKL-induced osteoclast differentiation, and thus maintaining physiological bone remodeling. Therapeutically targeting these mechanisms would therefore avoid long-term side effects caused by blockade of physiological bone remodeling. Anti-inflammatory therapy, such as TNF inhibitors, is often a double-edged sword that treats inflammation but meanwhile leads to immunorepressive side effects. Identification of alternative strategies that selectively target pathological bone resorption would help alleviate such undesirable treatment effects, such as the RBP-J mediated mechanisms discussed in this review. Collectively, the intrinsic inhibitory mechanisms selectively involved in TNF-mediated osteoclastogenesis have promising translational implications in treating inflammatory bone resorption.

AUTHOR CONTRIBUTIONS

The author confirms being the sole contributor of this work and has approved it for publication.

FUNDING

This work was supported by grants from the National Institutes of Health (AR068970 and AR071463 to BZ) and The Tow

Foundation (for the David Z. Rosensweig Genomics Center at the Hospital for Special Surgery). The content of this manuscript is solely the responsibilities of the author and does not necessarily represent the official views of the NIH.

ACKNOWLEDGMENTS

I thank Courtney Ng for proof-reading the manuscript.

REFERENCES

- Schett G, Gravalles E. Bone erosion in rheumatoid arthritis: mechanisms, diagnosis and treatment. *Nat Rev Rheumatol* (2012) 8(11):656–64. doi: 10.1038/nrrheum.2012.153
- Novack DV, Teitelbaum SL. The osteoclast: friend or foe? *Annu Rev Pathol* (2008) 3:457–84. doi: 10.1146/annurev.pathmechdis.3.121806.151431
- Schett G, Teitelbaum SL. Osteoclasts and arthritis. *J Bone Mineral Res* (2009) 24(7):1142–6. doi: 10.1359/jbmr.090533
- Boyce BF, Yao Z, Zhang Q, Guo R, Lu Y, Schwarz EM, et al. New roles for osteoclasts in bone. *Ann N Y Acad Sci* (2007) 1116:245–54. doi: 10.1196/annals.1402.084
- Sato K, Takayanagi H. Osteoclasts, rheumatoid arthritis, and osteoimmunology. *Curr Opin Rheumatol* (2006) 18(4):419–26. doi: 10.1097/01.bor.000.0231912.24740.a5
- Zhao B. TNF and Bone Remodeling. *Curr Osteoporos Rep* (2017) 15(3):126–34. doi: 10.1007/s11914-017-0358-z
- Teitelbaum SL. Osteoclasts: culprits in inflammatory osteolysis. *Arthritis Res Ther* (2006) 8(1):201. doi: 10.1186/ar1857
- Boyce BF, Xiu Y, Li J, Xing L, Yao Z. NF-kappaB-Mediated Regulation of Osteoclastogenesis. *Endocrinol Metab (Seoul)* (2015) 30(1):35–44. doi: 10.3803/EnM.2015.30.1.35
- Dougall WC, Glaccum M, Charrier K, Rohrbach K, Brasel K, De Smedt T, et al. RANK is essential for osteoclast and lymph node development. *Genes Dev* (1999) 13(18):2412–24. doi: 10.1101/gad.13.18.2412
- Pettit AR, Ji H, von Stechow D, Muller R, Goldring SR, Choi Y, et al. TRANCE/RANKL knockout mice are protected from bone erosion in a serum transfer model of arthritis. *Am J Pathol* (2001) 159(5):1689–99. doi: 10.1016/S0002-9440(10)63016-7
- Yarilina A, Xu K, Chen J, Ivashkiv LB. TNF activates calcium-nuclear factor of activated T cells (NFAT)c1 signaling pathways in human macrophages. *Proc Natl Acad Sci U S A* (2011) 108(4):1573–8. doi: 10.1073/pnas.1010030108
- Boyce BF, Schwarz EM, Xing L. Osteoclast precursors: cytokine-stimulated immunomodulators of inflammatory bone disease. *Curr Opin Rheumatol* (2006) 18(4):427–32. doi: 10.1097/01.bor.0000231913.32364.32
- Lam J, Takeshita S, Barker JE, Kanagawa O, Ross FP, Teitelbaum SL. TNF-alpha induces osteoclastogenesis by direct stimulation of macrophages exposed to permissive levels of RANK ligand. *J Clin Invest* (2000) 106(12):1481–8. doi: 10.1172/JCI11176
- Li J, Sarosi I, Yan XQ, Morony S, Capparelli C, Tan HL, et al. RANK is the intrinsic hematopoietic cell surface receptor that controls osteoclastogenesis and regulation of bone mass and calcium metabolism. *Proc Natl Acad Sci U S A* (2000) 97(4):1566–71. doi: 10.1073/pnas.97.4.1566
- Kim N, Kadono Y, Takami M, Lee J, Lee SH, Okada F, et al. Osteoclast differentiation independent of the TRANCE-RANK-TRAF6 axis. *J Exp Med* (2005) 202(5):589–95. doi: 10.1084/jem.20050978
- Kobayashi K, Takahashi N, Jimi E, Udagawa N, Takami M, Kotake S, et al. Tumor necrosis factor alpha stimulates osteoclast differentiation by a mechanism independent of the ODF/RANKL-RANK interaction. *J Exp Med* (2000) 191(2):275–86. doi: 10.1084/jem.191.2.275
- Azuma Y, Kaji K, Katogi R, Takeshita S, Kudo A. Tumor necrosis factor-alpha induces differentiation of and bone resorption by osteoclasts. *J Biol Chem* (2000) 275(7):4858–64. doi: 10.1074/jbc.275.7.4858
- Anandarajah AP, Schwarz EM, Totterman S, Monu J, Feng CY, Shao T, et al. The effect of etanercept on osteoclast precursor frequency and enhancing bone marrow oedema in patients with psoriatic arthritis. *Ann Rheum Dis* (2008) 67(3):296–301. doi: 10.1136/ard.2007.076091
- Yao Z, Li P, Zhang Q, Schwarz EM, Keng P, Arbin A, et al. Tumor necrosis factor-alpha increases circulating osteoclast precursor numbers by promoting their proliferation and differentiation in the bone marrow through up-regulation of c-Fms expression. *J Biol Chem* (2006) 281(17):11846–55. doi: 10.1074/jbc.M512624200
- Li P, Schwarz EM, O'Keefe RJ, Ma L, Looney RJ, Ritchlin CT, et al. Systemic tumor necrosis factor alpha mediates an increase in peripheral CD11bhigh osteoclast precursors in tumor necrosis factor alpha-transgenic mice. *Arthritis Rheum* (2004) 50(1):265–76. doi: 10.1002/art.11419
- Zhang Q, Guo R, Schwarz EM, Boyce BF, Xing L. TNF inhibits production of stromal cell-derived factor 1 by bone stromal cells and increases osteoclast precursor mobilization from bone marrow to peripheral blood. *Arthritis Res Ther* (2008) 10(2):R37. doi: 10.1186/ar2391
- Kitaura H, Kimura K, Ishida M, Kohara H, Yoshimatsu M, Takano-Yamamoto T. Immunological reaction in TNF-alpha-mediated osteoclast formation and bone resorption in vitro and in vivo. *Clin Dev Immunol* (2013) 2013:181849. doi: 10.1155/2013/181849
- Walsh MC, Choi Y. Biology of the RANKL-RANK-OPG System in Immunity, Bone, and Beyond. *Front Immunol* (2014) 5:511. doi: 10.3389/fimmu.2014.00511
- Kopan R, Ilagan MX. The canonical Notch signaling pathway: unfolding the activation mechanism. *Cell* (2009) 137(2):216–33. doi: 10.1016/j.cell.2009.03.045
- Zhao B, Grimes SN, Li S, Hu X, Ivashkiv LB. TNF-induced osteoclastogenesis and inflammatory bone resorption are inhibited by transcription factor RBP-J. *J Exp Med* (2012) 209(2):319–34. doi: 10.1084/jem.20111566
- Xu H, Zhu J, Smith S, Foldi J, Zhao B, Chung AY, et al. Notch-RBP-J signaling regulates the transcription factor IRF8 to promote inflammatory macrophage polarization. *Nat Immunol* (2012) 13(7):642–50. doi: 10.1038/ni.2304
- Hu X, Chung AY, Wu I, Foldi J, Chen J, Ji JD, et al. Integrated regulation of Toll-like receptor responses by Notch and interferon-gamma pathways. *Immunity* (2008) 29(5):691–703. doi: 10.1016/j.immuni.2008.08.016
- Shimizu T, Kagawa T, Inoue T, Nonaka A, Takada S, Aburatani H, et al. Stabilized beta-catenin functions through TCF/LEF proteins and the Notch/RBP-Jkappa complex to promote proliferation and suppress differentiation of neural precursor cells. *Mol Cell Biol* (2008) 28(24):7427–41. doi: 10.1128/MCB.01962-07
- Plaisance S, Vanden Berghe W, Boone E, Fiers W, Haegeman G. Recombination signal sequence binding protein Jkappa is constitutively bound to the NF-kappaB site of the interleukin-6 promoter and acts as a negative regulatory factor. *Mol Cell Biol* (1997) 17(7):3733–43. doi: 10.1128/MCB.17.7.3733
- Izumiya Y, Izumiya C, Hsia D, Ellison TJ, Luciw PA, Kung HJ. NF-kappaB serves as a cellular sensor of Kaposi's sarcoma-associated herpesvirus latency and negatively regulates K-Rta by antagonizing the RBP-Jkappa coactivator. *J Virol* (2009) 83(9):4435–46. doi: 10.1128/JVI.01999-08
- Swarnkar G, Karuppaiah K, Mbalaviele G, Chen TH, Abu-Amer Y. Osteopetrosis in TAK1-deficient mice owing to defective NF-kappaB and NOTCH signaling. *Proc Natl Acad Sci U S A* (2015) 112(1):154–9. doi: 10.1073/pnas.1415213112
- Li S, Miller CH, Giannopoulos E, Hu X, Ivashkiv LB, Zhao B. RBP-J imposes a requirement for ITAM-mediated costimulation of osteoclastogenesis. *J Clin Invest* (2014) 124(11):5057–73. doi: 10.1172/JCI71882
- Hayward SD. Viral interactions with the Notch pathway. *Semin Cancer Biol* (2004) 14(5):387–96. doi: 10.1016/j.semcancer.2004.04.018
- Taniguchi Y, Furukawa T, Tun T, Han H, Honjo T. LIM protein KyoT2 negatively regulates transcription by association with the RBP-J DNA-binding protein. *Mol Cell Biol* (1998) 18(1):644–54. doi: 10.1128/MCB.18.1.644

35. Beres TM, Masui T, Swift GH, Shi L, Henke RM, MacDonald RJ. PTF1 is an organ-specific and Notch-independent basic helix-loop-helix complex containing the mammalian Suppressor of Hairless (RBP-J) or its paralogue, RBP-L. *Mol Cell Biol* (2006) 26(1):117–30. doi: 10.1128/MCB.26.1.117-130.2006
36. Maillard I, Fang T, Pear WS. Regulation of lymphoid development, differentiation, and function by the Notch pathway. *Annu Rev Immunol* (2005) 23:945–74. doi: 10.1146/annurev.immunol.23.021704.115747
37. Foldi J, Shang Y, Zhao B, Ivashkiv LB, Hu X. RBP-J is required for M2 macrophage polarization in response to chitin and mediates expression of a subset of M2 genes. *Protein Cell* (2016) 7(3):201–9. doi: 10.1007/s13238-016-0248-7
38. Caton ML, Smith-Raska MR, Reizis B. Notch-RBP-J signaling controls the homeostasis of CD8⁺ dendritic cells in the spleen. *J Exp Med* (2007) 204(7):1653–64. doi: 10.1084/jem.20062648
39. Shang Y, Smith S, Hu X. Role of Notch signaling in regulating innate immunity and inflammation in health and disease. *Protein Cell* (2016) 7(3):159–74. doi: 10.1007/s13238-016-0250-0
40. Ma J, Liu YL, Hu YY, Wei YN, Zhao XC, Dong GY, et al. Disruption of the transcription factor RBP-J results in osteopenia attributable to attenuated osteoclast differentiation. *Mol Biol Rep* (2013) 40(3):2097–105. doi: 10.1007/s11033-012-2268-6
41. Bai S, Kopan R, Zou W, Hilton MJ, Ong CT, Long F, et al. NOTCH1 regulates osteoclastogenesis directly in osteoclast precursors and indirectly via osteoblast lineage cells. *J Biol Chem* (2008) 283(10):6509–18. doi: 10.1074/jbc.M707000200
42. Long CL, Humphrey MB. Osteoimmunology: the expanding role of immunoreceptors in osteoclasts and bone remodeling. *BoneKey Rep* (2012) 1:59–65. doi: 10.1038/bonekey.2012.59
43. Hamidi H, Gustafson D, Pellegrini M, Gasson J. Identification of novel targets of CSL-dependent Notch signaling in hematopoiesis. *PLoS One* (2011) 6(5):e20022. doi: 10.1371/journal.pone.0020022
44. Castel D, Mourikis P, Bartels SJ, Brinkman AB, Tajbakhsh S, Stunnenberg HG. Dynamic binding of RBPJ is determined by Notch signaling status. *Genes Dev* (2013) 27(9):1059–71. doi: 10.1101/gad.211912.112
45. Wang H, Zou J, Zhao B, Johannsen E, Ashworth T, Wong H, et al. Genome-wide analysis reveals conserved and divergent features of Notch1/RBPJ binding in human and murine T-lymphoblastic leukemia cells. *Proc Natl Acad Sci U S A* (2011) 108(36):14908–13. doi: 10.1073/pnas.1109023108
46. Miller CH, Smith SM, Elguindy M, Zhang T, Xiang JZ, Hu X, et al. RBP-J-Regulated miR-182 Promotes TNF- α -Induced Osteoclastogenesis. *J Immunol* (2016) 196(12):4977–86. doi: 10.4049/jimmunol.1502044
47. Inoue K, Deng Z, Chen Y, Giannopoulou E, Xu R, Gong S, et al. Bone protection by inhibition of microRNA-182. *Nat Communications* (2018) 9(1):4108. doi: 10.1038/s41467-018-06446-0
48. Inoue K, Hu X, Zhao B. Regulatory network mediated by RBP-J/NFATc1-miR182 controls inflammatory bone resorption. *FASEB J* (2020) 34(2):2392–407. doi: 10.1096/fj.201902227R
49. Vaira S, Johnson T, Hirbe AC, Alhawagiri M, Anwise I, Sammut B, et al. RelB is the NF- κ B subunit downstream of NIK responsible for osteoclast differentiation. *Proc Natl Acad Sci U S A* (2008) 105(10):3897–902. doi: 10.1073/pnas.0708576105
50. Otero JE, Dai S, Alhawagiri MA, Darwech I, Abu-Amer Y. IKK β activation is sufficient for RANK-independent osteoclast differentiation and osteolysis. *J Bone Mineral Res* (2010) 25(6):1282–94. doi: 10.1002/jbmr.4
51. Asagiri M, Takayanagi H. The molecular understanding of osteoclast differentiation. *Bone* (2007) 40(2):251–64. doi: 10.1016/j.bone.2006.09.023
52. Novack DV, Yin L, Hagen-Stapleton A, Schreiber RD, Goeddel DV, Ross FP, et al. The IkappaB function of NF- κ B p100 controls stimulated osteoclastogenesis. *J Exp Med* (2003) 198(5):771–81. doi: 10.1084/jem.20030116
53. Maruyama T, Fukushima H, Nakao K, Shin M, Yasuda H, Weih F, et al. Processing of the NF- κ B precursor p100 to p52 is critical for RANKL-induced osteoclast differentiation. *J Bone Mineral Res* (2010) 25(5):1058–67. doi: 10.1359/jbmr.091032
54. Yao Z, Xing L, Boyce BF. NF- κ B p100 limits TNF-induced bone resorption in mice by a TRAF3-dependent mechanism. *J Clin Invest* (2009) 119(10):3024–34. doi: 10.1172/JCI38716
55. Soysa NS, Alles N, Weih D, Lovas A, Mian AH, Shimokawa H, et al. The pivotal role of the alternative NF- κ B pathway in maintenance of basal bone homeostasis and osteoclastogenesis. *J Bone Mineral Res* (2010) 25(4):809–18. doi: 10.1359/jbmr.091030
56. Lee J, Kim K, Kim JH, Jin HM, Choi HK, Lee SH, et al. Id helix-loop-helix proteins negatively regulate TRANCE-mediated osteoclast differentiation. *Blood* (2006) 107(7):2686–93. doi: 10.1182/blood-2005-07-2798
57. Chan AS, Jensen KK, Skokos D, Doty S, Lederman HK, Kaplan RN, et al. Id1 represses osteoclast-dependent transcription and affects bone formation and hematopoiesis. *PLoS One* (2009) 4(11):e7955. doi: 10.1371/journal.pone.0007955
58. Hu R, Sharma SM, Bronisz A, Srinivasan R, Sankar U, Ostrowski MC. Eos, MITF, and PU.1 recruit corepressors to osteoclast-specific genes in committed myeloid progenitors. *Mol Cell Biol* (2007) 27(11):4018–27. doi: 10.1128/MCB.01839-06
59. Kim K, Kim JH, Lee J, Jin HM, Kook H, Kim KK, et al. MafB negatively regulates RANKL-mediated osteoclast differentiation. *Blood* (2007) 109(8):3253–9. doi: 10.1182/blood-2006-09-048249
60. Zhao B, Takami M, Yamada A, Wang X, Koga T, Hu X, et al. Interferon regulatory factor-8 regulates bone metabolism by suppressing osteoclastogenesis. *Nat Med* (2009) 15(9):1066–71. doi: 10.1038/nm.2007
61. Miyauchi Y, Ninomiya K, Miyamoto H, Sakamoto A, Iwasaki R, Hoshi H, et al. The Blimp1-Bcl6 axis is critical to regulate osteoclast differentiation and bone homeostasis. *J Exp Med* (2010) 207(4):751–62. doi: 10.1084/jem.20091957
62. Nishikawa K, Iwamoto Y, Kobayashi Y, Katsuoka F, Kawaguchi S, Tsujita T, et al. DNA methyltransferase 3a regulates osteoclast differentiation by coupling to an S-adenosylmethionine-producing metabolic pathway. *Nat Med* (2015) 21(3):281–7. doi: 10.1038/nm.3774
63. Fang C, Qiao Y, Mun SH, Lee MJ, Murata K, Bae S, et al. Cutting Edge: EZH2 Promotes Osteoclastogenesis by Epigenetic Silencing of the Negative Regulator IRF8. *J Immunol* (2016) 196(11):4452–6. doi: 10.4049/jimmunol.1501466
64. Marchesi I, Bagella L. Role of Enhancer of Zeste Homolog 2 Polycomb Protein and Its Significance in Tumor Progression and Cell Differentiation. In: D Radzioch, editor. *Chromatin Remodelling*. Rijeka: InTech (2013). p. Ch. 06. doi: 10.5772/55370
65. Tanaka Y, Bi K, Kitamura R, Hong S, Altman Y, Matsumoto A, et al. SWAP-70-like adapter of T cells, an adapter protein that regulates early TCR-initiated signaling in Th2 lineage cells. *Immunity* (2003) 18(3):403–14. doi: 10.1016/S1074-7613(03)00054-2
66. Gupta S, Lee A, Hu C, Fanzo J, Goldberg I, Cattoretti G, et al. Molecular cloning of IBP, a SWAP-70 homologous GEF, which is highly expressed in the immune system. *Hum Immunol* (2003) 64(4):389–401. doi: 10.1016/S0198-8859(03)00024-7
67. Chen Q, Gupta S, Pernis AB. Regulation of TLR4-mediated signaling by IBP/Def6, a novel activator of Rho GTPases. *J Leukoc Biol* (2009) 85(3):539–43. doi: 10.1189/jlb.0308219
68. Chen Q, Yang W, Gupta S, Biswas P, Smith P, Bhagat G, et al. IRF-4-binding protein inhibits interleukin-17 and interleukin-21 production by controlling the activity of IRF-4 transcription factor. *Immunity* (2008) 29(6):899–911. doi: 10.1016/j.immuni.2008.10.011
69. Binder N, Miller C, Yoshida M, Inoue K, Nakano S, Hu X, et al. Def6 Restrains Osteoclastogenesis and Inflammatory Bone Resorption. *J Immunol* (2017) 198(9):3436–47. doi: 10.4049/jimmunol.1601716
70. Stahl EA, Raychaudhuri S, Remmers EF, Xie G, Eyre S, Thomson BP, et al. Genome-wide association study meta-analysis identifies seven new rheumatoid arthritis risk loci. *Nat Genet* (2010) 42(6):508–14. doi: 10.1038/ng.582
71. Androutsellis-Theotokis A, Leker RR, Soldner F, Hoepfner DJ, Ravin R, Poser SW, et al. Notch signalling regulates stem cell numbers in vitro and in vivo. *Nature* (2006) 442(7104):823–6. doi: 10.1038/nature04940
72. Ivashkiv LB, Hu X. The JAK/STAT pathway in rheumatoid arthritis: pathogenic or protective? *Arthritis Rheum* (2003) 48(8):2092–6. doi: 10.1002/art.11095
73. Zhang H, Hilton MJ, Anolik JH, Welle SL, Zhao C, Yao Z, et al. NOTCH inhibits osteoblast formation in inflammatory arthritis via noncanonical NF- κ B. *J Clin Invest* (2014) 124(7):3200–14. doi: 10.1172/JCI68901

Conflict of Interest: The author declares that the research was conducted in the absence of any commercial or financial relationships that could be construed as a potential conflict of interest.

Copyright © 2020 Zhao. This is an open-access article distributed under the terms of the Creative Commons Attribution License (CC BY). The use, distribution or reproduction in other forums is permitted, provided the original author(s) and the copyright owner(s) are credited and that the original publication in this journal is cited, in accordance with accepted academic practice. No use, distribution or reproduction is permitted which does not comply with these terms.



Osteocytes and Bone Metastasis

Manuel A. Riquelme, Eduardo R. Cardenas and Jean X. Jiang*

Department of Biochemistry and Structural Biology, University of Texas Health Science Center, San Antonio, TX, United States

OPEN ACCESS

Edited by:

Lilian Irene Plotkin,
Indiana University Bloomington,
United States

Reviewed by:

Gabriel M. Pagnotti,
Stony Brook University, United States
Patricia Juarez,
Center for Scientific Research and
Higher Education in Ensenada
(CICESE), Mexico

*Correspondence:

Jean X. Jiang
jiangj@uthscsa.edu

Specialty section:

This article was submitted to
Bone Research,
a section of the journal
Frontiers in Endocrinology

Received: 30 May 2020

Accepted: 24 September 2020

Published: 14 October 2020

Citation:

Riquelme MA, Cardenas ER and
Jiang JX (2020) Osteocytes and
Bone Metastasis.
Front. Endocrinol. 11:567844.
doi: 10.3389/fendo.2020.567844

Bone is the most frequent site of breast cancer and prostate cancer metastasis, and one of the most common sites of metastasis for many solid tumors. Once cancer cells colonize in the bone, it imposes a major clinical challenge for the treatment of the disease, and fatality rates increase drastically. Bone, the largest organ in the body, provides a fertile microenvironment enriched with nutrients, growth factors and hormones, a generous reward for cancer cells. Dependent on cancer type, cancer cells can cause osteoblastic (bone forming) or osteolytic lesions to promote the net resorption and/or release of growth factors from the bone extracellular matrix. These processes activate a “vicious cycle”, leading to disruption of bone integrity and promoting cancer cell growth and migration. Cancer cells influence the bone microenvironment favoring their colonization and growth. In order to metastasize to the bone, cancer cells must first migrate from the site of origin, and once established within the bone, they must overcome the dormant inducing effects of resident cells. If successful, cancer cells can then colonize and continually disrupt bone homeostasis that is primarily maintained by osteocytes, the most abundant bone cell type. For example, it has been shown that exercise induces osteocytes to release anabolic factors that inhibit osteoclast resorptive activity, promote dormancy and the release of anti-cancer factors that inhibit breast cancer cell metastasis. In this review, we will summarize recent research findings and provide mechanistic insights related to the role of osteocytes in osteolytic metastasis.

Keywords: osteocyte, bone, cancer, metastasis, microenvironment

INTRODUCTION: CANCER BONE METASTASIS

The bone is a mineralized tissue highly regulated to adapt and meet the diverse needs of the host relative to physical demand, hormones, metabolic state, and environmental stimulation. Bone remodeling involves three major bone cell types; osteoblasts (bone forming cells) and osteoclasts (bone resorbing cells) that function in maintaining the structural balance, and the osteocytes that function in bone remodeling in response to environmental and mechanical signals and stimuli (1). The osteocyte, which is the most abundant cell type (~95%) in the bone, is the primary cell responsible for bone remodeling and homeostasis. Embedded inside the bone mineral matrix, osteocytes are connected and able to sense and respond coordinately to environmental cues, such as hormones, physical stress, and mechanical loading and unloading. These properties allow osteocytes to modulate the bone microenvironment by promoting the release of factors that regulate bone formation or resorption with respect to demands. Disease and aging can disrupt bone homeostasis, create structural defects, and alter the bone macro- and microenvironment, ultimately leading to

cancer cells colonizing within the tissue (2). The bone, along with the liver and lung, is one of the most frequent sites of cancer metastasis (2). Bone metastasis is an unfortunate outcome of many solid tumors, typically breast, lung, prostate, thyroid, renal carcinoma, melanoma, gastrointestinal tumors, and head and neck cancers (2, 3). Tumors that originate in the bone represent a small fraction of diagnosed cancers. Originating from cells found in bone tissue of osteosarcomas, these cancers are of transformed osteoblastic lineage, and occur most often in adolescents (4, 5). Other cancers, such as multiple myeloma arise from the bone marrow, but do not come from mesenchymal lineage. Approximately 80% of bone lesions and tumors originate in the bone marrow as multiple myeloma (3, 6, 7). The process of other cancers metastasizing to the bone is as complicated as one would expect considering that it is not one single cancer type that favors bone metastasis. This article primarily focuses on cancer bone metastasis from cancer not originating from the bone. Bone metastasis greatly affects the quality of life of patients, causing complications, such as pain, nerve root or spine cord compression, vertebral or peripheral fractures, hypercalcemia, and bone marrow infiltration that lead to cytopenia (3, 8).

The reasons why tumor cells metastasize to the bone are poorly understood. Bone tissue provides an ideal microenvironment for metastatic tumor cells. Bone marrow endothelium, adipocytes, and the immune response all participate in maintaining bone homeostasis in ways that are only partially understood. Although solid tumor metastasis to the bone is common, not all cancers preferably metastasize to the bone. Thus, disseminated tumor cells homing to the bone may be a targeted, and/or the microenvironment found in the bone, including cellular, hormonal or otherwise is not suitable for the growth of certain cancer types (8, 9). Interestingly, highly vascularized bone containing red bone marrow and cancellous bone (e.g. pelvis and long bones) are common sites of metastasis (rarely hand and foot bones) (3). It has been shown that primary tumors from near and distal regions of the body organize and make ready premetastatic niches. For instance, myeloid cells can be recruited from the bone marrow by tumor-derived exosomes that release a plethora of soluble factors, including, proteins, enzymes, and small nucleic acids, which are capable of homing in circulating tumor cells to the newly forming metastatic niche (10).

$\alpha v \beta 3$ integrins (acting as cell surface adhesion receptors) have been found to play a key role in mediating the metastatic MDA-MB-231 and Chinese Hamster Ovary tumor cells into the bone (11, 12). Metastatic cancer cells are attracted and retained in the bone marrow through the sensing and signaling of chemokines, for example, the C-X-C motif chemokine ligand 12 (CXCL12), which is expressed in bone marrow stromal cells, attracts tumor cells overexpressing the C-X-C chemokine receptor type 4 (CXCR4) (13). In another study by Cox et al., lysyl oxidase (LOX) was identified in hypoxic ER-negative breast tumor cells to play a key role in preparing the bone metastatic niche. LOX induces osteoclastogenesis independent of RANKL, disrupts bone homeostasis, ultimately leading to the formation of premetastatic bone lesions (14). Moreover, high LOX activity has been clinically associated with increased collagen cross-

linking, fibrosis, and elevated risk of cancer metastasis (15). LOX, secreted by primary tumor cells, is responsible for catalyzing the cross-linking of both collagen and elastin, which increases matrix stiffness, alignment, and total ECM volume. The increase of ECM stiffness facilitates the activation of integrins and augments Rho-generated cytoskeletal tension promoting focal adhesion formation and cell motility (14, 15).

Adaptive immune cells also play a role in setting up the bone metastatic niche. Immune-competent mice orthotopically injected with metastatic 4T1 breast cancer cells are shown to have increased osteoclastogenesis; this induces the pre-metastatic osteolytic niche required for colony formation. It is further shown that the primary tumor environment promotes the differentiation of helper T cells (CD4⁺), and the tumor-specific Th17 cells expressing RANKL, which stimulates osteoclast activation and induces osteolytic bone lesions, ultimately promoting breast cancer colonization in the bone (16).

The seemingly self-perpetuating metastatic growth to bone has been described as a 'vicious cycle'. In an intricate process inside the bone, tumor cells secrete osteoclastogenic factors (e.g., IL-1, IL-6, IL-11, PDGF, MIP1 α , TNF, M-CSF, RANKL, and PTHrP) that help stimulate the recruitment and activity of osteoclast, key players in the formation of osteolytic lesions (17). This process disrupts bone homeostasis and induces the release of growth factors, including, activin, transforming growth factor β (TGF β), fibroblast growth factor (FGF), and platelet-derived growth factor (PDGF) from the bone mineral matrix. In turn, these released factors promote tumor cell growth and increase further bone resorption (**Figure 1**, step ①) (18). This feedback loop, or 'vicious cycle', increases the incidence of metastatic lesions in the bone and eventually leads to related ailments, e.g. bone fractures, and high levels of blood calcium (hypercalcemia).

As mentioned, an important player in the vicious cycle is osteoclasts, large bone resorbing multinucleated cells originating from the fusion of bone marrow-derived monocytes/macrophages. Activated osteoclasts adhere to bone surfaces, forming an acting ring that covers a space in which bone demineralizing enzymes and proteases are secreted. Key players in osteoclast differentiation include adenosine nucleotides, receptor activator of nuclear factor κ -B ligand (RANKL), macrophage colony-stimulating factor (M-CSF), and other molecules (19), which are principally generated from nearby osteoblasts, osteocytes, and immune cells (20). Osteoclast generation and activation is achieved directly, or indirectly by RANKL production by neighboring cells, or by bone trophic tumor cells. These activities are eventually used by tumor derived cells to create the bone niche, leading to further osteoclastogenesis and bone resorption. The mechanistic comprehension of bone turnover in tumor growth has led to the clinical use of osteoclast inhibiting bisphosphonates, and Denosumab (anti-RANKL antibody) in patients with bone metastasis, and has become the standard of care to improve quality of life by limiting bone turnover (**Figure 1**, step ②) (21). In addition to molecules directly involved in bone resorption, other factors involved in bone resorption include interleukins-6 and 11 (22), parathyroid hormone-related peptide (PTHrP) (23,

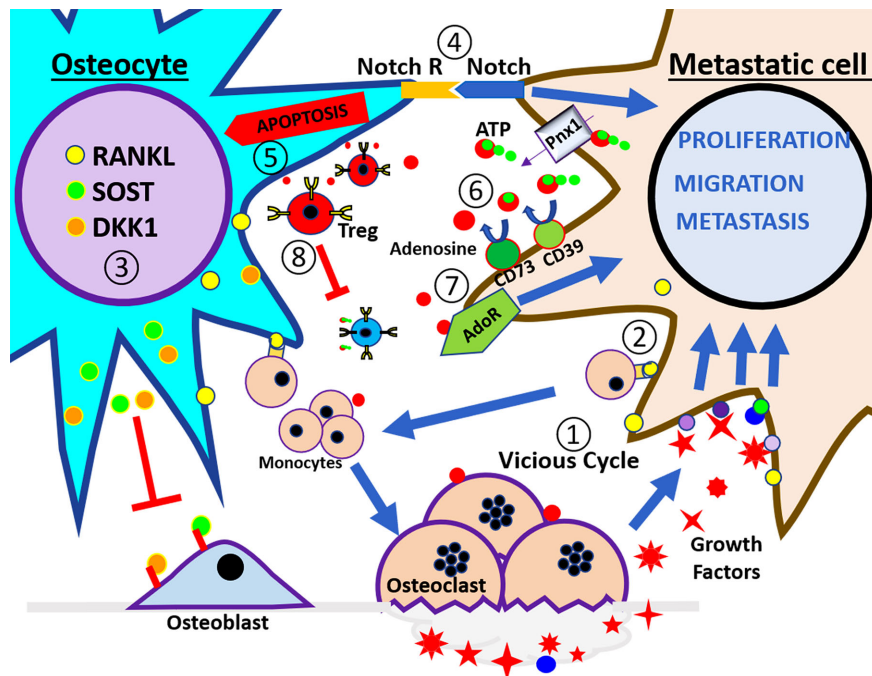


FIGURE 1 | Schematic illustration of tumor microenvironment in the bone. At the left side of the panel is the osteocyte and the right side is the breast cancer cell. These cells interact in a bone catabolic environment. The numbers indicate the steps of events that may happen during breast metastasis described in the review. ① The vicious cycle; cancer cells interact with monocytes to increase the osteoclast number and activity in order to release growth factors embedded in the bone. ② RANKL expressed by osteocytes and cancer cells increases the recruitment of monocytes and stimulates the osteoclast differentiation. ③ Under this condition osteocytes increase the release of Sost and DKK1 that inhibit osteoblast activity and increase the expression of RANKL. ④ Notch signaling pathway induces apoptosis in the osteocytes and increases the proliferation of cancer cells. ⑤ Osteocytes apoptosis signals promote osteoclasts for bone resorption. ⑥ eATP is hydrolyzed to adenosine through CD39/CD73 enzyme activation, and generated adenosine activates adenosine receptor in cancer cells, leading to increased proliferation, migration, and metastasis. ⑦ Extracellular adenosine increases osteoclast activity, ⑧ also promotes Treg activity, and increases immune tolerance.

24), soluble intercellular adhesion molecule 1 (ICAM-1) (25), Wnt molecules (26, 27), macrophage-stimulating protein (MSP) (28), and extracellular adenosine (**Figure 1**, step ③) (29).

Although crucial to bone metastasis and creating the metastatic niche, osteoclasts are not the only cell type to participate in bone metastasis, and osteoblasts also play a vital role. Osteoblasts participate in matrix mineralization, which provides strength (hardness) to the bone (30). Osteoblasts are derived from skeletal bone marrow stromal cells that differentiate into preosteoblasts and secrete numerous factors, including RANKL that directly impact osteoclastogenesis (**Figure 1**, step ③) (30). These cells eventually differentiate into mature osteoblasts, which secrete the mineral matrix proteins and mineralize bone (30). Some osteoblasts may become bone lining cells or become embedded in lacunae where they differentiate into fully mature mechanosensing osteocytes (1, 30). While studies show osteoclasts can induce tumor proliferation by releasing growth factors stored within the mineral matrix, osteoblast activity has been associated with tumor cell growth and tumor cell dormancy. Preosteoblasts and osteoblasts express tumor-promoting osteoprotegerin (OPG) (31), hepatocyte growth factor (HGF), and secrete connective tissue growth factor (CTGF) and TGF β (22). Furthermore, osteoblasts express IL-6, which increases osteoclastogenesis, and

has been shown to drive proliferation of multiple myeloma plasma cells (24, 32).

Tumor–osteoblast interactions have been shown to be critical in establishing bone metastasis (33, 34). Circulating (prostate) metastatic cells have been shown to have an affinity for the bone endosteal surface where they interact with osteoblasts through annexin2/annexin2 receptor interactions (33, 34). These micro-metastases are formed in regions of new bone formation, where differentiating and actively mineralizing osteoblasts are located. Furthermore, osteoblast and breast tumor interaction is shown to require adherent junction formation for tumor cell proliferation (9), supporting the notion that factors produced during osteogenesis promote cancer proliferation. Disseminated cancer cells must also compete for the endosteal surface of the bone, a niche occupied by non-proliferating long-term hematopoietic stem cells (LT-HSCs) (**Figure 2**, step ①). The mechanisms of cell cycle arrest of breast cancer cells once established in the endosteal niche are likely the same mechanisms that induce the non-proliferating status of long-term resident hematopoietic stem cells, unfortunately, only to later escape dormancy and proliferate (35, 36). In one study using a 3D co-culture model (osteoblast/breast cancer), it was identified that the addition of bone remodeling cytokines, tumor necrosis factor (TNF)- α and interleukin (IL)-1 β and tumor necrosis factor resulted in

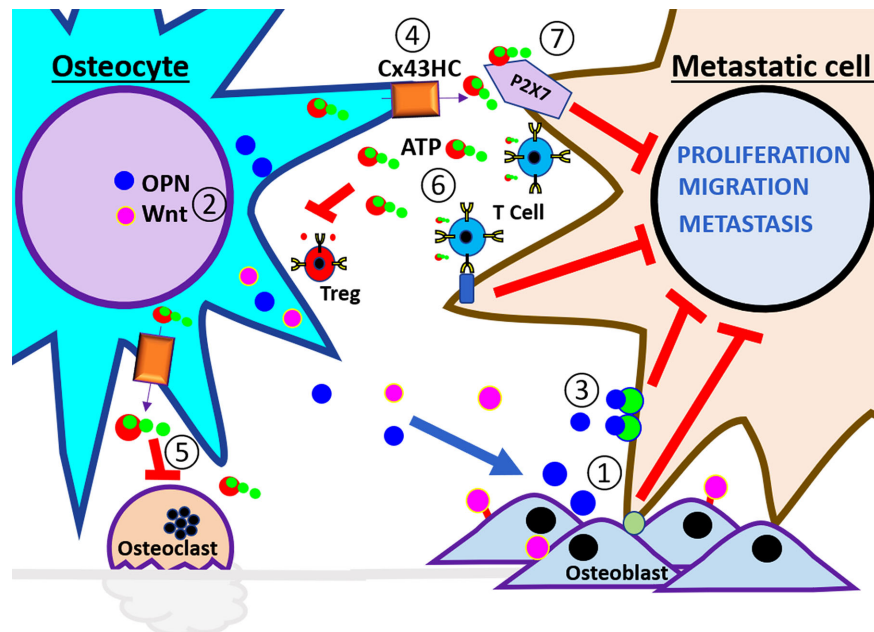


FIGURE 2 | Schematic illustration of anti-tumor microenvironment in the bone. At the left side of the panel are the osteocytes and the right side are the breast cancer cells. These cells interact in a healthy bone environment. The numbers indicate the steps of events that may happen during breast metastasis described in the review. ① The interaction of metastatic cells with osteoblast promotes dormancy. ② Physiological level of mechanical loading stimulates osteocyte release of anabolic factors, Wnt, and OPN, to increase osteoblast differentiation, activity, and bone strength. ③ High concentration of OPN reduces EMT in metastatic cells. ④ Mechanical loading increases opening of Cx43 hemichannels and the release of ATP. ⑤ eATP inhibits osteoclast activity and ⑥ also inhibits Treg formation and stimulates immune surveillance. ⑦ eATP activates P2X receptor and reduces the proliferation, migration, and metastatic potential of cancer cells.

increased proliferation in the breast cancer cell line MDA-MB-231 BMRS1 (37). The inhibition of $\text{TNF-}\alpha$ and $\text{IL-1}\beta$ downstream targets, cyclooxygenase (COX) and PGE2 receptors, resulted in decreased cancer cell proliferation (37). Moreover, osteoblasts and osteocytes also secrete leukemia inhibitory factor (LIF), and the activation of LIF receptors present in breast cancer cells is shown to maintain them in a dormant state. Loss of LIFR resulted in decreased expression of genes associated with cell dormancy. LIFR knockdown increased cancer cell migration and invasion, proliferation, and osteoclastogenesis. Interestingly, overexpression of PTHrP also decreased LIFR signaling. (38).

An early study by Kobayashi et al. found bone stromal cells induced dormancy by the release of bone morphogenic protein 7 (BMP7) and activation of prostate BMP receptor 2. BMP7-treated prostate cancer cells resulted in activated p38 MAPK, increased expression of p21 and the metastasis suppressor gene, NDRG1 (N-myc downstream-regulated gene 1) (39). Key studies have given further insight into the mechanisms in which osteoblasts may induce dormancy in disseminated tumor cells (40, 41). In another study, osteoblast conditioned media increased cellular quiescence of prostate cancer cells. TGF- β 2 and growth differentiation factor (GDF)10 were identified as osteoblast secretory factors that induced quiescence in several prostate cancer cell lines. The binding of these factors to the TGF- β RIII receptor expressed in prostate cancer cell lines activated (phosphorylation at Thr180/Tyr182) p38 mitogen activated protein kinase (MAPK). Activated p38-MAPK phosphorylation of downstream target retinoblastoma

protein (Rb) resulted in the inhibition of cancer cell-cycle progression (40). In another study of prostate cancer metastasis to the bone, Yumoto et al. identified osteoblast-derived ligand growth arrest specific 6 (GAS6) and the tumoral tyrosine kinase receptor Axl as required for the TGF- β 2-induced response towards prostate cancer cell dormancy (41). Multiple myeloma cells have also been shown to be affected by the bone microenvironment. These cells can occupy the endosteal niche, remain dormant, and escape therapies that largely target dividing cells. The interaction of multiple myeloma cells with cells of osteoblastic lineage along the endosteal bone surface was associated with single, non-dividing tumor cells. Interestingly, dormant myeloma cells that were insensitive to melphalan, a chemotherapeutic agent, could be reactivated upon osteoclast activation with the soluble form of RANKL (42).

The bone is home to the hematopoietic system, and it integrates an assortment of systemic physiological signals. Bone homeostasis is affected directly or indirectly by many pathological conditions, including diabetes, gastrointestinal diseases, physical stress, etc. (43–48). One example is the increased risk of cancer and tumor growth under inflammatory conditions (32, 49) or the propensity of cells metastasizing to fractures sites (50). Similar correlations have been associated with surgical procedures (51–53), which intrinsically induce trauma, inflammation, and an increase in innate immune cells needed for tissue repair. These responses have been shown to promote conditions conducive to metastatic growth at non-surgical sites (51, 53).

Bone, like other organs, changes with age, which includes an accumulation of senescent cells, such as, osteoblasts, and resident bone cells harboring genetic mutations (54–56). The loss of bone density with age is well known. Equally concerning is how the accumulated damage to cells and their genetic makeup, caused by environmental toxins, or byproducts of cellular respiration, can result in an environment primed for tumor growth and metastasis (57). How does an increase in senescent bone cells affect certain cancers metastasizing to the bone, or dormant cells in the bone being released from dormancy? As discussed here and shown in numerous studies, senescent osteoblasts can promote osteoclastogenesis, which leads to increased metastasis, dissemination, and metastatic growth of cancer in the bone. This supports and explains the possible mechanisms in which elder cancer patients in remission with dormant cancer cells in the bone often relapse. A possible underlying reason is that cancer cells can take residence in the bone through the contribution of senescent cells accumulated over time (42, 58). An important detail to keep in mind is that most experimental studies have not used aged animal models (59, 60). Studies delving into how age affects metastasis are in dire need.

Bone impacts metastasis in unexpected and sometimes complex manners. Mechanical loading inhibits secondary growth and osteolytic capability of metastatic tumors in nude mice by modulating osteoblastic/osteoclastic activities and communication between osteocytes and tumor cells (61). Osteocytic release of osteopontin (OPN) (Figure 2, step ②), a secreted phosphoprotein with a high avidity to bone mineral matrix, has been reported to induce activators of the EMT process (62). Interestingly, lower OPN levels (0.1 to 0.5 µg/ml) induce EMT markers. Low levels of mechanical loading (1 N) are shown to increase the expression and secretion of OPN (Fan, 2020 #82). The increase in OPN in turn inhibits the expression of TGF-β in osteocytes, increases the adhesion of tumoral cells, thus possibly inhibiting growth and migration by anchoring tumor cells at the primary site. This bone microenvironmental condition is pro-mesenchymal to epithelial transition (MET) reducing the aggressiveness and allowing the settlement of secondary tumor (Figure 2, step ③) (63). Similar intensities of mechanical loading inhibiting tumor growth in nude mice have been previously reported (61). As studies have shown, high loading intensity of the bone enhances breast cancer cell malignancy; therefore, the extent of mechanical loading should be carefully monitored (63). Taken together, studies indicate osteocytes are an important player in providing the ‘soil’ for bone metastasis/progression as well as associated skeletal diseases (27, 64–66).

INTRICATE FUNCTION OF OSTEOCYTES IN BONE HOMEOSTASIS AND CANCER BONE METASTASIS

The extensive lacuna–canaliculi network allows osteocytes to directly communicate with one another. It also allows for osteocytes to respond to local and distant signals, including

mechanical (bone stress) or biological (paracrine and endocrine) (1, 67). Osteocytes control bone remodeling through regulation of bone-forming and bone-destroying cells. During bone demineralization, osteocytes decrease osteoblast differentiation and function through secreted factors, including the Wnt signaling antagonists sclerostin and Dickkopf Wnt signaling pathway inhibitor 1 (DKK1) (67). Osteocytes are the main sclerostin producer in the bone, and this protein inhibits the association of Wnt ligands with their receptor in osteocytes and osteoblast. Therefore, the key bone formation inhibitor, sclerostin, has been given much attention as a targeted therapeutic approach for low bone density (66, 68). Bone RANKL is primarily produced by osteocytes (Figure 1, step ③). RANKL promotes monocyte differentiation into bone resorbing osteoclasts. Neutralization of RANKL with the antibody Denosumab is currently in use to reduce fracture incidence in low bone density, bone metastasis, and rare bone cancers (Figure 3, step ①) (69, 70). The Denosumab Clinical trial (ABCSG-18) showed that postmenopausal breast cancer patients under aromatase inhibitor treatment had a significant latency of apparition of bone fracture with Denosumab as an adjuvant (71). This was also true in metastatic breast cancers and new primary malignancies.

In contrast, in a clinical trial (D-CARE study) of patients with stage II/III breast cancer, Denosumab treatment did not improve bone metastasis free survival. Denosumab did increase the incidence of osteonecrosis of the jaw (5 *versus* <1%) and hypocalcaemia (7 *versus* 4%) in comparison with placebo (72). Although the above mentioned trials do not corroborate Denosumab having a beneficial effect on survival, the results obtained from these two trials have a significant difference. The D-care trial patient profile was of early stage high risk breast cancer patients, while the ABCSC-18 study focused on early stage low risk breast cancer patients. It is also important to note the trials were conducted with different Denosumab schedules and endpoints (70).

As mentioned above, bones inevitably age and undergo numerous changes, including bone loss, osteocyte apoptosis, and increased oxidative stress. Osteocyte apoptosis is a key stimulus that triggers bone resorption (Figure 1, step ⑤) (73, 74). The slowed production of sex hormones that comes with aging promotes osteoclast activity (75, 76), osteocyte apoptosis (73), elevated oxidative stress (76, 77), and a reduction in osteoblast function (78). Thus, reduction in sex hormones culminates in bone fragility and bone loss. This bone destructive environment is further enhanced by a decline in immune surveillance and increased fat formation; this disturbs the balance of critical osteoclastogenic proteins, RANKL, and OPG, towards bone destruction (79). The AZURE phase 3 clinical trial for post-menopausal women was designed to study the effects of adjuvant zoledronic acid treatment in early high risk breast cancer patients. The AZURE trial showed that with treatment, incidence of bone metastasis was reduced. Critical to our understanding, this benefit was restricted to postmenopausal women and those under ovarian suppression treatments with hormone-receptor-positive breast cancer. This

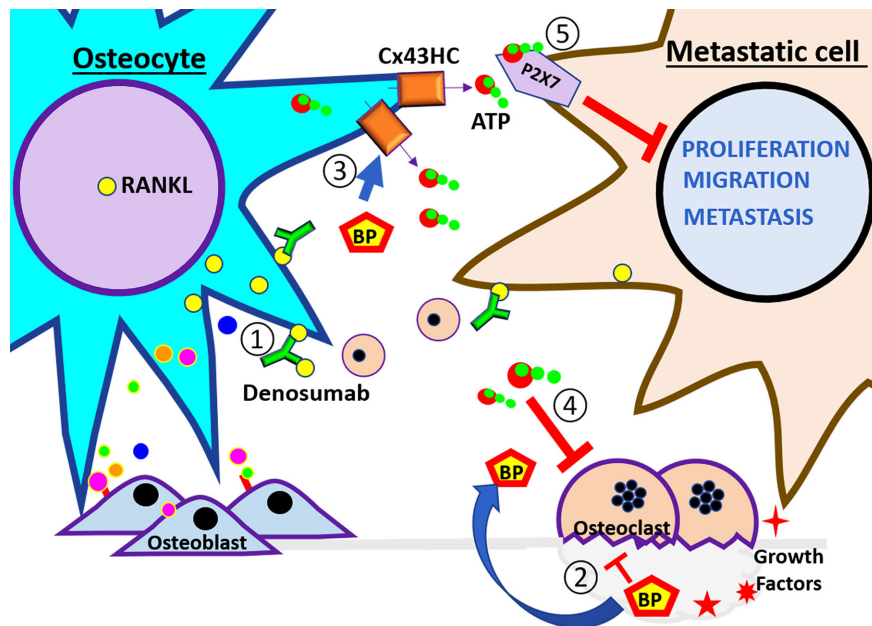


FIGURE 3 | Schematic illustration of therapeutic agents used to treat bone metastasis. At the left side of the panel are the osteocytes and the right side are the breast cancer cells. These cells are subjected to the therapeutic treatment under the bone environment. The numbers indicate the steps of events that may happen during breast metastasis described in the review. ① Denosumab, a RANKL neutralizing antibody, binds RankL expressed by osteocytes and cancer cells, and inhibits the recruitment of monocytes and osteoclast differentiation. ② Bisphosphonates (BPs) inhibit osteoclast activity. Also, ③ BP increases osteocyte survival and induces opening of Cx43 hemichannels and the release of ATP. ④ eATP inhibits osteoclast activity. ⑤ eATP activates P2X7 receptor and reduces the proliferation, migration, and metastatic potential of cancer cells. The effects of the pharmacological agents reduce the activity of the vicious cycle.

observation highlights how critical it is to understand the differences between old and young bones in metastasis (80, 81).

Emerging studies indicate how osteocytes could have a positive impact on tumor growth, motility, and survival, a scenario leading to poor outcomes in cancer patients. The interaction between prostate cancer cells and osteocytes induces the osteocytic production and release growth-derived factor 15 (GDF15) promoting prostate cancer cell proliferation, migration, and invasion of prostate cell in the bone (82). MLO-Y4 osteocytes stimulated by hydrostatic pressure, similar to what is observed in bone metastasis, increased the viability of prostate, breast, and lung cancer cell lines. Hydrostatic pressure also improved motile and invasive capacity through increased expression of chemokine (C-C motif) ligand 5 (CCL5, also known as RANTES) and MMPs (83). Likewise, high intensity shear stress increased survival and migration in the MDA-MBA-231 breast cancer cell line (63, 84). However, these studies also show how intensity of load impacts opposing effects on survival and migration. This underscores the importance of osteocytes in the modulation of the bone microenvironment with regard to tumor progression particularly with respect to the relationship between the magnitude of mechanical stimulation and breast cancer cell apoptosis or migration (84).

Increased osteocyte apoptosis within lytic bone lesions has been found in patients with multiple myeloma (85). During the progression of multiple myeloma, osteocytes directly interact with multiple myeloma cells, which stimulate osteocytes to produce

sclerostin and RANKL. This results in the recruitment of osteoclast precursors and a reduction of Wnt signaling, leading to the inhibition of osteoblast differentiation (**Figure 1**, step ③). Concomitantly, cell to cell interactions reduce osteocyte viability due to apoptosis triggered Notch signaling and sustained by multiple myeloma derived $\text{TNF}\alpha$. Furthermore, Notch signaling interaction increases the proliferation of multiple myeloma by increasing cyclin D1 RNA levels and accelerating cell proliferation (**Figure 1**, step ④) (27). This highlights how osteocytes play a constant integrative role of endocrine, paracrine, and mechanical signals, and the output of those signals results in bone formation or resorption responses. The complexity of such integration makes it particularly difficult to predict the impact of osteocytes on cancer cells metastasized to the bone.

PROTECTIVE ROLES OF OSTEOCYTES AGAINST CANCER BONE METASTASIS

The skeleton is a dynamic organ that responds to physical stress by promoting bone remodeling, which includes the addition and removal of bone. Although several resident bone cells are involved in mechanosensing, osteocytes are regarded as the major mechanosensory cell within the bone (67, 86). The long dendritic processes of osteocytes form gap junction channels composed primarily by gap junction proteins (connexins). These

gap junction networks connect not only neighboring osteocytes, but also cells on the bone surface, including osteoblasts and osteoclasts (1, 67). The mechanosensing osteocytes form connexin 43 (Cx43) hemichannels (half a gap junction channel) which allows for the communication between the internal environment of the cell and its extracellular environment. Gap junction channels are involved in the global regulation and fine tuning of bone formation and resorption as it was evidenced by the altered levels of serum remodeling markers N-terminal propeptide of type I procollagen and C-terminal telopeptide of type I collagen, respectively (87). Osteocyte hemichannels likely play a predominant role in its response to mechanical stimulation; given that bone and osteocytes are constantly subjected to mechanical stimuli as a result of physical movement, gravity, and blood circulation. This is evident by the major impact that Cx43 hemichannels have on the expression of OPG and RANKL, and osteocyte viability, which are essential for bone integrity and longevity (87, 88). Concordantly, the anti-apoptotic effect of bisphosphonates on osteoblasts and osteocytes has been shown to be through regulation of Cx43 hemichannels (**Figure 3**, step ③) (89). Bisphosphonates are the gold standard for therapy for bone diseases in cancer patients (6, 80) as they inhibit osteoclast activity and prevent bone loss induced by cancer cells, thus reducing fracture risk (21, 28). *In vivo*, osteocyte Cx43 hemichannel activity is an important mediator of the growth inhibitory effects of bisphosphonates in breast cancer (65). *In vitro* and *in vivo* studies by our group further underscore the key role of Cx43 in mediating the tumor inhibitory effects of bisphosphonates. Bisphosphonate conditioned media from osteocytes inhibited breast cancer cell growth (MDA-MB-231), migration, and invasion. These effects were abrogated by treating with Cx43 hemichannel specific blocking antibody (65). Moreover, mice with impaired Cx43 gap junctions and hemichannels showed significantly increased tumor burden and a reduced effect of bisphosphonates on tumor growth compared to mice with impaired Cx43 gap junction channel function or wild type (65). This implies Cx43 hemichannels in osteocytes are responsive to bisphosphonates, thus making Cx43 a promising novel drug target for the treatment of breast cancer metastasis to the bone. In a previous study, we have shown that these effects are mediated by adenosine triphosphate (ATP) released by osteocyte Cx43 hemichannel opening (**Figure 2**, steps ④ and ⑦) (**Figure 3**, steps ③ and ④) (90). These important findings highlight that more work is needed to determine exactly how osteocytes impact various cancers metastatic potential, and if these cells can be targeted to stop bone metastasis.

ATP RELEASE BY OSTEOCYTES, A KEY COMPONENT FOR THE HOSTILE MICROENVIRONMENT FOR CANCER

As a response to tissue damage and cellular stress, cells, including osteocytes, secrete/release ATP to the extracellular space (**Figure 2**, step ④) (65, 91, 92). The intracellular concentration of ATP is

~3–10 mM, and the extracellular ATP (eATP) is about 10 nM. The big difference between intracellular and extracellular ATP is from active ATP degradation through ectonucleotidases in the extracellular compartment (93). The presence of eATP has been shown to inhibit the growth of pancreatic, colon, prostate, breast, liver, ovarian, colorectal, esophageal, melanoma, and leukemia (94). Intravenous ATP used in clinical trials of patients with pre-terminal lung cancer, showed an increase in survival rate and had a beneficial effect on weight and muscle strength (95–97). Multiple studies show an anticancer action of eATP or eATP analogs by binding to P2 purinergic receptors (90, 98). eATP is rapidly degraded to adenosine, a well-known tumorigenic factor (92, 93, 99). Additionally, eATP or P2 receptor agonist decreases osteoclast activity and bone resorption (**Figure 2**, step ⑤) (100), reduces the number of T regulatory lymphocytes (Tregs) (101), and prolongs the activity of T lymphocytes (**Figure 2**, step ⑥) (102). However, ATP metabolites through P1 purinergic receptor activation also mediate pro-tumorigenic effects in prostate and breast cancer cells (90, 103). This suggests that ATP and/or ATP metabolite balance plays a key role in the tumor microenvironment. The solid tumor microenvironment is usually hypoxic and/or inflammatory, and the extracellular concentration of nucleotides (ATP/adenosine) is higher in comparison to normal tissue (92, 103, 104). In this hypoxic/inflammatory microenvironment, adenosine promotes cancer cell migration and chemotaxis in breast cancer and melanoma cells, along with an increase in osteoclastic activity and bone resorption (**Figure 1**, ⑥ and ⑦) (29). This microenvironment also results in poor immune surveillance with high lymphocytic tolerance (**Figure 1**, steps ⑥ and ⑧) (92, 105, 106). The main pathway leading to high extracellular adenosine levels is the hydrolysis of eATP by a family of enzymes known as ectonucleotidases, such as CD39 and CD73, which hydrolyze ATP and ADP to AMP, and AMP further to adenosine (**Figure 1**, step ⑥) (93, 105). CD73 has been associated with a pro-metastatic phenotype in breast cancer, and CD73 knockdown leads to suppression of breast cancer cell growth, migration, and invasion both *in vivo* and *in vitro* (105). Therefore, we must practice caution since the function of eATP on tumorigenesis could largely depend on the activity of ecto-ATPases in the tissue.

Adenosine and ATP bind to specific purinergic receptors at the cell surface, which are divided into P1 receptors, with adenosine as the main ligand, and P2 receptors, with ATP and ADP as the main agonists. P1 receptors have four subtypes: A1, A2a, A2b, and A3. There are two major P2 receptor subtypes, seven P2X, and eight P2Y subtypes (92, 107). The presence of P2Y subtypes has been shown to play important roles in cell survival under mechanical stress, although the role of specific P2X subtypes remains unclear. It has been suggested that autocrine activation of breast cancer P2X7 receptors participates in the activation of cell proliferation, cancer cell process elongation, and further ATP release (99). The tumor microenvironment rich in ATP is shown to either promote or inhibit cell migration, enough to activate multiple P2 receptors, but not enough to induce cell death through P2X7 activation. The study by Zhou et al. provides

clues to clarify the mixed effects of ATP. They showed that the addition of a non-hydrolysable P2X receptor agonist resulted in an inhibitory effect on cancer cell migration and growth. This inhibitory effect was dependent on P2X7 activation (**Figure 2**, step ⑦) (**Figure 3**, step ⑤) (90). A2A receptor activation, on the other hand, resulted in a stimulatory effect on breast cancer cell migration and growth (**Figure 1**, step ⑦) (90). Cancer cell-specific expression of P1 receptor subtypes has been reported, for example, in breast cancer. A2b receptors are absent on ER-positive MCF-7 cells, whereas MDA-MB-231 cells express very high levels of A2b (90). In order to understand and establish strategies to control tumor growth and metastasis, it is very important to evaluate the presence and expression levels of the specific P1 or P2 receptor subtypes in cancer cells. These are likely key factors determining if a cellular response to adenosine nucleotides will be elicited.

CONCLUSION AND FUTURE DIRECTIONS

The osteocyte is a key player modulating the bone cancer microenvironment. Metastatic cancer cells have shown the potential to utilize osteocyte signaling by turning the bone microenvironment osteoclastogenic and transforming osteocytes into pro-tumorigenic cells. Moreover, osteocytic overproduction of Wnt inhibitors contributes to the suppression of bone formation. In addition, metastatic cancer cells colonized in the bone reduce osteocyte viability, resulting in reduced cell capacity to maintain bone homeostasis. However, the bone forming ability of osteocytes is related with an anti-resorptive microenvironment. This condition reduces osteocyte apoptosis, enhances Cx43 hemichannel activity, increases bone strength, and reduces osteoclast recruitment and activity. Taken together, these osteoclast activities will inhibit the overall

activation of metastatic dormant cells, and tumor growth, and motility. Although we have just started a fascinating journey to understand the functional relationship between cancer and osteocytes, targeting osteocyte signaling pathways and molecular messengers has already shown to have a positive impact on preventing/improving bone pathologies associated with cancers. These results offer encouraging and supportive ideas of a targeted approach on osteocytes that reside in the cancer niche. These studies may offer guidance and a map to develop new therapies for cancers metastasized to bone, or the prevention thereof.

In conclusion, osteocytes play a large role as gate keepers of the bone and bone homeostasis. By having a broader knowledge on how osteocytes influence cancer cells, osteoblasts, and osteoclasts, we may improve and increase pharmacological strategies to help keep the bone healthy and free of cancer. Further work is needed to uncover key events and players that coordinate the communication between cancer cells and bone cells. The goal is to identify target points that can disrupt the initial and key steps of bone metastasis. Osteocytes may prove to be a key ally in combating cancer cell progression in the bone.

AUTHOR CONTRIBUTIONS

All authors contributed to the article and approved the submitted version.

FUNDING

JJ was supported by the US National Institutes of Health grant CA196214, US Department of Defense grant BC161273, and Welch Foundation grant AQ-1507.

REFERENCES

1. Bonewald LF. The amazing osteocyte. *J Bone Mineral Res* (2011) 26:229–38. doi: 10.1002/jbmr.320
2. Buenrosto D, Mulcrone PL, Owens P, Sterling JA. The Bone Microenvironment: a Fertile Soil for Tumor Growth. *Curr Osteoporos Rep* (2016) 14:151–8. doi: 10.1007/s11914-016-0315-2
3. Chin H, Kim J. Bone Metastasis: Concise Overview. Federal practitioner : for the health care professionals of the VA. *DoD PHS* (2015) 32:24–30.
4. Moore DD, Luu HH. Osteosarcoma. *Cancer Treat Res* (2014) 162:65–92. doi: 10.1007/978-3-319-07323-1_4
5. de Azevedo JWV, de Medeiros Fernandes TAA, Fernandes JV Jr., de Azevedo JCV, Lanza DCF, Bezerra CM, et al. Biology and pathogenesis of human osteosarcoma. *Oncol Lett* (2020) 19:1099–116. doi: 10.3892/ol.2019.11229
6. Terpos E, Berenson J, Raje N, Roodman GD. Management of bone disease in multiple myeloma. *Expert Rev Hematol* (2014) 7:113–25. doi: 10.1586/17474086.2013.874943
7. Minnie SA, Hill GR. Immunotherapy of multiple myeloma. *J Clin Invest* (2020) 130:1565–75. doi: 10.1172/JCI129205
8. Hernandez RK, Wade SW, Reich A, Piroli M, Liede A, Lyman GH. Incidence of bone metastases in patients with solid tumors: analysis of oncology electronic medical records in the United States. *BMC Cancer* (2018) 18:44. doi: 10.1186/s12885-017-3922-0
9. Wang H, Yu C, Gao X, Welte T, Muscarella AM, Tian L, et al. The osteogenic niche promotes early-stage bone colonization of disseminated breast cancer cells. *Cancer Cell* (2015) 27:193–210. doi: 10.1016/j.ccell.2014.11.017
10. Liu Y, Cao X. Characteristics and Significance of the Pre-metastatic Niche. *Cancer Cell* (2016) 30:668–81. doi: 10.1016/j.ccell.2016.09.011
11. Kwakwa KA, Sterling JA. Integrin alphavbeta3 Signaling in Tumor-Induced Bone Disease. *Cancers* (2017) 9. doi: 10.3390/cancers9070084
12. Pecheur I, Peyruchaud O, Serre CM, Guglielmi J, Volland C, Bourre F, et al. Integrin alpha(v)beta3 expression confers on tumor cells a greater propensity to metastasize to bone. *FASEB J* (2002) 16:1266–8. doi: 10.1096/fj.01-0911fje
13. Weidle UH, Birzele F, Kollmorgen G, Ruger R. Molecular Mechanisms of Bone Metastasis. *Cancer Genomics Proteomics* (2016) 13:1–12. doi: 10.21873/cgp.20004
14. Cox TR, Rumney RMH, Schoof EM, Perryman L, Hoye AM, Agrawal A, et al. The hypoxic cancer secretome induces pre-metastatic bone lesions through lysyl oxidase. *Nature* (2015) 522:106–10. doi: 10.1038/nature14492
15. Walker C, Mojares E, Del Rio Hernández A. Role of Extracellular Matrix in Development and Cancer Progression. *Int J Mol Sci* (2018) 19. doi: 10.3390/ijms19103028

16. Monteiro AC, Leal AC, Gonçalves-Silva T, Mercadante AC, Kestelman F, Chaves SB, et al. T cells induce pre-metastatic osteolytic disease and help bone metastases establishment in a mouse model of metastatic breast cancer. *PLoS One* (2013) 8:e68171. doi: 10.1371/journal.pone.0068171
17. Wu MY, Li CJ, Yang GT, Cheng YL, Tsai AP, Hou YT, et al. Molecular Regulation of Bone Metastasis Pathogenesis. *Cell Physiol Biochem Int J Exp Cell Physiol Biochem Pharmacol* (2018) 46:1423–38. doi: 10.1159/000489184
18. Chen YC, Sosnoski DM, Mastro AM. Breast cancer metastasis to the bone: mechanisms of bone loss. *Breast Cancer Res BCR* (2010) 12:215. doi: 10.1186/bcr2781
19. Pellegatti P, Falzoni S, Donvito G, Lemaire I, Di Virgilio F. P2X7 receptor drives osteoclast fusion by increasing the extracellular adenosine concentration. *FASEB J* (2011) 25:1264–74. doi: 10.1096/fj.10-169854
20. Kearns AE, Khosla S, Kostenuik PJ. Receptor activator of nuclear factor kappaB ligand and osteoprotegerin regulation of bone remodeling in health and disease. *Endocr Rev* (2008) 29:155–92. doi: 10.1210/er.2007-0014
21. Gralow J, Tripathy D. Managing metastatic bone pain: the role of bisphosphonates. *J Pain Symptom Manage* (2007) 33:462–72. doi: 10.1016/j.jpainsymman.2007.01.001
22. Kang Y, Siegel PM, Shu W, Drobnjak M, Kakonen SM, Cordon-Cardo C, et al. A multigenic program mediating breast cancer metastasis to bone. *Cancer Cell* (2003) 3:537–49. doi: 10.1016/S1535-6108(03)00132-6
23. Soki FN, Park SI, McCauley LK. The multifaceted actions of PTHrP in skeletal metastasis. *Future Oncol (Lond Engl)* (2012) 8:803–17. doi: 10.2217/fon.12.76
24. Weilbaecher KN, Guise TA, McCauley LK. Cancer to bone: a fatal attraction. *Nat Rev Cancer* (2011) 11:411–25. doi: 10.1038/nrc3055
25. Ell B, Mercatali L, Ibrahim T, Campbell N, Schwarzenbach H, Pantel K, et al. Tumor-induced osteoclast miRNA changes as regulators and biomarkers of osteolytic bone metastasis. *Cancer Cell* (2013) 24:542–56. doi: 10.1016/j.ccr.2013.09.008
26. Colombo M, Thummler K, Mirandola L, Garavelli S, Todoerti K, Apicella L, et al. Notch signaling drives multiple myeloma induced osteoclastogenesis. *Oncotarget* (2014) 5:10393–406. doi: 10.18632/oncotarget.2084
27. Delgado-Calle J, Anderson J, Gregor MD, Hiasa M, Chirgwin JM, Carlesso N, et al. Bidirectional Notch Signaling and Osteocyte-Derived Factors in the Bone Marrow Microenvironment Promote Tumor Cell Proliferation and Bone Destruction in Multiple Myeloma. *Cancer Res* (2016) 76:1089–100. doi: 10.1158/0008-5472.CAN-15-1703
28. Andrade K, Fornetti J, Zhao L, Miller SC, Randall RL, Anderson N, et al. RON kinase: A target for treatment of cancer-induced bone destruction and osteoporosis. *Sci Trans Med* (2017) 9. doi: 10.1126/scitranslmed.aai9338
29. Knowles HJ. The Adenosine A2B Receptor Drives Osteoclast-Mediated Bone Resorption in Hypoxic Microenvironments. *Cells* (2019) 8. doi: 10.3390/cells8060624
30. Dirckx N, Moorer MC, Clemens TL, Riddle RC. The role of osteoblasts in energy homeostasis. *Nat Rev Endocrinol* (2019) 15:651–65. doi: 10.1038/s41574-019-0246-y
31. Weichhaus M, Chung ST, Connelly L. Osteoprotegerin in breast cancer: beyond bone remodeling. *Mol Cancer* (2015) 14:117. doi: 10.1186/s12943-015-0390-5
32. Tawara K, Oxford JT, Jorcyk CL. Clinical significance of interleukin (IL)-6 in cancer metastasis to bone: potential of anti-IL-6 therapies. *Cancer Manage Res* (2011) 3:177–89. doi: 10.2147/CMAR.S18101
33. Shiozawa Y, Havens AM, Jung Y, Ziegler AM, Pedersen EA, Wang J, et al. Annexin II/annexin II receptor axis regulates adhesion, migration, homing, and growth of prostate cancer. *J Cell Biochem* (2008) 105:370–80. doi: 10.1002/jcb.21835
34. Shiozawa Y, Pedersen EA, Havens AM, Jung Y, Mishra A, Joseph J, et al. Human prostate cancer metastases target the hematopoietic stem cell niche to establish footholds in mouse bone marrow. *J Clin Invest* (2011) 121:1298–312. doi: 10.1172/JCI43414
35. Capulli M, Hristova D, Valbret Z, Carys K, Arjan R, Maurizi A, et al. Notch2 pathway mediates breast cancer cellular dormancy and mobilisation in bone and contributes to haematopoietic stem cell mimicry. *Br J Cancer* (2019) 121:157–71. doi: 10.1038/s41416-019-0501-y
36. Widner DB, Park SH, Eber MR, Shiozawa Y. Interactions Between Disseminated Tumor Cells and Bone Marrow Stromal Cells Regulate Tumor Dormancy. *Curr Osteoporos Rep* (2018) 16:596–602. doi: 10.1007/s11914-018-0471-7
37. Sosnoski DM, Norgard RJ, Grove CD, Foster SJ, Mastro AM. Dormancy and growth of metastatic breast cancer cells in a bone-like microenvironment. *Clin Exp Metastasis* (2015) 32:335–44. doi: 10.1007/s10585-015-9710-9
38. Johnson RW, Finger EC, Olcina MM, Vilalta A, Aguilera T, Miao Y, et al. Erratum: Induction of LIFR confers a dormancy phenotype in breast cancer cells disseminated to the bone marrow. *Nat Cell Biol* (2016) 18:1260. doi: 10.1038/ncb3433
39. Kobayashi A, Okuda H, Xing F, Pandey PR, Watabe M, Hirota S, et al. Bone morphogenetic protein 7 in dormancy and metastasis of prostate cancer stem-like cells in bone. *J Exp Med* (2011) 208:2641–55. doi: 10.1084/jem.20110840
40. Yu-Lee LY, Yu G, Lee YC, Lin SC, Pan J, Pan T, et al. Osteoblast-Secreted Factors Mediate Dormancy of Metastatic Prostate Cancer in the Bone via Activation of the TGFβRIII-p38MAPK-pS249/T252RB Pathway. *Cancer Res* (2018) 78:2911–24. doi: 10.1158/0008-5472.CAN-17-1051
41. Yumoto K, Eber MR, Wang J, Cackowski FC, Decker AM, Lee E, et al. Axl is required for TGF-β2-induced dormancy of prostate cancer cells in the bone marrow. *Sci Rep* (2016) 6:36520. doi: 10.1038/srep36520
42. Lawson MA, McDonald MM, Kovacic N, Hua Khoo W, Terry RL, Down J, et al. Osteoclasts control reactivation of dormant myeloma cells by remodelling the endosteal niche. *Nat Commun* (2015) 6:8983. doi: 10.1038/ncomms9983
43. Botolin S, McCabe LR. Bone loss and increased bone adiposity in spontaneous and pharmacologically induced diabetic mice. *Endocrinology* (2007) 148:198–205. doi: 10.1210/en.2006-1006
44. Burghardt AJ, Issever AS, Schwartz AV, Davis KA, Masharani U, Majumdar S, et al. High-resolution peripheral quantitative computed tomographic imaging of cortical and trabecular bone microarchitecture in patients with type 2 diabetes mellitus. *J Clin Endocrinol Metab* (2010) 95:5045–55. doi: 10.1210/jc.2010-0226
45. Vestergaard P. Discrepancies in bone mineral density and fracture risk in patients with type 1 and type 2 diabetes—a meta-analysis. *Osteoporos Int J established as result cooperation between Eur Foundation Osteoporos Natl Osteoporos Foundation USA* (2007) 18:427–44. doi: 10.1007/s00198-006-0253-4
46. Zong JC, Wang X, Zhou X, Wang C, Chen L, Yin LJ, et al. Gut-derived serotonin induced by depression promotes breast cancer bone metastasis through the RUNX2/PTHrP/RANKL pathway in mice. *Oncol Rep* (2016) 35:739–48. doi: 10.3892/or.2015.4430
47. Campbell JP, Karolak MR, Ma Y, Perrien DS, Masood-Campbell SK, Penner NL, et al. Stimulation of host bone marrow stromal cells by sympathetic nerves promotes breast cancer bone metastasis in mice. *PLoS Biol* (2012) 10:e1001363. doi: 10.1371/journal.pbio.1001363
48. Katz S, Weinerman S. Osteoporosis and gastrointestinal disease. *Gastroenterol Hepatol* (2010) 6:506–17.
49. Balkwill F, Mantovani A. Inflammation and cancer: back to Virchow? *Lancet (Lond Engl)* (2001) 357:539–45. doi: 10.1016/S0140-6736(00)04046-0
50. Lee JY, Murphy SM, Scanlon EF. Effect of trauma on implantation of metastatic tumor in bone in mice. *J Surg Oncol* (1994) 56:178–84. doi: 10.1002/jso.2930560311
51. Alieva M, van Rheenen J, Broekman MLD. Potential impact of invasive surgical procedures on primary tumor growth and metastasis. *Clin Exp Metastasis* (2018) 35:319–31. doi: 10.1007/s10585-018-9896-8
52. Demicheli R, Retsky MW, Hrushesky WJ, Baum M, Gukas ID. The effects of surgery on tumor growth: a century of investigations. *Ann Oncol* (2008) 19:1821–8. doi: 10.1093/annonc/mdn386
53. Krall JA, Reinhardt F, Mercury OA, Pattabiraman DR, Brooks MW, Dougan M, et al. The systemic response to surgery triggers the outgrowth of distant immune-controlled tumors in mouse models of dormancy. *Sci Trans Med* (2018) 10. doi: 10.1126/scitranslmed.aan3464
54. Campisi J, d'Adda di Fagnana F. Cellular senescence: when bad things happen to good cells. *Nat Rev Mol Cell Biol* (2007) 8:729–40. doi: 10.1038/nrm2233
55. Alspach E, Fu Y, Stewart SA. Senescence and the pro-tumorigenic stroma. *Crit Rev Oncogenesis* (2013) 18:549–58. doi: 10.1615/CritRevOncog.2014.010630

56. Luo X, Fu Y, Loza AJ, Murali B, Leahy KM, Ruhland MK, et al. Stromal-Initiated Changes in the Bone Promote Metastatic Niche Development. *Cell Rep* (2016) 14:82–92. doi: 10.1016/j.celrep.2015.12.016
57. Li Y, Terauchi M, Vikulina T, Roser-Page S, Weitzmann MN. B Cell Production of Both OPG and RANKL is Significantly Increased in Aged Mice. *Open Bone J* (2014) 6:8–17. doi: 10.2174/1876525401406010008
58. Ottewill PD, Wang N, Brown HK, Reeves KJ, Fowles CA, Croucher PJ, et al. Zoledronic acid has differential antitumor activity in the pre- and postmenopausal bone microenvironment in vivo. *Clin Cancer Res* (2014) 20:2922–32. doi: 10.1158/1078-0432.CCR-13-1246
59. Schosserer M, Grillari J, Breitenbach M. The Dual Role of Cellular Senescence in Developing Tumors and Their Response to Cancer Therapy. *Front Oncol* (2017) 7:278. doi: 10.3389/fonc.2017.00278
60. Lee S, Schmitt CA. The dynamic nature of senescence in cancer. *Nat Cell Biol* (2019) 21:94–101. doi: 10.1038/s41556-018-0249-2
61. Lynch ME, Brooks D, Mohanan S, Lee MJ, Polamraju P, Dent K, et al. In vivo tibial compression decreases osteolysis and tumor formation in a human metastatic breast cancer model. *J Bone Mineral Res* (2013) 28:2357–67. doi: 10.1002/jbmr.1966
62. Kothari AN, Arffa ML, Chang V, Blackwell RH, Syn WK, Zhang J, et al. Osteopontin-A Master Regulator of Epithelial-Mesenchymal Transition. *J Clin Med* (2016) 5. doi: 10.3390/jcm5040039
63. Fan Y, Jalali A, Chen A, Zhao X, Liu S, Teli M, et al. Skeletal loading regulates breast cancer-associated osteolysis in a loading intensity-dependent fashion. *Bone Res* (2020) 8:9. doi: 10.1038/s41413-020-0083-6
64. Delgado-Calle J, Bellido T, Roodman GD. Role of osteocytes in multiple myeloma bone disease. *Curr Opin Support Palliative Care* (2014) 8:407–13. doi: 10.1097/SPC.0000000000000090
65. Zhou JZ, Riquelme MA, Gu S, Kar R, Gao X, Sun L, et al. Osteocytic connexin hemichannels suppress breast cancer growth and bone metastasis. *Oncogene* (2016) 35:5597–607. doi: 10.1038/ncr.2016.101
66. McDonald MM, Delgado-Calle J. Sclerostin: an Emerging Target for the Treatment of Cancer-Induced Bone Disease. *Curr Osteoporosis Rep* (2017) 15:532–41. doi: 10.1007/s11914-017-0403-y
67. Robling AG, Bonewald LF. The Osteocyte: New Insights. *Annu Rev Physiol* (2020) 82:485–506. doi: 10.1146/annurev-physiol-021119-034332
68. Delgado-Calle J, Sato AY, Bellido T. Role and mechanism of action of sclerostin in bone. *Bone* (2017) 96:29–37. doi: 10.1016/j.bone.2016.10.007
69. Xiong J, Piemontese M, Onal M, Campbell J, Goellner JJ, Dusevich V, et al. Osteocytes, not Osteoblasts or Lining Cells, are the Main Source of the RANKL Required for Osteoclast Formation in Remodeling Bone. *PLoS One* (2015) 10:e0138189. doi: 10.1371/journal.pone.0138189
70. D'Oronzo S, Silvestris E, Paradiso A, Cives M, Tucci M. Role of Bone Targeting Agents in the Prevention of Bone Metastases from Breast Cancer. *Int J Mol Sci* (2020) 21. doi: 10.3390/ijms21083022
71. Gnant M, Pfeiler G, Steger GG, Egle D, Greil R, Fitzal F, et al. Adjuvant denosumab in postmenopausal patients with hormone receptor-positive breast cancer (ABCSG-18): disease-free survival results from a randomised, double-blind, placebo-controlled, phase 3 trial. *Lancet Oncol* (2019) 20:339–51. doi: 10.1016/S1470-2045(18)30862-3
72. Coleman R, Finkelstein DM, Barrios C, Martin M, Iwata H, Hegg R, et al. Adjuvant denosumab in early breast cancer (D-CARE): an international, multicentre, randomised, controlled, phase 3 trial. *Lancet Oncol* (2020) 21:60–72. doi: 10.1016/S1470-2045(19)30687-4
73. Plotkin LI, Gortazar AR, Davis HM, Condon KW, Gabilondo H, Maycas M, et al. Inhibition of osteocyte apoptosis prevents the increase in osteocytic receptor activator of nuclear factor kappaB ligand (RANKL) but does not stop bone resorption or the loss of bone induced by unloading. *J Biol Chem* (2015) 290:18934–42. doi: 10.1074/jbc.M115.642090
74. McCutcheon S, Majeska RJ, Spray DC, Schaffler MB, Vazquez M. Apoptotic Osteocytes Induce RANKL Production in Bystanders via Purinergic Signaling and Activation of Pannexin Channels. *J Bone Mineral Res* (2020) 35:966–77. doi: 10.1002/jbmr.3954
75. Kameda T, Mano H, Yuasa T, Mori Y, Miyazawa K, Shiokawa M, et al. Estrogen inhibits bone resorption by directly inducing apoptosis of the bone-resorbing osteoclasts. *J Exp Med* (1997) 186:489–95. doi: 10.1084/jem.186.4.489
76. Ma L, Hua R, Tian Y, Cheng H, Fajardo RJ, Pearson JJ, et al. Connexin 43 hemichannels protect bone loss during estrogen deficiency. *Bone Res* (2019) 7:11. doi: 10.1038/s41413-019-0050-2
77. Li J, Karim MA, Che H, Geng Q, Miao D. Deletion of p16 prevents estrogen deficiency-induced osteoporosis by inhibiting oxidative stress and osteocyte senescence. *Am J Trans Res* (2020) 12:672–83.
78. Kousteni S, Bellido T, Plotkin LI, O'Brien CA, Bodenner DL, Han L, et al. Nongenotropic, sex-nonspecific signaling through the estrogen or androgen receptors: dissociation from transcriptional activity. *Cell* (2001) 104:719–30. doi: 10.1016/S0092-8674(01)00268-9
79. Takeshita S, Fumoto T, Naoe Y, Ikeda K. Age-related marrow adipogenesis is linked to increased expression of RANKL. *J Biol Chem* (2014) 289:16699–710. doi: 10.1074/jbc.M114.547919
80. Coleman R, Cameron D, Dodwell D, Bell R, Wilson C, Rathbone E, et al. Adjuvant zoledronic acid in patients with early breast cancer: final efficacy analysis of the AZURE (BIG 01/04) randomised open-label phase 3 trial. *Lancet Oncol* (2014) 15:997–1006. doi: 10.1016/S1470-2045(14)70302-X
81. Early Breast Cancer Trialists' Collaborative Group (EBCTCG). Adjuvant bisphosphonate treatment in early breast cancer: meta-analyses of individual patient data from randomised trials. *Lancet (Lond Engl)* (2015) 386:1353–61. doi: 10.1016/S0140-6736(15)60908-4
82. Wang W, Yang X, Dai J, Lu Y, Zhang J, Keller ET. Prostate cancer promotes a vicious cycle of bone metastasis progression through inducing osteocytes to secrete GDF15 that stimulates prostate cancer growth and invasion. *Oncogene* (2019) 38:4540–59. doi: 10.1038/s41388-019-0736-3
83. Sottnik JL, Dai J, Zhang H, Campbell B, Keller ET. Tumor-induced pressure in the bone microenvironment causes osteocytes to promote the growth of prostate cancer bone metastases. *Cancer Res* (2015) 75:2151–8. doi: 10.1158/0008-5472.CAN-14-2493
84. Ma YV, Lam C, Dalmia S, Gao P, Young J, Middleton K, et al. Mechanical regulation of breast cancer migration and apoptosis via direct and indirect osteocyte signaling. *J Cell Biochem* (2018) 119:5665–75. doi: 10.1002/jcb.26745
85. Giuliani N, Ferretti M, Bolzoni M, Storti P, Lazzaretti M, Dalla Palma B, et al. Increased osteocyte death in multiple myeloma patients: role in myeloma-induced osteoclast formation. *Leukemia* (2012) 26:1391–401. doi: 10.1038/leu.2011.381
86. Riquelme MA, Cardenas ER, Xu H, Jiang JX. The Role of Connexin Channels in the Response of Mechanical Loading and Unloading of Bone. *Int J Mol Sci* (2020) 21. doi: 10.3390/ijms21031146
87. Xu H, Gu S, Riquelme MA, Burra S, Callaway D, Cheng H, et al. Connexin 43 channels are essential for normal bone structure and osteocyte viability. *J Bone Mineral Res* (2015) 30:436–48. doi: 10.1002/jbmr.2374
88. Kar R, Riquelme MA, Werner S, Jiang JX. Connexin 43 channels protect osteocytes against oxidative stress-induced cell death. *J Bone Mineral Res* (2013) 28:1611–21. doi: 10.1002/jbmr.1917
89. Bellido T, Plotkin LI. Novel actions of bisphosphonates in bone: preservation of osteoblast and osteocyte viability. *Bone* (2011) 49:50–5. doi: 10.1016/j.bone.2010.08.008
90. Zhou JZ, Riquelme MA, Gao X, Elies LG, Sun LZ, Jiang JX. Differential impact of adenosine nucleotides released by osteocytes on breast cancer growth and bone metastasis. *Oncogene* (2015) 34:1831–42. doi: 10.1038/ncr.2014.113
91. Genetos DC, Kephart CJ, Zhang Y, Yellowley CE, Donahue HJ. Oscillating fluid flow activation of gap junction hemichannels induces ATP release from MLO-Y4 osteocytes. *J Cell Physiol* (2007) 212:207–14. doi: 10.1002/jcp.21021
92. Di Virgilio F, Sarti AC, Falzoni S, De Marchi E, Adinolfi E. Extracellular ATP and P2 purinergic signalling in the tumour microenvironment. *Nat Rev Cancer* (2018) 18:601–18. doi: 10.1038/s41568-018-0037-0
93. Feng LL, Cai YQ, Zhu MC, Xing LJ, Wang X. The yin and yang functions of extracellular ATP and adenosine in tumor immunity. *Cancer Cell Int* (2020) 20:110. doi: 10.1186/s12935-020-01195-x
94. Rapaport E, Fishman RF, Gercel C. Growth inhibition of human tumor cells in soft-agar cultures by treatment with low levels of adenosine 5'-triphosphate. *Cancer Res* (1983) 43:4402–6.
95. Beijer S, Hupperets PS, van den Borne BE, Eussen SR, van Herten AM, van den Beuken-van Everdingen M, et al. Effect of adenosine 5'-triphosphate infusions on the nutritional status and survival of preterminal cancer patients. *Anti-cancer Drugs* (2009) 20:625–33. doi: 10.1097/CAD.0b013e32832d4f22

96. Agteresch HJ, Burgers SA, van der Gaast A, Wilson JH, Dagnelie PC. Randomized clinical trial of adenosine 5'-triphosphate on tumor growth and survival in advanced lung cancer patients. *Anti-cancer Drugs* (2003) 14:639–44. doi: 10.1097/00001813-200309000-00009
97. Agteresch HJ, Dagnelie PC, van der Gaast A, Stijnen T, Wilson JH. Randomized clinical trial of adenosine 5'-triphosphate in patients with advanced non-small-cell lung cancer. *J Natl Cancer Institute* (2000) 92:321–8. doi: 10.1093/jnci/92.4.321
98. White N, Burnstock G. P2 receptors and cancer. *Trends Pharmacol Sci* (2006) 27:211–7. doi: 10.1016/j.tips.2006.02.004
99. Furlow PW, Zhang S, Soong TD, Halberg N, Goodarzi H, Mangrum C, et al. Mechanosensitive pannexin-1 channels mediate microvascular metastatic cell survival. *Nat Cell Biol* (2015) 17:943–52. doi: 10.1038/ncb3194
100. Miyazaki T, Iwasawa M, Nakashima T, Mori S, Shigemoto K, Nakamura H, et al. Intracellular and extracellular ATP coordinately regulate the inverse correlation between osteoclast survival and bone resorption. *J Biol Chem* (2012) 287:37808–23. doi: 10.1074/jbc.M112.385369
101. Schenk U, Frascoli M, Proietti M, Geffers R, Traggiai E, Buer J, et al. ATP inhibits the generation and function of regulatory T cells through the activation of purinergic P2X receptors. *Sci Signaling* (2011) 4:ra12. doi: 10.1126/scisignal.2001270
102. Canale FP, Ramello MC, Nunez N, Araujo Furlan CL, Bossio SN, Gorosito Serran M, et al. CD39 Expression Defines Cell Exhaustion in Tumor-Infiltrating CD8(+) T Cells. *Cancer Res* (2018) 78:115–28. doi: 10.1158/0008-5472.CAN-16-2684
103. Kazemi MH, Raoofi Mohseni S, Hojjat-Farsangi M, Anvari E, Ghalamfarsa G, Mohammadi H, et al. Adenosine and adenosine receptors in the immunopathogenesis and treatment of cancer. *J Cell Physiol* (2018) 233:2032–57. doi: 10.1002/jcp.25873
104. Pellegatti P, Raffaghello L, Bianchi G, Piccardi F, Pistoia V, Di Virgilio F. Increased level of extracellular ATP at tumor sites: in vivo imaging with plasma membrane luciferase. *PloS One* (2008) 3:e2599. doi: 10.1371/journal.pone.0002599
105. Allard D, Allard B, Stagg J. On the mechanism of anti-CD39 immune checkpoint therapy. *J Immunotherapy Cancer* (2020) 8. doi: 10.1136/jitc-2019-000186
106. Hirata Y, Furuhashi K, Ishii H, Li HW, Pinho S, Ding L, et al. CD150(high) Bone Marrow Tregs Maintain Hematopoietic Stem Cell Quiescence and Immune Privilege via Adenosine. *Cell Stem Cell* (2018) 22:445–53.e5. doi: 10.1016/j.stem.2018.01.017
107. Vijayan D, Young A, Teng MWL, Smyth MJ. Targeting immunosuppressive adenosine in cancer. *Nat Rev Cancer* (2017) 17:709–24. doi: 10.1038/nrc.2017.86

Conflict of Interest: The authors declare that the research was conducted in the absence of any commercial or financial relationships that could be construed as a potential conflict of interest.

Copyright © 2020 Riquelme, Cardenas and Jiang. This is an open-access article distributed under the terms of the Creative Commons Attribution License (CC BY). The use, distribution or reproduction in other forums is permitted, provided the original author(s) and the copyright owner(s) are credited and that the original publication in this journal is cited, in accordance with accepted academic practice. No use, distribution or reproduction is permitted which does not comply with these terms.



The Hyperglycemia and Hyperketonemia Impaired Bone Microstructures: A Pilot Study in Rats

Qi Liu^{1*†}, Zhou Yang^{2†}, Chuhan Xie¹, Long Ling¹, Hailan Hu¹, Yanming Cao¹, Yan Huang¹, Qingan Zhu^{3*} and Yue Hua^{4*}

¹ Department of Orthopaedic Surgery, The Second Affiliated Hospital of Guangzhou Medical University, Guangzhou, China,

² Department of Orthopaedic Surgery, Southern University of Science and Technology Hospital, Shenzhen, China, ³ Division of Spine Surgery, Department of Orthopedics, Nanfang Hospital, Southern Medical University, Guangzhou, China, ⁴ School of Traditional Chinese Medicine, Southern Medical University, Guangzhou, China

OPEN ACCESS

Edited by:

Lilian Irene Plotkin,
Indiana University Bloomington,
United States

Reviewed by:

Subhashis Pal,
Emory University, United States
Paula H. Stern,
Northwestern University,
United States

*Correspondence:

Qi Liu
liuqi@i.smu.edu.cn
Qingan Zhu
qinganzhu@gmail.com
Yue Hua
bohemia999@foxmail.com

[†]These authors have contributed
equally to this work

Specialty section:

This article was submitted to
Bone Research,
a section of the journal
Frontiers in Endocrinology

Received: 02 August 2020

Accepted: 22 September 2020

Published: 22 October 2020

Citation:

Liu Q, Yang Z, Xie C, Ling L, Hu H,
Cao Y, Huang Y, Zhu Q and Hua Y
(2020) The Hyperglycemia and
Hyperketonemia Impaired Bone
Microstructures: A Pilot Study in Rats.
Front. Endocrinol. 11:590575.
doi: 10.3389/fendo.2020.590575

Though diabetes mellitus (DM) is one of the known causes of osteoporosis, it is also realized that ketogenic diet (KD), an effective regimen for epilepsy, impairs bone microstructures. However, the similarities and differences of effects between these two factors are still unknown. The purpose of this study is to identify different effects between hyperglycemia and hyperketonemia, which are manifestations of DM and KD, on bone in rats. Thirty male Sprague-Dawley rats were randomly divided into three groups: the sham, DM, and KD groups. Hyperglycemia was achieved by intravenous injection of streptozotocin in DM group, while hyperketonemia was induced by application of ketogenic diet (carbohydrates-to-fat as 1:3) in KD group. The body weight, blood ketone body, and blood glucose were recorded, and the bone turnover markers, bone length, bone microstructures, bone biomechanics and histomorphology were measured after 12 weeks intervention. Compared with the control and KD groups, a significant body weight loss was found in the DM group, and the bone lengths of tibia and femur of the group were shortened. The blood glucose and blood ketone were noticeably increased in the DM and KD rats, respectively. Microstructures and properties of cancellous bone were significantly deteriorated in both the DM and KD groups compared with the sham group, as the bone volumes were decreased and the bone trabecula structures were disturbed. Meanwhile, the thickness and strength of cortical bone was reduced more in the DM group than those in the sham and KD groups. The HE staining showed that bone trabecula was significantly decreased in both the DM and KD groups, and more adipose tissue was observed in the KD rats. The activity of osteoblasts was decreased more in both the KD and DM groups than that in the sham group, while the activity of osteoclasts of the two groups was remarkably increased. The present study indicates that both hyperglycemia and hyperketonemia have adverse effects on bone. Therefore, it is worth paying more attention to the bone status of patients with hyperglycemia and hyperketonemia in clinic.

Keywords: diabetes mellitus, ketogenic diet, cancellous bone, cortical bone, bone turnover

INTRODUCTION

Metabolic syndrome and osteoporosis are medical conditions that must not be overlooked, since both may lead to serious problems in the aged (1). Metabolic syndrome is characterized by abdominal obesity, impaired glucose tolerance, hypertension and dyslipidemia (2). The accumulating studies reported that metabolic disturbance might be a risk factor for osteoporosis. Increased insulin resistance promotes osteolysis of inflammatory cytokines in patients with metabolic syndrome, triggering osteoporosis (3). Moreover, higher serum lipid level resulting from metabolic syndrome is considered to play a critical factor in pathogenesis of osteoporosis (4).

Diabetes mellitus is a metabolic disease which is characterized as hyperglycemia resulted from defects in insulin action and/or insulin secretion (5). It has negative effects on skeletal disorders, including osteopenia or osteoporosis (6). It is known that type 1 diabetes mellitus (T1DM) compromises bone microstructures by suppressing growth potential and worsening insulin resistance and glycemic control (7). By carrying out an MRI-based assessment, Naiemh et al. (8) found that young women with T1DM were more likely to suffer from trabecular bone volume and trabecular numbers reduction. Shortened femur length, reduced growth plate thickness, compromised cancellous and cortical bone, and decreased collagen II expression were observed in streptozotocin-induced diabetic animal models (9, 10).

Ketogenic diet (KD) is a well-established therapeutic intervention for patients with refractory epilepsy (11). By maintaining a high-fat and low-carbohydrate diet with restricted protein intake, systemic ketosis raises seizure threshold for intractable epilepsy treatment (12). However, it was firstly reported by Hahn that KD had deleterious effects on bone mass in children who maintained this regimen in long term (13). Our previous studies also confirmed that KD compromised bone micro-structures and reduced bone biomechanics in rodents (14–18). However, the different effects of streptozotocin-induced hyperglycemia and KD-induced hyperketonemia on bone micro-structures and biomechanics have not been elucidated.

The purpose of this study is to investigate the effects of hyperglycemia and hyperketonemia on appendicular bone. Micro-CT scan and biomechanical test were performed to evaluate the bone mass and biomechanical properties, and both the serological and histological bone turnover markers were observed to evaluate the activities of osteoblasts and osteoclasts after intervention.

MATERIALS AND METHODS

Animals

A total of thirty Sprague Dawley male rats, purchased at 12 weeks of age from the Experimental Animal Center of Southern Medical University, were randomly divided into three groups: the sham group, the diabetes mellitus (DM) group, and the ketogenic diet (KD) group. The rats in the DM group were

injected intravenously with streptozotocin (STZ; Fisher Scientific) at the dose of 50 mg/kg (10), while the rats in the KD group were fed with the ketogenic diet (Jielikang Inc., Shenzhen, China), which containing a ratio of fat to carbohydrate and protein of 3:1. All rats were kept in a wire hanging cage with a 12-h light–dark cycle, and a constant temperature of 25°C and humidity of 48%. And they had free access to food and water during the entire experiment.

Specimens Collection

All the rats were anesthetized by 1% pentobarbitone sodium after 12-weeks interventions. The blood samples were collected with a 5 ml syringe from abdominal vein, and then centrifuged under 3000rpm for 20 min to obtain the serum samples. The left tibiae and left femora were fixed in 4% p-formaldehyde for 48 h before analyzing the bone microstructures, histology and immunohistochemistry, and the right tibiae and right femora were frozen in -20°C until biomechanical properties analysis.

Measurement of Body Weight, Length of Tibia and Femur, Blood Ketone Body, and Blood Glucose

The rats were weighed at 12 weeks using a CS 200 balance (Ohaus, Pine Brook, NJ, USA). The full lengths of the tibia and femur were measured with a vernier caliper. The blood ketone and glucose levels were measured by cutting tail veins. Yicheng Blood Ketone Meter T-1 (Sentest Inc., China) and Medisense Precision Xtra monitor (Abbott Laboratories, Canada) were used to determine the blood ketone concentrations, while the blood glucose levels were tested with monitor JPS-5 (Leapon Inc., China).

Analysis of Bone Turnover Biomarkers in the Serum

The collected serum samples were used to test the bone turnover biomarkers. The serological calcium and phosphorus concentrations, as well as the concentrations of the specific markers of bone turnover biomarkers, including bone-specific alkaline phosphatase (ALP), tartrate-resistant acid phosphatase (TRAP), insulin-like growth factor 1 (IGF-1), N-terminal propeptide of type I procollagen (P1NP), and C-telopeptide fragments of collagen type I $\alpha 1$ chains (β -CTX), were measured by available assay kit (Beckman Coulter, Suzhou, China) according to the manufacturer's protocols.

Micro-CT Scan

Each specimen was washed with tap water for 2 h and kept straight in the tube for micro-CT scanning after fixation. Refer to the guidelines for assessment of the bone microstructures in rodents using micro-CT (19), the trabecular microstructures of left tibiae were analyzed using a micro-CT system (μ CT80, SCANCO MEDICAL, Switzerland) at resolutions of 12 μ m with a tube voltage of 50 kV and a tube current of 0.1 mA. The region of interest (ROI) was defined as 180 slices approximately 2.0 mm from the growth plate of the proximal tibia. Bone morphometric parameters, included the tissue

mineral density (TMD), the connection density (Conn.D), the bone volume/tissue volume (BV/TV), the trabecular number (Tb.N), the trabecular thickness (Tb.Th) and the trabecular separation (Tb.Sp), were obtained *via* analysis of the ROI. The 180 slices of left femur mid-diaphysis were selected to analyze the parameters of cortical bone, including the total cross-sectional area inside the periosteal envelope (Tarea), the bone area (Barea) and the thickness (Ct.Th).

The micro-finite element analysis (micro-FEA) of compressive test (SCANCO Medical AG, Version 1.13) was used to assess the biomechanical characteristics in cancellous bone based on the micro-structures from micro-CT images. The simulations were done within the framework of linear elasticity, and the detailed operation was shown in our previous study (17). The simulation yielded the compressive stiffness and failure load of cancellous bones.

Three-Point Bending Test

The three-point bending test was performed to evaluate the biomechanical properties of cortical bone. After thawing 1 h at room temperature, the proximal tibiae were placed on a base consisting of an aluminum block with one rounded edge-free notches on top and the mid-shaft of femora were placed on two supports separated by a distance of 20 mm for biomechanical test. A compressive force was applied at a constant speed of 2 mm/min by the material testing machine (Instron ElectroPuls, E1000, USA). The maximum load (Max.L), stiffness, and energy absorption were obtained based on the load-deformation curve after the specimen was broken.

Histological and Immunohistochemical Staining

The proximal tibiae were embedded into olefin after micro-CT scan, and then decalcification in 10% EDTA for 4–5 weeks. All samples were stained with the hematoxylin–eosin and immunohistochemical (IHC) staining according to standard conditions. The hematoxylin–eosin staining was performed to observe the histomorphology of trabecula, while the osteocalcin (OCN) staining (Abcam Cambridge, UK) and the tartrate-resistant acid phosphatase (TRAP) staining (Sigma–Aldrich, St. Louis, USA) were performed to evaluate the osteoblasts cell activity and the presence of osteoclasts in the trabecular bone. The results of IHC staining were evaluated by cell number counting and computerized optical density (OD) measurements. Cells per bone surface (B.S) were used to calculate the number of positive cells, and integrated optical density per area of positive cells (IOD/area, mean density) was used to semi-quantify the staining intensity by detecting in 10 different images taken at 400× magnification every slide with Image Pro Plus 6.0 software (Media Cybernetics, MD, USA).

Statistical Analysis

All data were analyzed by SPSS 20.0 software and showed as mean ± SD. The differences in the body weight, the blood ketone and glucose levels, the serological biomarkers, the micro-CT parameters, the biomechanical results, and the histological results were analyzed by one-way ANOVA with least-

significant difference (LSD) *post hoc* test among groups. $P < 0.05$ was considered statistically significant.

RESULTS

Changes of Body Weight, Blood Ketone and Blood Glucose Concentrations, and Bone Lengths

The detailed data of body weight and the levels of blood ketone and glucose are shown in **Table 1**. The body weight of the DM group was significantly decreased compared with the sham and KD groups ($P < 0.05$), while no significant difference was shown between the sham group and the KD group ($P > 0.05$). The blood ketone of the KD group was noticeably higher than that of the sham group or the DM group (the blood ketone concentrations were 0.40 ± 0.14 mmol/L, 0.55 ± 0.21 mmol/L and 1.13 ± 0.12 mmol/L in the sham, DM and KD groups, respectively). The DM rats exhibited higher blood glucose levels than those in the sham and KD groups (the blood glucose concentrations were 7.10 ± 1.15 mmol/L, 6.1 ± 0.47 mmol/L and >33.33 mmol/L in the sham, KD and DM groups, respectively).

The bone length showed a trend similar to the body weight. The tibia and femur lengths of DM group were the shortest among all the groups (**Figure 1**). The lengths of tibia and femur of DM group were 0.47 mm and 0.52 mm, respectively, shorter than those in the sham group (**Table 2**).

Analysis of Serum Calcium, Phosphorus, and Bone Turnover Biomarkers

The serum concentrations of calcium and phosphorus showed no significant difference among the groups, yet there were great differences among the bone turnover biomarkers (**Table 3**). The ALP level was significantly decreased in the KD group compared with the sham group (the ALP level was 0.78 fold in the DM group relative to the sham group, $P < 0.05$). The concentrations of TRAP were increased remarkably in both DM and KD groups than that in the sham group (the TRAP levels were $113.0 \mu\text{mol/L}$, $206.3 \mu\text{mol/L}$ and $192.3 \mu\text{mol/L}$ in the sham, DM and KD groups, respectively).

IGF-1, as a growth factor rich in bone tissue, stimulates proliferation of preosteoblastic cells and enhances differentiated functions of the osteoblast. The concentrations of IGF-1 were significantly decreased in the DM and KD rats compared with that in the sham rats (629.0 ng/ml, 230.8 ng/ml, and 339.5 ng/ml in the sham, DM and KD groups, respectively). P1NP and β -CTX are biomarkers of bone formation and resorption, which are

TABLE 1 | The body weight, blood glucose, and blood ketone among groups.

Groups	Body weight (g)	Blood Ketone (mmol/L)	Blood Glucose (mmol/L)
Sham	508.33 ± 15.41	0.40 ± 0.14	7.10 ± 1.15
DM	$290.12 \pm 50.15^*$	0.55 ± 0.21	$>33.33^*$
KD	507.33 ± 22.23	$1.13 \pm 0.12^*$	6.1 ± 0.47

Data are represented as means ± SD. *** means $P < 0.05$ compared to Sham group.



FIGURE 1 | The general picture of bone length of tibia and femur in the sham, diabetes mellitus (DM) and ketogenic diet (KD) groups.

TABLE 2 | The bone length of tibia and femur among groups.

Groups	Tibia (mm)	Femur (mm)
Sham	4.52 ± 0.15	4.10 ± 0.12
DM	4.05 ± 0.09*	3.58 ± 0.11*
KD	4.36 ± 0.11	4.00 ± 0.08

Data are represented as means ± SD. *** means $P < 0.05$ compared to Sham group.

TABLE 3 | The serum parameters of calcium, phosphate, and bone turnover biomarkers among groups.

Parameters	Sham	DM	KD
Calcium (mol/L)	2.22 ± 0.09	2.21 ± 0.11	2.25 ± 0.08
Phosphorus (mol/L)	2.28 ± 0.32	2.24 ± 0.27	2.13 ± 0.20
ALP (μmol/L)	3.01 ± 0.34	2.65 ± 0.18*	2.25 ± 0.39*
TRAP (μmol/L)	113.02 ± 6.18	206.25 ± 41.21*	192.34 ± 19.67*
IGF-1 (ng/ml)	629.04 ± 66.53	230.84 ± 54.02*	339.51 ± 64.51*
P1NP (ng/ml)	12.83 ± 1.86	5.62 ± 0.90*	8.83 ± 1.19*
β-CTX (ng/ml)	16.02 ± 2.72	38.93 ± 10.20*	22.27 ± 2.95*#

Data are represented as means ± SD. *** means $P < 0.05$ compared to Sham group, and # means $P < 0.05$ between DM and KD groups.

recommended for clinical application. The concentrations of P1NP were decreased by 56.2% and 31.2% in the DM and KD groups compared with the sham group, while the β-CTX levels were increased by 143.1% and 39% in the DM and KD groups, respectively (Table 3). Moreover, the β-CTX concentration of the DM group was increased more significantly than that of the KD group (38.93 ng/ml and 22.27 ng/ml in the DM and KD groups, respectively).

Changes of Bone Microstructures

The micro-CT data showed that the cancellous bone was significantly compromised in the DM and KD groups compared with the sham group (Figure 2). The TMD and Conn.D were obviously reduced in both the DM and KD

groups (the TMD and Conn.D were 172.5 mg HA/ccm and 62.9 mm³, 65.2 mg HA/ccm and 21.8 mm³, 71.4 mg HA/ccm and 16.8 mm³ in the sham, DM and KD groups, respectively). And the DM and KD rats exhibited lower BV/TV and Tb.N with higher Tb.Sp than those in the sham group (the BV/TV was 22.1%, 7.2%, and 9.3% in the sham, DM and KD groups, respectively). While the Tb.Th of DM group was thinner than that of the KD group, no significant difference of Tb.Th was shown between the KD rats and the sham rats.

The cortical bone of the DM rats was impaired as well. The Barea and the Tarea of cortical bone were significantly decreased in the DM group compared with the sham and KD groups (Figure 3). The Ct.Th of the DM group was thinner than that of the sham and KD groups, although it was decreased in the KD group compared with the sham group (Figure 3).

Assessments of Biomechanical Properties

In order to verify the biomechanical properties of the cortical bone, the three-point bending test was performed on the proximal tibia (Figure 4A) and the mid-shaft femur (Figure 4B). It was showed that the Max.L, stiffness and the energy adoption of cortical bone of tibia and femur in the DM group were significantly decreased compared with the sham group (Figure 4). And the Max.L and the energy adoption of tibia and femur in the KD group were decreased more noticeably than those in the sham group (Figure 4).

The results of micro-FEA has shown that the stiffness and the failure load were significantly weakened in both the DM and KD groups compared with the sham group, and there was no significant difference between the DM and KD groups (the stiffness and failure load were 2127.3 ± 842.3 N/mm and 777.3 ± 279.6 N, 357.0 ± 117.4 N/mm and 132.1 ± 46.3 N, 734.5 ± 307.7 N/mm and 212.1 ± 100.9 N in the sham, DM and KD groups, respectively) (Figure 5).

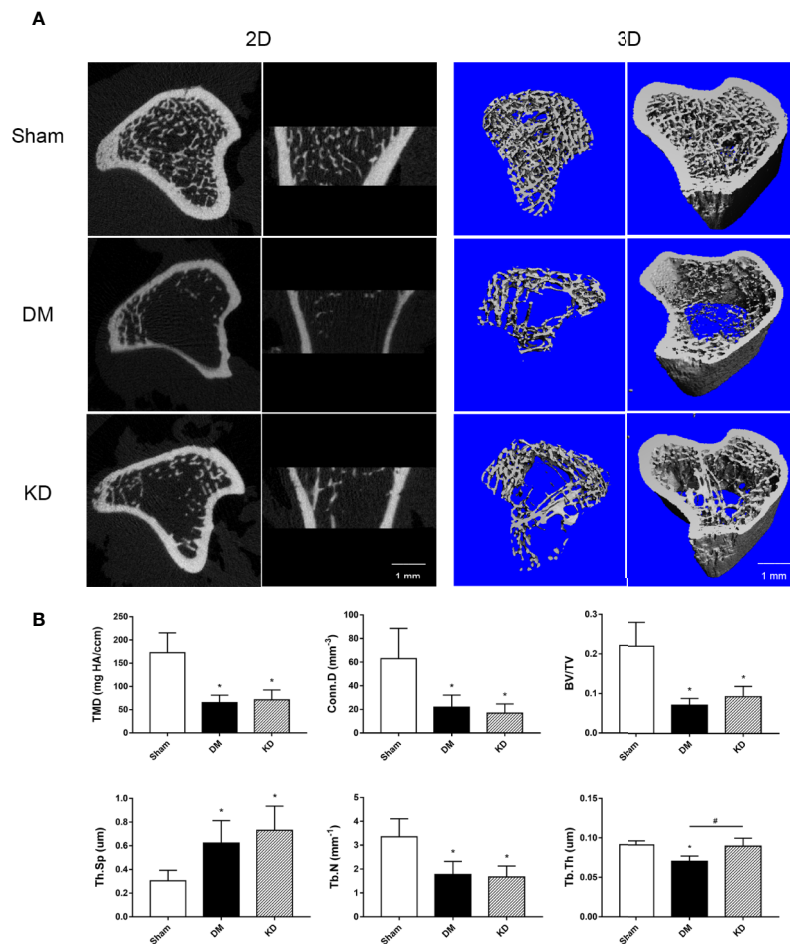


FIGURE 2 | The micro-CT pictures and bone parameters of cancellous bone in the proximal tibia. **(A)** The 2D and 3D pictures of bone microstructures in the sham, diabetes mellitus (DM) and ketogenic diet (KD) groups. **(B)** The trabecular parameters of cancellous bone among groups. “*” means $P < 0.05$ compared to sham group, “#” means $P < 0.05$ between the DM and KD groups.

Evaluations of Histology and Immunohistochemistry Staining

The HE staining results indicated that the number of trabeculae significantly decreased in both the DM and KD groups compared with the sham group (**Figure 6**). Meanwhile, more adipose tissue was found in the KD group than that in the sham and DM groups. Based on the immunohistochemical results, the activity of osteoblast cell was significantly decreased in the DM and KD groups, while the activity of osteoclast cell was increased. An obviously lower expression of OCN and remarkably higher expression of TRAP were identified in both the DM and KD groups relative to the sham group (**Figure 7**).

DISCUSSION

This study proved that both hyperglycemia and hyperketonemia induce bone compromising in rats by reducing bone mass, disturbing the balance of osteoblast and osteoclast, and

impairing the biomechanical properties. Nevertheless the effects of these two kind of metabolic disturbance on bone had some differences. Hyperketonemia induced by KD resulted in more compromised more in cancellous bone with little effect on cortical bone, while hyperglycemia caused by DM had adverse effects on both the cancellous bone and cortical bone, influencing the bone length as well.

It has been long thought that diabetes mellitus negatively affects bone metabolism. Using high-resolution peripheral quantitative computed tomography and magnetic resonance imaging, several cross-sectional studies revealed that both cortical and trabecular bone tend to be more fragile in diabetes patients, which increases fracture risk (20, 21). Diabetes mellitus reduces bone density and bone strength by inhibiting osteoblast activity and enhancing osteoclast activity (22). Guo et al. (23) found that ALP activity and TRAP activity in serum were significantly decreased in the STZ-injected rats. Meanwhile, other researchers found that serum ALP level was greatly increased in diabetic rats and serum TRAP level was also

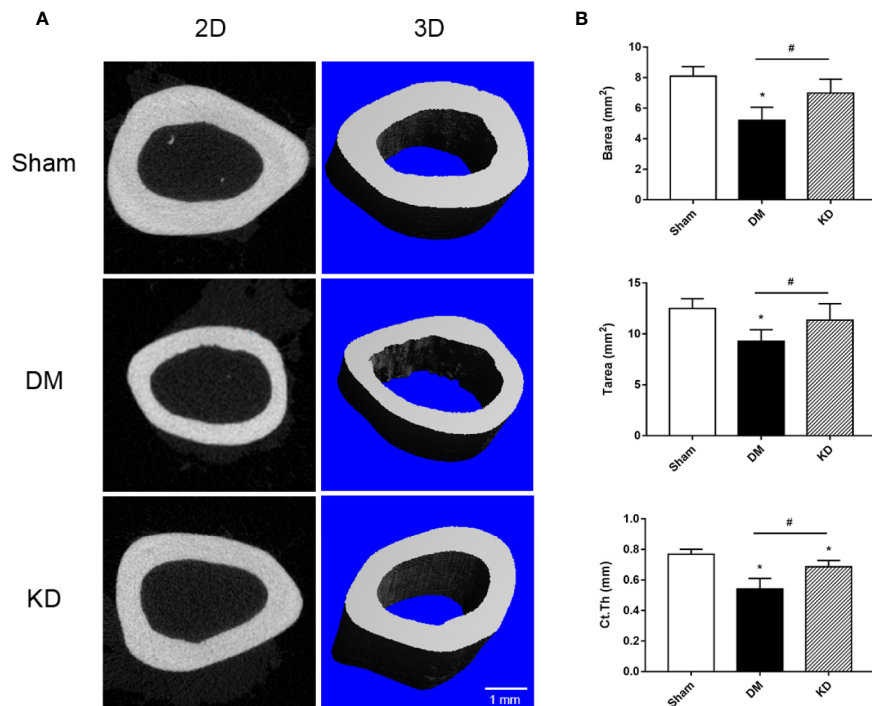


FIGURE 3 | The micro-CT pictures and the bone parameters of cortical bone in the mid-shaft femur. **(A)** The 2D and 3D pictures of bone microstructures in the sham, diabetes mellitus (DM) and ketogenic diet (KD) groups. **(B)** The parameters of cortical bone in the sham, DM and KD groups. “**” means $P < 0.05$ compared to sham group, “#” means $P < 0.05$ between the DM and KD groups.

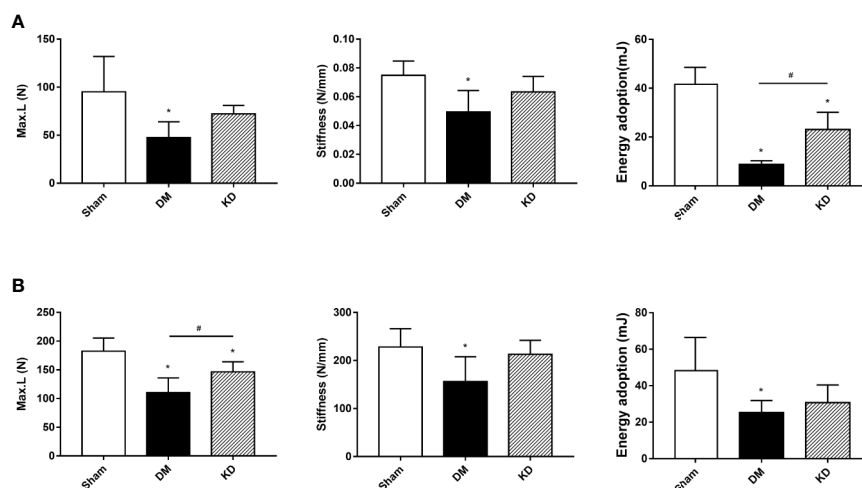


FIGURE 4 | The biomechanical strengths of cortical bone in the proximal tibia **(A)** and mid-shaft femur **(B)** from the three-bending test. “**” means $P < 0.05$ compared to sham group, “#” means $P < 0.05$ between the diabetes mellitus (DM) and ketogenic diet (KD) groups.

greatly increased (24). The findings of TRAP activity were consistent, though the ALP level showed differences among studies. In the present study, the ALP level was remarkably reduced in the DM rats, and the TRAP concentration was significantly raised. Moreover, N-terminal propeptide of type I

procollagen (P1NP) and C-telopeptide of type I collagen (CTX), as the specific biomarkers of bone formation and resorption, have been recommended for clinical application. A clinical research study into the bone turnover biomarkers showed that a corrective relationship exists between serum P1NP level and

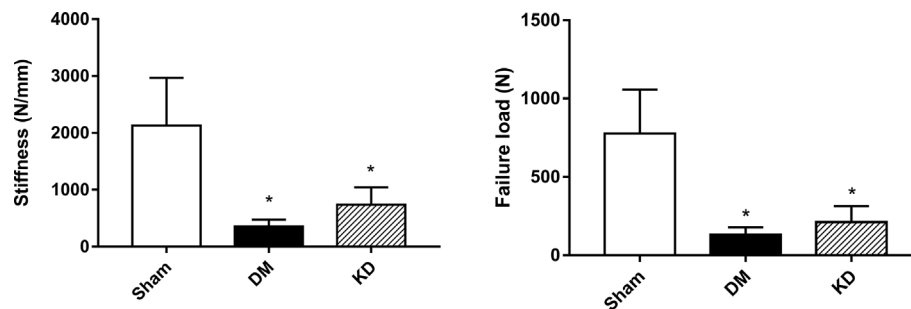


FIGURE 5 | The biomechanical properties of cancellous bone in the proximal tibia from the micro-FEA. “*” means $P < 0.05$ compared to sham group.

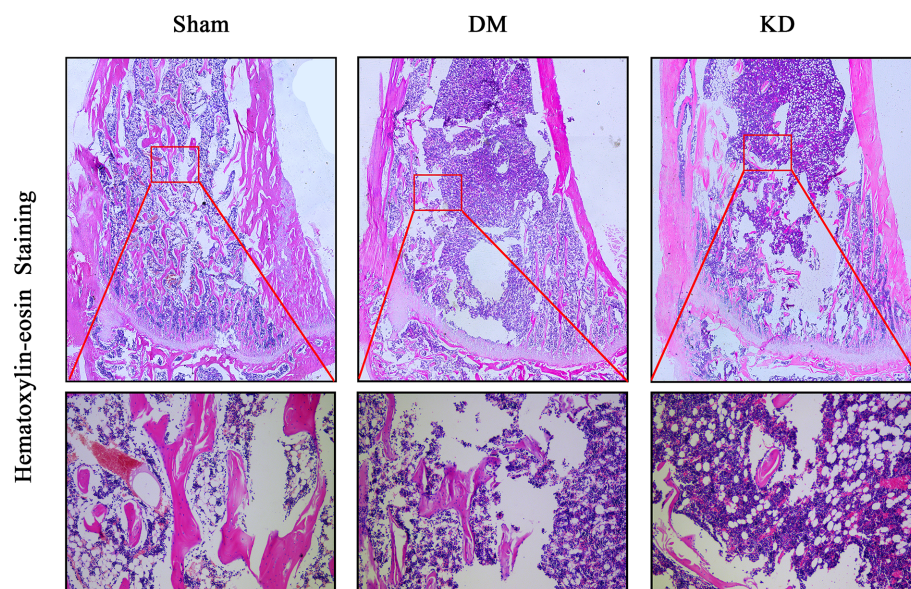


FIGURE 6 | The hematoxylin-eosin stain in the proximal tibia. The trabeculae was significantly decreased in both diabetes mellitus (DM) and ketogenic diet (KD) groups compared with the sham group, and the adipose tissue (showed in red frame) in the KD group was risen compared with the sham and DM groups.

histomorphometric bone formation estimates, and between serum CTX and histomorphometric bone resorption estimates (25). The present study found that the PINP concentration of the DM group was decreased by 56.2% and the β -CTX level increased by 143.1% in comparison with the sham group. We are inclined to the view that the functions of osteoblasts and osteoclasts were responsible for the bone loss in the DM rats which occurred at least 3 months later.

Abnormal bone metabolism indicators bring about deteriorated bone microarchitectures. Ma et al. (26) found a trabecular number and volume decrease and trabecular separation increase of femur in diabetic rats. In the present study, a remarkable TMD and Conn.D decrease was found in the diabetic rats with less bone volume fraction, lower trabecular number, thinner trabecular thickness, and wider trabecular separation. Similarly, diabetes deteriorates cortical bone and

shortens bone length. Hyperglycemia increases the osteocyte lacunar density by decreasing osteocytic territorial matrix volume, thus increasing cellularity of cortical bone as well as affecting the bone length (27). The STZ-rats displayed an apparently smaller cortical area and a higher cortical porosity (28). The micro-CT data showed that the bone area, the total area and cortical thickness of the mid-shaft of femur were significantly decreased in the DM rats than those in the sham rats. The lengths of tibia and femur of the diabetic rats were remarkably shortened. The bone trabecular and cortical bone parameters exhibited that diabetes not only affects the status of cancellous bone and cortical bone, but also affects the bone growth.

The status of cortical bone plays a critical role in bone strength. Supportive findings have shown that diabetes mellitus is associated with increased risk of hip fracture and other fractures (29). In the

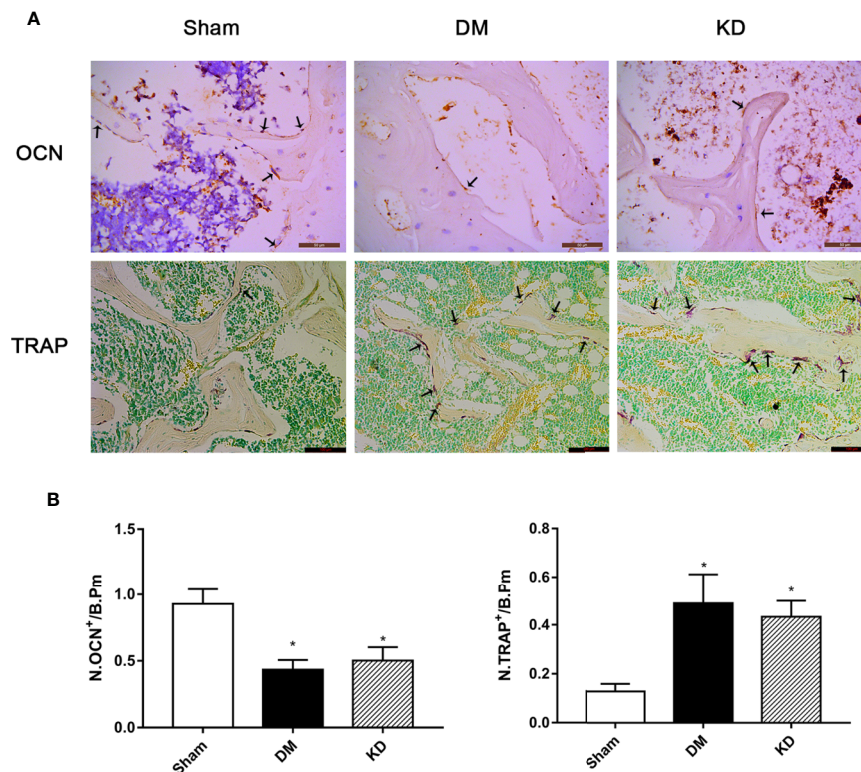


FIGURE 7 | The osteocalcin (OCN) and tartrate-resistant acid phosphatase (TRAP) staining in the proximal tibia (A), and the results of semi-quantitative analysis (B). The activity of the osteoblast cell was significantly decreased, while the osteoclast cell was increased in diabetes mellitus (DM) and ketogenic diet (KD) groups. There was significantly lower expression of OCN and remarkably higher expression of TRAP in both DM and KD groups compared with the sham group (arrows refer to positive cells). *** means $P < 0.05$ compared to sham group.

rodent models, diabetes significantly weakened bone strengths by impairing cortical bone microarchitectures (30, 31). Three-point bending test has been proven as a useful method to measure biomechanical properties of cortical bone in rodents (32). In this study, the biomechanical properties of cortical bone of the diabetic rats were significantly weakened, which was manifested as lower maximum load, stiffness and energy absorption, compared with the sham group. Moreover, simulated compressive test based on micro-finite element analysis is an effective technique for evaluation of cancellous bone since it has an irregular structures. Consistent with the bone parameters from micro-CT, the micro-FEA results also showed that the stiffness and failure load were significantly decreased in the DM group compared with the sham group. The results from the biomechanical tests indicated that both the cortical bone and cancellous bone were deteriorated in the diabetic rats.

Researches on the effects of hyperketonemia induced by KD on bone microstructures and bone qualities in rodents were performed in our previous studies. KD deteriorated microstructures of cancellous bone by decreasing bone mass and impairing biomechanical properties, as well as inhibiting osteogenic process and enhancing osteoclastic process in the BMSCs (15, 17). Akihiro et al. (33) found that ketone bodies bidirectionally modulate osteoblast functions, which suggests

that ketone bodies is an important endogenous factor that regulates bone metabolism in both physiological and pathological situations. And they pointed out that β -hydroxybutyrate significantly reduced the ALP activity and mineralization in osteoblasts. It was confirmed in this study that hyperketonemia severely impaired cancellous bone and its' biomechanical properties, and cortical bone was partly affected. The underlying mechanism might be that hyperketonemia inhibits the osteoblast activity and increases the osteoclast activity.

Both hyperglycemia and hyperketonemia have obvious adverse effects on bone. The results of this study showed that both hyperglycemia and hyperketonemia deteriorated cancellous bone and weakened its biomechanical properties, which might be attributed to the changes of activity of osteoblasts and osteoclasts. However, there were differences existing between the two effects. Firstly, hyperglycemia had more adverse effects on cortical bone than hyperketonemia. It was found that the DM rats exhibited smaller Barea and Tarea, and thinner Ct.Th than the sham and KD rats. The Ct.Th was thinner in the KD rats compared to the sham group, which was consistent with the results of biomechanical properties. Secondly, hyperglycemia induced by diabetes significantly inhibited the bone growth. The lengths of tibia and femur in the DM rats were remarkably shorter than those in the sham and KD groups. In addition, hyperglycemia

induced by diabetes and hyperketonemia induced by ketogenic diets provided similar effects on the bone turnover markers, which were decreasing the activity of osteoblasts and promoting the activity of osteoclasts. However, there was still a slight difference. According to the HE staining result, more adipocytes were found in the bone marrow cavity of the KD rats when compared with the sham and DM rats. This indicates that KD might have a stronger ability to differentiate BMSCs from osteoblasts to adipocytes.

It should be noted that the affecting mechanisms of hyperglycemia and hyperketonemia on bone are still unknown. Insulin-like growth factor 1 (IGF-1) plays a central role in growth, development and metabolism, and it contributes to normal longitudinal bone growth and cortical bone size as well as the maintenance of bone mass in adults (34). IGF-1 is highly expressed in osteoblasts and chondrocytes, and it brings its bone anabolic effects into play through promoting osteoblasts differentiation and bone mineralization (35, 36). IGF-1's stimulation of osteoblast differentiation is a result of activation of mammalian target of rapamycin (mTOR) through the PI3K/Akt pathway (37). Ma et al. (26) indicated that diabetes may damage bone microarchitectures and bone strengths through Sema3A/IGF-1/ β -catenin signaling pathway. In our previous study, KD reduced serological IGF-1 and delayed the spinal fusion (38). Bielohuby et al. (39) pointed out that diet-induced reduction in GH/IGF system components probably aggravated the bone phenotype, which might be an important factor in the KD-induced bone loss. The serological IGF-1 level decreased in both the DM and KD groups, with a lower trend in the DM group. Therefore, the systemic changes of IGF-1 might, in some extent, explain the mechanism of hyperglycemia and hyperketonemia on bone growth, bone development, and bone mass accrual. In addition, advanced glycation end products (AGEs) are diverse compounds that generated *via* a non-enzymatic reaction between reducing sugars and the amine residues on proteins, lipids, and nucleic acids. Growing evidence concerning bone fracture in patients with diabetes mellitus indicates the crucial roles of AGEs in aggravating bone fragility (40). However, ketogenic diet improves glycemic control in type 2 diabetes (41), and 3- β -hydroxybutyrate (the main component of a ketone body) inhibits the glycation process, decreases glucose binding to the protein, and prevents the formation of AGEs (42). Therefore, AGEs might not be a common role in the bone deterioration induced by hyperglycemia and hyperketonemia, but further study is needed.

Certain limitations of this study must be mentioned. On one hand, the effects of hyperglycemia and hyperketonemia on bone were observed at a single time point. The different time points and dynamic changes of bone microstructures and histomorphometry (such as calcein stain) need to be further studied. On the other hand, the present study has only indicated that hyperglycemia and hyperketonemia have adverse effects on bone structures, but the underlying mechanisms should be further investigated.

In conclusion, the present study comprehensively compared the effects of hyperglycemia and hyperketonemia on the bone structures from various perspectives, such as serum biomarkers, bone length, biomechanical characteristics, bone microarchitectures, and the histomorphometry. The disturbance of carbohydrate metabolism and lipid metabolism have significant adverse effects on the bone tissues, which is worth calling more attention to in clinical practice.

DATA AVAILABILITY STATEMENT

All datasets generated for this study are included in the article/supplementary files.

ETHICS STATEMENT

The animal study was reviewed and approved by Animal Ethics Committee of Southern Medical University.

AUTHOR CONTRIBUTIONS

QL, QZ and YuH contributed to the design of the experiment. QL and ZY performed the experiments, researched data, and wrote the manuscript. CX, LL and HH collected the data. YC and YaH provided statistical analyses. QL and YuH reviewed and edited the manuscript. All authors contributed to the article and approved the submitted version.

FUNDING

This work was supported by a grant from National Natural Science Foundation of China (No. 81574002).

REFERENCES

1. Terzi R, Dindar S, Terzi H, Demirtas O. Relationships among the metabolic syndrome, bone mineral density, bone turnover markers, and hyperglycemia. *Metab Syndr Relat Disord* (2015) 13(2):78–83. doi: 10.1089/met.2014.0074
2. Ford ES, Giles WH, Dietz WH. Prevalence of the metabolic syndrome among US adults: findings from the third National Health and Nutrition Examination Survey. *JAMA* (2002) 287(3):356–9. doi: 10.1001/jama.287.3.356
3. Rhee EJ, Kim YC, Lee WY, Jung CH, Sung KC, Ryu SH, et al. Comparison of insulin resistance and serum high-sensitivity C-reactive protein levels according to the fasting blood glucose subgroups divided by the newly recommended criteria for fasting hyperglycemia in 10059 healthy Koreans. *Metabolism* (2006) 55(2):183–7. doi: 10.1016/j.metabol.2005.08.010
4. Meier CR, Schlienger RG, Kraenzlin ME, Schlegel B, Jick H. HMG-CoA reductase inhibitors and the risk of fractures. *JAMA* (2000) 283(24):3205–10. doi: 10.1001/jama.283.24.3205
5. Thomas CC, Philipson LH. Update on diabetes classification. *Med Clin North Am* (2015) 99(1):1–16. doi: 10.1016/j.mcna.2014.08.015
6. Schwartz AV. Diabetes Mellitus: Does it Affect Bone? *Calcif Tissue Int* (2003) 73(6):515–9. doi: 10.1007/s00223-003-0023-7
7. Dunger DB, Acerini CL. IGF-I and diabetes in adolescence. *Diabetes Metab* (1998) 24(2):101–7.

8. Abdalrahman N, McComb C, Foster JE, McLean J, Lindsay RS, McClure J, et al. Deficits in Trabecular Bone Microarchitecture in Young Women With Type 1 Diabetes Mellitus. *J Bone Miner Res* (2015) 30(8):1386–93. doi: 10.1002/jbmr.2465
9. Coe LM, Zhang J, McCabe LR. Both spontaneous Ins2(+/-) and streptozotocin-induced type I diabetes cause bone loss in young mice. *J Cell Physiol* (2013) 228(4):689–95. doi: 10.1002/jcp.24177
10. Silva MJ, Brodt MD, Lynch MA, McKenzie JA, Tanouye KM, Nyman JS, et al. Type 1 diabetes in young rats leads to progressive trabecular bone loss, cessation of cortical bone growth, and diminished whole bone strength and fatigue life. *J Bone Miner Res* (2009) 24(9):1618–27. doi: 10.1359/jbmr.090316
11. Keene DL. A systematic review of the use of the ketogenic diet in childhood epilepsy. *Pediatr Neurol* (2006) 35(1):1–5. doi: 10.1016/j.pediatrneurol.2006.01.005
12. Neal EG, Chaffe H, Schwartz RH, Lawson MS, Edwards N, Fitzsimmons G, et al. The ketogenic diet for the treatment of childhood epilepsy: a randomised controlled trial. *Lancet Neurol* (2008) 7(6):500–6. doi: 10.1016/S1474-4422(08)70092-9
13. Hahn TJ, Halstead LR, DeVivo DC. Disordered mineral metabolism produced by ketogenic diet therapy. *Calcif Tissue Int* (1979) 28(1):17–22. doi: 10.1007/BF02441213
14. Wu X, Ding J, Xu X, Wang X, Liu J, Jiang J, et al. Ketogenic diet compromises vertebral microstructure and biomechanical characteristics in mice. *J Bone Miner Metab* (2019) 37(6):957–66. doi: 10.1007/s00774-019-01002-2
15. Xu X, Ding J, Wu X, Huang Z, Kong G, Liu Q, et al. Bone microstructure and metabolism changes under the combined intervention of ketogenic diet with intermittent fasting: an in vivo study of rats. *Exp Anim* (2019) 68(3):371–80. doi: 10.1538/expanim.18-0084
16. Ding J, Xu X, Wu X, Huang Z, Kong G, Liu J, et al. Bone loss and biomechanical reduction of appendicular and axial bones under ketogenic diet in rats. *Exp Ther Med* (2019) 17(4):2503–10. doi: 10.3892/etm.2019.7241
17. Liu Q, Xu X, Yang Z, Liu Y, Wu X, Huang Z, et al. Metformin Alleviates the Bone Loss Induced by Ketogenic Diet: An In Vivo Study in Mice. *Calcif Tissue Int* (2019) 104(1):59–69. doi: 10.1007/s00223-018-0468-3
18. Wu X, Huang Z, Wang X, Fu Z, Liu J, Huang Z, et al. Ketogenic Diet Compromises Both Cancellous and Cortical Bone Mass in Mice. *Calcif Tissue Int* (2017) 101(4):412–21. doi: 10.1007/s00223-017-0292-1
19. Bouxsein ML, Boyd SK, Christiansen BA, Guldberg RE, Jepsen KJ, Muller R. Guidelines for assessment of bone microstructure in rodents using micro-computed tomography. *J Bone Miner Res* (2010) 25(7):1468–86. doi: 10.1002/jbmr.141
20. Farr JN, Drake MT, Amin S, Melton LR, McCready LK, Khosla S. In vivo assessment of bone quality in postmenopausal women with type 2 diabetes. *J Bone Miner Res* (2014) 29(4):787–95. doi: 10.1002/jbmr.2106
21. Burghardt AJ, Issever AS, Schwartz AV, Davis KA, Masharani U, Majumdar S, et al. High-resolution peripheral quantitative computed tomographic imaging of cortical and trabecular bone microarchitecture in patients with type 2 diabetes mellitus. *J Clin Endocrinol Metab* (2010) 95(11):5045–55. doi: 10.1210/jc.2010-0226
22. Wongdee K, Charoenphandhu N. Update on type 2 diabetes-related osteoporosis. *World J Diabetes* (2015) 6(5):673–8. doi: 10.4239/wjd.v6.i5.673
23. Guo CJ, Xie JJ, Hong RH, Pan HS, Zhang FG, Liang YM. Puerarin alleviates streptozotocin (STZ)-induced osteoporosis in rats through suppressing inflammation and apoptosis via HDAC1/HDAC3 signaling. *Biomed Pharmacother* (2019) 115:108570. doi: 10.1016/j.biopha.2019.01.031
24. Rao SS, Ranganath PKS, Potu BK, Bhat KM. Beneficial Effect of Cissus quadrangularis Linn. on Osteopenia Associated with Streptozotocin-Induced Type 1 Diabetes Mellitus in Male Wistar Rats. *Adv Pharmacol Sci* (2014) 2014:483051. doi: 10.1155/2014/483051
25. Chavassieux P, Portero-Muzy N, Roux JP, Garnero P, Chapurlat R. Are Biochemical Markers of Bone Turnover Representative of Bone Histomorphometry in 370 Postmenopausal Women? *J Clin Endocrinol Metab* (2015) 100(12):4662–8. doi: 10.1210/jc.2015-2957
26. Ma R, Wang L, Zhao B, Liu C, Liu H, Zhu R, et al. Diabetes Perturbs Bone Microarchitecture and Bone Strength through Regulation of Sema3A/IGF-1/ β -Catenin in Rats. *Cell Physiol Biochem* (2017) 41(1):55–66. doi: 10.1159/000455936
27. Ay B, Parolia K, Liddell RS, Qiu Y, Grasselli G, Cooper D, et al. Hyperglycemia compromises Rat Cortical Bone by Increasing Osteocyte Lacunar Density and Decreasing Vascular Canal Volume. *Commun Biol* (2020) 3(1):20. doi: 10.1038/s42003-019-0747-1
28. Zeitoun D, Caliperoumal G, Bensidhoum M, Constans JM, Anagnostou F, Bousson V. Microcomputed tomography of the femur of diabetic rats: alterations of trabecular and cortical bone microarchitecture and vasculature—a feasibility study. *Eur Radiol Exp* (2019) 3(1):17. doi: 10.1186/s41747-019-0094-5
29. Schwartz AV, Sellmeyer DE. Diabetes, fracture, and bone fragility. *Curr Osteoporosis Rep* (2007) 5(3):105–11. doi: 10.1007/s11914-007-0025-x
30. Eckhardt BA, Rowsey JL, Thicke BS, Fraser DG, O'Grady KL, Bondar OP, et al. Accelerated osteocyte senescence and skeletal fragility in mice with type 2 diabetes. *JCI Insight* (2020) 5(9):e135236. doi: 10.1172/jci.insight.135236
31. Wang JY, Cheng YZ, Yang SL, An M, Zhang H, Chen H, et al. Dapagliflozin Attenuates Hyperglycemia Related Osteoporosis in ZDF Rats by Alleviating Hypercalciuria. *Front Endocrinol (Lausanne)* (2019) 10:700. doi: 10.3389/fendo.2019.00700
32. Turner CH, Burr DB. Basic biomechanical measurements of bone: a tutorial. *Bone* (1993) 14(4):595–608. doi: 10.1016/8756-3282(93)90081-k
33. Saito A, Yoshimura K, Miyamoto Y, Kaneko K, Chikazu D, Yamamoto M, et al. Enhanced and suppressed mineralization by acetoacetate and β -hydroxybutyrate in osteoblast cultures. *Biochem Biophys Res Commun* (2016) 473(2):537–44. doi: 10.1016/j.bbrc.2016.03.109
34. Tahimic CG, Wang Y, Bikle DD. Anabolic effects of IGF-1 signaling on the skeleton. *Front Endocrinol (Lausanne)* (2013) 4:6. doi: 10.3389/fendo.2013.00006
35. Sheng MH, Lau KH, Baylink DJ. Role of Osteocyte-derived Insulin-Like Growth Factor I in Developmental Growth, Modeling, Remodeling, and Regeneration of the Bone. *J Bone Miner Metab* (2014) 21(1):41–54. doi: 10.11005/jbm.2014.21.1.41
36. Kawai M, Rosen CJ. The insulin-like growth factor system in bone: basic and clinical implications. *Endocrinol Metab Clin North Am* (2012) 41(2):323–33, vi. doi: 10.1016/j.ecl.2012.04.013
37. Crane JL, Cao X. Function of matrix IGF-1 in coupling bone resorption and formation. *J Mol Med (Berl)* (2014) 92(2):107–15. doi: 10.1007/s00109-013-1084-3
38. Liu Q, Wang X, Huang Z, Liu J, Ding J, Xu X, et al. Ketogenic diet delays spinal fusion and decreases bone mass in posterolateral lumbar spinal fusion: an in vivo rat model. *Acta Neurochir (Wien)* (2018) 160(10):1909–16. doi: 10.1007/s00701-018-3616-7
39. Bielohuby M, Matsuura M, Herbach N, Kienzle E, Slawik M, Hoeflich A, et al. Short-term exposure to low-carbohydrate, high-fat diets induces low bone mineral density and reduces bone formation in rats. *J Bone Miner Res* (2010) 25(2):275–84. doi: 10.1359/jbmr.090813
40. Goh SY, Cooper ME. Clinical review: The role of advanced glycation end products in progression and complications of diabetes. *J Clin Endocrinol Metab* (2008) 93(4):1143–52. doi: 10.1210/jc.2007-1817
41. Hussain TA, Mathew TC, Dashti AA, Asfar S, Al-Zaid N, Dashti HM. Effect of low-calorie versus low-carbohydrate ketogenic diet in type 2 diabetes. *Nutrition* (2012) 28(10):1016–21. doi: 10.1016/j.nut.2012.01.016
42. Gharib R, Khatibi A, Khodarahmi R, Haidari M, Husseinazadeh S. Study of glycation process of human carbonic anhydrase II as well as investigation concerning inhibitory influence of 3- β -hydroxybutyrate on it. *Int J Biol Macromol* (2020) 149:443–9. doi: 10.1016/j.jbiomac.2020.01.192

Conflict of Interest: The authors declare that the research was conducted in the absence of any commercial or financial relationships that could be construed as a potential conflict of interest.

Copyright © 2020 Liu, Yang, Xie, Ling, Hu, Cao, Huang, Zhu and Hua. This is an open-access article distributed under the terms of the Creative Commons Attribution License (CC BY). The use, distribution or reproduction in other forums is permitted, provided the original author(s) and the copyright owner(s) are credited and that the original publication in this journal is cited, in accordance with accepted academic practice. No use, distribution or reproduction is permitted which does not comply with these terms.



Control of Bone Matrix Properties by Osteocytes

Amy Creecy^{1†}, John G. Damrath^{2†} and Joseph M. Wallace^{1*}

¹ Department of Biomedical Engineering, Indiana University-Purdue University at Indianapolis, Indianapolis, IN, United States,

² Weldon School of Biomedical Engineering, Purdue University, West Lafayette, IN, United States

OPEN ACCESS

Edited by:

Deborah Veis,
Washington University School of
Medicine in St. Louis, United States

Reviewed by:

Laoise Maria McNamara,
National University of Ireland Galway,
Ireland

Connie M. Weaver,
Purdue University, United States
Marian Young,
National Institutes of Health (NIH),
United States

*Correspondence:

Joseph M. Wallace
jmwalla@iupui.edu

[†]These authors have contributed
equally to this work

Specialty section:

This article was submitted to
Bone Research,
a section of the journal
Frontiers in Endocrinology

Received: 30 June 2020

Accepted: 01 December 2020

Published: 18 January 2021

Citation:

Creecy A, Damrath JG and
Wallace JM (2021) Control of Bone
Matrix Properties by Osteocytes.
Front. Endocrinol. 11:578477.
doi: 10.3389/fendo.2020.578477

Osteocytes make up 90–95% of the cellular content of bone and form a rich dendritic network with a vastly greater surface area than either osteoblasts or osteoclasts. Osteocytes are well positioned to play a role in bone homeostasis by interacting directly with the matrix; however, the ability for these cells to modify bone matrix remains incompletely understood. With techniques for examining the nano- and microstructure of bone matrix components including hydroxyapatite and type I collagen becoming more widespread, there is great potential to uncover novel roles for the osteocyte in maintaining bone quality. In this review, we begin with an overview of osteocyte biology and the lacunar–canalicular system. Next, we describe recent findings from *in vitro* models of osteocytes, focusing on the transitions in cellular phenotype as they mature. Finally, we describe historical and current research on matrix alteration by osteocytes *in vivo*, focusing on the exciting potential for osteocytes to directly form, degrade, and modify the mineral and collagen in their surrounding matrix.

Keywords: perilacunar remodeling, lacunocanalicular network, extracellular matrix, collagen, mineral, mechanical loading

INTRODUCTION

Embedded within the mineralized matrix of bone, osteocytes, a cell population of growing importance in bone biology and medicine, find great longevity despite their apparently isolated location. Osteocytes are increasingly recognized as cells that govern the process of bone remodeling by directing bone forming osteoblasts and bone resorbing osteoclasts. While these actions play an important role in determining the location and time-course of bone remodeling, osteocytes themselves are positioned to readily access immense quantities of bone tissue. Making up over 90% of the cellular content of bone, osteocytes form a rich network of dendrites that communicate with roughly 50 neighboring osteocytes, resulting in a total surface area that greatly exceeds that of osteoblasts and osteoclasts combined. Therefore, any stimulus that triggers osteocytes to directly interact with the bone matrix could have a great positive or negative impact on the overall integrity of bone. In this review, we begin with a brief discussion of how osteocytes direct the activities of osteoblasts and osteoclasts. Next, we cover the important role of the lacunar–canalicular network (LCN) in osteocyte communication and remodeling. Finally, we discuss the exciting potential for osteocytes to directly modify the organic and inorganic components of the bone matrix, which may form an important basis for future treatment strategies aimed at improving bone mass and tissue quality.

OSTEOCYTE-DIRECTED MATRIX MODIFICATION BY OSTEOBLASTS AND OSTEOCLASTS

At the end of their period of bone formation, late-stage osteoblasts are directed *via* unknown cues to either undergo apoptosis or terminal differentiation (1, 2). One option is for osteoblasts to differentiate into quiescent bone lining cells, which cover the bone surface and are thought to mediate remodeling in localized bone areas (1). Some osteoblasts further differentiate into osteocytes. Late osteoblasts transition to early osteocytes by forming dendrites *via* upregulation of the gene *E11/gp38*, or podoplanin (3). Upregulation of *MT1-MMP*, a metalloproteinase that cleaves collagen, is also required for osteocyte dendrite formation and maintains cell viability throughout differentiation (4, 5). These findings may suggest that osteocyte embedding is an active, proteolytic process, in contrast to initial studies that suggested osteocyte embedding is a process of passive entrapment within the matrix (6, 7). Recently, however, studies utilizing intravital imaging have suggested that there may be multiple mechanisms for osteocyte embedding that involve some combination of the above processes, as well as lacunar reshaping prior to differentiation (8). Once embedded, the osteocyte begins its role in coordinating the actions of osteoblasts and osteoclasts as a part of the rich osteocyte network.

Osteocyte Communication With Osteoblasts

The activities of osteoblasts and osteoclasts are highly regulated by signals originating from osteocytes, although the mechanisms by which signals reach these cells are poorly understood. Osteoblasts are responsible for new bone formation, which primarily occurs on trabecular and cortical bone surfaces (9). Bone formation is notably induced by the Wnt signaling pathway. The canonical pathway involves Wnt binding to low-density lipoprotein receptor-related protein 5/6 (*Lrp5/6*) and its co-receptor, *Frizzled* (10). This binding inhibits the intracellular activity of glycogen synthase kinase 3 (*GSK3*) and its complex consisting of *Axin* and adenomatous polyposis coli (*APC*), which results in hypophosphorylation of the transcription factor β -catenin (11). Translocation of intact β -catenin to the nucleus results in the expression of genes that enhance osteoblast survival and bone formation activity. Osteocytes are an important regulator of this process *via* the secretion of *Sclerostin* (*Sost*). *Sost* is a potent suppressor of Wnt signaling by binding *Lrp5/6*, competitively inhibiting Wnt binding (12). This results in uninhibited phosphorylation of β -catenin and its subsequent degradation by the proteasome. *Sclerostin* has also been shown to inhibit bone morphogenetic protein (*BMP*)-related bone formation (13). In humans, mutations in *Sost* result in sclerosteosis, a condition characterized by increased bone formation resulting in high bone mass and cranial neuropathies due to nerve compression (14). Therefore, osteocytes have the potential to control when and where bone formation occurs and interfering with this process can have dramatic effects on human health.

Osteocyte Communication With Osteoclasts

Interestingly, osteocytes also mediate the process of bone resorption by osteoclasts. One method of regulation is through osteocyte secretion of receptor activator of nuclear factor kappa B ligand (*RANKL*) through their dendrites, which binds the *RANK* receptor on osteoclast precursors and drives their differentiation into mature osteoclasts (15). *RANKL* expression by osteocytes is essential for trabecular bone remodeling and is secreted by osteocytes in regions of osteocytic apoptosis (16, 17). Additionally, osteocytes secrete osteoprotegerin (*OPG*), a molecule that competes with *RANKL* for the *RANK* receptor (18). This interaction suppresses osteoclast activity and is the basis for the anti-resorptive osteoporosis drug *denosumab* (19, 20). Frequently, the overall secreted *RANKL/OPG* ratio is measured in *in vitro* and *in vivo* models, and in humans, to approximate the degree of osteoclastogenesis in the bone (21). Therefore, osteocytes can modify the total content and activity of mature osteoblasts and osteoclasts, demonstrating their important regulatory role in the process of bone remodeling.

Repair of bone microdamage has also been shown to be dependent on the coordinated actions of osteocytes and osteoclasts. Microdamage, or small cracks or breaks in the bone, trigger osteocyte apoptosis and induce intracortical remodeling, a process that is atypical in rodent cortical bone (22). Further, regions of bone remodeling colocalize with regions of osteocyte apoptosis in the context of microdamage or estrogen deficiency (22, 23). *In vitro* studies have demonstrated that apoptotic osteocytes stimulate their neighbors to release *RANKL*, which acts as a chemotactic signal for osteoclasts to migrate into the regions of apoptosis and remodel the bone (24). Therefore, osteocytes also utilize osteoclasts to repair regions of microdamage through the controlled release of *RANKL* while preserving undamaged regions of the bone.

The process of remodeling is slow and deliberate, but evidence demonstrating decreased whole body bone mineral content in lactating women suggests that rapid changes in systemic mineral demands must be met by liberating mineral from the bone (25). Furthermore, bone matrix components must rapidly reform to maintain bone strength when mineral demands are lifted. Indeed, weaning triggers osteoclast apoptosis and a decrease in *RANKL* levels within the bone while osteoblastic activity remains elevated, favoring bone formation (26). However, considering that the resorption and formation processes by osteoclasts and osteoblasts, respectively, primarily occur on bone surfaces, it is logical that osteocytes may utilize their large surface area to release bone mineral during lactation and reconstruct their surrounding matrix after weaning. Therefore, due to their large population, extensive network, and sprawling surface area, researchers have begun investigating the osteocyte as a potential candidate for rapid bone alterations when subjected to stimuli that alter bone formation and resorption (27). The remainder of this review will focus on observations from *in vitro* and *in vivo* studies examining the potential for osteocytes to control the structure and composition

of bone by modulating the activity of osteoblasts and osteoclasts and by direct interaction with the extracellular matrix.

LACUNAR–CANALICULAR NETWORK AND ITS ROLE IN TRANSMITTING MECHANICAL STIMULI

Osteocyte cells are embedded in the mineralized matrix in protected lacunae which surround the cell body. The cells are connected to one another by dendritic cell processes which reside in canaliculi. Together, these form the lacunar–canalicular network (LCN). This interconnected network of cells may be relevant to mechanical sensing and is important for signaling and solute transport (28). As extracellular fluid flows through the LCN, the osteocytes release chemicals such as nitric oxide, prostaglandin, and other factors (29). Additionally, the level of mechanical stimuli is related to osteocyte apoptosis which promotes osteoclastogenesis and is a mechanism by which osteocytes regulate bone repair and shape (28). Loading enhances fluid flow and the shape of the LCN may affect how fluid flows through the system, as observed by the use of injected tracers, where there is an increase in labeled osteocytes with loading (30). Ciani et al. saw an increase in the percentage of osteocytes labeled with an injected tracer in loaded tibiae compared to non-loaded tibiae of rats. However, this only occurred in cancellous bone, not cortical bone (30). This increase of fluid flow with loading has also been speculated with numerical methods. Multiple groups have attempted to quantify the forces placed on the LCN using finite element analysis (FEA) and numerical models which indicate that the shape of the network influences the shear stress the cell is exposed to (31–33). The model in Gatti et al. indicated that vascular porosity plays a role as well, with idealized models showing a decrease in fluid velocity with an increase in vascular porosity (33). Using a fluid–structure interaction model to model a single cell, Joukar et al. indicated cells in rounded lacunae experienced less shear stress than elliptical ones under different modes of loading (32). The overall organization and shape of the LCN affect the ability of the osteocyte to sense stimuli, communicate with other cells, and effectively modulate bone quality.

The LCN can be imaged multiple ways, in two and three dimensions to provide quantitative measures of the LCN and osteocyte shape and organization. Two dimensional methods include scanning electron microscopy (11) with silver staining or quantitative backscatter imaging. Three dimensional methods allow for data analysis on connections between the osteocytes. These include high resolution micro-computed tomography, second harmonic generation, and confocal microscopy when combined with staining (34). In addition to the LCN shape, the osteocyte cell can be imaged using a combination of staining and confocal microscopy. Recent research has utilized green fluorescence protein (GFP)-labeled osteocytes and other dyes to image cellular aspects of the osteocyte such as the cytoskeleton along with the dendritic connections in relation to the

surrounding collagen (35). This approach has yielded some evidence that vesicles may be released by the osteocyte as it embeds itself within the LCN and that collagen may be produced by the osteocyte. It is important to note that quantifying the number of lacunae is not the same as quantifying occupied lacunae (36). After an osteocyte dies, the lacunae will remain empty until it is gradually filled with mineralized debris.

Quantitative analysis of the LCN structure must be done to determine if alterations to the shape and organization of the network are occurring. Lacunar area or volume, lacunar density, canalicular length, and canalicular density are some of the measurements that can be made to quantify changes. The LCN can also be quantified in a manner similar to quantification of the connectivity of the trabecular bone network. This is essentially a measure of how many connections would have to be broken to separate the network into two (37). Additionally, the LCN can be analyzed in terms of connectomics. In this analysis, the LCN is considered as a system of nodes linked together by edges. Nodes can be either lacunae or places where at least three canaliculi connect. This analysis could be useful to determine how the organization of the LCN affects the osteocyte's ability to communicate with other cells and respond to loading. Nodal centers with higher numbers of connections may indicate fewer and more utilized routes of communication. Connectomics analysis has been reviewed in depth elsewhere (38). Less work has been done using connectomics analysis, but there have been some studies that have utilized this technique. Mabilieu et al. have indicated that high fat diet caused an increase in node degree in mice (39). Additionally, connectomics analysis has been used to analyze differences in the LCN structure between sheep and mouse bone, albeit on a limited number of samples (40). The network of sheep bone was more regularly organized but less connected than mouse bone, but properties such as edges per node and edge length were similar between species.

Changes to the LCN have been observed based on the organization of the surrounding matrix, during aging, disease, and in response to environmental factors. More spherical lacunae are likely to be found in woven bone versus the more organized lamellar bone (41). Osteocytes have been seen to elongate perpendicular to the long axis of bones in amphibians, reptiles, and mammals (42). High fat diet caused an increase in lacunar area in mice (39). The LCN also changes with aging, as lacunae become flatter and the canaliculi become more interconnected with maturity, a trend that reverses once bone is aged (43). There are changes to the LCN in osteogenesis imperfecta (OI) as OI mice have been observed to have more spherical lacunae with more canaliculi than wild-type mice (44). Mechanical unloading also results in changes to the LCN. Sciatic neurectomy to immobilize one limb in growing rats resulted in lower lacunar density and volume (45). Similarly, growing mice were found to have a reduced cell volume and number of processes with sciatic neurectomy in both cortical and cancellous bone (46). It is important to note that these experiments were both done in growing rodents. Immobilized female patients had a lower osteocyte density and reduced connectivity than postmenopausal controls (47). Fluid flow as

determined by finite element analysis (FEA) was shown to decrease in ovariectomized rats that had lower lacunar density and porosity (33).

The LCN may have a direct effect on bone quality. In cases of spaceflight where the lacunar volume was shown to decrease and become more spherical, nanoindentation indicated that the hardness and stiffness of the matrix also decreased (48). Another study used nanoindentation to assess the area close to (1 to 5 μm) and further away from the lacunae (16 to 20 μm) in ovariectomized rats with treatment. While there were no differences between treatment groups (PTH, alendronate, raloxifene, PTH and alendronate, and PTH and raloxifene), Young's modulus was lower in the perilacunar region compared to the area further away (49). Modulus was also higher further away from the lacunae and canaliculi in healthy 4-month old female rats (50). Mounting evidence supports that actions coordinated by osteocytes in the LCN directly impact matrix quality.

The pericellular matrix (PCM) surrounds the osteocyte and separates the cell from the walls of the lacunae and canaliculi. This matrix contains proteoglycans and hyaluronic acid and may amplify the impacts of mechanical loading to allow osteocyte to sense more load than what would be calculated by tissue strain alone. Tethering elements between the matrix wall and the cells that could amplify force through shear drag forces in response to fluid flow were first postulated with computational modeling (51) prior to transverse elements between the matrix wall and cell being visually confirmed with TEM imaging (52). Perlecan has been speculated to form the tethering elements in the PCM. MLO-Y4 cells express perlecan protein and immunogold labeling indicated the presence of perlecan along the osteocyte bodies and walls of the canaliculi (53). Perlecan deficient mice have shown higher solute diffusivity, but lacked the anabolic response to *in vivo* tibial loading (54) indicating its importance for mechanical sensing (54). Additionally, integrins have been speculated to form part of the PCM and affect the osteocyte response to mechanical stimulation. TEM images have indicated the canalicular walls may have protrusions into the pericellular space (55, 56). A theoretical model incorporating tethering elements along with focal adhesion complexes mathematically predicted a high amplification of strain that was an order of magnitude higher than previous strain amplification models (56). This focal adhesion complex has been speculated to be $\beta 3$ -integrin as immunohistochemistry has indicated the presence of $\beta 3$ -integrin along the walls of canaliculi of murine cortical bone (55). *In vitro*, inhibition of $\alpha \nu \beta 3$ integrin attachment sites in MLO-Y4 cells reduced the Ca^{2+} response to probe stimulation (57). Structured Illumination Super Resolution Microscopy has found membrane proteins associated with mechanotransduction to be colocalized with $\beta 3$ -integrin foci *in vivo*, though this did not find a colocalization with connexin 43 (58). The PCM may also alter with age. Osteocytes isolated from aged mice were able to produce less PCM than osteocytes from young mice *in vitro*. Aged cells also had fewer plasma membrane disruptions than young cells in response to fluid shear stress, indicating the mechanical response may be dependent on the PCM (59). This is an aspect of osteocyte control of the environment that needs to be further studied.

IN VITRO MODELS OF PERILACUNAR REMODELING

Due to their preference of remaining embedded within the bone matrix, osteocytes have proven difficult to study when removed from their natural enclosure. Indeed, studies on primary osteocytes have demonstrated complications including low yield, poor viability when grown in 2D culture, and limited dendrite formation. Therefore, most studies to date have utilized immortalized cellular models of osteocytes. These cell lines represent various stages of the osteocyte life cycle, including late transitioning osteoblasts, early osteocytes, late osteocytes, and lines that gradually differentiate through all three stages. Despite being derived from osteocytes, each cell line responds differently to mechanical, endocrine, and paracrine signals. Therefore, we will begin our analysis of osteocyte matrix modeling and remodeling by examining what has been learned using *in vitro* models.

Cellular Models of Osteocytes

The most frequently used cell line in osteocyte research is the MLO-Y4 line. These cells were derived from the long bones of female mice and immortalized using an SV40 T-cell antigen coupled to the osteocalcin promoter (60). MLO-Y4 cells are mechanosensitive, as studies utilizing fluid shear stress have demonstrated robust increases in intracellular calcium currents, ATP production, and release of prostaglandin E2 (PGE2) and nitric oxide (NO) (61–63), all of which are essential components of the osteocyte response to mechanical stimulation. Additionally, they express large amounts of connexin 43 (Cx43) and produce a dendritic network. In response to short-term unidirectional and oscillatory fluid flow, MLO-Y4 cells increase RANKL expression while greatly increasing OPG expression, resulting in a decrease in the RANKL/OPG ratio (64, 65). This finding may indicate that osteocytes respond to loading by reducing osteoclast activity through paracrine signaling. Importantly, MLO-Y4 cells do not typically express Sost, a potent inhibitor of bone formation by osteoblasts. This shortcoming is also noted in MLO-A5 cells, a model of late transitioning osteoblasts (66). Interestingly, long-term fluid shear may increase Sost expression in MLO-Y4 cells despite their lack of natural Sost expression, although conflicting evidence exists (67, 68). In terms of anabolic functions, conditioned media taken from MLO-Y4 cultures increases alkaline phosphatase (34) and osteocalcin (OCN) expression in osteoblasts, indicating the presence of additional secreted factors that increase osteoblast activity (69).

Two models of differentiated osteocytes are the Ocy454 and IDG-SW3 cell lines. Each of these lines utilizes an interferon- γ driven T-cell antigen promoter to induce immortalization followed by temperature-driven differentiation. The mechanical response of Ocy454 cells to fluid shear are more variable than MLO-Y4 cells, with fewer cells demonstrating increased calcium currents with occasional high magnitude calcium waves (70). Unlike MLO-Y4 cells, Ocy454 osteocytes express abundant DMP1 and Sost, and Sost expression can be lowered by fluid

shear (68). Increasing the duration of fluid shear gradually increases Sost expression and the RANKL/OPG ratio in both lines (68). Like Ocy454 cells, the IDG-SW3 cell line expresses classic osteocytic genes when they reach maturity. In the early stages of differentiation, IDG-SW3 cells express osteoblastic genes including ALP and type I collagen (colla1) (71). As they transition into early osteocytes, dentin matrix protein 1 (DMP1), matrix extracellular phosphoglycoprotein (MEPE), and phosphate-regulating neutral endopeptidase (PheX) levels increase (71). Finally, as late osteocytes, IDG-SW3 cells begin expressing high levels of Sost and fibroblast growth factor 23 (FGF23), demonstrating their utility in studying osteocyte paracrine and endocrine signaling (71).

While osteoblasts and osteoclasts are the classic cell types involved with forming and shaping bone, emerging research has demonstrated that many of the cues that drive these cells may also trigger osteocytes to participate in these functions. The process of bone matrix alteration by osteocytes is currently known as perilacunar remodeling (PLR), a concept that is gaining popularity in the bone community. Utilizing the idea that osteocytes also modify their activity in response to cues that would normally change bone mass, we next examine how bone-altering signals may modify osteocyte function to alter their surrounding extracellular matrix using the aforementioned *in vitro* models.

Osteocyte Responses to Endocrine, Paracrine, and Mechanical Stimuli

One of the most important signals the bone receives is from parathyroid hormone (PTH), a peptide hormone secreted from the parathyroid gland in response to low serum calcium. In addition to increasing calcium absorption from the intestine, sustained elevations in PTH are known to cause mineral release from the bone, as seen in hypercalcemia of malignancy and chronic kidney disease (72, 73). Studies using IDG-SW3 cells have demonstrated that PTH upregulates ATPase H⁺ Transporting V0 Subunit D2 (ATP6V0D2), a proton pump on the cell membrane that acidifies the extracellular environment, indicating that osteocytes can acidify their extracellular environment to degrade mineral (74). PTH-related Peptide (PTHrP) has also been shown to stimulate acidification of the osteocyte extracellular environment by upregulating ATP6V0D2 during lactation, and this process is dependent on intact PTH signaling in osteocytes (75). IDG-SW3 cells naturally upregulate several osteoclastic genes throughout their 28-day differentiation including tartrate-resistant acid phosphatase (TRAP), carbonic anhydrase I and II (CA1/2), and cathepsin K (CTSK), indicating that mature osteocytes are poised to participate in PLR (76). While matrix acidification is required for mineral removal, it also promotes the collagenolytic activity of CTSK, indicating that osteocytes can degrade both mineral and collagen (77, 78). In addition to PTH, Sost signaling has also been shown to upregulate TRAP, CA, and CTSK in neighboring MLO-Y4 osteocytes (79). Therefore, osteocytes may increase the bone resorbing activity of nearby osteocytes in addition to reducing

osteoblast activity *via* Sost signaling (76, 79). Finally, TGF β also upregulates several osteoclastic genes *via* the YAP/TAZ signaling pathway in MLO-Y4 and Ocy454 cells. In MLO-Y4 cells, treatment with TGF β results in extracellular acidification and upregulation of CTSK and matrix metalloproteinase 13 and 14 (MMP13/14) while glucocorticoid treatment decreases MMP13 expression (80). A similar finding was shown in Ocy454 cells, which upregulated CTSK and MMP14, but not MMP13 (78). While these two osteocyte models differ slightly in their responses, they each suggest that osteocytes participate in matrix remodeling by adopting an osteoclast-like phenotype.

As mentioned above, mechanical loading alters osteocyte signaling to osteoblasts and osteoclasts. However, whether loading influences the process of PLR remains unclear. When fluid shear stress is applied to MLO-Y4 cells, increased E11/gp38 expression drives increased dendrite formation and elongation (80). For this process to occur *in vivo*, however, osteocyte dendrites must express genes that allow them to degrade local mineral and collagen to extend through the bone. Indeed, a recent study seeding IDG-SW3 cells into an MMP-sensitive hydrogel demonstrated increased dendricity, Cx43, and MMPs 2 and 13 throughout differentiation (81). These cells also maintained elevated ALP expression through day 28 of differentiation while ALP expression diminishes in 2D culture. Another study in 3D culture demonstrated that MLO-Y4 cells display increased colla1 expression over time (82). Therefore, 3D culture models may be necessary to capture the ability for osteocytes to form matrix components. However, studies examining perilacunar modeling and remodeling by osteocytes in 3D cell culture with loading or other physiologic stimuli remain to be performed. Altogether, these *in vitro* findings suggest that bone-forming osteoblasts can differentiate into mechanosensitive osteocytes that coordinate the activities of osteoblasts and osteoclasts, and eventually gain osteoclastic resorptive abilities. Strikingly, while osteocytes reduce their osteoblastic activity over time, these functions are not entirely lost as they mature in a 3D environment. Therefore, further research probing the ability for osteocytes to form mineral and collagen are imperative to understand the contribution of osteocytes to the microstructure and overall integrity of bone.

MODIFICATION OF MINERAL BY THE OSTEOCYTE

Osteocyte modification of the mineral in the surrounding matrix has been observed in cases where PLR removes mineral such as in lactation (83) and hibernation (84), and lack of PLR can result in hypermineralization such as in the case of exposure to microgravity (48). This has been supported by changes to lacunar area. In the case of lactation, it has been suggested that the osteocyte can also replace the mineral in its surrounding bone if recovery after weaning is allowed, as double fluorochrome labeling has indicated new mineral formation around the osteocyte (75). The osteocyte can alter the overall porosity of

bone by either removing or adding mineral to its lacunae. The osteocyte network appears to influence the quality of the mineral as well. Using small angle X-ray scattering (SAXS) combined with confocal microscopy, a study showed that in areas with a high density of osteocytes that were well aligned, the mineral platelet thickness and particle orientation was higher than in less organized areas (85). The mineral thickness and particle orientation were lower in the areas closer to the lacunae themselves, indicating that the osteocytes may control the quality of the mineral over time (85). In another study looking at mice that underwent treadmill running, the mineral to matrix ratio (MMR) of the matrix surrounding the osteocyte was lower than the MMR of the matrix further away, indicating the osteocyte altering its bone matrix (86). Interestingly, mice that underwent treadmill running and showed lower MMR in their perilacunar region had higher post-yield work in bending tests of their tibiae, indicating that PLR may improve bone's overall mechanical properties (86). An effect on mechanical properties has also been observed elsewhere as the elastic modulus as measured by microindentation of the bone decreased with lactation (87). Thus, changes to the mineral by the osteocyte may affect overall bone quality.

COLLAGEN PRODUCTION AND ALTERATION BY OSTEOCYTES

Type I collagen is the most prevalent organic component of the bone extracellular matrix and provides the tissue with tensile ductility and fracture toughness by limiting crack formation and propagation (88–90). Collagen is primarily produced by osteoblasts during bone formation alongside mineral. The helical structure of collagen is composed of Gly-X-Y repeats where X and Y are typically proline and hydroxyproline, respectively (91). Collagen consists of two pro- $\alpha 1$ and one pro- $\alpha 2$ peptide chains that are translated by ribosomes embedded within the endoplasmic reticulum (ER) membrane. Next, post-translational modifications including hydroxylation of proline and lysine residues and glycosylation of some prolines occurs within the ER. The chains twist into a triple helix and are shuttled to the Golgi apparatus as procollagen. Upon secretion from the osteoblast, the N- and C-terminal domains are cleaved, forming tropocollagen. Finally, tropocollagen strands self-assemble into fibrils and neighboring tropocollagen molecules are crosslinked at their hydroxylysine residues by lysyl oxidase, stabilizing the fibrillar structure (92).

The overall quality of collagen is dependent on the correct level of post-translational modifications, proper crosslinking, incorporation into the bone, and alignment within the bone tissue. Importantly, the alignment of collagen fibrils is related to the types of loads that each bone experiences. During physiologic loading of the lower limb, the anterior portion of the femur and tibia typically experiences tension while the posterior portion is under compression (93). Studies utilizing polarized light microscopy have determined that collagen fibrils tend to be aligned perpendicular to transverse sections of bones under tension while they are aligned parallel to transverse sections in compressive regions. Intriguingly, collagen fibrils tend to align with the major axis of osteocytes and their lacunae (41).

Additionally, it has been shown that osteoblasts initially secrete disorganized collagen that eventually aligns with the osteoblast major axis or the axis under the greatest mechanical strain (94, 95).

While osteoblasts follow mechanical cues from their environment to determine collagen orientation and placement, mechanosensory cues from osteocytes may also be required to instruct osteoblast collagen deposition. Further, it stands that osteocytes themselves may be responsible for forming and aligning collagen in the perilacunar region. One of the earliest studies examining this possibility placed bones from egg-laying hens in media containing radiolabeled proline, a highly prevalent amino acid in all collagens (96). In hens fed a calcium-rich diet after egg laying, it was reported that osteoblasts and osteocytes demonstrated widespread uptake of proline, indicating that osteocytes may replenish matrix collagen following lactation (97). Modern intravital imaging studies have also demonstrated that early osteocytes may be able to synthesize parts of the collagen matrix surrounding their lacunae while also exerting mechanical forces on the existing collagen matrix (8). Eventually, this process results in a collagenous matrix that aligns with the major axis of osteocyte lacunae, but whether this process is mechanically driven remains unknown.

As discussed earlier, *in vitro* models of osteocytes have the capacity to degrade collagen in response to catabolic stimuli including PTH. The importance of this finding has also been established *in vivo*, as lactating mice fail to resorb mineral from their lacunae if collagen degrading genes including CTSK and MMP-13 are knocked out in osteocytes (98, 99). Therefore, collagen degradation is an essential step in perilacunar remodeling. Additionally, MMP-13 expression by osteocytes is critical to maintenance of bone fracture toughness, or the ability of bone to resist crack formation and propagation, a property that is highly dependent on proper collagen incorporation and crosslinking (99, 100). There are implications that TGF- β may be involved as well. It has been demonstrated that inhibiting TGF- β receptor pharmacologically in mice resulted in a reduction of gene expression of genes associated with PLR and reduced canaliculi length (76). The same study examined a knock-out mouse of osteocyte specific TGF- β receptor in bone which resulted in a similar decline in PLR gene expression and decrease in canalicular length and lacunar–canalicular area. Fracture resistance was notably lower in the knock-out mice (76). Taken together, there is striking preliminary evidence to warrant a deeper investigation of the osteocytes ability to modify, align, and produce collagen within their lacunae. Future work may require the use of 3D scaffolds in order to capture these effects *in vitro* while *in vivo* studies will likely benefit from the use of emerging techniques to analyze bone composition and mechanical properties on the microscale in animal models of post-lactation recovery, space flight, and other instances of mineral challenge. Furthermore, while collagen is the most prevalent protein in bone, genetic knockouts of non-collagenous proteins (NCPs) including biglycan, fibrillin-2, and bone sialoprotein among others have demonstrated altered microarchitecture and/or reduced mechanical properties (101–103). Biglycan in particular is required for proper collagen assembly into organized fibrils, and knockouts resemble the

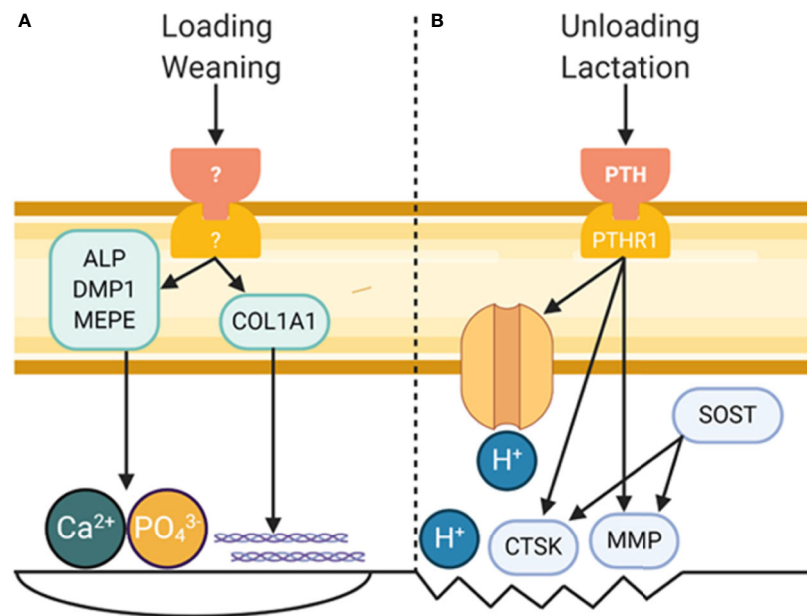


FIGURE 1 | Role of Osteocytes in Modifying Bone Matrix Properties. **(A)** Mechanical loading and wearing are known to increase bone formation, and osteocytes are known to play a critical role in each. While a definite pathway leading to bone formation by osteocytes remains to be discovered, a small amount of bone formation by osteocytes could have a profound effect on bone material properties. **(B)** Perilacunar remodeling by osteocytes occurs in response to unloading and lactation, processes in which PTH is a major player. This results in decreased pH in the perilacunar space and increased expression of collagenolytic enzymes. Figure created with BioRender.com.

phenotype of Ehlers–Danlos syndrome (104). However, material tests such as fracture toughness testing and tissue-level analyses have largely not been performed on these genetic models. While NCPs are known to impact bone formation, whether osteocytes can interact with and alter NCPs, or whether NCPs control the ability for osteocytes to model and remodel their surrounding matrix remains largely unknown. Taken together, understanding the full extent of the osteocytes capabilities will require a combination of robust cellular models, modern imaging modalities, and tissue-level analyses that can distinguish material, structural, and compositional properties on the micro- and nano-scales in and around the LCN, enhancing our ability to devise new treatments for bone diseases.

CONCLUSION

The osteocyte has a profound effect on the bone matrix through signaling to osteoblasts and osteoclasts and by directly modifying

its environment (**Figure 1**). The structure of the LCN relates to the structure and quality of the surrounding matrix. There is also *in vitro* and *in vivo* evidence indicating the osteocyte can directly modify mineral and collagen in its surroundings. Thus, the osteocyte must be considered when examining the effects of disease and treatments on the bone matrix.

AUTHOR CONTRIBUTIONS

AC, JD, and JW planned and wrote the document. All authors contributed to the article and approved the submitted version.

FUNDING

This work was supported by the National Institutes of Health [JW: AR072609; AC: AR065971; JD: DK121399].

REFERENCES

- Manolagas SC. Birth and Death of Bone Cells: Basic Regulatory Mechanisms and Implications for the Pathogenesis and Treatment of Osteoporosis*. *Endocrine Rev* (2000) 21:115–37. doi: 10.1210/er.21.2.115
- Jilka RL, Weinstein RS, Bellido T, Parfitt AM, Manolagas SC. Osteoblast Programmed Cell Death (Apoptosis): Modulation by Growth Factors and Cytokines. *J Bone Mineral Res* (1998) 13:793–802. doi: 10.1359/jbmr.1998.13.5.793
- Wetterwald A, Hofstetter W, Cecchini MG, Lanske B, Wagner C, Fleisch H, et al. Characterization and cloning of the E11 antigen, a marker expressed by Rat Osteoblasts and Osteocytes. *Bone* (1996) 18:125–32. doi: 10.1016/8756-3282(95)00457-2
- Karsdal MA, Andersen TA, Bonewald L, Christiansen C. Matrix Metalloproteinases (MMPs) Safeguard Osteoblasts from Apoptosis during Transdifferentiation into Osteocytes: MT1-MMP Maintains Osteocyte Viability. *DNA Cell Biol* (2004) 23:155–65. doi: 10.1089/104454904322964751

5. Holmbeck K, Bianco P, Pidoux I, Inoue S, Billingham RC, Wu W, et al. The metalloproteinase MT1-MMP is required for normal development and maintenance of osteocyte processes in bone. *J Cell Sci* (2005) 118:147. doi: 10.1242/jcs.01581
6. Palumbo C, Palazzini S, Zaffe D, Marotti G. Osteocyte differentiation in the tibia of newborn rabbit: an ultrastructural study of the formation of cytoplasmic processes. *Acta Anat (Basel)* (1990) 137:350–8. doi: 10.1159/000146907
7. Franz-Odenaal TA, Hall BK, Witten PE. Buried alive: how osteoblasts become osteocytes. *Dev Dyn* (2006) 235:176–90. doi: 10.1002/dvdy.20603
8. Shiflett LA, Tiede-Lewis LM, Xie Y, Lu Y, Ray EC, Dallas SL. Collagen Dynamics During the Process of Osteocyte Embedding and Mineralization. *Front Cell Dev Biol* (2019) 7:178. doi: 10.3389/fcell.2019.00178
9. Eriksen EF. Normal and Pathological Remodeling of Human Trabecular Bone: Three Dimensional Reconstruction of the Remodeling Sequence in Normals and in Metabolic Bone Disease*. *Endocrine Rev* (1986) 7:379–408. doi: 10.1210/edrv-7-4-379
10. Wodarz A, Nusse R. MECHANISMS OF WNT SIGNALING IN DEVELOPMENT. *Annu Rev Cell Dev Biol* (1998) 14:59–88. doi: 10.1146/annurev.cellbio.14.1.59
11. Li VS, Ng SS, Boersema PJ, Low TY, Karthaus WR, Gerlach JP, et al. Wnt Signaling through Inhibition of β -Catenin Degradation in an Intact Axin1 Complex. *Cell* (2012) 149:1245–56. doi: 10.1016/j.cell.2012.05.002
12. Poole KES, Van Bezooijen RL, Loveridge N, Hamersma H, Papapoulos SE, Löwik CW, et al. Sclerostin is a delayed secreted product of osteocytes that inhibits bone formation. *FASEB J* (2005) 19:1842–4. doi: 10.1096/fj.05-4221fje
13. Bezooijen R, Dijke P.t., Papapoulos SE, Löwik CW. SOST/sclerostin, an osteocyte-derived negative regulator of bone formation. *Cytokine Growth Factor Rev* (2005) 16:319–27. doi: 10.1016/j.cytogfr.2005.02.005
14. Truswell AS. OSTEOPTOROSIS WITH SYNDACTYLY. *J Bone Joint Surg* (1958) British volume 40-B:208–18. doi: 10.1302/0301-620X.40B2.208
15. Honma M, Ikebuchi Y, Kariya Y, Hayashi M, Hayashi N, Aoki S, et al. RANKL subcellular trafficking and regulatory mechanisms in osteocytes. *J Bone Mineral Res* (2013) 28:1936–49. doi: 10.1002/jbmr.1941
16. Nakashima T, Hayashi M, Fukunaga T, Kurata K, Oh-hora M, Feng JQ, et al. Evidence for osteocyte regulation of bone homeostasis through RANKL expression. *Nat Med* (2011) 17:1231–4. doi: 10.1038/nm.2452
17. Xiong J, Onal M, Jilka RL, Weinstein RS, Manolagas SC, O'Brien CA. Matrix-embedded cells control osteoclast formation. *Nat Med* (2011) 17:1235–41. doi: 10.1038/nm.2448
18. Lacey DL, Timms E, Tan HL, Kelley MJ, Dunstan CR, Burgess T, et al. Osteoprotegerin Ligand Is a Cytokine that Regulates Osteoclast Differentiation and Activation. *Cell* (1998) 93:165–76. doi: 10.1016/S0092-8674(00)81569-X
19. Delmas PD. Clinical Potential of RANKL Inhibition for the Management of Postmenopausal Osteoporosis and Other Metabolic Bone Diseases. *J Clin Densitometry* (2008) 11:325–38. doi: 10.1016/j.jocd.2008.02.002
20. Boyle WJ, Simonet WS, Lacey DL. Osteoclast differentiation and activation. *Nature* (2003) 423:337–42. doi: 10.1038/nature01658
21. Hofbauer LC, Schoppert M. Clinical Implications of the Osteoprotegerin/RANKL/RANK System for Bone and Vascular Diseases. *JAMA* (2004) 292:490–5. doi: 10.1001/jama.292.4.490
22. Kennedy OD, Lendhey M, Mauer P, Philip A, Basta-Pljakic J, Schaffler MB. Microdamage induced by in vivo Reference Point Indentation in mice is repaired by osteocyte-apoptosis mediated remodeling. *Bone* (2017) 95:192–8. doi: 10.1016/j.bone.2016.11.029
23. Emerton KB, Hu B, Woo AA, Sinofsky A, Hernandez C, Majeska RJ, et al. Osteocyte apoptosis and control of bone resorption following ovariectomy in mice. *Bone* (2010) 46:577–83. doi: 10.1016/j.bone.2009.11.006
24. McCutcheon S, Majeska RJ, Spray DC, Schaffler MB, Vazquez M. Apoptotic Osteocytes Induce RANKL Production in Bystanders via Purinergic Signaling and Activation of Pannexin Channels. *J Bone Miner Res* (2020) 35:966–77. doi: 10.1002/jbmr.3954
25. Hopkinson JM, Butte NF, Ellis K, Smith EOB. Lactation Delays Postpartum Bone Mineral Accretion and Temporarily Alters Its Regional Distribution in Women. *J Nutr* (2000) 130:777–83. doi: 10.1093/jn/130.4.777
26. Ardeshirpour L, Dann P, Adams DJ, Nelson T, VanHouten J, Horowitz MC, et al. Weaning Triggers a Decrease in Receptor Activator of Nuclear Factor- κ B Ligand Expression, Widespread Osteoclast Apoptosis, and Rapid Recovery of Bone Mass after Lactation in Mice. *Endocrinology* (2007) 148:3875–86. doi: 10.1210/en.2006-1467
27. Marotti G, Ferretti M, Remaggi F, Palumbo C. Quantitative evaluation on osteocyte canalicular density in human secondary osteons. *Bone* (1995) 16:125–8. doi: 10.1016/8756-3282(95)80022-I
28. Wang B, Zhou X, Price C, Li W, Pan J, Wang L. Quantifying load-induced solute transport and solute-matrix interaction within the osteocyte lacunar-canalicular system. *J Bone Mineral Res* (2013) 28:1075–86. doi: 10.1002/jbmr.1804
29. Robling AG, Bonewald LF. The Osteocyte: New Insights. *Annu Rev Physiol* (2020) 82:485–506. doi: 10.1146/annurev-physiol-021119-034332
30. Ciani C, Sharma D, Doty SB, Fritton SP. Ovariectomy enhances mechanical load-induced solute transport around osteocytes in rat cancellous bone. *Bone* (2014) 59:229–34. doi: 10.1016/j.bone.2013.11.026
31. Fan L, Pei S, Lucas Lu X, Wang L. A multiscale 3D finite element analysis of fluid/solute transport in mechanically loaded bone. *Bone Res* (2016) 4:16032. doi: 10.1038/boneres.2016.32
32. Joukar A, Niroomand-Oscuii H, Ghalichi F. Numerical simulation of osteocyte cell in response to directional mechanical loadings and mechanotransduction analysis: Considering lacunar-canalicular interstitial fluid flow. *Comput Methods Progr Biomed* (2016) 133:133–41. doi: 10.1016/j.cmpb.2016.05.019
33. Gatti V, Azoulay EM, Fritton SP. Microstructural changes associated with osteoporosis negatively affect loading-induced fluid flow around osteocytes in cortical bone. *J Biomechanics* (2018) 66:127–36. doi: 10.1016/j.jbiomech.2017.11.011
34. Schneider P, Meier M, Wepf R, Müller R. Towards quantitative 3D imaging of the osteocyte lacuno-canalicular network. *Bone* (2010) 47:848–58. doi: 10.1016/j.bone.2010.07.026
35. Kamel-ElSayed SA, Tiede-Lewis LM, Lu Y, Veno PA, Dallas SL. Novel approaches for two and three dimensional multiplexed imaging of osteocytes. *Bone* (2015) 76:129–40. doi: 10.1016/j.bone.2015.02.011
36. Qiu S, Rao DS, Palnitkar S, Parfitt AM. Reduced Iliac Cancellous Osteocyte Density in Patients With Osteoporotic Vertebral Fracture. *J Bone Mineral Res* (2003) 18:1657–63. doi: 10.1359/jbmr.2003.18.9.1657
37. Odgaard A, Gundersen HJG. Quantification of connectivity in cancellous bone, with special emphasis on 3-D reconstructions. *Bone* (1993) 14:173–82. doi: 10.1016/8756-3282(93)90245-6
38. Weinkamer R, Kollmannsberger P, Fratzl P. Towards a Connectomic Description of the Osteocyte Lacunocanalicular Network in Bone. *Curr Osteoporosis Rep* (2019) 17:186–94. doi: 10.1007/s11914-019-00515-z
39. Mabilieu G, Perrot R, Flatt PR, Irwin N, Chappard D. High fat-fed diabetic mice present with profound alterations of the osteocyte network. *Bone* (2016) 90:99–106. doi: 10.1016/j.bone.2016.06.008
40. Kollmannsberger P, Kerschnitzki M, Repp F, Wagermaier W, Weinkamer R, Fratzl P. The small world of osteocytes: connectomics of the lacunocanalicular network in bone. *New J Phys* (2017) 19:073019. doi: 10.1088/1367-2630/aa764b
41. Kerschnitzki M, Wagermaier W, Roschger P, Seto J, Shahar R, Duda GN, et al. The organization of the osteocyte network mirrors the extracellular matrix orientation in bone. *J Struct Biol* (2011) 173:303–11. doi: 10.1016/j.jsb.2010.11.014
42. Cao L, Moriishi T, Miyazaki T, Iimura T, Hamagaki M, Nakane A, et al. Comparative morphology of the osteocyte lacunocanalicular system in various vertebrates. *J Bone Mineral Metab* (2011) 29:662–70. doi: 10.1007/s00774-011-0268-6
43. Okada S, Yoshida S, Ashrafi SH, Schraufnagel DE. The Canalicular Structure of Compact Bone in the Rat at Different Ages. *Microscopy Microanalysis* (2002) 8:104–15. doi: 10.1017/S1341927601020037
44. Carriero A, Doube M, Vogt M, Busse B, Zustin J, Levchuk A, et al. Altered lacunar and vascular porosity in osteogenesis imperfecta mouse bone as revealed by synchrotron tomography contributes to bone fragility. *Bone* (2014) 61:116–24. doi: 10.1016/j.bone.2013.12.020
45. Britz HM, Carter Y, Jokihaara J, Leppänen OV, Järvinen TLN, Belev G, et al. Prolonged unloading in growing rats reduces cortical osteocyte lacunar density and volume in the distal tibia. *Bone* (2012) 51:913–9. doi: 10.1016/j.bone.2012.08.112

46. Sugawara Y, Kamioka H, Ishihara Y, Fujisawa N, Kawanabe N, Yamashiro T. The early mouse 3D osteocyte network in the presence and absence of mechanical loading. *Bone* (2013) 52:189–96. doi: 10.1016/j.bone.2012.09.033
47. Rolvien T, Milovanovic P, Schmidt FN, von Kroge S, Wölfel EM, Krause M, et al. Long-Term Immobilization in Elderly Females Causes a Specific Pattern of Cortical Bone and Osteocyte Deterioration Different From Postmenopausal Osteoporosis. *J Bone Mineral Res N/A* (2020) 35(7):1343–51. doi: 10.1002/jbmr.3970
48. Gerbaix M, Gnyubkin V, Farlay D, Olivier C, Ammann P, Courbon G, et al. One-month spaceflight compromises the bone microstructure, tissue-level mechanical properties, osteocyte survival and lacunae volume in mature mice skeletons. *Sci Rep* (2017) 7:2659. doi: 10.1038/s41598-017-09608-0
49. Stern AR, Yao X, Wang Y, Berhe A, Dallas M, Johnson ML, et al. Effect of osteoporosis treatment agents on the cortical bone osteocyte microenvironment in adult estrogen-deficient, osteopenic rats. *Bone Rep* (2018) 8:115–24. doi: 10.1016/j.bonr.2018.02.005
50. Zhang S, Bach-Gansmo FL, Xia D, Besenbacher F, Birkedal H, Dong M. Nanostructure and mechanical properties of the osteocyte lacunar-canalicular network-associated bone matrix revealed by quantitative nanomechanical mapping. *Nano Res* (2015) 8:3250–60. doi: 10.1007/s12274-015-0825-8
51. Weinbaum S, Cowin SC, Zeng Y. A model for the excitation of osteocytes by mechanical loading-induced bone fluid shear stresses. *J Biomechanics* (1994) 27:339–60. doi: 10.1016/0021-9290(94)90010-8
52. You L-D, Weinbaum S, Cowin SC, Schaffler MB. Ultrastructure of the osteocyte process and its pericellular matrix. *Anatomical Record Part A: Discov Mol Cell Evolutionary Biol* (2004) 278A:505–13. doi: 10.1002/ar.a.20050
53. Thompson WR, Modla S, Grindel BJ, Czymmek KJ, Kirn-Safran CB, Wang L, et al. Perlecan/Hspg2 deficiency alters the pericellular space of the lacunocanalicular system surrounding osteocytic processes in cortical bone. *J Bone Mineral Res* (2011) 26:618–29. doi: 10.1002/jbmr.236
54. Wang B, Lai X, Price C, Thompson WR, Li W, Quabili TR, et al. Perlecan-Containing Pericellular Matrix Regulates Solute Transport and Mechanosensing Within the Osteocyte Lacunar-Canalicular System. *J Bone Mineral Res* (2014) 29:878–91. doi: 10.1002/jbmr.2105
55. McNamara LM, Majeska RJ, Weinbaum S, Friedrich V, Schaffler MB. Attachment of Osteocyte Cell Processes to the Bone Matrix. *Anatomical Record* (2009) 292:355–63. doi: 10.1002/ar.20869
56. Wang Y, McNamara LM, Schaffler MB, Weinbaum S. A model for the role of integrins in flow induced mechanotransduction in osteocytes. *Proc Natl Acad Sci U S A* (2007) 104:15941–6. doi: 10.1073/pnas.0707246104
57. Thi MM, Suadicanio SO, Schaffler MB, Weinbaum S, Spray DC. Mechanosensory responses of osteocytes to physiological forces occur along processes and not cell body and require $\alpha V\beta 3$ integrin. *Proc Natl Acad Sci U S A* (2013) 110:21012–7. doi: 10.1073/pnas.1321210110
58. Cabahug-Zuckerman P, Stout RF Jr, Majeska RJ, Thi MM, Spray DC, Weinbaum S, et al. Potential role for a specialized $\beta 3$ integrin-based structure on osteocyte processes in bone mechanosensation. *J Orthopaedic Res* (2018) 36:642–52. doi: 10.1002/jor.23792
59. Hagan ML, Yu K, Zhu J, Vinson BN, Roberts RL, Montesinos Cartagena M, et al. Decreased pericellular matrix production and selection for enhanced cell membrane repair may impair osteocyte responses to mechanical loading in the aging skeleton. *Aging Cell* (2020) 19:e13056–6. doi: 10.1111/acer.13056
60. Kato Y, Windle JJ, Koop BA, Mundy GR, Bonewald LF. Establishment of an Osteocyte-like Cell Line, MLO-Y4. *J Bone Mineral Res* (1997) 12:2014–23. doi: 10.1359/jbmr.1997.12.12.2014
61. Kamel MA, Picconi JL, Lara-Castillo N, Johnson ML. Activation of β -catenin signaling in MLO-Y4 osteocytic cells versus 2T3 osteoblastic cells by fluid flow shear stress and PGE₂: Implications for the study of mechanosensation in bone. *Bone* (2010) 47:872–81. doi: 10.1016/j.bone.2010.08.007
62. Rath AL, Bonewald LF, Ling J, Jiang JX, Van Dyke ME, Nicoletta DP. Correlation of cell strain in single osteocytes with intracellular calcium, but not intracellular nitric oxide, in response to fluid flow. *J Biomechanics* (2010) 43:1560–4. doi: 10.1016/j.jbiomech.2010.01.030
63. Genetos DC, Kephart CJ, Zhang Y, Yellowley CE, Donahue HJ. Oscillating fluid flow activation of gap junction hemichannels induces ATP release from MLO-Y4 osteocytes. *J Cell Physiol* (2007) 212:207–14. doi: 10.1002/jcp.21021
64. You L, Temiyasathit S, Lee P, Kim CH, Tummala P, Yao W, et al. Osteocytes as mechanosensors in the inhibition of bone resorption due to mechanical loading. *Bone* (2008) 42:172–9. doi: 10.1016/j.bone.2007.09.047
65. Li J, Rose E, Frances D, Sun Y, You L. Effect of oscillating fluid flow stimulation on osteocyte mRNA expression. *J Biomech* (2012) 45:247–51. doi: 10.1016/j.jbiomech.2011.10.037
66. Yang D, Gronthos S, Isenmann S, Morris HA, Atkins GJ. The Late Osteoblast/Preosteocyte Cell Line MLO-A5 Displays Mesenchymal Lineage Plasticity In Vitro and In Vivo. *Stem Cells Int* (2019) 2019:9838167. doi: 10.1155/2019/9838167
67. Li X, Liu C, Li P, Li S, Zhao Z, Chen Y, et al. Connexin 43 is a potential regulator in fluid shear stress-induced signal transduction in osteocytes. *J Orthopaedic Res* (2013) 31:1959–65. doi: 10.1002/jor.22448
68. Spatz JM, Wein MN, Gooi JH, Qu Y, Garr JL, Liu S, et al. The Wnt Inhibitor Sclerostin Is Up-regulated by Mechanical Unloading in Osteocytes In Vitro. *J Biol Chem* (2015) 290:16744–58. doi: 10.1074/jbc.M114.628313
69. Heino TJ, Hentunen TA, Väänänen HK. Conditioned medium from osteocytes stimulates the proliferation of bone marrow mesenchymal stem cells and their differentiation into osteoblasts. *Exp Cell Res* (2004) 294:458–68. doi: 10.1016/j.yexcr.2003.11.016
70. Xu LH, Shao H, Ma Y-HV, You L. OCY454 Osteocytes as an in Vitro Cell Model for Bone Remodeling Under Mechanical Loading. *J Orthopaedic Res* (2019) 37:1681–9. doi: 10.1002/jor.24302
71. Woo SM, Rosser J, Dusevich V, Kalajic I, Bonewald LF. Cell line IDG-SW3 replicates osteoblast-to-late-osteocyte differentiation in vitro and accelerates bone formation in vivo. *J Bone Mineral Res* (2011) 26:2634–46. doi: 10.1002/jbmr.465
72. Stewart AF. Hypercalcemia Associated with Cancer. *N Engl J Med* (2005) 352:373–9. doi: 10.1056/NEJMcp042806
73. Levin A, Bakris GL, Molitch M, Smulders M, Tian J, Williams LA, et al. PTH, calcium, and phosphorus in patients with chronic kidney disease: Results of the study to evaluate early kidney disease. *Kidney Int* (2007) 71:31–8. doi: 10.1038/sj.ki.5002009
74. Jähn K, Kelkar S, Zhao H, Xie Y, Tiede-Lewis LM, Dusevich V, et al. Osteocytes Acidify Their Microenvironment in Response to PTHrP In Vitro and in Lactating Mice In Vivo. *J Bone Mineral Res* (2017) 32:1761–72. doi: 10.1002/jbmr.3167
75. Qing H, Ardeshirpour L, Divieti Pajevic P, Dusevich V, Jähn K, Kato S, et al. Demonstration of osteocytic perilacunar/canalicular remodeling in mice during lactation. *J Bone Miner Res* (2012) 27:1018–29. doi: 10.1002/jbmr.1567
76. Dole NS, Mazur CM, Acevedo C, Lopez JP, Monteiro DA, Fowler TW, et al. Osteocyte-Intrinsic TGF- β Signaling Regulates Bone Quality through Perilacunar/Canalicular Remodeling. *Cell Rep* (2017) 21:2585–96. doi: 10.1016/j.celrep.2017.10.115
77. Hou WS, Brömme D, Zhao Y, Mehler E, Dushey C, Weinstein H, et al. Characterization of novel cathepsin K mutations in the pro and mature polypeptide regions causing pycnodysostosis. *J Clin Invest* (1999) 103:731–8. doi: 10.1172/JCI653
78. Bossard MJ, Tomaszek TA, Thompson SK, Amegadzie BY, Hanning CR, Jones C, et al. Proteolytic activity of human osteoclast cathepsin K. Expression, purification, activation, and substrate identification. *J Biol Chem* (1996) 271:12517–24. doi: 10.1074/jbc.271.21.12517
79. Fowler TW, Acevedo C, Mazur CM, Hall-Glenn F, Fields AJ, Bale HA, et al. Glucocorticoid suppression of osteocyte perilacunar remodeling is associated with subchondral bone degeneration in osteonecrosis. *Sci Rep* (2017) 7:44618. doi: 10.1038/srep44618
80. Zhang K, Barragan-Adjemian C, Ye L, Kotha S, Dallas M, Lu Y, et al. E11/gp38 Selective Expression in Osteocytes: Regulation by Mechanical Strain and Role in Dendrite Elongation. *Mol Cell Biol* (2006) 26:4539. doi: 10.1128/MCB.02120-05
81. Aziz AH, Wilmoth RL, Ferguson VL, Bryant SJ. IDG-SW3 Osteocyte Differentiation and Bone Extracellular Matrix Deposition Are Enhanced in a 3D Matrix Metalloproteinase-Sensitive Hydrogel. *ACS Appl Bio Mater* (2020) 3:1666–80. doi: 10.1021/acsbm.9b01227
82. Tanaka T, Hoshijima M, Sunaga J, Nishida T, Hashimoto M, Odagaki N, et al. Analysis of Ca²⁺ response of osteocyte network by three-dimensional time-lapse imaging in living bone. *J Bone Mineral Metab* (2018) 36:519–28. doi: 10.1007/s00774-017-0868-x

83. Wysolmerski JJ. Osteocytes remove and replace perilacunar mineral during reproductive cycles. *Bone* (2013) 54:230–6. doi: 10.1016/j.bone.2013.01.025
84. McGee-Lawrence ME, Stoll DM, Mantila ER, Fahrner BK, Carey HV, Donahue SW. Thirteen-lined ground squirrels (*Thomomys talpini*) show microstructural bone loss during hibernation but preserve bone macrostructural geometry and strength. *J Exp Biol* (2011) 214:1240. doi: 10.1242/jeb.053520
85. Kerschnitzki M, Kollmannsberger P, Burghammer M, Duda GN, Weinkamer R, Wagermaier W, et al. Architecture of the osteocyte network correlates with bone material quality. *J Bone Mineral Res* (2013) 28:1837–45. doi: 10.1002/jbmr.1927
86. Gardinier JD, Al-Omaishi S, Morris MD, Kohn DH. PTH signaling mediates perilacunar remodeling during exercise. *Matrix Biol* (2016) 52–54:162–75. doi: 10.1016/j.matbio.2016.02.010
87. Kaya S, Basta-Pljakic J, Seref-Ferlengez Z, Majeska RJ, Cardoso L, Bromage TG, et al. Lactation-Induced Changes in the Volume of Osteocyte Lacunar-Canalicular Space Alter Mechanical Properties in Cortical Bone Tissue. *J Bone Mineral Res* (2017) 32:688–97. doi: 10.1002/jbmr.3044
88. Rho J-Y, Kuhn-Spearing, Liisa, Zioupos, Peter, Mechanical properties and the hierarchical structure of bone. *Med Eng Phys* (1998) 20:92–102. doi: 10.1016/S1350-4533(98)00007-1
89. Burton B, Gaspar A, Josey D, Tupy J, Grynpas MD, Willett TL. Bone embrittlement and collagen modifications due to high-dose gamma-irradiation sterilization. *Bone* (2014) 61:71–81. doi: 10.1016/j.bone.2014.01.006
90. Cabral WA, Perdivara I, Weis M, Terajima M, Blissett AR, Chang W, et al. Abnormal Type I Collagen Post-translational Modification and Crosslinking in a Cyclophilin B KO Mouse Model of Recessive Osteogenesis Imperfecta. *PLoS Genet* (2014) 10:e1004465. doi: 10.1371/journal.pgen.1004465
91. Ramshaw JAM, Shah NK, Brodsky B. Gly-X-Y Tripeptide Frequencies in Collagen: A Context for Host–Guest Triple-Helical Peptides. *J Struct Biol* (1998) 122:86–91. doi: 10.1006/jsbi.1998.3977
92. Wu M, Cronin K, Crane JS. *Collagen Synthesis, Biochemistry*. Treasure Island, FL: StatPearls Publishing LLC (2020).
93. Yang P-F, Sanno M, Ganse B, Koy T, Brüggemann G-P, Müller LP, et al. Torsion and Antero-Posterior Bending in the In Vivo Human Tibia Loading Regimes during Walking and Running. *PLoS One* (2014) 9:e94525. doi: 10.1371/journal.pone.0094525
94. Jones SJ, Boyde A, Pawley JB. Osteoblasts and collagen orientation. *Cell Tissue Res* (1975) 159:73–80. doi: 10.1007/BF00231996
95. Matsugaki A, Fujiwara N, Nakano T. Continuous cyclic stretch induces osteoblast alignment and formation of anisotropic collagen fiber matrix. *Acta Biomater* (2013) 9:7227–35. doi: 10.1016/j.actbio.2013.03.015
96. Krane SM. The importance of proline residues in the structure, stability and susceptibility to proteolytic degradation of collagens. *Amino Acids* (2008) 35:703. doi: 10.1007/s00726-008-0073-2
97. Zamboni Zallone A, Teti A, Primavera MV, Pace G. Mature osteocytes behaviour in a repletion period: the occurrence of osteoplastic activity. *Basic Appl Histochem* (1983) 27:191–204. 6196018.
98. Lotinun S, Ishihara Y, Nagano K, Kiviranta R, Carpentier VT, Neff L, et al. Cathepsin K-deficient osteocytes prevent lactation-induced bone loss and parathyroid hormone suppression. *J Clin Invest* (2019) 129:3058–71. doi: 10.1172/JCI122936
99. Tang SY, Herber R-P, Ho SP, Alliston T. Matrix metalloproteinase-13 is required for osteocytic perilacunar remodeling and maintains bone fracture resistance. *J Bone Miner Res* (2012) 27:1936–50. doi: 10.1002/jbmr.1646
100. McNerny EMB, Gong B, Morris MD, Kohn DH. Bone Fracture Toughness and Strength Correlate With Collagen Cross-Link Maturity in a Dose-Controlled Lathyrism Mouse Model. *J Bone Mineral Res* (2015) 30:455–64. doi: 10.1002/jbmr.2356
101. Xu T, Bianco P, Fisher LW, Longenecker G, Smith E, Goldstein S, et al. Targeted disruption of the biglycan gene leads to an osteoporosis-like phenotype in mice. *Nat Genet* (1998) 20:78–82. doi: 10.1038/1746
102. Arteaga-Solis E, Sui-Arteaga L, Kim M, Schaffler MB, Jepsen KJ, Pleshko N, et al. Material and mechanical properties of bones deficient for fibrillin-1 or fibrillin-2 microfibrils. *Matrix Biol* (2011) 30:188–94. doi: 10.1016/j.matbio.2011.03.004
103. Malaval L, Wade-Guée NM, Boudiffa M, Fei J, Zirngibl R, Chen F, et al. Bone sialoprotein plays a functional role in bone formation and osteoclastogenesis. *J Exp Med* (2008) 205:1145–53. doi: 10.1084/jem.20071294
104. Corsi A, Xu T, Chen XD, Boyde A, Liang J, Mankani M, et al. Phenotypic effects of biglycan deficiency are linked to collagen fibril abnormalities, are synergized by decorin deficiency, and mimic Ehlers-Danlos-like changes in bone and other connective tissues. *J Bone Miner Res* (2002) 17:1180–9. doi: 10.1359/jbmr.2002.17.7.1180

Conflict of Interest: The authors declare that the research was conducted in the absence of any commercial or financial relationships that could be construed as a potential conflict of interest.

The reviewer CW declared a shared affiliation with one of the authors, JD, to the handling editor at time of review.

Copyright © 2021 Creecy, Damrath and Wallace. This is an open-access article distributed under the terms of the Creative Commons Attribution License (CC BY). The use, distribution or reproduction in other forums is permitted, provided the original author(s) and the copyright owner(s) are credited and that the original publication in this journal is cited, in accordance with accepted academic practice. No use, distribution or reproduction is permitted which does not comply with these terms.



Interleukin-6 Knockout Inhibits Senescence of Bone Mesenchymal Stem Cells in High-Fat Diet-Induced Bone Loss

Yujue Li^{1,2}, Lingyun Lu^{1,3}, Ying Xie¹, Xiang Chen¹, Li Tian¹, Yan Liang⁴, Huifang Li⁴, Jie Zhang⁴, Yi Liu⁵ and Xijie Yu^{1*}

¹ Department of Endocrinology and Metabolism, Laboratory of Endocrinology and Metabolism, Rare Disease Center, West China Hospital, Sichuan University, Chengdu, China, ² Department of General Practice, West China Hospital, Sichuan University, Chengdu, China, ³ Department of Integrated Traditional Chinese and Western Medicine, West China Hospital, Sichuan University, Chengdu, China, ⁴ Research Core Facility, West China Hospital, Sichuan University, Chengdu, China, ⁵ Department of Rheumatology and Immunology, Rare Disease Center, West China Hospital, Sichuan University, Chengdu, China

OPEN ACCESS

Edited by:

Deborah Veis,
Washington University School of
Medicine in St. Louis, United States

Reviewed by:

Sadiq Umar,
University of Illinois at Chicago,
United States
Yong-Can Huang,
Peking University Shenzhen Hospital,
China

*Correspondence:

Xijie Yu
xijieyu@hotmail.com;
xijieyu@scu.edu.cn

Specialty section:

This article was submitted to
Bone Research,
a section of the journal
Frontiers in Endocrinology

Received: 29 October 2020

Accepted: 31 December 2020

Published: 19 February 2021

Citation:

Li Y, Lu L, Xie Y, Chen X, Tian L,
Liang Y, Li H, Zhang J, Liu Y and Yu X
(2021) Interleukin-6 Knockout Inhibits
Senescence of Bone Mesenchymal
Stem Cells in High-Fat
Diet-Induced Bone Loss.
Front. Endocrinol. 11:622950.
doi: 10.3389/fendo.2020.622950

Obesity, a chronic low-grade inflammatory state, not only promotes bone loss, but also accelerates cell senescence. However, little is known about the mechanisms that link obesity, bone loss, and cell senescence. Interleukin-6 (IL-6), a pivotal inflammatory mediator increased during obesity, is a candidate for promoting cell senescence and an important part of senescence-associated secretory phenotype (SASP). Here, wild type (WT) and (IL-6 KO) mice were fed with high-fat diet (HFD) for 12 weeks. The results showed IL-6 KO mice gain less weight on HFD than WT mice. HFD induced trabecular bone loss, enhanced expansion of bone marrow adipose tissue (BMAT), increased adipogenesis in bone marrow (BM), and reduced the bone formation in WT mice, but it failed to do so in IL-6 KO mice. Furthermore, IL-6 KO inhibited HFD-induced clone formation of bone marrow cells (BMCs), and expression of senescence markers (p53 and p21). IL-6 antibody inhibited the activation of STAT3 and the senescence of bone mesenchymal stem cells (BMSCs) from WT mice *in vitro*, while rescued IL-6 induced senescence of BMSCs from IL-6 KO mice through the STAT3/p53/p21 pathway. In summary, our data demonstrated that IL-6 KO may maintain the balance between osteogenesis and adipogenesis in BM, and restrain senescence of BMSCs in HFD-induced bone loss.

Keywords: IL-6, obesity, osteoporosis, senescence, bone mesenchymal stem cells

INTRODUCTION

Obesity and osteoporosis are common diseases with increasing prevalence worldwide. Obesity is often accompanied by metabolic complications, including insulin resistance, type 2 diabetes (T2D) and liver steatosis (1, 2). Osteoporosis is characterized by low bone mass with microstructure disruption, resulting in skeletal fragility and increased risk of fracture (3, 4). For a long time, obesity was recognized as a condition with positive effects on bone, mainly because weight gain on bone has

been considered to increase mechanical loading exerted on the skeleton, and then bone mass would increase to accommodate weight gain (5). However, some epidemiologic studies indicate that obesity is associated with increased incidence of fractures (6, 7). In general, the increase of mechanical load caused by obesity initially promotes the increase of bone mass, while the metabolic disorders caused by long-term obesity leading to the decrease of bone formation and bone turnover (8). In recent years, studies on obesity and bone metabolism have attracted academic attention. However, the mechanisms underlying the bone mass acquired in obesity remains not well known.

There are two main imbalances in the development of osteoporosis (OP): one is the uncoupled bone remodeling involving bone-forming osteoblasts and bone-resorbing osteoclasts, the other lies in bone-fat imbalance (9). Current evidence indicates that the differentiation potential of bone mesenchymal stem cells (BMSCs) is strictly regulated by the bone marrow (BM) microenvironment, including cytokines and hormones in BM (10). Changes in the BM microenvironment determine the commitment of BMSCs into the osteoblast or adipocyte lineage (11, 12). The balance between adipogenesis and osteogenesis of BMSCs would be broken when the BM microenvironment changes. The eWAT-derived cytokines may dysregulate the interaction between adipogenesis and osteogenesis of BMSCs through endocrine pathway. Bone marrow adipose tissue (BMAT) exerts influence on osteoblasts, osteoclasts and hematopoietic cells through paracrine pathway (13). Obesity causes chronic low-grade inflammatory state. The adipose tissue derived inflammatory cytokines promote obesity-related metabolic disorders. The level of inflammatory cytokine is discrepant in different adipose tissues, and visceral adipose tissue (VAT) produces more pro-inflammatory cytokines than subcutaneous adipose tissue (SAT) (14). Although the underlying mechanism is not clear, increased levels of inflammatory factors (such as TNF- α , IL-1, IL-6, and IL-17) have been traditionally thought to contribute to bone loss (15–17).

IL-6, a multifunctional cytokine, is produced by adipocytes, monocytes, endotheliocytes and hepatocytes (18). As one important mediator of chronic low-grade inflammation, the level of IL-6 is higher in VAT than SAT in mice (19). However, the level of IL-6 in BM is not exactly known. IL-6 initiates intracellular signal transduction by binding to its membrane-bound receptor IL-6R α or its soluble receptor sIL-6R (20). Studies have shown that levels of IL-6 and sIL-6R increase during the osteogenic differentiation of BMSCs. Then, the IL-6/sIL-6R complex could activate the downstream signal transducer and activator of transcription 3 (STAT3) signaling pathway, promote the osteogenic differentiation of BMSCs through autocrine or paracrine feedback loops (21, 22). The IL-6/sIL-6R complex could enhance alkaline phosphatase (ALP) activity of human (MG-63) and murine (MC3T3-E1) osteoblastic cell lines as well as primary murine calvaria cells (23, 24). However, the activation of the gp130 signaling pathway by the IL-6/sIL-6R complex was initially thought to regulate osteoclast formation in bone (25). Early research also suggested

that IL-6 inhibited bone nodule formation by rat calvaria cells *in vitro*, revealing that IL-6 may inhibit osteoblast differentiation (26). In obesity, elevated level of IL-6 may lead to a low-grade inflammatory state and bone metabolism imbalance, but the mechanism remains unclear.

It was reported that obesity accelerated senescence of BMSCs (including the increased expression of senescence markers p53 and p21) in the BM microenvironment, thereby preventing BMSCs recruitment for bone remodeling and leading to bone fragility (27). IL-6 may be involved in the pathogenesis of senescence (28–33). The combination of IL-6/sIL-6R complex and gp130 activates the JAK/STAT signal transduction pathway and transmits the signal from cell membrane to nucleus, which is critical to cell cycle transition from G1 to S (34). Previously, IL-6/sIL-6R induced premature senescence in normal human fibroblasts through STAT3/p53 pathway, and there was a potential binding site (5'-TTnnnnGA-3') of p-STAT3 in the p53 promoter region (30, 35). Moreover, IL-6 activated intracellular STAT3/p53/p21 signal transduction and induced senescence of vascular smooth muscle cells (36). However, it is unclear whether IL-6 involved in the senescence of BMSCs in high-fat diet (HFD)-induced obesity. In summary, current knowledge about the roles of IL-6 in differentiation and senescence of BMSCs is limited in HFD-induced obesity. In this study, we used IL-6 gene knockout (IL-6 KO) mice to investigate the effect of IL-6 on bone metabolism and the potential mechanism in HFD-induced obesity. Our study demonstrated that IL-6 KO may inhibit the senescence of BMSCs, thus led to attenuated bone loss.

MATERIALS AND METHODS

Experimental Animals

All animal experiments have been approved by the Institutional Animal Care and Treatment Committee of Sichuan University in China (Permit number: 2020136A) and were carried out in accordance with the approved guidelines. The male wild type (WT) and IL-6 KO mice generated on C57BL/6 background were purchased from Jackson Laboratory (Bar Harbor, ME, USA). Mice were housed in cages at a temperature of $23 \pm 1^\circ\text{C}$ with a 12 h light-dark cycle and had free access to food and water. Eight-week-old WT and IL-6 KO mice were randomly divided into standard diet (SD) and HFD groups. The composition of SD and HFD from Beijing HFK Bioscience Corporation was shown in **Table 1**. Four groups of mice were given diet intervention for 12 weeks: (1) WT mice, fed on SD (WT-SD group); (2) WT mice, fed on HFD (WT-HFD group); (3) IL-6 KO mice, fed on SD (IL-6 KO-SD group); (4) IL-6 KO mice, fed on HFD (IL-6 KO-HFD group). Body weight was measured weekly. Mice were fasted for 12 h at the end of the experiment and euthanized under a general anesthesia. Blood was collected from retroorbital vein prior to sacrifice. Enzyme-linked immunosorbent assay (ELISA) kits (Mbbiology biological, Jiangsu, China) were used for detecting levels of IL-6 and procollagen I N-terminal peptide (PINP).

TABLE 1 | The composition of standard diet (SD) and high fat diet (HFD).

Composition	SD		HFD	
Protein	19.2 g%	20 kcal%	26 g%	20 kcal%
Casein	189.58 g	758.32 kcal	258.45 g	1033.80 kcal
Cystine	2.84 g	11.36 kcal	3.88 g	15.52 kcal
Carbohydrate	67.3 g%	70 kcal%	26 g%	20 kcal%
Corn starch	298.59 g	1194.36 kcal	0	0
Maltodextrin	33.18 g	132.72 kcal	161.53 g	646.12 kcal
Saccharose	331.77 g	1327.08 kcal	88.91 g	355.64 kcal
Fat	4.3 g%	10 kcal%	35 g%	60 kcal%
Soybean oil	23.70 g	213.30 kcal	32.31 g	290.79 kcal
Lard oil	18.96 g	170.64 kcal	316.60 g	2849.40 kcal
Cellulose	47.40 g	0	64.61 g	0
Others	53.98 g	37.92 kcal	73.71 g	51.68 kcal
Total	1000 g	3845.70 kcal	1000 g	5242.95 kcal

Others: mineral mixture, calcium hydrophosphate, calcium carbonate, potassium citrate, vitamin mixture, etc.

Analysis of Bone Microstructure

Left femurs and L3 vertebrae were isolated from soft tissues and immersed into fixative solution for μ CT analysis (37). The high-resolution μ CT system (vivaCT80; Scanco Medical, Switzerland) was used to analyze the bone microstructure of trabecular bone of distal femoral metaphysis and L3 vertebra, and cortical bone of femoral mid-diaphysis. The scanner was set at a voltage of 55 kVp, a current of 145 μ A and a voxel size of 10 μ m. The three-dimensional (3D) reconstruction and analysis were performed using the Scanco software version 5.0. One hundred contiguous cross-sectional slices were selected for analysis of trabecular and cortical bone. The domain of trabecular and cortical analysis was manually profiled and intermediate sections were interpolated with the contouring algorithm to choose a region of interest (ROI). The parameters including bone volume per tissue volume (BV/TV), connect density (Conn. D), structure model index (SMI), trabecular number (Tb. N), trabecular thickness (Tb. Th) and trabecular spacing (Tb. Sp) were achieved for analysis of trabecular bone, while BV/TV, cortical thickness (Ct. Th) and bone surface per bone volume (BS/BV) for cortical bone.

Quantification and Imaging of BMAT by Osmium- μ CT

The BMAT was quantified by osmium tetroxide (osmic acid) staining combined with μ CT imaging (Quantum GX, PerkinElmer, USA) (38). The right tibias were dissected from soft tissues, fixed for 24 h, washed for 10 min, and immersed into 20% ethylenediaminetetraacetic acid (EDTA) solution to decalcify at 37°C for 14–17 d. The decalcification solution was changed every 3 d until the bones were flexible. One part 5% solution of potassium dichromate and one part 2% solution of osmium tetroxide were added to a 2-ml microtube, each with 3–4 bones inside. The bones were immersed in the dye for 48 to 60 h at room temperature and washed repeatedly with distilled water for 2 h. The μ CT system was used to perform 2D analysis of BMAT in tibias. The scanner was set at a voltage of 90 kVp, a current of 88 μ A and a voxel size of 50 μ m. The analysis of the osmium density (white color in BM cavity) of tibial sagittal plane was used to assess the content of BMAT with Image J software.

Histological Analysis

The left tibias were dissected from soft tissues, fixed for 12 h, washed for 10 min, and decalcified at 37°C until the bones were flexible. The tibias were then dehydrated, embedded in paraffin, cut to 5 μ m sections, dried, and kept at room temperature. Longitudinal sections from the proximal tibias were stained with either hematoxylin-eosin (H&E) or tartrate-resistant acid phosphatase (TRAP) (Sigma, Merck, Germany). Lipid droplets were counted and calculated to assess BM adiposity using Image J software. TRAP-positive multinucleated cells were observed along the bone edge. Osteoclast surface per bone surface (OcS/BS) was calculated at five different visual fields with Image J software to evaluate osteoclast formation.

Isolation of Bone Marrow Cells (BMCs)

Both femurs and tibias of WT and IL-6 KO mice were collected and cleaned in PBS. The femoral and tibial diaphysis were snipped and the BMCs were isolated as previously described (39). Bones were placed vertically in a 0.5-ml microtube that was cut open at the bottom. The 0.5-ml microtube was placed into a 1.5-ml microtube. Fresh BM was spun out by quick centrifuge (from 0 to 10,000 rpm within 10 s) at room temperature. Red blood cells were lysed using erythrocyte lysing buffer (Beyotime, Shanghai, China) and the BM suspension was allowed to stand for 5–10 min to make low-density bone marrow adipocytes (BMAs) released and floating. After centrifugation (3,000 rpm for 3 min), the bottom BMCs were collected and washed with PBS for the follow-up experiments. BMCs contained BMSCs, hematopoietic cells, immune cells, etc. but not BMAs or erythrocytes.

Colony Formation

BMCs harvested from femoral and tibial cavities of WT and IL-6 KO mice after diet intervention were plated at a density of 5×10^5 cells/well in 6-well culture plates (40). BMCs were cultured with MEM alpha modification (α MEM, HyClone, Thermo Fisher Scientific, USA), containing 10% fetal bovine serum (FBS, Gibco, Thermo Fisher Scientific, USA) and 1% penicillin-streptomycin solution. After 24 h of adhesion, nonadherent cells were discarded and the culture medium was changed every other day. Colonies were cultured for 14 d in growth culture medium. Then the medium was removed and cells were stained with 0.1% crystal violet (Beyotime) after fixed with 4% paraformaldehyde solution. Colonies were counted in three different wells with Image J software.

Replicative Senescent BMSCs

BMCs from WT and IL-6 KO mice were cultured in α MEM, digested and passaged with TrypLE Express Enzyme (Gibco). BMCs were cultured for passage 9 (P9) to achieve replicative senescent BMSCs as described previously (41), with minor modification. BMCs from WT mice were cultured with or without 100 ng/ml mouse IL-6 neutralization antibody (R&D Systems, USA), while cells from IL-6 KO mice were cultured with or without 2 ng/ml recombinant mouse IL-6 (Solarbio, Beijing, China). The medium was changed every other day. BMCs,

containing hematopoietic cells, immune cells etc., were purified into BMSCs through culturing and passaging. The senescent BMSCs were used for senescence-associated- β -galactosidase (SA- β -gal) staining, and analysis of related mRNA and protein expression.

SA- β -Gal (Senescence-Associated- β -Galactosidase) Staining

SA- β -gal staining of BMSCs was conducted as previously described (42). Senescence β -galactosidase staining kit and X-gal were purchased from Cell Signaling Technology (CST, USA). Briefly, cells were fixed in fix solution at room temperature for 15 min and stained with fresh staining solution at 37°C overnight. SA- β -gal-positive cells were counted in randomly selected five fields by Image J software.

RNA Extraction, cDNA Synthesis, and Quantitative RT-PCR (qRT-PCR)

Total RNA was extracted from the distal metaphysis of right femurs, BMCs and cultured BMSCs according to the protocol provided by the manufacturer with TRIzol reagent (Invitrogen, Thermo Fisher Scientific, USA). The total RNA (1 μ g) was converted to cDNA using PrimeScript RT reagent Kit with gDNA Eraser (Takara, Japan). Gene expression analysis was performed using LightCycler 96 Real-Time PCR System (Roche, Switzerland) and TB Green Premix Ex Taq II (Takara). Primer sequences were summarized in **Table 2**. The relative mRNA levels of target genes were normalized to that of β -actin. Data analysis was performed with the $2^{-\Delta\Delta CT}$ method.

Western Blot Analysis

The total protein from BMCs and cultured BMSCs was obtained by using RIPA lysis buffer with general protease inhibitor cocktail and general phosphatase inhibitor cocktail (Absin, Shanghai, China). Protein lysates were quantified using a BCA quantification kit (Absin), subjected to sodium dodecyl sulfate-polyacrylamide gels (SDS-PAGE) and electrotransferred to PVDF membranes (GE Life Sciences, USA). The membranes were blocked with 5% milk solution, incubated with primary and secondary antibodies in sequence. The primary antibodies against β -actin, p21, p53, STAT3 and phospho-STAT3, as well as secondary antibodies were from CST. The results of western blot analysis were obtained by ChemiDoc XRS+ system (Bio-Rad, USA) with ECL reagents (GE Life Sciences).

TABLE 2 | Primer sequences.

Target gene	Forward (5' to 3')	Reverse (5' to 3')
β -actin	AGATTACTGCTCTGGCTCCTAGC	ACTCATCGTACTCCTGCTTGCT
Col1a1	CTGGCGGTTTCAGGTCCAAT	TTCCAGGCAATCCACGAGC
Col1a2	CCCAGAGTGGACACGCGATT	ATGAGTTCTTCGCTGGGGTG
Adipoq	ATCTGGAGGTGGGAGACCAA	GGGCTATGGGTAGTTGCAGT
Pparg	CACTCGCATTCTTTGACATC	CGCACTTTGGTATTCTTGAG
Lepr	GGTCCTCTTCTTCTGGAGCCT	AGAACTGCTTTTCAGGGTCTGG
p53	TCAGCCTCTTGATGACTGCC	ATCGTCCATGCAGTGAGGTG
p21	GTGAGGAGGAGCATGAATGGA	GAACAGGTGGACATCACCA
p16	CGCTTCTCACCTCGCTTGT	TGACCAAGAACCTGCGGACC

Statistical Analysis

Results were presented as mean \pm standard deviation (SD). Statistical analysis was performed using SPSS 5.0 software. Statistically significant differences between two groups were determined using unpaired, two-tailed Student's *t* test, and two-way ANOVA (genotype \times diet) with post-hoc test was used for multiple group comparisons. Actual *P* values have been shown in each graph or statistically significant *p* values were labeled as follows: * *P* < 0.05, ** *P* < 0.01, *** *P* < 0.001 (compared to the same genotype); # *P* < 0.05, ## *P* < 0.01, ### *P* < 0.001 (compared to the same diet).

RESULTS

IL-6 KO Restrained Trabecular Bone Loss in HFD-induced Obesity

The obesity models were established with WT and IL-6 KO mice after HFD for 12 weeks. Compared with the SD, the weight of WT mice was increased by 25%, 36%, and 41% after HFD for 4, 8, and 12 weeks, while the weight of IL-6 KO mice was increased by 9%, 20%, and 22% (**Figures 1A, B**). Moreover, we found that the levels of IL-6 in serum increased significantly after HFD in WT mice (**Table 3**). To evaluate the effects of HFD and IL-6 on the bone mass and bone microstructure, μ CT was used to assay the trabecular bone of distal femoral metaphysis, L3 vertebra, and the cortical bone of femoral mid-diaphysis. On the SD, no difference was observed between WT and IL-6 KO mice in the trabecular bone of the distal femoral metaphysis (**Figure 2A**) and the L3 vertebra (**Figure 2B**). On the HFD, the distal femoral metaphysis of WT mice showed obvious reduction in trabecular BV/TV, Conn. D, Tb. N and Tb. Th, and prominent increase in SMI and Tb. Sp, the L3 vertebra of WT mice showed distinct reduction in trabecular BV/TV and Tb. Th, and significant increase in SMI and Tb. Sp. The distal femoral metaphysis and L3 vertebra of IL-6 KO mice showed no significant changes in bone mass and bone microstructure after HFD. Additionally, no significant changes were detected in cortical BV/TV, Ct. Th and BS/BV in the femoral mid-diaphysis of WT and IL-6 KO mice after HFD (**Figure 2C**). These results indicated that IL-6 KO retained trabecular bone loss in HFD-induced obesity.

IL-6 KO Rescued the Decreased Osteogenesis in HFD-induced Obesity

To investigate the possible contributor of bone loss after HFD, we further analyzed the bone turnover indicators. TRAP staining of proximal tibia showed no significant difference between WT and IL-6 KO mice after SD or HFD (**Figure 3A**). The level of serum bone formation biomarker PINP was significantly decreased in WT mice (14.3 to 8.7 ng/ml) after HFD, while it kept a similar level in IL-6 KO mice (11.8 to 12.9 ng/ml) after HFD (**Figure 3B**). In addition, mRNA levels of collagen type 1 alpha 1 chain (Col1a1) and Col1a2 in metaphysis of WT mice were significantly reduced, while those in IL-6 KO mice did not show notable changes after HFD

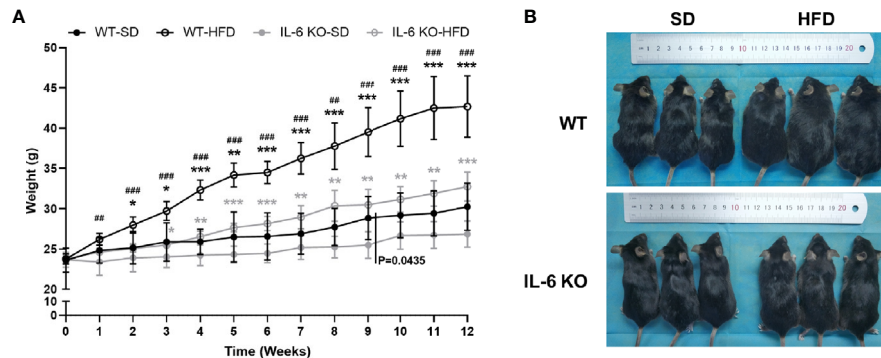


FIGURE 1 | The obesity models were established with WT and IL-6 KO mice. **(A)** Body weight curves of WT and IL-6 KO mice after SD or HFD ($n = 5$). **(B)** Photographs of mice in each group after 12 weeks of dietary intervention. Data were expressed as mean \pm SD, * $P < 0.05$, ** $P < 0.01$, *** $P < 0.001$: compared to the same genotype; # $P < 0.05$, ## $P < 0.01$, ### $P < 0.001$: compared to the same diet.

TABLE 3 | The levels of IL-6 in serum and culture medium of BMSCs in WT mice after SD or HFD.

Mice	Serum ($n = 7$)	Culture medium of primary BMSCs ($n = 8$)
WT-SD	15.2 \pm 6.4 pg/ml	11.0 \pm 1.0 pg/ml
WT-HFD	28.9 \pm 7.1 pg/ml **	20.8 \pm 2.5 pg/ml ***

Data were expressed as mean \pm SD. ** $P < 0.01$, *** $P < 0.001$: WT-HFD mice versus WT-SD mice.

(Figure 3C). These results suggested that HFD inhibited osteogenic differentiation, while IL-6 KO rescued the HFD-induced decreased osteogenesis.

IL-6 KO Attenuated Adipogenesis of BM in HFD-induced Obesity

HFD induced significant obesity in mice of both strains, while the weight gain of IL-6 KO-HFD mice was significantly lower than that of WT-HFD mice. Obesity-induced osteoporosis is closely related to osteogenesis and adipogenesis in the BM. We next investigated BM adiposity *via* osmium- μ CT and H&E staining. On the SD, IL-6 KO mice exhibited less BMAT, compared with WT mice (Figure 4A). The osmium signal was increased in WT mice, while it was not statistically changed in IL-6 KO mice after HFD. In addition, the amounts of adipocytes in proximal tibia by H&E staining were statistically increased only in WT mice, but not in IL-6 KO mice (Figure 4B). These data indicated that HFD induced a greater amount of BMAT in WT mice than that in IL-6 KO mice.

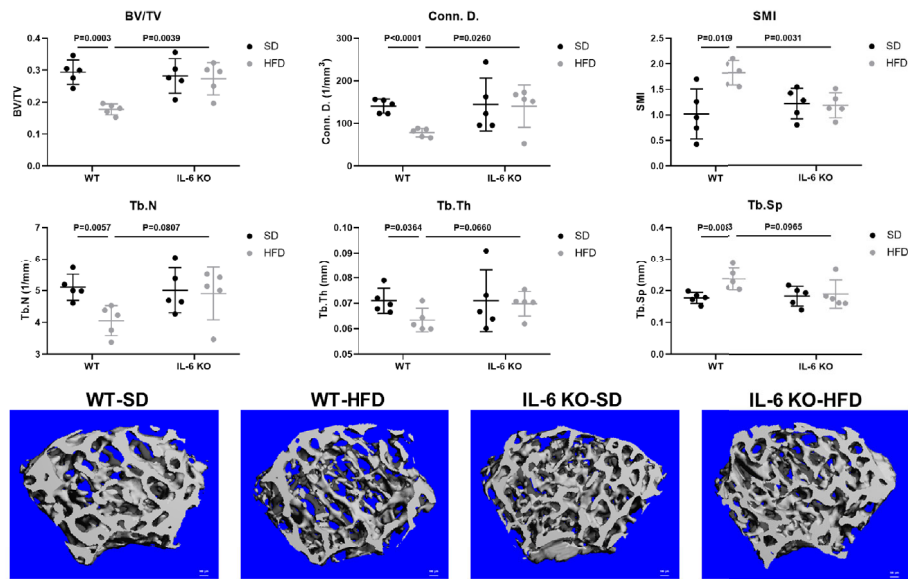
Since the osteogenesis and adipogenesis of BMSCs created a tug-of-war between osteoblasts and adipocytes, we next examined the mRNA levels of adipogenic differentiation genes in bone marrow cells (BMCs). BMCs contained BMSCs, hematopoietic cells, immune cells, etc. but not BMAs or erythrocytes. The BMCs from WT-HFD mice exhibited increased adipocytic differentiation capacity compared with WT-SD mice measured by mRNA gene expression of adipogenic genes (Adipoq, Pparg, Lepr), indicating that HFD

increased an adipogenic cell population in BM (Figure 4C). However, the adipogenic gene expression (Adipoq, Pparg) in the BMCs from IL-6 KO mice was not significantly changed after HFD, which suggested that IL-6 KO restrained HFD-induced BMAT expansion. These results implied that IL-6 might enhance the adipogenic potential of BMSCs to accelerate trabecular bone loss in HFD-induced obesity.

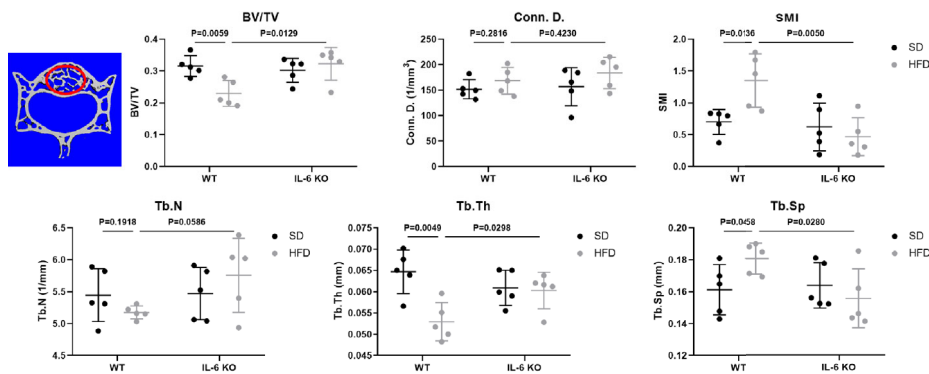
IL-6 KO Attenuated Senescence of BMCs in HFD-induced Bone Loss

We have observed the differences in the increase of adipogenesis and the decrease of osteogenesis in BM of the two strains of mice in HFD-induced obesity, and obesity can also accelerate cellular senescence (27, 43, 44). As an important component of senescence-associated secretory phenotype (SASP), IL-6 can enhance cell senescence through autocrine and paracrine pathways (45). The HFD induced distinct increase in IL-6 levels of the culture supernatant of primary BMSCs in WT mice (Table 3), suggesting the senescent phenotype of BMSCs. Considering the senescence of BMSCs promoted bone loss (27), we explored whether IL-6 KO could inhibit senescence of BMSCs. Bone marrow cells (BMCs), containing hematopoietic cells, immune cells etc., were purified into BMSCs through culturing. The number of colonies from BMCs was significantly decreased in WT mice after HFD, while it remained similarly in IL-6 KO mice after HFD (Figure 5A). The changes in mRNA levels of typical senescence marker p16 were not statistically significant in the four groups of mice (Figure 5B). However, p21, another typical aging marker, in BMCs was significantly increased in WT-HFD mice while it did not change observably in IL-6 KO-HFD mice (Figures 5B, C). Although the mRNA level of p53 in WT mice showed only a slight increase after HFD, the protein level was significantly increased. Moreover, the protein level of p53 in BMCs was not significantly changed in IL-6 KO mice after HFD. It was reported that IL-6 activated intracellular STAT3/p53/p21 signal transduction and induced senescence of vascular smooth muscle cells (36). As IL-6/sIL-6R was involved in the

A Trabecular bone of distal femoral metaphysis



B Trabecular bone of L3 vertebra



C Cortical bone of femoral mid-diaphysis

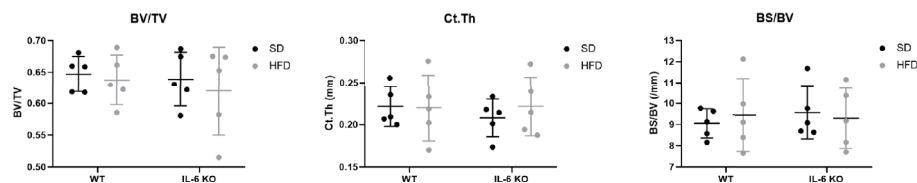


FIGURE 2 | IL-6 KO restrained the trabecular bone loss in HFD-induced obesity. **(A)** The trabecular bone parameters at distal femoral metaphysis were evaluated as BV/TV, Conn. D., SMI, Tb. N, Tb. Th and Tb. Sp from WT and IL-6 KO mice after SD or HFD treatment. Representative images for μ CT 3D reconstruction were shown in lower panel (scale bar = 100 μ m). **(B)** The trabecular bone parameters at the L3 vertebra were measured via μ CT from WT and IL-6 KO mice after SD or HFD treatment. The red circles indicate the ROI. **(C)** The cortical bone parameters at femoral mid-diaphysis measurement were evaluated as BV/TV, Ct. Th and BS/BV from WT and IL-6 KO mice after SD or HFD treatment. Data were expressed as mean \pm SD.

pathogenesis of cell senescence through IL-6/sIL-6R/STAT3 axis (30, 32–34), we explored this pathway in the process of senescence in BMCs. HFD induced a similar protein level of p-STAT3 in WT and IL-6 KO mice (**Figure 5C**). These results suggested IL-6 KO attenuated the reduced proliferation of BMCs and the enhanced expression of senescence markers in HFD-induced bone loss, which implied that IL-6 promoted senescence of BMCs.

IL-6 Might Accelerate Senescence of BMSCs through IL-6/STAT3 Pathway

BMSCs are the common ancestor of osteoblasts and adipocytes. The status of BMSCs accurately reflects the potential of adipogenic and osteogenic differentiation. To further investigate the role of IL-6 on BMSCs senescence, we generated replicative senescent BMSCs from BMCs of WT and IL-6 KO mice by

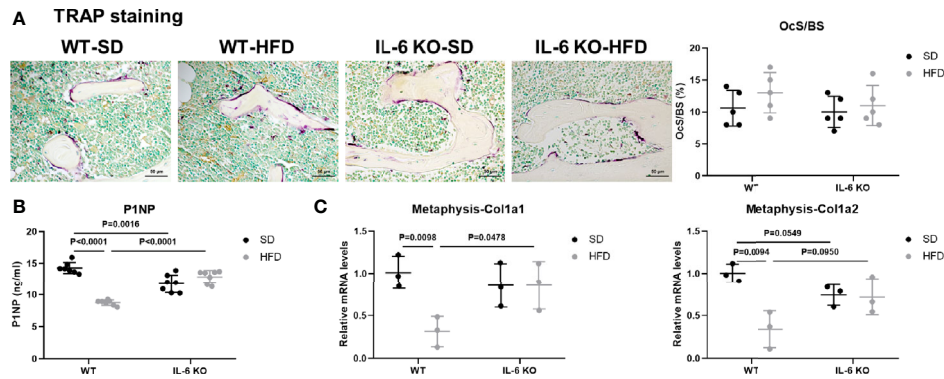


FIGURE 3 | IL-6 KO rescued the decreased osteogenesis in HFD-induced obesity. **(A)** Histopathological analysis on bone sections from tibia stained with TRAP staining from WT and IL-6 KO mice after SD or HFD treatment (scale bar = 50 μ m). Osteoclast surface per bone surface (OcS/BS) was evaluated in tibia (right panel). **(B)** Bone formation marker PINP was measured in serum of WT and IL-6 KO mice after SD or HFD. **(C)** The mRNA levels of osteogenic markers Col1a1 and Col1a2 were measured in metaphysis of WT and IL-6 KO mice after SD or HFD. Data were expressed as mean \pm SD.

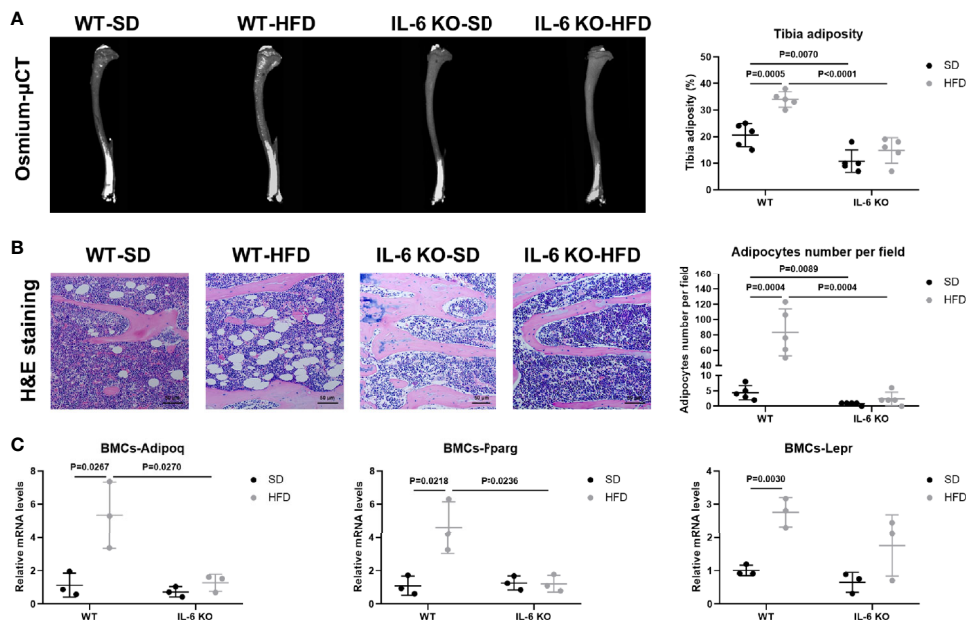


FIGURE 4 | IL-6 KO attenuated adipogenesis of BM in HFD-induced obesity. **(A)** Representative images of BMAT from full-length tibial sagittal plane of WT and IL-6 KO mice fed with SD or HFD by μ CT. Quantification of the osmium density in tibial sagittal plane was expressed as tibia adiposity (right panel). **(B)** Histopathological analysis on bone sections from tibia stained with H&E staining from WT and IL-6 KO mice after SD or HFD treatment (scale bar = 50 μ m). Adipocyte number per field on H&E section was evaluated by Image J software (right panel). **(C)** The mRNA levels of adipogenic genes in bone marrow cells (BMCs) of WT and IL-6 KO mice after SD or HFD. Data were expressed as mean \pm SD.

cultivation and passage. SA- β -gal is a key feature in the process of cell senescence. The SA- β -gal positive BMSCs from IL-6 KO mice were significantly less than that from WT mice when cultured for passage 9 (P9) (**Figure 6A**). IL-6 neutralization antibody exposure resulted in significant reduction in SA- β -gal positive cells in WT mice, while BMSCs from IL-6 KO mice showed more positive cells after being treated with recombinant IL-6. Furthermore, the mRNA and protein levels of senescence

markers (p53, p21) in BMSCs from WT were markedly decreased after IL-6 antibody treatment (**Figures 6B, C**). In contrast, the mRNA and protein levels of senescence markers (p53, p21) in BMSCs from IL-6 KO mice were significantly increased after recombinant IL-6 treatment (**Figures 6D, E**). The protein level of p-STAT3 was notably decreased in senescent BMSCs from WT mice with IL-6 antibody treatment, while expression of p-STAT3 showed significant increase in BMSCs from IL-6 KO mice after

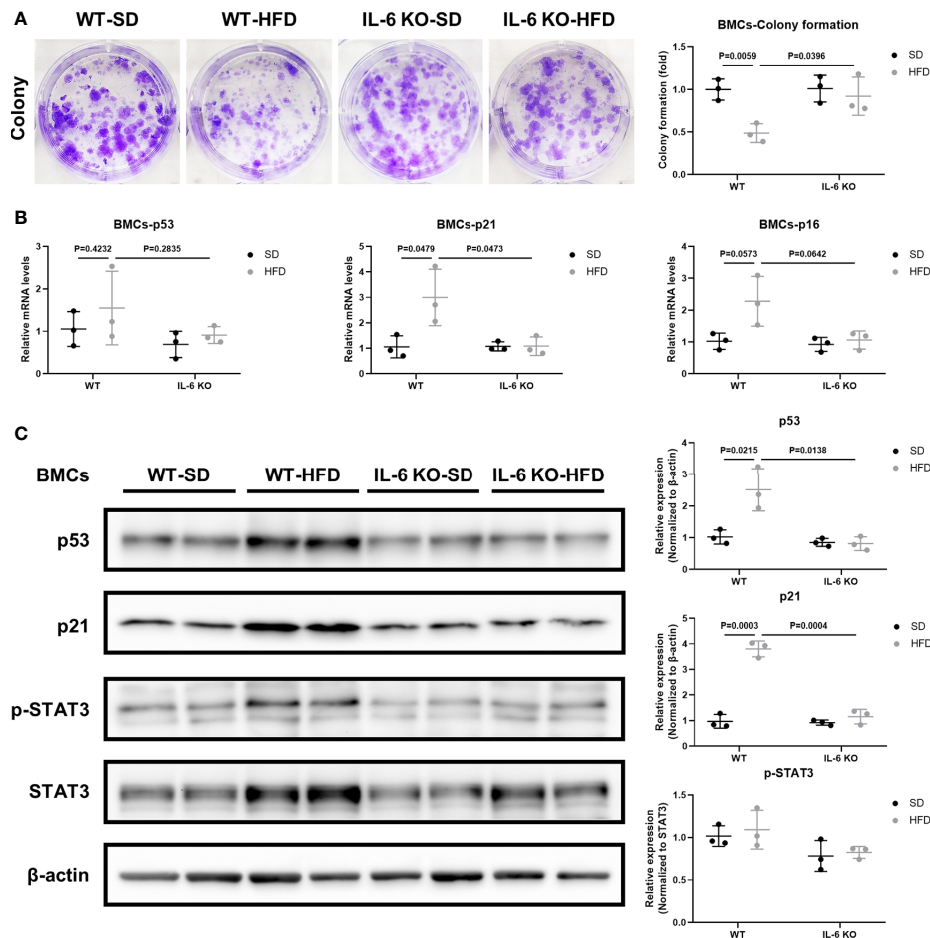


FIGURE 5 | IL-6 KO attenuated senescence of BMSCs in HFD-induced bone loss. **(A)** Representative images for colony formation of bone marrow cells (BMCs) from WT and IL-6 KO mice after SD or HFD treatment. The number of colonies per well was counted and calculated (right panel). **(B)** The mRNA levels of typical aging markers (p53, p21, p16) in BMCs from WT and IL-6 KO mice after SD or HFD. **(C)** Western blot analysis of indicated proteins (p53, p21, p-STAT3, STAT3, β-actin) in BMCs of WT and IL-6 KO mice fed with SD or HFD for 12 weeks. The expression of p53 and p21 was normalized against β-actin, and the expression of p-STAT3 was normalized against STAT3. Quantitative analysis with Image J software was shown on the right panel. Data were expressed as mean ± SD.

recombinant IL-6 treatment (**Figures 6C, E**). Taken together, these results implied that IL-6 accelerated senescent phenotype of BMSCs through the IL-6/STAT3 pathway, suggesting a potential mechanism for bone loss in HFD-induced obesity.

DISCUSSION

The body weight of WT and IL-6 KO mice was increased significantly after HFD, while IL-6 KO mice gained less weight than WT mice (**Figures 1A, B**). The changes of body weight were consistent with the previous study (46), but not exactly as the same as the results of several other studies due to the different dietary intervention time, the consistency of the initial body weight of the two strains of mice, and the animal conditions (47–49). Previous study has suggested that the trabecular BV/TV, Tb. N and Tb. Th of IL-6 KO mice were higher than those of WT

mice through bone histomorphometry after SD (47). In our study, the high-resolution μ CT system was used to analyze the bone microstructure of WT and IL-6 KO mice, and we found similar levels of BV/TV, Conn. D, SMI, Tb. N, Tb. Th and Tb. Sp between WT-SD and IL-6 KO-SD mice. The dietary intervention time and detection methods in our study were different from the previous study (47), which may help explain the inconsistent results of bone phenotypes. In the present study, we found 12-week HFD treatment obviously enhanced trabecular bone loss in WT mice, but it failed to do so in IL-6 KO mice (**Figures 2A, B**).

Evidence has shown that HFD led to chronic low-grade inflammation and local lipid accumulation (50). There are two main imbalances in the development of osteoporosis (OP): one is bone-fat imbalance, the other lies on the uncoupled bone remodeling (9). Bone resorption marker TRAP staining showed no significant difference between WT and IL-6 KO mice after SD or HFD (**Figure 3A**). Furthermore, both the

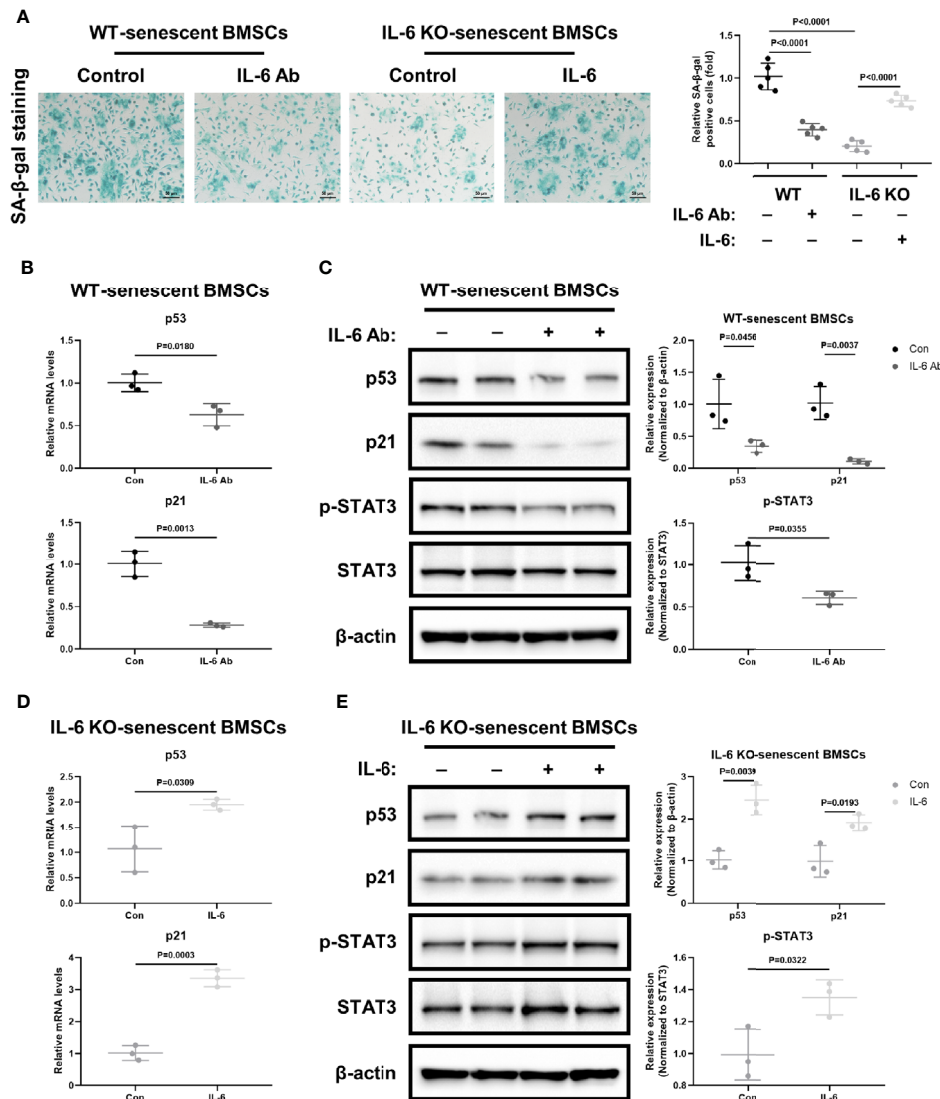


FIGURE 6 | IL-6 accelerated senescence of BMSCs through IL-6/STAT3 pathway. **(A)** Representative images for SA-β-Gal staining of replicative BMSCs with or without IL-6 neutralization antibody from WT mice, and with or without recombinant mouse IL-6 treatment from IL-6 KO mice. (Cell nucleus: dark blue, SA-β-gal-positive cell: cyan, scale bar = 50 μm). Quantification of SA-β-Gal positive cells evaluated with Image J software (right panel). **(B)** The mRNA levels of p53 and p21 in replicative BMSCs with or without IL-6 antibody treatment from WT mice. **(C)** Western blot analysis of indicated proteins (p53, p21, p-STAT3, STAT3, β-actin) in replicative BMSCs with or without IL-6 antibody treatment from WT mice. The expression of p53 and p21 was normalized against β-actin, and the expression of p-STAT3 was normalized against STAT3. Quantitative analysis with Image J software was shown on the right panel. **(D)** The mRNA levels of p53 and p21 in replicative BMSCs with or without IL-6 treatment from IL-6 KO mice. **(E)** Western blot analysis of indicated proteins in replicative BMSCs with or without recombinant IL-6 treatment from IL-6 KO mice. The expression of p53 and p21 was normalized against β-actin, and the expression of p-STAT3 was normalized against STAT3. Quantitative analysis with Image J software was shown on the lower panel. Data were expressed as mean ± SD.

levels of PINP in serum and the mRNA levels of osteogenic markers in metaphysis indicated that IL-6 KO restrained HFD-induced decrease of osteogenesis (Figures 3B, C). It was widely accepted that abnormal expansion of BMAT plays a crucial role in the onset and progression of OP, in part because both adipocytes and osteoblasts originate from a common ancestor lineage and there is a competitive relationship between adipogenic and osteogenic differentiation of BMSCs (51). Marrow adipocytes are dynamic: their size and number can

change in response to environmental, nutritional, and hormonal cues (39). In our study, IL-6 KO suppressed HFD-induced BMAT expansion (Figures 4A, B). In addition, IL-6 KO restrained the increase of adipogenic genes (Adipoq, Pparg) in BMCs induced by HFD (Figure 4C). Therefore, IL-6 KO inhibited the adipogenesis in BM, arrested the shift of BMSCs from the osteoblast lineage to the adipocyte lineage.

BM adiposity is a manifestation of BMSCs senescence, and obesity accelerates cell senescence (27, 43, 44). Tencerova

et al. found BMAT accumulation and BMSCs senescence were increased in BM cavity in obesity (27, 43). Moreover, obesity results in the accumulation of senescent glial cells in proximity to the lateral ventricle, while senescent glial cells exhibit excessive fat deposits (44). As one of the most important inflammatory mediators in obesity, IL-6 was also involved in the pathogenesis of cell senescence. IL-6 KO inhibited aging-related accumulation of p53 in mouse myocardium (52). Cell senescence involves in multiple signaling pathways (53). The senescence associated gene p21 is a well-known target gene of p53 that has been shown to play a critical role during the process of p53 induced cellular senescence (54). We hypothesized that IL-6 KO may restrain HFD-induced accelerated senescent phenotype in the BM microenvironment. Several lines of experimental evidence supported this hypothesis. First, IL-6 KO inhibited the HFD-induced decrease in the number of colonies from BMCs (**Figure 5A**). Secondly, IL-6 KO inhibited HFD-induced increase of senescence-specific markers in BMCs (**Figures 5B, C**). This may explain the possible molecular mechanism of IL-6 KO preventing HFD-induced bone loss. IL-6 KO may prevent HFD-induced BMSCs exhaustion and the creation of a senescent BM microenvironment, thereby relieving bone fragility in HFD-induced obesity.

Senescent cells secrete multiple inflammatory factors, chemokines and matrix proteases, known as senescence-associated secretory phenotype (SASP). IL-6 is an important component of SASP. IL-6 can enhance cell senescence through autocrine and paracrine pathways (45). Replicative BMSCs derived from WT mice when grown in medium supplemented with IL-6 antibody, exhibited consistently less SA- β -gal staining and lower levels of senescent markers (p53, p21) than controls (**Figures 6A–C**). The recombinant IL-6 administration led to increased SA- β -gal staining and higher levels of senescent markers (p53, p21) in replicative BMSCs from the IL-6 KO mice, when compared to controls (**Figures 6A, D, E**).

It was reported that the IL-6/sIL-6R complex activates the JAK/STAT3 signal transduction pathway and inhibits G1 to S phase transition of cell cycle (34, 36, 52). Previously, IL-6/sIL-6R induced premature senescence in normal human fibroblasts through STAT3/p53 pathway, and there was a potential binding site (5'-TTnnnnGA-3') of p-STAT3 in the p53 promoter region (30, 35). Moreover, IL-6 activated intracellular STAT3/p53/p21 signal transduction and induced senescence of vascular smooth muscle cells (36). In our study, although BMCs from IL-6 KO mice expressed similar levels of p-STAT3 with WT mice after HFD (**Figure 5C**), less p-STAT3 expression was detected when the effects of IL-6 were removed in replicative senescent model using BMSCs from WT and IL-6 KO mice (**Figures 6C, E**). This supports the hypothesis that the activation of IL-6/STAT3 promotes the senescence of BMSCs in BM, suggesting a potential mechanism for trabecular bone loss in HFD-induced obesity.

In summary, we demonstrated the effect of IL-6 on differentiation and senescence of BMSCs in HFD-induced obesity. IL-6 KO restrained HFD-induced trabecular bone loss and BMAT increase. IL-6 might promote BMAT expansion and

break the balance between osteogenesis and adipogenesis of BMSCs in HFD-induced bone fragility. IL-6 promoted BMSCs senescence through IL-6/STAT3 pathway, suggesting a potential mechanism for bone loss. Therefore, IL-6 KO contributed to the maintenance of bone mass after HFD. Our results showed, for the first time, that the IL-6 may be involved in the potential mechanism of HFD-induced trabecular bone loss by breaking the balance between osteogenesis and adipogenesis of BMSCs and promoting senescence of BMSCs in HFD-induced obesity.

DATA AVAILABILITY STATEMENT

The original contributions presented in the study are included in the article/supplementary material. Further inquiries can be directed to the corresponding author.

ETHICS STATEMENT

The animal study was reviewed and approved by the Institutional Animal Care and Treatment Committee of Sichuan University.

AUTHOR CONTRIBUTIONS

XY designed this research. YJL, LL, YX, XC, LT, YaL, HL, and JZ were responsible for the experiments. Among them, YJL, LL, YX, XC, and HL were in charge of the animal experiments, cellular experiments, and molecular experiments. YaL and JZ were mainly responsible for the histopathological part. YJL, LT, YiL, and XY were responsible for the revision of the whole article. All authors contributed to the article and approved the submitted version.

FUNDING

This work was supported by grants from the National Natural Science Foundation of China (no. 81770875, 81902246), the Project of Health Commission of Sichuan Province (no. 19PJ096), 1.3.5 Project for Disciplines of Excellence of West China Hospital (no. 2020HXXFH008, ZYJC18003), and the Post-Doctor Research Project of West China Hospital (no. 19HXBH053).

ACKNOWLEDGMENTS

The authors thank Miss Xiao Yu from the University of Michigan Ann Arbor, for help with editing the language. The authors also thank Mr Bo Su from Histology and Imaging Platform, Research Core Facility, West China Hospital, Sichuan University, for assistance with imaging of BMAT by osmium- μ CT.

REFERENCES

- Kahn SE, Hull RL, Utzschneider KM. Mechanisms linking obesity to insulin resistance and type 2 diabetes. *Nature* (2006) 444:840–6. doi: 10.1038/nature05482
- Willebrords J, Pereira IV, Maes M, Crespo Yanguas S, Colle I, Van Den Bossche B, et al. Strategies, models and biomarkers in experimental non-alcoholic fatty liver disease research. *Prog Lipid Res* (2015) 59:106–25. doi: 10.1016/j.plipres.2015.05.002
- Mpalaris V, Anagnostis P, Goulis DG, Iakovou I. Complex association between body weight and fracture risk in postmenopausal women. *Obes Rev* (2015) 16:225–33. doi: 10.1111/obr.12244
- Nih Consensus Development Panel on Osteoporosis Prevention D. Therapy. Osteoporosis prevention, diagnosis, and therapy. *JAMA* (2001) 285:785–95. doi: 10.1001/jama.285.6.785
- Evans AL, Paggiosi MA, Eastell R, Walsh JS. Bone density, microstructure and strength in obese and normal weight men and women in younger and older adulthood. *J Bone Miner Res* (2015) 30:920–8. doi: 10.1002/jbmr.2407
- Cohen A, Dempster DW, Recker RR, Lappe JM, Zhou H, Zwahlen A, et al. Abdominal fat is associated with lower bone formation and inferior bone quality in healthy premenopausal women: a transiliac bone biopsy study. *J Clin Endocrinol Metab* (2013) 98:2562–72. doi: 10.1210/jc.2013-1047
- Compston JE, Flahive J, Hooven FH, Anderson FA Jr., Adachi JD, Boonen S, et al. Obesity, health-care utilization, and health-related quality of life after fracture in postmenopausal women: Global Longitudinal Study of Osteoporosis in Women (GLOW). *Calcif Tissue Int* (2014) 94:223–31. doi: 10.1007/s00223-013-9801-z
- Lecka-Czernik B, Stechschulte LA, Czernik PJ, Dowling AR. High bone mass in adult mice with diet-induced obesity results from a combination of initial increase in bone mass followed by attenuation in bone formation; implications for high bone mass and decreased bone quality in obesity. *Mol Cell Endocrinol* (2015) 410:35–41. doi: 10.1016/j.mce.2015.01.001
- Li J, Chen X, Lu L, Yu X. The relationship between bone marrow adipose tissue and bone metabolism in postmenopausal osteoporosis. *Cytokine Growth Factor Rev* (2020) 52:88–98. doi: 10.1016/j.cytogfr.2020.02.003
- Tencerova M, Kassem M. The Bone Marrow-Derived Stromal Cells: Commitment and Regulation of Adipogenesis. *Front Endocrinol (Lausanne)* (2016) 7:127. doi: 10.3389/fendo.2016.00127
- Abdallah BM, Kassem M. New factors controlling the balance between osteoblastogenesis and adipogenesis. *Bone* (2012) 50:540–5. doi: 10.1016/j.bone.2011.06.030
- Jafari A, Qanie D, Andersen TL, Zhang Y, Chen L, Postert B, et al. Legumain Regulates Differentiation Fate of Human Bone Marrow Stromal Cells and Is Altered in Postmenopausal Osteoporosis. *Stem Cell Rep* (2017) 8:373–86. doi: 10.1016/j.stemcr.2017.01.003
- Veldhuis-Vlug AG, Rosen CJ. Clinical implications of bone marrow adiposity. *J Intern Med* (2018) 283:121–39. doi: 10.1111/joim.12718
- Amano SU, Cohen JL, Vangala P, Tencerova M, Nicoloso SM, Yaw JC, et al. Local proliferation of macrophages contributes to obesity-associated adipose tissue inflammation. *Cell Metab* (2014) 19:162–71. doi: 10.1016/j.cmet.2013.11.017
- McLean RR. Proinflammatory cytokines and osteoporosis. *Curr Osteoporosis Rep* (2009) 7:134–9. doi: 10.1007/s11914-009-0023-2
- Schett G. Effects of inflammatory and anti-inflammatory cytokines on the bone. *Eur J Clin Invest* (2011) 41:1361–6. doi: 10.1111/j.1365-2362.2011.02545.x
- Souza PP, Lerner UH. The role of cytokines in inflammatory bone loss. *Immunol Invest* (2013) 42:555–622. doi: 10.3109/08820139.2013.822766
- Mohamed-Ali V, Goodrick S, Rawesh A, Katz DR, Miles JM, Yudkin JS, et al. Subcutaneous adipose tissue releases interleukin-6, but not tumor necrosis factor- α , in vivo. *J Clin Endocrinol Metab* (1997) 82:4196–200. doi: 10.1210/jcem.82.12.4450
- Tchkonia T, Morbeck DE, Von Zglinicki T, Van Deursen J, Lustgarten J, Scrable H, et al. Fat tissue, aging, and cellular senescence. *Aging Cell* (2010) 9:667–84. doi: 10.1111/j.1474-9726.2010.00608.x
- Schaper F, Rose-John S. Interleukin-6: Biology, signaling and strategies of blockade. *Cytokine Growth Factor Rev* (2015) 26:475–87. doi: 10.1016/j.cytogfr.2015.07.004
- Sims NA, Jenkins BJ, Quinn JM, Nakamura A, Glatt M, Gillespie MT, et al. Glycoprotein 130 regulates bone turnover and bone size by distinct downstream signaling pathways. *J Clin Invest* (2004) 113:379–89. doi: 10.1172/JCI19872
- Xie Z, Tang S, Ye G, Wang P, Li J, Liu W, et al. Interleukin-6/interleukin-6 receptor complex promotes osteogenic differentiation of bone marrow-derived mesenchymal stem cells. *Stem Cell Res Ther* (2018) 9:13. doi: 10.1186/s13287-017-0766-0
- Bellido T, Borba VZ, Roberson P, Manolagas SC. Activation of the Janus kinase/STAT (signal transducer and activator of transcription) signal transduction pathway by interleukin-6-type cytokines promotes osteoblast differentiation. *Endocrinology* (1997) 138:3666–76. doi: 10.1210/endo.138.9.5364
- Nishimura R, Moriyama K, Yasukawa K, Mundy GR, Yoneda T. Combination of interleukin-6 and soluble interleukin-6 receptors induces differentiation and activation of JAK-STAT and MAP kinase pathways in MG-63 human osteoblastic cells. *J Bone Miner Res* (1998) 13:777–85. doi: 10.1359/jbmr.1998.13.5.777
- Roodman GD. Interleukin-6: an osteotropic factor? *J Bone Miner Res* (1992) 7:475–8. doi: 10.1002/jbmr.5650070502
- Hughes FJ, Howells GL. Interleukin-6 inhibits bone formation in vitro. *Bone Miner* (1993) 21:21–8. doi: 10.1016/s0169-6009(08)80117-1
- Tencerova M, Frost M, Figeac F, Nielsen TK, Ali D, Lauterlein JL, et al. Obesity-Associated Hypermetabolism and Accelerated Senescence of Bone Marrow Stromal Stem Cells Suggest a Potential Mechanism for Bone Fragility. *Cell Rep* (2019) 27:2050–62.e6. doi: 10.1016/j.celrep.2019.04.066
- Ersler WB. Interleukin-6: a cytokine for gerontologists. *J Am Geriatr Soc* (1993) 41:176–81. doi: 10.1111/j.1532-5415.1993.tb02054.x
- Erol A. Interleukin-6 (IL-6) is still the leading biomarker of the metabolic and aging related disorders. *Med Hypotheses* (2007) 69:708. doi: 10.1016/j.mehy.2007.01.021
- Kojima H, Kunimoto H, Inoue T, Nakajima K. The STAT3-IGFBP5 axis is critical for IL-6/gp130-induced premature senescence in human fibroblasts. *Cell Cycle* (2012) 11:730–9. doi: 10.4161/cc.11.4.19172
- Kuilman T, Michaloglou C, Vredeveld LC, Douma S, van Doorn R, Desmet CJ, et al. Oncogene-induced senescence relayed by an interleukin-dependent inflammatory network. *Cell* (2008) 133:1019–31. doi: 10.1016/j.cell.2008.03.039
- Ren C, Cheng X, Lu B, Yang G. Activation of interleukin-6/signal transducer and activator of transcription 3 by human papillomavirus early proteins 6 induces fibroblast senescence to promote cervical tumorigenesis through autocrine and paracrine pathways in tumor microenvironment. *Eur J Cancer* (2013) 49:3889–99. doi: 10.1016/j.ejca.2013.07.140
- Hodge DR, Peng B, Cherry JC, Hurt EM, Fox SD, Kelley JA, et al. Interleukin 6 supports the maintenance of p53 tumor suppressor gene promoter methylation. *Cancer Res* (2005) 65:4673–82. doi: 10.1158/0008-5472.CAN-04-3589
- Hirano T, Ishihara K, Hibi M. Roles of STAT3 in mediating the cell growth, differentiation and survival signals relayed through the IL-6 family of cytokine receptors. *Oncogene* (2000) 19:2548–56. doi: 10.1038/sj.onc.1203551
- Kojima H, Inoue T, Kunimoto H, Nakajima K. IL-6-STAT3 signaling and premature senescence. *JAKSTAT* (2013) 2:e25763. doi: 10.4161/jkst.25763
- Xu D, Zeng F, Han L, Wang J, Yin Z, Lv L, et al. The synergistic action of phosphate and interleukin-6 enhances senescence-associated calcification in vascular smooth muscle cells depending on p53. *Mech Ageing Dev* (2019) 182:111124. doi: 10.1016/j.mad.2019.111124
- Beamer WG, Shultz KL, Ackert-Bicknell CL, Horton LG, Delahunty KM, Coombs HF3rd, et al. Genetic dissection of mouse distal chromosome 1 reveals three linked BMD QTLs with sex-dependent regulation of bone phenotypes. *J Bone Miner Res* (2007) 22:1187–96. doi: 10.1359/jbmr.070419
- Scheller EL, Troiano N, Vanhoutan JN, Boussein MA, Fretz JA, Xi Y, et al. Use of osmium tetroxide staining with microcomputerized tomography to visualize and quantify bone marrow adipose tissue in vivo. *Methods Enzymol* (2014) 537:123–39. doi: 10.1016/B978-0-12-411619-1.00007-0
- Fan Y, Hanai JI, Le PT, Bi R, Maridas D, DeMambro V, et al. Parathyroid Hormone Directs Bone Marrow Mesenchymal Cell Fate. *Cell Metab* (2017) 25:661–72. doi: 10.1016/j.cmet.2017.01.001

40. Sun P, Jia K, Zheng C, Zhu X, Li J, He L, et al. Loss of Lgr4 inhibits differentiation, migration and apoptosis, and promotes proliferation in bone mesenchymal stem cells. *J Cell Physiol* (2019) 234:10855–67. doi: 10.1002/jcp.27927
41. Deng L, Ren R, Liu Z, Song M, Li J, Wu Z, et al. Stabilizing heterochromatin by DGC88 alleviates senescence and osteoarthritis. *Nat Commun* (2019) 10:3329. doi: 10.1038/s41467-019-10831-8
42. Debacq-Chainiaux F, Erusalimsky JD, Campisi J, Toussaint O. Protocols to detect senescence-associated beta-galactosidase (SA-beta-gal) activity, a biomarker of senescent cells in culture and in vivo. *Nat Protoc* (2009) 4:1798–806. doi: 10.1038/nprot.2009.191
43. Tencerova M, Figeac F, Ditzel N, Taipaleenmaki H, Nielsen TK, Kassem M. High-Fat Diet-Induced Obesity Promotes Expansion of Bone Marrow Adipose Tissue and Impairs Skeletal Stem Cell Functions in Mice. *J Bone Miner Res* (2018) 33:1154–65. doi: 10.1002/jbmr.3408
44. Ogrodnik M, Zhu Y, Langhi LGP, Tchkonja T, Kruger P, Fielder E, et al. Obesity-Induced Cellular Senescence Drives Anxiety and Impairs Neurogenesis. *Cell Metab* (2019) 29:1061–77.e8. doi: 10.1016/j.cmet.2018.12.008
45. Mosteiro L, Pantoja C, de Martino A, Serrano M. Senescence promotes in vivo reprogramming through p16(INK)(4a) and IL-6. *Aging Cell* (2018) 17:e12711. doi: 10.1111/accel.12711
46. Chen F, Chen D, Zhao X, Yang S, Li Z, Sanchis D, et al. Interleukin-6 deficiency facilitates myocardial dysfunction during high fat diet-induced obesity by promoting lipotoxicity and inflammation. *Biochim Biophys Acta Mol Basis Dis* (2017) 1863:3128–41. doi: 10.1016/j.bbdis.2017.08.022
47. Feng W, Liu B, Liu D, Hasegawa T, Wang W, Han X, et al. Long-Term Administration of High-Fat Diet Corrects Abnormal Bone Remodeling in the Tibiae of Interleukin-6-Deficient Mice. *J Histochem Cytochem* (2016) 64:42–53. doi: 10.1369/0022155415611931
48. Wang C, Tian L, Zhang K, Chen Y, Chen X, Xie Y, et al. Interleukin-6 gene knockout antagonizes high-fat-induced trabecular bone loss. *J Mol Endocrinol* (2016) 57:161–70. doi: 10.1530/JME-16-0076
49. Chen X, Gong Q, Wang CY, Zhang K, Ji X, Chen YX, et al. High-Fat Diet Induces Distinct Metabolic Response in Interleukin-6 and Tumor Necrosis Factor-alpha Knockout Mice. *J Interferon Cytokine Res* (2016) 36:580–8. doi: 10.1089/jir.2016.0022
50. Airaksinen K, Jokkala J, Ahonen I, Auriola S, Kolehmainen M, Hanhineva K, et al. High-Fat Diet, Betaine, and Polydextrose Induce Changes in Adipose Tissue Inflammation and Metabolism in C57BL/6J Mice. *Mol Nutr Food Res* (2018) 62:e1800455. doi: 10.1002/mnfr.201800455
51. Song L, Liu M, Ono N, Bringhurst FR, Kronenberg HM, Guo J. Loss of wnt/beta-catenin signaling causes cell fate shift of preosteoblasts from osteoblasts to adipocytes. *J Bone Miner Res* (2012) 27:2344–58. doi: 10.1002/jbmr.1694
52. Bonda TA, Dziemidowicz M, Cieslinska M, Tarasiuk E, Wawrusiewicz-Kurylonek N, Bialuk I, et al. Interleukin 6 Knockout Inhibits Aging-Related Accumulation of p53 in the Mouse Myocardium. *J Gerontol A Biol Sci Med Sci* (2019) 74:176–82. doi: 10.1093/gerona/gly105
53. Kim YY, Jee HJ, Um JH, Kim YM, Bae SS, Yun J. Cooperation between p21 and Akt is required for p53-dependent cellular senescence. *Aging Cell* (2017) 16:1094–103. doi: 10.1111/accel.12639
54. Brugarolas J, Chandrasekaran C, Gordon JI, Beach D, Jacks T, Hannon GJ. Radiation-induced cell cycle arrest compromised by p21 deficiency. *Nature* (1995) 377:552–7. doi: 10.1038/377552a0

Conflict of Interest: The authors declare that the research was conducted in the absence of any commercial or financial relationships that could be construed as a potential conflict of interest.

Copyright © 2021 Li, Lu, Xie, Chen, Tian, Liang, Li, Zhang, Liu and Yu. This is an open-access article distributed under the terms of the Creative Commons Attribution License (CC BY). The use, distribution or reproduction in other forums is permitted, provided the original author(s) and the copyright owner(s) are credited and that the original publication in this journal is cited, in accordance with accepted academic practice. No use, distribution or reproduction is permitted which does not comply with these terms.



Muscle-Bone Crosstalk in the Masticatory System: From Biomechanical to Molecular Interactions

Sonja Buvinic^{1,2*}, Julián Balanta-Melo^{3,4,5}, Kornelius Kupczik⁶, Walter Vásquez¹, Carolina Beato¹ and Viviana Toro-Ibacache^{1,6}

¹ Institute for Research in Dental Sciences, Faculty of Dentistry, Universidad de Chile, Santiago, Chile, ² Center for Exercise, Metabolism and Cancer Studies CEMC2016, Faculty of Medicine, Universidad de Chile, Santiago, Chile, ³ School of Dentistry, Faculty of Health, Universidad del Valle, Cali, Colombia, ⁴ Evidence-Based Practice Unit Univalle, Hospital Universitario del Valle, Cali, Colombia, ⁵ Max Planck Weizmann Center for Integrative Archaeology and Anthropology, Max Planck Institute for Evolutionary Anthropology, Leipzig, Germany, ⁶ Department of Human Evolution, Max Planck Institute for Evolutionary Anthropology, Leipzig, Germany

OPEN ACCESS

Edited by:

Lilian Irene Plotkin,
Indiana University Bloomington,
United States

Reviewed by:

Marco P. Brotto,
University of Texas at Arlington,
United States
Andrea Bonetto,
Indiana University, United States

*Correspondence:

Sonja Buvinic
sbuvinic@u.uchile.cl

Specialty section:

This article was submitted to
Bone Research,
a section of the journal
Frontiers in Endocrinology

Received: 16 September 2020

Accepted: 31 December 2020

Published: 01 March 2021

Citation:

Buvinic S, Balanta-Melo J, Kupczik K, Vásquez W, Beato C and Toro-Ibacache V (2021) Muscle-Bone Crosstalk in the Masticatory System: From Biomechanical to Molecular Interactions. *Front. Endocrinol.* 11:606947. doi: 10.3389/fendo.2020.606947

The masticatory system is a complex and highly organized group of structures, including craniofacial bones (maxillae and mandible), muscles, teeth, joints, and neurovascular elements. While the musculoskeletal structures of the head and neck are known to have a different embryonic origin, morphology, biomechanical demands, and biochemical characteristics than the trunk and limbs, their particular molecular basis and cell biology have been much less explored. In the last decade, the concept of muscle-bone crosstalk has emerged, comprising both the loads generated during muscle contraction and a biochemical component through soluble molecules. Bone cells embedded in the mineralized tissue respond to the biomechanical input by releasing molecular factors that impact the homeostasis of the attaching skeletal muscle. In the same way, muscle-derived factors act as soluble signals that modulate the remodeling process of the underlying bones. This concept of muscle-bone crosstalk at a molecular level is particularly interesting in the mandible, due to its tight anatomical relationship with one of the biggest and strongest masticatory muscles, the masseter. However, despite the close physical and physiological interaction of both tissues for proper functioning, this topic has been poorly addressed. Here we present one of the most detailed reviews of the literature to date regarding the biomechanical and biochemical interaction between muscles and bones of the masticatory system, both during development and in physiological or pathological remodeling processes. Evidence related to how masticatory function shapes the craniofacial bones is discussed, and a proposal presented that the masticatory muscles and craniofacial bones serve as secretory tissues. We furthermore discuss our current findings of myokines-release from masseter muscle in physiological conditions, during functional adaptation or pathology, and their putative role as bone-modulators in the craniofacial system. Finally, we address the physiological implications of the crosstalk between muscles and bones in the

masticatory system, analyzing pathologies or clinical procedures in which the alteration of one of them affects the homeostasis of the other. Unveiling the mechanisms of muscle-bone crosstalk in the masticatory system opens broad possibilities for understanding and treating temporomandibular disorders, which severely impair the quality of life, with a high cost for diagnosis and management.

Keywords: musculoskeletal system, masticatory muscles, craniofacial bones, paracrine communication, bone biomechanical

INTRODUCTION

A strong positive-association between bone mass and muscle mass throughout life has been attributed to their shared function (1–5). This mechano-functional theory has been built upon studies using different approaches. Among these, clinical studies have shown simultaneous decreases in bone and muscle mass when musculoskeletal activity decreases, as in neuronal lesions leading to paralysis, neuromuscular dystrophies, microgravity, immobilizations or prolonged rest (2, 6–8). Likewise, the concomitant loss of both muscle and bone mass in the elderly (sarcopenia and osteoporosis, respectively) leads to a reduction in motility and increases the risk of falls and fractures, heightening morbidity and mortality. How this relationship occurs is not only relevant for basic science; due to the progressive aging of the world population, musculoskeletal disorders are reaching an epidemic status (9, 10). Thus, providing knowledge on the topic can help to the development of prevention and treatment strategies.

Muscle-bone crosstalk, long regarded as exclusively biomechanical, has, over the last decades, been opened to the idea of an additional biochemical component. Thus, muscles and bones are considered secretory tissues capable of releasing soluble molecules to regulate each other (3, 6, 11, 12).

The masticatory system is a highly organized group of craniofacial structures, including bones (maxillae and mandible), teeth, joints, neurovascular elements, and the muscles responsible for moving the mandible. Mandibular movements are required for vital functions such as mastication. These are made possible by the coordinated action of the masticatory muscles (jaw closing and jaw opening) that displace the mandible in a wide range of motions in the tri-dimensional space. That displacement is also guided by the articular surfaces of the temporomandibular joint (TMJ) (13). The biomechanical input from masticatory muscles is not only required for mandibular movement but also for TMJ maintenance (14, 15). The functional and/or structural alterations in one or more of the structures of the TMJ are recognized as temporomandibular disorders (TMDs), grouped by muscular, articular, or developmental conditions (16, 17).

The masticatory system is a highly coordinated machine, where minimal deregulation in one of the components evokes dramatic alterations in the whole system. Because of this, it is an exciting model to study muscle-bone crosstalk. To date, the molecular basis for muscle plasticity or muscle-bone interaction has not been studied in the masticatory system,

hindering the development of proper therapies against direct targets in TMDs. Considering that jaw muscles are anatomically and biochemically different to those of the trunk and limb (18–20), it is essential to study them at the cellular and molecular level. Some of the masticatory muscles unique features are: 1) In the embryo, they develop from the mesoderm of the first pharyngeal arch, while the trunk and limb muscles derive from the somites; 2) They express a broader range of myosin heavy chain (MyHC) in adulthood (in addition to type I-IIA-IIX), such as neonatal and cardiac isoforms; 3) They have a high number of hybrid fibers (one fiber expressing several MyHC subtypes), which leads to the development of high force in a fatigue-resistant mode; 4) Their fiber morphology is unusual, with type II fibers smaller in diameter than type I; 5) The velocity of shortening of their type I and type II fibers is even slower and faster, respectively, than their counterparts in the trunk and limbs (**Figure 1**) (20, 21). Moreover, masticatory muscles are highly moldable, depending on genetic and environmental factors (21).

Besides, compared to the postcranial skeleton, the jaws present some unique developmental and morphological features (**Figure 2**). They derive from the embryonic neural crest cells instead of the embryonic mesoderm; they support teeth, which means that they are exposed to additional developmental processes (anatomical and molecular) until young adulthood; they undergo pathologies that are not present in other bones (many of them related to the presence of teeth); as part of the axial skeleton, they contain more red bone marrow than yellow bone marrow; their regeneration capacity is higher than that of the other axial bones; and they are under the constant mechanical stimulus produced by chewing, speech, and swallowing (22–25) (**Figure 2**).

Most of the muscle-bone functional relationship has been addressed through bone biomechanics, i.e. how loading and movement impact bone shape through modeling and remodeling. The cellular processes responsible of this relationship were however not broadly studied. In addition, in the last decade, the molecular crosstalk between bone and muscle has received increasing attention. The present review gathers and organizes for the first time the current evidence of the cross-communication between muscles and bones in the masticatory apparatus, starting from their intimate biomechanical relationship to the current knowledge on molecular cross-talk generated by our own work and the work of other researchers. We propose that, as it occurs with other features of the masticatory apparatus, the muscles and bones of this territory

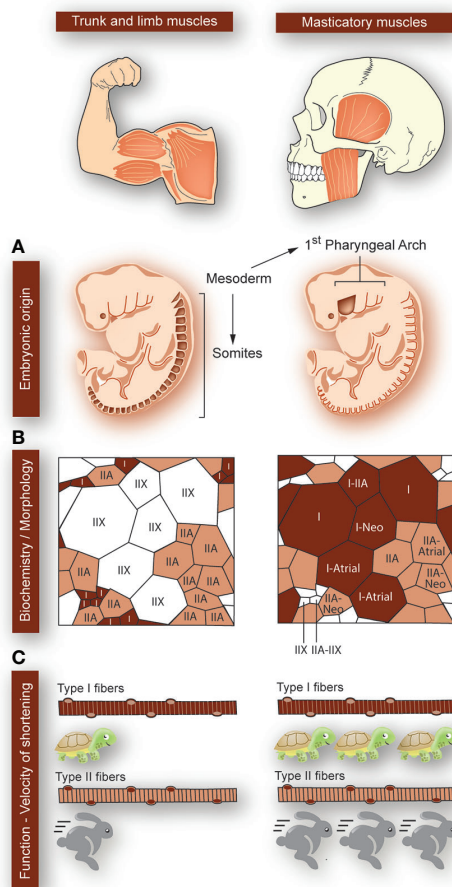


FIGURE 1 | Particularities of masticatory muscles with respect to that of the trunk and limbs. Differences between trunk and limb muscles (left panels) and masticatory muscles (right panels) are depicted, as indicated at the top of the figure. **(A)** While the trunk and limb muscles form from the mesoderm-derived somites, the masticatory muscles are derived from mesodermic-derived cells at the first pharyngeal arch (origin sites colored in dark-brown). **(B)** The trunk and limb muscles express myosin heavy chains (MyHC) type I, IIA, or IIX. Each myofiber expresses a single type of MyHC, and type II fast-fibers have a larger diameter than type I slow-fibers. In masticatory muscles, apart from the classic MyHC types (I, IIA, IIX), the neonatal and cardiac (atrial) types are expressed. There is a large proportion of “hybrid” fibers, simultaneously expressing several MyHCs types. This means that the fibers can have great force-generating properties, with high resistance to fatigue. Additionally, in masticatory muscles, type I fibers are larger in diameter than type II. **(C)** In masticatory muscles, type I myofibers are even 10-fold slower than in trunk and limbs. Moreover, the velocity of shortening of type II myofibers is faster in masticatory muscles as compared to the trunk and limbs ones.

hold a particular biochemical communication through secreted molecules mediating auto/paracrine responses, in particular “myokines” and “osteokines.” Finally, we address how the dysregulation of the masticatory muscles affects the bone component and vice versa, in pathologies, adaptations, or interventions. The latter reinforces the functional interrelation of the components of the masticatory apparatus and challenges to elucidate the molecular bases that mediate this process.

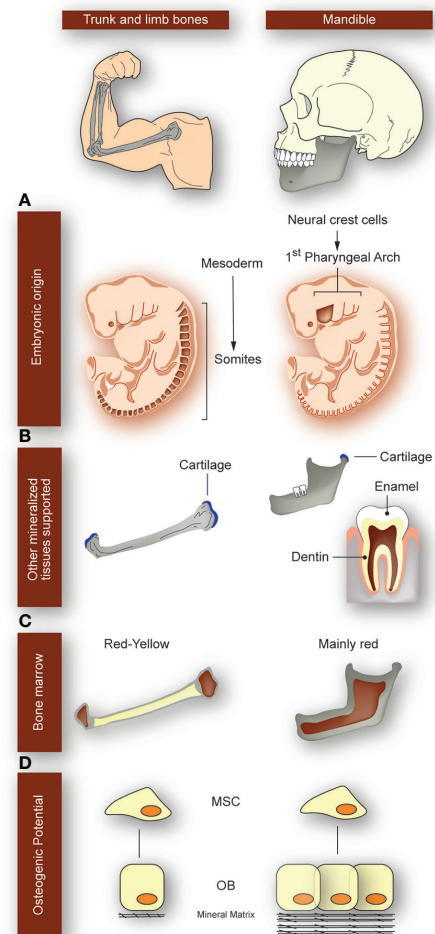


FIGURE 2 | Particularities of the mandibular bone with respect to the trunk and limb bones. Differences between long bones of the appendicular skeleton (left panels) and mandible (right panels) are depicted, as indicated at the top of the figure. **(A)** While long bones derive from embryonic mesoderm, mandibular bone derives from cells of the 1st pharyngeal arch coming from the neural crest (origin sites colored in dark-brown). **(B)** Mandible is the only structure supporting the four main mineralized tissues: bone, cartilage, enamel, and dentin. Instead, long bones only have bone and cartilage. Because jaws support the teeth, they are exposed to additional developmental processes until adulthood and undergo pathologies that are not present in other bones. **(C)** While long bones contain both red and yellow bone marrow, the jaws mainly have red bone marrow. **(D)** Mesenchymal stem cells (MSC) derived from mandible have better osteogenic potential than derived from long bones; they have a higher proliferation rate and mineralization, with an increased regeneration capacity. OB: osteoblasts.

BIOMECHANICAL INTERACTION BETWEEN MUSCLES AND BONES IN THE MASTICATORY SYSTEM; FROM FUNCTION TO SHAPE

Mechanical stimulation, which at a tissue level results in microdeformation of the cells and the extracellular matrix, is an essential factor for bone development and determining bone

shape in adults. The mechanostat hypothesis by Harold Frost (26, 27), is still widely accepted among researchers in biomechanics. It proposes that when mechanical stimulation produces bone strains in or above the 1,500–3,000 microstrain range, bone modeling increases bone mass. In comparison, strains below the 100–300 microstrain range activate bone resorption, which reduces unnecessary bone that is metabolically expensive. Low strain magnitudes acting at high frequency are also important in promoting bone formation (28, 29). For this to occur, bone cells responsible for bone deposition and resorption must sense such changes in mechanical stimuli. During muscle contraction and during loading due to e.g., body weight, the deformation of bone tissue, intertrabecular spaces, bone canaliculi and movement of interstitial fluids cause mechanical stimuli that osteocytes sense through mechanoreceptors. This signal is then transduced to different parts within the cell until a target molecule is activated (30).

Although research in this field of mechanoreception and mechanotransduction is still ongoing, some aspects have been elucidated. Among the mechanoreceptors, there are mechanosensitive ion channels that change the polarization status of a cell; integrins that connect the cell membrane with the extracellular matrix and have the inherent capacity to initiate signal transduction; connexins that allow cells in a network to “inform” the others about the mechanical milieu; lipid rafts associated to cytoplasmic second-messengers; and the same cell membrane and primary cilia which during deformation causes conformational changes in molecules that cause the transduction of signals (30–33). During mechanotransduction the cytoskeleton is deformed, which moves organelles and proteins, deforms the nucleus, and activates ion channels and G-protein receptors; in addition, second messengers are activated following the activation of a mechanoreceptor (30, 31). Mechanotransduction ends with the expression of genes and synthesis of proteins such as the receptor activator of nuclear factor kappa-B ligand (RANKL), sclerostin, osteopontin, and fibroblast growth factor 23, among others relevant for bone homeostasis (30, 33).

The masticatory apparatus produces loads of variable magnitude and high frequency on the teeth and jaws. Unlike in the appendicular skeleton, the loads cause complex patterns of bone deformation during normal function. These cause bone modeling and remodeling, which ultimately shapes the adult form of the jaw to a mechanically fit morphology. These loads are produced directly by tension in the entheses, but perhaps more markedly, by microdeformation of the entire structure as a result of the different force vectors acting on it. During the power stroke of mastication, maximal muscle activity and bone strain occur. Forces acting on the jaw during the power stroke can be represented in a simplified manner using lever mechanics, where the TMJ acts as the fulcrum, the distance of muscle insertion to the TMJ is the force arm, and the biting force is the resistance arm. The more anterior the biting point, the lower the resulting biting force, and vice versa. In a frontal plane, a more laterally placed biting point (e.g., at the posterior teeth of animals with wide palates like humans) is close to the TMJ, reducing the length

of the resistance arm and increasing bite force. The logical conclusion is that biting in posterior teeth is more efficient in terms of the use of muscle force. A more detailed review on the mechanics of biting in humans can be found in Hylander (34) and Lieberman (35). In this simplified model, not only the biting point and the entheses (at the cranium and mandible) are loaded, but also the TMJ surfaces. The applied muscle force magnitude decomposes at the biting point and the TMJ. Thus, if a large muscle force is generated during contraction, a large bite force reduces the reaction force at the TMJ. The resulting forces produced during biting cause the deformation of the jaw (**Figure 3**). Due to its simpler anatomy compared to the maxilla, the mandible has undergone most of the studies in this regard. Using experimental and theoretical approaches in humans and non-human primates, it has been shown that the mandible deforms in three main patterns: bending of the sagittal plane, transversal bending (also called “wishboning”), and twisting of the corpus and symphysis (37–40) (**Figure 3**). Studies by Daegling (37) and Fukase (41) analyzing the morphology of the mandible in macaques and humans, respectively, concluded that a thick cortical bone is located in the anterior part of the mandible and towards the posterior end of the corpus, precisely where strains during biting are the largest.

The study of the primate cranium has presented a comparable level of evidence regarding the impact of biting forces on bone strain and, thus, morphology. Bromage found that the orientation of collagen fibers in the circumorbital region of macaques follows the directions of strains produced on it during biting (42). These strains,

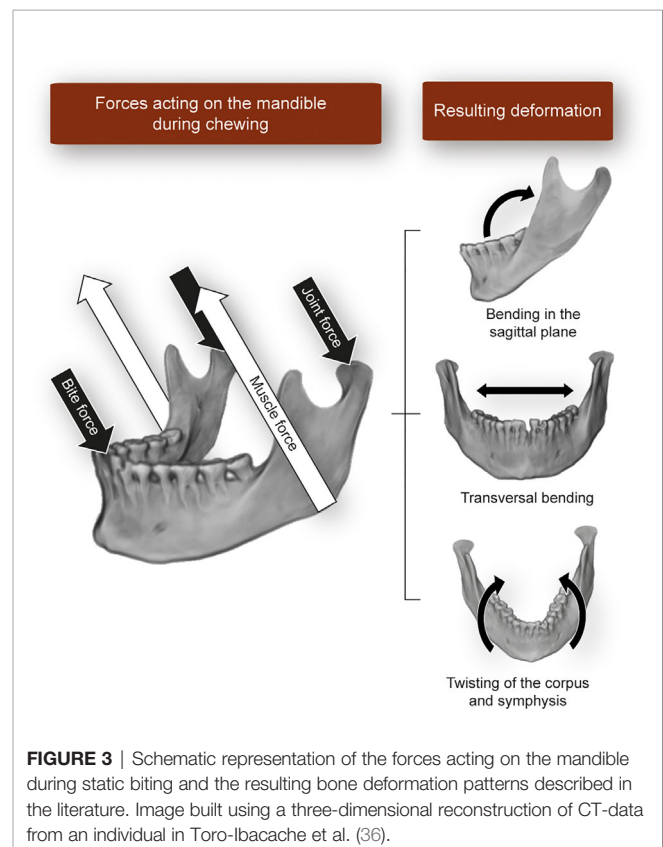


FIGURE 3 | Schematic representation of the forces acting on the mandible during static biting and the resulting bone deformation patterns described in the literature. Image built using a three-dimensional reconstruction of CT-data from an individual in Toro-Ibacache et al. (36).

however, although enough to have an impact at the tissue level, would not be the cause of presence of the supraorbital torus in these animals (43). In a series of experimental and observational studies, Toro-Ibacache et al. showed that during incisor and molar biting in humans, the most strained areas of the face are the alveolar process in relation to the loaded tooth and the frontal and zygomatic processes of the maxilla (44–46). These areas at the same time are formed by dense bone that forms the cranial buttresses and also show evidence of bone deposition (47). The deformation pattern in the human cranium does not vary much from that of non-human primates, consisting of a ventral bending of the anterior part of the maxilla during incisor biting (45, 48), and compression of the lateral aspect of the orbit during molar biting (45, 49).

Considering the evidence above, it is then logical to assume that a modification of masticatory forces also affects skull form. Experimental work in animal models has shown that the impairment of masticatory muscle activity and/or softening food consistency leads to a reduction in the thickness of the trabecular bone of the condylar process (50, 51), to a reorganization of it (51, 52), and to a gracilization in the form of the entire skull (53, 54). Observational studies in humans agree with these results. Raphael et al. (55) showed in women with TMJ disorders that those who had received intramuscular injections of botulinum toxin had a decreased bone density of the condylar process in compared to women who did not receive the injections. Overloading of the TMJ could also lead to degeneration of the joint components (56, 57). Egli et al. found in people affected by Duchenne muscular dystrophy that they progressively developed malocclusions, which are associated with lowering bite forces and a detriment of the masticatory function (58). Moreover, it has been proposed that the diet of the modern, urban populations, based mainly on highly extraorally processed food items, is the cause of a reduction in jaw size that results in dental malocclusions in modern humans which are not found in their ancestors (59–61). In addition, dental malocclusions reduce masticatory efficiency (62), and altered maxillomandibular relationships are at the same time associated to broad ranges of craniofacial shape variation (36, 63, 64).

From a developmental perspective, an optimal masticatory function should act by canalizing craniofacial form. However, this does not seem to be the rule in modern humans. Although it is possible to find a relationship between the intensity of masticatory activity and the shape of the craniofacial skeleton, this seems relatively modest, increasing only when functional limits are reached, i.e. when either very high/low/infrequent force magnitudes or altered force vectors are produced. In this regard, Toro-Ibacache et al. found that modifying the patterns of masticatory muscle activity (i.e. the relative force produced by each jaw-closing muscle during biting) changes the peak strain magnitudes, but not where these are located; only large, asymmetric modifications were able to change the location of TMJ peak strains from the balancing to the working side (45). Moreover, the same author described a weak covariation between masticatory muscle force and craniofacial shape in humans (46) and found differences in mandibular and cranial shape only among groups of individuals with marked differences in diet consistency/dental occlusion pattern

(36, 63). Shape covariation between the upper and lower jaws/dental arches is also lower in humans when compared with other animals (65), which has been associated with the comparatively lower mechanical and kinetic constraints underwent by humans during the normal masticatory function. Conversely, stronger covariation has been found in individuals with malocclusions when compared with those with normal occlusion (64, 66). Taken together, these antecedents support the idea that in humans, there has been a reduction in the constraining role of the masticatory function on the shape of the craniofacial skeleton. This means that under physiological conditions that do not involve intense nor too low masticatory forces, the human cranium displays a broad range of morphologies, which may be the result of other, non-mechanical factors. However, outside these functional limits, there are morphological consequences on craniofacial bones, as seen in the aforementioned studies with congenital and induced muscle paralysis and dental malocclusions. How this can be of use in the clinical context has been in part explored; changes in how the musculoskeletal system works is the basis of orthopedics and other related disciplines, such as orthodontics and management of TMJ disorders. However, achieving predictable, long-term results is sometimes challenging. For example, some malocclusions relapse after the end of orthodontic treatment, and some individuals do not respond to the orthopedic management of TMJ disorders. At the same time, the use of extreme functional settings or the use of large external forces to induce bone changes can also cause tissue damage. Thus, how to achieve a fine-tuning of the relationship between forces and bone (and articular tissues) morphology is yet to be understood.

In conclusion, chewing generates forces that cause the deformation of the skeleton. This deformation is sensed at the cellular level, eliciting a response that can result in bone resorption or deposition. These processes modify the shape of the loaded bone, turning it into a structure able to withstand the new loading scenario. This relationship, however, is not always linear. In humans, whose masticatory activity is less intense compared to that of other mammals, the shape of the craniofacial skeleton is remarkably variable, and it does not necessarily correlate to masticatory function parameters. However, under extreme functional situations, the form of the jaws is more prone to reflect the loading scenario. Controlling this non-linear relationship between form and function could be key in achieving predictable, long-term results in clinical situations where functional or externally applied forces are the therapeutic tools.

MASTICATORY MUSCLES AND BONES AS SECRETORY TISSUES. MUSCLE-BONE INTERACTION THROUGH SIGNALING MOLECULES

Muscle-Bone Crosstalk; Looking Beyond Mechanics

The relationship between muscles and bones in health and disease has been mainly considered as a mechanical process in which bone provides an attachment site for muscles and muscles

apply load to bone (67). It is known that bone adjusts its mass and architecture to changes in mechanical load, so it is strongly influenced by muscle contraction (68). In recent years, the idea has emerged that beyond this mechanical coupling of muscle and bones, there is a biochemical crosstalk through secreted molecules (11). In effect, both muscle and bone produce factors that circulate and act on distant tissues, the classical definition of an endocrine signal. Therefore, molecular communication with its adjacent tissue is even more likely to occur. Understanding this apparent biochemical coupling between muscles and bones is an exciting new avenue of research (2, 3, 6, 69). Muscles and bones have been recently defined as endocrine organs, secreting “myokines” and “osteokines,” respectively. These molecules are secreted after a wide range of stimuli and run autocrine, paracrine, and endocrine effects in several tissues. A recent review by Kirk et al. summarizes the current knowledge about molecules involved in musculoskeletal communication, including not only myokines and osteokines, but also adipokines (12). The list of currently defined myokines includes myostatin, interleukin (IL)-5,6,7,8,15, brain-derived neurotrophic factor (BDNF), Irisin, Insulin-Like Growth Factor (IGF), β -aminoisobutyric acid (BAIBA), matrix metalloproteinase-2, and Fibroblast Growth Factor (FGF)-2, which mediate the crosstalk between skeletal muscles and adipose tissues, blood vessels, central nervous system, and/or bone (3, 6, 70–72). Muscle-derived exosomes and miRNAs have been found in the circulation and influenced by exercise and disease, but their paracrine/endocrine role on other tissues has been not well-established (73, 74). Actually, efforts are directed towards muscle secretome elucidation (75, 76). Likewise, bone cells, which historically have been considered a target of the endocrine system, have been described in recent years as secretory entities of signaling molecules for controlling local or long-distance processes (77–79). Molecules suggested as osteokines include Osteocalcin (80), Sclerostin (81), Prostaglandin-E2 (PGE2) (81), Fibroblast Growth Factor 23 (FGF-23) (82), Transforming Growth Factor β (TGF- β) (83), RANKL (84, 85), and Wnt3a (81, 86).

The intimate muscle-bone relation is strongly evidenced by the fact that in open fractures, if muscle injury is also extensive, or if muscle atrophy develops, healing of the fracture is significantly impaired (11, 87, 88). In contrast, when the fracture area is covered with muscle flaps, even without tendon attachment, bone repair is significantly improved (88). This reinforces the communication between muscles and bones through soluble molecules, complementary to signaling by mechanical loading. In a mouse model of deep penetrating bone fracture and muscle injury, the exogenous administration of recombinant myostatin significantly reduced bone callus formation, while increasing fibrous tissue in skeletal muscle (87). Furthermore, assays using conditioned media coming from C2C12 cultured myotubes demonstrated that skeletal muscle-secreted factors protect the osteocytes against apoptosis evoked by glucocorticoids, by activating the β -catenin pathway (89). In the opposite way, conditioned media derived from osteocytes evokes calcium transients and myogenesis of a C2C12 cell line,

mimicked by the bone-released factor prostaglandin E2 (PGE2) (81).

Biochemical Muscle-Bone Crosstalk in the Masticatory System—From *In Vitro* to Preclinical Evidence

As previously described, the muscle-bone relationship in the masticatory system has been mostly studied from a biomechanical perspective. However, differentiating the mechanical component and the biochemical signaling by secreted molecules is not straightforward. Nowadays, there are no studies available that address biochemical crosstalk between muscles and bones in the masticatory system. However, several molecules described as myokines or osteokines in the musculoskeletal system of the trunk and limbs have been reported acting in the masticatory region, allowing to propose their putative role in bone-muscle communication.

A common criticism of the idea of biochemical communication between muscles and bones is that the molecules released from one of them must pass multiple tissue barriers to move from one tissue to another. The presence of physical barriers such as endomysium, perimysium, and epimysium in muscle and periosteum in bone is always mentioned. However, it has been demonstrated the presence of vessels coming from muscle in bone, in direct relation to osteocytes (3), which would allow a rapid endocrine effect between them. In particular, the injection of bone marrow mononuclear cells into rat masseter muscle has been shown to help repair bone after mid-palate expansion procedures (90). Therefore, if cell migration between the masseter and the palate occurs, communication *via* molecules is highly probable.

Next, we list several molecules well-described as muscle-bone interactors in the trunk and limbs and analyze the background suggesting their involvement in the masticatory apparatus.

Myostatin

Myostatin (GDF-8) is a member of the TGF-superfamily. It is released by muscle cells and acts as an autocrine negative regulator of muscle mass (91). An increase in myostatin levels is related to conditions of skeletal muscle injury, disuse, or sarcopenia (92, 93), and limits the bone formation/resorption index (94). In contrast, reduction of myostatin expression by using genetic approaches or pharmacological inhibitors highly increases skeletal muscle mass, bone formation, and bone regeneration (95–98). The effect of myostatin on bone remodeling has historically been attributed to its direct effect on muscles and their biomechanical role on the skeleton. However, it is currently known that myostatin has a direct impact on bone cells, such as the acceleration of osteoclasts formation evoked by RANKL (99) and the inhibition of osteoblasts differentiation by controlling the content of the exosomes derived from osteocytes (74). This is why myostatin has emerged as one of the candidates in muscle-bone crosstalk. Knockout mice lacking myostatin, called “mighty mice,” have higher morphologic dimensions of the mandibular condylar process, corpus, and symphysis (100). Moreover, they have

increased mineralization at the corpus (101), as well as in the condylar subchondral bone and mandible neck (102). Myostatin-deficient mice have longer and “rocker-shaped” mandibles, with shorter and wider crania compared to controls (103).

Insulin-Like Growth Factor 1

IGF-1 is mainly produced in the liver, but it is also expressed in skeletal muscle and highly increases after exercise (104). In addition, IGF-1 is the main growth factor in the bone matrix (105); it is expressed by osteocytes and upregulated in response to mechanical loading (106). It is also well known that IGF-1 is a relevant anabolic factor in muscle and bone and has been proposed as a potential muscle-bone crosstalk molecule (107). Several functional changes in skeletal muscle, such as unloading, overloading, or denervation, modify the expression of proteins of the IGF-1 signaling pathway, which relates to changes in muscle fiber type (104, 108). When rats are fed with a soft diet immediately after weaning, the mRNA levels for IGF-1, IGF-2, IGF receptor (IGFR) 2, IGF binding proteins (IGFBP) four and six in masseter muscle are reduced (109). Furthermore, in the masseter muscles of mice feeding a soft diet after weaning, there is a reduction in IGF-1, IGF-2, and IGFBP5 expression (110). In parallel, murine models of masticatory reduction through soft diet consumption show alterations in morphology and molecular markers in masseter muscle and mandible (**Table 1, Figure 4**). A decrease in masseter muscle activity has been reported (114, 115). Furthermore, a reduction in masseter muscle mass and fibers diameter have been demonstrated in rats (110, 117) and mice (111, 118, 124) after soft-diet consumption. MyHCIIb (fast glycolytic) expression levels are increased in a 580%, and MyHCIIa (fast-oxidative) mRNA levels are reduced in a 70% in rats fed with a soft diet (109), consistent with observed in all muscle disuse models. It has been established that the increased expression of genes related to hypercatabolism works as a molecular marker of muscle atrophy. Of these, the most studied are the ubiquitin ligases muscle RING finger 1 (Murf1) and muscle atrophy F-box (MAFbx or Atrogin), relevant components of the ATP-dependent ubiquitin-proteasome pathway (130). We have recently reported an increase in atrophy markers Atrogin and Murf in the masseter muscle of adult mice, as early as 2 days after start eating a soft-diet (4- and 20-fold increase, respectively). After 30 days of consuming the soft diet, the levels of Atrogin and Murf expression were increased by 35- and 150-fold, respectively, compared with mice eating regular pellets (118, 124). In mice and rats, the soft-diet consumption modifies both mandible and condylar morphology, by reducing mandible ramus height and robustness and condylar width (54, 57, 113, 115, 117). A reduction in bone volume fraction of the mandibular condyle and masseter muscle attachment sites have been observed, as well as a reduction in articular cartilage thickness (112, 115, 116, 131).

On the other hand, it has been recently demonstrated that a mouse model of increased mastication by hard-diet consumption shows raised levels of IGF-1 and a decrease in sclerostin expression in osteocytes. In this model, an increase in bone formation at the enthesis of the masseter muscle was observed (132).

Then, the IGF-1 signaling either decreases or increases after hypo- or hyperfunction of the masticatory system, respectively. IGF-1 is expressed by both the masseter muscle fibers and mandibular osteocytes, which makes it a strong candidate for mediating muscle-bone crosstalk in this territory (**Figure 4**).

Interleukin-6 (IL-6)

IL-6 family of cytokines comprises ten members, such as IL-6, IL-11, leukemia inhibitor factor (LIF), and oncostatin M (OSM). IL-6 synthesis and release have been historically related to immune cells, for mediating B- and T-cells development with a pro-inflammatory role (133). However, nowadays, it is known that there are several sources of IL-6, such as epithelial cells, fibroblasts, osteoblasts, synovial cells, cancer cells, and skeletal muscle fibers, leading to either pro- or anti-inflammatory events (134, 135). IL-6 is a 26 kDa glycopeptide that binds a specific IL-6 receptor (IL-6R, either membrane-associated or soluble (sIL-6R)) (134). IL-6 was the first molecule defined as “myokine” when Pedersen and colleagues demonstrated a link between IL-6 and exercise (136). IL-6 is a myokine released from skeletal muscles during exercise, with a plethora of physiological effects in autocrine, paracrine and endocrine ways (135, 137, 138). The magnitude of the plasma-IL-6 increase depends on the exercise duration, intensity, and muscle mass involved. Plasma levels of IL-6 increase up to 100-fold after exercise, without any sign of muscle damage, nor an associated inflammatory response. Furthermore, the concentration of IL-6 in the interstice of the exercised muscles, measured by microdialysis, is up to 100 times higher than the plasma concentration, suggesting a possible local role (139).

IL-6, in an autocrine-loop, improves insulin sensitivity in skeletal muscle cells for increasing glucose uptake (140, 141). In addition, IL-6 produced in response to strenuous and prolonged exercises increases satellite cells proliferation, leading to regeneration of damaged muscle myofibers and hypertrophy (142, 143). However, a pivotal role of IL-6 in skeletal muscle has been proposed, being related to both skeletal muscle renewal and wasting. Under some pathological conditions, IL-6 leads to muscular atrophy. During cachexia [muscle wasting associated with underlying chronic diseases such as cancer, chronic heart failure, and chronic kidney disease (144)] it has been proposed that increased IL-6 plasma levels mediate proteolysis at the skeletal muscle in patients. In a mice model of cancer-evoked cachexia, activation of the IL-6 signaling pathway has been demonstrated in skeletal muscles, increasing both phosphorylation and nuclear localization of STAT3 (145). Moreover, pharmacological or molecular blockade of the IL-6/STAT3 signaling pathway prevents tumor-induced muscle atrophy in mice (146). Either IL-6 infusion in wild type mice or the transgenic mouse models for IL-6 overexpression, evoke muscle atrophy by reducing protein synthesis and promoting catabolic pathways (147–149). Several pharmacological therapies targeting the IL-6 signaling pathway, mainly by using anti-IL-6 or anti-IL-6R antibodies or blockers, have had preventive effects in cancer-evoked cachexia (150, 151), restored muscle function

TABLE 1 | Summary of adaptations in the masseter muscle and mandible in murine models of masticatory hypofunction.**A. Soft diet consumption**

Reference	Effect on masseter	Effect on mandible	Myokines/Osteokines
Vilman et al (111).	↓ Fibers diameter		
Saito et al (109).	↓ Type IIA fibers ↑ Type IIB and type IIX fibers		↓ IGF-1 and IGF-2 expression
Urushiyama et al (110).	↓ Muscle mass ↓ Fibers diameter		↓ IGF-2 expression
Tanaka et al (112).		↓ Degree of mineralization in the trabecular bone of the mandibular condylar process	
Odman et al (113).		↓ Posterior height of the mandibular corpus and the height of the angular process	
Kawai et al (114).	↓ Muscle activity ↓ Type IIA fibers ↑ Type IIB fibers ↓ Cross-sectional area of type IIB and IIX fibers		
Hichijo et al (115).	↓ Muscle activity	↓ Condylar articular cartilage thickness ↓ Mandibular ramus height	
Hichijo et al (116).		↓ BV/TV of the mandibular condyle and the masseter attachment sites	
Spasov et al (54).	↓ Muscle mass	Horizontally-oriented coronoid process and smaller mandibular condylar process articular surface	
Shi et al (117).	↓ Muscle mass	↓ Tb.Th and Tb.N of the mandibular condylar process ↓ Condylar articular cartilage thickness	
Rojas-Beato et al (118).	↓ Muscle mass ↑ Atrophy markers (Atrogin/MuRF)		↑ IL-6 expression and synthesis

B. Masseter muscle intervention with BoNTA

Reference	Animal (age)	Effect on masseter	Effect on mandible	Myokines/Osteokines
Tsai et al (119).	Male rats (4 wks)	↓ Muscle mass	↓ Total mandibular length	
Tsai et al (120).	Male rats (8 wks)	↓ Muscle mass	↓ Mandible dimensions, BMD, Cortical Bone Thickness and Trabecular Bone Area to Total Bone Surface	
Tsai et al (121).	Male rats (10 wks)	↓ Muscle activity (transient, up to 4 wks)		
Kün-Darbois et al (122).	Male rats (18 wks)		↓ B.Ar/T.Ar of the alveolar and the mandibular condylar process	
Dutra et al (123).	Female mice (5 wks)		↓ BV/TV, Tb.Th, width and tissue density of the mandibular condylar process ↑ Apoptosis and ↓ proliferation in both subchondral bone and articular cartilage of the mandibular condylar process	
Shi et al (117).	Female rats (5 wks)	↓ Muscle mass	↓ BV/TV, Tb.Th, Tb.N, width and length of the mandibular condylar process ↓ Condylar articular cartilage thickness ↑ Tb.Sp of the mandibular condylar process	
Balanta-Melo et al (50).	Male mice (8 wks)	↓ Muscle mass ↓ Fibers diameter ↑ Atrophy markers (Atrogin/MuRF) and Myogenin mRNA expression	↓ B.Ar/T.Ar and Tb.Th of the mandibular condyle	↑ RANKL mRNA expression in the mandibular condylar process
Balanta-Melo 2018b (124).	Male mice (8 wks)			↑ IL-6 expression
Balanta-Melo et al (51).	Male mice (8 wks)	↓ Muscle mass	↓ BV/TV, Tb.Th and shape changes of the mandibular condylar process	
Balanta-Melo et al (125).	Male mice (8 wks)		↓ BV/TV and Tb.Th in the middle portion of the mandibular condylar process ↓ BMD of the mandibular condylar process	

(Continued)

TABLE 1 | Continued

B. Masseter muscle intervention with BoNTA

Reference	Animal (age)	Effect on masseter	Effect on mandible	Myokines/Osteokines
Dutra and Yadav (126).	Female mice (6 wks)		↓ BV/TV and articular cartilage thickness of the mandibular condylar process (not transient, up to 8 wks) ↑ Apoptosis in articular cartilage of the mandibular condylar process	
Vásquez et al (127).	Male mice (8 wks)	↓ Muscle mass ↓ Fibers diameter ↑ Atrophy markers (Atrogin/MuRF) and Myogenin mRNA expression		↑ IL-6 expression

Evidence regarding morphological and biochemical changes in the masseter muscle and/or the mandible in murine models of soft-diet consumption (A) or masseter paralysis evoked by BoNTA injection (B) are listed. Changes in expression of molecules classically described as myokines or osteokines are highlighted.

wks, weeks; mo, months; BV/TV, bone volume fraction; Tb.Th, trabecular thickness; Tb.N, trabecular number; Tb.Sp, trabecular space; B.Ar/T.Ar, bone area per tissue area; BMD, bone mineral density; IGF, Insulin Growth Factor.

in a mouse model of muscular dystrophy (152), and ameliorated muscle atrophy induced by tail suspension in mice (153).

In bone physiology, IL-6 also shows a dual role. IL-6 influences both osteoclasts and osteoblasts differentiation through contradictory mechanisms. It sustains bone formation, but it also drives bone loss in various osteolytic pathologies (134). Osteoblasts express low levels of IL-6R; therefore, sIL6R is required for maximum IL-6 effects. IL-6 family members increase osteoblast markers expression and matrix mineralization nodules, all mediated through the STAT3 activation (154, 155). In contrast, IL-6 type cytokines (IL-6, IL-11, LIF, and OSM) inhibit bone formation *in vitro*, with potent pro-apoptotic effects, all mediated by PKC δ and ERK1/2 pathways. IL-6 clearly stimulates the osteoblastic production of RANKL and PGE2, both involved in differentiation and activation of osteoclasts; this has been described as the critical event leading to pro-resorption action evoked by IL-6, and is mediated by STAT3 signaling (156–158). In contrast, other research groups have described that IL-6 inhibits osteoclast formation and bone resorption in pre-osteoclasts primary cultures or cell lines (159, 160). By using genetic strategies, it has been demonstrated that the IL-6 deficient mice have increased bone formation, whereas IL-6 overexpression showed a decrease in osteoblasts and osteoid, but also in osteoclasts and bone resorption. Then, it has been proposed that IL-6 could contribute to bone turnover *in vivo* (134). An essential role of IL-6 in osteoarticular pathologies has been established. IL6^{-/-} mice are protected from joint inflammation and destruction in a mouse model of arthritis, and from bone loss evoked by estrogen depletion. Inhibition of IL-6R with the drug Tocilizumab improves the clinical response and suppresses the biochemical markers of osteoclast-mediated bone destruction in patients with rheumatoid arthritis (161, 162). In contrast, IL-6 stimulates fracture healing and bone resistance (163). All of this data suggests that IL-6 can lead to bone formation or resorption, depending on its pathophysiological context. The role of IL-6 in bone turnover is then indisputable; however, it is not easy to directly associate it to a specific effect, due to it appears as a double-edged sword.

At the masticatory system, the role of IL-6 in muscle homeostasis has been demonstrated. An increase in masticatory activity in a mice model of restrained/gnawing raises IL-6 mRNA

and protein levels in the masseter muscle. The increase in IL-6 production and release is dependent on a previous rise in IL1 α - β , and then promotes the glucose uptake in the masseter muscle. Authors suggest that a highly coordinated loop happens, where masseter muscle activity releases some myokine that “calls to” IL-1 positive cells around blood vessels; then, IL-1 evokes IL6 expression and release from masseter muscle, improving the glucose homeostasis and muscle performance and preventing muscle fatigability (164). Ono et al. also reported an increase in IL-6 in rat masseter muscle when stimulated electrically *in situ* (100 Hz for 200 ms, 800 ms between stimulations, 10–30–60 min total stimulation time) (165). In masseter muscles isolated after the electrical stimulation protocol, they observed a 3-fold increase in IL-6 mRNA levels, with no changes in IL-1 β mRNA levels. These authors propose that considering that IL-1 β is a well-known pro-inflammatory cytokine, the increase in IL-6 in masseter muscle would not respond to inflammatory infiltration, but a local synthesis in muscle fibers. When carrageenan was directly injected in rat masseter muscles, which is an inductor of local acute inflammation, both IL-6 and IL-1 β mRNA levels increased. When the electrical stimulation was performed after muscle contraction blockade with dantrolene, the increase in IL-6 mRNA was blocked, suggesting that muscle contraction is relevant to evoke IL-6 expression. The authors reinforce the idea that masseter muscle contraction stimulates IL-6 expression, independent on inflammation processes (165).

Some of us have recently demonstrated that electrical stimulation of isolated masseter muscle *in vitro* (20 Hz, 270 pulses, 0.3 ms each), resembling motoneuron stimulation, evokes an increase in IL-6 mRNA expression, as well as IL-6 protein synthesis and release (118). Thus, masseter muscle synthesizes and releases IL-6 during activity. However, as previously described, IL-6 has a pivotal role, as it has either anabolic or catabolic effects in the musculoskeletal system. We have recently demonstrated basal increases in IL-6 production and secretion in mouse models of masseter muscle atrophy. In the previously described model of adult mice consuming a soft diet, a 2-fold increase in IL-6 mRNA was observed in the masseter muscle, as early as 2 days after soft-feeding. Two weeks later, resting levels of IL-6 mRNA and protein increased 12-fold and 2-fold,

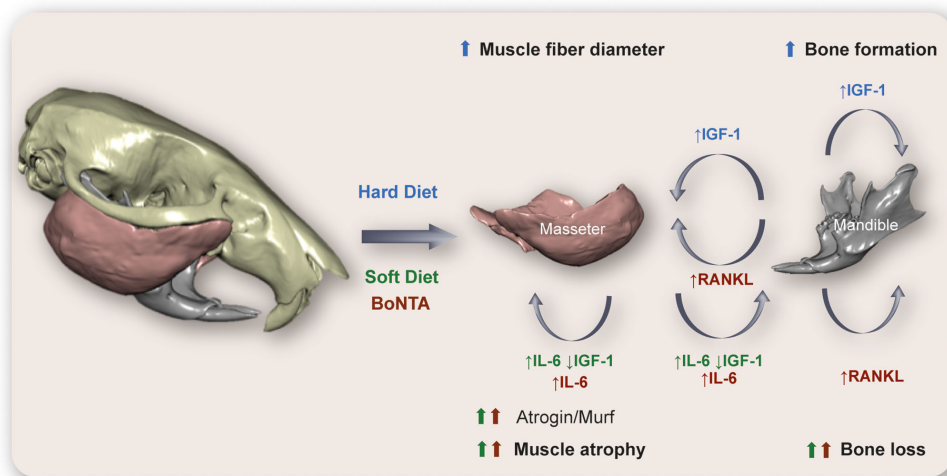


FIGURE 4 | Hypothetical model of cross-communication between muscles and bones at the murine masticatory system. Here we relate in a graphic outline the main changes described in rat/mouse models subjected to a reduction (Soft Diet) or an increase (Hard Diet) in diet consistency, as well as those described after paralysis of the masseter muscle by injection of botulinum toxin type A (BoNTA). In the hypofunctional models (Soft-diet, BoNTA), an increase in interleukin-6 (IL-6) expression and release, as well as a reduction in insulin-like growth factor 1 (IGF-1) in masseter muscle could mediate the muscle atrophy and bone loss, together with the reduced mechanical stimulation. In addition, the increased levels of RANK ligand (RANKL) in mandibular condyle after BoNTA injection could mediate both the osteoclastogenesis leading to bone loss and the muscle atrophy observed. On the other hand, consumption of a hard diet evokes an increase in IGF-1 expression in mandibular osteocytes, which could act as an anabolic factor in muscle and bone, leading to increased muscle mass and bone formation described in this model. *Technical information:* 3D rendering of murine skull, mandible, and masseter muscles corresponds to PTA contrast-enhanced high-resolution microCT data taken at the Max Planck Institute for Evolutionary Anthropology (Leipzig, Germany). Skull and mandible segmented with Avizo 9.2 (Thermo Scientific™, USA); masseter muscles segmented with the Biomedical Segmentation App (Biomedisa) (128). 3D rendering of hard and soft tissues performed with DRAGONFLY 4.1 (Object Research Systems, Canada). Image built using data from an individual in Balanta-Melo et al. (129).

respectively, compared with mice eating regular pellets (118, 124, 166, 167). Thus, IL-6 is highly overexpressed in a mouse model of masseter muscle atrophy by underuse. We also developed a mouse model of unilateral injection of Botulinum Toxin type A (BoNTA) in the masseter muscle, specifically to address putative alterations in the associated bone (mandibular condylar process) evoked by muscle paralysis. This is highly relevant in dentistry because BoNTA is used as an off-label therapeutic tool for the management of several TMDs (125, 168). In adult mice, we injected the right masseter with 0.2U/10 μ l BoNTA, and the left masseter with saline solution. As early as 7 days after the intervention, an increase in molecular markers of muscle atrophy (Atrogin and Murf1) was observed, with histological signs of atrophy after 14 d (50, 127, 167, 169). A reduction in masseter muscle activity, muscle mass and fibers diameter have also been observed after BoNTA injection in masseter muscles of rats and mice (50, 117, 119–121, 170). Interestingly, we demonstrated an increase in IL-6 mRNA levels in muscles as early as 2 days after BoNTA injection (50, 127, 167, 169). Just 2 days after BoNTA injection in masseter muscle, a significant increase in a molecular marker of bone resorption (RANKL) was also observed in the ipsilateral mandibular condylar process. Two weeks after BoNTA injection, qualitative bone loss was detected in the right mandibular condyle (BoNTA-side), with highly impaired bone parameters detected by microcomputed tomography (μ CT). In contrast, contralateral saline-injected masseter muscle and its

adjacent condylar process remained as healthy as that in control untreated mice (51, 125). Several other authors have observed severe damages in mandibular morphology and microstructure after BoNTA injection in masseter muscles of murine, with high impact in the articular cartilage and subchondral bone (117, 119, 120, 122, 123, 126, 170). Then, BoNTA injection evokes both muscle atrophy and bone loss at the mandibular condylar process (as summarized in **Table 1** and **Figure 4**). We are currently studying the putative role of IL-6 myokine in both muscle atrophy and bone loss evoked by BoNTA injection. Taken together, these results support the idea that IL-6 is released from masseter muscle either during activity and during paralysis/atrophy, reinforcing its dual role in physiology and pathology of the musculoskeletal system.

Interestingly, IL-6 level at the synovial fluid has been widely associated with TMD (171). IL-6 level is undetectable in synovial fluid from healthy controls (172, 173), but it is increased in that from patients with chronic TMD (174). Moreover, in TMD patients, IL-6 level at the synovial fluid is significantly higher in the joints with bony changes in the condylar processes than when these are not affected (175). Then, IL-6 could be associated with bone remodeling during TMDs. It has always been considered that, in TMD, the IL-6 at the synovial fluid comes from synoviocytes, chondrocytes, or inflammatory cells as the main source. But, depending on the TMD-type, masticatory muscles should be a new source to keep in mind, considering its great contribution to the biomass of the system.

MUSCLE-BONE CROSSTALK AT THE MASTICATORY SYSTEM IN HEALTH AND DISEASE—MOVING TO CLINICAL EVIDENCE

In the present section, we discuss clinical data suggesting a biochemical communication between muscle and bone at the masticatory system. To this end, we reviewed the evidence on several muscular pathologies or clinical interventions leading to bone remodeling, as well as bone pathologies leading to muscle remodeling. We focus on the presence of molecules described in the previous sections as myokines or osteokines.

Muscular Conditions With Potential Bone Implications in the Masticatory System

During prolonged tooth clenching, the masseter muscle exhibits a lower recovery capacity for tissue reoxygenation (176, 177), which favors the development of skeletal muscle inflammation. Britto et al. have demonstrated that hypoxia-evoked inflammation leads to skeletal muscle hypertrophy through the IL-6/STAT3 pathway in human legs (178). These results may explain the potential mechanism behind the masseter hypertrophy in patients with parafunctional masticatory activity (179, 180). The expression of IL-6 is also increased during other inflammatory conditions of the masticatory system, such as myofascial pain (181), which is part of the group of craniofacial musculoskeletal diseases known as TMDs (182, 183). Increased levels of IL-6 have been reported in masseter muscles of adult women with myofascial pain compared to healthy controls, levels that are even higher during tooth clenching (184). Considering the dual role of IL-6 in bone formation and resorption, is highly possible that muscle-derived IL-6 mediate mandibular bone remodeling observed in TMDs.

Masseter hypertrophy is often associated with parafunctional activities such as bruxism (179), but it also may have an idiopathic background (i.e., benign masseter hypertrophy) (185). In both cases, the aesthetic impairment caused by the increase of masseter volume mass can be solved either using surgical techniques or by inducing muscle atrophy with botulinum toxin type A (BoNTA) (186, 187). The BoNTA is a neurotoxin that blocks the release of neurotransmitters in the skeletal muscle, leading to hypofunction and atrophy (188). Therefore, BoNTA-induced atrophy is effective in reducing the thickness of the masseter muscle (189). This desired aesthetic outcome, however, may involve deleterious consequences on mandibular bone homeostasis (51, 125). In patients that underwent repetitive BoNTA injections to treat masseter hypertrophy, a reduction of bone volume at the mandibular angle was found after 6 months (190). Another study found bone loss in the anterior portion of the mandibular condylar process 1 year after a single injection of BoNTA in both the masseter and the temporalis muscles (191). Using a similar design, a retrospective study identified in adult women a cortical bone thinning in the mandibular condylar processes after two BoNTA injections within a 6-month interval (192). In this context, the

BoNTA intervention resulted in a more deleterious effect at the cortical bone of the mandibular condylar process of postmenopausal women, when compared with premenopausal women (192). In adult women with myofascial pain, a randomized clinical trial demonstrated a significant reduction of the volume of the mandibular condylar process at 3 months, after a high BoNTA dose injection in both the temporalis (25 U) and the masseter (75 U) muscles but not at lower doses (20 U and 50 U, respectively) (193). These results are consistent with a cohort study, which showed no bone loss at the mandibular condylar process in adult women with myofascial pain that underwent BoNTA interventions under 40 U in the masseter muscles when compared to match control population (194). These results support the hypothesis that masticatory muscle hypofunction negatively impacts mandibular bone homeostasis in humans, especially at the condylar process, when high doses of BoNTA are used. Based on our results in a mouse model, it is advisable to characterize how the negative effect of BoNTA-induced masseter atrophy on the mandibular bone occurs. Is it limited to a biomechanical interaction, or does it respond to alteration on the secretory activity of soluble factors from the injected muscles, such as IL-6? The answer to this question may help to develop strategies to avoid BoNTA's deleterious effect on the mandible.

Bone Conditions With Potential Muscle Implications in the Masticatory System

As mentioned above, the jaws undergo pathologies that are specific to them, but they are also affected by more general conditions such as bone loss during aging (195). Since bone also works as an endocrine organ (12), pathological conditions that affect the capacity of the mandibular bone to release osteokines could also affect muscle-bone molecular crosstalk. Here we analyze how mandible-changes could lead to masticatory muscles remodeling during aging, microgravity, and periodontal disease in humans.

In postmenopausal women, a lower mandibular bone density and higher plasma levels of osteocalcin were determined when compared with premenopausal women (195). These results found as a consequence of aging are consistent with those identified during space flight conditions (i.e., microgravity) (196). In adults of both sexes, the use of simulated microgravity promotes a reduction of bone mineral density in the mandibular bone and an increase in the plasma and salivary levels of osteocalcin (197). Interestingly, in an animal study under microgravity conditions, the masticatory muscles were not atrophied, in contrast with those from the hindlimbs (198). The fact that the activity of the masticatory muscles seems not to be affected by the lack of gravity may shed light on their structural and physiological differences to postcranial muscles.

Osteocalcin has been linked to muscle hypertrophy (12). In a mouse model of forceful mastication, an increase of osteoblasts positive for osteocalcin in the enthesis between the masseter and mandibular bone was observed (132). Even more, recently has been described that a muscle-bone axis comprising IL-6 released by muscles and osteocalcin released and processed by osteoblasts/osteoclasts is relevant to improve muscle

performance during exercise (80). It seems contradictory, then, to observe increased plasma levels of osteocalcin in older adults and hypogravity models, which present a clear decrease in muscle mass in the trunk and limbs. One possibility is that, since osteocalcin is regulating the levels of IL-6 secreted by the muscle, it may also promote the adverse catabolic effects of IL-6 on muscles and bones. Probably a fine-tuned muscle-bone axis is controlling anabolic or catabolic final effects, depending on myokines/osteokines concentrations, or modulated by additional microenvironment stimuli. It is still unknown how these molecular pathways differentially affect masticatory versus trunk and limbs musculoskeletal system. The existence of features that appear contradictory, such as bone loss with an increased osteocalcin production and a preserved muscle activity, presents an exciting opportunity to investigate the functional peculiarities of the musculoskeletal components of the masticatory apparatus.

In addition, while mandibular osteocytes are activated during high load masticatory activity (132), the aging process seems to affect their number only in the bones of the hindlimbs but not in those of the craniofacial skeleton, including the mandible (199, 200). *In vitro*, it has been shown that osteocytes also produce osteokines that impair skeletal muscle homeostasis (12, 201). One of these osteocyte-derived osteokines is sclerostin (202). Since masticatory function suppresses the release of sclerostin from mandibular osteocytes (132), a reduced masticatory function during aging increases the levels of this osteokine, which may impact the masticatory muscles negatively through a molecular (and not purely mechanical) mechanism.

The inflammatory periodontal disease that causes alveolar bone loss (i.e., periodontitis) increases the level of osteokines like osteocalcin in the gingival crevicular fluid (GCF) of postmenopausal women (203). This increase, however, was not found in the saliva or plasma of the periodontally ill patients (203). Moreover, there is a lack of correlation between the presence of systemic bone disease (osteopenia and osteoporosis) and osteocalcin levels in either salivary, plasma or GCF samples (203–205). Another recognized osteokine, sclerostin, is also increased in the GCF of periodontally ill patients (12, 206). In bone tissue, sclerostin is a negative regulator of bone mass through the inhibition of the Wnt signaling in the osteoblast lineage (206). The osteoblast population of the human mandible, however, exhibits a higher Wnt signaling response to external vibration when compared with osteoblast from the iliac bone (207). In adults with moderate to severe periodontitis, a significant increase of sclerostin in the GCF was determined when compared with healthy patients (208). In contrast, Wnt proteins levels in the GCF were not significantly different between periodontally ill and healthy patients but were increased in individual sampled sites (periodontally compromised) when compared with healthy sites (208). Taken together, the results of this clinical study suggest both sclerostin and Wnt proteins as a promising diagnostic tool for periodontitis (208). Since sclerostin has been presented as an osteokine with catabolic potential on muscle cells, these results allow us to hypothesize a molecular

(and not purely mechanical) link between periodontitis and the reduction of the masticatory muscle thickness that has been found in periodontally ill patients (209).

The osteocyte population is a crucial regulator of both sclerostin and RANKL local expression during active periodontal disease (210). The sclerostin and RANKL are negative bone mass regulators by inhibiting Wnt signaling and by inducing osteoclastogenesis, respectively (210–212). Specifically, the receptor of RANKL, RANK, is expressed in the skeletal muscle tissue (213) and a deleterious effect of RANKL on muscle homeostasis has been suggested (212, 214). Although periodontitis is known to increase the systemic inflammatory burden affecting, e.g., the cardiovascular system (215), it is reasonable to hypothesize that inflammatory diseases of the jaws can affect masticatory muscle homeostasis, as these are anatomically closer and linked through the vascular network.

CONCLUDING REMARKS AND FURTHER PERSPECTIVES

In this review, we summarized and discussed the available information regarding the muscle-bone interaction in the masticatory apparatus, with an emphasis in the molecular crosstalk between both tissues, an emerging research area that shows promising applications in clinics. The structures of the masticatory apparatus present biochemical, structural, and functional characteristics that make them physiologically very different from the musculoskeletal components of the trunk and limbs. The bones in the masticatory apparatus also have a high rate of remodeling, not only during development and postnatal growth but well into adulthood. In addition, an essential morphofunctional relationship between the muscles and bones has been described in this region.

To date, the approach to study the muscle-bone crosstalk in the masticatory apparatus has been mostly biomechanical. Here, we present the evidence suggesting that the communication between the jaws and masticatory muscles also occurs *via* secreted molecules, which opens a new field of research. Molecules defined as “myokines” (e.g., IGF-1 and IL-6) or “osteokines” (e.g., Osteocalcin, Sclerostin, RANKL) have been described as expressed in the masticatory apparatus. The levels of these mediators are altered both in animal models of use/disuse of the masticatory apparatus, as well as in pathophysiological conditions in humans. Due to the large biomass component provided by the masticatory muscles, it is highly probable that they contribute through myokines in the pathogenesis of temporomandibular disorders. Molecules such as IL-6, which have been reported elevated in the synovial fluid of individuals affected by TMDs, and have been essentially associated with chondrocytes or inflammatory cells, could well be derived from masticatory muscles. Likewise, the molecules that mediate bone resorption associated with periodontitis could cross-affect masticatory muscles and contribute to the loss in their volume.

It is already challenging to experimentally separate the biomechanical from the biochemical component in the musculoskeletal system, but even more so in the masticatory apparatus, which due to its structural characteristics makes it difficult to work with isolated cells. For example, the culture of isolated fibers is of common use to study limb muscles. It is, however, very complex in multipennate muscles such as the masseter, with fibers of very different lengths, orientations, and firmly attached to bone and tendons. To our knowledge, obtaining isolated masseter muscle fibers has been briefly described in only one article (216), but to date, no cellular or biochemical studies have been reported that use them *in vitro*. Likewise, obtaining bone precursors for *in vitro* cultures, which is easy from long bones such as the femur or the tibia, is operationally much more challenging in the mandible (217). It therefore remains a challenge to find experimental designs that allow for evaluating the biochemical muscle-bone crosstalk in the masticatory apparatus. Probably, genetic manipulation approaches, directed to proteins in specific cell types, will be relevant in this mission.

The understanding of how the cells of the masticatory apparatus (muscle, bone, cartilage, immune) communicate through molecules, both in health and disease, will contribute to the global understanding of how the masticatory apparatus remodels. More importantly, it will allow for having precise therapeutic targets, focused not only to alleviate the symptoms but to tackle some prevalent orofacial pathologies from their bases.

AUTHOR CONTRIBUTIONS

SB proposed the concept of the review. SB, JB-M, KK, and VT-I wrote and edited the manuscript. WV and CB contributed new

data for the topic discussion. SB, JB-M, and VT-I designed the figures. All authors contributed to the article and approved the submitted version.

FUNDING

This work was financed by Fondecyt-Chile Grant N°1201385 (SB, VT-I, KK, JB-M) and Universidad de Chile VID-Enlace Fondecyt 2019 Grant N° ENL29-19 (SB).

ACKNOWLEDGMENTS

We are thankful to Jean-Jaques Hublin from the Max Planck Institute for Evolutionary Anthropology for providing access to the microCT scanning facilities. We thank Andrea Eyquem from the Universidad de Chile for segmenting both the skull and the mandible data of a murine sample; Maximilian Bemmman, Edwin Dickinson, David Plotzki and Tina Kotteck from the Max Planck Weizmann Center for Integrative Archaeology and Anthropology (Max Planck Institute for Evolutionary Anthropology) for their assistance during the microCT scanning (DP), the enhanced-contrast protocol of the muscles (TK) and the segmentation of soft tissues from microCT data of a murine sample (MB and ED). We also thank to Object Research Systems (ORS, Canada) for providing the academic license of DRAGONFLY 4.1 software to the Digital Dentistry and Health Sciences Research Lab (School of Dentistry, Universidad del Valle), which was used for 3D rendering of the murine hypothetical model (skull, mandible, and masseter muscles).

REFERENCES

- Bajaj D, Allerton BM, Kirby JT, Miller F, Rowe DA, Pohlig RT, et al. Muscle volume is related to trabecular and cortical bone architecture in typically developing children. *Bone* (2015) 81:217–27. doi: 10.1016/j.bone.2015.07.014
- Laurent MR, Dubois V, Claessens F, Verschueren SM, Vanderschueren D, Gielen E, et al. Muscle-bone interactions: From experimental models to the clinic? A critical update. *Mol Cell Endocrinol* (2016) 432:14–36. doi: 10.1016/j.mce.2015.10.017
- Maurel DB, Jahn K, Lara-Castillo N. Muscle-Bone Crosstalk: Emerging Opportunities for Novel Therapeutic Approaches to Treat Musculoskeletal Pathologies. *Biomedicine* (2017) 5(62):1–18. doi: 10.3390/biomedicine5040062
- Novotny SA, Warren GL, Hamrick MW. Aging and the muscle-bone relationship. *Physiology (Bethesda)* (2015) 30:8–16. doi: 10.1152/physiol.00033.2014
- Sun Y, Kueh V, Liu Y, Tickner J, Yuan Y, Chen L, et al. MiR-214 is an important regulator of the musculoskeletal metabolism and disease. *J Cell Physiol* (2018) 234:231–45. doi: 10.1002/jcp.26856
- Brotto M, Bonewald L. Bone and muscle: Interactions beyond mechanical. *Bone* (2015) 80:109–14. doi: 10.1016/j.bone.2015.02.010
- Perrini S, Laviola L, Carreira MC, Cignarelli A, Natalicchio A, Giorgino F. The GH/IGF1 axis and signaling pathways in the muscle and bone: mechanisms underlying age-related skeletal muscle wasting and osteoporosis. *J Endocrinol* (2010) 205:201–10. doi: 10.1677/JOE-09-0431
- Thompson WR, Rubin CT, Rubin J. Mechanical regulation of signaling pathways in bone. *Gene* (2012) 503:179–93. doi: 10.1016/j.gene.2012.04.076
- Khosla S. Pathogenesis of age-related bone loss in humans. *J Gerontol A Biol Sci Med Sci* (2013) 68:1226–35. doi: 10.1093/gerona/gls163
- Mitchell WK, Williams J, Atherton P, Larvin M, Lund J, Narici M. Sarcopenia, dynapenia, and the impact of advancing age on human skeletal muscle size and strength; a quantitative review. *Front Physiol* (2012) 3:260. doi: 10.3389/fphys.2012.00260
- Brotto M, Johnson ML. Endocrine crosstalk between muscle and bone. *Curr Osteoporos Rep* (2014) 12:135–41. doi: 10.1007/s11914-014-0209-0
- Kirk B, Feehan J, Lombardi G, Duque G. Muscle, Bone, and Fat Crosstalk: the Biological Role of Myokines, Osteokines, and Adipokines. *Curr Osteoporos Rep* (2020) 18:388–400. doi: 10.1007/s11914-020-00599-y
- Koolstra JH. Dynamics of the human masticatory system. *Crit Rev Oral Biol Med* (2002) 13:366–76. doi: 10.1177/154411130201300406
- de Jong WC, Korfage JA, Langenbach GE. The role of masticatory muscles in the continuous loading of the mandible. *J Anat* (2011) 218:625–36. doi: 10.1111/j.1469-7580.2011.01375.x
- Tsouknidas A, Jimenez-Rojo L, Karatsis E, Michailidis N, Mitsiadis TA. A Bio-Realistic Finite Element Model to Evaluate the Effect of Masticatory Loadings on Mouse Mandible-Related Tissues. *Front Physiol* (2017) 8:273. doi: 10.3389/fphys.2017.00273
- Ahmad M, Schiffman EL. Temporomandibular Joint Disorders and Orofacial Pain. *Dent Clin North Am* (2016) 60:105–24. doi: 10.1016/j.cden.2015.08.004
- Okeon JP, de Leeuw R. Differential diagnosis of temporomandibular disorders and other orofacial pain disorders. *Dent Clin North Am* (2011) 55:105–20. doi: 10.1016/j.cden.2010.08.007
- Korfage JA, Koolstra JH, Langenbach GE, van Eijden TM. Fiber-type composition of the human jaw muscles—(part 1) origin and functional

- significance of fiber-type diversity. *J Dent Res* (2005) 84:774–83. doi: 10.1177/154405910508400901
19. Korfage JA, Koolstra JH, Langenbach GE, van Eijden TM. Fiber-type composition of the human jaw muscles—(part 2) role of hybrid fibers and factors responsible for inter-individual variation. *J Dent Res* (2005) 84:784–93. doi: 10.1177/154405910508400902
 20. Sciote JJ, Horton MJ, Rowleson AM, Link J. Specialized cranial muscles: how different are they from limb and abdominal muscles? *Cells Tissues Organs* (2003) 174:73–86. doi: 10.1159/000070576
 21. Isola G, Anastasi GP, Matarese G, Williams RC, Cutroneo G, Bracco P, et al. Functional and molecular outcomes of the human masticatory muscles. *Oral Dis* (2018) 24:1428–41. doi: 10.1111/odi.12806
 22. Akintoye SO. The distinctive jaw and alveolar bone regeneration. *Oral Dis* (2018) 24:49–51. doi: 10.1111/odi.12761
 23. Akintoye SO, Lam T, Shi S, Ibrahim J, Collins MT, Robey PG. Skeletal site-specific characterization of orofacial and iliac crest human bone marrow stromal cells in same individuals. *Bone* (2006) 38:758–68. doi: 10.1016/j.bone.2005.10.027
 24. Li C, Wang F, Zhang R, Qiao P, Liu H. Comparison of Proliferation and Osteogenic Differentiation Potential of Rat Mandibular and Femoral Bone Marrow Mesenchymal Stem Cells In Vitro. *Stem Cells Dev* (2020) 29:728–36. doi: 10.1089/scd.2019.0256
 25. Singhal V, Torre Flores LP, Stanford FC, Toth AT, Carmine B, Misra M, et al. Differential associations between appendicular and axial marrow adipose tissue with bone microarchitecture in adolescents and young adults with obesity. *Bone* (2018) 116:203–6. doi: 10.1016/j.bone.2018.08.009
 26. Frost HM. Bone “mass” and the “mechanostat”: a proposal. *Anat Rec* (1987) 219:1–9. doi: 10.1002/ar.1092190104
 27. Frost HM. Bone’s mechanostat: a 2003 update. *Anat Rec A Discov Mol Cell Evol Biol* (2003) 275:1081–101. doi: 10.1002/ar.a.10119
 28. Hsieh YF, Turner CH. Effects of loading frequency on mechanically induced bone formation. *J Bone Miner Res* (2001) 16:918–24. doi: 10.1359/jbmr.2001.16.5.918
 29. Lad SE, McGraw WS, Daegling DJ. Haversian remodeling corresponds to load frequency but not strain magnitude in the macaque (*Macaca fascicularis*) skeleton. *Bone* (2019) 127:571–6. doi: 10.1016/j.bone.2019.07.027
 30. Ethier CR. *Introductory biomechanics from cells to organisms*. Cambridge: Cambridge University Press (2007). doi: 10.1017/CBO9780511809217
 31. Bullock WAP, Plotkin LI, Robling AG, Pavalko FM. Mechanotransduction in Bone Formation and Maintenance. In: Bilezikian JP, Bouillon R, Clemens T, Compston J, Bauer DC, Ebeling PR, et al., editors. *Primer on the Metabolic Bone Diseases and Disorders of Mineral Metabolism*. (2018). p. 75–83. doi: 10.1002/9781119266594.ch10
 32. Rubin J, Rubin C, Jacobs CR. Molecular pathways mediating mechanical signaling in bone. *Gene* (2006) 367:1–16. doi: 10.1016/j.gene.2005.10.028
 33. Uda Y, Azab E, Sun N, Shi C, Pajevic PD. Osteocyte Mechanobiology. *Curr Osteoporos Rep* (2017) 15:318–25. doi: 10.1007/s11914-017-0373-0
 34. Hylander WL. *Functional anatomy and biomechanics of the masticatory apparatus, Temporomandibular disorders: an evidenced approach to diagnosis and treatment*. New York: Quintessence Pub Co. (2006).
 35. Lieberman D. *The evolution of the human head*. Cambridge, Mass.: Belknap Press of Harvard University Press (2011).
 36. Toro-Ibáñez V, Ugarte F, Morales C, Eyquem A, Aguilera J, Astudillo W. Dental malocclusions are not just about small and weak bones: assessing the morphology of the mandible with cross-section analysis and geometric morphometrics. *Clin Oral Investig* (2019) 23:3479–90. doi: 10.1007/s00784-018-2766-6
 37. Daegling DJ. The relationship of in vivo bone strain to mandibular corpus morphology in *Macaca fascicularis*. *J Hum Evol* (1993) 25:247–69. doi: 10.1006/jhev.1993.1048
 38. Gröning F, Liu J, Fagan MJ, O’Higgins P. Why do humans have chins? Testing the mechanical significance of modern human symphyseal morphology with finite element analysis. *Am J Phys Anthropol* (2011) 144:593–606. doi: 10.1002/ajpa.21447
 39. Hylander WL. Stress and strain in the mandibular symphysis of primates: a test of competing hypotheses. *Am J Phys Anthropol* (1984) 64:1–46. doi: 10.1002/ajpa.1330640102
 40. Hylander WL. Mandibular Function and Biomechanical Stress and Scaling. *Am Zool* (1985) 25:315–30. doi: 10.1093/icb/25.2.315
 41. Fukase H. Functional significance of bone distribution in the human mandibular symphysis. *Anthropol Sci* (2007) 115:55–62. doi: 10.1537/ase.060329
 42. Bromage T. *Microstructural organization and biomechanics of the macaque circumorbital region, Structure, function and evolution of teeth*. London: Freund Publishing House (1992). p. 257–72.
 43. Kupczik K, Dobson CA, Crompton RH, Phillips R, Oxnard CE, Fagan MJ, et al. Masticatory loading and bone adaptation in the supraorbital torus of developing macaques. *Am J Phys Anthropol* (2009) 139:193–203. doi: 10.1002/ajpa.20972
 44. Toro-Ibáñez V, Fitton LC, Fagan MJ, O’Higgins P. Validity and sensitivity of a human cranial finite element model: implications for comparative studies of biting performance. *J Anat* (2016) 228:70–84. doi: 10.1111/joa.12384
 45. Toro-Ibáñez V, O’Higgins P. The Effect of Varying Jaw-elevator Muscle Forces on a Finite Element Model of a Human Cranium. *Anat Rec* (2016) 299:828–39. doi: 10.1002/ar.23358
 46. Toro-Ibáñez V, Zapata Muñoz V, O’Higgins P. The relationship between skull morphology, masticatory muscle force and cranial skeletal deformation during biting. *Ann Anat* (2016) 203:59–68. doi: 10.1016/j.aanat.2015.03.002
 47. Brachetta-Aporta N, Gonzalez PN, Bernal V. Variation in facial bone growth remodeling in prehistoric populations from southern South America. *Am J Phys Anthropol* (2019) 169:422–34. doi: 10.1002/ajpa.23857
 48. Fitton LC, Prôa M, Rowland C, Toro-Ibáñez V, O’Higgins P. The Impact of Simplifications on the Performance of a Finite Element Model of a *Macaca fascicularis* Cranium. *Anat Rec* (2015) 298:107–21. doi: 10.1002/ar.23075
 49. Strait DS, Richmond BG, Spencer MA, Ross CF, Dechow PC, Wood BA. Masticatory biomechanics and its relevance to early hominid phylogeny: An examination of palatal thickness using finite-element analysis. *J Hum Evol* (2007) 52:585–99. doi: 10.1016/j.jhevol.2006.11.019
 50. Balanta-Melo J, Toro-Ibáñez V, Torres-Quintana MA, Kupczik K, Vega C, Morales C, et al. Early molecular response and microanatomical changes in the masseter muscle and mandibular head after botulinum toxin intervention in adult mice. *Ann Anat* (2018) 216:112–9. doi: 10.1016/j.aanat.2017.11.009
 51. Balanta-Melo J, Torres-Quintana MA, Bemmman M, Vega C, Gonzalez C, Kupczik K, et al. Masseter muscle atrophy impairs bone quality of the mandibular condyle but not the alveolar process early after induction. *J Oral Rehabil* (2019) 46:233–41. doi: 10.1111/joor.12747
 52. Terhune CE, Sylvester AD, Scott JE, Ravosa MJ. Internal architecture of the mandibular condyle of rabbits is related to dietary resistance during growth. *J Exp Biol* (2020) 223:jeb220988. doi: 10.1242/jeb.220988
 53. Menegaz RA, Sublett SV, Figueroa SD, Hoffman TJ, Ravosa MJ, Aldridge K. Evidence for the influence of diet on cranial form and robusticity. *Anat Rec (Hoboken)* (2010) 293:630–41. doi: 10.1002/ar.21134
 54. Spassov A, Toro-Ibáñez V, Krautwald M, Brinkmeier H, Kupczik K. Congenital muscle dystrophy and diet consistency affect mouse skull shape differently. *J Anat* (2017) 231:736–48. doi: 10.1111/joa.12664
 55. Raphael KG, Tadinada A, Bradshaw JM, Janal MN, Sirois DA, Chan KC, et al. Osteopenic consequences of botulinum toxin injections in the masticatory muscles: a pilot study. *J Oral Rehabil* (2014) 41:555–63. doi: 10.1111/joor.12180
 56. Comisso MS, Martínez-Reina J, Mayo J. A study of the temporomandibular joint during bruxism. *Int J Oral Sci* (2014) 6:116–23. doi: 10.1038/ijos.2014.4
 57. Tanaka E, Detamore MS, Mercuri LG. Degenerative disorders of the temporomandibular joint: etiology, diagnosis, and treatment. *J Dent Res* (2008) 87:296–307. doi: 10.1177/154405910808700406
 58. Egli F, Botteron S, Morel C, Kiliaridis S. Growing patients with Duchenne muscular dystrophy: longitudinal changes in their dentofacial morphology and orofacial functional capacities. *Eur J Orthod* (2018) 40:140–8. doi: 10.1093/ejo/cjx038
 59. Corruccini RS. An epidemiologic transition in dental occlusion in world populations. *Am J Orthod* (1984) 86:419–26. doi: 10.1016/S0002-9416(84)90035-6
 60. Lieberman DE, Krovitz GE, Yates FW, Devlin M, St M. Claire. Effects of food processing on masticatory strain and craniofacial growth in a retrognathic face. *J Hum Evol* (2004) 46:655–77. doi: 10.1016/j.jhevol.2004.03.005

61. Sarig R, Slon V, Abbas J, May H, Shpack N, Vardimon AD, et al. Malocclusion in early anatomically modern human: a reflection on the etiology of modern dental misalignment. *PLoS One* (2013) 8:e80771–1. doi: 10.1371/journal.pone.0080771
62. English JD, Buschang PH, Throckmorton GS. Does malocclusion affect masticatory performance? *Angle Orthod* (2002) 72:21–7. doi: 10.1043/0003-3219(2002)072<0021:DMAMP>2.0.CO;2
63. Eyquem AP, Kuzminsky SC, Aguilera J, Astudillo W, Toro-Ibache V. Normal and altered masticatory load impact on the range of craniofacial shape variation: An analysis of pre-Hispanic and modern populations of the American Southern Cone. *PLoS One* (2019) 14:e0225369–e0225369. doi: 10.1371/journal.pone.0225369
64. Toro-Ibache V, Cortés Araya J, Díaz Muñoz A, Manríquez Soto G. Morphologic variability of nonsyndromic operated patients affected by cleft lip and palate: a geometric morphometric study. *Am J Orthod Dentofacial Orthop* (2014) 146:346–54. doi: 10.1016/j.ajodo.2014.06.002
65. Stelzer S, Gunz P, Neubauer S, Spoor F. Hominoid arcade shape: Pattern and magnitude of covariation. *J Hum Evol* (2017) 107:71–85. doi: 10.1016/j.jhevol.2017.02.010
66. Alarcón JA, Bastir M, García-Espona I, Menéndez-Núñez M, Rosas A. Morphological integration of mandible and cranium: Orthodontic implications. *Arch Oral Biol* (2014) 59:22–9. doi: 10.1016/j.archoralbio.2013.10.005
67. Avin KG, Bloomfield SA, Gross TS, Warden SJ. Biomechanical aspects of the muscle-bone interaction. *Curr Osteoporos Rep* (2015) 13:1–8. doi: 10.1007/s11914-014-0244-x
68. Ferretti JL, Cointy GR, Capozza RF, Frost HM. Bone mass, bone strength, muscle-bone interactions, osteopenias and osteoporoses. *Mech Ageing Dev* (2003) 124:269–79. doi: 10.1016/S0047-6374(02)00194-X
69. Karsenty G, Mera P. Molecular bases of the crosstalk between bone and muscle. *Bone* (2017) 115:43–49. doi: 10.1016/j.bone.2017.04.006
70. Bonewald L. Use it or lose it to age: A review of bone and muscle communication. *Bone* (2019) 120:212–8. doi: 10.1016/j.bone.2018.11.002
71. Giudice J, Taylor JM. Muscle as a paracrine and endocrine organ. *Curr Opin Pharmacol* (2017) 34:49–55. doi: 10.1016/j.coph.2017.05.005
72. Kitase Y, Vallejo JA, Gutheil W, Vemula H, Jahn K, Yi J, et al. beta-aminobutyric Acid, I-BAIBA, Is a Muscle-Derived Osteocyte Survival Factor. *Cell Rep* (2018) 22:1531–44. doi: 10.1016/j.celrep.2018.01.041
73. Qin W, Dallas SL. Exosomes and Extracellular RNA in Muscle and Bone Aging and Crosstalk. *Curr Osteoporos Rep* (2019) 17:548–59. doi: 10.1007/s11914-019-00537-7
74. Qin Y, Peng Y, Zhao W, Pan J, Ksiezak-Reding H, Cardozo C, et al. Myostatin inhibits osteoblastic differentiation by suppressing osteocyte-derived exosomal microRNA-218: A novel mechanism in muscle-bone communication. *J Biol Chem* (2017) 292:11021–33. doi: 10.1074/jbc.M116.770941
75. Huh JY. The role of exercise-induced myokines in regulating metabolism. *Arch Pharm Res* (2018) 41:14–29. doi: 10.1007/s12272-017-0994-y
76. Little HC, Tan SY, Cali FM, Rodriguez S, Lei X, Wolfe A, et al. Multiplex Quantification Identifies Novel Exercise-regulated Myokines/Cytokines in Plasma and in Glycolytic and Oxidative Skeletal Muscle. *Mol Cell Proteomics* (2018) 17:1546–63. doi: 10.1074/mcp.RA118.000794
77. Dallas SL, Prideaux M, Bonewald LF. The osteocyte: an endocrine cell ... and more. *Endocr Rev* (2013) 34:658–90. doi: 10.1210/er.2012-1026
78. DiGirolamo DJ, Clemens TL, Kousteni S. The skeleton as an endocrine organ. *Nat Rev Rheumatol* (2012) 8:674–83. doi: 10.1038/nrrheum.2012.157
79. Sanchez C, Mazzuchelli G, Lambert C, Comblain F, DePauw E, Henrotin Y. Comparison of secretome from osteoblasts derived from sclerotic versus non-sclerotic subchondral bone in OA: A pilot study. *PLoS One* (2018) 13: e0194591. doi: 10.1371/journal.pone.0194591
80. Chowdhury S, Schulz L, Palmisano B, Singh P, Berger JM, Yadav VK, et al. Muscle-derived interleukin 6 increases exercise capacity by signaling in osteoblasts. *J Clin Invest* (2020) 130:2888–902. doi: 10.1172/JCI133572
81. Mo C, Romero-Suarez S, Bonewald L, Johnson M, Brotto M. Prostaglandin E2: from clinical applications to its potential role in bone- muscle crosstalk and myogenic differentiation. *Recent Pat Biotechnol* (2012) 6:223–9. doi: 10.2174/1872208311206030223
82. Wacker MJ, Touchberry CD, Silswal N, Brotto L, Elmore CJ, Bonewald LF, et al. Skeletal Muscle, but not Cardiovascular Function, Is Altered in a Mouse Model of Autosomal Recessive Hypophosphatemic Rickets. *Front Physiol* (2016) 7:173. doi: 10.3389/fphys.2016.00173
83. Waning DL, Mohammad KS, Reiken S, Xie W, Andersson DC, John S, et al. Excess TGF-beta mediates muscle weakness associated with bone metastases in mice. *Nat Med* (2015) 21:1262–71. doi: 10.1038/nm.3961
84. Bonnet N, Bourgoin L, Biver E, Douni E, Ferrari S. RANKL inhibition improves muscle strength and insulin sensitivity and restores bone mass. *J Clin Invest* (2019) 129:3214–23. doi: 10.1172/JCI125915
85. Hamoudi D, Marcadet L, Piette Boulanger A, Yagita H, Bouredji Z, Argaw A, et al. An anti-RANKL treatment reduces muscle inflammation and dysfunction and strengthens bone in dystrophic mice. *Hum Mol Genet* (2019) 28:3101–12. doi: 10.1093/hmg/ddz124
86. Huang J, Romero-Suarez S, Lara N, Mo C, Kaja S, Brotto L, et al. Crosstalk between MLO-Y4 osteocytes and C2C12 muscle cells is mediated by the Wnt/beta-catenin pathway. *JBM Plus* (2017) 1:86–100. doi: 10.1002/jbm4.10015
87. Elkasrawy M, Immel D, Wen X, Liu X, Liang LF, Hamrick MW. Immunolocalization of myostatin (GDF-8) following musculoskeletal injury and the effects of exogenous myostatin on muscle and bone healing. *J Histochem Cytochem* (2012) 60:22–30. doi: 10.1369/0022155411425389
88. Harry LE, Sandison A, Paleolog EM, Hansen U, Pearse MF, Nanchahal J. Comparison of the healing of open tibial fractures covered with either muscle or fasciocutaneous tissue in a murine model. *J Orthop Res* (2008) 26:1238–44. doi: 10.1002/jor.20649
89. Jahn K, Lara-Castillo N, Brotto L, Mo CL, Johnson ML, Brotto M, et al. Skeletal muscle secreted factors prevent glucocorticoid-induced osteocyte apoptosis through activation of beta-catenin. *Eur Cell Mater* (2012) 24:197–209; discussion 209–10. doi: 10.22203/eCM.v024a14
90. Che X, Guo J, Li X, Wang L, Wei S. Intramuscular injection of bone marrow mononuclear cells contributes to bone repair following midpalatal expansion in rats. *Mol Med Rep* (2016) 13:681–8. doi: 10.3892/mmr.2015.4578
91. McPherron AC, Lawler AM, Lee SJ. Regulation of skeletal muscle mass in mice by a new TGF-beta superfamily member. *Nature* (1997) 387:83–90. doi: 10.1038/387083a0
92. Carnac G, Vernus B, Bonniou A. Myostatin in the pathophysiology of skeletal muscle. *Curr Genomics* (2007) 8:415–22. doi: 10.2174/138920207783591672
93. White TA, LeBrasseur NK. Myostatin and sarcopenia: opportunities and challenges - a mini-review. *Gerontology* (2014) 60:289–93. doi: 10.1159/000356740
94. Buehring B, Binkley N. Myostatin—the holy grail for muscle, bone, and fat? *Curr Osteoporos Rep* (2013) 11:407–14. doi: 10.1007/s11914-013-0160-5
95. Elkasrawy MN, Hamrick MW. Myostatin (GDF-8) as a key factor linking muscle mass and bone structure. *J Musculoskelet Neuronal Interact* (2010) 10:56–63.
96. Hamrick MW, Samadder T, Pennington C, McCormick J. Increased muscle mass with myostatin deficiency improves gains in bone strength with exercise. *J Bone Miner Res* (2006) 21:477–83. doi: 10.1359/JBMR.051203
97. Lodberg A, van der Eerden BCJ, Boers-Sijmons B, Thomsen JS, Bruel A, van Leeuwen J, et al. A follistatin-based molecule increases muscle and bone mass without affecting the red blood cell count in mice. *FASEB J* (2019) 33:6001–10. doi: 10.1096/fj.201801969RR
98. Wallner C, Jaurich H, Wagner JM, Becerikli M, Harati K, Dadras M, et al. Inhibition of GDF8 (Myostatin) accelerates bone regeneration in diabetes mellitus type 2. *Sci Rep* (2017) 7:9878. doi: 10.1038/s41598-017-10404-z
99. Dankbar B, Fennen M, Brunert D, Hayer S, Frank S, Wehmeyer C, et al. Myostatin is a direct regulator of osteoclast differentiation and its inhibition reduces inflammatory joint destruction in mice. *Nat Med* (2015) 21:1085–90. doi: 10.1038/nm.3917
100. Ravosa MJ, Lopez EK, Menegaz RA, Stock SR, Stack MS, Hamrick MW. Using “Mighty Mouse” to understand masticatory plasticity: myostatin-deficient mice and musculoskeletal function. *Integr Comp Biol* (2008) 48:345–59. doi: 10.1093/icb/icn050
101. Ravosa MJ, Klopp EB, Pinchoff J, Stock SR, Hamrick MW. Plasticity of mandibular biomineralization in myostatin-deficient mice. *J Morphol* (2007) 268:275–82. doi: 10.1002/jmor.10517

102. Nicholson EK, Stock SR, Hamrick MW, Ravosa MJ. Biom mineralization and adaptive plasticity of the temporomandibular joint in myostatin knockout mice. *Arch Oral Biol* (2006) 51:37–49. doi: 10.1016/j.archoralbio.2005.05.008
103. Vecchione L, Miller J, Byron C, Cooper GM, Barbano T, Cray J, et al. Age-related changes in craniofacial morphology in GDF-8 (myostatin)-deficient mice. *Anat Rec (Hoboken)* (2010) 293:32–41. doi: 10.1002/ar.21024
104. Goldspink G. Mechanical signals, IGF-I gene splicing, and muscle adaptation. *Physiology (Bethesda)* (2005) 20:232–8. doi: 10.1152/physiol.00004.2005
105. Giustina A, Mazziotti G, Canalis E. Growth hormone, insulin-like growth factors, and the skeleton. *Endocr Rev* (2008) 29:535–59. doi: 10.1210/er.2007-0036
106. Reijnders CM, Bravenboer N, Tromp AM, Blankenstein MA, Lips P. Effect of mechanical loading on insulin-like growth factor-I gene expression in rat tibia. *J Endocrinol* (2007) 192:131–40. doi: 10.1677/joe.1.06880
107. Bikle DD, Tahimic C, Chang W, Wang Y, Philippou A, Barton ER. Role of IGF-I signaling in muscle bone interactions. *Bone* (2015) 80:79–88. doi: 10.1016/j.bone.2015.04.036
108. Kineman RD, Del Rio-Moreno M, Sarmento-Cabral A. 40 YEARS of IGF1: Understanding the tissue-specific roles of IGF1/IGF1R in regulating metabolism using the Cre/loxP system. *J Mol Endocrinol* (2018) 61:T187–t198. doi: 10.1530/JME-18-0076
109. Saito T, Fukui K, Akutsu S, Nakagawa Y, Ishibashi K, Nagata J, et al. Effects of diet consistency on the expression of insulin-like growth factors (IGFs), IGF receptors and IGF binding proteins during the development of rat masseter muscle soon after weaning. *Arch Oral Biol* (2004) 49:777–82. doi: 10.1016/j.archoralbio.2004.02.014
110. Urushiyama T, Akutsu S, Miyazaki J, Fukui T, Diekwisch TG, Yamane A. Change from a hard to soft diet alters the expression of insulin-like growth factors, their receptors, and binding proteins in association with atrophy in adult mouse masseter muscle. *Cell Tissue Res* (2004) 315:97–105. doi: 10.1007/s00441-003-0787-0
111. Vilmann H, Kirkeby S, Kronborg D. Histomorphometrical analysis of the influence of soft diet on masticatory muscle development in the muscular dystrophic mouse. *Arch Oral Biol* (1990) 35:37–42. doi: 10.1016/0003-9969(90)90112-N
112. Tanaka E, Sano R, Kawai N, Langenbach GE, Brugman P, Tanne K, et al. Effect of food consistency on the degree of mineralization in the rat mandible. *Ann BioMed Eng* (2007) 35:1617–21. doi: 10.1007/s10439-007-9330-x
113. Odman A, Mavropoulos A, Kiliaridis S. Do masticatory functional changes influence the mandibular morphology in adult rats. *Arch Oral Biol* (2008) 53:1149–54. doi: 10.1016/j.archoralbio.2008.07.004
114. Kawai N, Sano R, Korfage JA, Nakamura S, Kinouchi N, Kawakami E, et al. Adaptation of rat jaw muscle fibers in postnatal development with a different food consistency: an immunohistochemical and electromyographic study. *J Anat* (2010) 216:717–23. doi: 10.1111/j.1469-7580.2010.01235.x
115. Hichijo N, Kawai N, Mori H, Sano R, Ohnuki Y, Okumura S, et al. Effects of the masticatory demand on the rat mandibular development. *J Oral Rehabil* (2014) 41:581–7. doi: 10.1111/joor.12171
116. Hichijo N, Tanaka E, Kawai N, van Ruijven LJ, Langenbach GE. Effects of Decreased Occlusal Loading during Growth on the Mandibular Bone Characteristics. *PLoS One* (2015) 10:e0129290. doi: 10.1371/journal.pone.0129290
117. Shi Z, Lv J, Xiaoyu L, Zheng LW, Yang XW. Condylar Degradation from Decreased Occlusal Loading following Masticatory Muscle Atrophy. *BioMed Res Int* (2018) 2018:6947612. doi: 10.1155/2018/6947612
118. Rojas-Beato C. PhD Thesis: Efecto de la actividad masticatoria sobre la producción y liberación de IL-1b e IL-6 a través de la señalización por ATP extracelular en fibras de músculo masetero de ratón. Santiago, Chile: Faculty of Medicine, Universidad de Chile (2019). p. 120.
119. Tsai CY, Chiu WC, Liao YH, Tsai CM. Effects on craniofacial growth and development of unilateral botulinum neurotoxin injection into the masseter muscle. *Am J Orthod Dentofacial Orthop* (2009) 135:142.e1–6; discussion 142–3. doi: 10.1016/j.ajodo.2008.06.020
120. Tsai CY, Huang RY, Lee CM, Hsiao WT, Yang LY. Morphologic and bony structural changes in the mandible after a unilateral injection of botulinum neurotoxin in adult rats. *J Oral Maxillofac Surg* (2010) 68:1081–7. doi: 10.1016/j.joms.2009.12.009
121. Tsai CY, Lei YY, Yang LY, Chiu WC. Changes of masseter muscle activity following injection of botulinum toxin type A in adult rats. *Orthod Craniofac Res* (2015) 18:202–11. doi: 10.1111/ocr.12095
122. Kün-Darbois JD, Libouban H, Chappard D. Botulinum toxin in masticatory muscles of the adult rat induces bone loss at the condyle and alveolar regions of the mandible associated with a bone proliferation at a muscle enthesis. *Bone* (2015) 77:75–82. doi: 10.1016/j.bone.2015.03.023
123. Dutra EH, MH OB, Lima A, Kalajic Z, Tadinada A, Nanda R, et al. Cellular and Matrix Response of the Mandibular Condylar Cartilage to Botulinum Toxin. *PLoS One* (2016) 11:e0164599. doi: 10.1371/journal.pone.0164599
124. Balanta-Melo J, Beato C, Vásquez V, Kupczik K, Toro-Ibacache V, Buvinic S. Extracellular nucleotides in muscle-bone crosstalk at the masticatory system, 2018. *J Dent Res* (2018) 97(Special Issue C):oral1004.
125. Balanta-Melo J, Toro-Ibacache V, Kupczik K, Buvinic S. Mandibular Bone Loss after Masticatory Muscles Intervention with Botulinum Toxin: An Approach from Basic Research to Clinical Findings. *Toxins (Basel)* (2019) 11:1–16. doi: 10.3390/toxins11020084
126. Dutra EH, Yadav S. The effects on the mandibular condyle of Botox injection into the masseter are not transient. *Am J Orthod Dentofacial Orthop* (2019) 156:193–202. doi: 10.1016/j.ajodo.2018.08.023
127. Vásquez W. M.Sc. Thesis: Efectos de la inyección de toxina botulínica tipo A sobre la vía de señalización del ATP extracelular en músculo masetero de ratón. Santiago, Chile: Faculty of Medicine, Universidad de Chile (2020). p. 61.
128. Losel PD, van de Kamp T, Jayme A, Ershov A, Farago T, Pichler O, et al. Introducing Biomedisa as an open-source online platform for biomedical image segmentation. *Nat Commun* (2020) 11:5577. doi: 10.1038/s41467-020-19303-w
129. Balanta-Melo JE, Eyquem A, Toro-Ibacache V, Torres-Quintana M, Kupczik K, Buvinic S. Quantifying Jaw Muscle Volumes Following Masseter Hypofunction With Contrast-Enhanced Micro-CT, IADR/ADR/CADR General Session 98th General Session. *J Dent Res* (2020) 99 (Spec Iss A):2770.
130. Bodine SC, Baehr LM. Skeletal muscle atrophy and the E3 ubiquitin ligases MuRF1 and MAFbx/atrogin-1. *Am J Physiol Endocrinol Metab* (2014) 307: E469–84. doi: 10.1152/ajpendo.00204.2014
131. Enomoto A, Watahiki J, Yamaguchi T, Irie T, Tachikawa T, Maki K. Effects of mastication on mandibular growth evaluated by microcomputed tomography. *Eur J Orthod* (2010) 32:66–70. doi: 10.1093/ejo/cjp060
132. Inoue M, Ono T, Kameo Y, Sasaki F, Ono T, Adachi T, et al. Forceful mastication activates osteocytes and builds a stout jawbone. *Sci Rep* (2019) 9:4404. doi: 10.1038/s41598-019-40463-3
133. Dayer JM, Choy E. Therapeutic targets in rheumatoid arthritis: the interleukin-6 receptor. *Rheumatology (Oxford)* (2010) 49:15–24. doi: 10.1093/rheumatology/kep329
134. Blanchard F, Duplomb L, Baud'huin M, Brounais B. The dual role of IL-6-type cytokines on bone remodeling and bone tumors. *Cytokine Growth Factor Rev* (2009) 20:19–28. doi: 10.1016/j.cytogfr.2008.11.004
135. Pedersen BK, Febbraio MA. Muscle as an endocrine organ: focus on muscle-derived interleukin-6. *Physiol Rev* (2008) 88:1379–406. doi: 10.1152/physrev.90100.2007
136. Pedersen BK, Steensberg A, Fischer C, Keller C, Keller P, Plomgaard P, et al. Searching for the exercise factor: is IL-6 a candidate? *J Muscle Res Cell Motil* (2003) 24:113–9. doi: 10.1023/A:1026070911202
137. Hiscock N, Chan MH, Bisucci T, Darby IA, Febbraio MA. Skeletal myocytes are a source of interleukin-6 mRNA expression and protein release during contraction: evidence of fiber type specificity. *FASEB J* (2004) 18:992–4. doi: 10.1096/fj.03-1259fj
138. Ostrowski K, Rohde T, Asp S, Schjerling P, Pedersen BK. Pro- and anti-inflammatory cytokine balance in strenuous exercise in humans. *J Physiol* (1999) 515(Pt 1):287–91. doi: 10.1111/j.1469-7793.1999.287ad.x
139. Rosendal L, Sogaard K, Kjaer M, Sjøgaard G, Langberg H, Kristiansen J. Increase in interstitial interleukin-6 of human skeletal muscle with repetitive low-force exercise. *J Appl Physiol* (1985) 98(2005):477–81. doi: 10.1152/japplphysiol.00130.2004
140. Febbraio MA, Hiscock N, Sacchetti M, Fischer CP, Pedersen BK. Interleukin-6 is a novel factor mediating glucose homeostasis during skeletal muscle contraction. *Diabetes* (2004) 53:1643–8. doi: 10.2337/diabetes.53.7.1643

141. Pedersen BK, Febbraio MA. Muscles, exercise and obesity: skeletal muscle as a secretory organ. *Nat Rev Endocrinol* (2012) 8:457–65. doi: 10.1038/nrendo.2012.49
142. Cantini M, Massimino ML, Rapizzi E, Rossini K, Catani C, Dalla Libera L, et al. Human satellite cell proliferation in vitro is regulated by autocrine secretion of IL-6 stimulated by a soluble factor(s) released by activated monocytes. *Biochem Biophys Res Commun* (1995) 216:49–53. doi: 10.1006/bbrc.1995.2590
143. Serrano AL, Baeza-Raja B, Perdiguerro E, Jardi M, Munoz-Canoves P. Interleukin-6 is an essential regulator of satellite cell-mediated skeletal muscle hypertrophy. *Cell Metab* (2008) 7:33–44. doi: 10.1016/j.cmet.2007.11.011
144. Evans WJ, Morley JE, Argiles J, Bales C, Baracos V, Guttridge D, et al. Cachexia: a new definition. *Clin Nutr* (2008) 27:793–9. doi: 10.1016/j.clnu.2008.06.013
145. Bonetto A, Aydogdu T, Kunzevitzky N, Guttridge DC, Khuri S, Koniaris LG, et al. STAT3 activation in skeletal muscle links muscle wasting and the acute phase response in cancer cachexia. *PLoS One* (2011) 6:e22538. doi: 10.1371/journal.pone.0022538
146. Bonetto A, Aydogdu T, Jin X, Zhang Z, Zhan R, Puzis L, et al. JAK/STAT3 pathway inhibition blocks skeletal muscle wasting downstream of IL-6 and in experimental cancer cachexia. *Am J Physiol Endocrinol Metab* (2012) 303: E410–21. doi: 10.1152/ajpendo.00039.2012
147. Haddad F, Zaldivar F, Cooper DM, Adams GR. IL-6-induced skeletal muscle atrophy. *J Appl Physiol* (1985) 98(2005):911–7. doi: 10.1152/japplphysiol.01026.2004
148. Tsujinaka T, Ebisui C, Fujita J, Kishibuchi M, Morimoto T, Ogawa A, et al. Muscle undergoes atrophy in association with increase of lysosomal cathepsin activity in interleukin-6 transgenic mouse. *Biochem Biophys Res Commun* (1995) 207:168–74. doi: 10.1006/bbrc.1995.1168
149. Tsujinaka T, Fujita J, Ebisui C, Yano M, Kominami E, Suzuki K, et al. Interleukin 6 receptor antibody inhibits muscle atrophy and modulates proteolytic systems in interleukin 6 transgenic mice. *J Clin Invest* (1996) 97:244–9. doi: 10.1172/JCI118398
150. Ando K, Takahashi F, Kato M, Kaneko N, Doi T, Ohe Y, et al. Tocilizumab, a proposed therapy for the cachexia of Interleukin6-expressing lung cancer. *PLoS One* (2014) 9:e102436. doi: 10.1371/journal.pone.0102436
151. Zaki MH, Nemeth JA, Trikha M, CNTO 328, a monoclonal antibody to IL-6, inhibits human tumor-induced cachexia in nude mice. *Int J Cancer* (2004) 111:592–5. doi: 10.1002/ijc.20270
152. Wada E, Tanihata J, Iwamura A, Takeda S, Hayashi YK, Matsuda R. Treatment with the anti-IL-6 receptor antibody attenuates muscular dystrophy via promoting skeletal muscle regeneration in dystrophin-/utrophin-deficient mice. *Skelet Muscle* (2017) 7:23. doi: 10.1186/s13395-017-0140-z
153. Yakabe M, Ogawa S, Ota H, Iijima K, Eto M, Ouchi Y, et al. Inhibition of interleukin-6 decreases atrogenic expression and ameliorates tail suspension-induced skeletal muscle atrophy. *PLoS One* (2018) 13:e0191318. doi: 10.1371/journal.pone.0191318
154. Itoh S, Udagawa N, Takahashi N, Yoshitake F, Narita H, Ebisu S, et al. A critical role for interleukin-6 family-mediated Stat3 activation in osteoblast differentiation and bone formation. *Bone* (2006) 39:505–12. doi: 10.1016/j.bone.2006.02.074
155. Takeuchi Y, Watanabe S, Ishii G, Takeda S, Nakayama K, Fukumoto S, et al. Interleukin-11 as a stimulatory factor for bone formation prevents bone loss with advancing age in mice. *J Biol Chem* (2002) 277:49011–8. doi: 10.1074/jbc.M207804200
156. Kaneshiro S, Ebina K, Shi K, Higuchi C, Hirao M, Okamoto M, et al. IL-6 negatively regulates osteoblast differentiation through the SHP2/MEK2 and SHP2/Akt2 pathways in vitro. *J Bone Miner Metab* (2014) 32:378–92. doi: 10.1007/s00774-013-0514-1
157. Palmqvist P, Persson E, Conaway HH, Lerner UH. IL-6, leukemia inhibitory factor, and oncostatin M stimulate bone resorption and regulate the expression of receptor activator of NF-kappa B ligand, osteoprotegerin, and receptor activator of NF-kappa B in mouse calvariae. *J Immunol* (2002) 169:3353–62. doi: 10.4049/jimmunol.169.6.3353
158. Yokota K, Sato K, Miyazaki T, Kitaura H, Kayama H, Miyoshi F, et al. Combination of tumor necrosis factor alpha and interleukin-6 induces mouse osteoclast-like cells with bone resorption activity both in vitro and in vivo. *Arthritis Rheumatol* (2014) 66:121–9. doi: 10.1002/art.38218
159. Duplomb L, Baud'huin M, Charrier C, Berreur M, Trichet V, Blanchard F, et al. Interleukin-6 inhibits receptor activator of nuclear factor kappaB ligand-induced osteoclastogenesis by diverting cells into the macrophage lineage: key role of Serine727 phosphorylation of signal transducer and activator of transcription 3. *Endocrinology* (2008) 149:3688–97. doi: 10.1210/en.2007-1719
160. Yoshitake F, Itoh S, Narita H, Ishihara K, Ebisu S. Interleukin-6 directly inhibits osteoclast differentiation by suppressing receptor activator of NF-kappaB signaling pathways. *J Biol Chem* (2008) 283:11535–40. doi: 10.1074/jbc.M607999200
161. Karsdal MA, Schett G, Emery P, Harari O, Byrjalsen I, Kenwright A, et al. IL-6 receptor inhibition positively modulates bone balance in rheumatoid arthritis patients with an inadequate response to anti-tumor necrosis factor therapy: biochemical marker analysis of bone metabolism in the tocilizumab RADIATE study (NCT00106522). *Semin Arthritis Rheum* (2012) 42:131–9. doi: 10.1016/j.semarthrit.2012.01.004
162. Terpos E, Fragiadakis K, Konsta M, Bratengeier C, Papatheodorou A, Sfrikakis PP. Early effects of IL-6 receptor inhibition on bone homeostasis: a pilot study in women with rheumatoid arthritis. *Clin Exp Rheumatol* (2011) 29:921–5.
163. Rozen N, Lewinson D, Bick T, Jacob ZC, Stein H, Soudry M. Fracture repair: modulation of fracture-callus and mechanical properties by sequential application of IL-6 following PTH 1-34 or PTH 28-48. *Bone* (2007) 41:437–45. doi: 10.1016/j.bone.2007.04.193
164. Chiba K, Tsuchiya M, Koide M, Hagiwara Y, Sasaki K, Hattori Y, et al. Involvement of IL-1 in the Maintenance of Masseter Muscle Activity and Glucose Homeostasis. *PLoS One* (2015) 10:e0143635. doi: 10.1371/journal.pone.0143635
165. Ono T, Maekawa K, Watanabe S, Oka H, Kuboki T. Muscle contraction accelerates IL-6 mRNA expression in the rat masseter muscle. *Arch Oral Biol* (2007) 52:479–86. doi: 10.1016/j.archoralbio.2006.10.025
166. Beato C, Vicencio N, Casas M, Buvinic S. Mouse masseter muscle activity induces IL1 β and IL6 expression mediated by extracellular ATP signaling. *Experimental Biology. FASEB J San Diego CA U S A* (2018) 32:857.5–857.5. doi: 10.1096/fasebj.2018.32.1_supplement.857.5
167. Buvinic S. Muscle-Bone crosstalk at the masticatory system: unveiling molecular mediators in health and disease. In: *Annual Meeting of the Chilean Society for Physiological Sciences*. Santa Cruz, Chile: In Vitro (2019). p. 23. Available at: https://revistainvitro.cl/wp-content/uploads/2019/09/201909_SCHCF_programa_resumenenes.pdf?fb8a078.
168. Balanta-Melo J, Buvinic S. Mandibular bone loss: a hidden side effect of botulinum toxin type A injection in masticatory muscles. *J Oral Res* (2018) 7:44–6. doi: 10.17126/joralres.2018.014
169. Vásquez W, Arias-Calderón M, Beato C, Balanta-Melo J, Hernández N, Llanos P, et al. La parálisis inducida por Toxina Botulínica tipo A exacerbó la vía de ATP extracelular en el músculo masetero de ratón. In: *Annual Meeting of the Chilean Society for Physiological Sciences*. Santa Cruz, Chile: In Vitro (2019). p. 66. Available at: https://revistainvitro.cl/wp-content/uploads/2019/09/201909_SCHCF_programa_resumenenes.pdf?fb8a078&fb8a078.
170. Kim JY, Kim ST, Cho SW, Jung HS, Park KT, Son HK. Growth effects of botulinum toxin type A injected into masseter muscle on a developing rat mandible. *Oral Dis* (2008) 14:626–32. doi: 10.1111/j.1601-0825.2007.01435.x
171. Zwiri A, Al-Hatamleh MAI, Wma WA, Ahmed Asif J, Khoo SP, Husein A, et al. Biomarkers for Temporomandibular Disorders: Current Status and Future Directions. *Diagnostics (Basel)* (2020) 10:1–18. doi: 10.3390/diagnostics10050303
172. Kim YK, Kim SG, Kim BS, Lee JY, Yun PY, Bae JH, et al. Analysis of the cytokine profiles of the synovial fluid in a normal temporomandibular joint: preliminary study. *J Craniomaxillofac Surg* (2012) 40:e337–41. doi: 10.1016/j.jcms.2012.02.002
173. Kristensen KD, Alstergren P, Stoustrup P, Kuseler A, Herlin T, Pedersen TK. Cytokines in healthy temporomandibular joint synovial fluid. *J Oral Rehabil* (2014) 41:250–6. doi: 10.1111/joor.12146
174. Shinoda C, Takaku S. Interleukin-1 beta, interleukin-6, and tissue inhibitor of metalloproteinase-1 in the synovial fluid of the temporomandibular joint with respect to cartilage destruction. *Oral Dis* (2000) 6:383–90. doi: 10.1111/j.1601-0825.2000.tb00131.x

175. Kaneyama K, Segami N, Sato J, Nishimura M, Yoshimura H. Interleukin-6 family of cytokines as biochemical markers of osseous changes in the temporomandibular joint disorders. *Br J Oral Maxillofac Surg* (2004) 42:246–50. doi: 10.1016/S0266-4356(03)00258-4
176. Satokawa C, Nishiyama A, Suzuki K, Uesugi S, Kokai S, Ono T. Evaluation of tissue oxygen saturation of the masseter muscle during standardised teeth clenching. *J Oral Rehabil* (2020) 47:19–26. doi: 10.1111/joor.12863
177. Suzuki S, Castrillon EE, Arima T, Kitagawa Y, Svensson P. Blood oxygenation of masseter muscle during sustained elevated muscle activity in healthy participants. *J Oral Rehabil* (2016) 43:900–10. doi: 10.1111/joor.12450
178. Britto FA, Gnimassou O, De Groote E, Balan E, Warnier G, Everard A, et al. Acute environmental hypoxia potentiates satellite cell-dependent myogenesis in response to resistance exercise through the inflammation pathway in human. *FASEB J* (2020) 34:1885–900. doi: 10.1096/fj.201902244R
179. Aguilera SB, Brown L, Perico VA. Aesthetic Treatment of Bruxism. *J Clin Aesthet Dermatol* (2017) 10:49–55.
180. Yoshida Y, Suganuma T, Takaba M, Ono Y, Abe Y, Yoshizawa S, et al. Association between patterns of jaw motor activity during sleep and clinical signs and symptoms of sleep bruxism. *J Sleep Res* (2017) 26:415–21. doi: 10.1111/jsr.12481
181. Ayoub S, Berberi A, Fayyad-Kazan M. Cytokines, Masticatory Muscle Inflammation, and Pain: an Update. *J Mol Neurosci* (2020) 70:790–5. doi: 10.1007/s12031-020-01491-1
182. Beaumont S, Garg K, Gokhale A, Heaphy N. Temporomandibular Disorder: a practical guide for dental practitioners in diagnosis and management. *Aust Dent J* (2020) 65:172–80. doi: 10.1111/adj.12785
183. Takeuchi T, Arima T, Ernberg M, Yamaguchi T, Ohata N, Svensson P. Symptoms and physiological responses to prolonged, repeated, low-level tooth clenching in humans. *Headache* (2015) 55:381–94. doi: 10.1111/head.12528
184. Louca Jounger S, Christidis N, Svensson P, List T, Ernberg M. Increased levels of intramuscular cytokines in patients with jaw muscle pain. *J Headache Pain* (2017) 18:30. doi: 10.1186/s10194-017-0737-y
185. Kebede B, Megersa S. Idiopathic masseter muscle hypertrophy. *Ethiop J Health Sci* (2011) 21:209–12.
186. Fedorowicz Z, van Zuuren EJ, Schoones J. Botulinum toxin for masseter hypertrophy. *Cochrane Database Syst Rev* (2013) 2013:CD007510. doi: 10.1002/14651858.CD007510.pub3
187. Kamburoglu K, Sonmez G, Nalcaci R, Yurttutan E, Tuzunel AO. Ultrasonographic Evaluation Of The Masseter Muscle Before And After Botulinum Toxin Injection In Patients With Bruxism. *Oral Surg Oral Med Oral Pathol Oral Radiol* (2019) 128:e174. doi: 10.1016/j.oooo.2019.01.059
188. Salari M, Sharma S, Jog MS. Botulinum Toxin Induced Atrophy: An Uncharted Territory. *Toxins (Basel)* (2018) 10:1–11. doi: 10.3390/toxins10080313
189. Park G, Choi YC, Bae JH, Kim ST. Does Botulinum Toxin Injection into Masseter Muscles Affect Subcutaneous Thickness? *Aesthet Surg J* (2018) 38:192–8. doi: 10.1093/asj/sjx102
190. Lee HJ, Kim SJ, Lee KJ, Yu HS, Baik HS. Repeated injections of botulinum toxin into the masseter muscle induce bony changes in human adults: A longitudinal study. *Korean J Orthod* (2017) 47:222–8. doi: 10.4041/kjod.2017.47.4.222
191. Kahn A, Kun-Darbois JD, Bertin H, Corre P, Chappard D. Mandibular bone effects of botulinum toxin injections in masticatory muscles in adult. *Oral Surg Oral Med Oral Pathol Oral Radiol* (2020) 129:100–8. doi: 10.1016/j.oooo.2019.03.007
192. Hong SW, Kang JH. Decreased mandibular cortical bone quality after botulinum toxin injections in masticatory muscles in female adults. *Sci Rep* (2020) 10:3623. doi: 10.1038/s41598-020-60554-w
193. De la Torre Canales G, Alvarez-Pinzon N, Munoz-Lora VRM, Vieira Peroni L, Farias Gomes A, Sanchez-Ayala A, et al. Efficacy and Safety of Botulinum Toxin Type A on Persistent Myofascial Pain: A Randomized Clinical Trial. *Toxins (Basel)* (2020) 12:1–13. doi: 10.3390/toxins12060395
194. Raphael KG, Janal MN, Tadinada A, Santiago V, Sirois DA, Lurie AG. Effect of Multiple Injections of Botulinum Toxin into Painful Masticatory Muscles on Bone Density in the Temporomandibular Complex. *J Oral Rehabil* (2020) 47:1319–29. doi: 10.1111/joor.13087
195. Thanakun S, Pornprasertsuk-Damrongsri S, Na Mahasarakham CP, Techatanawat S, Izumi Y. Increased Plasma Osteocalcin, Oral Disease, and Altered Mandibular Bone Density in Postmenopausal Women. *Int J Dent* (2019) 2019:3715127. doi: 10.1155/2019/3715127
196. Strollo F, Gentile S, Strollo G, Mambro A, Vernikos J. Recent Progress in Space Physiology and Aging. *Front Physiol* (2018) 9:1551. doi: 10.3389/fphys.2018.01551
197. Rai B, Kaur J, Catalina M. Bone mineral density, bone mineral content, gingival crevicular fluid (matrix metalloproteinases, cathepsin K, osteocalcin), and salivary and serum osteocalcin levels in human mandible and alveolar bone under conditions of simulated microgravity. *J Oral Sci* (2010) 52:385–90. doi: 10.2334/josnusd.52.385
198. Philippou A, Minozzo FC, Spinazzola JM, Smith LR, Lei H, Rassier DE, et al. Masticatory muscles of mouse do not undergo atrophy in space. *FASEB J* (2015) 29:2769–79. doi: 10.1096/fj.14-267336
199. Stigler RG, Becker K, Hasanov E, Hormann R, Gassner R, Lepperdinger G. Osteocyte numbers decrease only in postcranial but not in cranial bones in humans of advanced age. *Ann Anat* (2019) 226:57–63. doi: 10.1016/j.aanat.2019.06.006
200. Stigler RG, Becker K, Kloss FR, Gassner R, Lepperdinger G. Long-lived murine osteocytes are embodied by craniofacial skeleton in young and old animals whereas they decrease in number in postcranial skeletons at older ages. *Gerodontology* (2018) 35:391–7. doi: 10.1111/ger.12362
201. Wood CL, Pajevic PD, Gooi JH. Osteocyte secreted factors inhibit skeletal muscle differentiation. *Bone Rep* (2017) 6:74–80. doi: 10.1016/j.bonr.2017.02.007
202. Battafarano G, Rossi M, Marampon F, Minisola S, Del Fattore A. Bone Control of Muscle Function. *Int J Mol Sci* (2020) 21:1–14. doi: 10.3390/ijms21041178
203. Bullon P, Goberna B, Guerrero JM, Segura JJ, Perez-Cano R, Martinez-Sahuquillo A. Serum, saliva, and gingival crevicular fluid osteocalcin: their relation to periodontal status and bone mineral density in postmenopausal women. *J Periodontol* (2005) 76:513–9. doi: 10.1902/jop.2005.76.4.513
204. Kersch-Schindl K, Boschitsch E, Marculescu R, Gruber R, Pietschmann P. Bone turnover markers in serum but not in saliva correlate with bone mineral density. *Sci Rep* (2020) 10:11550. doi: 10.1038/s41598-020-68442-z
205. Betsy J, Ahmed JM, Mohasin AK, Mohammed A, Nabeeh AA. Diagnostic accuracy of salivary biomarkers of bone turnover in identifying patients with periodontitis in a Saudi Arabian population. *J Dent Sci* (2019) 14:269–76. doi: 10.1016/j.jds.2019.03.002
206. Holdsworth G, Roberts SJ, Ke HZ. Novel actions of sclerostin on bone. *J Mol Endocrinol* (2019) 62:R167–85. doi: 10.1530/JME-18-0176
207. Pravitharangul A, Suttapreyasri S, Leethanakul C. Mandible and iliac osteoblasts exhibit different Wnt signaling responses to LMHF vibration. *J Oral Biol Craniofac Res* (2019) 9:355–9. doi: 10.1016/j.jobcr.2019.09.005
208. Chatzopoulos GS, Mansky KC, Lunos S, Costalonga M, Wolff LF. Sclerostin and WNT-5a gingival protein levels in chronic periodontitis and health. *J Periodontol Res* (2019) 54:555–65. doi: 10.1111/jre.12659
209. Tasdemir Z, Etoz M, Koy O, Soydan D, Alkan A. Masseter muscle thickness and elasticity in periodontitis. *J Oral Sci* (2020) 62:43–7. doi: 10.2334/josnusd.18-0341
210. de Vries TJ, Huesa C. The Osteocyte as a Novel Key Player in Understanding Periodontitis Through its Expression of RANKL and Sclerostin: a Review. *Curr Osteoporos Rep* (2019) 17:116–21. doi: 10.1007/s11914-019-00509-x
211. Kitaura H, Marahleh A, Ohori F, Noguchi T, Shen WR, Qi J, et al. Osteocyte-Related Cytokines Regulate Osteoclast Formation and Bone Resorption. *Int J Mol Sci* (2020) 21:1–24. doi: 10.3390/ijms21145169
212. Ono T, Hayashi M, Sasaki F, Nakashima T. RANKL biology: bone metabolism, the immune system, and beyond. *Inflamm Regen* (2020) 40:2. doi: 10.1186/s41232-019-0111-3
213. Dufresne SS, Dumont NA, Boulanger-Piette A, Fajardo VA, Gamu D, Kake-Guena SA, et al. Muscle RANK is a key regulator of Ca²⁺ storage, SERCA activity, and function of fast-twitch skeletal muscles. *Am J Physiol Cell Physiol* (2016) 310:C663–72. doi: 10.1152/ajpcell.00285.2015

214. Colaianni G, Storlino G, Sanesi L, Colucci S, Grano M. Myokines and Osteokines in the Pathogenesis of Muscle and Bone Diseases. *Curr Osteoporos Rep* (2020) 18:401–7. doi: 10.1007/s11914-020-00600-8
215. Sanz M, Del Castillo AM, Jepsen S, Gonzalez-Juanatey JR, D'Aiuto F, Bouchard P, et al. Periodontitis and Cardiovascular Diseases. Consensus Report. *Glob Heart* (2020) 15:1. doi: 10.5334/gh.400
216. Keire P, Shearer A, Shefer G, Yablonka-Reuveni Z. Isolation and culture of skeletal muscle myofibers as a means to analyze satellite cells. *Methods Mol Biol* (2013) 946:431–68. doi: 10.1007/978-1-62703-128-8_28
217. Aghaloo TL, Chaichanasakul T, Bezouglaia O, Kang B, Franco R, Dry SM, et al. Osteogenic potential of mandibular vs. long-bone marrow stromal cells. *J Dent Res* (2010) 89:1293–8. doi: 10.1177/0022034510378427

Conflict of Interest: The authors declare that the research was conducted in the absence of any commercial or financial relationships that could be construed as a potential conflict of interest.

The handling editor declared a past co-authorship with the authors SB, JB-M.

Copyright © 2021 Buvinic, Balanta-Melo, Kupczik, Vásquez, Beato and Toro-Ibacache. This is an open-access article distributed under the terms of the Creative Commons Attribution License (CC BY). The use, distribution or reproduction in other forums is permitted, provided the original author(s) and the copyright owner(s) are credited and that the original publication in this journal is cited, in accordance with accepted academic practice. No use, distribution or reproduction is permitted which does not comply with these terms.



Sclerostin and Osteocalcin: Candidate Bone-Produced Hormones

Jialiang S. Wang^{1†}, Courtney M. Mazur^{1†} and Marc N. Wein^{1,2,3*}

¹ Endocrine Unit, Department of Medicine, Massachusetts General Hospital, Harvard Medical School, Boston, MA, United States, ² Broad Institute of Massachusetts Institute of Technology (MIT) and Harvard, Cambridge, MA, United States, ³ Harvard Stem Cell Institute, Cambridge, MA, United States

OPEN ACCESS

Edited by:

Lilian Irene Plotkin,
Indiana University Bloomington,
United States

Reviewed by:

Stavroula Kousteni,
Columbia University, United States
Natalie A. Sims,
University of Melbourne, Australia

*Correspondence:

Marc N. Wein
mnwein@mgm.harvard.edu

[†]These authors have contributed
equally to this work

Specialty section:

This article was submitted to
Bone Research,
a section of the journal
Frontiers in Endocrinology

Received: 16 July 2020

Accepted: 13 January 2021

Published: 10 March 2021

Citation:

Wang JS, Mazur CM and
Wein MN (2021) Sclerostin
and Osteocalcin: Candidate
Bone-Produced Hormones.
Front. Endocrinol. 12:584147.
doi: 10.3389/fendo.2021.584147

In addition to its structural role, the skeleton serves as an endocrine organ that controls mineral metabolism and energy homeostasis. Three major cell types in bone - osteoblasts, osteoclasts, and osteocytes - dynamically form and maintain bone and secrete factors with systemic activity. Osteocalcin, an osteoblast-derived factor initially described as a matrix protein that regulates bone mineralization, has been suggested to be an osteoblast-derived endocrine hormone that regulates multiple target organs including pancreas, liver, muscle, adipose, testes, and the central and peripheral nervous system. Sclerostin is predominantly produced by osteocytes, and is best known as a paracrine-acting regulator of WNT signaling and activity of osteoblasts and osteoclasts on bone surfaces. In addition to this important paracrine role for sclerostin within bone, sclerostin protein has been noted to act at a distance to regulate adipocytes, energy homeostasis, and mineral metabolism in the kidney. In this article, we aim to bring together evidence supporting an endocrine function for sclerostin and osteocalcin, and discuss recent controversies regarding the proposed role of osteocalcin outside of bone. We summarize the current state of knowledge on animal models and human physiology related to the multiple functions of these bone-derived factors. Finally, we highlight areas in which future research is expected to yield additional insights into the biology of osteocalcin and sclerostin.

Keywords: osteoblast, osteocyte, osteocalcin, sclerostin, bone homeostasis

INTRODUCTION

Traditionally considered as a structural organ, the skeleton provides mechanical support and protection for soft organs and facilitates mobility. To maintain skeletal integrity, the three major cell types within bone - osteoblasts, osteocytes, and osteoclasts - remodel bone through coupled processes. Osteoclasts are multinucleated hematopoietic cells of the monocyte-macrophage lineage that resorb bone along its surfaces (1). Osteoblasts originate from mesenchymal progenitor cells and produce bone matrix proteins to facilitate bone formation on the surface (2, 3). Some osteoblasts acquire long dendritic processes and embed within bone to become terminally-differentiated

osteocytes (4). Osteocytes remodel their surrounding bone matrix and orchestrate the activity of osteoblasts and osteoclasts (4).

One way that osteoblasts, osteocytes, and osteoclasts communicate is through production of paracrine signaling molecules that act on neighboring cells. Well known bone-derived paracrine factors include sclerostin (osteocyte-derived inhibitor of Wnt signaling), receptor activator of NF- κ B ligand (RANKL, a key regulator of osteoclast differentiation produced mainly by mesenchymal osteoblast-lineage cells), monocyte/macrophage colony stimulating factor (M-CSF, osteoblast-derived stimulator of myeloid cell survival and osteoclastogenesis) and osteoprotegerin (OPG, osteoblast-derived inhibitor of osteoclastogenesis) (5–10). Beyond well-established bone-derived paracrine-acting factors that participate in cross-talk between cell types within bone, bone-derived *endocrine* factors have also been reported.

Other than its classic structural role, the paracrine and endocrine functions of bone are essential for organismal homeostasis. Fibroblast growth factor 23 (FGF-23) is mainly secreted by osteoblasts and osteocytes and plays an important role in regulating phosphate homeostasis (11). Osteocalcin (OCN), the most abundant non-collagenous bone matrix protein, is produced specifically by osteoblasts and is suggested to regulate the biological processes of multiple organs including bone, brain, liver, pancreas, testes, muscle, the parasympathetic nervous system, and adipose tissue (11). Recent studies demonstrate that osteoblast-derived lipocalin 2 (LCN2) regulates glucose tolerance, insulin sensitivity, and insulin secretion to maintain glucose homeostasis (12). In addition to its paracrine roles, effects of sclerostin on adipose tissue and mineral metabolism have also been reported recently, with an additional possible role in preventing vascular calcification (13–15). Given the established role of FGF-23 in regulating renal phosphate handling and the relatively limited information on LCN2, this review will focus on osteocalcin and sclerostin. Here, we will bring together the recent data on osteocalcin and sclerostin in bone and distant target organs, primarily focusing on important new insights into the role of these circulating factors learned from animal models.

OSTEOCALCIN

Osteocalcin, or bone γ -carboxyglutamic acid (Gla) protein, is an osteoblast-derived circulating protein. Osteocalcin is initially synthesized as a prohormone (95 amino acids) and then cleaved to form the mature peptide (46 amino acids) that contains three γ -carboxyglutamic acid residues at positions 13, 17 and 20 (16). In human, the mature peptide has 49 amino acids and is γ -carboxylated at positions 17, 21 and 24 (17). γ -carboxylation increases the affinity of osteocalcin to the mineral component of the extracellular matrix. This leads to the accumulation of γ -carboxylated osteocalcin in bone (18). Osteoclast resorption, on the other hand, creates an acidic environment where osteocalcin is de-carboxylated. Under-

carboxylated osteocalcin has lower affinity to bone matrix and is released into the bloodstream where it can function as an endocrine hormone (19, 20).

OCN is encoded by a single gene (*BGLAP*) in human, while mice have a cluster of three genes (*Bglap*, *Bglap2*, and *Bglap3*) within a 25 kb genomic region (21–23). *Bglap* and *Bglap2* are highly expressed in bone, while *Bglap3* has a relatively lower expression in bone, but higher expression in kidney and lung (23–25). The amino acid sequences of γ -carboxylated Ocn encoded by *Bglap* and *Bglap2* are identical. The sequence encoded by *Bglap3* is different from the sequences encoded by *Bglap* and *Bglap2* by four amino acid residues (26).

OSTEOCALCIN IN SKELETAL DEVELOPMENT

To study and understand the role of osteocalcin in bone formation, Karsenty and colleagues generated the first *Ocn*-deficient mouse (*Osc⁻/Osc⁻*) in 1996 (27). Mice homozygous for the deletion of *Bglap* and *Bglap2* were generated in embryonic stem (ES) cells by homologous recombination. Exon4 of *Bglap* and the entire sequence of *Bglap2* were replaced by a PGK-Neo cassette. *Osc⁻/Osc⁻* pups are viable, fertile and there are no skeletal defects at birth. At 6 and 9-months of age, osteocalcin null mice showed significantly increased bone mass, bone strength and bone formation, without changes in osteoblast numbers or bone resorption. A subsequent study on the role of osteocalcin in extracellular matrix using fourier-transform infrared imaging (FTIR) showed larger hydroxyapatite crystal size (28). More recently, it was reported that osteocalcin null mice on a pure C57BL/6J background show increased carbonate-to-mineral ratio in cortical bone (29).

More recently, studies of two independently-generated osteocalcin knockout mouse models were published in *PLOS Genetics*. In an article by Diegel and colleagues, the authors generated a *Bglap* and *Bglap2* double-knockout (*Bglap2^{dko/dko}*) strain using CRISPR/Cas9-mediated gene editing (26). More specifically, they designed guide RNAs that target *Bglap* and *Bglap2*, but not *Bglap3*. In one founder allele, a 6.8-kb fragment was deleted which leads to a functional junction between exon 2 of *Bglap* to exon 4 of *Bglap2*. The authors reported no differences in bone mass or bone strength between homozygous mutants and wild-type mice. Further FTIR analysis revealed that *Bglap2^{dko/dko}* mice have increased crystal size and higher carbonate-to-mineral ratio. Moriishi and colleagues also reported a novel *Ocn* knockout strain (*Ocn^{-/-}*) using homologous recombination by replacing the genomic region encompassing *Bglap* and *Bglap2* with the gene conferring neomycin resistance (30). Both trabecular and cortical bone mass are similar in wild-type and *Ocn* knockout mice. While most skeletal parameters analyzed were normal, these authors did observe disrupted orientation of hydroxyapatite crystals along collagen fibrils in their *Ocn^{-/-}* strain.

Several possible explanations exist for differences in skeletal phenotypes among three osteocalcin knockout models, including mouse genetic background, sex, differences in age of analysis,

effects of mutated alleles on neighboring genes and, potentially, technical differences between homologous recombination and CRISPR/Cas9-mediated gene editing. In all 3 osteocalcin-null models, complete genome sequencing has not been performed, which leaves open the possibility that ‘off-target’ effects related to traditional or CRISPR/Cas9-mediated target gene modification may drive phenotypic differences. Though the specificity of Cas9 is determined by the 20-base pair (bp) sequence of the sgRNA and the NGG trinucleotide (the protospacer-adjacent motif, PAM) adjacent to the target sequence, off-target mutations can be induced at sites that differ slightly from the on-target sites (31–33). Sensitive and comprehensive approaches are therefore required to detect off-target sites. Currently developed and widely-adapted methods include deep sequencing, web-based in silico prediction tools, and ChIP-seq (34–37). Compared to CRISPR-Cas9 gene editing, conventional homologous recombination leads to rare off-target effects (38). Whole genome sequencing of all three osteocalcin mutant mouse strains may therefore prove useful to clarify potential differences between these models at the level of locus modification and potential off-target changes. *Osc*^{−/−} mice from Karsenty and colleagues were initially generated and characterized in the mixed BL6/129 background; more recently, studies related to energy metabolism, male fertility and neurobiology on that studies have been performed on a ‘pure’ 129 background (39–41). *Bglap*/*2*^{dko/dko} mice generated by Diegel and colleagues were on a mixed BL6/C3H background

(back-crossed to C57BL/6 for 2 generations). *Ocn*^{−/−} mice were generated in the pure C57BL/6 background by Moriishi and colleagues. Studies from Berezovaska and colleagues do support genetic background as a contributing factor to different osteocalcin null phenotypes (29). When *Osc*^{−/−}/*Osc*^{−/−} mice were backcrossed to pure C57BL/6J mice (more than 8 generations), reduced bone strength was observed. Other than genetic background, Moriishi et al. used mice with different ages and sexes compared to *Osc*^{−/−}/*Osc*^{−/−} mice generated by Karsenty and colleagues.

In summary, there are both consistent and inconsistent findings when comparing skeletal traits in the three reported osteocalcin knockout mouse models (Figure 1). Beyond some questions about the role of osteocalcin in bone, different potential roles of osteocalcin as an endocrine factor will be discussed below in detail. At present, additional work is needed to clarify this active controversy (42–45). Potential future strategies that could be considered to address this controversy might include a blinded, side-by-side comparison of the 3 different osteocalcin-null models with appropriate age- and sex-matched littermate controls. This approach may help to tease apart the relative role of methodological differences in assessing metabolic phenotypes (see below) versus inherent intrinsic differences between different osteocalcin mutant strains in driving different observations. An additional, constructive approach may be to backcross to ‘purity’ all mouse models on the same genetic background and then rigorously re-analyze each model.





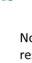
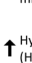






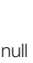


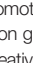


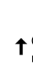






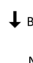
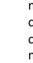
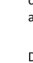




 <i>Osc</i> ^{−/−} (Ducy et al: cited by 1738)		 <i>Bglap</i> / <i>2</i> ^{dko/dko} (Diegel et al: cited by 8)		 <i>Ocn</i> ^{−/−} (Moriishi et al: cited by 20)	
C57BL6 x 129 mixed background Homologous recombination: delete <i>Bglap</i> (exon4) and <i>Bglap2</i>		C57BL6 background (backcross 2 generations) CRISPR/Cas9: join <i>Bglap</i> (exon2) and <i>Bglap2</i> (exon4)		C57BL6 background Homologous recombination: delete <i>Bglap</i> and <i>Bglap2</i>	
Skeleton	Endocrine	Skeleton	Endocrine	Skeleton	Endocrine
 ↑ Bone mass  ↑ Bone strength  ↑ Bone formation No change in bone resorption and mineralization  ↑ Hydroxyapatite (HA) crystal size	 ↑ Glucose level  ↓ Insulin synthesis  ↓ β-cell proliferation  ↑ lipids  ↑ Body fat  ↓ Muscle weight  ↓ Testis size  ↓ Testis weight  ↓ Testosterone level	 No change in: bone mass, bone strength, bone formation, bone resorption  ↑ Hydroxyapatite crystal size  ↑ Carbonate-to-mineral ratio	 No change in: glucose level  N/A  No change in: body fat  N/A  No change in: testis size, testosterone level	 No change in: bone mass, bone formation, bone resorption  ↓ Bone strength  No change in: mineralization, crystallinity, carbonate-to-mineral ratio, collagen fiber alignment  Disrupted axis orientation of HA  N/A  No change in: body fat  No change in: muscle weight  No change in: testis size, testosterone level, spermatogenesis	

FIGURE 1 | Summary of three osteocalcin null mouse models and their observed phenotypes in different tissues. Karsenty and colleagues generated the first *Ocn*-deficient mouse (*Osc*^{−/−}) in 1996. *Bglap* and *Bglap2* were deleted in embryonic stem cells using homologous recombination. Diegel and colleagues generated the *Bglap* and *Bglap2* double-knockout (*Bglap*/*2*^{dko/dko}) strain using CRISPR/Cas9-mediated gene editing. Moriishi and colleagues generated the novel *Ocn* knockout mouse (*Ocn*^{−/−}) using homologous recombination by replacing the genomic region encompassing *Bglap* and *Bglap2* with the neomycin resistant gene. *Osc*^{−/−} mice showed increased bone mass and bone formation, while *Bglap*/*2*^{dko/dko} and *Ocn*^{−/−} mice showed similar bone mass/formation compared to their control littermates. Many investigators reported the endocrine role of osteocalcin by studying *Osc*^{−/−} mice. Circulating osteocalcin stimulates β-cell proliferation and insulin synthesis in pancreas. Under-carboxylated osteocalcin may also increase insulin sensitivity in adipose tissue and liver. Elevated osteocalcin increases nutrient uptake in muscle and exercise capacity. In addition, osteocalcin promotes male fertility by increasing testosterone synthesis. However, initial analyses on *Bglap*/*2*^{dko/dko} and *Ocn*^{−/−} mice demonstrated that osteocalcin has no effect on glucose level, body fat, muscle weight, and testis size. N/A, not assessed. This figure was created using Servier Medical Art templates, which are licensed under a Creative Commons Attribution 3.0 Unported License; <https://smart.servier.com>

OSTEOCALCIN IN ENERGY METABOLISM (PANCREAS, LIVER, ADIPOSE AND MUSCLE)

The first demonstration of a potential endocrine function of osteocalcin came with the description that *Osc*^{-/-} mice have high blood glucose levels, increased fat mass, glucose intolerance due to decreased insulin synthesis and beta cell proliferation, and insulin resistance (39). In contrast, *Esp*^{-/-} mice with ablation of osteo-testicular protein tyrosine phosphatase have opposite metabolic phenotypes as *Osc*^{-/-} animals: decreased fat mass, increased β -cell proliferation and enhanced insulin sensitivity (46, 47). The authors went on to show that *Esp*^{-/-} mice exhibit a gain-of-function of osteocalcin phenotype since the encoded phosphatase is a negative regulator of osteocalcin activation. *Esp*-deficient mice have decreased γ -carboxylated osteocalcin and therefore show increased serum osteocalcin levels. Further studies showed that exogenous un-carboxylated osteocalcin can also increase glucose tolerance and insulin sensitivity (39, 48, 49). Reciprocal regulation of osteocalcin by insulin has also been demonstrated: insulin-treatment of MC3T3-E1 cells increased osteocalcin promoter activity and gene expression (50). Mice with deletion of the insulin receptor from osteoblasts show increased body fat, impaired glucose metabolism, reduced levels of circulating uncarboxylated osteocalcin, and impaired insulin sensitivity (49, 50). These analyses suggest a bone-pancreas endocrine loop where insulin induces osteocalcin expression and then in turn promotes insulin secretion. The receptor *Gprc6a* may mediate the osteocalcin function in pancreatic islets. *In vivo*, *Gprc6a*^{-/-} pancreas showed decreased β -cell mass, β -cell proliferation and impaired capacity of insulin secretion (48). However, Diegel and colleagues showed no differences in blood glucose (with or without fasting) and body weight between *Bglap*/*2*^{dko/dko} and wild-type littermates (26). These phenotypes align with previous reports on *Bglap* knockout rats. Osteocalcin null rats exhibit no change in glucose levels and insulin resistance (51). Moriishi and colleagues also examined the role of osteocalcin in glucose metabolism and observed similar blood glucose between *Ocn*^{-/-} and wild-type mice in both sexes at all ages. Both glucose tolerance tests (GTTs) and insulin tolerance tests (ITTs) showed no change of serum glucose levels in *Ocn*^{-/-} mice in both sexes, at all ages and with both normal and high fat diet fed animals (30).

At present there is no unifying explanation to account for these apparently discrepant findings. A large body of evidence published in high quality, peer-reviewed journals strongly supports a role for osteocalcin in regulating energy metabolism (43, 52). The recent CRISPR/Cas9-generated osteocalcin-null models reported limited numbers of mice analyzed for analysis of glucose metabolism phenotypes. As detailed above, a 'contemporaneous replication' strategy (53), if possible, may be helpful to build confidence in potentially-controversial preclinical findings. In addition, in an important perspective relevant to this issue, the topic of inter-lab variability in the setting of preclinical energy metabolism models has recently been addressed in a productive manner by top scientists from the pharmaceutical industry (54). As noted above, differences in

strain background and off-target effects may play an important role in driving different observations between osteocalcin mutant strains reported to date. In addition, important methodologic differences must be acknowledged in how metabolic phenotypes were assessed in the 'newer' osteocalcin mutant strains versus the extensive metabolic phenotyping performed by Karsenty and colleagues over many years and multiple publications. For example, Diegel and colleagues measured fasting blood glucose in n=8-11 six month old *Bglap*/*2*^{dko/dko} mice, without measuring insulin levels, performing dynamic testing such as oral glucose tolerance tests or insulin tolerance tests, or investigating glucose-related phenotypes at other ages (26). Moriishi et al. did perform dynamic testing (30), though methodologic differences appear to exist between doses of glucose and insulin used in their studies versus those previous reported by Karsenty and colleagues (39). In addition, it is possible that differences in housing conditions (bedding, animal diet, local microbiome), sex of mice analyzed, and experimental sample size may be present between the different studies as well. These same methodologic issues may contribute to differences noted between strains with respect to assessment of fertility and gonadal hormone levels. **Figure 1** summarizes the currently-available mouse osteocalcin mutant models.

In addition to glucose intolerance and insulin resistance, *Osc*^{-/-} *Osc*^{-/-} mice showed liver steatosis, adipose tissue inflammation, and reduced exercise capacity (46, 47). Since osteocalcin knockout mice (*Osc*^{-/-}/*Osc*^{-/-}) showed accumulation of body fat, several research groups examined the role of *Ocn* as a potential mediator of crosstalk between bone and adipose tissue. The direct role of osteocalcin in adipocytes was demonstrated first through *in vitro* analyses. *In vitro* uncarboxylated osteocalcin treatment of adipocytes increased the expression of peroxisome-proliferator-activated receptor γ (master regulator of adipogenesis) and adiponectin (an adipokine that regulates glucose and lipid metabolism) via the *Gprc6a* receptor (49, 55). *In vivo* treatment of mice with recombinant osteocalcin can also upregulate adipocyte adiponectin in white and brown adipose tissues (46). Though *Gprc6a*^{-/-} mice also had increased fat mass, further studies are needed to reveal whether osteocalcin interacts with *Gprc6a* or other potential receptors in adipose tissue (56). Two studies reported that adiponectin plays a role in regulating insulin sensitivity in high fat diet-fed mice (57) and adiponectin can regulate bone mass in normal diet-fed mice without affecting glucose levels (58). It still remains unknown how osteocalcin affects fat mass. Uncarboxylated osteocalcin treatment can promote the expression of adipose triglyceride lipase (ATGL) and further lead to the induction of lipolysis though the cAMP-PKA-ERK-CREB signaling *in vitro* (59). Livers in *Osc*^{-/-}/*Osc*^{-/-} mice show accumulation of lipids and steatosis (49). Mice treated with osteocalcin have no accumulation of lipids and show normal liver morphology though fed with high fat diet (60, 61). The current understanding of how osteocalcin regulates lipid accumulation is still unclear. One potential mechanism is through the receptor *Gprc6a* since *Gprc6a*^{-/-} mice also develop hepatic steatosis (56).

Ocn-deficient (*Osc*^{-/-}/*Osc*^{-/-}) mice show reduced muscle mass (62). To further investigate the role of osteocalcin in muscle, the

receptor *Gprc6a* was conditionally deleted in myofibers using *Mck-Cre* (63). *Gprc6a* may also serve as the osteocalcin receptor in skeletal muscle since *Gprc6a*-deficient mice have impaired exercise capacity and are resistant to osteocalcin treatment (56, 63, 64). The analysis showed that osteocalcin is necessary to increase exercise capacity. The level of circulating under-carboxylated osteocalcin increases during exercising. The increasing *Ocn* can increase nutrient uptake and ATP production. The potential mechanism of osteocalcin in regulating muscle function is by promoting the expression of interleukin-6 (IL-6) (65). Increased IL-6 level results in bone resorption and in turn, de-carboxylates osteocalcin (66). These studies outline a feed-forward loop between bone and muscle. Further, both *Ocn* levels and muscle mass decrease with aging. Treatment with osteocalcin augments exercise capacity in both young and old mice (63, 64). This suggests that osteocalcin is necessary and sufficient to maintain/increase muscle mass in older mice. However, Moriishi et al. recently showed that there are no differences in muscle weight or fiber area between *Ocn*^{-/-} mice and wild-type littermates (30).

Another recent review also addressed some of the controversial actions of uncarboxylated osteocalcin in adipocytes and hepatocytes (26, 30). Although recombinant osteocalcin does show intriguing effects, another possibility is that osteocalcin-deficient mice might acquire compensatory mechanisms during development. For example, *Gprc6a* may use other ligands instead of osteocalcin. Similar to osteocalcin null mice, *Gprc6a* deficient mice also showed discrepancies in the metabolic functions as reported by different laboratories (30).

OSTEOCALCIN IN MALE FERTILITY

A distinct role of osteocalcin as an endocrine factor related to male fertility has been described. Oury and colleagues were the first to show that osteocalcin favors male fertility (41). Male *Osc*⁻/*Osc*⁻ mice have lower litter frequencies, testis size and weights, and testosterone levels. These phenotypes caused by osteocalcin deficiency could be rescued by supplementing male mice with exogenous, uncarboxylated osteocalcin. Moreover, in the gain-of-function model of osteocalcin [*Esp*^{-/-}, (40, 48, 67)], hyperandrogenism is noted. The study further identified the G-protein coupled receptor *Gprc6a* as the receptor for mediating testosterone synthesis. Mice lacking *Gprc6a* in Leydig cells showed decreased testis size, weight and testosterone levels. The role of osteocalcin in modulating male reproduction was also identified in humans by examining patients with primary testicular failure due to *GPRC6A* mutations (68). However, both Diegel et al. and Moriishi et al. showed discrepant results compared to Karsenty group regarding the role of osteocalcin in male fertility (*Bglap*/*2*^{dko/dko} and *Ocn*^{-/-}) (26, 30). Diegel and colleagues reported that there are no differences in testis size and blood testosterone levels between *Bglap*/*2*^{dko/dko} and wild-type mice. Moriishi and colleagues also demonstrated that testis size, serum testosterone levels, testosterone synthesis and spermatogenesis are normal in *Ocn*^{-/-} mice compared to wild-

type mice. As discussed in detail above, side-by-side analysis of distinct strains of osteocalcin-deficient mice may be helpful to resolve the role of osteocalcin in male fertility in mice. In addition, careful review of potential methodologic differences between studies may help clarify these apparent discrepancies. Moreover, identification of additional humans with rare and common osteocalcin/*GPRC6A* variants linked to male fertility phenotypes is needed to further understand the role of osteocalcin as an LH-independent regulator of testicular testosterone synthesis. Additional (non-osteocalcin) ligands for *Gprc6a* have been proposed. As such, an improved structure/function understanding of how this receptor control Leydig cell testosterone synthesis, and how *Gprc6a* variants affect the function of this receptor (69), is needed (70).

OSTEOCALCIN IN THE CENTRAL AND PERIPHERAL NERVOUS SYSTEM

Studies on a potential role for osteocalcin in the central nervous system (CNS) were prompted by the initial observation that *Osc*⁻/*Osc*⁻ mice displayed an extremely passive phenotype during routine animal handling (27). Since this phenotype was present in both male and female mice, it was unlikely to be related to male-specific hypogonadism discussed above. Rather, it was noted that under-carboxylated osteocalcin could cross the blood-brain barrier where it accumulated in the midbrain and brainstem. Formal behavioral testing revealed anxiety-like phenotypes with learning defects in *Osc*⁻/*Osc*⁻ mice (41). Neuroanatomic analysis of brains from *Osc*⁻/*Osc*⁻ mice showed hippocampal atrophy (specifically in the dentate gyrus region) with frequent absence of the corpus callosum. These neuroanatomic abnormalities were associated with dramatic changes in overall CNS neurotransmitter levels: *Osc*⁻/*Osc*⁻ mice show reduced brainstem monoamines and increased GABA levels. At the electrophysiologic level, *Osc*⁻/*Osc*⁻ mice show increased activation potential of brainstem neurons in the locus coeruleus. Direct delivery of recombinant uncarboxylated osteocalcin into the CNS corrected molecular and phenotypic abnormalities in *Osc*⁻/*Osc*⁻ mice. Interestingly, the role of osteocalcin in CNS development seems to be due to the ability of circulating maternal uncarboxylated osteocalcin to cross the placenta and the fetal blood-brain barrier. In humans, decreased circulating osteocalcin levels are associated with poor cognitive performance (71, 72). Highlighting the potential function of CNS-active uncarboxylated osteocalcin to restore cognitive function in aging, injection of plasma from young control, but not *Osc*⁻/*Osc*⁻ mice improved cognitive function and anxiety-related behaviors in aged mice. Osteocalcin appears to accomplish these effects by promoting synaptic transport of vesicles containing the neurotrophic factor BDNF in a pathway in hippocampal neurons involving the histone binding protein RbAp48 (73, 74).

While the peripheral extra-skeletal functions of osteocalcin appear to be mediated via *GPRC6A*, osteocalcin uses a distinct G protein coupled receptor to regulate neurons in the central and

peripheral nervous system. GPR158 is a neuronally-expressed class C GPCR required for the CNS effects of osteocalcin. Mice lacking this GPCR in brain show similar learning defects and anxiety-related phenotypes as *Osc⁻/Osc⁻* mice, and studies using compound heterozygotes for both genes show that they function in a similar genetic pathway (73). In neurons, GPR158 signals through a Gαq-dependent pathway to promote IP₃ generation. It remains possible that additional CNS osteocalcin receptors exist since the pattern of GPR158 expression does not perfectly match the pattern of CNS uncarboxylated osteocalcin binding.

In addition to its proposed role in the central nervous system, more recently it has also been reported that osteocalcin regulates output of parasympathetic neurons during the “fight or flight” (acute stress) response (ASR) (75). Exposure of rodents and humans to stressful stimuli acutely increases circulating bioactive osteocalcin levels in a manner dependent on the amygdala. Interestingly, treatment of osteoblasts with the excitatory neurotransmitter glutamate rapidly increases osteocalcin production, and glutamatergic nerve terminals can be found immediately adjacent to osteoblasts in bone. Therefore, the model emerges that the ASR increases sympathetic input to bone which in turn rapidly promotes osteoblastic osteocalcin production. In the ASR, *Osc⁻/Osc⁻* mice show blunted physiologic changes such as heat generation, increased oxygen consumption, and increased serum glucose levels. Osteocalcin promotes the acute stress response by binding to GPRC6A expressed in parasympathetic neurons. Upon binding to parasympathetic nerves, osteocalcin inhibits their firing and blunts parasympathetic tone and therefore promotes sympathetic output in the ASR. By linking bone and the acute stress response, osteocalcin may serve as an endocrine link between the ability of an organism to quickly run away from danger and promote physiologic changes to facilitate this rapid response (75).

Taken together, this line of investigation supports a role for bone-derived osteocalcin as a factor that modulates brain development and function, thereby linking bone homeostasis with whole body physiology and higher order cognitive functions (76). That being said, careful review of potential neuronal functions of osteocalcin in independent models, as reviewed above, will be helpful to build confidence in these findings. Future studies are needed to better define the role of the putative CNS osteocalcin receptor GPR158 in human nervous phenotypes, and to explore whether other CNS osteocalcin receptors may exist.

SCLEROSTIN

Sclerostin is a secreted glycoprotein expressed predominantly by mature osteocytes that is best known as a negative regulator of bone formation (77). Sclerostin was originally discovered because of inactivating mutations in the coding and enhancer regions of the *SOST* gene that cause the rare high bone mass disorders sclerosteosis and van Buchem disease (78). Although sclerostin was initially described as a BMP antagonist (79, 80), it

is now primarily studied as a negative regulator of Wnt signaling (81). Sclerostin antagonizes Wnt signaling by occupying Wnt coreceptors LRP5/6 and preventing their binding to Wnt ligands, which inhibits downstream canonical Wnt signaling (78, 82). Sclerostin also binds directly to LRP4, a membrane-bound protein that facilitates its interactions with LRP5/6 (83). Since active canonical Wnt signaling promotes osteogenic differentiation and osteoblast maturation and survival, low sclerostin expression leads to bone anabolism whereas high expression inhibits bone formation (77). The regulation of sclerostin in bone in response to mechanical and biochemical cues and its role in regulating bone homeostasis has been reviewed elsewhere (79, 80).

The possibility that sclerostin can exert endocrine effects on non-skeletal tissues is inspired by the detection of sclerostin protein in circulation. Whereas sclerosteosis patients have no detectable protein in circulation, heterozygous carriers of *SOST* mutations have serum sclerostin levels approximately half that of control subjects (84) and bone mineral density (BMD) values higher than age-matched controls (85). In mice, sclerostin overexpression in the liver causes increases in serum sclerostin and loss of trabecular bone mass (86). Dozens of clinical studies have reported correlations between serum sclerostin levels and age, sex, bone mass, and disease (87). While most studies agree that circulating sclerostin increases with age (88–90), puzzling inconsistencies and contradictions exist, such as reports of both positive (89, 91, 92) and negative (93) associations between serum sclerostin and bone mass. The extent to which sclerostin measured in serum typically represents an active mediator of Wnt signaling versus a biomarker of ongoing disease (discussed more later), remains to be determined.

Bona fide endocrine effects of sclerostin would require that the protein be transported from the cell of origin to distant tissues. Sclerostin is a marker of mature osteocytes, and the osteocyte lacuno-canalicular network provides a pathway for secreted osteocyte factors to enter the circulation (94, 95). Inactivation of the *Sost* gene in mice with osteoblast and osteocyte-targeted Cre recombinases results in undetectable serum sclerostin, suggesting that osteocytes are the primary source of sclerostin in circulation (96). At least two clinical studies have found that circulating sclerostin does not correlate with *SOST* mRNA in bone biopsies (91, 97). However, the relationship between serum sclerostin and mRNA in bone biopsies is inherently sensitive to the mechanical environment of the biopsy site, the cortical/cancellous composition of the biopsy, and differences in clearance rates between subjects, so these studies do not necessarily detract from the animal work demonstrating that osteocytes are the primary source of circulating sclerostin. It is worth noting that *Sost* ablation with Prx1-Cre-mediated recombination does not fully reduce serum sclerostin, likely due to contributions from osteocytes in the axial skeleton. However, the high bone mass phenotype in the appendicular skeleton of these mice matches that seen with systemic *Sost* deletion better than *Dmp1*- and *Col1*-Cre models (96). Together these models indicate that sclerostin regulates bone mass through primarily paracrine signaling from

osteoblasts, osteocytes, and additional cells derived from the limb mesenchyme. At various points in normal development and in disease, low levels of *SOST* mRNA or sclerostin protein have been detected in additional locations including cementocytes, hypertrophic chondrocytes, synovial fibroblasts, vascular smooth muscle cells, and kidney (79, 80, 98). There is no evidence to date to support that cells other than osteocytes contribute significantly to sclerostin in the circulation.

While questions remain regarding the accuracy and utility of measuring circulating sclerostin, many groups have gone on to test hypotheses regarding the role of sclerostin on non-bone tissues. Here we review the effects of sclerostin on adipose tissue, renal mineral metabolism, and the cardiovascular system. As more evidence is gathered to determine whether bone-derived sclerostin is implicated in these outcomes, the endocrine capacity of sclerostin will be decided.

SCLEROSTIN IN ADIPOGENESIS

Wnt signaling plays a key role in mesenchymal progenitor differentiation. Activation of Wnt signaling drives osteogenic differentiation of early mesenchymal precursors, while suppression of Wnt signaling promotes adipogenesis (99). Through its interactions with LRP4/5/6, sclerostin inhibits canonical Wnt signaling and could therefore stimulate adipogenesis. Studies of body adiposity in sclerosteosis patients have not been reported, and clinical descriptions that discuss patient weight compared to control subjects attribute slight increases to the extreme density of the skeleton (100). Nevertheless, correlations between circulating sclerostin and fat mass or metabolic disorders have inspired investigations into possible endocrine effects of sclerostin on adipose tissue.

Clinical Evidence

Clinical studies demonstrate that serum sclerostin levels are positively correlated with fat mass and incidence of metabolic disorders. Serum sclerostin is positively correlated with abdominal fat mass, android and gynoid fat mass, and body mass index (BMI) in men and women (89, 92, 101) and with vertebral bone marrow fat content in men (102). Men and women with type 2 diabetes have significantly higher serum sclerostin than non-diabetic controls (103–105). Even in prediabetes, when insulin resistance and secretion are first altered, circulating sclerostin is elevated and positively correlated with fasting glucose production and metrics of insulin resistance (106). Inactivating mutations in *LRP6*, as well as single nucleotide polymorphisms (SNPs) in *LRP5* that are associated with low bone mass, are correlated with increases in metabolic syndrome and diabetes in humans, similar to mice that overexpress sclerostin (13, 107, 108). Individuals with a gain of function mutation in *LRP5* that causes high bone mass have decreased upper-to-lower body fat ratio and increased insulin sensitivity, consistent with the metabolic phenotype of mice that do not express *Sost* (13, 107). These studies support a role for sclerostin and Wnt signaling in the regulation of adipose tissue

and whole-body metabolism, but they need to be interpreted with caution for several reasons.

First, cross-sectional/case-control studies are insufficient to demonstrate causal relationships between sclerostin levels and disease phenotypes. While individual-level data allows strong correlations to be drawn, these human studies lack interventions that would help to rule out confounding variables. None of the clinical trials evaluating therapeutic sclerostin-neutralizing antibodies (Scl Ab) to date report fat mass or insulin resistance as outcomes. This interventional design would be ideal for assessing the effects of sclerostin in humans. Second, the accuracy and consistency of assays for circulating sclerostin is not well established. Significantly different sclerostin concentrations have been found in serum and plasma from the same patients using three different assays (87). When two commercially available assays were compared directly, they also produced significantly different results (109). Care must therefore be taken when conducting meta-analyses of studies that utilize different sclerostin assays, and individual studies would ideally use a consistent assay for all subjects and report their validation strategy. Third, the extent to which circulating sclerostin levels represent active protein is not entirely certain. In cross-sectional studies, circulating sclerostin is often positively correlated with BMD even though high sclerostin levels would be expected to suppress bone formation (89, 91, 92). Mendelian randomization studies clarified this relationship, showing that high serum sclerostin is causally related to low BMD and that high BMD causes high serum sclerostin (93). In this case, serum sclerostin measurements may include both bioactive molecules and biomarkers of osteocyte activity. Furthermore, most studies do not investigate whether changes in serum sclerostin arise from changes in skeletal production or in renal clearance. Therefore, serum sclerostin levels and metabolic disorders may both reflect underlying differences in kidney function rather than pathogenic overproduction of sclerostin. Fourth, serum sclerostin measurements may be disrupted when Scl Ab is administered. Several animal studies that measure serum sclerostin after treatment with Scl Ab report increases in circulating sclerostin even though β -catenin activity and bone mass increase (13, 110). One potential explanation is that the antibodies used to quantify serum sclerostin detect the protein whether it is biologically active or bound and inactivated by the therapeutic neutralizing antibody (110). Well-controlled interventional studies will be needed in order to reliably correlate bioavailable sclerostin with the endocrine functions it exerts.

In Vitro Evidence

In vitro experiments have demonstrated the direct effects of sclerostin on adipogenesis in primary and immortalized cells. Sclerostin positively regulates the differentiation of the 3T3-L1 preadipocyte cell line. Treatment with recombinant sclerostin or with osteocyte conditioned media increases expression of adipogenic transcription factors *Pparg* and *Cebpa* and increases lipid accumulation as measured by oil red O staining (111, 112). Primary adipocytes treated with recombinant sclerostin respond

by increasing expression of adipocyte differentiation markers, increasing fatty acid synthesis, and increasing oil red O staining. Primary cells also reduce their metabolism of fatty acids in response to sclerostin, as evidenced by downregulation of genes such as *Cpt1a* and reduced oleate oxidation (13, 113). Mesenchymal stromal cells from mouse bone marrow, mouse ear tissue, and human bone marrow also respond to treatment with recombinant sclerostin and osteocyte conditioned media with increased expression of *Cebpa* and *Pparg* and increased oil red O staining (111). Thus when isolated *in vitro*, sclerostin consistently stimulates adipocyte differentiation and increases cell lipid content through enhanced fatty acid synthesis and reduced catabolism.

Evidence From Animal Studies

The positive regulation of adipogenesis by sclerostin is further supported by studies of white adipose tissue and metabolism in animals. Mice with systemic ablation of *Sost* (*Sost*^{-/-} mice) have lower overall fat mass as measured by qNMR and reduced mass of white adipose tissue from gonadal, inguinal, and retroperitoneal fat pads. Within the white adipose tissue of *Sost*^{-/-} mice, individual adipocytes were also smaller, and Wnt target genes were upregulated (13). In mice injected with an AAV causing overexpression of sclerostin the same relationship was supported; *Sost*-AAV-treated mice had significantly increased fat mass, increased weight of individual fat pads, increased adipocyte size, and down-regulation of Wnt target gene expression in white adipose tissue depots (13).

The effects of sclerostin on white adipose tissue *in vivo* appear to be both pro-anabolic and anti-catabolic. Genes associated with adipocyte differentiation and lipid synthesis were increased in fat pads from mice treated with *Sost*-AAV and downregulated in *Sost*^{-/-} mice (13). Fatty acid synthesis, as measured by ³H-acetate incorporation, was also reduced in *Sost*^{-/-} mice. At the same time, genes associated with fatty acid oxidation and markers of beige adipocytes, such as *Cpt1a*, *Ppargc1a*, and *Ucp1*, were increased when *Sost* was ablated. Beige adipocytes are cells in white adipose tissue that express UCP1 and take on a thermogenic brown adipocyte-like phenotype with improved insulin sensitivity and glucose metabolism (114). *Sost*^{-/-} mice and Scl Ab-treated mice (1 dose/week, 30 mg/kg, 8 weeks) show increased oxidation of the fatty acid oleate in adipose tissue explants (13). These findings are in agreement with *in vitro* studies on primary and immortalized adipocytes. However, they do not demonstrate whether sclerostin predominantly acts on adipocytes or on mesenchymal progenitor cells to induce adipogenesis.

The ability of sclerostin to act directly on adipose tissue *in vivo* was investigated in mice made conditionally insensitive to sclerostin with deletion of *Lrp4* from white and brown adipocytes (83). These mice showed small adipocytes with reduced expression of *Cebpa*, though fat mass and weight of individual fat pads was not affected. By further reducing sclerostin availability with compound heterozygous mice expressing one allele of *Lrp4* in adipocytes and one allele of *Sost* systemically, fat mass and adipocyte size were reduced (113). Two studies found that deletion of *Lrp4* from osteoblast-lineage cells leads to high

bone mass and increased circulating sclerostin, due to either increased sclerostin production in bone or the loss of local sequestration by LRP4 (113, 115). This model of high circulating sclerostin also increased fat mass in white adipose tissue depots (113). These studies indicate that sclerostin can act directly on adipocytes *in vivo*, but progenitor cells targeted by circulating sclerostin during development likely also contribute to the full white adipose tissue phenotype of mice with systemic *Sost* overexpression or ablation.

Sclerostin may also play a broader role in metabolism in mice. Feeding wild-type mice with a high fat diet for 4 or 8 weeks leads to increased white adipose tissue mass, increased *Sost* mRNA in bone, and increased serum sclerostin (13). Leptin-deficient *ob/ob* and *db/db* mice also have elevated serum sclerostin compared to wild-type littermates (13). *Sost*^{-/-} mice fed a high fat diet, however, gain less body weight and fat mass than their wild-type counterparts. Scl Ab treatment (1 dose/week, 30 mg/kg, 8 weeks) also partially protected mice from high fat diet-induced increases in body weight and fat mass. Along with differences in white adipose tissue mass, *Sost*^{-/-} mice showed improved glucose handling in glucose tolerance and insulin sensitivity tests compared to wild-type littermates on normal or high fat diets. These results are supported in Scl Ab-treated mice. *Sost*-AAV-treated mice, on the other hand, have higher random-fed insulin levels, are worse at regulating blood glucose levels, and are less sensitive to insulin (13). Reducing adipocyte sensitivity to sclerostin through *Lrp4* deletion and additionally reducing circulating sclerostin both cause improvements in glucose handling, suggesting that sclerostin's effects on adipose tissue can have a systemic impact (113).

In addition to these endocrine effects on white adipose tissue, sclerostin also positively regulates adipose tissue in the bone marrow. Marrow adipose tissue - distinct from the white adipose tissue found in subcutaneous and visceral fat depots - is dynamically regulated with age, diet, hormones, and disease, though its function in skeletal homeostasis is still being determined (114). Effects of sclerostin on immune cells in the marrow, recently reviewed elsewhere (116), and on marrow adipose tissue may be best classified as paracrine, but we will discuss the available research on marrow adipose tissue here.

Consistent with the effects of *Sost* ablation on white adipose tissue, *Sost*^{-/-} mice have decreased bone marrow adipose tissue volume as detected by osmium tetroxide micro-CT (117). Likewise, mice treated with Scl Ab for 3 weeks (1 dose/week, 100 mg/kg) end with lower marrow adipocyte number and size (118). In a separate study, 3 weeks of Scl Ab treatment (2 doses/week, 25 mg/kg) did not significantly affect bone marrow adipocyte number in healthy mice, nor did it decrease the number of adipocytes surrounding a fracture callus (110). These studies all used young male mice (6-11 weeks old), though the differences in animal age and antibody dose may explain the discrepancy in outcomes.

Male and female rats treated with Scl Ab (1 dose/week, 3 or 50 mg/kg) for 4 or 26 weeks presented a more complex response (119). After 26 weeks of treatment, both sexes showed significant dose-dependent decreases in tissue adiposity driven by decreased

adipocyte number, consistent with prior studies in mice. However, when adipocyte numbers were normalized to bone marrow area, which decreases as bone mass increases in treated animals, the significant effects of sclerostin antibody on marrow adiposity were limited to males. Whether normalized to tissue area or marrow area, marrow adiposity of female rats increased in the first four weeks of Scl Ab treatment, again in a dose-dependent manner, whereas male rats showed no changes in the first four weeks of treatment. Sex-dependent differences in baseline trabecular bone volume and marrow adiposity may drive the sex-specific differences in early response to Scl Ab. Also notable was that marrow adiposity increased with age, an effect that was only partially blocked by Scl Ab treatment. In sum, these studies illustrate a predominantly positive relationship between sclerostin and marrow adiposity, but reconciling the age-, sex-, and dose-dependent effects of Scl Ab treatment will require further study.

In disease models where marrow adiposity is elevated, a protective role of sclerostin antibody treatment has been reported. Rabbits treated with Scl Ab for five months (2 doses/week, 13 mg/kg) were protected from the increase in marrow fat fraction caused by ovariectomy. While adipocytes in untreated ovariectomized rabbits increased in diameter and density, those in rabbits that also received Scl Ab were indistinguishable from sham-operated animals (120). Streptozotocin-induced diabetic mice have higher bone marrow adiposity than non-diabetic mice. In this model, Scl Ab treatment slightly attenuates the additional increase in adipocyte density seen around a fracture callus (3 weeks, 2 doses/week, 25 mg/kg) (110). This raises the possibility that sclerostin acts as a mediator in disease even if it is not a primary regulator of adipogenesis in bone marrow. Additional *in vivo* studies with conditional deletion of LRP6 from adipocytes and from mesenchymal progenitor cells are needed to determine the extent to which sclerostin acts directly on marrow adipocytes versus altering the commitment of bipotential precursor cells to cause these phenotypes.

In vitro studies, animal experiments, and clinical trials have provided evidence that sclerostin can act on adipose tissue to regulate Wnt signaling, adipogenesis, and metabolism. Together this body of work suggests an overall positive regulatory relationship between sclerostin and adipogenesis, but the extent of its regulatory capabilities and its importance relative to other endocrine and paracrine factors in homeostasis and in disease is not entirely clear. In humans, all studies published to date linking sclerostin levels and metabolic phenotypes are associative. While *in vitro* and *in vivo* studies show that sclerostin is capable of regulating adipocyte behavior, its importance within physiological concentrations and in concert with other signaling molecules is not yet clear. In mouse models, global deletion of sclerostin or mutations in Wnt signaling-related proteins may cause secondary changes in bone that in turn regulate adipocyte biology, rather than direct effects of sclerostin protein on adipocytes. The careful experiments describing cell type-specific contributions of *Sost* to regulation of bone mass (96) have not been conducted with adipose outcomes. Future studies using bone-specific sclerostin mutant animals will be helpful to isolate the effects of bone-derived sclerostin on distant tissues in mice.

SCLEROSTIN IN MINERAL METABOLISM

The extreme high bone mass phenotype seen in people with sclerosteosis and in *Sost*^{-/-} mice likely requires a shift in systemic mineral homeostasis to support absorption and retention of the required calcium and phosphorus. In neutral calcium balance, the dietary calcium absorbed in the intestines is offset by the amount of calcium filtered and then reabsorbed or excreted *via* the kidneys. Calcium and phosphorus balance are carefully maintained through the coordinated control of circulating hormones including PTH, FGF-23, and vitamin D (121, 122). Since sclerostin plays a major role in regulating bone homeostasis, whether this same factor may modulate renal mineral metabolism or the actions of calciotropic hormones is of particular interest.

Indeed, *Sost*^{-/-} mice demonstrate alterations in mineral metabolism resulting in enhanced absorption and reduced excretion of calcium and phosphorus. Active vitamin D (1 α ,25(OH)₂D) concentrations were significantly elevated in the serum of *Sost*^{-/-} mice, which would be expected to promote calcium and phosphorus absorption in the kidney and intestines. Accordingly, urinary calcium excretion was reduced, serum phosphorus was elevated, and serum FGF-23, which promotes phosphate excretion, was low in *Sost*^{-/-} mice (14). In wild-type mice and in a mouse model of X-linked hypophosphatemia, sclerostin-neutralizing antibody treatment (4 weeks, 2 doses/week, 25 mg/kg) significantly increased serum phosphate and decreased circulating FGF-23 (123). Therefore, sclerostin deficiency leads to alterations in mineral metabolism to enhance absorption and reduce excretion of calcium and phosphorus.

Since vitamin D regulates mineral absorption in both the kidney and the intestines, the possibility of direct action of sclerostin on vitamin D metabolism has been investigated. Inactive vitamin D prehormone (25(OH)D) must be converted to the active form (1 α ,25(OH)₂D) by 25-hydroxyvitamin D 1 α -hydroxylase (1 α -hydroxylase, encoded by *Cyp27b1*), which primarily occurs in the kidney. *Cyp27b1* expression is slightly elevated in the kidneys of *Sost*^{-/-} mice and is significantly repressed in proximal tubule cells after treatment with recombinant sclerostin, consistent with the elevated levels of 1 α ,25(OH)₂D in serum of *Sost*^{-/-} mice (14). High serum PTH, low serum phosphorus, and low FGF-23 could also cause high 1 α -hydroxylase activity, but of these factors, *Sost*^{-/-} mice only have low serum FGF-23 (124–126). Together these results suggest that sclerostin, through direct effects on proximal tubule cells and indirectly through FGF-23, negatively regulates the synthesis of 1 α ,25(OH)₂D. The ability of sclerostin to regulate systemic mineral metabolism may therefore be regulated by a combination of vitamin D-mediated effects and direct action on the kidney to control calcium excretion. The potential endocrine effects of sclerostin on mineral metabolism and on adipogenesis as studied in cell and animal models are shown in **Figure 2**. For schematics describing the role of sclerostin in bone, we again refer the reader to existing reviews (79, 80).

To date, the effects of sclerostin overexpression on mineral metabolism remain to be determined, and many outstanding questions remain regarding potential renal actions of sclerostin

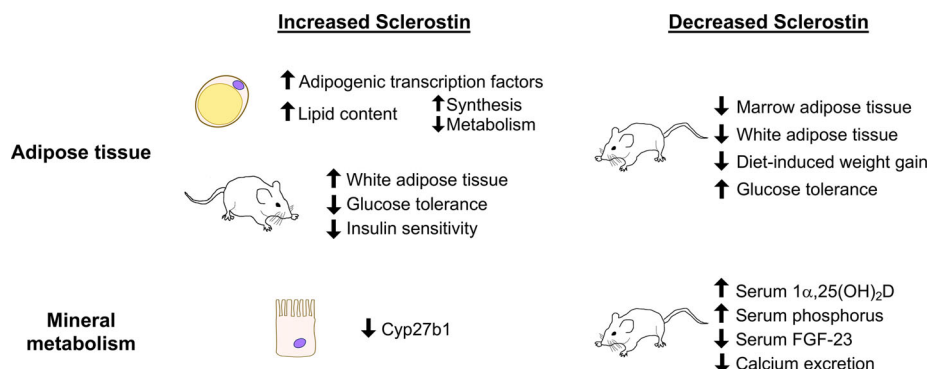


FIGURE 2 | Summary of sclerostin-mediated effects on adipose tissue and on mineral metabolism. Recombinant sclerostin exerts direct effects on adipocytes and kidney proximal tubule cells in culture. Mice overproducing sclerostin demonstrate increased adiposity and reduced glucose tolerance. Reduced sclerostin *in vivo*, achieved through inactivating mutations, conditional ablation, or neutralizing antibodies, leads to reduced adiposity, improved glucose handling, and altered mineral metabolism in mice.

(127). For example, does FGF-23 act independently of sclerostin or mediate its effects on $1\alpha,25(\text{OH})_2\text{D}$ synthesis? Which nephron segment in the kidney responds to sclerostin to regulate calcium excretion? Do these processes involve canonical Wnt signaling? The extent to which sclerostin functions as a normal part of processing dietary calcium, versus only in a disease state, also remains to be determined. Supporting the importance of sclerostin in the kidney, though, a meta-analysis of genomewide association studies found robust association between SNPs in *B4GALNT3*, which is highly expressed in the kidney, and serum sclerostin (93). Thus, the kidney may participate in regulating the levels of circulating sclerostin available to act on it by modulating expression of *B4GALNT3*. Further mechanistic studies are needed to validate the role of renal *B4GALNT3* in regulating sclerostin availability and clearance.

Studies with adult sclerosteosis patients have found normal urinary calcium excretion, plasma PTH, $25(\text{OH})\text{D}$ prehormone, serum calcium, and serum phosphorus (84, 128). van Lierop et al. reviewed 96 cases of sclerosteosis and determined that active $1\alpha,25(\text{OH})_2\text{D}$ is elevated in sclerosteosis patients compared to carriers (129). Children with sclerosteosis have high serum phosphorus and calcium, and they may better match the developmental stage of mice used in research (128). Interpretation of clinical trials studying sclerostin-neutralizing antibodies blosozumab and romosozumab is complicated by the simultaneous administration of calcium and vitamin D supplements. Blosozumab caused slight elevation of serum $1\alpha,25(\text{OH})_2\text{D}$ and PTH compared to placebo that did not reach statistical significance (130). Romosozumab caused a transient decrease in serum calcium and a slight dose-dependent increase in serum PTH compared to baseline, but vitamin D was not reported after baseline (131, 132). In the first single-dose studies of romosozumab (then called AMG 785) when calcium and vitamin D supplements were not given, serum calcium and PTH reacted similarly, but vitamin D was not measured (133). In the relatively healthy people studied in

these trials, sclerostin deficiency appears to have a small effect on mineral metabolism. However, given the careful balance of sclerostin, PTH, and FGF-23 [reviewed by (134)], sclerostin may play a bigger role in patients with chronic kidney disease (135).

Because of the frequency of bone phenotypes in patients with chronic kidney disease, the role of circulating sclerostin has been studied extensively in this population. In two cross-sectional studies of patients with chronic kidney disease, serum sclerostin levels were higher in patients with the lower glomerular filtration rates characteristic of advanced disease (136, 137). Rather than reflecting reduced renal clearance, however, the urinary excretion of sclerostin also increased as kidney disease progressed (137). This along with immunohistochemistry of bone biopsies from chronic kidney disease patients suggests that increased production of sclerostin by osteocytes may be a factor in the development of chronic kidney disease (138, 139). This is further supported by bone biopsies from patients undergoing kidney transplant. Serum sclerostin measurements were significantly correlated with the percentage of sclerostin-positive osteocytes measured by immunohistochemistry and negatively associated with residual renal function in end-stage kidney disease (140). As needed with studies of adiposity, careful interventional clinical trials and animal studies with tissue-specific sclerostin overexpression or ablation will be necessary to isolate the effects of sclerostin on mineral metabolism.

SCLEROSTIN IN VASCULAR CALCIFICATION

The individual effects of sclerostin on bone, adipose tissue, and kidney suggest that sclerostin-neutralizing antibodies should have net positive benefits on human health, and clinical trials thus far have reported few adverse events from sclerostin-neutralizing antibodies (130–132, 141, 142). While sclerosteosis can lead to life-threatening elevation of intracranial pressure caused by

thickening of the skull, health of people with sclerosteosis and van Buchem's disease is considered good overall, without involvement of the heart or lungs (143). Furthermore, sclerosteosis carriers have high bone mass without intracranial hypertension. However, a numeric imbalance in serious cardiovascular adverse events was reported in romosozumab-treated women compared to alendronate-treated women in the ARCH trial (144) as well as in romosozumab-treated men compared to placebo-treated men in the BRIDGE trial (145). While the absolute risk for adverse cardiovascular events remained quite small, these findings led the U.S. FDA to include a black box packaging warning for potential cardiac risks associated with romosozumab. It is not yet known why this effect on cardiovascular adverse events was not apparent in women in the placebo-controlled trial (131). It is possible that the placebo-controlled trial in women included younger patients with fewer risk factors for cardiac events or that alendronate is somewhat cardioprotective. These clinical findings also raise the possibility that circulating sclerostin exerts effects on the vasculature in a cardioprotective manner.

A recent genetics study supports the idea that inhibition of sclerostin elevates risk of cardiovascular adverse events (15). Bovijn et al. found that two common *SOST* variants associated with high BMD were also associated with reduced expression of *SOST* and a small increase in lifetime risk of myocardial infarction, coronary heart disease, and other adverse cardiovascular events. One mechanism by which sclerostin could prevent cardiovascular adverse events is through inhibition of vascular calcification, though correlations between sclerostin and vascular calcification have identified both positive and negative relationships (146). In support of a protective role for sclerostin, a multivariate logistic regression model of patients with chronic kidney disease found that lower circulating sclerostin was significantly associated with aortic calcification (147). In another human study, biopsies from aortic aneurysms contained less sclerostin protein than healthy aortic tissue (148). *ApoE*^{-/-} mice stimulated with angiotensin II develop aortic aneurysms and atherosclerotic plaques, but when these mice also overexpressed human sclerostin or were injected with recombinant mouse sclerostin they were protected from aortic aneurysms and atherosclerosis (148).

On the other hand, sclerostin is also positively associated with cardiovascular disease in some cases. When vascular smooth muscle cells are induced toward calcification *in vitro*, they express more sclerostin (149). In a mouse model of chronic kidney disease-mineral and bone disorder, aortic calcification and circulating sclerostin were significantly increased compared to healthy mice (150). In a mixed population of people with and without type 2 diabetes, serum sclerostin was positively associated with the presence of aortic calcifications and cardiovascular mortality over the eight-year longitudinal study (151). Finally, in end-stage renal disease, coronary artery & epigastric artery calcification positively correlated with serum sclerostin. Since no specific sclerostin mRNA or protein expression was detected in the vessels, it appeared that circulating sclerostin produced elsewhere was responsible for the vascular calcification (152). In these associative studies, it is still not known whether sclerostin is

involved in the cause or response to calcification. Furthermore, many of these studies were performed in the context of chronic kidney disease where sclerostin also correlates with age, male gender, and glomerular filtration rate, so its individual effect on the vasculature is difficult to discern.

A safety study sponsored by Amgen Inc., Astellas, and UCB Pharma reported no effects of sclerostin-neutralizing antibody on the cardiovascular system in multiple animal models (153). Healthy rats and cynomolgus monkeys as well as angiotensin II-infused *ApoE*^{-/-} mice and ovariectomized *ApoE*^{-/-} mice on a high fat diet were administered romosozumab and monitored for toxicity and cardiovascular function. In healthy animals and in mouse models of atherosclerosis, effects of sclerostin neutralization on cardiovascular function, vascular calcification, and transcription were nonsignificant. Only the supraphysiological dose of 300 mg/kg romosozumab in monkeys elicited a response - sporadic increases in heart rate and blood pressure - which was discounted by the authors. While this study gives ample evidence that romosozumab is unlikely to exert direct effects on the cardiovascular system, many questions remain regarding the extent to which sclerostin itself functions in the vasculature and the mechanisms by which romosozumab induces cardiovascular adverse events in humans. The effects of sclerostin on cardiovascular health will doubtless be a focus of research in the future as more patients are prescribed sclerostin-neutralizing antibodies to increase bone mass and reduce fracture risk.

Further work will be needed to determine the extent to which bone-derived sclerostin regulates adipogenesis, renal mineral metabolism, cardiovascular health, and other potential non-skeletal tissues. Of particular importance are animal studies in which sclerostin is ablated specifically from osteoblast lineage cells, animal studies in which potential target cells are rendered insensitive to sclerostin, and clinical trials that measure the effects of sclerostin or sclerostin neutralizing antibodies on non-skeletal tissues in a prospective, interventional manner. As the full endocrine capacity of sclerostin is elucidated, it may lead to exciting new roles for osteocytes in systemic homeostasis.

CONCLUSIONS AND FUTURE PERSPECTIVES

As summarized here, multiple extra-skeletal functions of osteocalcin and sclerostin have been proposed based on preclinical models. Given the central role of bone in whole organism physiology, it is not surprising that crosstalk between the skeleton and other organs exists and is mediated by bone-specific factors. It is likely that osteocalcin and sclerostin represent the tip of the iceberg with respect to how bone-derived factors regulate the function of other organs. As outlined above, future studies are needed to validate findings from preclinical models and to rigorously test hypotheses in humans. In addition, it will be important to consider how the organs targeted by bone-derived factors signal to the skeleton in order to maintain organismal homeostasis.

AUTHOR CONTRIBUTIONS

JW, CM, and MW wrote and edited the manuscript. All authors contributed to the article and approved the submitted version.

FUNDING

CM acknowledges support from the NIH (T32DK007028). MW acknowledges support from the American Society of Bone and

Mineral Research (Rising Star award) and the NIH (DK116716 and DK011794).

ACKNOWLEDGMENTS

We thank members of the Wein laboratory for stimulating discussions.

REFERENCES

- Teitelbaum SL. Bone resorption by osteoclasts. *Science* (2000) 289 (5484):1504–8. doi: 10.1126/science.289.5484.1504
- Olsen BR, Reginato AM, Wang W. Bone development. *Annu Rev Cell Dev Biol* (2000) 16:191–220. doi: 10.1146/annurev.cellbio.16.1.191
- Jensen ED, Gopalakrishnan R, Westendorf JJ. Regulation of gene expression in osteoblasts. *Biofactors* (2010) 36(1):25–32. doi: 10.1002/biof.72
- Bonewald LF. The amazing osteocyte. *J Bone Miner Res* (2011) 26(2):229–38. doi: 10.1002/jbmr.320
- Winkler DG, Sutherland MK, Geoghegan JC, Yu C, Hayes T, Skonier JE, et al. Osteocyte control of bone formation via sclerostin, a novel BMP antagonist. *EMBO J* (2003) 22(23):6267–76. doi: 10.1093/emboj/cdg599
- Nakashima T, Hayashi M, Fukunaga T, Kurata K, Oh-Hora M, Feng JQ, et al. Evidence for osteocyte regulation of bone homeostasis through RANKL expression. *Nat Med* (2011) 17(10):1231–4. doi: 10.1038/nm.2452
- Yoshida H, Hayashi S, Kunisada T, Ogawa M, Nishikawa S, Okamura H, et al. The murine mutation osteopetrosis is in the coding region of the macrophage colony stimulating factor gene. *Nature* (1990) 345(6274):442–4. doi: 10.1038/345442a0
- Udagawa N, Takahashi N, Yasuda H, Mizuno A, Itoh K, Ueno Y, et al. Osteoprotegerin produced by osteoblasts is an important regulator in osteoclast development and function. *Endocrinology* (2000) 141(9):3478–84. doi: 10.1210/endo.141.9.7634
- Pederson L, Ruan M, Westendorf JJ, Khosla S, Oursler MJ. Regulation of bone formation by osteoclasts involves Wnt/BMP signaling and the chemokine sphingosine-1-phosphate. *Proc Natl Acad Sci USA* (2008) 105 (52):20764–9. doi: 10.1073/pnas.0805133106
- Kimura H, Kwan KM, Zhang Z, Deng JM, Darnay BG, Behringer RR, et al. Cthrc1 is a positive regulator of osteoblastic bone formation. *PLoS One* (2008) 3(9):e3174. doi: 10.1371/journal.pone.0003174
- Lang F, Leibrock C, Pandya AA, Stournaras C, Wagner CA, Foller M. Phosphate Homeostasis, Inflammation and the Regulation of FGF-23. *Kidney Blood Press Res* (2018) 43(6):1742–8. doi: 10.1159/000495393
- Mosialou I, Shikhel S, Liu JM, Maurizi A, Luo N, He Z, et al. MC4R-dependent suppression of appetite by bone-derived lipocalin 2. *Nature* (2017) 543(7645):385–90. doi: 10.1038/nature21697
- Kim SP, Frey JL, Li Z, Kushwaha P, Zoch ML, Tomlinson RE, et al. Sclerostin influences body composition by regulating catabolic and anabolic metabolism in adipocytes. *Proc Natl Acad Sci USA* (2017) 114(52):E11238–47. doi: 10.1073/pnas.1707876115
- Ryan ZC, Ketha H, McNulty MS, McGee-Lawrence M, Craig TA, Grande JP, et al. Sclerostin alters serum vitamin D metabolite and fibroblast growth factor 23 concentrations and the urinary excretion of calcium. *Proc Natl Acad Sci USA* (2013) 110(15):6199–204. doi: 10.1073/pnas.1221255110
- Bovijn J, Krebs K, Chen CY, Boxall R, Censin JC, Ferreira T, et al. Evaluating the cardiovascular safety of sclerostin inhibition using evidence from meta-analysis of clinical trials and human genetics. *Sci Transl Med* (2020) 12(549). doi: 10.1126/scitranslmed.aay6570
- Hauschka PV, Lian JB, Cole DE, Gundersen CM. Osteocalcin and matrix Gla protein: vitamin K-dependent proteins in bone. *Physiol Rev* (1989) 69 (3):990–1047. doi: 10.1152/physrev.1989.69.3.990
- Morris DP, Stevens RD, Wright DJ, Stafford DW. Processive post-translational modification. Vitamin K-dependent carboxylation of a peptide substrate. *J Biol Chem* (1995) 270(51):30491–8. doi: 10.1074/jbc.270.51.30491
- Hoang QQ, Sicheri F, Howard AJ, Yang DS. Bone recognition mechanism of porcine osteocalcin from crystal structure. *Nature* (2003) 425(6961):977–80. doi: 10.1038/nature02079
- Malashkevich VN, Almo SC, Dowd TL. X-ray crystal structure of bovine 3 Glu-osteocalcin. *Biochemistry* (2013) 52(47):8387–92. doi: 10.1021/bi4010254
- Mizokami A, Kawakubo-Yasukochi T, Hirata M. Osteocalcin and its endocrine functions. *Biochem Pharmacol* (2017) 132:1–8. doi: 10.1016/j.bcp.2017.02.001
- Celeste AJ, Rosen V, Buecker JL, Kriz R, Wang EA, Wozney JM. Isolation of the human gene for bone gla protein utilizing mouse and rat cDNA clones. *EMBO J* (1986) 5(8):1885–90. doi: 10.1002/j.1460-2075.1986.tb04440.x
- Rahman S, Oberdorf A, Montecino M, Tanhauser SM, Lian JB, Stein GS, et al. Multiple copies of the bone-specific osteocalcin gene in mouse and rat. *Endocrinology* (1993) 133(6):3050–3. doi: 10.1210/endo.133.6.8243336
- Desbois C, Hogue DA, Karsenty G. The mouse osteocalcin gene cluster contains three genes with two separate spatial and temporal patterns of expression. *J Biol Chem* (1994) 269(2):1183–90. doi: 10.1016/S0021-9258(17)42240-X
- Sato M, Tada N. Preferential expression of osteocalcin-related protein mRNA in gonadal tissues of male mice. *Biochem Biophys Res Commun* (1995) 215(1):412–21. doi: 10.1006/bbrc.1995.2480
- Petrucchi M, Paquette Y, Leblond FA, Pichette V, Bonnardeaux A. Evidence that the mouse osteocalcin-related gene does not encode nephrocalcin. *Nephron Exp Nephrol* (2006) 104(4):e140–6. doi: 10.1159/000094965
- Diegel CR, Hann S, Ayturk UM, Hu JCW, Lim KE, Droscha CJ, et al. An osteocalcin-deficient mouse strain without endocrine abnormalities. *PLoS Genet* (2020) 16(5):e1008361. doi: 10.1371/journal.pgen.1008361
- Ducy P, Desbois C, Boyce B, Pinero G, Story B, Dunstan C, et al. Increased bone formation in osteocalcin-deficient mice. *Nature* (1996) 382(6590):448–52. doi: 10.1038/382448a0
- Boskey AL, Gadaleta S, Gundersen C, Doty SB, Ducy P, Karsenty G. Fourier transform infrared microspectroscopic analysis of bones of osteocalcin-deficient mice provides insight into the function of osteocalcin. *Bone* (1998) 23(3):187–96. doi: 10.1016/S8756-3282(98)00092-1
- Berezovska O, Yildirim G, Budell WC, Yagerman S, Pidhayny B, Bastien C, et al. Osteocalcin affects bone mineral and mechanical properties in female mice. *Bone* (2019) 128:115031. doi: 10.1016/j.bone.2019.08.004
- Moriishi T, Ozasa R, Ishimoto T, Nakano T, Hasegawa T, Miyazaki T, et al. Osteocalcin is necessary for the alignment of apatite crystallites, but not glucose metabolism, testosterone synthesis, or muscle mass. *PLoS Genet* (2020) 16(5):e1008586. doi: 10.1371/journal.pgen.1008586
- Fu Y, Foden JA, Khayter C, Maeder ML, Reyon D, Joung JK, et al. High-frequency off-target mutagenesis induced by CRISPR-Cas nucleases in human cells. *Nat Biotechnol* (2013) 31(9):822–6. doi: 10.1038/nbt.2623
- Hsu PD, Scott DA, Weinstein JA, Ran FA, Konermann S, Agarwala V, et al. DNA targeting specificity of RNA-guided Cas9 nucleases. *Nat Biotechnol* (2013) 31(9):827–32. doi: 10.1038/nbt.2647
- Pattanayak V, Lin S, Guilinger JP, Ma E, Doudna JA, Liu DR. High-throughput profiling of off-target DNA cleavage reveals RNA-programmed Cas9 nuclease specificity. *Nat Biotechnol* (2013) 31(9):839–43. doi: 10.1038/nbt.2673

34. Cho SW, Kim S, Kim Y, Kweon J, Kim HS, Bae S, et al. Analysis of off-target effects of CRISPR/Cas-derived RNA-guided endonucleases and nickases. *Genome Res* (2014) 24(1):132–41. doi: 10.1101/gr.162339.113
35. Ran FA, Hsu PD, Wright J, Agarwala V, Scott DA, Zhang F. Genome engineering using the CRISPR-Cas9 system. *Nat Protoc* (2013) 8(11):2281–308. doi: 10.1038/nprot.2013.143
36. Heigwer F, Kerr G, Boutros M. E-CRISP: fast CRISPR target site identification. *Nat Methods* (2014) 11(2):122–3. doi: 10.1038/nmeth.2812
37. Singh R, Kescu C, Quinlan A, Qi Y, Adli M. Cas9-chromatin binding information enables more accurate CRISPR off-target prediction. *Nucleic Acids Res* (2015) 43(18):e118. doi: 10.1093/nar/gkv575
38. Hendel A, Fine EJ, Bao G, Porteus MH. Quantifying on- and off-target genome editing. *Trends Biotechnol* (2015) 33(2):132–40. doi: 10.1016/j.tibtech.2014.12.001
39. Lee NK, Sowa H, Hinoi E, Ferron M, Ahn JD, Confavreux C, et al. Endocrine regulation of energy metabolism by the skeleton. *Cell* (2007) 130(3):456–69. doi: 10.1016/j.cell.2007.05.047
40. Oury F, Sumara G, Sumara O, Ferron M, Chang H, Smith CE, et al. Endocrine regulation of male fertility by the skeleton. *Cell* (2011) 144(5):796–809. doi: 10.1016/j.cell.2011.02.004
41. Oury F, Khirman L, Denny CA, Gardin A, Chamouni A, Goeden N, et al. Maternal and offspring pools of osteocalcin influence brain development and functions. *Cell* (2013) 155(1):228–41. doi: 10.1016/j.cell.2013.08.042
42. Diegel CR, Hann S, Ayturk UM, Hu JCW, Lim KE, Droscha CJ, et al. Independent validation of experimental results requires timely and unrestricted access to animal models and reagents. *PLoS Genet* (2020) 16(6):e1008940. doi: 10.1371/journal.pgen.1008940
43. Karsenty G. The facts of the matter: What is a hormone? *PLoS Genet* (2020) 16(6):e1008938. doi: 10.1371/journal.pgen.1008938
44. Moriishi T, Komori T. Lack of reproducibility in osteocalcin-deficient mice. *PLoS Genet* (2020) 16(6):e1008939. doi: 10.1371/journal.pgen.1008939
45. Manolagas SC. Osteocalcin promotes bone mineralization but is not a hormone. *PLoS Genet* (2020) 16(6):e1008714. doi: 10.1371/journal.pgen.1008714
46. Ferron M, Lacombe J. Regulation of energy metabolism by the skeleton: osteocalcin and beyond. *Arch Biochem Biophys* (2014) 561:137–46. doi: 10.1016/j.abb.2014.05.022
47. Karsenty G. Update on the Biology of Osteocalcin. *Endocr Pract* (2017) 23(10):1270–4. doi: 10.4158/EP171966.RA
48. Wei J, Hanna T, Suda N, Karsenty G, Ducy P. Osteocalcin promotes beta-cell proliferation during development and adulthood through Gprc6a. *Diabetes* (2014) 63(3):1021–31. doi: 10.2337/db13-0887
49. Ferron M, Hinoi E, Karsenty G, Ducy P. Osteocalcin differentially regulates beta cell and adipocyte gene expression and affects the development of metabolic diseases in wild-type mice. *Proc Natl Acad Sci USA* (2008) 105(13):5266–70. doi: 10.1073/pnas.071119105
50. Fulzele K, Riddle RC, DiGirolamo DJ, Cao X, Wan C, Chen D, et al. Insulin receptor signaling in osteoblasts regulates postnatal bone acquisition and body composition. *Cell* (2010) 142(2):309–19. doi: 10.1016/j.cell.2010.06.002
51. Lambert LJ, Challa AK, Niu A, Zhou L, Tucholski J, Johnson MS, et al. Increased trabecular bone and improved biomechanics in an osteocalcin-null rat model created by CRISPR/Cas9 technology. *Dis Model Mech* (2016) 9(10):1169–79. doi: 10.1242/dmm.025247
52. Ducy P. Bone Regulation of Insulin Secretion and Glucose Homeostasis. *Endocrinology* (2020) 161(10):1–12. doi: 10.1210/endo/bqaa149
53. Rosen CJ, Zaidi M. Contemporaneous reproduction of preclinical science: a case study of FSH and fat. *Ann N Y Acad Sci* (2017) 1404(1):17–9. doi: 10.1111/nyas.13457
54. von Herrath M, Pagni PP, Grove K, Christoffersson G, Tang-Christensen M, Karlens AE, et al. Case Reports of Pre-clinical Replication Studies in Metabolism and Diabetes. *Cell Metab* (2019) 29(4):795–802. doi: 10.1016/j.cmet.2019.02.004
55. Hill HS, Grams J, Walton RG, Liu J, Moellering DR, Garvey WT. Carboxylated and uncarboxylated forms of osteocalcin directly modulate the glucose transport system and inflammation in adipocytes. *Horm Metab Res* (2014) 46(5):341–7. doi: 10.1055/s-0034-1368709
56. Pi M, Chen L, Huang MZ, Zhu W, Ringhofer B, Luo J, et al. GPRC6A null mice exhibit osteopenia, feminization and metabolic syndrome. *PLoS One* (2008) 3(12):e3858. doi: 10.1371/journal.pone.0003858
57. Yamauchi T, Kamon J, Waki H, Terauchi Y, Kubota N, Hara K, et al. The fat-derived hormone adiponectin reverses insulin resistance associated with both lipodystrophy and obesity. *Nat Med* (2001) 7(8):941–6. doi: 10.1038/90984
58. Kajimura D, Lee HW, Riley KJ, Arteaga-Solis E, Ferron M, Zhou B, et al. Adiponectin regulates bone mass via opposite central and peripheral mechanisms through FoxO1. *Cell Metab* (2013) 17(6):901–15. doi: 10.1016/j.cmet.2013.04.009
59. Otani T, Matsuda M, Mizokami A, Kitagawa N, Takeuchi H, Jimi E, et al. Osteocalcin triggers Fas/FasL-mediated necroptosis in adipocytes via activation of p300. *Cell Death Dis* (2018) 9(12):1194. doi: 10.1038/s41419-018-1257-7
60. Ferron M, McKee MD, Levine RL, Ducy P, Karsenty G. Intermittent injections of osteocalcin improve glucose metabolism and prevent type 2 diabetes in mice. *Bone* (2012) 50(2):568–75. doi: 10.1016/j.bone.2011.04.017
61. Zhou B, Li H, Xu L, Zang W, Wu S, Sun H. Osteocalcin reverses endoplasmic reticulum stress and improves impaired insulin sensitivity secondary to diet-induced obesity through nuclear factor-kappaB signaling pathway. *Endocrinology* (2013) 154(3):1055–68. doi: 10.1210/en.2012-2144
62. Karsenty G, Olson EN. Bone and Muscle Endocrine Functions: Unexpected Paradigms of Inter-organ Communication. *Cell* (2016) 164(6):1248–56. doi: 10.1016/j.cell.2016.02.043
63. Mera P, Laue K, Wei J, Berger JM, Karsenty G. Osteocalcin is necessary and sufficient to maintain muscle mass in older mice. *Mol Metab* (2016) 5(10):1042–7. doi: 10.1016/j.molmet.2016.07.002
64. Mera P, Laue K, Ferron M, Confavreux C, Wei J, Galan-Diez M, et al. Osteocalcin Signaling in Myofibers Is Necessary and Sufficient for Optimum Adaptation to Exercise. *Cell Metab* (2016) 23(6):1078–92. doi: 10.1016/j.cmet.2016.05.004
65. Pedersen BK, Febbraio MA. Muscles, exercise and obesity: skeletal muscle as a secretory organ. *Nat Rev Endocrinol* (2012) 8(8):457–65. doi: 10.1038/nrendo.2012.49
66. Ferron M, Wei J, Yoshizawa T, Del Fattore A, DePinho RA, Teti A, et al. Insulin signaling in osteoblasts integrates bone remodeling and energy metabolism. *Cell* (2010) 142(2):296–308. doi: 10.1016/j.cell.2010.06.003
67. Pi M, Wu Y, Quarles LD. GPRC6A mediates responses to osteocalcin in beta-cells in vitro and pancreas in vivo. *J Bone Miner Res* (2011) 26(7):1680–3. doi: 10.1002/jbmr.390
68. Oury F, Ferron M, Huizhen W, Confavreux C, Xu L, Lacombe J, et al. Osteocalcin regulates murine and human fertility through a pancreas-bone-testis axis. *J Clin Invest* (2013) 123(6):2421–33. doi: 10.1172/JCI65952
69. Pi M, Xu F, Ye R, Nishimoto SK, Kesterson RA, Williams RW, et al. Humanized GPRC6A(KGKY) is a gain-of-function polymorphism in mice. *Sci Rep* (2020) 10(1):11143. doi: 10.1038/s41598-020-68113-z
70. Jorgensen CV, Brauner-Osborne H. Pharmacology and physiological function of the orphan GPRC6A receptor. *Basic Clin Pharmacol Toxicol* (2020) 126 Suppl 6:77–87. doi: 10.1111/bcpt.13397
71. Bradburn S, McPhee JS, Bagley L, Sipila S, Stenroth L, Narici MV, et al. Association between osteocalcin and cognitive performance in healthy older adults. *Age Ageing* (2016) 45(6):844–9. doi: 10.1093/ageing/afw137
72. Puig J, Blasco G, Daunis-i-Estadella J, Moreno M, Molina X, Alberich-Bayarri A, et al. Lower serum osteocalcin concentrations are associated with brain microstructural changes and worse cognitive performance. *Clin Endocrinol (Oxf)* (2016) 84(5):756–63. doi: 10.1111/cen.12954
73. Khirman L, Obri A, Ramos-Brossier M, Rousseaud A, Moriceau S, Nicot AS, et al. Gpr158 mediates osteocalcin's regulation of cognition. *J Exp Med* (2017) 214(10):2859–73. doi: 10.1084/jem.20171320
74. Kosmidis S, Polyzos A, Harvey L, Youssef M, Denny CA, Dranovsky A, et al. RbAp48 Protein Is a Critical Component of GPR158/OCN Signaling and Ameliorates Age-Related Memory Loss. *Cell Rep* (2018) 25(4):959–973 e6. doi: 10.1016/j.celrep.2018.09.077
75. Berger JM, Singh P, Khirman L, Morgan DA, Chowdhury S, Arteaga-Solis E, et al. Mediation of the Acute Stress Response by the Skeleton. *Cell Metab* (2019) 30(5):890–902 e8. doi: 10.1016/j.cmet.2019.08.012
76. Obri A, Khirman L, Karsenty G, Oury F. Osteocalcin in the brain: from embryonic development to age-related decline in cognition. *Nat Rev Endocrinol* (2018) 14(3):174–82. doi: 10.1038/nrendo.2017.181

77. Baron R, Kneissel M. WNT signaling in bone homeostasis and disease: from human mutations to treatments. *Nat Med* (2013) 19(2):179–92. doi: 10.1038/nm.3074
78. Li X, Zhang Y, Kang H, Liu W, Liu P, Zhang J, et al. Sclerostin binds to LRP5/6 and antagonizes canonical Wnt signaling. *J Biol Chem* (2005) 280(20):19883–7. doi: 10.1074/jbc.M413274200
79. Delgado-Calle J, Sato AY, Bellido T. Role and mechanism of action of sclerostin in bone. *Bone* (2017) 96:29–37. doi: 10.1016/j.bone.2016.10.007
80. Holdsworth G, Roberts SJ, Ke HZ. Novel actions of sclerostin on bone. *J Mol Endocrinol* (2019) 62(2):R167–85. doi: 10.1530/JME-18-0176
81. van Bezooijen RL, Roelen BA, Visser A, van der Wee-Pals L, de Wilt E, Karperien M, et al. Sclerostin is an osteocyte-expressed negative regulator of bone formation, but not a classical BMP antagonist. *J Exp Med* (2004) 199(6):805–14. doi: 10.1084/jem.20031454
82. Semenov M, Tamai K, He X. SOST is a ligand for LRP5/LRP6 and a Wnt signaling inhibitor. *J Biol Chem* (2005) 280(29):26770–5. doi: 10.1074/jbc.M504308200
83. Leupin O, Piters E, Halleux C, Hu S, Kramer I, Morvan F, et al. Bone overgrowth-associated mutations in the LRP4 gene impair sclerostin facilitator function. *J Biol Chem* (2011) 286(22):19489–500. doi: 10.1074/jbc.M110.190330
84. van Lierop AH, Hamdy NA, Hamersma H, van Bezooijen RL, Power J, Loveridge N, et al. Patients with sclerosteosis and disease carriers: human models of the effect of sclerostin on bone turnover. *J Bone Miner Res* (2011) 26(12):2804–11. doi: 10.1002/jbmr.474
85. Gardner JC, van Bezooijen RL, Mervin B, Hamdy NA, Lowik CW, Hamersma H, et al. Bone mineral density in sclerosteosis; affected individuals and gene carriers. *J Clin Endocrinol Metab* (2005) 90(12):6392–5. doi: 10.1210/jc.2005-1235
86. Zhang D, Park BM, Kang M, Nam H, Kim EJ, Bae C, et al. The systemic effects of sclerostin overexpression using PhiC31 integrase in mice. *Biochem Biophys Res Commun* (2016) 472(3):471–6. doi: 10.1016/j.bbrc.2016.01.178
87. Clarke BL, Drake MT. Clinical utility of serum sclerostin measurements. *Bonekey Rep* (2013) 2:361. doi: 10.1038/bonekey.2013.95
88. Modder UI, Hoey KA, Amin S, McCreedy LK, Achenbach SJ, Riggs BL, et al. Relation of age, gender, and bone mass to circulating sclerostin levels in women and men. *J Bone Miner Res* (2011) 26(2):373–9. doi: 10.1002/jbmr.217
89. Amrein K, Amrein S, Drexler C, Dimai HP, Dobnig H, Pfeifer K, et al. Sclerostin and its association with physical activity, age, gender, body composition, and bone mineral content in healthy adults. *J Clin Endocrinol Metab* (2012) 97(1):148–54. doi: 10.1210/jc.2011-2152
90. Ardawi MS, Al-Kadi HA, Rouzi AA, Qari MH. Determinants of serum sclerostin in healthy pre- and postmenopausal women. *J Bone Miner Res* (2011) 26(12):2812–22. doi: 10.1002/jbmr.479
91. Reppe S, Noer A, Grimholt RM, Halldorsson BV, Medina-Gomez C, Gautvik VT, et al. Methylation of bone SOST, its mRNA, and serum sclerostin levels correlate strongly with fracture risk in postmenopausal women. *J Bone Miner Res* (2015) 30(2):249–56. doi: 10.1002/jbmr.2342
92. Urano T, Shiraki M, Ouchi Y, Inoue S. Association of circulating sclerostin levels with fat mass and metabolic disease-related markers in Japanese postmenopausal women. *J Clin Endocrinol Metab* (2012) 97(8):E1473–7. doi: 10.1210/jc.2012-1218
93. Zheng J, Maerz W, Gergei I, Kleber M, Drechsler C, Wanner C, et al. Mendelian Randomization Analysis Reveals a Causal Influence of Circulating Sclerostin Levels on Bone Mineral Density and Fractures. *J Bone Miner Res* (2019) 34(10):1824–36. doi: 10.1002/jbmr.3803
94. Dallas SL, Prideaux M, Bonewald LF. The osteocyte: an endocrine cell ... and more. *Endocr Rev* (2013) 34(5):658–90. doi: 10.1210/er.2012-1026
95. Poole KE, van Bezooijen RL, Loveridge N, Hamersma H, Papapoulos SE, Lowik CW, et al. Sclerostin is a delayed secreted product of osteocytes that inhibits bone formation. *FASEB J* (2005) 19(13):1842–4. doi: 10.1096/fj.05-4221fje
96. Yee CS, Manilay JO, Chang JC, Hum NR, Murugesh DK, Bajwa J, et al. Conditional Deletion of Sost in MSC-Derived Lineages Identifies Specific Cell-Type Contributions to Bone Mass and B-Cell Development. *J Bone Miner Res* (2018) 33(10):1748–59. doi: 10.1002/jbmr.3467
97. Roforth MM, Fujita K, McGregor UI, Kirmani S, McCreedy LK, Peterson JM, et al. Effects of age on bone mRNA levels of sclerostin and other genes relevant to bone metabolism in humans. *Bone* (2014) 59:1–6. doi: 10.1016/j.bone.2013.10.019
98. Weivoda MM, Youssef SJ, Oursler MJ. Sclerostin expression and functions beyond the osteocyte. *Bone* (2017) 96:45–50. doi: 10.1016/j.bone.2016.11.024
99. Ross SE, Hemati N, Longo KA, Bennett CN, Lucas PC, Erickson RL, et al. Inhibition of adipogenesis by Wnt signaling. *Science* (2000) 289(5481):950–3. doi: 10.1126/science.289.5481.950
100. Hamersma H, Gardner J, Beighton P. The natural history of sclerosteosis. *Clin Genet* (2003) 63(3):192–7. doi: 10.1034/j.1399-0004.2003.00036.x
101. Confavreux CB, Casey R, Varennes A, Goudable J, Chapurlat RD, Szulc P. Has sclerostin a true endocrine metabolic action complementary to osteocalcin in older men? *Osteoporos Int* (2016) 27(7):2301–9. doi: 10.1007/s00198-016-3540-8
102. Ma YH, Schwartz AV, Sigurdsson S, Hue TF, Lang TF, Harris TB, et al. Circulating sclerostin associated with vertebral bone marrow fat in older men but not women. *J Clin Endocrinol Metab* (2014) 99(12):E2584–90. doi: 10.1210/jc.2013-4493
103. Gennari L, Merlotti D, Valenti R, Ceccarelli E, Ruvio M, Pietrini MG, et al. Circulating sclerostin levels and bone turnover in type 1 and type 2 diabetes. *J Clin Endocrinol Metab* (2012) 97(5):1737–44. doi: 10.1210/jc.2011-2958
104. Garcia-Martin A, Rozas-Moreno P, Reyes-Garcia R, Morales-Santana S, Garcia-Fontana B, Garcia-Salcedo JA, et al. Circulating levels of sclerostin are increased in patients with type 2 diabetes mellitus. *J Clin Endocrinol Metab* (2012) 97(1):234–41. doi: 10.1210/jc.2011-2186
105. van Lierop AH, Hamdy NA, van der Meer RW, Jonker JT, Lamb HJ, Rijzewijk LJ, et al. Distinct effects of pioglitazone and metformin on circulating sclerostin and biochemical markers of bone turnover in men with type 2 diabetes mellitus. *Eur J Endocrinol* (2012) 166(4):711–6. doi: 10.1530/EJE-11-1061
106. Daniele G, Winnier D, Mari A, Bruder J, Fourcaudot M, Pengou Z, et al. Sclerostin and Insulin Resistance in Prediabetes: Evidence of a Cross Talk Between Bone and Glucose Metabolism. *Diabetes Care* (2015) 38(8):1509–17. doi: 10.2337/dc14-2989
107. Loh NY, Neville MJ, Marinou K, Hardcastle SA, Fielding BA, Duncan EL, et al. LRP5 regulates human body fat distribution by modulating adipose progenitor biology in a dose- and depot-specific fashion. *Cell Metab* (2015) 21(2):262–73. doi: 10.1016/j.cmet.2015.01.009
108. Mani A, Radhakrishnan J, Wang H, Mani A, Mani MA, Nelson-Williams C, et al. LRP6 mutation in a family with early coronary disease and metabolic risk factors. *Science* (2007) 315(5816):1278–82. doi: 10.1126/science.1136370
109. McNulty M, Singh RJ, Li X, Bergstralh EJ, Kumar R. Determination of serum and plasma sclerostin concentrations by enzyme-linked immunoassays. *J Clin Endocrinol Metab* (2011) 96(7):E1159–62. doi: 10.1210/jc.2011-0254
110. Yee CS, Xie L, Hatsell S, Hum N, Murugesh D, Economides AN, et al. Sclerostin antibody treatment improves fracture outcomes in a Type I diabetic mouse model. *Bone* (2016) 82:122–34. doi: 10.1016/j.bone.2015.04.048
111. Fairfield H, Falank C, Harris E, Demambro V, McDonald M, Pettitt JA, et al. The skeletal cell-derived molecule sclerostin drives bone marrow adipogenesis. *J Cell Physiol* (2018) 233(2):1156–67. doi: 10.1002/jcp.25976
112. Ukita M, Yamaguchi T, Ohata N, Tamura M. Sclerostin Enhances Adipocyte Differentiation in 3T3-L1 Cells. *J Cell Biochem* (2016) 117(6):1419–28. doi: 10.1002/jcb.25432
113. Kim SP, Da H, Li Z, Kushwaha P, Beil C, Mei L, et al. Lrp4 expression by adipocytes and osteoblasts differentially impacts sclerostin's endocrine effects on body composition and glucose metabolism. *J Biol Chem* (2019) 294(17):6899–911. doi: 10.1074/jbc.RA118.006769
114. Wu J, Bostrom P, Sparks LM, Ye L, Choi JH, Giang AH, et al. Beige adipocytes are a distinct type of thermogenic fat cell in mouse and human. *Cell* (2012) 150(2):366–76. doi: 10.1016/j.cell.2012.05.016
115. Chang MK, Kramer I, Huber T, Kinzel B, Guth-Gundel S, Leupin O, et al. Disruption of Lrp4 function by genetic deletion or pharmacological blockade increases bone mass and serum sclerostin levels. *Proc Natl Acad Sci USA* (2014) 111(48):E5187–95. doi: 10.1073/pnas.1413828111
116. Donham C, Manilay JO. The Effects of Sclerostin on the Immune System. *Curr Osteoporos Rep* (2020) 18(1):32–7. doi: 10.1007/s11914-020-00563-w
117. Wang J, Liu R, Wang F, Hong J, Li X, Chen M, et al. Ablation of LGR4 promotes energy expenditure by driving white-to-brown fat switch. *Nat Cell Biol* (2013) 15(12):1455–63. doi: 10.1038/ncb2867
118. Fulzele K, Lai F, Deddic C, Saini V, Uda Y, Shi C, et al. Osteocyte-Secreted Wnt Signaling Inhibitor Sclerostin Contributes to Beige Adipogenesis in

- Peripheral Fat Depots. *J Bone Miner Res* (2017) 32(2):373–84. doi: 10.1002/jbmr.3001
119. Costa S, Fairfield H, Reagan MR. Inverse correlation between trabecular bone volume and bone marrow adipose tissue in rats treated with osteoanabolic agents. *Bone* (2019) 123:211–23. doi: 10.1016/j.bone.2019.03.038
 120. Li S, Huang B, Jiang B, Gu M, Yang X, Yin Y. Sclerostin Antibody Mitigates Estrogen Deficiency-Induced Marrow Lipid Accumulation Assessed by Proton MR Spectroscopy. *Front Endocrinol (Lausanne)* (2019) 10:159. doi: 10.3389/fendo.2019.00159
 121. Potts JT. Parathyroid hormone: past and present. *J Endocrinol* (2005) 187(3):311–25. doi: 10.1677/joe.1.06057
 122. Pi M, Quarles LD. Novel bone endocrine networks integrating mineral and energy metabolism. *Curr Osteoporos Rep* (2013) 11(4):391–9. doi: 10.1007/s11914-013-0178-8
 123. Carpenter KA, Ross RD. Sclerostin Antibody Treatment Increases Bone Mass and Normalizes Circulating Phosphate Levels in Growing Hyp Mice. *J Bone Miner Res* (2020) 35(3):596–607. doi: 10.1002/jbmr.3923
 124. Garabedian M, Holick MF, Deluca HF, Boyle IT. Control of 25-hydroxycholecalciferol metabolism by parathyroid glands. *Proc Natl Acad Sci USA* (1972) 69(7):1673–6. doi: 10.1073/pnas.69.7.1673
 125. Tanaka Y, Deluca HF. The control of 25-hydroxyvitamin D metabolism by inorganic phosphorus. *Arch Biochem Biophys* (1973) 154(2):566–74. doi: 10.1016/0003-9861(73)90010-6
 126. Shimada T, Kakitani M, Yamazaki Y, Hasegawa H, Takeuchi Y, Fujita T, et al. Targeted ablation of Fgf23 demonstrates an essential physiological role of FGF23 in phosphate and vitamin D metabolism. *J Clin Invest* (2004) 113(4):561–8. doi: 10.1172/JCI200419081
 127. Kumar R, Vallon V. Reduced renal calcium excretion in the absence of sclerostin expression: evidence for a novel calcium-regulating bone kidney axis. *J Am Soc Nephrol* (2014) 25(10):2159–68. doi: 10.1681/ASN.2014020166
 128. Epstein S, Hamersma H, Beighton P. Endocrine function in sclerosteosis. *S Afr Med J* (1979) 55(27):1105–10.
 129. van Lierop AH, Appelman-Dijkstra NM, Papapoulos SE. Sclerostin deficiency in humans. *Bone* (2017) 96:51–62. doi: 10.1016/j.bone.2016.10.010
 130. Recker RR, Benson CT, Matsumoto T, Bolognese MA, Robins DA, Alam J, et al. A randomized, double-blind phase 2 clinical trial of romosozumab, a sclerostin antibody, in postmenopausal women with low bone mineral density. *J Bone Miner Res* (2015) 30(2):216–24. doi: 10.1002/jbmr.2351
 131. Cosman F, Crittenden DB, Adachi JD, Binkley N, Czerwinski E, Ferrari S, et al. Romosozumab Treatment in Postmenopausal Women with Osteoporosis. *N Engl J Med* (2016) 375(16):1532–43. doi: 10.1056/NEJMoa1607948
 132. McClung MR, Grauer A, Boonen S, Bolognese MA, Brown JP, Diez-Perez A, et al. Romosozumab in postmenopausal women with low bone mineral density. *N Engl J Med* (2014) 370(5):412–20. doi: 10.1056/NEJMoa1305224
 133. Padhi D, Jang G, Stouch B, Fang L, Posvar E. Single-dose, placebo-controlled, randomized study of AMG 785, a sclerostin monoclonal antibody. *J Bone Miner Res* (2011) 26(1):19–26. doi: 10.1002/jbmr.173
 134. Drake MT, Khosla S. Hormonal and systemic regulation of sclerostin. *Bone* (2017) 96:8–17. doi: 10.1016/j.bone.2016.12.004
 135. Brandenburg VM, Verhulst A, Babler A, D'Haese PC, Evenepoel P, Kaesler N. Sclerostin in chronic kidney disease-mineral bone disorder think first before you block it! *Nephrol Dial Transplant* (2019) 34(3):408–14. doi: 10.1093/ndt/gfy129
 136. Pelletier S, Dubourg L, Carlier MC, Hadj-Aissa A, Fouque D. The relation between renal function and serum sclerostin in adult patients with CKD. *Clin J Am Soc Nephrol* (2013) 8(5):819–23. doi: 10.2215/CJN.07670712
 137. Cejka D, Marculescu R, Kozakowski N, Plischke M, Reiter T, Gessl A, et al. Renal elimination of sclerostin increases with declining kidney function. *J Clin Endocrinol Metab* (2014) 99(1):248–55. doi: 10.1210/jc.2013-2786
 138. Sabbagh Y, Gracioli FG, O'Brien S, Tang W, dos Reis LM, Ryan S, et al. Repression of osteocyte Wnt/beta-catenin signaling is an early event in the progression of renal osteodystrophy. *J Bone Miner Res* (2012) 27(8):1757–72. doi: 10.1002/jbmr.1630
 139. Gracioli FG, Neves KR, Barreto F, Barreto DV, Dos Reis LM, Canziani ME, et al. The complexity of chronic kidney disease-mineral and bone disorder across stages of chronic kidney disease. *Kidney Int* (2017) 91(6):1436–46. doi: 10.1016/j.kint.2016.12.029
 140. Mare A, Verhulst A, Cavalier E, Delanaye P, Behets GJ, Meijers B, et al. Clinical Inference of Serum and Bone Sclerostin Levels in Patients with End-Stage Kidney Disease. *J Clin Med* (2019) 8(12). doi: 10.3390/jcm8122027
 141. Glorieux FH, Devogelaer JP, Durigova M, Goemaere S, Hemsley S, Jakob F, et al. BPS804 Anti-Sclerostin Antibody in Adults With Moderate Osteogenesis Imperfecta: Results of a Randomized Phase 2a Trial. *J Bone Miner Res* (2017) 32(7):1496–504. doi: 10.1002/jbmr.3143
 142. Seefried L, Baumann J, Hemsley S, Hofmann C, Kunstmann E, Kiese B, et al. Efficacy of anti-sclerostin monoclonal antibody BPS804 in adult patients with hypophosphatasia. *J Clin Invest* (2017) 127(6):2148–58. doi: 10.1172/JCI83731
 143. Appelman-Dijkstra NM, Papapoulos SE. From disease to treatment: from rare skeletal disorders to treatments for osteoporosis. *Endocrine* (2016) 52(3):414–26. doi: 10.1007/s12020-016-0888-7
 144. Saag KG, Petersen J, Brandt ML, Karaplis AC, Lorentzon M, Thomas T, et al. Romosozumab or Alendronate for Fracture Prevention in Women with Osteoporosis. *N Engl J Med* (2017) 377(15):1417–27. doi: 10.1056/NEJMoa1708322
 145. Lewiecki EM, Blicharski T, Goemaere S, Lippuner K, Meisner PD, Miller PD, et al. A Phase III Randomized Placebo-Controlled Trial to Evaluate Efficacy and Safety of Romosozumab in Men With Osteoporosis. *J Clin Endocrinol Metab* (2018) 103(9):3183–93. doi: 10.1210/jc.2017-02163
 146. Zeng C, Guo C, Cai J, Tang C, Dong Z. Serum sclerostin in vascular calcification and clinical outcome in chronic kidney disease. *Diabetes Vasc Dis Res* (2018) 15(2):99–105. doi: 10.1177/1479164117742316
 147. Claes KJ, Viaene L, Heye S, Meijers B, d'Haese P, Evenepoel P. Sclerostin: Another vascular calcification inhibitor? *J Clin Endocrinol Metab* (2013) 98(8):3221–8. doi: 10.1210/jc.2013-1521
 148. Krishna SM, Seto SW, Jose RJ, Li J, Morton SK, Biros E, et al. Wnt Signaling Pathway Inhibitor Sclerostin Inhibits Angiotensin II-Induced Aortic Aneurysm and Atherosclerosis. *Arterioscler Thromb Vasc Biol* (2017) 37(3):553–66. doi: 10.1161/ATVBAHA.116.308723
 149. Zhu D, Mackenzie NC, Millan JL, Farquharson C, MacRae VE. The appearance and modulation of osteocyte marker expression during calcification of vascular smooth muscle cells. *PLoS One* (2011) 6(5):e19595. doi: 10.1371/journal.pone.0019595
 150. Fang Y, Ginsberg C, Sugatani T, Monier-Faugere MC, Malluche H, Hruska KA. Early chronic kidney disease-mineral bone disorder stimulates vascular calcification. *Kidney Int* (2014) 85(1):142–50. doi: 10.1038/ki.2013.271
 151. Novo-Rodriguez C, Garcia-Fontana B, Luna-Del Castillo JD, Andujar-Vera F, Avila-Rubio V, Garcia-Fontana C, et al. Circulating levels of sclerostin are associated with cardiovascular mortality. *PLoS One* (2018) 13(6):e0199504. doi: 10.1371/journal.pone.0199504
 152. Qureshi AR, Olauson H, Witasp A, Haarhaus M, Brandenburg V, Wernerson A, et al. Increased circulating sclerostin levels in end-stage renal disease predict biopsy-verified vascular medial calcification and coronary artery calcification. *Kidney Int* (2015) 88(6):1356–64. doi: 10.1038/ki.2015.194
 153. Turk JR, Deaton AM, Yin J, Stolina M, Felix M, Boyd G, et al. Nonclinical cardiovascular safety evaluation of romosozumab, an inhibitor of sclerostin for the treatment of osteoporosis in postmenopausal women at high risk of fracture. *Regul Toxicol Pharmacol* (2020) 115:104697. doi: 10.1016/j.yrtph.2020.104697

Conflict of Interest: MW receives research funding from Radius Health and Galapagos NV on projects unrelated to this review. These funders had no role in preparation of this review manuscript or decision to publish.

The remaining authors declare that the research was conducted in the absence of any commercial or financial relationships that could be construed as a potential conflict of interest.

Copyright © 2021 Wang, Mazur and Wein. This is an open-access article distributed under the terms of the Creative Commons Attribution License (CC BY). The use, distribution or reproduction in other forums is permitted, provided the original author(s) and the copyright owner(s) are credited and that the original publication in this journal is cited, in accordance with accepted academic practice. No use, distribution or reproduction is permitted which does not comply with these terms.



Circulating Carboxylated Osteocalcin Correlates With Skeletal Muscle Mass and Risk of Fall in Postmenopausal Osteoporotic Women

OPEN ACCESS

Jacopo Antonino Vitale¹, Veronica Sansoni², Martina Faraldi², Carmelo Messina^{3,4}, Chiara Verdelli⁵, Giovanni Lombardi^{2,6*} and Sabrina Corbetta^{7,8}

Edited by:

Lucas R. Brun,
National University of Rosario,
Argentina

Reviewed by:

Jan Josef Stepan,
Charles University, Czechia
Subhashis Pal,
Emory University, United States

*Correspondence:

Giovanni Lombardi
giovanni.lombardi@
grupposandonato.it

Specialty section:

This article was submitted to
Bone Research,
a section of the journal
Frontiers in Endocrinology

Received: 19 February 2021

Accepted: 12 April 2021

Published: 05 May 2021

Citation:

Vitale JA, Sansoni V,
Faraldi M, Messina C, Verdelli C,
Lombardi G and Corbetta S (2021)
Circulating Carboxylated
Osteocalcin Correlates With
Skeletal Muscle Mass and
Risk of Fall in Postmenopausal
Osteoporotic Women.
Front. Endocrinol. 12:669704.
doi: 10.3389/fendo.2021.669704

¹ Laboratory of Movement and Sport Science, IRCCS Istituto Ortopedico Galeazzi, Milan, Italy, ² Laboratory of Experimental Biochemistry and Molecular Biology, IRCCS Istituto Ortopedico Galeazzi, Milan, Italy, ³ Radiology Unit, IRCCS Istituto Ortopedico Galeazzi, Milan, Italy, ⁴ Department of Biomedical Sciences for Health, University of Milan, Milan, Italy, ⁵ Laboratory of Experimental Endocrinology, IRCCS Istituto Ortopedico Galeazzi, Milan, Italy, ⁶ Department of Athletics, Strength and Conditioning, Poznań University of Physical Education, Poznań, Poland, ⁷ Endocrinology and Diabetology Service, IRCCS Istituto Ortopedico Galeazzi, Milan, Italy, ⁸ Department of Biomedical, Surgical and Dental Sciences, University of Milan, Milan, Italy

Background: Bone and skeletal muscle represent a single functional unit. We cross-sectionally investigated body composition, risk of fall and circulating osteocalcin (OC) isoforms in osteoporotic postmenopausal women to test the hypothesis of an involvement of OC in the bone-muscle crosstalk.

Materials and Methods: Twenty-nine non-diabetic, non-obese, postmenopausal osteoporotic women (age 72.4 ± 6.8 years; BMI 23.0 ± 3.3 kg/m²) underwent to: 1) fasting blood sampling for biochemical and hormone assays, including carboxylated (cOC) and uncarboxylated (uOC) osteocalcin; 2) whole-body dual energy X-ray absorptiometry (DXA) to assess total and regional body composition; 3) magnetic resonance imaging to determine cross-sectional muscle area (CSA) and intermuscular adipose tissue (IMAT) of thigh muscles; 4) risk of fall assessment through the OAK system.

Results: Appendicular skeletal muscle index (ASMMI) was low in 45% of patients. Forty percent got a low OAK score, consistent with moderate-severe risk of fall, which was predicted by low legs lean mass and increased total fat mass. Circulating cOC levels showed significantly correlated with β CTx-I, lean mass parameters including IMAT, and OAK score. Fractured and unfractured women did not differ for any of the analyzed parameters, though cOC and uOC positively correlated with legs lean mass, OAK score and bone markers only in fractured women.

Conclusions: Data supported the relationship between OC and skeletal muscle mass and function in postmenopausal osteoporotic women. Serum cOC, but not uOC, emerges as mediator in the bone-muscle crosstalk. Circulating cOC and uOC levels may be differentially regulated in fractured and unfractured osteoporotic women, suggesting underlying differences in bone metabolism.

Keywords: osteocalcin, skeletal muscle mass, risk of fall, osteoporosis, fragility fractures

INTRODUCTION

Aging results in the progressive and parallel loss of bone, known as osteopenia, and in skeletal muscles, known as sarcopenia. Sarcopenia is defined as the loss of skeletal muscle mass and quality, which accelerates with aging and is associated with functional decline. Osteopenia and sarcopenia are two main determinants of aging-related fragility (1), and sarcopenia represents one of the main causes of increased risk of falls and, directly or indirectly, fractures (2). Sarcopenia in elderly women associated with an increased risk of all-cause mortality (3, 4). Moreover, in older adults, the coexistence of osteopenia and sarcopenia, namely osteosarcopenia, has to be regarded as the major risk factor for fractures and further functional decline due to low physical performance (5–7). Among the lean tissues, skeletal muscles exert a strong positive effect on bone mass (8–10), while the impact of fat is weaker and likely indirect (11, 12).

Bone and muscle are functionally related, not only biomechanically since the direct connection, but also based on the emerging intense endocrine crosstalk (13–16).

Osteocalcin (OC) is mainly secreted by osteoblasts during bone formation, in part also by osteocytes, and it binds to the mineralized matrix (17). Its role in skeletal remodeling is debated as OC knockout mice showed normal bone mineral density though they display a crystals misalignment along the collagen fibrils consistent with a low degree of crystal maturation and increased brittleness (18, 19). OC overexpression in mice does not affect bone mineralization, but it promotes recruitment and differentiation of circulating monocytes and osteoclast precursors, suggesting a role in the osteoblast-osteoclast interaction (20).

Among other metabolic abnormalities and the substantially unmodified bony phenotype, mice in which *Gprc6a*, the putative receptor for OC, has been knocked out experienced decreased muscle mass, while the knockout mice of *Esp*, a phosphatase that inhibits the function of OC, has increased muscle mass. Further evidence that OC may solve a relevant role in muscle mass gain and muscle function is that supplementation with OC restores reduced exercise capacity in aged mice and increases muscle strength. Aerobic exercise increases circulating bioactive OC levels (i.e., uncarboxylated OC) and induces OC signaling in muscle leading to the expression of the myokine IL-6 (21, 22).

OC regulates muscle mass independently of its effects on energy expenditure, acting by direct activation of the receptor GPRC6A (21–23). Uncarboxylated OC (uOC) seems to directly promote protein synthesis in mice myotubes, explaining why this

hormone is responsible for muscle maintenance during aging (21, 22). Moreover, uOC induces myoblast proliferation *via* sequential activation of the PI3K/Akt and p38 MAPK pathways in C2C12 murine myoblasts, while it enhances myogenic differentiation *via* a mechanism involving GPRC6A-ERK1/2 signaling (23).

However, many studies were published using animal models, and they need to be confirmed in humans. Some differences between murine and human OC should be considered. OC is carboxylated on glutamic acid residues (Glu→Gla) 13, 17, and 20 in the mouse protein and on Glu 17, 21, and 24 in humans. Moreover, regarding the circadian rhythm, in mice OC levels peak during the daytime and are at lowest during nighttime, whereas in humans, the levels fall in the early morning, rise in the afternoon and peak at night (14, 24).

The primary aim of the present study was to investigate the associations between circulating carboxylated (cOC) and uOC, body composition (i.e., bone, fat and muscle mass) and risk of fall in a series of postmenopausal osteoporotic elderly women. Secondly, we aimed to examine the pairwise differences in body composition, risk of fall and circulating cOC and uOC levels between fractured and unfractured osteoporotic women. We tested the hypothesis that cOC and/or uOC are involved in the bone-muscle crosstalk in osteoporotic elderly women.

MATERIALS AND METHODS

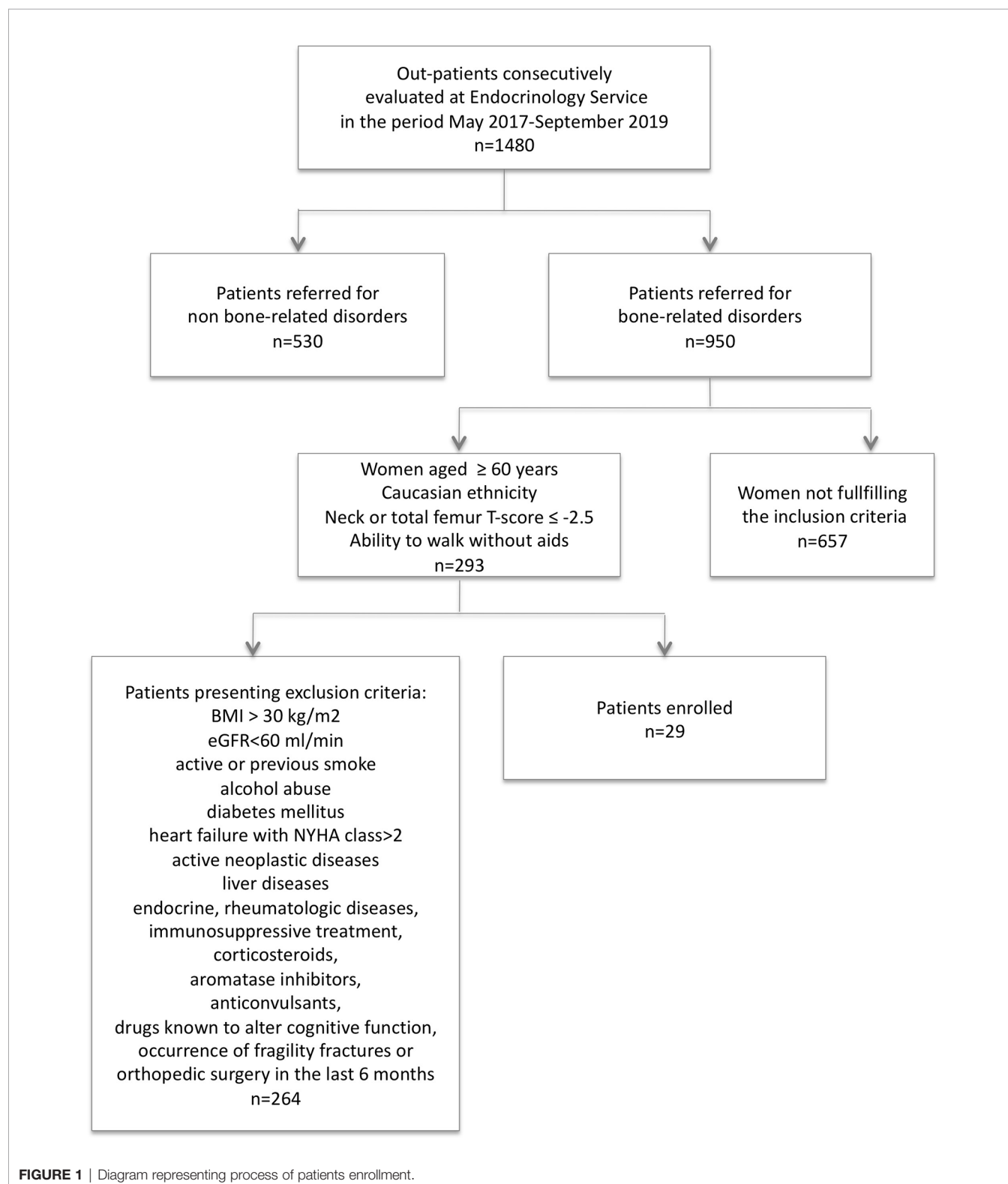
Study Design

This is an observational cross-sectional study conducted in accordance with the STROBE guidelines for cross-sectional studies (25) and was approved by the Ethical Committee of Vita-Salute San Raffaele University (ref.no.17/INT/2017). Before the beginning of the study, all the participants signed their written informed consent to participate. All study procedures were performed in compliance with the laws and regulations governing the use of human subjects (Declaration of Helsinki) and the study protocol was registered at clinicaltrials.gov (ref.no. NCT03382366). All patients enrolled were investigated by: a) clinical and anthropometric evaluation; b) risk of fall evaluation by the OAK system (Khymeia, Noventa Padovana, Italy); c) fasting blood sample for biochemical and hormonal assays, and d) total body dual energy x-ray absorptiometry scan (DXA) for body composition assessment. Moreover, magnetic resonance imaging (MRI) was performed to measure the cross-sectional muscle area (CSA) and the intermuscular adipose tissue (IMAT) of thigh muscles.

Study Population

The final series was represented by 29 postmenopausal non-obese women (mean age 72.4 ± 6.8 , range 60-85 years; BMI 23.0 ± 3.3 kg/m², range 18.1-29.3) from the outpatients referred to the Endocrinology

Service of IRCCS Istituto Ortopedico Galeazzi in Milan. Women were consecutively enrolled between May 2017 and September 2019 as illustrated in **Figure 1**. Inclusion criteria were: Caucasian ethnicity, age ≥ 60 years, a DXA-based diagnosis of osteoporosis at



proximal hip (neck or total femur bone mineral density (BMD) T-score ≤ -2.5), and ability to walk without aids. Exclusion criteria included: age < 60 years, BMI $> 30 \text{ kg/m}^2$, estimated GFR $> 60 \text{ ml/min}$, active or previous smoke, alcohol abuse, diabetes mellitus, heart failure with NYHA class > 2 , active neoplastic diseases, liver diseases, ascertained endocrine and rheumatologic diseases, immunosuppressive treatment including corticosteroids, treatment with aromatase inhibitors, anticonvulsants, drugs known to alter cognitive function, occurrence of fragility fractures or orthopedic surgery in the last 6 months before the enrollment. All women, included those with previous fragility fractures, were free from anti-osteoporotic drugs, calcium and vitamin D supplementation since at least 6 months.

Fall Risk Assessment by OAK Device

The OAK device is a safe and validated device used for the assessment of fall risk [26]; it provides an automated version of the Brief-BESTest, a clinical tool examining balance performance in six specific context of postural control (26). The risk of fall reflects bone frailty, chronic, and/or degenerative conditions associated with physical, sensory, and cognitive changes in advancing age (27). The OAK system works semi-automatically and an experienced investigator assisted every session. The OAK system comprises two stabilometric platforms, three sensorized bars, four antennas and a Human Machine Interface providing audio and video instructions to the subjects. Before the beginning of the test, all subjects wore a portable device connected to a set of four inertial-magnetic sensors, located on the wrists and the thighs through gloves and rip-ties, to interact with the OAK system. Data from sensors, platforms and bars were then collected and integrated to calculate balance scores for each task. The global score ranges between 0 and 24 points: a score between 17 and 24 classifies a subject as low risk of fall, while a score between 0 and 16 identifies a subject as medium/high risk of fall (28). A familiarization session was performed before the text execution; the time range needed to complete the whole test was 9–15 minutes.

Body Composition Analysis

A whole-body DXA scan was performed to measure total and regional body composition (Hologic QDR-Discovery 139 W densitometer; Hologic Inc., Bedford, MA, USA). Regions of interest were automatically defined by the software including six different body districts: total body, trunk, upper limbs (left and right arms), lower limbs (left and right legs). For each region, the exam provided the weight of total mass, fat mass, and lean mass, all expressed in grams (g), as well as regional BMD values, expressed in g/cm^2 . The precision of the BMD measurement by DXA has coefficients of variation (CV) at different sites between 0.4% (lumbar spine) to 1.3% (femoral neck) and 2% to 6% for body composition, in line with previous report (29).

The total amount of lean mass was also investigated by using the Appendicular Skeletal Muscle Mass Index (ASMMI), which is the amount of muscle in the upper and lower limbs, corrected by the individuals' square of the height (appendicular lean mass/height²). The most valid and widely accepted cut-off

value for ASMMI with the whole-body DXA in women is reported to be 5.7 kg/m^2 , with subjects under this threshold being diagnosed with low muscle mass (30, 31). Diagnosis of osteoporosis was established in presence of BMD of -2.5 standard deviation or more below the mean of a young healthy adult (T-score) (32). DXA-measured femoral neck BMD (33) and ASMMI (31, 33) are considered the gold standard values for the diagnosis of osteoporosis and low muscle mass, respectively (34, 35).

Magnetic Resonance Imaging (MRI)

MRI was performed in twenty-four women; the remaining patients refused to undergo this additional procedure due to claustrophobia. All scans were performed with a 1.5T MR system (Avanto, Siemens Medical Solution, Erlangen, Germany) and 15 slices with a thickness of 5 mm were acquired covering a total length of 7.5 cm at the middle third of the right thigh. MRI protocol included a transverse T1-weighted sequence (for anatomic reference) and a transverse Dixon sequence (for quantitative analysis), for a total examination time of about 10 minutes. More in detail, intermuscular adipose tissue (IMAT) quantification was performed by using Dixon MRI sequences, which produce four sets of MRI images providing information on water and fat content separately, therefore offering the possibility for precise fat quantification (36, 37). The segmentation of the thigh muscles was performed for each slice of that in which the muscle-tendon junction of the gluteus maximus muscle was visible with the use of ImageJ, an open-source software (38), by a single expert operator (C.M.). The whole muscle area was selected as a single unit. Two quantitative parameters were finally calculated using ImageJ15: the thigh cross-sectional muscle area (CSA), expressed in mm^2 , and the thigh IMAT, representing the IMAT absolute value of the total muscle CSA and expressed in mm^2 . Subcutaneous fat, major blood vessels and the bony femur were excluded from the segmentation.

Laboratory Examination

Fasting blood samples were collected from each patient by standard venipuncture. Total calcium, phosphate, total alkaline phosphatase activity (ALP), creatinine, and the bone resorption marker type I collagen C-terminal cross-linked telopeptide ($\beta\text{CTx-I}$) were measured by routine assays in serum tubes with clot activator (SSTII Advance Vacutainer, Becton Dickinson, Franklin Lakes, NJ, USA). Dipotassium ethylenediaminetetraacetate (K2EDTA)-anticoagulated plasma PTH (K2EDTA Vacutainer, Becton Dickinson) and serum 25-hydroxyvitamin D [25-(OH)D] were assayed by Roche. Plasma cOC and uOC were measured by the means of two specific monoclonal antibody-based sandwich immunoassays (Undercarboxylated OC EIA kit and Gla-Type OC EIA kit, Takara Bio Inc., Otsu-Shi, SHG, Japan). The lower limit of detection (LLD) was 0.25 ng/mL for both assays. As reported by the manufacturer, intra-assay (CV_w) and interassay (CV_b) coefficients of variation were 4.58% and 5.67% for uOC and 3.3% and 1.0% for cOC, respectively (39). All samples were tested in duplicate and according to the most up-to-date pre-analytical warnings (40, 41).

Statistical Analysis

Sample size was calculated by G*power3.1, considering as significant a correlation with a slope of at least 0.48, an α -error of 0.05 and a power of 0.80 in a model of linear bivariate regression. Continuous variables were given as mean \pm standard error media (SEM). Numeration data were described as percentages (%). The normality of the distribution of clinical, radiological and laboratory variables for the fractured (n=13) and unfractured group (n=16) were checked using graphical methods and the Shapiro-Wilk test. Data homogeneity between groups was tested through un-paired Student t-tests or with the Mann-Whitney rank test for non-normally distributed variables. Significance was set at $p < 0.05$. In addition, the normality of the distribution of clinical, radiological and laboratory variables were checked using graphical methods and the Shapiro-Wilk test for the entire group of subjects. The existence of a correlation between outcomes was tested by the Pearson's correlation index. The same approach was adopted to test the existence of possible correlations between cOC or uOC and the other outcomes for the group of fractured and unfractured women separately. Correlations were considered significant when $r > 0.25$ and $P < 0.05$. Multivariate analysis considering OAK score and cOC as dependent variables have been performed to test the hypothesis they could be predictive of muscle parameters. Statistical analysis was performed using GraphPad Prism version 6.00 (GraphPad Software, San Diego, CA, USA) and by Past3.14 (42).

RESULTS

Body Composition in the Series of Postmenopausal Osteoporotic Women

Mean ASMMI was $5.69 \pm 0.13 \text{ kg/m}^2$. Considering a cut-off of 5.7 kg/m^2 for the diagnosis of low muscle mass in elderly women according the Consensus Report produced by European Working Group on Sarcopenia in Older People 2 (EWGSOP2) (30), low muscle mass was detected in 13 (45%) out of the 29 osteoporotic women, with ASMMI ranging between 4.20 and 5.62 kg/m^2 . In the present series of osteoporotic postmenopausal women, ASMMI did not correlate with age, while it positively correlated with BMI value ($r = 0.599$, $p = 0.006$); therefore, the muscle mass index was normalized by BMI, and appendicular skeletal muscle (ASM)/BMI was considered. ASM/BMI negatively correlated with total fat mass ($r = -0.644$, $p = 0.0002$) (Figure 2A) and in particular with the trunk fat mass ($r = -0.724$, $p = 0.0001$) (Figure 2B). Despite ASM/BMI did not show any significant correlation with segmental bone mineral density, considering the lean mass of each leg, a significant positive correlation with the corresponding segmental bone mineral density (BMD) emerged (Figures 2C, D).

We further gained insight about skeletal muscle mass features in elderly osteoporotic women investigating the muscle and fat components of thigh by MRI. The thigh CSA ranged 5323–10759 mm^2 , and positively correlated with ASM/BMI ($r = 0.415$, $p = 0.044$) (Figure 3A) and with leg BMD ($r = 0.554$, $p = 0.014$) (Figure 3B).

The extracellular adipose tissue found beneath the fascia and in-between muscle groups, evaluated as IMAT, ranged between 741 mm^2 and 1881 mm^2 , representing 10–25% of the thigh CSA. IMAT positively correlated with CSA ($r = 0.471$, $p = 0.020$) (Figure 3C), and with the leg fat mass measured by DXA ($r = 0.564$, $p = 0.012$) (Figure 3D).

Fall risk was evaluated using the OAK score derived by the OAK system. Mean OAK score was 17.8 ± 4.7 point-score out of 24.0; 12 women (41%) showed an OAK score between 0–16 consistent with moderate-high risk of fall. OAK scores negatively correlated with age (Figure 3E). Interestingly, OAK scores positively correlated with ASM/BMI ($r = 0.645$, $p = 0.0002$) (Figure 3F), with CSA ($r = 0.436$, $p = 0.033$) (Figure 3G), and negatively with total fat mass ($r = -0.527$, $p = 0.003$) (Figure 3H). A multivariate model considering OAK score as the dependent variable, and age, ASM/BMI, CSA, and total fat mass as the independent variables, indicated that OAK score is significantly related to age ($r^2 = 0.334$, $p = 0.004$) as well as to ASM/BMI ($r^2 = 0.416$, $p = 0.005$).

Circulating Osteocalcin Levels in Osteoporotic Postmenopausal Women

OC is released by activated osteoblasts (17). Though both plasma cOC and uOC did not show any significant correlation with segmental BMDs nor with total or segmental fat masses (data not shown), in the series of osteoporotic women, both serum cOC and uOC levels positively correlated with serum $\beta\text{CTx-I}$ levels, while any significant correlation could be detected with the mineral metabolic markers (Table 1). It is note of worth that plasma cOC, but not uOC, levels positively correlated with the ASM/BMI (Table 1). Considering the different skeletal muscle segments, plasma cOC, but not uOC, levels positively correlated with trunk lean mass as well as with legs lean mass (Table 1). In line with finding in DXA-derived lean mass parameters, plasma cOC levels positively correlated with CSA and with IMAT measured by MRI (Table 1). Interestingly, plasma cOC levels also positively correlated with muscle function assessed as OAK score (Table 1). In a multivariate model considering plasma cOC levels as the dependent variable, and serum $\beta\text{CTx-I}$ levels, legs lean mass, IMAT, and OAK score, as the independent variables, cOC levels were significantly related to serum $\beta\text{CTx-I}$ levels ($r^2 = 0.147$, $p = 0.011$) and to legs lean mass ($r^2 = 0.319$, $p = 0.017$).

Differences Between Fractured and Unfractured Osteoporotic Women

Thirteen women (45%) experienced previous fragility fractures: at least one vertebral fracture (clinical and morphometric vertebral fractures, detected by dorsal and lumbar conventional x-ray imaging) was diagnosed in 10 women, femur neck fracture in 1 woman, and distal radius fractures in 2 women. Fractured osteoporotic women did not show evident differences in their body composition when compared with unfractured women (Table 2).

We further investigated about differences in cOC and uOC correlations between fractured and unfractured osteoporotic women (Table 3). The most striking difference between the two groups consists in the strong positive relationship between

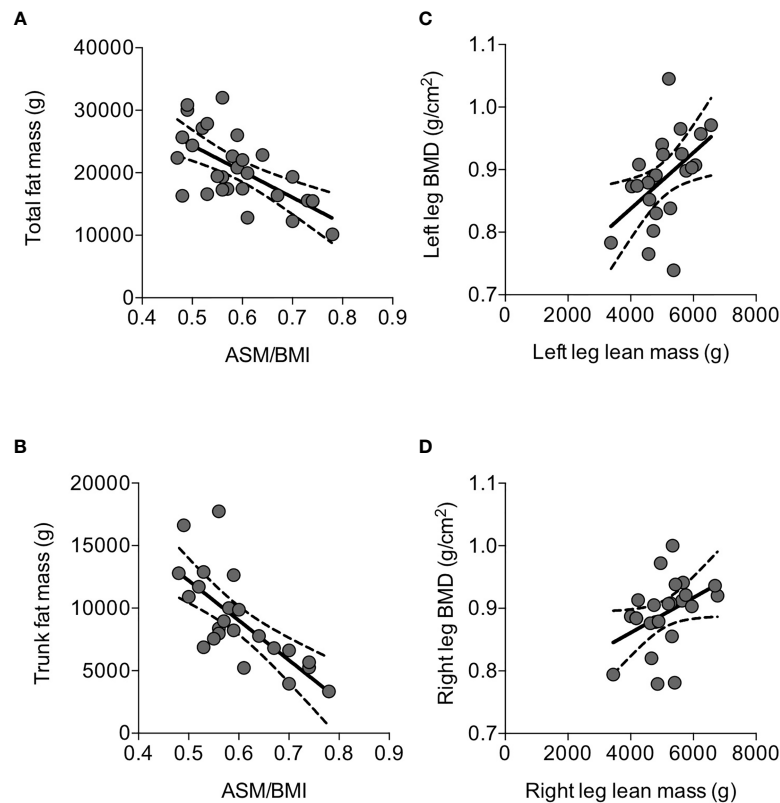


FIGURE 2 | Correlations between parameters of body composition detected by DXA in osteoporotic postmenopausal women. ASM/BMI negatively correlated with total fat mass **(A)** and, in particular, with trunk fat mass **(B)**. Left leg lean mass positively correlated with the corresponding segmental BMD **(C)**; similar correlation was detected between the right lean mass and the corresponding segmental BMD **(D)**. Lines represent regressions, dot lines represent 95% confidence intervals. Data were analyzed by Pearson coefficient of correlation.

serum cOC and uOC levels in fractured women ($r=0.852$, $p=0.0002$), which was definitely abolished in unfractured women. In unfractured women, circulating cOC was confirmed to correlate with muscle mass parameters, such as legs lean mass, thigh CSA and IMAT. In fractured women, both cOC and uOC correlated with lean mass parameters, namely ASM/BMI and legs lean mass, with the OAK score-related risk of fall, and with bone markers, suggesting that the intense crosstalk among bone, and muscle mass and function mediated by cOC is more active in fractured osteoporotic women with respect to unfractured women.

DISCUSSION

Osteoporosis and sarcopenia are serious health problems in postmenopausal women. In the present study, the interaction between bone and skeletal muscle was investigated in non-obese, non-diabetic, vitamin D-sufficient, older than 60 years postmenopausal osteoporotic women, free from anti-osteoporotic drugs and from any other treatment known to affect bone metabolism. The hypothesis that circulating carboxylated and/or uncarboxylated osteocalcin levels may mediate the bone-muscle interaction has been tested. Low muscle mass affected about a half of

osteoporotic women, and data obtained by MRI suggested that elderly osteoporotic women with conserved lean mass may have, indeed, increased intramuscular fat infiltration, measured as IMAT. This finding is relevant because as IMAT increases, muscle quality, and possibly muscle function, decreases (43). Moreover, the frequently occurring low muscle mass at legs level and reduced thigh cross-sectional muscle area are known to be associated with reduced bone mineral densities, in line with a previous report (44), underscoring the relationship between bone and skeletal muscle in elderly osteoporotic women.

A consistent subset (40%) of osteoporotic postmenopausal women had a moderate-high increased risk of fall as evaluated by the automated system OAK. Interestingly, OAK score well correlated with muscle parameters, namely ASM/BMI and thigh CSA, supporting the hypothesis that a reduced muscle mass increases the risk of fall in osteoporotic women. Increased fat mass also emerged as a negative factor determining the risk of fall, though the role seems minor than that of age and ASM/BMI. Therefore, impaired muscle mass and function frequently occur in osteoporotic postmenopausal women and are related with BMD.

Experimental evidence suggest an intense crosstalk between bone and skeletal muscle through mechanic stimulation and hormones, including myokines, adipokines, and osteokines

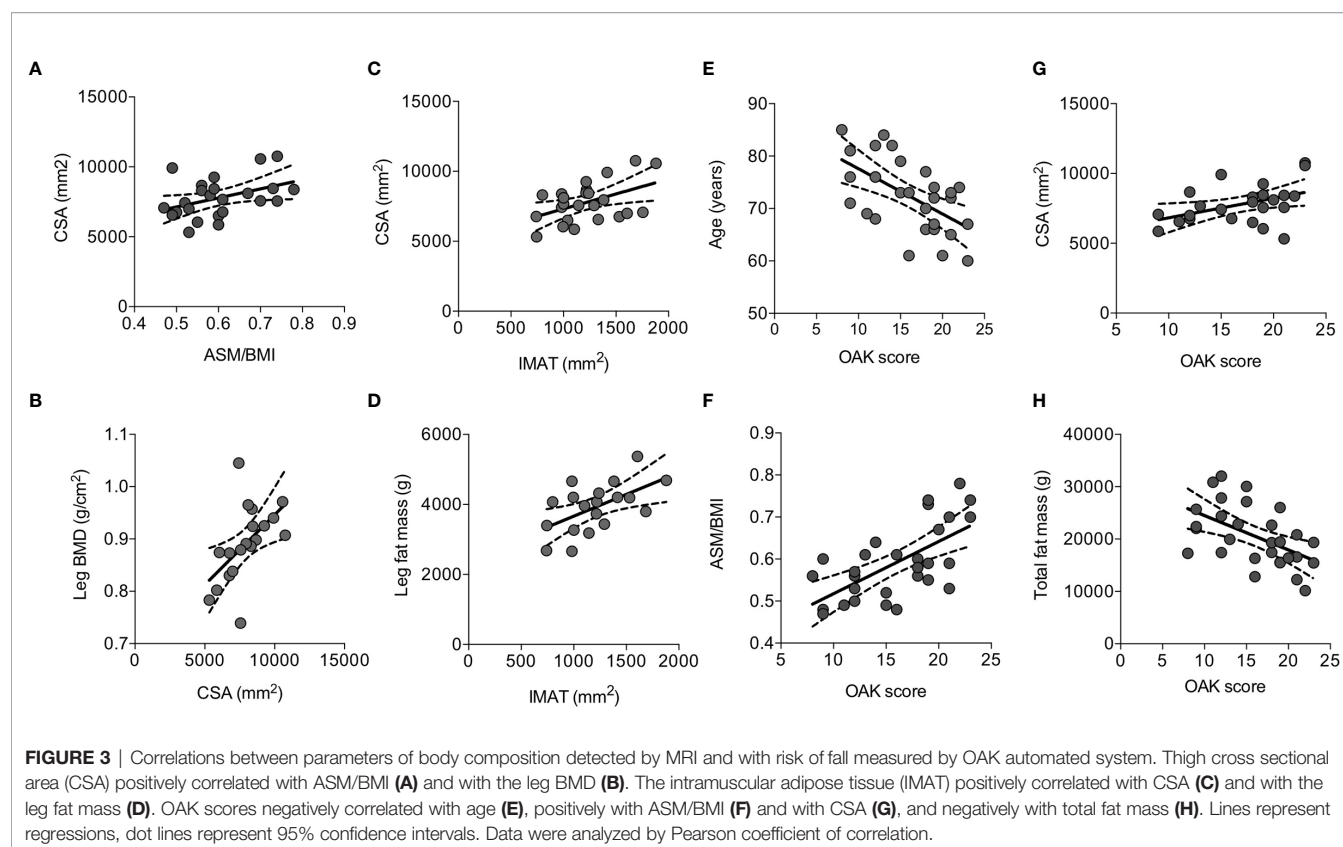


TABLE 1 | Significant correlations between plasma cOC and uOC levels and parameters related to bone, muscle mass, and muscle function.

Pearson	cOC		uOC	
	r	P	r	P
Bone parameters				
β CTx-I	0.620	0.039	0.707	<0.0001
Muscle mass				
ASM/BMI	0.458	0.013	0.009	0.961
Trunk lean mass	0.458	0.012	0.186	0.400
Legs lean mass	0.565	0.001	-0.134	0.542
CSA	0.519	0.009	0.153	0.475
IMAT	0.435	0.034	-0.022	0.917
Muscle function				
OAK score	0.431	0.020	0.014	0.944

cOC, carboxylated osteocalcin; uOC, uncarboxylated osteocalcin; r, coefficient of correlation by Pearson test; P, statistical significance; β CTx-I, beta-crosslinked C-terminal telopeptide of type I collagen; ASM/BMI, appendicular skeletal muscle mass corrected for BMI; CSA, Cross-sectional muscle area of the thigh; IMAT, Intermuscular fat of the thigh. Bold values highlighted statistical significant values.

(15, 16). We focused attention on osteocalcin, whose endocrine function is emerging, though data are controversial (45). Gender differences in serum osteocalcin levels and their modulation have been reported (20), so to avoid this potential confounding bias, postmenopausal women have been analyzed in the present study. Moreover, osteoporotic women with diabetes and obesity were excluded, since the potential involvement of this hormone in the regulation of energy metabolism and endocrine pancreas function, at least in rodent models (46). Investigating both the carboxylated and uncarboxylated forms in a series of postmenopausal osteoporotic women, we found that both cOC

and uOC levels positively correlated with serum β CTx-I levels, in line with what previously reported (47, 48), suggesting that OC is related with osteoclastic resorptive activity. We found that circulating cOC levels correlated with body composition, namely ASM/BMI, in particular with the trunk and legs lean masses, and with total fat mass in osteoporotic women. Of note, legs lean mass is mainly associated with circulating cOC levels, supporting the narrow relationship between skeletal muscle and bone-derived cOC in osteoporotic elder women. This finding represents a discrepancy with reports in mice, where uOC display endocrine action. The association we found between

TABLE 2 | Pairwise comparisons between fractured (n=13) and unfractured (n=16) osteoporotic women for clinical, body composition and bone metabolism variables.

Parameters	Fractured women (n=13)	Unfractured women (n=16)	Significance
Age (years)	74.7±1.6	70.6±1.8	0.107
Bone mineral density			
L1-L4 T-score	-2.70±0.31	-3.00±0.26	0.448
Neck T-score	-2.74±0.09	-2.60±0.13	0.410
Femur T-score	-2.34±0.19	-2.51±0.15	0.487
Arm sBMD (g/cm ²)	1.194±0.201	1.199±0.080	0.926
Legs BMD (g/cm ²)	1.709±0.310	1.630±0.509	0.656
Fat mass			
BMI (kg/m ²)	24.2±0.9	22.1±0.8	0.075
Total fat mass (g)	22109.0±1817.0	19283.0±1187.0	0.190
Arms fat mass (g)	3107.0±1272.0	2567.0±1242.2	0.316
Legs fat mass (g)	7735.0±1699.0	7889.0±1507.4	0.821
Trunk fat (g)	9988.0±1307.0	8163.0±872.0	0.251
Lean mass			
ASM/BMI	0.248±0.033	0.251±0.029	0.773
Arms lean mass (g)	3634.0±373.3	3258.0±404.9	0.016
Legs lean mass (g)	10487.0±1222.0	9665.0±1628.0	0.144
Trunk lean mass (g)	17260.0±522.5	16225.0±590.7	0.207
Thigh muscle CSA (mm ²)	7998.8±1163.2	7637.1±1574.9	0.545
IMAT (mm ²)	1265±52.6	1190±102.9	0.571
Muscle function			
Physical activity (hr/week)	1.08±1.38	2.19±3.10	0.243
OAK score (0-to-24)	15.5±4.3	16.4±4.8	0.578
Circulating bone markers			
cOC (ng/ml)	10.2±1.0	10.3±0.9	0.936
uOC (ng/ml)	3.7±0.6	4.5±0.9	0.509
Total ALP (U/L)	74.0±26.1	66.0±13.4	0.256
βCTx-I (ng/ml)	0.245±0.144	0.259±0.162	0.888
Total calcium (mg/dl)	9.3±0.3	9.4±0.5	0.427
PTH (pg/ml)	50.7±24.3	84.1±37.5	0.226
25-(OH)D (ng/ml)	36.4±12.8	33.7±14.3	0.900

Data are reported as mean ± SD. BMD, Bone Mineral Density; BMI, Body-Mass Index; ASM/BMI, Appendicular Skeletal Muscle Mass Index; CSA, Cross-sectional muscle area of the thigh; IMAT, Intermuscular fat of the thigh; cOC, carboxylated osteocalcin; uOC, uncarboxylated osteocalcin; ALP, alkaline phosphatase activity; PTH, Parathyroid hormone; 25-(OH)D, serum 25-hydroxyvitamin D; βCTx-I, beta-crosslinked C-terminal telopeptide of type I collagen.

Bold values highlighted statistical significant values.

TABLE 3 | Correlations between cOC or uOC with the body composition parameters and bone markers in fractured and unfractured women.

Parameters	Fractured				Unfractured			
	cOC		uOC		cOC		uOC	
	r	P	r	P	r	P	r	P
Muscle mass								
ASM/BMI	0.433	0.139	0.716	0.006	0.100	0.712	-0.013	0.962
Legs lean mass (g)	0.661	0.014	0.499	0.084	0.595	0.029	-0.117	0.665
CSA (mm ²)	0.378	0.282	0.050	0.891	0.569	0.034	0.190	0.515
IMAT (g)	-0.355	0.315	-0.453	0.189	0.640	0.014	0.095	0.747
Muscle function								
OAK score	0.645	0.017	0.591	0.034	0.170	0.530	-0.122	0.652
Fat mass								
BMI (kg/m ²)	-0.200	0.521	-0.521	0.068	0.147	0.587	0.276	0.300
Total fat mass (g)	-0.221	0.468	-0.493	0.087	0.058	0.830	0.066	0.806
Circulating bone markers								
Total ALP (U/L)	0.786	0.007	0.794	0.006	0.494	0.214	0.665	0.072
βCTx-I (ng/ml)	0.855	0.0002	0.855	0.0002	0.063	0.817	0.678	0.004
25-(OH)D (ng/ml)	-0.689	0.019	-0.468	0.146	0.035	0.923	-0.494	0.147
uOC (ng/ml)	0.852	0.0002	–	–	-0.013	0.963	–	–

OC, carboxylated osteocalcin; uOC, uncarboxylated osteocalcin; fractured, osteoporotic women experiencing previous fragility fracture; unfractured, osteoporotic women without evidence of clinical or morphometric fractures; r, coefficient of correlation by Pearson test; P, statistical significance; ASM/BMI, appendicular skeletal muscle mass corrected for BMI; BMI, Body-Mass Index; CSA, Cross-sectional muscle area of the thigh; IMAT, Intermuscular fat of the thigh; ALP, alkaline phosphatase activity; βCTx-I, beta-crosslinked C-terminal telopeptide of type I collagen; 25-(OH)D, serum 25-hydroxyvitamin D.

Bold values highlighted statistical significant values.

cOC and leg composition may be related to the muscular activity that, in humans, included the elderly, is prominent in the lower limbs. However, this finding should be confirmed and its physiological meaning might be investigated. Nonetheless, it is in line with the intervention study by Kyla Shea et al. (49) demonstrating that uOC was not cross-sectionally associated with appendicular lean mass or fat mass in older community-dwelling men or women, and that reduction of uOC levels following vitamin K supplementation affected neither lean nor fat mass over 3 years. Moreover, a positive correlation between circulating osteocalcin and lean mass has been reported in trained and untrained young women (50) and in middle-aged and elderly Chinese subjects (51). Moreover, exercise enhances osteocalcin serum levels in adult women (22), while osteocalcin circulating levels decrease during aging, when exercise capacity declines. By contrast, in community-dwelling middle-aged and elderly adults, Moriawaki et al. failed to detect any relationship between OC and muscle parameters (52).

Further, we focused the attention on the two subgroups of osteoporotic elder women who experienced at least one fracture and those who never suffered fractures, including screening for morphometric vertebral deformities. All fractures occurred at least 6 months before the enrollment in the study, when bone turnover markers return to baseline (53).

We failed in detecting any difference in body composition parameters, OAK score, as well as in circulating bone markers between the two groups. Nonetheless, fractured women were characterized by a positive relationship between circulating cOC and uOC, which was absent in unfractured women. Moreover, plasma cOC and uOC levels well correlated with total ALP and β CTx-I in fractured women, but not in unfractured women. These findings suggest that bone remodeling differ in osteoporotic fractured women compared with osteoporotic unfractured. In the present series of osteoporotic elder women, serum β CTx-I emerged as a determinant of circulating cOC, suggesting that osteoclast-related resorptive activity, which is known to be associated with an increased risk of fractures (54, 55), may be involved in modulation of cOC levels, throughout its release from the matrix. Moreover, in fractured women, plasma cOC and uOC correlated with the lean mass parameters and OAK score, showing that relatively low circulating levels of cOC and uOC may be predictive of low legs lean mass and, hence, increased risk of fall in fractured osteoporotic women. Besides, unfractured women displayed a significant positive correlation of plasma cOC levels with IMAT and with legs lean mass, highlighting that relative high cOC levels may reflect conserved muscle mass though of reduced quality. This finding suggested that bone turnover rate may differ in fractured and unfractured osteoporosis and that, likely, differently influenced the release of the different forms of OC. The different correlations between cOC and uOC and the parameters of the musculoskeletal system, such as risk of fall and intramuscular fat infiltration, are consistent with a complexity in the modulation of the OC effect on skeletal muscle mass.

A limit of the present study is represented by the small sample size, that, though adherent to the power analysis calculation, is limited due to extensive exclusion criteria aimed to avoid a number

of diseases and therapies known to independently affect bone mass and metabolism, as well as skeletal muscle mass and function. Second, study design prevents any inference about cause-effect relationship between plasma carboxylated osteocalcin and the different parameters analyzed. Third, vitamin K status, which is known to affect OC carboxylation, has not been evaluated in the present series due to unavailability of accurate tools such as high-performance liquid chromatography–tandem mass spectrometry for the assessment of vitamin K homologues, phyloquinone (vitamin K1) and menaquinones (MK-4 and MK-7). However, it is of note that measuring uncarboxylated vitamin K-dependent protein (i.e., osteocalcin) levels is considered the most accurate and convenient method for assessing tissue-specific vitamin K deficiency or insufficiency (56). Indeed, here failure in detecting association between plasma uOC levels and most of the parameters related with body composition, may suggest that vitamin K replenishment is not a major determinant of the potential relationship with muscle mass and function. Lastly, vitamin D was not routinely administered, though at the enrollment all women were checked for circulating 25-(OH)D levels and in all participants serum 25-(OH)D levels were above 20 ng/ml, a threshold considered consistent with a sufficient condition of vitamin D repletion (57).

Strengths of the present study are body composition analysis by DXA and risk of fall assessment by an automated system. DXA is the gold-standard technique in the analysis of body composition, providing assessment and quantification of fat mass, lean mass and bone mineral content, both in a single body region of interest and at whole-body level (35). The OAK system incorporates movement and balance sensors and accelerometers for the assessment of fall risk in a single examination. The diagnostic test accuracy of the OAK device has been recently investigated and the results showed good accuracy of OAK system in assessing risk of fall (discriminative power of AUC values above 80%) and the device also showed a sensitivity of 84% and a specificity of 67% (28). Diagnostic accuracy of OAK system was similar to the sensitivity levels obtained with other fall risk assessment, such as the Brief-BESTest. Moreover, data about skeletal muscle fat infiltration analyzed by lower leg MRI has been provided. Lastly, both circulating cOC and uOC levels were analyzed in the same sample, at variance with most clinical studies provided data about total OC and/or uOC.

In conclusion, data here presented supported the relationship between OC and skeletal muscle mass and function detected in mice, though in osteoporotic postmenopausal women cOC, but not uOC, emerges as mediator in the bone-muscle crosstalk. Though the release of cOC and uOC was similar, circulating levels may be differentially regulated in fractured and unfractured women, suggesting that bone metabolism differs in the two groups.

DATA AVAILABILITY STATEMENT

The datasets presented in this study can be found in online repositories. The names of the repository and accession number can be found below: ZENODO <http://doi.org/10.5281/zenodo.4558652>.

ETHICS STATEMENT

The studies involving human participants were reviewed and approved by Ospedale San Raffaele in Milan (ref.no.17/INT/2017). The patients/participants provided their written informed consent to participate in this study. All participants gave their signed informed consent to participation.

AUTHOR CONTRIBUTIONS

SC, GL, and JV designed the study and prepared the first draft of the paper. SC is guarantor. JV, CM, and SC enrolled and clinically evaluated the patients. VS, MF, and CV contributed to the experimental work performing the assays. MF and SC were

responsible for statistical analysis of the data. All authors agree to be accountable for the work and to ensure that any questions relating to the accuracy and integrity of the paper are investigated and properly resolved. All authors gave their approval and consent to publication; there is any restriction by government authorities. All authors contributed to the article and approved the submitted version.

FUNDING

The study has been funded by the “Bando CARIPLO sulla ricerca biomedica legata alle malattie dell’invecchiamento 2018” for the project OSTMARK (no.2018-0458) and by Italian Ministry of Health.

REFERENCES

- Curtis E, Litwic A, Cooper C, Dennison E. Determinants of Muscle and Bone Aging. *J Cell Physiol* (2015) 230:2618–25. doi: 10.1002/jcp.25001
- Scott D, Seibel M, Cumming R, Naganathan V, Blyth F, Le Couteur DG, et al. Sarcopenic Obesity and its Temporal Associations With Changes in Bone Mineral Density, Incident Falls, and Fractures in Older Men: The Concord Health and Ageing in Men Project. *J Bone Miner Res* (2017) 32:575–83. doi: 10.1002/jbmr.3016
- Batsis JA, Mackenzie TA, Barre LK, Lopez-Jimenez F, Bartels SJ. Sarcopenia, Sarcopenic Obesity and Mortality in Older Adults: Results From the National Health and Nutrition Examination Survey Iii. *Eur J Clin Nutr* (2014) 68:1001–7. doi: 10.1038/ejcn.2014.117
- Vitale JA, Bonato M, La Torre A, Banfi G. The Role of the Molecular Clock in Promoting Skeletal Muscle Growth and Protecting Against Sarcopenia. *Int J Mol Sci* (2019) 20:4318. doi: 10.3390/ijms20174318
- Drey M, Sieber CC, Bertsch T, Bauer JM, Schmidmaier RFIAT intervention group. Osteosarcopenia is More Than Sarcopenia and Osteopenia Alone. *Aging Clin Exp Res* (2016) 28:895–9. doi: 10.1007/s40520-015-0494-1
- Messina C, Vitale JA, Pedone L, Chianca V, Vicentin I, Albano D, et al. Critical Appraisal of Papers Reporting Recommendation on Sarcopenia Using the AGREE II Tool: A EuroAIM Initiative. *Eur J Clin Nutr* (2020) 74:1164–72. doi: 10.1038/s41430-020-0638-z
- Vitale JA, Bonato M, Borghi S, Messina C, Albano D, Corbetta S, et al. Home-Based Resistance Training for Older Subjects During the COVID-19 Outbreak in Italy: Preliminary Results of a Six-Months RCT. *Int J Environ Res Public Health* (2020) 17:9533. doi: 10.3390/ijerph17249533
- Lee I, Ha C, Kang H. Association of Sarcopenia and Physical Activity With Femur Bone Mineral Density in Elderly Women. *J Exerc Nutr Biochem* (2016) 20:23–8. doi: 10.20463/jenb.2016.03.20.1.8
- Santos VR, Christofaro DG, Gomes IC, Júnior IF, Gobbo LA. Relationship Between Obesity, Sarcopenia, Sarcopenic Obesity, and Bone Mineral Density in Elderly Subjects Aged 80 Years and Over. *Rev Bras Ortop* (2017) 53:300–5. doi: 10.1016/j.rboe.2017.09.002
- Papageorgiou M, Sathyapalan T, Schutte R. Muscle Mass Measures and Incident Osteoporosis in a Large Cohort of Postmenopausal Women. *J Cachexia Sarcopenia Muscle* (2019) 1:131–9. doi: 10.1002/jcsm.12359
- Ho-Pham LT, Nguyen UD, Nguyen TV. Association Between Lean Mass, Fat Mass, and Bone Mineral Density: A Meta-Analysis. *J Clin Endocrinol Metab* (2014) 99:30–8. doi: 10.1210/jc.2014-v99i12-30A
- Liu PY, Ilich JZ, Brummel-Smith K, Ghosh S. New Insight Into Fat, Muscle and Bone Relationship in Women: Determining the Threshold At Which Body Fat Assumes Negative Relationship With Bone Mineral Density. *Int J Prev Med* (2014) 5:1452–63.
- Bonewald L. Use it or Lose it to Age: A Review of Bone and Muscle Communication. *Bone* (2019) 120:212–8. doi: 10.1016/j.bone.2018.11.002
- Battafarano G, Rossi M, Marampon F, Minisola S, Del Fattore A. Bone Control of Muscle Function. *Int J Mol Sci* (2020) 21:1178. doi: 10.3390/ijms21041178
- Gomarasca M, Banfi G, Lombardi G. Myokines: The Endocrine Coupling of Skeletal Muscle and Bone. *Adv Clin Chem* (2020) 94:155–218. doi: 10.1016/bbsacc.2019.07.010
- Kirk B, Feehan J, Lombardi G, Duque G. Muscle, Bone and Fat Crosstalk: The Biological Role of Myokines, Osteokines and Adipokines. *Curr Osteoporos Rep* (2020) 18:388–400. doi: 10.1007/s11914-020-00599-y
- Hauschka PV, Lian JB, Cole DE, Gundersberg CM. Osteocalcin and Matrix Gla Protein: Vitamin K-dependent Proteins in Bone. *Physiol Rev* (1989) 69:990–1047. doi: 10.1152/physrev.1989.69.3.990
- Ducy P, Desbois C, Boyce B, Pinero G, Story B, Dunstan C, et al. Increased Bone Formation in Osteocalcin-Deficient Mice. *Nature* (1996) 382:448–52. doi: 10.1038/382448a0
- Boskey AL, Gadaleta S, Gundersberg C, Doty SB, Ducy P, Karsenty G. Fourier Transform Infrared Microspectroscopic Analysis of Bones of Osteocalcin-Deficient Mice Provides Insight Into the Function of Osteocalcin. *Bone* (1998) 23:187–96. doi: 10.1016/s8756-3282(98)00092-1
- Li J, Zhang H, Yang C, Li Y, Dai Z. An Overview of Osteocalcin Progress. *J Bone Miner Metab* (2016) 34:367–79. doi: 10.1007/s00774-015-0734-7
- Mera P, Laue K, Wei J, Berger JM, Karsenty G. Osteocalcin is Necessary and Sufficient to Maintain Muscle Mass in Older Mice. *Mol Metab* (2016) 5:1042–7. doi: 10.1016/j.molmet.2016.07.002
- Mera P, Laue K, Ferron M, Confavreux C, Wei J, Galan-Diez M, et al. Osteocalcin Signaling in Myofibers is Necessary and Sufficient for Optimum Adaptation to Exercise. *Cell Metab* (2017) 23:1078–92. doi: 10.1016/j.cmet.2016.12.003
- Liu S, Gao F, Wen L, Ouyang M, Wang Y, Wang Q, et al. Osteocalcin Induces Proliferation Via Positive Activation of the PI3K/Akt, P38 MAPK Pathways and Promotes Differentiation Through Activation of the GPRC6A-ERK1/2 Pathway in C2C12 Myoblast Cells. *Cell Physiol Biochem* (2017) 43:1100–12. doi: 10.1159/000481752
- Lombardi G, Perego S, Luzi L, Banfi G. A Four-Season Molecule: Osteocalcin. Updates in its Physiological Roles. *Endocrine* (2015) 48:394–404. doi: 10.1007/s12020-014-0401-0
- von Elm E, Altman DG, Egger M, Pocock SJ, Göttsche PC, Vandenbroucke JP. The Strengthening the Reporting of Observational Studies in Epidemiology (STROBE) Statement: Guidelines for Reporting Observational Studies. *Lancet* (2007) 370:1453–7. doi: 10.1016/S0140-6736(07)61602-X
- Padgett PK, Jacobs JV, Kasser SL. Is the BESTest At its Best? A Suggested Brief Version Based on Interrater Reliability, Validity, Internal Consistency, and Theoretical Construct. *Phys Ther* (2012) 92:1197–207. doi: 10.2522/ptj.20120056
- Sutter T, Duboeuf F, Chapurlat R, Cortet B, Lespessailles E, Roux JP. DXA Body Composition Corrective Factors Between Hologic Discovery Models to Conduct Multicenter Studies. *Bone* (2021) 142:115683. doi: 10.1016/j.bone.2020.115683

28. Castellini G, Gianola S, Stucovitz E, Tramacere I, Banfi G, Moja L. Diagnostic Test Accuracy of an Automated Device as a Screening Tool for Fall Risk Assessment in Community-Residing Elderly: A STARD Compliant Study. *Med (United States)* (2019) 98:e17105. doi: 10.1097/MD.00000000000017105
29. Houry D, Florence C, Baldwin G, Stevens J, McClure R. The CDC Injury Center's Response to the Growing Public Health Problem of Falls Among Older Adults. *Am J Lifestyle Med* (2016) 10:74–7. doi: 10.1177/1559827615600137
30. Albano D, Messina C, Vitale J, Sconfienza LM. Imaging of Sarcopenia: Old Evidence and New Insights. *Eur Radiol* (2020) 30:64:2199–208. doi: 10.1007/s00330-019-06573-2
31. Cruz-Jentoft AJ, Bahat G, Bauer J, Boirie Y, Bruyère O, Cederholm T, et al. Sarcopenia: Revised European Consensus on Definition and Diagnosis. *Age Ageing* (2019) 48:16–31. doi: 10.1093/ageing/afz046
32. Kanis JA, Adachi JD, Cooper C, Clark P, Cummings SR, Diaz-Curiel M, et al. Standardising the Descriptive Epidemiology of Osteoporosis: Recommendations From the Epidemiology and Quality of Life Working Group of IOF. *Osteoporos Int* (2013) 24:2763–4. doi: 10.1007/s00198-013-2413-7
33. Kanis JA, McCloskey EV, Johansson H, Oden A, Melton J, Khaltav N. A Reference Standard for the Description of Osteoporosis. *Bone* (2008) 42:467–75. doi: 10.1016/j.bone.2007.11.001
34. Messina C, Maffi G, Vitale JA, Olivieri FM, Guglielmi G, Sconfienza LM. Diagnostic Imaging of Osteoporosis and Sarcopenia: A Narrative Review. *Quant Imaging Med Surg* (2018) 8:86–99. doi: 10.21037/qims.2018.01.01
35. Guglielmi G, Ponti F, Agostini M, Amadori M, Battista G, Bazzocchi A. The Role of DXA in Sarcopenia. *Aging Clin Exp Res* (2016) 28:1047–60. doi: 10.1007/s40520-016-0589-3
36. Grimm A, Meyer H, Nickel MD, Nittka M, Raithel E, Chaudry O, et al. Evaluation of 2-Point, 3-Point, and 6-Point Dixon Magnetic Resonance Imaging With Flexible Echo Timing for Muscle Fat Quantification. *Eur J Radiol* (2018) 103:57–64. doi: 10.1016/j.ejrad.2018.04.011
37. Grimm A, Meyer H, Nickel MD, Nittka M, Raithel E, Chaudry O, et al. Repeatability of Dixon Magnetic Resonance Imaging and Magnetic Resonance Spectroscopy for Quantitative Muscle Fat Assessments in the Thigh. *J Cachexia Sarcopenia Muscle* (2018) 9:1093–100. doi: 10.1002/jcsm.12343
38. Schneider CA, Rasband WS, Eliceiri KW. Nih Image to ImageJ: 25 Years of Image Analysis. *Nat Methods* (2012) 9:671–5. doi: 10.1038/nmeth.2089
39. Sansoni V, Vernillo G, Perego S, Barbuti A, Merati G, Schena F, et al. Bone Turnover Response is Linked to Both Acute and Established Metabolic Changes in Ultra-Marathon Runners. *Endocrine* (2017) 56:196–204. doi: 10.1007/s12020-016-1012-8
40. Lombardi G, Lanteri P, Colombini A, Banfi G. Blood Biochemical Markers of Bone Turnover: Pre-Analytical and Technical Aspects of Sample Collection and Handling. *Clin Chem Lab Med* (2012) 50:771–89. doi: 10.1515/cclm-2011-0614
41. Lombardi G, Barbaro M, Locatelli M, Banfi G. Novel Bone Metabolism-Associated Hormones: The Importance of the Pre-Analytical Phase for Understanding Their Physiological Roles. *Endocrine* (2017) 56:460–84. doi: 10.1007/s12020-017-1239-z
42. Hammer Ø, Harper DAT, Ryan PD. Past: Paleontological Statistics Software Package for Education and Data Analysis. *Palaeontol Electron* (2001) 4(1):9.
43. Correa-de-Araujo R, Addison O, Miljkovic I, Goodpaster BH, Bergman BC, Clark RV, et al. Myosteatosis in the Context of Skeletal Muscle Function Deficit: An Interdisciplinary Workshop At the National Institute on Aging. *Front Physiol* (2020) 11:963. doi: 10.3389/fphys.2020.00963
44. Yin L, Xu Z, Wang L, Li W, Zhao Y, Su Y, et al. Associations of Muscle Size and Density With Proximal Femur Bone in a Community Dwelling Older Population. *Front Endocrinol (Lausanne)* (2020) 11:503. doi: 10.3389/fendo.2020.00503
45. Manolagas SC. Osteocalcin Promotes Bone Mineralization But is Not a Hormone. *PLoS Genet* (2020) 16:e1008714. doi: 10.1371/journal.pgen.1008714
46. Ferron M, Hinoi E, Karsenty G, Ducy P. Osteocalcin Differentially Regulates Beta Cell and Adipocyte Gene Expression and Affects the Development of Metabolic Diseases in Wild-Type Mice. *Proc Natl Acad Sci USA* (2008) 105:5266–70. doi: 10.1073/pnas.0711191105
47. Levinger I, Scott D, Nicholson GC, Stuart AL, Duque G, McCorquodale T, et al. Undercarboxylated Osteocalcin, Muscle Strength and Indices of Bone Health in Older Women. *Bone* (2014) 64:8–12. doi: 10.1016/j.bone.2014.03.008
48. Kersch-Schindl K, Boschitsch E, Marculescu R, Gruber R, Pietschmann P. Bone Turnover Markers in Serum But Not in Saliva Correlate With Bone Mineral Density. *Sci Rep* (2020) 10:11550. doi: 10.1038/s41598-020-68442-z
49. Shea MK, Dawson-Hughes B, Gundberg CM, Booth SL. Reducing Undercarboxylated Osteocalcin With Vitamin K Supplementation Does Not Promote Lean Tissue Loss or Fat Gain Over 3 Years in Older Women and Men: A Randomized Controlled Trial. *J Bone Miner Res* (2017) 32:243–9. doi: 10.1002/jbmr.2989
50. Jackman SR, Scott S, Randers MB, Orntoft C, Blackwell J, Zar A, et al. Musculoskeletal Health Profile for Elite Female Footballers Versus Untrained Young Women Before and After 16 Weeks of Football Training. *J Sports Sci* (2013) 31:1468–74. doi: 10.1080/02640414.2013.796066
51. Xu Y, Ma X, Shen Y, Gu C, Tang J, Bao Y. Role of Hyperglycaemia in the Relationship Between Serum Osteocalcin Levels and Relative Skeletal Muscle Index. *Clin Nutr* (2019) 38:2704–11. doi: 10.1016/j.clnu.2018.11.025
52. Moriaki K, Matsumoto H, Tanishima S, Tanimura C, Osaki M, Nagashima H, et al. Association of Serum Bone- and Muscle-Derived Factors With Age, Sex, Body Composition, and Physical Function in Community-Dwelling Middle-Aged and Elderly Adults: A Cross-Sectional Study. *BMC Musculoskelet Disord* (2019) 20:276. doi: 10.1186/s12891-019-2650-9
53. Højsager FD, Rand MS, Pedersen SB, Nissen N, Jørgensen NR. Fracture-Induced Changes in Biomarkers CTX, Pinp, OC, and BAP—a Systematic Review. *Osteoporos Int* (2019) 30:2381–9. doi: 10.1007/s00198-019-05132-1
54. Dai Z, Wang R, Ang LW, Yuan JM, Koh WP. Bone Turnover Biomarkers and Risk of Osteoporotic Hip Fracture in an Asian Population. *Bone* (2016) 83:171–7. doi: 10.1016/j.bone.2015.11.005
55. Garnero P, Mulleman D, Munoz F, Sornay-Rendu E, Delmas PD. Long-Term Variability of Markers of Bone Turnover in Postmenopausal Women and Implications for Their Clinical Use: The OFELY Study. *J Bone Miner Res* (2003) 18:1789–94. doi: 10.1359/jbmr.2003.18.10.1789
56. Tsugawa N, Shiraki M. Vitamin K Nutrition and Bone Health. *Nutrients* (2020) 12:1909. doi: 10.3390/nu12071909
57. Sempos CT, Heijboer AC, Bikle DD, Bollerslev J, Bouillon R, Brannon PM, et al. Vitamin D Assays and the Definition of Hypovitaminosis D: Results From the First International Conference on Controversies in Vitamin D. *Br J Clin Pharmacol* (2018) 84:2194–207. doi: 10.1111/bcp.13652

Conflict of Interest: The authors declare that the research was conducted in the absence of any commercial or financial relationships that could be construed as a potential conflict of interest.

Copyright © 2021 Vitale, Sansoni, Faraldi, Messina, Verdelli, Lombardi and Corbetta. This is an open-access article distributed under the terms of the Creative Commons Attribution License (CC BY). The use, distribution or reproduction in other forums is permitted, provided the original author(s) and the copyright owner(s) are credited and that the original publication in this journal is cited, in accordance with accepted academic practice. No use, distribution or reproduction is permitted which does not comply with these terms.



Hematopoietic Wnts Modulate Endochondral Ossification During Fracture Healing

Kenon Chua^{1,2,3}, Victor K. Lee⁴, Cheri Chan³, Andy Yew², Eric Yeo⁴ and David M. Virshup^{1,5*}

¹ Programme in Cancer and Stem Cell Biology, Duke-NUS Medical School, Singapore, Singapore, ² Department of Orthopedic Surgery, Singapore General Hospital, Singapore, Singapore, ³ Programme in Musculoskeletal Sciences Academic Clinical Program, SingHealth/Duke-NUS, Singapore, Singapore, ⁴ Department of Pathology, National University of Singapore, Singapore, Singapore, ⁵ Department of Pediatrics, Duke University, Durham, NC, United States

OPEN ACCESS

Edited by:

Uma Sankar,
Purdue University Indianapolis,
United States

Reviewed by:

Stéphane Blouin,
Ludwig Boltzmann Institute of
Osteology (LBIO), Austria
Robin Mark Howard Rumney,
University of Portsmouth,
United Kingdom

*Correspondence:

David M. Virshup
david.virshup@duke-nus.edu.sg

Specialty section:

This article was submitted to
Bone Research,
a section of the journal
Frontiers in Endocrinology

Received: 13 February 2021

Accepted: 09 April 2021

Published: 24 May 2021

Citation:

Chua K, Lee VK, Chan C, Yew A,
Yeo E and Virshup DM (2021)
Hematopoietic Wnts Modulate
Endochondral Ossification During
Fracture Healing.
Front. Endocrinol. 12:667480.
doi: 10.3389/fendo.2021.667480

Wnt signaling plays a critical role in bone formation, homeostasis, and injury repair. Multiple cell types in bone have been proposed to produce the Wnts required for these processes. The specific role of Wnts produced from cells of hematopoietic origin has not been previously characterized. Here, we examined if hematopoietic Wnts play a role in physiological musculoskeletal development and in fracture healing. Wnt secretion from hematopoietic cells was blocked by genetic knockout of the essential Wnt modifying enzyme PORCN, achieved by crossing *Vav-Cre* transgenic mice with *Porcn*^{flox} mice. Knockout mice were compared with their wild-type littermates for musculoskeletal development including bone quantity and quality at maturation. Fracture healing including callus quality and quantity was assessed in a diaphyseal fracture model using quantitative micro computer-assisted tomographic scans, histological analysis, as well as biomechanical torsional and 4-point bending stress tests. The hematopoietic *Porcn* knockout mice had normal musculoskeletal development, with normal bone quantity and quality on micro-CT scans of the vertebrae. They also had normal gross skeletal dimensions and normal bone strength. Hematopoietic Wnt depletion in the healing fracture resulted in fewer osteoclasts in the fracture callus, with a resultant delay in callus remodeling. All calluses eventually progressed to full maturation. Hematopoietic Wnts, while not essential, modulate osteoclast numbers during fracture healing. These osteoclasts participate in callus maturation and remodeling. This demonstrates the importance of diverse Wnt sources in bone repair.

Keywords: fracture healing, bone formation, Wnt signaling, osteoclast, hematopoietic Wnts

HIGHLIGHTS

- Hematopoietic Wnts are dispensable for normal skeletal development, growth and maturation.
- Bone mass accrual and bone quality are not adversely affected by hematopoietic Wnt depletion.
- Depletion of hematopoietic Wnts results in fewer osteoclasts and delayed maturation of the fracture callus after bone injury.
- Hematopoietic Wnts are dispensable for completion of fracture healing.

INTRODUCTION

Bone is a complex tissue that is structurally important for force transmission and locomotion, as well as mineral metabolism and hematopoiesis. The Wnt signaling pathway is a key modulator of bone formation (1–4). Wnts influence prenatal skeletal development, as well as post-partum skeletal growth and maturation. Wnts are also critically important in bone mass accrual and adult bone hemostasis in the skeletally mature individual.

There are 19 distinct Wnt ligands in the human genome that function *via* short range cell to cell signaling (5–8). Different Wnts can function in different processes, broadly categorized into β -catenin dependent and independent pathways, both of which are involved in bone formation at different time points during development and fracture healing. Early in bone development, Wnt/ β -catenin signaling through Frizzled and LRP5/6 receptors inhibits chondrogenesis. Conversely, WNT5A interacts with its receptor ROR2 to antagonize the Wnt/ β -catenin pathway to induce local chondrogenesis by stimulating cartilage nodule formation (9, 10). Wnt/ β -catenin signaling, in contrast, promotes osteoblastic differentiation (11) and mineralization (12). This is important in late phase fracture callus maturation as well as bone growth. Besides maintaining the osteoblasts, Wnts also enhance proliferation and prevent differentiation of the osteoclast precursor cells, regulating the number of mature osteoclasts that are critical for callus remodeling. Wnt signaling is thus extremely important for multiple aspects of fracture healing (13–16).

The Wnts regulating bone formation and repair can be produced by multiple cell types, the most well-known being osteoblasts (11). Another potential source are the cells of hematopoietic origin (hereafter called hematopoietic Wnts). Hematopoietic stem cells differentiate and proliferate into various blood components every day. Bone plays a role in regulating hematopoiesis (17). Conversely, cells of hematopoietic origin, specifically monocytes and tissue macrophages, are important in injury repair (18–20). Macrophages migrate to sites of tissue injury and produce Wnts as well as multiple cytokines and other factors to aid in tissue repair (21, 22). Whether hematopoietic and macrophage derived Wnts also contribute to fracture healing and bone formation is not known.

Fracture non-unions and delayed unions are common clinical problems worldwide, with up to 18.5 percent incidence in tibia diaphyseal fractures reported (23). Non-union is defined clinically as the arrest of progression to union at the fracture site with persistent pain and mobility for six months or more. The causes of non-union are categorized into two broad groups. The first is due to mechanical factors that impair fracture healing, such as poor strain environment or excessive motion. The second is caused by biological factors. This includes a multitude of causes that have a cumulative or additive effects, including local bone marrow suppression, poor vascularity, immunosuppression, and aberrant cellular signaling (24–27). Introducing autologous bone graft and bone marrow aspirate concentrate to the fracture site to promote healing in fracture non-unions has proven to be clinically efficacious (28–31). These therapeutic interventions introduce several cell types, including cells of hematopoietic origin that are important for fracture healing (19). Hematopoietic cells are also known to

express multiple Wnt ligands, but their function is controversial. Kabiri et al. made the unexpected and surprising discovery, examining mice with genetic knockout of *Porcn* in cells of hematopoietic lineage using three (*Vav*, *Mx1*, and *Rosa26*) distinct Cre drivers, that intrinsic Wnt production was not required for the stemness, regeneration, nor differentiation of the hematopoietic compartment (32). Why then do hematopoietic cells make Wnts? Since we know that Wnts function as short-range signaling molecules, we hypothesized that Wnts secreted from cells of hematopoietic origin (hereafter designated as hematopoietic Wnts) at the site of injury might play an additive role in modulating bone formation.

To test the importance of hematopoietic Wnts in bone growth and fracture healing, we utilized the previously reported *Vav-Cre* x *Porcn*^{fllox} mouse model (**Figure 1**), where Wnt secretion is blocked specifically in cells of hematopoietic lineage (32). This is accomplished by knockout of the *Porcn* gene encoding an endoplasmic reticulum-resident membrane bound O-acyltransferase that responsible for palmitoleation of all Wnt molecules. This essential post-translational modification is required for the interaction with the Wnt transporter molecule WLS, which transports Wnts to the cell surface for secretion. Knockout of *Porcn* therefore results in an upstream inhibition of Wnt signaling, by inhibiting secretion of all Wnts (33, 34). We assessed skeletal development, growth and maturation, as well as fracture healing, in the absence of hematopoietic Wnts. We found that hematopoietic Wnts did indeed contribute quantitatively to fracture callus maturation. Hematopoietic Wnt depleted mice had fewer mature osteoclasts as well as more residual mineralized cartilage in the callus (**Figure 2**). We also observed a marginal decrease in skeletal length in the hematopoietic Wnt depleted mice. However, depletion of hematopoietic Wnts did not result in severe musculoskeletal abnormalities. This suggests that there is a physiological redundancy of secreted Wnts from other cell types for modulation of bone formation during development. Hematopoietic Wnts do play a role in modulating osteoclasts during fracture healing (**Figure 2**).

METHODS

Mice Strains

Mice with a *Porcn* conditional null allele (*Porcn*^{fllox}) were generated as described (35). The *Porcn*^{fllox} mice were crossed with *Vav-Cre* mice [9, 14] to generate *Vav-Cre/Porcn*^{Del} mice, with hematopoietic tissue-specific block in Wnt secretion (**Figure 1**). These mice were age and gender matched with their wild-type litter mates for comparison. Male mice and female mice were analyzed separately. Genotyping primer sequences are provided in the table **PRIMERS**. Animal housing, breeding and procedures were done in accordance with IACUC guidelines.

Measurement of Developmental Weight and Dimensions

Mice pups were weaned at 3 weeks old and weighed at weekly intervals until past skeletal maturity (100 days old). Measurements of mouse bone length (nose to pelvis), right femur length and cranial size were done at skeletal maturity using digital calipers, after

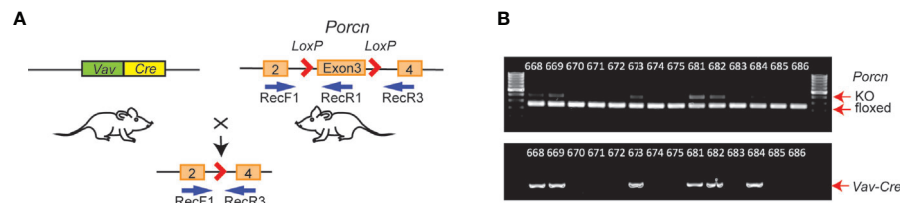


FIGURE 1 | Generation of hematopoietic Wnt-depleted mice. **(A)** *Porcn*^{lox} mice were crossed with *Vav-Cre* mice, resulting in *Vav-Cre/Porcn*^{lox} mice with excisional deletion of *Porcn* exon 3 in hematopoietic and other tissues expressing *Vav-Cre*. Relative annealing positions of complementary primers used for PCR from mouse genomic DNA is shown (RecF1, RecR1, and RecR3). **(B)** PCR genotyping using DNA from tail clippings. Each lane is from an individual mouse. Upper panel, *Vav-Cre/Porcn*^{lox} mice samples exhibited 2 bands, a faster 128 bp band from RecF1/RecR1 (floxed), and a slower 248 bp band from RecF1/RecR3 (KO, knockout), since the tail clippings contain both hematopoietic and non-hematopoietic tissue. *Porcn*^{lox} mice in the absence of *Vav-Cre* exhibit only a single PCR product (RecF1/RecR1).

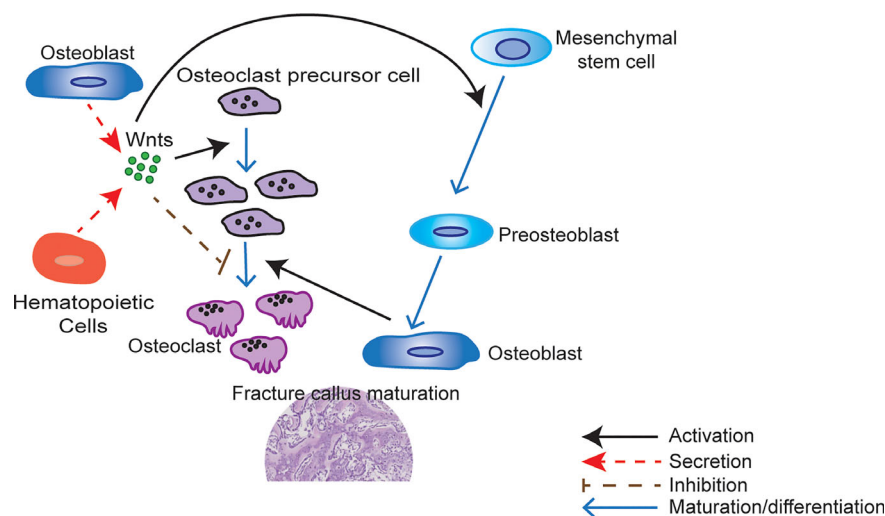


FIGURE 2 | Wnts modulate fracture callus maturation. Hematopoietic and other cells within the bone microenvironment secrete Wnts. Wnt upregulation activates osteoclastic precursor cell proliferation but inhibits osteoclastic precursor cell maturation to osteoclast. Carefully regulated Wnt activity is therefore required for the correct number of mature osteoclasts to develop during fracture healing. Wnts are also responsible for the activation of mesenchymal stem cell differentiation to osteoblasts. These mature osteoblasts are responsible for the formation of woven bone. Osteoclasts also play a key role in callus maturation by resorption of cartilage during callus remodeling. A quantitative shortfall in the secreted Wnts may therefore result in a less mature callus with more cartilage and less woven bone by inhibiting the proliferation of osteoclast precursor cells.

PRIMERS | Genotyping primer sequences.

Primer	Sequence
<i>PORCN</i> Forward	CTGTTAAACCAAGACATGACCTTCA
<i>PORCN</i> Reverse 1	TAAGTAGGACGCTTTGGGATAGGAT
<i>PORCN</i> Reverse 3	GTTCTGCCTTCCTAACCCATATAAC
<i>Vav</i> Forward	GGACATGTTCCAGGGACAGGCA
<i>Vav</i> Reverse	CTCTGATTCTGGCAATTTTCGGC

dissection of soft tissue. Both male and female mice were measured and analyzed. To facilitate readability and avoid figure redundancy, all figures henceforth are of female mice, since there were no gender specific differences in the results.

Whole-Mount Skeletal Staining

Mice were sacrificed at 3 weeks of age and stained as described by Rigueur and Lyons (36). Soft tissue was removed, including the

skin, fat, muscle and viscera, and the specimens were fixed in ethanol (95%). The whole mouse specimens were then sequentially stained with Alcian Blue and Alizarin Red stains.

Fracture Surgery

Tibia diaphyseal fracture model was performed as described (19) at ~100 days of age. A 1 cm incision was made centered on the proximal tibia. The patella was identified. A stainless-steel pin (Entochrysis Stainless Mounting Insect Pin, Size 00) was inserted *via* the tibia plateau to stabilize the subsequent tibia fracture, and a diaphyseal osteotomy was then performed. Care was taken to ensure that the localization of the osteotomy was consistent from mouse to mouse, by referencing to the tibia tubercle. Routine analgesia was given perioperatively and the mice were allowed to weight bear as tolerated upon recovery. The mice were sacrificed at 2 weeks, 3 weeks or 4 weeks after the osteotomy was performed for

callus analysis. The pin was removed from the tibia specimens after retrieval. Both male and female mice were analyzed separately at the 2-week, 3-week and 4-week time points after injury to exclude gender bias.

Micro-Computed Tomography (Micro-CT, μ CT)

Harvested specimens were dissected of soft tissue and scanned using high resolution micro-CT (Skyscan 1176, Bruker Micro-CT, Kontich, Belgium) at 9 μ m resolution. Image acquisition was performed at 50 kV, 800 μ A and 0.25 mm aluminum filter. Hydroxyapatite phantoms were scanned and used for bone mineral density (BMD) calibration.

Acquired images were reconstructed with NRecon and analyzed with CTAn (version 1.5.0, Skyscan, Bruker Micro-CT). For analysis of the cancellous bone, the region of interest encompassing the entire vertebrae body was manually defined to include the trabeculae bone only. Cortical bone was segmented out. This was used to generate a three-dimensional (3D) model CTvol (Skyscan Bruker Micro-CT) for analysis. For analysis of the tibial cortical bone, the midpoint of the tibia was used, and a 100-slice volume centered on this midpoint was defined as the region of interest. For analysis of the fracture callus, the midpoint of the callus was used to define a 3mm region of interest. The cortical bone from the fracture fragments within the callus was segmented out, leaving only the newly formed callus for analysis. The fibular callus was not included in our analysis.

Histology

Fracture calluses were decalcified in Osteosoft (Merck) for 5 days and paraffin embedded after μ CT scanning of bone. Serial sections of 3 μ m were deparaffinized and rehydrated to water for hematoxylin and eosin (H&E), toluidine blue and Von Kossa Stain.

For hematoxylin and eosin (H&E) staining, tissue sections were stained in Shandon hematoxylin solution, differentiated in 1% acid alcohol, and immersed in ammonia with washing between steps. The sections were subsequently rinsed in 95% alcohol, counterstained in eosin-phloxine solution and rinsed before mounting.

Toluidine blue stain was used to identify the cartilaginous components of the callus. Sections were stained with 1% toluidine blue before being dehydrated and mounted. After staining, cartilage appears blue to purple, nuclei dark blue and all other tissue green.

Von Kossa staining was employed to monitor the mineralization of bone. After the sections were degreased and rehydrated, 2% silver nitrate solution was applied to each section, and the slides were exposed to strong light for 30 minutes. After the silver nitrate was removed, 5% sodium thiosulfate was added to the section for prior to rinsing with distilled water. The sections were then incubated with van Gieson working solution before mounting. After von Kossa staining, the mineralized bone appeared black, and less mineralized bone appearing pink.

Tartrate resistant acid phosphatase (TRAP) staining was used to stain osteoclasts. Demineralized samples were incubated in freshly made TRAP staining solution at 37°C for 30 minutes. The slides were then rinsed with distilled water and counterstained with 0.02% Fast Green for 30 seconds and then rinsed again with

distilled water. Osteoclasts were stained red violet and the callus matrix was stained green.

Histomorphometry Analysis

Histology cross-sections were referenced to the corresponding micro-CT images to identify those which represented the center of the fracture callus, and mid-section of the vertebrae. These sections were digitized and analyzed using the BioQuant Osteo software package (<https://osteo.bioquant.com>, Nashville, TN, USA). Total cartilage volume, total tissue volume, total trabecular bone volume, total trabecular bone surface area, trabecular diameter, trabecular number, trabecular spacing, fibrosis volume, total osteoblast surface, total osteoblast number, and osteoblast number per bone surface were analyzed. The results for osteoblast number, osteoblast number per bone surface, cartilage volume, and cartilage to total volume ratio were verified manually by a trained clinical pathologist (VKL) reviewing the digitized images of the calluses.

Biomechanical Evaluation

Whole tibia fracture callus specimens were allocated for mechanical testing. All specimens were measured with a digital Vernier caliper (Mitutoyo Absolute, Mitutoyo, Japan), and the mid-point for the callus was determined. Intramedullary pins were removed prior to testing. A distance of 1.5 mm from the mid-point of the callus was marked superiorly and inferiorly. The 1.5 mm marking was used as a baseline to ensure that the tibia was centered, with equidistance from the mid-point of the callus. Superior and inferior ends of the tibia were embedded into stainless steel nuts using acrylic dental cement. Tibial specimens were wrapped in gauze soaked in saline solution to prevent the bone from dehydration and kept at 4°C. On the day of experiment, each specimen was mounted onto a torsion testing machine (Bionix[®] EM Torsion Test System, MTS, Eden Prairie, MN USA) and angularly displaced at a rate of 2 degrees per second. Angular displacement and torque were recorded for the duration of each test. Torsional stiffness was computed as the gradient of the most linear part of the torque versus angular displacement curve. Angular failure displacement and failure torque were determined as the yield point of the torque versus angular displacement curve.

Quantitative PCR Analysis

Fracture calluses were snap frozen in liquid nitrogen and processed using a bead beater with tungsten beads for homogenization. RNA was extracted from the cell lysate using Qiagen RNeasy RNA extraction kit. Total RNA was reverse transcribed into cDNA first strand using the Superscript II kit as per manufacturer's protocol. Target and endogenous control genes were amplified with validated primers. Reactions were performed in triplicate in a 96-well plate using OneStep Plus (Applied Biosystems) for 40 cycles. Differential expression was determined using the comparative Ct method.

Statistical Analysis

Results were presented graphically as a scatter plot of the individual sample values and expressed as a mean \pm standard deviation of the mean. This format of presentation provides both

the sample size in each group, as well as the result of each individual mice in the experiment. Sample normality was assessed with the Kolmogorov-Smirnov (KS) test prior to analysis. Statistical significance between all parametric sample groups was determined by performing an unpaired t test with Welch's correction at 5% statistical significance. Individual P values for each test was presented. All data was analyzed using GraphPad PRISM (version 8.4.2; San Diego, California, USA).

RESULTS

Loss of Hematopoietic Wnt Secretion Results in Marginal Decrease in Skeletal Size, but No Gross Defects

Wnts are implicated in both endochondral ossification and intramembranous ossification during skeletal growth and development. To investigate the role of hematopoietic Wnts in fetal skeletal development, we bred *Porcn^{fllox}* mice (32, 35) with *Vav-Cre* mice (37). This allowed us to generate mice with tissue specific deletion of *Porcn* in hematopoietic lineage cells (*Vav-Cre/Porcn^{Del}*) (Figure 1). *PORCN* is required for Wnt secretion and activity (33, 38, 39). Hematopoietic lineage cells in *Vav-Cre/Porcn^{Del}* mice therefore cannot produce active Wnts. *Porcn^{Del}* mice were confirmed by genotyping (Figure 1). Depletion of hematopoietic Wnts was well tolerated, with similar numbers of *Vav-Cre/Porcn^{Del}* and wild-type pups surviving.

If hematopoietic Wnts are important in fetal musculoskeletal development, we expect the *Vav-Cre/Porcn^{Del}* pups to differ phenotypically from their wild-type littermates. The *Vav-Cre/Porcn^{Del}* mice differed slightly in weight and size from the wild-type littermates but only at 3 months of age. They did not

demonstrate any gross skeletal abnormalities on whole mount skeletal staining of the mice pups at 3 weeks of age (Figure 3). The microarchitecture of the spine was grossly normal on H&E and Safranin O staining, with normal development of the vertebral body and intervertebral discs, with no gross deformities. The *Vav-Cre/Porcn^{Del}* mice pups also had normal weight gain over time until skeletal maturity and had normal long bone and cranial dimensions on maturation (Figure 3). There was a marginal decrease in the nose to pelvis length of *Vav-Cre/Porcn^{Del}* mice but overall, there were no significant gross musculoskeletal abnormalities in these developing mice. There was no increase in mortality in the *Vav-Cre/Porcn^{Del}* mice compared to their wild-type littermates, with similar numbers surviving beyond sexual maturity to late adulthood.

Hematopoietic Wnts Do Not Contribute to Bone Mass Accrual

Wnts are important in bone mass accrual and are implicated in osteoporosis. To determine if hematopoietic Wnts play an important role in bone mass accrual, we evaluated the microarchitecture of the *Vav-Cre/Porcn^{Del}* vertebral body at maturity using high resolution microcomputer tomography scans (μ CT) (Figure 4, male mice). The *Vav-Cre/Porcn^{Del}* demonstrated no difference in trabeculae bone volume, percentage trabeculae bone volume and bone mineral density compared to the wild-type mice. There was also no difference in cortical volume and thickness. Since the dimensions of the cortical bone were similar, we proceeded to evaluate the qualitative properties of the cortical bone of the *Vav-Cre/Porcn^{Del}* mice by measuring the stiffness and torque required for fracture (strength). If hematopoietic Wnts depletion resulted in quantitative or qualitative differences in bone development, we expect the cortical bone to have decreased mechanical strength. Again, there was no demonstrable difference in stiffness or torque strength between the

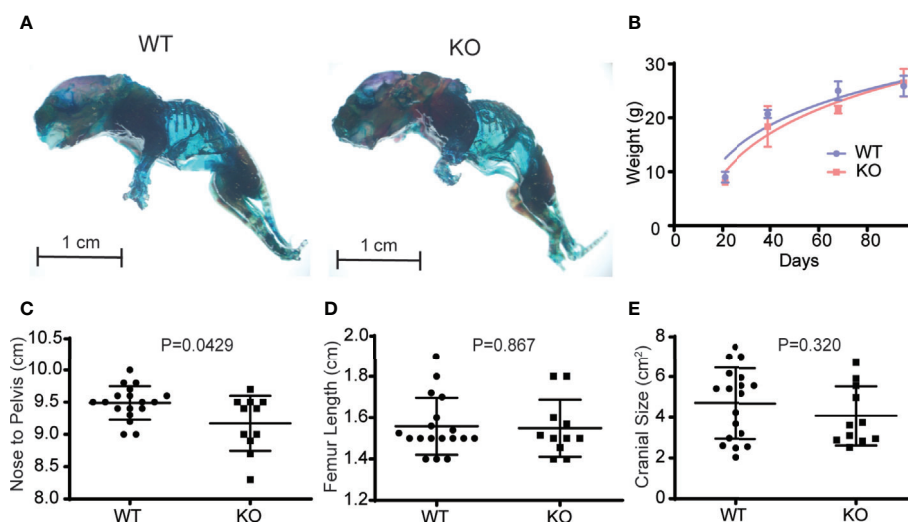


FIGURE 3 | Depletion of hematopoietic Wnts has a minimal effect on musculoskeletal development. (A) Whole-mount skeletal staining demonstrating similar gross skeletal structure in the wild type (WT) and knockout mice (KO). (B) Growth curves demonstrated no growth arrest or delay in the KO mice. (C) Nose to pelvis length, (D) femur length, (E) cranial size (cross sectional dimensions) were comparable for the KO and WT mice, with only nose to pelvis length demonstrating a marginal increase in the WT.

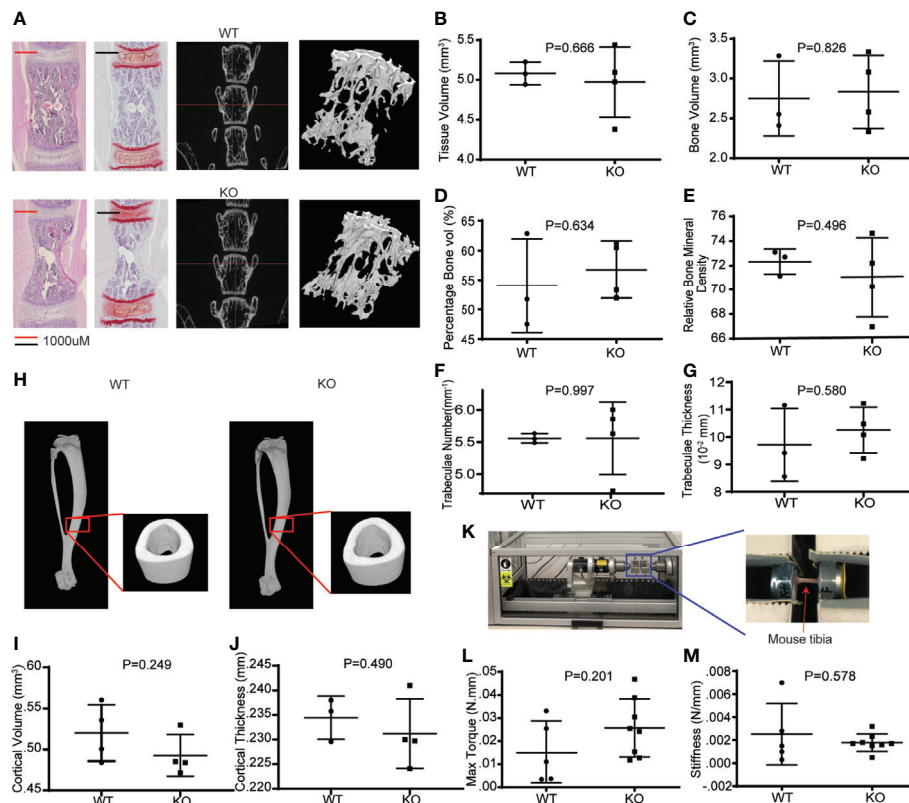


FIGURE 4 | Hematopoietic Wnt-depleted mice have normal bone quality. **(A)** L5 vertebral bodies from WT and KO mice assessed by hematoxylin and eosin (H&E) and safranin O staining and micro computer-assisted tomography (μCT) with reconstruction demonstrating similar trabecular bone microarchitecture. **(B–G)** μCT quantification revealed no major differences in the bone quality of the L5 vertebrae by tissue volume (mm³), bone volume (mm³), percentage bone volume (%) and relative bone mineral density, trabeculae number (mm⁻¹) and trabeculae thickness in the KO and WT mice. **(H)** μCT reconstruction of tibia cortical bone demonstrated minimal difference in **(I)** cortical volume (mm³), and **(J)** cortical thickness (mm) between the KO and WT mice. **(K)** Rotational torque machine. **(L)** The maximum tibia torque and **(M)** 4-point bending stiffness (Newton/mm) of the tibia were similar for both groups of mice.

Vav-Cre/Porcn^{Del} mice and their wild-type littermates, suggesting that hematopoietic Wnts production is dispensable for physiological bone development.

Hematopoietic Wnts Promote Fracture Callus Maturation by Up-Regulation of Osteoclasts

Fracture healing in long bones most frequently occurs by endochondral ossification. Direct healing only occurs when there is bone to bone apposition and compression at the fracture site, with absolute stability (40). The early phase of endochondral fracture healing involves an inflammatory process followed by the formation of a soft callus (41). This soft callus depends on chondrogenic differentiation of stromal mesenchymal stem cells, which then produce a cartilage scaffold around the fracture site. Specific Wnts (WNT9A, WNT5B) are known to play a key role in chondrocyte differentiation and soft callus formation (10). To investigate the role of hematopoietic Wnts in this early phase of fracture healing, we created an osteotomy in the tibia diaphysis of the *Vav-Cre/Porcn^{Del}* mice, stabilized with an intra-medullary steel

pin (**Figure 5**). We then evaluated the early fracture callus using high resolution micro-CT scans and histomorphometrically analysis at 2 weeks after the osteotomy had been performed. The hematopoietic Wnt depleted calluses were of normal volume and percentage bone volume compared to the wild-type calluses. There was only a marginal increase in the volume of cartilage, as well as the cartilage to total volume ratio in the hematopoietic Wnt-depleted callus (**Figure 6I**), indicating that the callus was less mature. However, this difference did not reach statistical significance. These results suggest that hematopoietic Wnts, specifically those implicated in chondrogenic differentiation, do not play an important role in the early phase of fracture healing.

We then investigated the effects of hematopoietic Wnt depletion in the 3-week-old callus. This allowed us to investigate the role of hematopoietic Wnts in the mineralization of the soft callus by osteoblasts. As expected, the wild-type callus demonstrated decreased cartilage composition, and increased woven bone and mineralization, compared to the 2-week-old callus. The *Vav-Cre/Porcn^{Del}* mice also demonstrated a similar increase in woven bone and mineralization in the 3-week-old callus compared to the 2-week-old callus. Interestingly, we found that the *Vav-Cre/Porcn^{Del}*

mice had a higher volume of cartilage and percentage of cartilage in the callus at 3 weeks compared to the wild-type mice (**Figure 6**). The wild-type mice callus had negligible cartilage at 3 weeks after fracture, indicating that the callus had almost completely matured to woven bone. This suggested that hematopoietic Wnts had a positive effect in ossification of the cartilaginous callus. However, by 4 weeks, both the wild-type mice and the *Vav-Cre/Porcrt^{Del}* mice had fully matured calluses with all woven bone and no more cartilage. Thus, hematopoietic Wnt depletion demonstrated a

clinically significant but dispensable role in callus formation and maturation. To identify how hematopoietic Wnt depletion resulted in a delay in callus remodeling to woven bone, we analyzed the osteoclasts and osteoblasts per bone surface area in the fracture calluses. We observed that the hematopoietic Wnt depleted callus had fewer osteoclasts at the 3-week mark (**Figure 7**). In contrast, the osteoblasts were not decreased.

We lysed the 3-week-old fracture callus to investigate the transcriptional changes in Wnt target genes and markers of

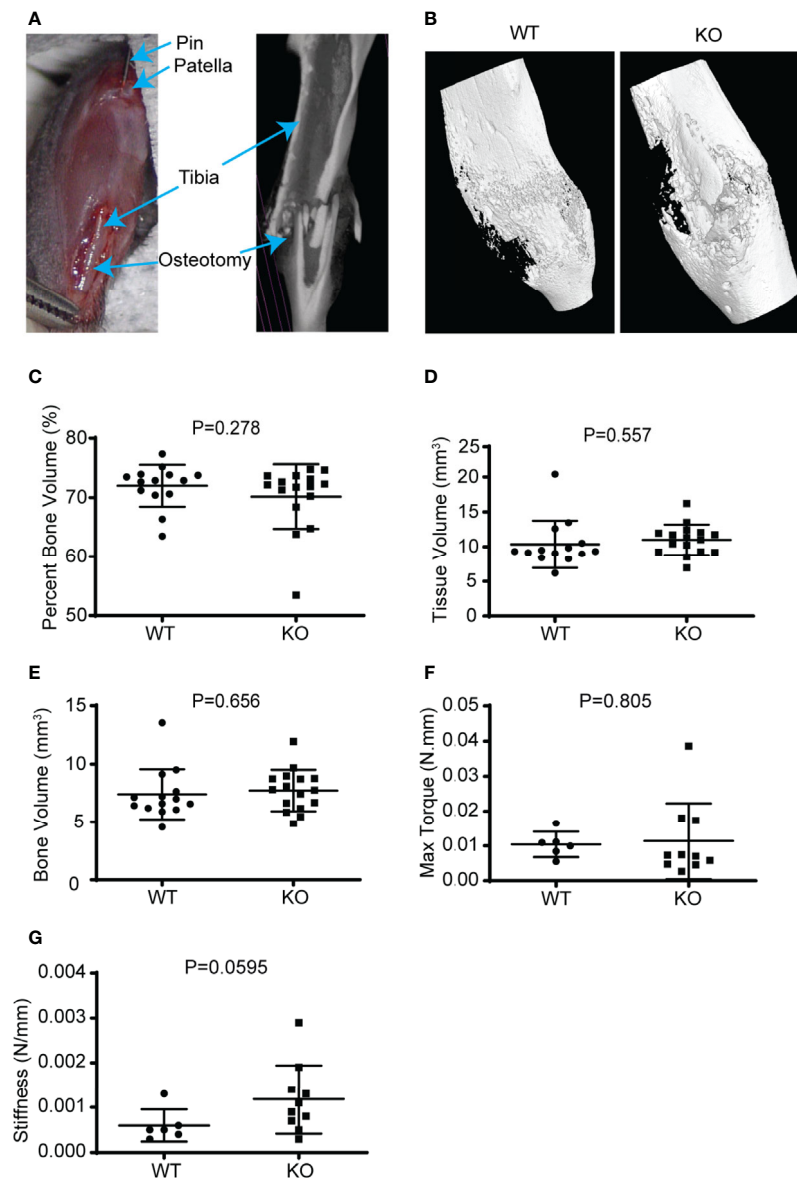


FIGURE 5 | Hematopoietic depletion of Wnt does not affect callus volume and early healing. **(A)** Illustration of murine fracture model with a diaphyseal osteotomy stabilized with an intramedullary stainless-steel pin. **(B)** μCT reconstructed 3D images showed that the KO mice healing fracture callus had similar gross dimensions compared to the WT, 3 weeks after injury. **(C–E)** μCT volumetric analysis of the 3-week-old fracture callus by percentage bone volume (%), tissue volume (mm³), and bone volume (mm³); showed that the KO mice had normal callus bony volume and density. **(F, G)** Mechanical evaluation of the fracture callus at 3 weeks by maximum torque (Newton.mm), and stiffness (Newton/mm) were similar for both the KO and WT mice.

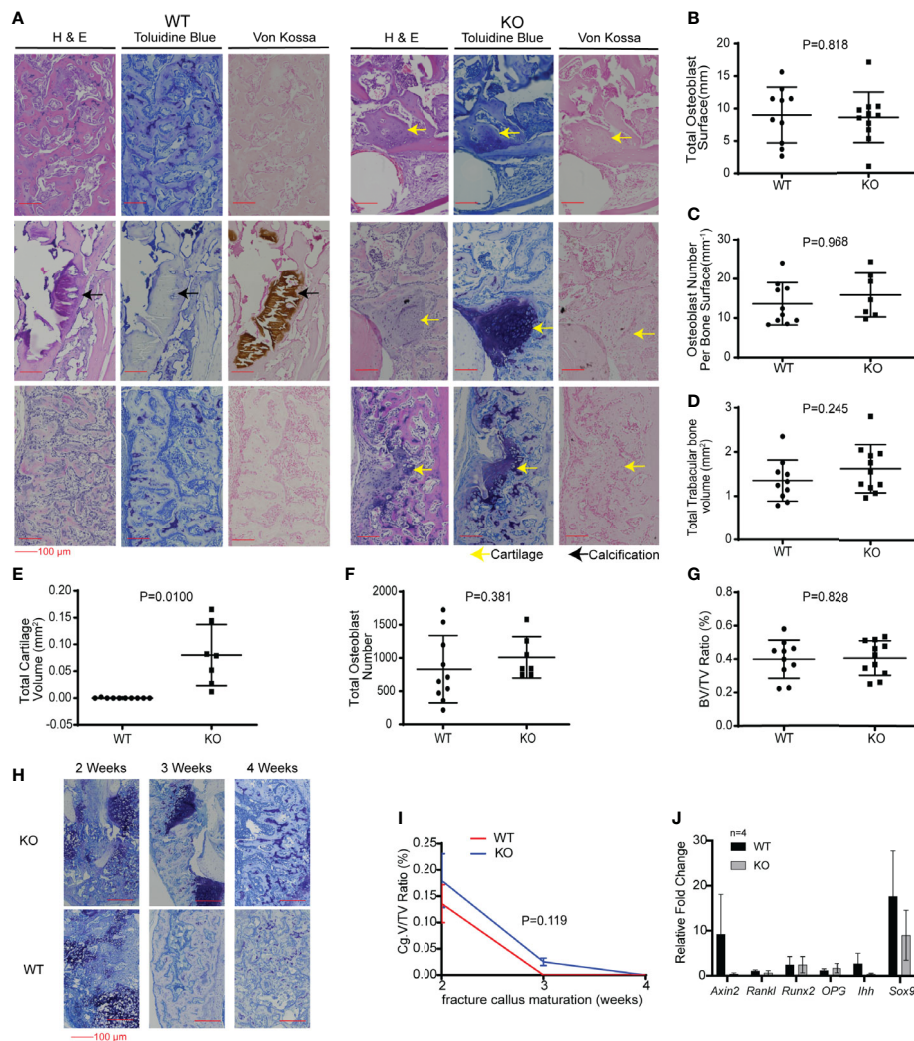
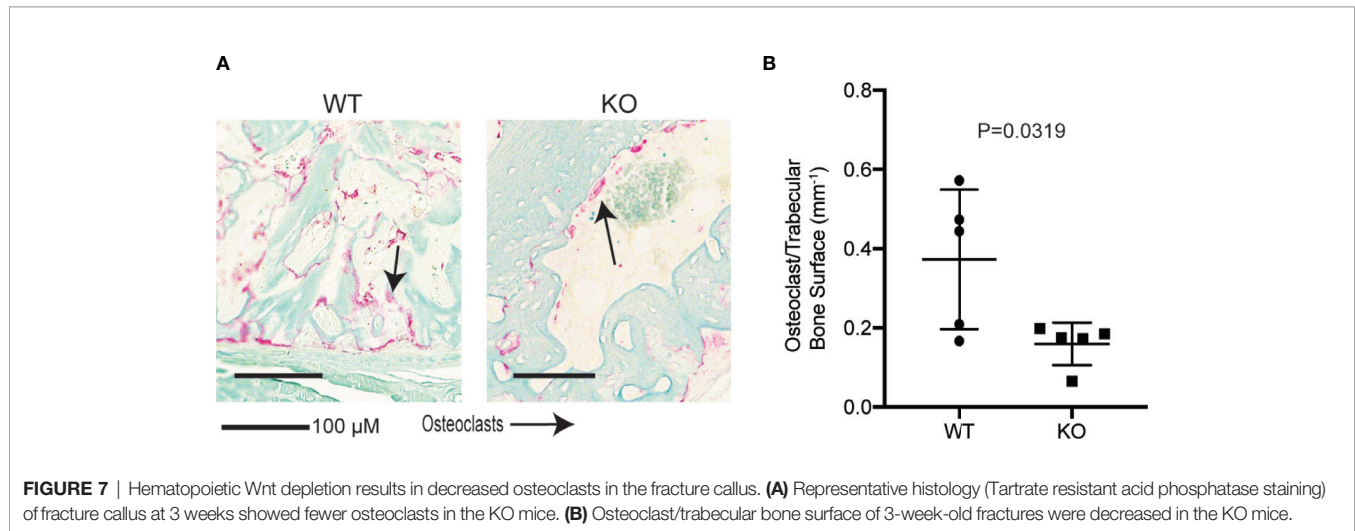


FIGURE 6 | Hematopoietic Wnt-depleted mice had delayed callus maturation with more cartilage. **(A)** Histology of representative mice callus samples 3 weeks after injury from each group, demonstrated increased cartilage in the callus in the KO compared to the WT mice. **(B–H)** Quantitative evaluation of the fracture callus 3 weeks after injury were done by determining the **(B)** Total osteoblast surface (mm), **(C)** osteoblast number per bone surface (mm³), **(D)** total trabecular bone volume (mm³), **(E)** total cartilage volume (mm³), **(F)** total osteoblast number and **(G)** bone volume to total callus volume ratio (%). Total cartilage volume **(E)** was significantly less in the KO compared to the WT callus samples. **(H)** Representative images showing progressive maturation of the fracture callus in hematopoietic Wnt-depleted mice (KO) and wild type mice (WT). **(I)** Cartilage volume to total volume ratio (%) during the first 4 weeks after injury, demonstrating that the fracture calluses from the KO mice matured to woven bone after 4 weeks. **(J)** Quantitative polymerase chain reaction (qPCR) evaluation of the fracture callus at 3 weeks for relative expression of Wnt target gene (*Axin2*), bone turnover (*Rankl*), osteoblastic genes (*Runx2*, *Opg*) and chondrogenic genes (*Ihh*, *Sox9*) revealed no significant difference in the 2 groups of mice. $N=4$ mice per group.

osteoblastic differentiation (**Figure 6J**, female mice). Despite the difference in the phenotype of the callus at 3 weeks, expression of the Wnt/ β -catenin target gene (*Axin2*) and the markers of osteoblastic differentiation (*Opg*, *Runx2*), bone resorption (*Rankl*) and early chondrogenesis (*Ihh* and *Sox9a*) were similar for both groups. This may be because the increase in Wnts secreted, and expression of the markers analyzed may have changed for only a short transient duration. This may have normalized at the time point of our analysis. There may also only be a difference in the ratio of specific Wnts rather than just a decrease in the quantity of β -catenin dependent Wnts in the KO callus compared to the wild-type callus.

DISCUSSION

This study sets out to investigate the role of hematopoietic Wnts in bone homeostasis and fracture healing. We know that bone marrow is important for hematopoiesis, but are hematopoietic cells important for bone formation? Do marrow cells play a role under normal physiological conditions in development or only in injury? These important questions can help us to understand how autologous bone marrow grafts assist in fracture healing. Stimulation of fracture healing by bone marrow or bone grafting has thus far been focused on the therapeutic effect of mesenchymal stem cells and the osteoconductive scaffold that the graft provides.



We do not know much about how the hematopoietic component of the marrow contributes to bone formation. Understanding how hematopoietic cells modulate fracture healing will also help us to predict how bone marrow suppression or failure may affect fracture healing.

In this study, we found that hematopoietic Wnts had only a marginal quantitative effect on musculoskeletal development during fetal development and post-partum growth. However, when we examined what happens during fracture, we identified that there was a delay in fracture callus maturation. This was demonstrated by a more cartilaginous callus matrix. Fracture callus maturation is depended on two sequential and overlapping processes. The first process is resorption of the mineralized cartilage in the soft callus by osteoclasts. The second process is the replacement of the resorbed cartilage with woven bone by osteoblasts. Disruption of either of these two processes can result in delay in callus maturation (40). We found that in the hematopoietic Wnt depleted mice callus, there was a significant decrease in the osteoclast to bone surface area. This phenotype of delayed callus remodeling that we observed was similar to what Lin et al. (42) reported following reduction of osteoclast numbers in a fracture model. Can a shortfall in Wnts result in a reduced number of osteoclasts? Wei et al. (43) demonstrated that Wnt inhibition in osteoclast lineage cells by β -catenin deletion resulted in inhibition of proliferation of osteoclast precursor cells. Wnt/ β -catenin activation stimulates GATA2/Evi1 expression which is required to generate osteoclast precursors. Constitutive Wnt/ β -catenin activation resulted in proliferation of osteoclast precursors, but inhibition of osteoclastic differentiation to mature osteoclasts. Wei also showed that Wnt/ β -catenin downregulation is needed for c-Jun activation, which in turn is required for the proliferation to differentiation switch in osteoclast precursors. This suggests that a very finely balanced, phased Wnt activation level is required for optimizing the number of mature osteoclasts. Although Wei's experiments were not done in a fracture model, it follows that an acute

shortfall in Wnt molecules during healing caused by hematopoietic Wnt depletion can disrupt this balance and result in fewer mature osteoclasts within the callus, specifically by inhibiting osteoclast precursor proliferation.

In contrast to the number of mature osteoclasts, the number of osteoblasts per bone volume was not decreased in the hematopoietic Wnt depleted callus. Osteoblasts play a key role in laying down bone during fracture healing, an essential step in callus maturation. Wnt signaling is a positive regulator of osteoblasts (44) and osteoblastic Wnt/ β -catenin inhibition results in fracture non-union (14). In our model, Wnt secretion from osteoblasts was not blocked, and so the osteoblasts could provide an alternative source of functional Wnts in our model.

Other hematopoietic cells, specifically myeloid cells including macrophages and osteoclasts, have also been reported to be important for late stage fracture healing. Schlundt (41) reported that macrophage reduction did not result in an obvious effect in the early phase of fracture healing but resulted in delayed hard callus formation. They also reported that the anti-inflammatory M2 macrophage enhancement improved fracture callus maturation. They concluded that the macrophages played an important role in immune modulation during healing. Linda et al. (19) also reported that macrophages were important in promoting osteoblastic differentiation during fracture healing. Our study suggests that hematopoietic cells may contribute to fracture healing in a multitude of ways, including secretion of Wnts to increase osteoclasts during callus remodeling. This has important implications for our understanding of basic fracture healing physiology.

DATA AVAILABILITY STATEMENT

The raw data supporting the conclusions of this article will be made available by the authors, without undue reservation.

ETHICS STATEMENT

The animal study was reviewed and approved by Institutional Animal Care and Use Committee.

AUTHOR CONTRIBUTIONS

Conception and design: KC and DV. Development of methodology: KC. Acquisition of data: KC, CC, AY, and EY. Analysis and interpretation of data: KC, VL, and DV. Writing, review, and/or revision of the paper: KC and DV. Administrative, technical, or material support: VL. Study supervision: KC and DV. All authors contributed to the article and approved the submitted version.

FUNDING

This work was by the National Research Foundation Singapore, administered by the Singapore Ministry of Health's National

Medical Research Council under Singapore Translational Research (STaR) Award MOH-000155 to DV.

ACKNOWLEDGMENTS

Technical assistance in performing the micro-CT was generously provided by Hoshiang Chueh, Nikita Agarwal and Way Cherng Chen, in collaboration with Bruker SBIC PCI Centre. We gratefully acknowledge Zahra Kabiri, Yun Ka Wong, Babita Madan, Edison and other members of the Virshup lab, Nurul Azizah Binte Johari of Program in Musculoskeletal Sciences Academic Clinical Program for technical help and support. We would also like to thank Bryan Ogden and staff of the Singapore Experimental Medicine Center for logistical support and veterinarian assistance. Finally, we would like to thank members of the Benjamin Alman lab at Duke University for assistance and guidance on experimental methodology along the way.

REFERENCES

- Baron R, Rawadi G. Targeting the Wnt/beta-catenin Pathway to Regulate Bone Formation in the Adult Skeleton. *Endocrinology* (2007) 148:2635–43. doi: 10.1210/en.2007-0270
- Baron R, Kneissel M. WNT Signaling in Bone Homeostasis and Disease: From Human Mutations to Treatments. *Nat Med* (2013) 19:179–92. doi: 10.1038/nm.3074
- Rudnicki MA, Williams BO. Wnt Signaling in Bone and Muscle. *Bone* (2015) 80:60–6. doi: 10.1016/j.bone.2015.02.009
- Chen Y, Alman BA. Wnt Pathway, an Essential Role in Bone Regeneration. *J Cell Biochem* (2009) 106:353–62. doi: 10.1002/jcb.22020
- Nusse R. Wnt Signaling. *Cold Spring Harb Perspect Biol* (2012) 4:a011163–a011163. doi: 10.1101/cshperspect.a011163
- Maruotti N, Corrado A, Neve A, Cantatore FP. Systemic Effects of Wnt Signaling. *J Cell Physiol* (2013) 228:1428–32. doi: 10.1002/jcp.24326
- Yu J, Virshup DM. Updating the Wnt Pathways. *Biosci Rep* (2014) 34:593–607. doi: 10.1042/BSR20140119
- Nusse R, Clevers H. Wnt/ β -Catenin Signaling, Disease, and Emerging Therapeutic Modalities. *Cell* (2017) 169:985–99. doi: 10.1016/j.cell.2017.05.016
- Sassi N, Laadhar L, Allouche M, Achek A, Kallel-Sellami M, Makni S, et al. WNT Signaling and Chondrocytes: From Cell Fate Determination to Osteoarthritis Pathophysiology. *J Recept Signal Transduct Res* (2014) 34:73–80. doi: 10.3109/10799893.2013.863919
- Ling IT, Rochard L, Liao EC. Distinct Requirements of Wls, Wnt9a, Wnt5b and Gpc4 in Regulating Chondrocyte Maturation and Timing of Endochondral Ossification. *Dev Biol* (2017) 421:219–32. doi: 10.1016/j.ydbio.2016.11.016
- Wan Y, Lu C, Cao J, Zhou R, Yao Y, Yu J, et al. Osteoblastic Wnts Differentially Regulate Bone Remodeling and the Maintenance of Bone Marrow Mesenchymal Stem Cells. *Bone* (2013) 55:258–67. doi: 10.1016/j.bone.2012.12.052
- Fukuda T, Kokabu S, Ohte S, Sasanuma H, Kanomata K, Yoneyama K, et al. Canonical Wnts and BMPs Cooperatively Induce Osteoblastic Differentiation Through a GSK3 β -Dependent and β -Catenin-Independent Mechanism. *Differentiation* (2010) 80:46–52. doi: 10.1016/j.diff.2010.05.002
- Xu H, Duan J, Ning D, Li J, Liu R, Yang R, et al. Role of Wnt Signaling in Fracture Healing. *BMB Rep* (2014) 47:666–72. doi: 10.5483/BMBRep.2014.47.12.193
- Chen Y, Whetstone HC, Lin AC, Nadesan P, Wei Q, Poon R, et al. Beta-Catenin Signaling Plays a Disparate Role in Different Phases of Fracture Repair: Implications for Therapy to Improve Bone Healing. *PloS Med* (2007) 4:e249. doi: 10.1371/journal.pmed.0040249
- Komatsu DE, Mary MN, Schroeder RJ, Robling AG, Turner CH, Warden SJ. Modulation of Wnt Signaling Influences Fracture Repair. *J Orthop Res* (2010) 28:928–36. doi: 10.1002/jor.21078
- Liu Y-B, Lin L-P, Zou R, Zhao Q-H, Lin F-Q. Silencing Long Non-Coding RNA MEG3 Accelerates Tibia Fracture Healing by Regulating the Wnt/ β -Catenin Signaling Pathway. *J Cell Mol Med* (2019) 23:3855–66. doi: 10.1111/jcmm.14229
- Kollet O, Dar A, Shvitiel S, Kalinkovich A, Lapid K, Sztainberg Y, et al. Osteoclasts Degrade Endosteal Components and Promote Mobilization of Hematopoietic Progenitor Cells. *Nat Med* (2006) 12:657–64. doi: 10.1038/nm1417
- Sinder BP, Pettit AR, McCauley LK. Macrophages: Their Emerging Roles in Bone. *J Bone Miner Res* (2015) 30:2140–9. doi: 10.1002/jbmr.2735
- Vi L, Baht GS, Whetstone H, Ng A, Wei Q, Poon R, et al. Macrophages Promote Osteoblastic Differentiation in-Vivo: Implications in Fracture Repair and Bone Homeostasis. *J Bone Miner Res* (2015) 30:1090–102. doi: 10.1002/jbmr.2422
- McCauley J, Bitsakis C, Cottrell J. Macrophage Subtype and Cytokine Expression Characterization During the Acute Inflammatory Phase of Mouse Bone Fracture Repair. *J Orthop Res* (2020) 1:1. doi: 10.1002/jor.24603
- Saha S, Aranda E, Hayakawa Y, Bhanja P, Atay S, Brodin NP, et al. Macrophage-Derived Extracellular Vesicle-Packaged WNTs Rescue Intestinal Stem Cells and Enhance Survival After Radiation Injury. *Nat Commun* (2016) 7:13096. doi: 10.1038/ncomms13096
- Wynn TA, Vannella KM. Macrophages in Tissue Repair, Regeneration, and Fibrosis. *Immunity* (2016) 44:450–62. doi: 10.1016/j.immuni.2016.02.015
- Fong K, Truong V, Foote CJ, Petrison B, Williams D, Ristevski B, et al. Predictors of Nonunion and Reoperation in Patients With Fractures of the Tibia: An Observational Study. *BMC Musculoskelet Disord* (2013) 14:103. doi: 10.1186/1471-2474-14-103
- Santolini E, West R, Giannoudis PV. Risk Factors for Long Bone Fracture Non-Union: A Stratification Approach Based on the Level of the Existing Scientific Evidence. *Injury* (2015) 46(Suppl 8):S8–S19. doi: 10.1016/S0020-1383(15)30049-8
- Burska AN, Giannoudis PV, Tan BH, Ilas D, Jones E, Ponchel F. Dynamics of Early Signaling Events During Fracture Healing and Potential Serum Biomarkers of Fracture non-Union in Humans. *J Clin Med* (2020) 9:492. doi: 10.3390/jcm9020492
- Gorter EA, Hamdy NAT, Appelman-Dijkstra NM, Schipper IB. The Role of Vitamin D in Human Fracture Healing: A Systematic Review of the Literature. *Bone* (2014) 64:288–97. doi: 10.1016/j.bone.2014.04.026
- Mills L, Tsang J, Hopper G, Keenan G, Simpson AHRW. The Multifactorial Aetiology of Fracture Nonunion and the Importance of Searching for Latent

- Infection. *Bone Joint Res* (2016) 5:512–9. doi: 10.1302/2046-3758.510.BJR-2016-0138
28. Gómez-Barrena E, Rosset P, Lozano D, Stanovici J, Ermthaller C, Gerbhard F. Bone Fracture Healing: Cell Therapy in Delayed Unions and Nonunions. *Bone* (2015) 70:93–101. doi: 10.1016/j.bone.2014.07.033
 29. Le Baron M, Vivona J-P, Maman P, Volpi R, Flecher X. Can the Reamer/Irrigator/Aspirator System Replace Anterior Iliac Crest Grafting When Treating Long Bone Nonunion? *Orthop Traumatol Surg Res* (2019) 105:529–33. doi: 10.1016/j.otsr.2018.12.011
 30. Yee MA, Hundal RS, Perdue AM, Hake ME. Autologous Bone Graft Harvest Using the Reamer–Irrigator–Aspirator. *J Orthop Trauma* (2018) 32:S20–1. doi: 10.1097/BOT.0000000000001195
 31. Attum B, Douleh D, Whiting PS, White-Dzuro GA, Dodd AC, Shen MS, et al. Outcomes of Distal Femur Nonunions Treated With a Combined Nail/Plate Construct and Autogenous Bone Grafting. *J Orthop Trauma* (2017) 31:e301–4. doi: 10.1097/BOT.0000000000000926
 32. Kabiri Z, Numata A, Kawasaki A, Blank E, Tenen DG, Virshup DM. Wnts are Dispensable for Differentiation and Self-Renewal of Adult Murine Hematopoietic Stem Cells. *Blood* (2015) 126:1–27. doi: 10.1182/blood-2014-09-598540
 33. Yu J, Chia J, Canning CA, Jones CM, Bard FA, Virshup DM. WLS Retrograde Transport to the Endoplasmic Reticulum During Wnt Secretion. *Dev Cell* (2014) 29:277–91. doi: 10.1016/j.devcel.2014.03.016
 34. Proffitt KD, Virshup DM. Precise Regulation of Porcupine Activity is Required for Physiological Wnt Signaling. *J Biol Chem* (2012) 287:34167–78. doi: 10.1074/jbc.M112.381970
 35. Biechele S, Cockburn K, Lanner F, Cox BJ, Rossant J. Porcn-Dependent Wnt Signaling is Not Required Prior to Mouse Gastrulation. *Development* (2013) 140:2961–71. doi: 10.1242/dev.094458
 36. Rigueur D, Lyons KM. Whole-Mount Skeletal Staining. *Methods Mol Biol* (2014) 1130:113–21. doi: 10.1007/978-1-62703-989-5_9
 37. de Boer J, Williams A, Skavdis G, Harker N, Coles M, Tolaini M, et al. Transgenic Mice With Hematopoietic and Lymphoid Specific Expression of Cre. *Eur J Immunol* (2003) 33:314–25. doi: 10.1002/immu.200310005
 38. Proffitt KD, Madan B, Ke Z, Pendharkar V, Ding L, Lee MA, et al. Pharmacological Inhibition of the Wnt Acyltransferase PORCN Prevents Growth of WNT-driven Mammary Cancer. *Cancer Res* (2013) 73:502–7. doi: 10.1158/0008-5472.CAN-12-2258
 39. Najdi R, Proffitt K, Sprowl S, Kaur S, Yu J, Covey TM, et al. A Uniform Human Wnt Expression Library Reveals a Shared Secretory Pathway and Unique Signaling Activities. *Differentiation* (2012) 84:203–13. doi: 10.1016/j.diff.2012.06.004
 40. Marsell R, Einhorn TA. The Biology of Fracture Healing. *Injury* (2011) 42:551–5. doi: 10.1016/j.injury.2011.03.031
 41. Schlundt C, Khassawna El T, Serra A, Dienelt A, Wendler S, Schell H, et al. Macrophages in Bone Fracture Healing: Their Essential Role in Endochondral Ossification. *Bone* (2015) 106:78–89. doi: 10.1016/j.bone.2015.10.019
 42. Lin H-N, O'Connor JP. Osteoclast Depletion With Clodronate Liposomes Delays Fracture Healing in Mice. *J Orthop Res* (2017) 35:1699–706. doi: 10.1002/jor.23440
 43. Wei W, Zeve D, Suh JM, Wang X, Du Y, Zerwekh JE, et al. Biphasic and Dosage-Dependent Regulation of Osteoclastogenesis by β -Catenin. *Mol Cell Biol* (2011) 31:4706–19. doi: 10.1128/MCB.05980-11
 44. Day T, Guo X, Garrettbeal L, Yang Y. Wnt/ β -Catenin Signaling in Mesenchymal Progenitors Controls Osteoblast and Chondrocyte Differentiation During Vertebrate Skeletogenesis. *Dev Cell* (2005) 8:739–50. doi: 10.1016/j.devcel.2005.03.016

Conflict of Interest: The authors declare that the research was conducted in the absence of any commercial or financial relationships that could be construed as a potential conflict of interest.

Copyright © 2021 Chua, Lee, Chan, Yew, Yeo and Virshup. This is an open-access article distributed under the terms of the Creative Commons Attribution License (CC BY). The use, distribution or reproduction in other forums is permitted, provided the original author(s) and the copyright owner(s) are credited and that the original publication in this journal is cited, in accordance with accepted academic practice. No use, distribution or reproduction is permitted which does not comply with these terms.



Decreased Sclerostin Secretion in Humans and Mice With Nonalcoholic Fatty Liver Disease

Fangli Zhou^{1,2}, Yan Wang¹, Yujue Li¹, Mengjia Tang¹, Shan Wan¹, Haoming Tian² and Xiang Chen^{1*}

¹ Department of Endocrinology, Laboratory of Endocrinology and Metabolism, West China Hospital, Sichuan University, Chengdu, China, ² Department of Endocrinology, West China Hospital, Sichuan University, Chengdu, China

OPEN ACCESS

Edited by:

Lilian Irene Plotkin,
Indiana University Bloomington,
United States

Reviewed by:

Subhashis Pal,
Emory University, United States
Thomas Levin Andersen,
University of Southern Denmark,
Denmark

*Correspondence:

Xiang Chen
onlycx@163.com

Specialty section:

This article was submitted
to Bone Research,
a section of the journal
Frontiers in Endocrinology

Received: 10 May 2021

Accepted: 23 July 2021

Published: 05 August 2021

Citation:

Zhou F, Wang Y, Li Y, Tang M,
Wan S, Tian H and Chen X (2021)
Decreased Sclerostin Secretion
in Humans and Mice With
Nonalcoholic Fatty Liver Disease.
Front. Endocrinol. 12:707505.
doi: 10.3389/fendo.2021.707505

Objectives: Growing evidence argues for a relationship between liver and bone metabolisms. Sclerostin is a secreted glycoprotein and could antagonize osteoblast-mediated bone formation. Previous studies indicated that circulating sclerostin levels may be associated with metabolic parameters with inconsistent results. This study was designed to evaluate serum sclerostin in patients with or without nonalcoholic fatty liver disease (NAFLD) and to analyze its relationship with metabolic parameters in different populations.

Methods: A cross-sectional study was designed and 168 NAFLD subjects and 85 control subjects were included in this study. Serum sclerostin and metabolic parameters were measured. Mouse models of NAFLD were also induced by high-fat diet. Bone structural parameters were determined using microCT and mRNA expression levels of sclerostin in bone and liver tissues were measured.

Results: Our study suggested that circulating sclerostin levels were significantly lower in NAFLD subjects compared with normal controls. In NAFLD subjects, sclerostin was negatively correlated with multiple metabolic parameters, including waist circumference, urea, hepatic enzyme, gamma-glutamyl transpeptidase, and triglyceride, while such correlation was not significant in control subjects. Circulating sclerostin was also negatively correlated with fatty liver index in NAFLD subjects but not in control subjects. Mice fed on a high-fat diet had reduced bone mass and lower sclerostin expression levels in both the bone and liver tissues.

Conclusions: Our study suggested that the liver-lipid-bone interactions may play a key role in the abnormal bone metabolism in NAFLD, and circulating sclerostin may be a surrogate marker to reflect bone metabolism status in NAFLD subjects.

Keywords: sclerostin, NAFLD, fatty liver index, bone metabolism, triglyceride

INTRODUCTION

Nonalcoholic fatty liver disease (NAFLD), which is closely associated with obesity, type 2 diabetes, and the metabolic syndrome, has become the most prevalent chronic liver disease today. In recent years, extrahepatic manifestations of NAFLD have attracted scientific attention (1, 2). Previous studies also indicated a possible liver - bone interaction (3). Low bone mineral density (BMD) and high risk of osteoporosis have been found in both pediatric and adult populations with NAFLD (4, 5). For example, Pardee et al. reported that obese children with NAFLD had significantly lower BMD Z-scores than obese children without NAFLD after controlling for age, sex, race, ethnicity, and total percent body fat (6). In Korean men, NAFLD has been demonstrated to be negatively associated with right-hip BMD and serum osteocalcin after adjusting for body mass index (BMI) and homeostasis model assessment of insulin resistance (HOMA-IR) in Korean men (7, 8). However, reverse results have also been reported. S. H. Lee et al. revealed a significantly negative association between the femoral neck (FN) BMD and NAFLD in men, while a positive correlation between lumbar spine BMD and NAFLD in postmenopausal women (7). It was suggested that fatty liver index (FLI), which is calculated using BMI, waist circumference (WC), serum triglyceride (TG), and gamma-glutamyltranspeptidase (γ -GGT) levels, was negatively associated with total hip, femoral neck, and whole-body BMD in Korean men, but not in women (9). A meta-analysis including studies in adults did not show a significant difference in BMD between patients with NAFLD and non-NAFLD (10), while meta-analysis including studies conducted in children or adolescents revealed significant differences in whole-body or lumbar BMD Z scores between children/adolescents with and without NAFLD (11). Therefore, the liver- bone interaction and the underlying mechanism deserve further investigations.

Sclerostin is a glycoprotein predominately secreted by osteocytes. Notably, although sclerostin could antagonize osteoblast-mediated bone formation through inhibiting the Wnt pathway, circulating sclerostin levels have been found to be positively associated with BMD in humans (12–14). It is speculated that circulating sclerostin may reflect numbers of osteocytes. Sclerostin has been found to be associated with metabolic abnormalities. Giuseppe Daniele et al. suggested that sclerostin levels were higher in impaired glucose regulation (IGR) subjects compared with normal glucose tolerant (NGT) individuals and are correlated with insulin resistance in skeletal muscle, liver, and adipose tissue (15). Higher sclerostin levels have also been found in type 2 diabetes (16, 17). NAFLD plays a key role in insulin resistance and type 2 diabetes. It is intriguing to explore whether sclerostin is correlated with NAFLD. S. A. Polyzos et al. found a progressive decline in serum sclerostin levels from the controls (76.1 ± 6.8 pmol/L) to nonalcoholic simple steatosis (SS) (53.5 ± 6.4 pmol/L) and steatohepatitis (NASH) (46.0 ± 8.1 pmol/L) patients ($p = 0.009$) (3). Our clinical study also demonstrated that circulating sclerostin levels were significantly lower in NAFLD subjects than normal controls and

were significantly correlated with multiple metabolic parameters. Although sclerostin is predominately expressed by osteocytes, sclerostin mRNA was also detected in liver tissues in human and mice. Therefore, we also built mouse models of NAFLD using a high-fat diet (HFD) to compare the mRNA expression levels of sclerostin in both the bone and liver tissues between mice fed on a control diet (CON) or HFD.

MATERIALS AND METHODS

Subjects

This study was approved by the Ethics Committee of the West China Hospital. All participants gave written informed consent. NAFLD group included patients with ultrasound found fatty liver, and there were no causes for secondary hepatic fat accumulation due to significant alcohol consumption, malnutrition, hepatitis B virus, and hepatitis C virus. Exclusion criteria include: (1). Patients with alcohol consumption more than 140g/week for males and 70g/week for females; (2). There was a past history of hepatitis B virus and hepatitis C virus; (3). Ultrasound showed hepatomegaly; (4). BMI < 16 and incomplete data. 168 NAFLD patients were included in our study. 85 age- matched control subjects without ultrasound found fatty liver were recruited from West China hospital's physical examination center. None of the participants were on any medications known to cause hepatic steatosis or taking vitamin supplements.

Anthropometric Measurements

Anthropometric measurements were performed for all participants and were recorded by trained staff. Body height, weight, blood pressure, and WC were recorded. BMI was calculated as weight (kg) divided by height (m²) squared. Measurements were carried out twice by two independent interviewers.

Laboratory Assessments

Venous blood samples were collected to measure lipids, liver function, and other biochemical parameters after fasting for ≥ 8 h. Total cholesterol (TC), TG, low-density lipoprotein cholesterol (LDL-C), high-density lipoprotein cholesterol (HDL-C), alanine transaminase (ALT), aspartate aminotransferase (AST), γ -GGT, urea, alkaline phosphatase (ALP), ferritin, and alpha-fetoprotein (AFP) were assessed in all the patients using automated, standardized equipment from the Clinical Laboratory of West China Hospital. Plasma glucose levels were tested using a hexokinase enzymatic technique. Serum insulin was measured using a radioimmunoassay (Beijing North Institute of Biological Technology). Circulating sclerostin levels were measured using an ELISA kit from Abcam (ab221836, Cambridge, UK). The detection limit of the assay is 6 pg/mL with a range of 31.1 – 2000 pg/mL. The intra- and inter-assay precisions are 4.8 and 8.6%, respectively. HOMA-IR was used to measure the insulin resistance as the equation: $\text{HOMA-IR} = [\text{fasting plasma glucose (mmol/L)} \times \text{fasting insulin (pmol/L)}] / 22.5$. Fatty liver index (FLI), calculated from serum TG, BMI, WC, and γ -GGT, has been used as a surrogate

marker of NAFLD and a screening test in epidemiologic studies. FLI was calculated by the following formula: $FLI = [e^{0.953 \times \ln(TG) + 0.139 \times BMI + 0.718 \times \ln(GGT) + 0.053 \times WC - 15.745} / (1 + e^{0.953 \times \ln(TG) + 0.139 \times BMI + 0.718 \times \ln(GGT) + 0.053 \times WC - 15.745})] \times 100$ (18).

Abdominal Ultrasonography

A high-resolution B-mode ultrasound probe (IU22, Philips, Netherlands) equipped with a 7.5 MHz linear array was used to measure the fatty liver. Participants were asked to maintain in the supine position with the right arm raised above the head during the examination. The liver's fatty infiltration was diagnosed by two experienced sonographers unaware of the study's aims and blinded to the laboratory results. A fatty liver was defined as the presence of hyperechogenic liver parenchyma compared to the kidney or spleen parenchyma.

Animals and Interventions

Male C57BL/6 mice were maintained in the temperature- and light-controlled pathogen-free barrier facility under a 12-h light–12-h dark cycle and had free access to water and diet. At the age of 8 weeks, mice were divided into 2 groups with 6 animals each either on a standard chow diet (64% carbohydrate, 10% fat, and 26% protein) or a high-fat diet (28% carbohydrate, 60% fat, and 12% protein) for 12 weeks.

At the end of the experiment, mice were euthanized with an intraperitoneal injection of sodium pentobarbital. Bone and liver tissues were fixed in 4% formalin, embedded in paraffin, and stained with Hematoxylin and Eosin for histopathological analysis. Oil Red O staining was also performed in the frozen liver sections. The left femora were immersed into 4% paraformaldehyde immediately for measurement of bone structural parameters.

Bone structural parameters of mice, including trabecular bone volume (Tb. BV/TV), cortical bone volume (Cort. BV/TV), trabecular number (Tb-N), trabecular thickness (Tb-Th), and trabecular separation (Tb-Sp), were measured using microcomputed tomography (μ CT) (MicroCT80, Scanco Medical AG, Bassersdorf, Switzerland), as previously described (19).

Total RNA was extracted from femur distal metaphyses (which was devoid of bone marrow) and liver tissues using Trizol reagent according to the manufacturer's protocol (Invitrogen, Frederick, USA). 1 μ g RNA was reversely transcribed into cDNA with PrimeScriptTM RT reagent kit (TaKaRa Biotechnology Co., Ltd., Dalian, China). Following reverse transcription, the cDNA (2 μ l) was amplified and quantified (Bio-Rad laboratories, Inc., California, USA). The sequence of oligonucleotide primers was listed in the following: sclerostin forward primer: CCTCATCTGCCTACTTGTGC (5'–3'); sclerostin reverse primer: GGTCTGGTTGTTCTCA GGAGG (5'–3'). Relative gene expression levels were normalized to beta-actin and analyzed with the $2^{-\Delta\Delta C_t}$ method.

Statistical Analysis

Data were analyzed using SPSS v. 16.0 software. Shapiro–Wilk's test was used to verify the normal distribution of continuous data before each analysis. Analysis showed that HOMA-IR, sclerostin,

ALT, TG, γ -GGT, ferritin and FLI were not distributed normally. Data are presented as mean \pm standard deviation (SD) for normally distributed data. Otherwise, non-normally distributed data were presented as median (quartiles) and were transformed, using the natural logarithms, before each analysis. The significance of group differences was evaluated using independent samples t-Test for continuous variables, while Chi-square test was performed for categorical variables. Pearson's correlation test or Spearman's correlation test was used to determine the correlation between sclerostin levels with various parameters. Partial correlation was used to eliminate the influence of potential confounding factors. The statistical significance was set at $p < 0.05$ (two-tailed).

RESULTS

Clinical Study

As expected, the metabolic parameters were significantly different between NAFLD subjects and normal controls (Table 1). NAFLD subjects had significantly higher BMI, WC, Waist-to-Hip ratio (WHR), blood pressure levels, urea, AST,

TABLE 1 | Baseline characteristics and biochemical indices.

	Control (n=85)	NAFLD (n=168)	<i>p</i> values
Age (years)	43.27 \pm 11.19	47.74 \pm 10.35	0.002
Gender (male/female)	48/37	119/49	0.000
Body weight (kg)	61.48 \pm 9.50	70.73 \pm 10.53	0.000
Height (cm)	163.27 \pm 7.97	165.08 \pm 8.47	0.111
BMI (kg/m ²)	22.99 \pm 2.67	25.86 \pm 2.48	0.000
Waist circumference (cm)	77.96 \pm 7.56	88.19 \pm 7.60	0.000
WHR	0.83 \pm 0.06	0.91 \pm 0.05	0.000
SBP (mmHg)	116.16 \pm 16.36	121.75 \pm 16.75	0.014
DBP (mmHg)	71.60 \pm 10.06	77.54 \pm 10.44	0.000
Urea (μ mol/L)	320.31 \pm 82.03	399.57 \pm 96.82	0.000
ALT (IU/L)	19.00(14.00–26.00)	38.00(24.00–56.75)	0.000
AST (IU/L)	23.00 \pm 9.15	32.27 \pm 15.48	0.000
Fasting plasma glucose (mmol/L)	5.14 \pm 0.52	5.87 \pm 1.84	0.000
Fasting insulin (pmol/L)	14.04 \pm 6.77	15.35 \pm 7.56	0.163
HOMA-IR	3.08(2.02–4.50)	3.62(2.36–5.22)	0.013
TC (mmol/L)	4.76 \pm 0.74	5.17 \pm 0.99	0.001
TG (mmol/L)	1.16 (0.90–1.62)	2.13(1.57–3.04)	0.001
LDL-C (mmol/L)	2.57 \pm 0.64	2.80 \pm 0.78	0.018
HDL-C (mmol/L)	1.59 \pm 0.41	1.27 \pm 0.30	0.000
γ -GGT (IU/L)	16.00 (12.00–23.00)	35.50(25.00–66.75)	0.000
ALP (IU/L)	67.18 \pm 18.43	78.38 \pm 21.39	0.000
Ferritin (ng/mL)	111.23 (53.27–152.84)	209.18(125.38–303.32)	0.000
AFP (ng/mL)	3.75 \pm 2.13	3.52 \pm 1.36	0.320
Sclerostin (pg/mL)	462.60(346.95–617.15)	362.25(189.78–489.40)	0.000
FLI	12.42 (6.19–23.20)	52.77 (34.63–70.47)	0.000

NAFLD, nonalcoholic fatty liver disease; BMI, body mass index; WC, waist circumference; WHR, Waist-to-Hip ratio; SBP, systolic blood pressure; DBP, diastolic blood pressure; ALT, alanine aminotransferase; AST, aspartate aminotransferase; HOMA-IR, homeostasis model assessment of insulin resistance; TC, total cholesterol; TG, triglyceride; LDL-C, low density lipoprotein; HDL-C, high-density lipoprotein; γ -GGT, gamma-glutamyltranspeptidase; ALP, alkaline phosphatase; AFP, alpha fetoprotein; FLI, fatty liver index.

ALT, fasting blood glucose levels, HOMA-IR, TC, TG, LDL-C, γ -GGT, ALP, and ferritin levels, as well as significantly lower HDL-C levels, compared with normal controls. Height, fasting insulin, and AFP levels were not different between the two groups. Circulating sclerostin levels were significantly lower in NAFLD subjects than normal controls.

For normal controls, circulating sclerostin was found to be positively associated with age, fasting insulin levels, and HOMA-IR and negatively correlated with HDL-C levels through Pearson analysis (**Table 2**). After adjusting for age and WC, these correlations were still significant (**Table 3**). For NAFLD subjects, sclerostin showed a positive correlation with age and a negative correlation with height, body weight, WC, DBP, urea, ALT, AST, fasting insulin levels, HOMA-IR, TC, TG, γ -GGT, and ALP levels by Pearson analysis (**Table 2**). After adjustment for age and WC, sclerostin was still negatively correlated with DBP, ALT, AST, HOMA-IR, TC, TG, γ -GGT, ALP and FLI (**Table 3**). Further analysis showed that the correlation between sclerostin with BW, BMI, WC, WHR, urea, insulin, HOMA-IR, TG and HDL-C are different between two groups (**Table 2**). It seems that sclerostin are closely associated with TG, BW and BW-related parameters in NAFLD subjects, while are closely correlated with insulin, HOMA-IR and HDL-C in controls (**Table 2**).

FLI serves as a surrogate marker for liver fat content. Our study revealed a negative correlation between circulating sclerostin with FLI in NAFLD subjects ($r=-0.243$, $p=0.002$), while no correlation was found in normal control ($r=0.178$, $p=0.111$) (**Figure 1**). Further analysis showed that the

TABLE 3 | Correlation between sclerostin and other parameters after adjustment of WC and age.

Parameters	Control		NAFLD	
	<i>r</i>	<i>p</i>	<i>r</i>	<i>p</i>
DBP (mmHg)	-0.216	0.058	-0.170	0.033
AST (U/L)	-0.123	0.284	-0.174	0.029
ALT (U/L)	-0.023	0.841	-0.200	0.012
Fasting insulin (pmol/L)	0.270	0.018	-0.130	0.104
HOMA-IR	0.269	0.017	-0.159	0.046
TC (mmol/L)	-0.070	0.545	-0.189	0.018
TG (mmol/L)	-0.100	0.384	-0.244	0.002
HDL-C (mmol/L)	-0.233	0.040	-0.112	0.164
γ -GGT (U/L)	-0.116	0.311	-0.186	0.020
ALP (μ g/L)	-0.179	0.116	-0.165	0.039
FLI	0.025	0.830	-0.161	0.045

WC, waist circumference; NAFLD, nonalcoholic fatty liver disease; DBP, diastolic blood pressure; AST, aspartate aminotransferase; ALT, alanine aminotransferase; HOMA-IR, homeostasis model assessment of insulin resistance; TC, total cholesterol; TG, triglyceride; HDL-C, high-density lipoprotein; γ -GGT, gamma-glutamyltranspeptidase; ALP, alkaline phosphatase; FLI, fatty liver index.

correlation of NAFLD and controls are statistically different (95% confidence interval: -0.663, -0.160; $p=0.002$). After adjustment for age and WC, the correlation was still significant in NAFLD subjects (**Table 3**).

Animal Study

Hematoxylin and Eosin and Oil Red O staining showed more lipid droplets accumulated in the liver tissues of HFD-fed mice

TABLE 2 | Correlation between sclerostin and other parameters.

Parameters	Control		NAFLD		Comparison of correlation		
	<i>r</i>	<i>p</i>	<i>r</i>	<i>p</i>	95% confidence interval		<i>p</i>
Age (years)	0.343	0.001	0.233	0.002	-0.136	0.340	0.374
Gender	-0.115	0.297	0.102	0.189	-0.470	0.047	0.107
Body weight (kg)	0.165	0.141	-0.224	0.004	0.128	0.632	0.004
Height (cm)	0.046	0.682	-0.183	0.020	-0.033	0.483	0.087
BMI (kg/m ²)	0.176	0.116	-0.128	0.104	0.041	0.551	0.023
Waist circumference (cm)	0.185	0.099	-0.183	0.020	0.106	0.612	0.006
WHR	0.175	0.117	-0.126	0.111	0.038	0.549	0.025
SBP (mmHg)	-0.056	0.582	-0.047	0.551	-0.268	0.253	0.947
DBP (mmHg)	-0.062	0.099	-0.236	0.002	-0.083	0.430	0.187
Urea	0.160	0.143	-0.176	0.022	0.073	0.582	0.012
ALT (U/L)	-0.034	0.755	-0.216	0.005	-0.077	0.438	0.170
AST (U/L)	-0.129	0.238	-0.217	0.005	-0.165	0.345	0.512
Fasting plasma glucose (mmol/L)	0.111	0.312	-0.055	0.480	-0.098	0.420	0.218
Fasting insulin (pmol/L)	0.217	0.047	-0.174	0.024	0.130	0.632	0.003
HOMA-IR	0.243	0.025	-0.161	0.037	0.144	0.643	0.002
TC (mmol/L)	-0.029	0.793	-0.173	0.025	-0.116	0.402	0.281
TG (mmol/L)	0.178	0.103	-0.256	0.001	0.174	0.675	0.001
LDL-C (mmol/L)	0.061	0.579	-0.121	0.118	-0.081	0.438	0.176
HDL-C (mmol/L)	-0.256	0.018	0.151	0.051	-0.645	-0.148	0.002
γ -GGT (U/L)	-0.067	0.541	-0.280	0.000	-0.042	0.467	0.103
ALP (μ g/L)	-0.076	0.489	-0.165	0.033	-0.169	0.348	0.504
Ferritin (ng/mL)	0.051	0.645	-0.136	0.079	-0.076	0.443	0.164
AFP (ng/mL)	-0.096	0.381	0.013	0.868	-0.365	0.155	0.419

NAFLD, nonalcoholic fatty liver disease; BMI, body mass index; WC, waist circumference; WHR, Waist-to-Hip ratio; SBP, systolic blood pressure; DBP, diastolic blood pressure; ALT, alanine aminotransferase; AST, aspartate aminotransferase; HOMA-IR, homeostasis model assessment of insulin resistance; TC, total cholesterol; TG, triglyceride; LDL-C, low density lipoprotein; HDL-C, high-density lipoprotein; γ -GGT, gamma-glutamyltranspeptidase; ALP, alkaline phosphatase; AFP, alpha fetoprotein.

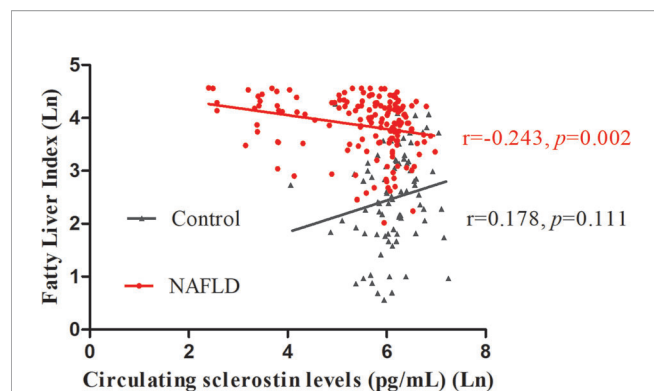


FIGURE 1 | Circulating sclerostin was negatively correlated with FLI in NAFLD subjects ($r = -0.243$, $p = 0.002$), but not in control subjects ($r = 0.178$, $p = 0.111$). FLI, fatty liver index; NAFLD, nonalcoholic fatty liver disease.

compared with mice fed on a control diet (**Figures 2A–D**). More fat vacuoles were found in the bone marrow of mice fed on a high-fat diet (**Figures 2E, F**). Tb. BV/TV and Cort. BV/TV were significantly decreased in mice fed on a high-fat diet compared to mice on a control diet, while Tb. N, Tb. Sp and Tb. Th were not significantly different between groups (**Figure 3**).

The mRNA expression levels of sclerostin were significantly lower in both the bone and liver tissues of HFD-fed mice than those of mice on a control diet (**Figures 4A, B**). Sclerostin expression levels in bone tissues were positively correlated with Cort. BV/TV (**Figure 4C**).

DISCUSSION

Our study suggested that circulating sclerostin levels were significantly lower in NAFLD subjects compared with normal controls, which was consistent with a previous study (3). Our study also indicated that sclerostin was correlated with multiple metabolic parameters, especially WC, hepatic enzyme, γ -GGT, and TG. Although sclerostin is predominantly expressed by osteocytes, sclerostin mRNA has been detected in other human and mouse tissues, including cartilage, liver, kidney, and heart (20). Research conducted by M. E. Brunkow et al. suggested that sclerostin expression levels in human and mouse liver were only lower than those of bone and cartilage (21). Therefore, we also conducted an animal study to compare the expression levels of sclerostin in bone and liver tissues of mice fed on either a control diet or HFD. Mice fed on HFD showed significantly lower sclerostin expression levels in both the bone and liver tissues,

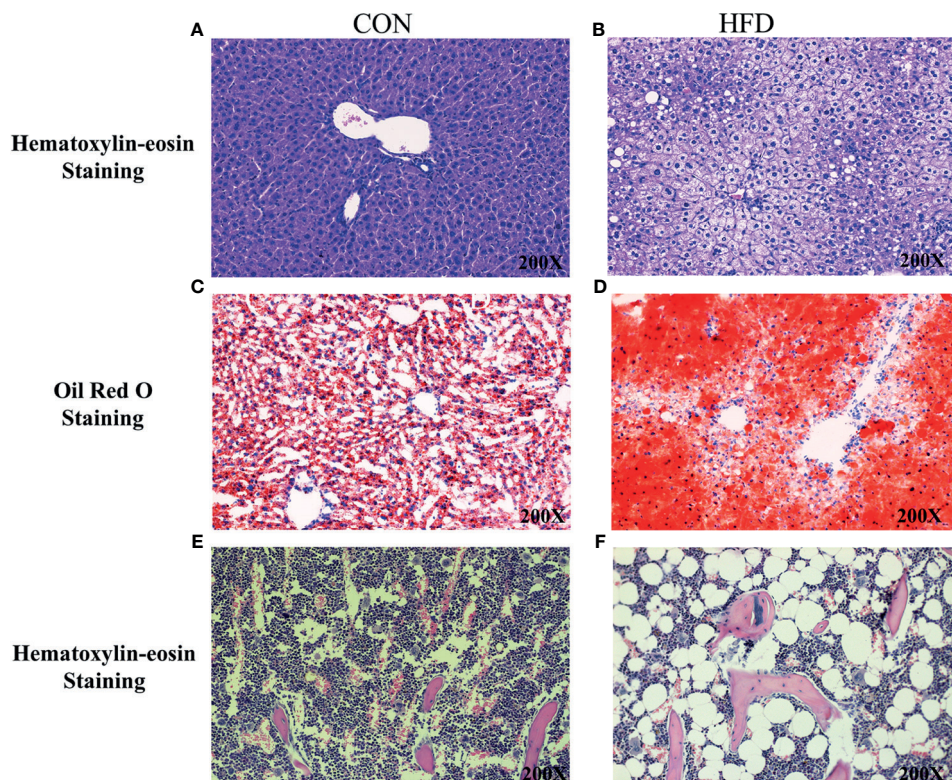


FIGURE 2 | Histological analyses of fat deposition in liver and bone marrow of mice. (**A, B**) Hematoxylin and Eosin staining showed more lipid droplets accumulated in the liver tissues of HFD-fed mice, compared with mice fed on control diets. (**C, D**) Oil Red O staining showed more lipid droplets accumulated in the liver tissues of HFD-fed mice. (**E, F**) Hematoxylin and Eosin staining revealed more fat vacuoles in the bone marrow of mice fed on HFD. CON, control; HFD, high-fat diet.

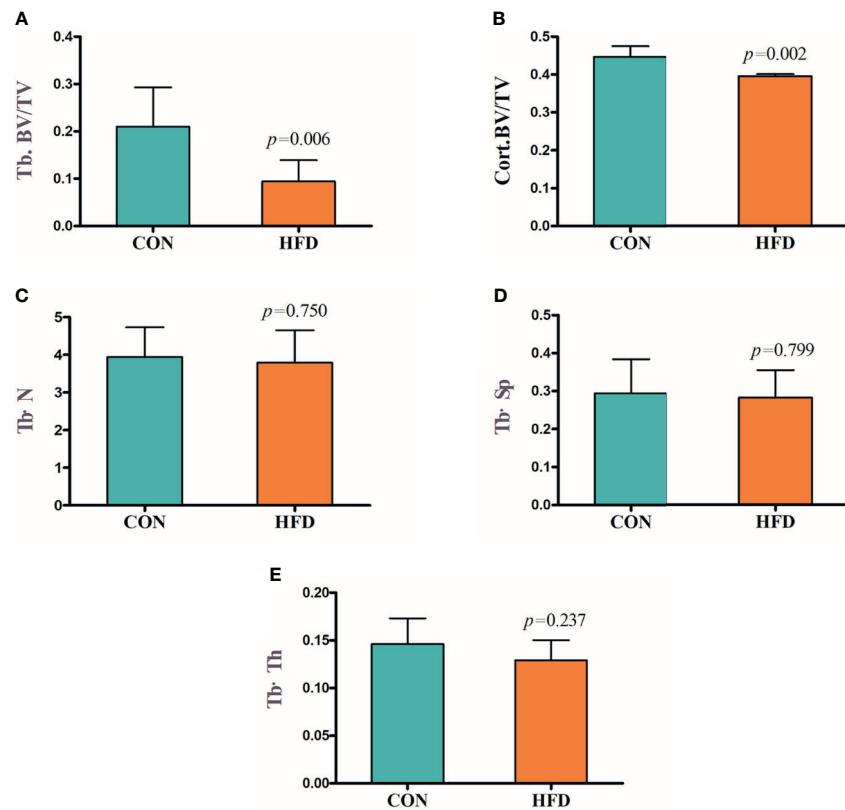


FIGURE 3 | Decreased bone mass in mice fed on a high-fat diet. **(A)** Trabecular bone volume (Tb. BV/TV). **(B)** Cortical bone volume (Cort. BV/TV). **(C)** Trabecular bone number (Tb. N). **(D)** Trabecular separation (Tb. Sp). **(E)** Trabecular bone thickness (Tb. Th). CON, control; HFD, high-fat diet.

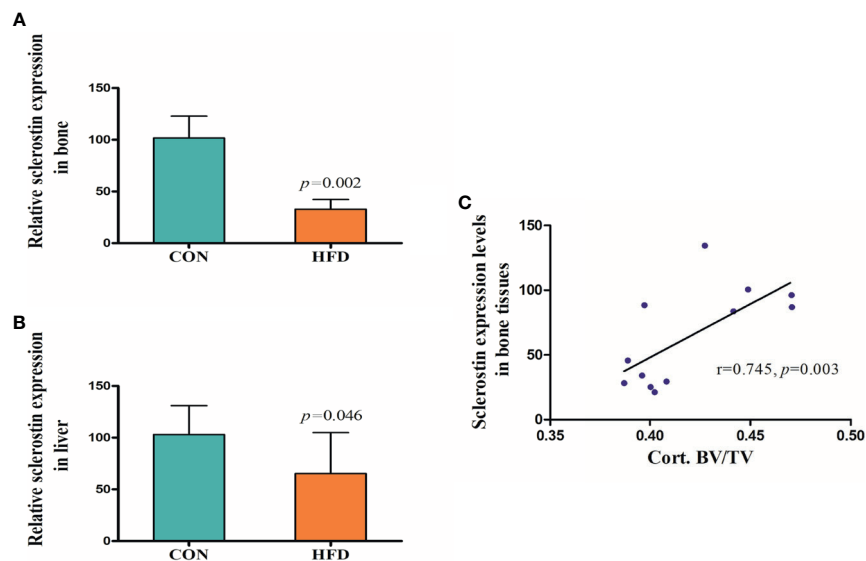


FIGURE 4 | Expression levels of sclerostin. **(A)** Sclerostin expression was significantly decreased in bone tissues of HFD-fed mice ($p=0.002$). **(B)** Sclerostin expression was significantly decreased in liver tissues of HFD-fed mice ($p=0.046$). **(C)** Sclerostin expression levels in bone tissues were positively correlated with Cort. BV/TV ($r=0.745$, $p=0.003$). CON, control; HFD, high-fat diet.

especially the bone tissues. Since the mRNA expression levels of sclerostin in liver tissues were extraordinarily low (data are not shown), when compared with the expression levels of sclerostin in bone tissues, it was speculated that the decreased sclerostin levels in NAFLD subjects may mainly reflect reduced sclerostin secretion from bone tissues.

Previous studies suggested that sclerostin expression is regulated by several factors, including age, estrogen, parathyroid hormone (PTH), and mechanical loading et al. (22). Our study also found a significantly positive correlation between sclerostin and age. Our study indicated that the correlation between sclerostin with metabolic parameters are different between two groups. In NAFLD subjects, sclerostin was closely and negatively correlated with TG, BW and BW-related indicators, while in controls, sclerostin was positively and significantly correlated with insulin and HOMA-IR, and negatively correlated with HDL-C. However, in subjects with NFALD, sclerostin was negatively associated with insulin and HOMA-IR. It seems that body weight gain and accompanying metabolic abnormalities may play a key role in the reduced sclerostin levels in NAFLD subjects. In this study, the sex distribution is significantly different between groups. However, our study indicated that gender may not play a role in the different sclerostin levels between two groups. In both the NAFLD patients and controls, circulating sclerostin levels were not different between male and female (**Supplementary Figure 1**), and no significant correlation between sclerostin and gender was found ($r=-0.115$, $p=0.297$ in NAFLD; $r=0.102$, $p=0.189$ in controls). WC, γ -GGT, and TG are also key risk factors of NAFLD and are used to calculate FLI. In this study, we also analyzed the possible association between sclerostin and FLI in different populations. Similarly, circulating sclerostin was significantly and negatively correlated with FLI in NAFLD subjects, while it was not associated with FLI in control subjects. Our study may suggest that in normal subjects without NAFLD, these metabolic indexes showed no obvious influence on sclerostin secretion, while in NAFLD subjects, these multiple metabolic abnormalities may inhibit sclerostin secretion mediated by a direct or indirect mechanism. The more obvious the metabolic abnormalities were, the more prominent the inhibitory effects on sclerostin expression.

NAFLD, defined by the presence of hepatic steatosis in the absence of other causes for hepatic fat accumulation, is actually a multisystemic clinical disease with extrahepatic manifestations including cardiovascular disease, type 2 diabetes, chronic kidney disease, hypothyroidism, polycystic ovarian syndrome, and psoriasis (1). Decreased BMD and increased risks of osteoporotic fractures have been observed in NAFLD subjects (5), and the underlying mechanism linking fat accumulation in the liver with abnormal bone metabolism has attracted increasing interest recently (5). Chronic inflammation, vitamin D deficiency, growth hormone (GH)/insulin-like growth factor 1 (IGF-1) axis, insulin resistance, limited physical activity, some adipokines like adiponectin and leptin, as well as marrow adipose tissue (MAT) have been proposed as possible mediators of mutual interactions among the skeleton, fatty tissue, and liver (23).

The liver plays a key role in lipid, glucose, and energy metabolism. NAFLD reflects a local manifestation of systemic

metabolic abnormalities. These abnormalities are closely associated with increased body fat content and abnormal lipid metabolism. Our previous and current studies have found a decreased bone mass and increased adipocytes in the bone marrow of mice fed on HFD, indicating MAT may be critically involved in the interplay between bone and liver (19). MAT, which is functionally distinct from both white and brown adipose, can contribute to systemic and skeletal metabolism (23). The previous study found no correlation between MAT with any measure of metabolic risk, including WHR, blood pressure, carotid intima-media thickness, insulin resistance, or lipid profile in young, healthy individuals, while such association was noticed in obese women as well as in patients with type 2 diabetes, indicating MAT may be activated by these metabolic abnormalities. Our present study also revealed similar phenomena. A significant and negative correlation was observed between sclerostin with multiple metabolic indexes, including FLI, in NAFLD subjects, while such correlation was not significant in control subjects without NAFLD. Sclerostin acts as a negative regulator of bone formation by inhibiting the Wnt pathway, while most previous studies revealed a positive correlation between circulating sclerostin levels and BMD in human subjects (24). Our animal study also found that sclerostin expression levels in bone tissues were positively correlated with Cort. BV/TV. Therefore, the decreased circulating sclerostin levels in NAFLD patients may reflect the reduced bone mass and abnormal bone metabolism in these subjects to some degree. MAT may be involved in this process, and the underlying mechanism needs further investigation.

It has been suggested that sclerostin could directly increase adipogenesis in mouse pre-adipocytes and enhance adipocyte differentiation in 3T3-L1 cells (25, 26). However, in our current study, we showed that mice on HFD had more adipocytes in bone marrow while lower sclerostin expression in bone tissues. The inhibited sclerostin expression may reflect lower bone mass with decreased osteocyte numbers in these mice on HFD. However, there may be an interaction between sclerostin and MAT, and enhanced MAT may show some regulatory effects on sclerostin expression. The relevant studies are under way.

Previous studies found increased sclerostin levels in type 2 diabetic patients compared with age-matched controls and type 1 diabetic patients, and sclerostin increased with the number of metabolic syndrome features (16, 17). In post-menopausal type 2 diabetic women with NAFLD and significant fibrosis, sclerostin levels were also higher than those of type 2 diabetic patients without NAFLD (27). In our study, a positive association between sclerostin levels with insulin and HOMA-IR was found in control subjects without NAFLD, while a negative correlation was found between sclerostin and HOMA-IR in NAFLD subjects. Furthermore, NAFLD patients showed a significant correlation between sclerostin levels with lipid profiles, especially TG levels, even after adjusting for confounding factors. These discrepancies may suggest that pathways involved in bone metabolism are different between T2DM and NAFLD.

Our study has certain limitations. First, the clinical study was a cross-sectional study, and thus no causal relationship

could be established. Second, the liver biopsy was not performed due to possible risks for participants. Furthermore, BMD and bone turnover markers, including bone-specific alkaline phosphatase (B-ALP), procollagen I N-terminal propeptide (PINP), and cross-linked type I collagen (CTx), have not been measured in the clinical study. However, the animal experiment was performed and showed from different aspects that sclerostin expression in both the bone and liver tissues was indeed decreased in mice with NAFLD induced by HFD. Our animal study also revealed a positive correlation between sclerostin expression levels in bone tissues and Cort. BV/TV.

CONCLUSIONS

Our study suggested that circulating sclerostin levels were significantly decreased in NAFLD subjects and were negatively correlated with multiple metabolic parameters, including FLI. Mice with NAFLD induced by HFD showed decreased bone mass and lower sclerostin expression in bone and liver tissues. Our study indicated that the liver-lipid-bone interactions may play a key role in the abnormal bone metabolism in NAFLD.

DATA AVAILABILITY STATEMENT

The original contributions presented in the study are included in the article/**Supplementary Material**. Further inquiries can be directed to the corresponding author.

ETHICS STATEMENT

The studies involving human participants were reviewed and approved by the Ethics Committee of the West China Hospital.

REFERENCES

- Li AA, Ahmed A, Kim D. Extrahepatic Manifestations of Nonalcoholic Fatty Liver Disease. *Gut Liver* (2020) 14(2):168–78. doi: 10.5009/gnl19069
- Selvakumar PKC, Kabbany MN, Nobili V, Alkhoury N. Nonalcoholic Fatty Liver Disease in Children: Hepatic and Extrahepatic Complications. *Pediatr Clin North Am* (2017) 64(3):659–75. doi: 10.1016/j.pcl.2017.01.008
- Polyzos SA, Anastasilakis AD, Kountouras J, Makras P, Papatheodorou A, Kokkoris P, et al. Circulating Sclerostin and Dickkopf-1 Levels in Patients With Nonalcoholic Fatty Liver Disease. *J Bone Miner Metab* (2016) 34(4):447–56. doi: 10.1007/s00774-015-0687-x
- Armstrong MJ, Adams LA, Canbay A, Syn WK. Extrahepatic Complications of Nonalcoholic Fatty Liver Disease. *Hepatology* (2014) 59(3):1174–97. doi: 10.1002/hep.26717
- Yilmaz Y. Review Article: Non-Alcoholic Fatty Liver Disease and Osteoporosis—Clinical and Molecular Crosstalk. *Aliment Pharmacol Ther* (2012) 36(4):345–52. doi: 10.1111/j.1365-2036.2012.05196.x
- Pardee PE, Dunn W, Schwimmer JB. Non-Alcoholic Fatty Liver Disease is Associated With Low Bone Mineral Density in Obese Children. *Aliment Pharmacol Ther* (2012) 35(2):248–54. doi: 10.1111/j.1365-2036.2011.04924.x
- Lee SH, Yun JM, Kim SH, Seo YG, Min H, Chung E, et al. Association Between Bone Mineral Density and Nonalcoholic Fatty Liver Disease in

The patients/participants provided their written informed consent to participate in this study. The animal study was reviewed and approved by the Ethics Committee of the West China Hospital.

AUTHOR CONTRIBUTIONS

FZ and XC designed research, collected data, and wrote the manuscript. YW, YL, MT, and SW performed animal study and collected clinical data. HT designed the study and revised paper. All authors contributed to the article and approved the submitted version.

FUNDING

The study was supported by West China Hospital, Sichuan University (Grant Nos. ZYGD18022 and 2020HXBH028 to FZ), China Postdoctoral Science Foundation (Grant No. 2020M670060ZX to FZ) and West China Hospital, Sichuan University (Grant No 2018HXFH009 to FZ). This work was also supported by the 1.3.5 project for disciplines of excellence, West China Hospital, Sichuan University (No. ZYGD18022 to HT).

SUPPLEMENTARY MATERIAL

The Supplementary Material for this article can be found online at: <https://www.frontiersin.org/articles/10.3389/fendo.2021.707505/full#supplementary-material>

Supplementary Figure 1 | Comparison of circulating sclerostin levels between male and female. (A) Controls. (B) NAFLD subjects.

- Korean Adults. *J Endocrinol Invest* (2016) 39(11):1329–36. doi: 10.1007/s40618-016-0528-3
- Yang HJ, Shim SG, Ma BO, Kwak JY. Association of Nonalcoholic Fatty Liver Disease With Bone Mineral Density and Serum Osteocalcin Levels in Korean Men. *Eur J Gastroenterol Hepatol* (2016) 28(3):338–44. doi: 10.1097/MEG.0000000000000535
- Ahn SH, Seo DH, Kim SH, Nam MS, Hong S. The Relationship Between Fatty Liver Index and Bone Mineral Density in Koreans: KNHANES 2010–2011. *Osteoporos Int* (2018) 29(1):181–90. doi: 10.1007/s00198-017-4257-z
- Upala S, Sanguankeo A, Jaruvongvanich V. Association Between Nonalcoholic Fatty Liver Disease and Bone Mineral Density: A Systematic Review and Meta-Analysis. *J Endocrinol Invest* (2015) 38(8):931–2. doi: 10.1007/s40618-015-0342-3
- Mantovani A, Gatti D, Zoppini G, Lippi G, Bonora E, Byrne CD, et al. Association Between Nonalcoholic Fatty Liver Disease and Reduced Bone Mineral Density in Children: A Meta-Analysis. *Hepatology* (2019) 70(3):812–23. doi: 10.1002/hep.30538
- Szulc P, Boutroy S, Vilaythiou N, Schoppet M, Rauner M, Chapurlat R, et al. Correlates of Bone Microarchitectural Parameters and Serum Sclerostin Levels in Men: The STRAMBO Study. *J Bone Miner Res* (2013) 28(8):1760–70. doi: 10.1002/jbmr.1888

13. Thorson S, Prasad T, Sheu Y, Danielson ME, Arasu A, Cummings SR, et al. Sclerostin and Bone Strength in Women in Their 10th Decade of Life. *J Bone Miner Res* (2013) 28(9):2008–16. doi: 10.1002/jbmr.1929
14. Polyzos SA, Anastasilakis AD, Bratengeier C, Woloszczuk W, Papatheodorou A, Terpos E. Serum Sclerostin Levels Positively Correlate With Lumbar Spinal Bone Mineral Density in Postmenopausal Women—The Six-Month Effect of Risedronate and Teriparatide. *Osteoporos Int* (2012) 23(3):1171–6. doi: 10.1007/s00198-010-1525-6
15. Daniele G, Winnier D, Mari A, Bruder J, Fourcaudot M, Pengou Z, et al. Sclerostin and Insulin Resistance in Prediabetes: Evidence of a Cross Talk Between Bone and Glucose Metabolism. *Diabetes Care* (2015) 38(8):1509–17. doi: 10.2337/dc14-2989
16. Napoli N, Strollo R, Defeudis G, Leto G, Moretti C, Zampetti S, et al. Serum Sclerostin and Bone Turnover in Latent Autoimmune Diabetes in Adults. *J Clin Endocrinol Metab* (2018) 103(5):1921–8. doi: 10.1210/jc.2017-02274
17. Gennari L, Merlotti D, Valenti R, Ceccarelli E, Ruvio M, Pietrini MG, et al. Circulating Sclerostin Levels and Bone Turnover in Type 1 and Type 2 Diabetes. *J Clin Endocrinol Metab* (2012) 97(5):1737–44. doi: 10.1210/jc.2011-2958
18. Bedogni G, Bellentani S, Miglioli L, Masutti F, Passalacqua M, Castiglione A, et al. The Fatty Liver Index: A Simple and Accurate Predictor of Hepatic Steatosis in the General Population. *BMC Gastroenterol* (2006) 6:33. doi: 10.1186/1471-230X-6-33
19. Chen X, Wang C, Zhang K, Xie Y, Ji X, Huang H, et al. Reduced Femoral Bone Mass in Both Diet-Induced and Genetic Hyperlipidemia Mice. *Bone* (2016) 93:104–12. doi: 10.1016/j.bone.2016.09.016
20. Weivoda MM, Youssef SJ, Oursler MJ. Sclerostin Expression and Functions Beyond the Osteocyte. *Bone* (2017) 96:45–50. doi: 10.1016/j.bone.2016.11.024
21. Brunkow ME, Gardner JC, Van Ness J, Paeper BW, Kovacevich BR, Proll S, et al. Bone Dysplasia Sclerosteosis Results From Loss of the SOST Gene Product, A Novel Cystine Knot-Containing Protein. *Am J Hum Genet* (2001) 68(3):577–89. doi: 10.1086/318811
22. Guerriere KI, Hughes JM, Gaffney-Stomberg E, Staab JS, Matheny RW Jr. Circulating Sclerostin Is Not Suppressed Following a Single Bout of Exercise in Young Men. *Physiol Rep* (2018) 6(10):e13695. doi: 10.14814/phy2.13695
23. Filip R, Radzki RP, Bienko M. Novel Insights Into the Relationship Between Nonalcoholic Fatty Liver Disease and Osteoporosis. *Clin Interv Aging* (2018) 13:1879–91. doi: 10.2147/CIA.S170533
24. Garnero P, Sornay-Rendu E, Munoz F, Borel O, Chapurlat RD. Association of Serum Sclerostin With Bone Mineral Density, Bone Turnover, Steroid and Parathyroid Hormones, and Fracture Risk in Postmenopausal Women: The OFELY Study. *Osteoporos Int* (2013) 24(2):489–94. doi: 10.1007/s00198-012-1978-x
25. Fairfield H, Rosen CJ, Reagan MR. Connecting Bone and Fat: The Potential Role for Sclerostin. *Curr Mol Biol Rep* (2017) 3(2):114–21. doi: 10.1007/s40610-017-0057-7
26. Ukita M, Yamaguchi T, Ohata N, Tamura M. Sclerostin Enhances Adipocyte Differentiation in 3T3-L1 Cells. *J Cell Biochem* (2016) 117(6):1419–28. doi: 10.1002/jcb.25432
27. Mantovani A, Sani E, Fassio A, Colecchia A, Viapiana O, Gatti D, et al. Association Between Non-Alcoholic Fatty Liver Disease and Bone Turnover Biomarkers in Post-Menopausal Women With Type 2 Diabetes. *Diabetes Metab* (2019) 45(4):347–55. doi: 10.1016/j.diabet.2018.10.001

Conflict of Interest: The authors declare that the research was conducted in the absence of any commercial or financial relationships that could be construed as a potential conflict of interest.

Publisher's Note: All claims expressed in this article are solely those of the authors and do not necessarily represent those of their affiliated organizations, or those of the publisher, the editors and the reviewers. Any product that may be evaluated in this article, or claim that may be made by its manufacturer, is not guaranteed or endorsed by the publisher.

Copyright © 2021 Zhou, Wang, Li, Tang, Wan, Tian and Chen. This is an open-access article distributed under the terms of the Creative Commons Attribution License (CC BY). The use, distribution or reproduction in other forums is permitted, provided the original author(s) and the copyright owner(s) are credited and that the original publication in this journal is cited, in accordance with accepted academic practice. No use, distribution or reproduction is permitted which does not comply with these terms.



The Associations of Serum Osteocalcin and Cortisol Levels With the Psychological Performance in Primary Hyperparathyroidism Patients

Shu-min Wang, Yang He, Min-ting Zhu, Bei Tao, Hong-yan Zhao, Li-hao Sun* and Jian-min Liu*

Department of Endocrine and Metabolic Diseases, Rui-jin Hospital, Shanghai Institute of Endocrine and Metabolic Diseases, Shanghai Clinical Center for Endocrine and Metabolic Diseases, Shanghai Jiao Tong University School of Medicine, Shanghai, China

OPEN ACCESS

Edited by:

Lilian Irene Plotkin,
Indiana University Bloomington,
United States

Reviewed by:

Ziyue Liu,
Purdue University Indianapolis,
United States
Ehab Shiban,
Augsburg University Hospital,
Germany

*Correspondence:

Li-hao Sun
leoslh@163.com
Jian-min Liu
ljm10586@rjh.com.cn

Specialty section:

This article was submitted
to Bone Research,
a section of the journal
Frontiers in Endocrinology

Received: 09 April 2021

Accepted: 19 July 2021

Published: 12 August 2021

Citation:

Wang S-M, He Y, Zhu M-T, Tao B, Zhao H-Y, Sun L-H and Liu J-M (2021) The Associations of Serum Osteocalcin and Cortisol Levels With the Psychological Performance in Primary Hyperparathyroidism Patients. *Front. Endocrinol.* 12:692722. doi: 10.3389/fendo.2021.692722

Objectives: The aim of this study was to investigate factors responsible for the psychological performance in primary hyperparathyroidism (PHPT) patients.

Methods: A group of 38 PHPT patients receiving questionnaires, including Beck Depression Inventory (BDI), State-Trait Anxiety Inventory (STAI), and 36-Item Short Form Survey (SF-36), was evaluated. The relationships between scores of questionnaires and clinical biomarkers were examined. Collinearity and linear regression model were applied to examine variables determining the scores of the questionnaire. In 192 PHPT patients, bivariate and partial correlation were used to analyze the relationships between serum concentrations of parathyroid hormone (PTH), calcium, osteocalcin (OCN), and cortisol.

Results: Among 38 patients receiving questionnaire tests, 50% (19/38) of the patients developed state anxiety, 60.5% (23/38) of the patients had the trait of developing anxiety. In addition, 18.4% (7/38) of the patients developed mild to severe depression. Serum cortisol at 8:00 was negatively and significantly correlated with social function ($r = -0.389$, $p = 0.041$) after controlling for age, sex, disease duration, serum PTH, calcium, phosphorus, and 25-hydroxyvitamin D [25(OH)D] concentration. OCN was significantly and negatively correlated with score of STAI-S ($r = -0.426$, $p = 0.027$). In the linear regression model for BDI score, variables with statistical significance were serum OCN ($\beta = -0.422$, $p = 0.019$) and cortisol at 0:00 ($\beta = 0.371$, $p = 0.037$). In 192 PHPT patients, the serum concentration of OCN ($r = 0.373$, $p = 0.000$) was positively correlated with PTH level. After controlling for age, sex, disease duration, serum 25(OH)D, phosphorus, and calcium concentration, the positive correlation between OCN and PTH was still statistically significant ($r = 0.323$, $p = 0.000$). The serum concentration of cortisol at 0:00 was significantly and positively correlated with serum calcium ($r = 0.246$, $p = 0.001$) in bivariate correlation analysis. After controlling for age, sex, disease duration, serum PTH, 25(OH)D,

and phosphorus concentration, serum cortisol at 0:00 was still positively and significantly correlated with serum calcium ($r = 0.245$, $p = 0.001$).

Conclusion: Serum levels of OCN and cortisol, rather than PTH and calcium, are associated with the development of anxiety and depression symptoms in PHPT patients.

Keywords: depression, anxiety, primary hyperparathyroidism, cortisol, osteocalcin

INTRODUCTION

Primary hyperparathyroidism (PHPT) is a disorder of parathyroid hormone (PTH) hypersecretion by parathyroid gland(s) in patients with normal renal function, resulting in increased serum calcium concentration (1). While most patients today are “asymptomatic”, lacking the classical skeletal and renal manifestations of PHPT, nonspecific neuropsychological symptoms are also investigated (2–5). Several studies suggested that PHPT was associated with impaired quality of life (QoL), anxiety, and depression as evaluated by questionnaires (6–8). Although these symptoms are concerning, there is a debate upon whether these symptoms are directly and specifically attributable to PHPT (7). There were mainly two facts contributing to this argument. For one thing, there is no consistent difference in the psychological performance between PHPT patients and control counterparts (7–9). For the other, the reversible role of parathyroidectomy on these psychologic features was not fully recognized (1, 9–11). Therefore, at the Third International Workshop on Asymptomatic Primary Hyperparathyroidism (12), studies on the psychological and cognitive features of PHPT were reviewed and were not considered to be an indication for parathyroidectomy (13). As for the primary exploration for factors of PHPT neuropsychological manifestations, studies were mainly concentrated on the relationship between psychological performance and PTH or calcium. However, neither the increased PTH nor calcium concentration was definitely reported to be the direct cause (1, 7).

In fact, a number of hypotheses have been proposed with regard to the mechanism of depression and anxiety development. “Hypothalamus pituitary adrenal (HPA) axis disorder” hypothesis (14) was a classic and widely accepted hypothesis for the pathophysiology of anxiety and depression. Glucocorticoids exerted damaging effects on psychological function. Mouse experiments showed that high-dose glucocorticoid reduced the neurogenesis of the hippocampus and olfactory bulb that were related to depression and anxiety behaviors (15–17). For humans, Cushing’s syndrome (CS) was a pathological model of hypercortisolemia. The psychiatric feature of hypercortisolism is a well-recognized manifestation of CS, as described decades ago (18). In a study by Kelly et al. (19), including 209 patients with active CS of all ages, depression was present in 57% of the patients, while anxiety was diagnosed in 12% of the patients. In addition to cortisol, recently, the beneficial effects of osteocalcin (OCN), a bone-derived protein, on improving neurological performance were reported, such as

cognition impairment (20, 21), neuromotor dysfunction (22), and anxiety and depression (21, 23). However, the changes of cortisol and OCN concentration in PHPT, especially their relationships with psychological features in PHPT patients, have not been investigated.

In this study, both serum cortisol and OCN concentration changes and the correlation of psychological features with serum OCN and cortisol were analyzed in a group of PHPT patients.

MATERIALS AND METHODS

Patients

In this study, psychological questionnaires, which were not a mandatory requirement for every patient in our department, were tested from August 2020. Until December 2020, questionnaire information in 38 out of 52 patients in this period was obtained. The inclusion criteria included: i) elevated serum calcium level with inappropriately high serum PTH level and ii) with a complete record of serum PTH, OCN, and cortisol concentration. The exclusion criteria included: i) secondary and tertiary hyperparathyroidism, ii) multiple endocrine neoplasms, iii) malignancy, iv) chronic kidney disease (CKD) stages 4 and 5 or $eGFR \leq 30$ ml/min, v) a history of head trauma or stroke, and vi) medications with glucocorticoid. In order to find out whether serum concentration of OCN and cortisol changed as PTH and calcium increased in PHPT patients, a total of 192 PHPT patients admitted to our department from January 2011 to December 2020, including the above 38 patients, were retrospectively evaluated, who met the above inclusion and none of the exclusion criteria. All the patients were managed by the standard protocol developed by our department. Due to the retrospective nature of this study, the written informed consent was waived, which was approved by the ethics committee of our hospital (2017-201).

Clinical Features

The age of onset was recorded according to the first identification of symptoms related to PHPT (bone pain, nephrolithiasis, pathological fractures, polydipsia and polyuria, digestive symptoms, neuropsychiatric manifestations, etc.) or an elevation in serum calcium or PTH concentrations. The anthropometric information was also collected, including sex, age at the time of diagnosis, and body mass index (BMI).

Biochemical Markers and Bone Mineral Density Measurements

Blood samples were collected in the morning after 10 h of fasting. Fasting serum albumin, calcium, phosphorus, and creatinine levels were measured using an automatic biochemical analyzer (Beckman Coulter, DXH 800, USA). Serum level of PTH was measured by intact immunoradiometric assay (ARCHITECT i2000sr, Abbott, Chicago, IL). Serum level of 25-hydroxyvitamin D [25(OH)D] was measured by electrochemiluminescence immunoassay (Roche Diagnostics, Indianapolis, IN, USA). Serum level of OCN was assayed by two methods: radioimmunoassay (Gamma radioimmunoassay counter GC-911, ZONKIA, China) and electrochemiluminescence (Cobas, E601, Roche) during different periods. Serum concentrations of Type I procollagen amino-terminal peptide (PINP) and Collagen I telopeptide- β (β -CTX) were examined through electrochemiluminescence method (Cobas, E601, Roche). Serum concentrations of cortisol (collected at 8:00, 16:00, and 0:00) and 24-h urinary cortisol were assayed by chemical luminescence assay (Beckman Coulter Corp., Brea, CA, USA). Plasma adrenocorticotrophic hormone (ACTH) level was tested by chemical luminescence assay (Mindray CL-600i, China). Area bone mineral densities (aBMDs) at the lumbar spines L1–L4 were measured by dual-energy X-ray absorptiometer (DXA, Lunar Prodigy; GE Medical Systems).

Psychological Testing in Primary Hyperparathyroidism Patients

Testing was conducted preoperatively by a doctor who was not blinded to disease state, lasting approximately 0.5 h for each. Psychological tests included State–Trait Anxiety Inventory (STAI) (24), Beck Depression Inventory (BDI) (25), and 36-Item Short Form Survey (SF-36) (9). In our study, only mental components (MCs) of SF-36 were analyzed, including social function (SF), role of emotion (RE), mental health (MH), and vitality (VI).

The STAI (24) measures anxiety and consists of two 20-item scales measuring trait anxiety (anxiety proneness) and state anxiety (a current emotional condition), with higher scores suggesting more obvious anxiety or more traits developing anxiety. As a reference, mean raw values (\pm SD) for working adults aged 50–69 years are 32.2 ± 8.7 for state anxiety and 31.8 ± 7.8 for trait anxiety. For BDI (25), higher scores indicate more symptoms: 0–13 indicates no or minimal depression; 14–19, mild depression; 20–28, moderate depression; and 29–63, severe depression. For items in SF-36 (9), a higher score indicates a better QoL; for mental components of SF-36, a higher score suggests better psychological performance.

Statistical Analysis

For results in this study, continuous variables were expressed as means \pm SD or median (minimum, maximum) according to their distributions. Categorical variables were summarized as group number/total number. The comparisons of continuous variables between groups were performed using t-test or one-way ANOVA for normally distributed variables; otherwise, nonparametric test. Categorical data were compared by

chi-square test. As serum concentration of OCN was tested by two different kinds of methods, OCN was transformed into categorical variables according to its tertile values. Pearson correlation analysis (two-tailed) was used to investigate the relationship of PTH, calcium with cortisol, as well as the association between the serum PTH, calcium, OCN, cortisol levels, and parameters of questionnaires. Kendall's tau-b was used to test the correlation between OCN and PTH or calcium, which were also transformed into categorical variables here. Partial correlation analysis (two-tailed) was used to examine the above associations when controlling for clinical features and biomedical markers. Linear regression analysis with backward mode was applied to examine determining variables of questionnaire score. In this part, age; sex; disease duration; serum PTH; calcium; phosphorus; 25(OH)D; OCN; cortisol of 8:00, 16:00, 0:00; and 24-h urinary free cortisol were considered. To get stable results, collinearity analysis was used to eliminate collinear variables in each questionnaire regression model. The cutoff value of the variance decomposition proportion for the diagnosis of multicollinearity is set to 0.3 in dimensions with condition index over 10 according to the work of Liao (26) and Kim (27). After screening, all the variance inflation factors became less than 2, indicating that no multicollinearity existed (26, 27). All statistical calculations were performed using the SPSS (version 23.0; IBM statistics). A p-value <0.05 was considered statistically significant.

RESULTS

Higher Serum Cortisol Concentration and Lower Serum Osteocalcin Level Were Correlated With Worse Psychological Manifestation in Primary Hyperparathyroidism Patients

Since only 38 out of 52 patients received psychological evaluation, including BDI, STAI, and SF-36 questionnaire during August 2020 to December 2020, a sensitivity analysis was performed between patients who had taken the tests and those who had not. As shown in the **Supplementary Table**, there were no between-group differences in age, sex, disease duration, body weight, height, BMI, systolic blood pressure (SBP), heart rate, BMD (L1–L4), serum concentrations of PTH, 25(OH)D, β -CTX, albumin, hemoglobin, HbA1c, and phosphorus (all $p > 0.05$). Serum calcium concentration ($p = 0.006$) was higher in patients receiving questionnaires. However, serum and urine cortisol concentrations had no statistical difference between the two groups ($p > 0.05$).

For PHPT patients receiving questionnaire tests, the SF-36 MC items' scores were 74.04 ± 23.32 for SF, 72.74 ± 18.71 for MH, 57.76 ± 22.17 for VI, and 66.67 (0,100) for RE, respectively. The score of STAI-S was 35.43 ± 11.56 , STAI-T 37.39 ± 10.34 , and BDI was 5 (0,46). According to the reference (24), out of the 38 patients receiving questionnaires, 50% of the patients (19/38) with a STAI-S score over 32.2 were in a state of anxiety; 60.5% of the patients (23/38) with the score of STAI-T over 31.8 have the trait of

developing anxiety; 44.74% of the patients (17/38) had both STAI-S over 32.2 and STAI-T over 31.8. As for BDI score (25), 18.4% patients (7/38) developed mild to severe depression. Here, 15.9% of the patients (6/38) developed both anxiety (STAI-S and STAI-T were higher than the reference) and depression.

In addition, we assessed associations of PTH, calcium, OCN, and cortisol concentrations with psychological performance, as evaluated by questionnaires. As shown in **Table 1**, in bivariate model, cortisol concentration at 8:00 was significantly and negatively correlated with SF ($r = -0.393$, $p = 0.015$), one feature of psychological health evaluation. Serum OCN concentration was significantly and negatively correlated with BDI ($r = -0.345$, $p = 0.0378$). Serum concentration of PTH and calcium was not correlated with any of the scores in the questionnaires ($p > 0.05$). After controlling for age, sex, and disease duration, serum concentration of cortisol at 8:00 was still significantly and negatively correlated with SF ($r = -0.391$, $p = 0.020$). When serum PTH, 25(OH)D, phosphorus, and calcium were further adjusted, the correlation of cortisol at 8:00 with the score of SF ($r = -0.389$, $p = 0.041$) was still significantly negative; the negative correlation of serum OCN concentration and STAI-S ($r = -0.426$, $p = 0.027$) was statistically significant.

OCN and Cortisol Levels Were the Determinants of Psychological Performance in Patients With Primary Hyperparathyroidism

As for the linear regression model of the BDI score, statistically significant variables were serum OCN ($\beta = -0.422$, $p = 0.019$) and cortisol at 0:00 ($\beta = 0.371$, $p = 0.037$), while variables excluded by collinearity analysis included age, serum PTH, 25(OH)D, calcium, cortisol at 8:00, and urinary free cortisol in 24 h. No significant variable was included in the equations of other questionnaires.

Serum Cortisol and Osteocalcin Were Positively Correlated With Serum Calcium and Parathyroid Hormone Concentration in Primary Hyperparathyroidism Patients

In these 38 patients, we found that OCN was associated with PTH ($r = 0.351$, $p = 0.031$) and marginally associated with calcium ($r = 0.304$, $p = 0.067$), while cortisol was not related with these two parameters. In order to further test whether these findings could be replicated in a larger sample size, we further explored the relationships among OCN, cortisol, PTH, and calcium in 192 PHPT patients.

The baseline characteristics of 192 PHPT patients in different PTH tertile groups were shown in **Table 2**. The mean age of the cohort was 52.7 ± 13.8 years, with 76.6% (147/192) females. In terms of bone biochemical markers, it was found that, as the serum PTH concentration increased, the serum concentration of calcium ($p = 0.000$), PINP ($p = 0.000$), and β -CTX ($p = 0.028$) increased and phosphorus decreased ($p = 0.000$) significantly. Also, with the increase of PTH concentration, the percentage of patients with upper tertile of OCN concentration increased ($p = 0.000$), while both the serum 25(OH)D concentration

TABLE 1 | Correlation between scores of questionnaires and biomarkers in PHPT patients.

	SF		RE		MH		VI		STAI-S		STAI-T		BDI	
	r	p	r	p	r	p	r	p	r	p	r	p	r	p
Model 1														
PTH	0.071	0.674	-0.175	0.0293	0.172	0.0303	0.156	0.0349	-0.148	0.0383	-0.168	0.0328	-0.166	0.0327
Calcium	-0.120	0.480	0.066	0.698	0.033	0.844	0.063	0.710	-0.060	0.726	0.049	0.782	0.027	0.874
Cortisol at 8:00	-0.393	0.015*	-0.159	0.341	-0.195	0.241	0.042	0.804	0.092	0.587	0.172	0.316	0.123	0.467
OCN	0.131	0.432	-0.012	0.942	0.298	0.069	0.240	0.147	-0.323	0.051	-0.250	0.141	-0.345	0.037*
Model 2														
Cortisol at 8:00	-0.391	0.020*	-0.136	0.436	-0.123	0.480	0.110	0.530	0.047	0.791	0.115	0.523	0.084	0.636
OCN	0.114	0.513	-0.046	0.795	0.308	0.072*	0.244	0.157	-0.334	0.053	-0.263	0.139	-0.326	0.060
Model 3														
Cortisol at 8:00	-0.389	0.041*	-0.072	0.716	-0.129	0.512	0.144	0.466	0.044	0.827	0.127	0.538	0.058	0.773
OCN	0.102	0.606	0.00	0.999	0.370	0.052	0.248	0.203	-0.426	0.027*	-0.363	0.069	-0.337	0.086

Model 1: bivariate correlation.

Model 2: controlling for age, sex, disease duration.

Model 3: controlling for age, sex, disease duration, PTH, calcium, phosphorus, and 25-hydroxyvitamin D [25(OH)D].

* $p < 0.05$.

SF, social function; RE, role of emotion; MH, mental health; VI, vitality; STAI-S/T, State-Trait Anxiety Inventory-State/Trait; BDI, Beck Depression Inventory; PHPT, primary hyperparathyroidism.

TABLE 2 | Baseline characteristics of PHPT patients in different PTH tertile groups.

	Total	Tertile 1 (pg/ml) <167.50	Tertile 2 (pg/ml) 167.50–318.90	Tertile 3 (pg/ml) >318.90	p-value
Sex (female/total, %)	147/192, 76.6	54/64, 84.4	48/64, 75	45/64, 71.9	–
Age (years old)	52.7 ± 13.8	54.9 ± 12.2	51.2 ± 13.5	52.1 ± 15.5	0.286
Disease duration (months)	12 (0.25, 360)	16.5 (0.5, 240)	13.0 (0.25, 360)	12 (0.25, 360)	0.592
Weight (kg)	61.22 ± 10.81	61.57 ± 10.26	61.86 ± 11.34	60.29 ± 10.96	0.702
Height (cm)	162.56 ± 7.45	162.43 ± 6.064	162.36 ± 7.68	162.89 ± 8.10	0.916
BMI (kg/m ²)	23.01 ± 3.06	23.15 ± 3.07	23.43 ± 3.14	22.41 ± 2.92	0.213
SBP (mmHg)	128.52 ± 16.98	129.77 ± 20.52	126.84 ± 14.84	128.91 ± 15.40	0.613
HR (bpm)	75.12 ± 11.75	75.41 ± 9.92	74.20 ± 12.03	75.73 ± 13.27	0.760
Serum 25(OH)D (nmol/L)	35.13 ± 16.02	42.22 ± 16.07	33.67 ± 15.42	24.49 ± 14.02	0.000***
Serum PINP (ng/ml)	84.59 (17.96, 1,200)	69.11 (20.54, 207.90)	80.59 (17.96, 262.30)	151.80 (28.42, 1,200.0)	0.000***
Serum β-CTX (ng/ml)	0.84 (0.09, 4.06)	0.72 (0.28, 2.11)	1.01 (0.09, 2.80)	0.945 (0.14, 4.06)	0.028*
Serum OCN (upper tertile/total, %)	63/192, 32.8	7/64, 10.9	17/64, 26.6	39/64, 60.9	0.000***
Serum calcium (mmol/L)	2.74 ± 0.25	2.60 ± 0.17	2.72 ± 0.22	2.89 ± 0.27	0.000***
Serum phosphorus (mmol/L)	0.85 (0.44, 10.50)	0.97 (0.59, 1.27)	0.85 (0.54, 10.50)	0.76 (0.44, 1.20)	0.000***
BMD (L1~L4) (g/cm ²)	0.957 ± 0.189	1.012 ± 0.162	0.992 ± 0.197	0.863 ± 0.173	0.000***
Albumin (g/L)	39.61 ± 3.58	39.78 ± 3.30	39.74 ± 3.60	39.31 ± 3.83	0.719
Serum creatinine (μmol/L)	65.52 ± 22.79	63.52 ± 16.48	65.57 ± 18.64	68.45 ± 30.59	0.445
Serum hemoglobin (g/L)	127.57 ± 20.14	129.23 ± 16.91	128.51 ± 21.15	125.03 ± 22.03	0.462
HbA1c (%)	5.55 ± 1.09	5.58 ± 0.65	5.39 ± 0.66	5.68 ± 1.66	0.338
Serum cortisol 8:00 (μg/dl)	11.28 ± 4.09	10.74 ± 3.32	11.05 ± 3.68	12.03 ± 5.02	0.175
Serum cortisol 16:00 (μg/dl)	5.28 (1.77, 21.19)	5.11 (2.19, 19.21)	5.02 (2.00, 15.76)	5.40 (1.77, 21.19)	0.859
Serum cortisol 0:00 (μg/dl)	2.65 (0.54, 18.84)	2.47 (0.54, 14.85)	2.46 (0.76, 18.12)	3.34 (0.96, 18.84)	0.021*
Urine cortisol (μg/24 h)	71.34 (1.90, 407.55)	70.00 (28.0, 144.96)	71.03 (3.31, 269.83)	73.16 (1.90, 407.55)	0.797
Serum ACTH (pg/ml)	25.83 (4.41, 105.92)	25.36 (4.41, 70.49)	26.20 (0.92, 105.92)	25.62 (6.4, 91.67)	0.681

BMI, body mass index; SBP, systolic blood pressure; HR, heart rate; 25(OH)D, 25-hydroxyvitamin D; PINP, Type I procollagen amino-terminal peptide; CTX-β, collagen I telopeptide-β; OCN, osteocalcin; BMD (L1~L4), bone mineral density (lumbar 1~4); HbA1c, glycosylated hemoglobin; ACTH, adrenocorticotrophic hormone; PHPT, primary hyperparathyroidism.

* $p < 0.05$, *** $p < 0.0001$.

($p = 0.000$) and BMD (L1~L4) level ($p = 0.000$) declined significantly. As for cortisol, the serum cortisol at 0:00 ($p = 0.021$) was significantly elevated with the increase of PTH concentration. As serum PTH concentration increased, no difference in serum ACTH, cortisol concentration at 8:00 and 16:00, and urinary cortisol excretion in 24 h was observed ($p > 0.05$).

When patients were grouped according to tertiles of serum calcium concentration, as shown in **Table 3**, with the increase of serum calcium concentration, serum PTH ($p = 0.000$), PINP ($p = 0.000$), β-CTX ($p = 0.001$), and the percentage of patients with upper tertile of OCN concentration ($p = 0.000$) increased significantly, while serum phosphorus concentration ($p = 0.002$) and BMD (L1~L4) ($p = 0.000$) decreased significantly. Serum concentration of 25(OH)D was significantly ($p = 0.000$) different between calcium tertile groups. However, the differences in body weight, height, and BMI were not statistically significant. It was again shown that with the increase of calcium concentration, serum cortisol concentration at 8:00, 16:00, and 0:00 and urinary cortisol excretion did not show a statistically significant difference ($p > 0.05$).

In addition, in the bivariate correlation model between serum PTH concentration and OCN, cortisol concentration showed that serum PTH was positively and significantly correlated with serum OCN ($r = 0.373$, $p = 0.000$). When controlling for age, sex, and disease duration, and additionally with phosphorus, calcium, and 25(OH)D, PTH was still positively and significantly correlated with serum OCN concentration ($r = 0.323$, $p = 0.000$).

However, serum PTH concentration was not significantly correlated with serum cortisol of different time points and urinary cortisol excretion ($p > 0.05$) in the bivariate and partial correlation model.

As to serum calcium level, it was positively and significantly correlated with serum OCN ($r = 0.240$, $p = 0.000$) and cortisol concentration at 0:00 ($r = 0.246$, $p = 0.001$). When controlling for age, sex, and duration, the correlation of serum calcium with OCN ($r = 0.248$, $p = 0.001$) and cortisol at 0:00 ($r = 0.249$, $p = 0.001$) was still significantly positive. When serum 25(OH)D and phosphorus were adjusted, serum calcium was still significantly and positively correlated with serum cortisol at 0:00 ($r = 0.251$, $p = 0.001$) and OCN ($r = 0.222$, $p = 0.003$). Even when serum PTH was further adjusted, the correlation between serum calcium and cortisol at 0:00 was still significantly positive ($r = 0.245$, $p = 0.001$), while the correlation between serum calcium and OCN ($r = 0.110$, $p = 0.143$) lost its significance.

DISCUSSION

The findings from this study lie in two aspects. Firstly, the balance of serum OCN and cortisol was associated with the psychological performance in PHPT patients. Secondly, with the elevation of serum calcium and PTH, the concentration of serum cortisol and OCN increased.

The effects of glucocorticoid (15–17, 19) and OCN (21, 23, 28) on the depression and anxiety symptoms in patients and related behavioral performance in animals were widely reported.

TABLE 3 | Baseline characteristics of PHPT patients in different calcium tertile groups.

	Total	Tertile 1 (mmol/L) <2.62	Tertile 2 (mmol/L) 2.62–2.81	Tertile 3 (mmol/L) >2.81	p-value
Sex (female/total, %)	147/192, 76.6	52/63, 82.5	47/66, 71.2	45/63, 71.4	–
Age (years old)	52.7 ± 13.8	54.9 ± 12.2	51.2 ± 13.5	52.1 ± 15.5	0.286
Disease duration (months)	12.0 (0.25, 360)	12.0 (0.25, 240)	12.0 (0.33, 180)	12.0 (0.25, 360.0)	0.986
Weight (kg)	61.22 ± 10.81	61.57 ± 10.26	61.86 ± 11.34	60.29 ± 10.96	0.702
Height (cm)	162.56 ± 7.45	162.43 ± 6.64	162.36 ± 7.68	162.89 ± 8.10	0.916
BMI (kg/m ²)	23.01 ± 3.06	23.15 ± 3.07	23.43 ± 3.14	22.41 ± 2.92	0.213
SBP (mmHg)	128.52 ± 16.98	129.77 ± 20.25	126.84 ± 14.84	128.91 ± 15.40	0.613
HR (bpm)	75.12 ± 11.75	75.41 ± 9.92	74.20 ± 12.03	75.73 ± 13.27	0.760
Serum PTH (pg/ml)	220.35 (74.70, 218.10)	149.5 (74.7, 1,939.9)	215.65 (94.30, 2,380.10)	398.2 (88.9, 2,680.1)	0.000***
Serum 25(OH)D (nmol/L)	35.13 ± 16.02	42.22 ± 16.07	33.67 ± 15.42	29.49 ± 14.02	0.000***
Serum PINP (ng/ml)	84.59 (17.96, 1,200)	69.11 (17.96, 418.90)	86.92 (24.09, 479.20)	110.7 (28.95, 1,200)	0.000***
Serum β-CTX (ng/ml)	0.835 (0.09, 4.06)	0.703 (0.11, 1.91)	0.93 (0.24, 1.95)	1.44 (0.09, 4.06)	0.001**
Serum OCN (upper tertile/total, %)	63/192, 32.8	11/63, 17.5	20/66, 30.3	32/63, 50.8	0.000***
Serum phosphorus (mmol/L)	0.85 (0.44, 10.50)	0.94 (0.44, 10.50)	0.85 (0.44, 1.32)	0.79 (0.50, 1.20)	0.002**
BMD (L1–L4) (g/cm ²)	0.957 ± 0.189	1.012 ± 0.162	0.992 ± 0.197	0.863 ± 0.1730	0.000***
Albumin (g/L)	39.61 ± 3.58	39.78 ± 3.30	39.74 ± 3.60	39.31 ± 3.83	0.719
Serum creatinine (μmol/L)	65.52 ± 22.79	63.52 ± 16.48	64.57 ± 18.64	68.45 ± 30.59	0.445
Serum hemoglobin (g/L)	127.57 ± 20.14	129.23 ± 16.91	128.51 ± 21.15	125.03 ± 22.03	0.462
HbA1c (%)	5.55 ± 1.09	5.58 ± 0.65	5.39 ± 0.66	5.68 ± 1.66	0.338
Serum cortisol 8:00 (μg/dl)	11.28 ± 4.09	10.74 ± 3.32	11.05 ± 3.68	12.03 ± 5.02	0.175
Serum cortisol 16:00 (μg/dl)	5.28 (1.77, 21.19)	4.71 (2.19, 19.21)	5.67 (2.00, 12.72)	5.56 (1.77, 21.19)	0.133
Serum cortisol 0:00 (μg/dl)	2.65 (0.54, 18.84)	2.61 (0.54, 14.85)	2.46 (0.91, 12.35)	2.91 (0.99, 18.84)	0.092
Urine cortisol (μg/24h)	71.34 (1.90, 407.55)	71.78 (43.44, 157.92)	71.72 (1.90, 222.14)	70.92 (3.31, 407.55)	0.999
Serum ACTH (pg/ml)	25.83 (4.41, 105.92)	25.48 (7.06, 91.67)	26.23 (4.41, 72.58)	23.82 (10.4, 105.92)	0.419

BMI, body mass index; SBP, systolic blood pressure; HR, heart rate; 25(OH)D, 25-hydroxyvitamin D; PINP, Type I procollagen amino-terminal peptide; CTX-β, collagen I telopeptide-β; OCN, osteocalcin; BMD (L1–L4), bone mineral density (lumbar 1–4); HbA1c, glycosylated hemoglobin; ACTH, adrenocorticotropic hormone; PHPT, primary hyperparathyroidism.

p* < 0.01, *p* < 0.0001.

Thus, changes of cortisol and OCN in PHPT patients and their relationships with scores of questionnaires were investigated in this study. We found that as serum PTH concentration increased, circulating OCN and cortisol levels increased significantly. Besides, through the correlation analysis, we found that cortisol and OCN were negatively and positively related with psychological performance in PHPT patients, respectively, independent of PTH and calcium.

To the best of our knowledge, the balance of cortisol and OCN has not been reported in studies concerning psychological performance in PHPT so far. In our study, we found that OCN and cortisol were two determinants of the psychological performance in PHPT patients, independent of PTH and calcium. Our finding was supported by previous clinical and animal studies. First of all, clinical studies revealed the opposite effects of cortisol and OCN on psychological performance and brain structure that was related to affective disorders. On the one hand, excessive cortisol was related to decreased volume of different brain areas of patients. It was reported that hypercortisolemia in CS leads to shrinkage of amygdala volume (29), an important brain structure involved in emotional response (30) and a target of cortisol hormone with abundant glucocorticoid receptors (31). It was also reported that amygdala volume was negatively and significantly correlated with scores of STAI-S and BDI in CS (29). Other findings in active CS patients revealed smaller volumes in comparison to healthy controls in gray matter of the medial frontal gyrus (32), cerebellar cortex, and gray matter volumes (33), which was observed in depression models (34). Besides, higher serum

cortisol at bedtime could reflect a flatter diurnal slope (35, 36), which was associated with an impaired psychological manifestation (37). In this study, we found that a flatter diurnal slope reflected by higher serum cortisol concentration at 0:00 was associated with worse psychological performance in PHPT patients. On the other hand, a recent study (38) revealed that OCN concentration was lower in depressive patients than that in healthy controls. In obese and control human subjects, lower serum levels of OCN were associated with lower cognitive performance together with cognitive and depressive brain microstructural changes, and serum OCN independently explained 10% of the variation in cognitive performance (28). The correlation between the decrease of OCN concentration and cognition impairment has also been noted in older adults (39). Secondly, experimental studies uncovered molecular mechanisms of harmful and protective effects of glucocorticoid and OCN for psychological features, respectively. Glucocorticoid was reported to be increased in depression and anxiety mice and was revealed to increase the hippocampus apoptosis *in vivo* and *in vitro* (40). In contrast, OCN was demonstrated to exhibit neuron-protective effects on dopaminergic neuron in a Parkinson's disease mouse model through regulating gut microbiota in our most recent study (41). It was also reported (40) that glucocorticoid elevation leads to decreased expression of brain-derived neurotrophic factor (BDNF) in depressive mouse hippocampus and in PC12 cells, while OCN exerted a protective effect for depression and anxiety by increasing BDNF expression through activation of cAMP/PKA signaling in mice (21). Thus, the above studies suggested that opposite to

glucocorticoid, OCN might exert protective effects on depression and anxiety in patients and mice. The net effect of this balance may explain the inconsistent findings regarding the psychological performance in PHPT from different studies (7–9). Also, since there is no report on changes of these parameters before and after surgery in PHPT patients, it is thus interesting to investigate whether its dynamic changes are related to the psychological performance in PHPT patients after parathyroidectomy (1, 9, 10).

It is noteworthy that in our multivariate correlation analysis, serum calcium rather than PTH was independently and positively correlated with cortisol concentration in PHPT patients. From a clinical perspective, Espiritu et al. (41) reported that PHPT patients with serum calcium over 2.47 mmol/L had more symptoms of depression than patients with lower calcium. Weber et al. (42) also found that serum calcium rather than PTH was related to depression. These observations were in line with our results that higher calcium was independently related to higher serum cortisol level, which was associated with more depression symptoms, as evidenced by SF score. From the perspective of mouse studies, serum calcium can stimulate the secretion of adrenal hormones, while PTH just acts like a calcium ionophore (43). To some extent, this finding could partly explain why no difference in depression and cognitive indices was reported in mild hypercalcemic and normocalcemic PHPT patients (7).

However, Bargren et al. (44) found that patients with milder hypercalcemia had more depression, suggesting that hypercalcemia might not mediate these symptoms. In our study, it was demonstrated that with the elevation of serum calcium level, both serum cortisol and OCN increased, thus it is of interest to investigate whether the findings from Bargren et al. (44) could be explained by the balance of cortisol and OCN. In addition, in the other study of Kearns et al. (11), baseline PTH level, but not calcium, was found to have a weak relationship with change in depressive symptoms after parathyroid surgery. This result seemed to contradict with our findings. In our study, both OCN and cortisol were increased along with the increase of PTH; however, after controlling PTH, although serum calcium was not related to OCN, it still significantly correlated with midnight serum cortisol level, while morning cortisol level was in a significantly negative association with SF independent of PTH. Furthermore, in our study, neither PTH nor calcium has any correlation with scores in questionnaires. Thus, investigating the relative contribution of PTH, calcium, OCN, and cortisol to the development of anxiety and depression behaviors in PHPT in a larger cohort, especially before and after parathyroidectomy, is very important.

Although we revealed the presence of psychoneurological phenotypes in PHPT and found the independent role of serum cortisol and OCN in PHPT patients, this study was just exploratory or hypothesis generating, instead of a confirmatory investigation. Some limitations should be mentioned here. First, the postoperative concentrations of cortisol and OCN as well as the psychological questionnaires were not examined and compared with the preoperative ones. Thus, we have no idea whether the balance of these two markers and patients'

psychological scores changed or not after parathyroidectomy. Second, in this study, we analyzed concentrations of total OCN, rather than uncarboxylated OCN (ucOCN), which is a metabolically active form of OCN at least in mouse studies (21). Third, the sample size of this study, especially those receiving questionnaires, was small; selection bias should be considered. In our sensitivity analysis, it was found that no significant difference of serum OCN and cortisol existed between those receiving questionnaires and their counterparts. Last, we did not measure body water distribution in PHPT patients who were usually treated with water repletion. It was recently shown that the ratio of extracellular water to total body water was related to cognitive function in diabetes patients (45).

To sum up, in this study, it was demonstrated that the serum levels of OCN and cortisol were independently associated with the development of psychological symptoms in PHPT patients. More basic and clinical studies are needed to test and verify this observation.

DATA AVAILABILITY STATEMENT

The raw data supporting the conclusions of this article will be made available by the authors, without undue reservation.

ETHICS STATEMENT

The studies involving human participants were reviewed and approved by Shanghai Ruijin Hospital. Written informed consent for participation was not required for this study in accordance with the national legislation and the institutional requirements.

AUTHOR CONTRIBUTIONS

J-ML and L-HS conceived the project. S-MW carried out most of the information collection and data analysis and wrote the manuscript. YH and M-TZ collected part of patients' clinical information. BT and H-YZ played a key role in maintaining and screening patients. All authors contributed to the article and approved the submitted version.

FUNDING

This study was funded by the Yang Fan Project of Shanghai Science and Technology Commission (19YF1430000).

SUPPLEMENTARY MATERIAL

The Supplementary Material for this article can be found online at: <https://www.frontiersin.org/articles/10.3389/fendo.2021.692722/full#supplementary-material>

REFERENCES

- Walker MD, McMahon DJ, Inabnet WB, Lazar RM, Brown I, Vardy S, et al. Neuropsychological Features in Primary Hyperparathyroidism: A Prospective Study. *J Clin Endocrinol Metab* (2009) 94(6):1951–8. doi: 10.1210/jc.2008-2574
- Silverberg SJ, Shane E, Jacobs TP, Siris E, Bilezikian JP. A 10-Year Prospective Study of Primary Hyperparathyroidism With or Without Parathyroid Surgery. *N Engl J Med* (1999) 341(17):1249–55. doi: 10.1056/NEJM199910213411701
- Walker MD, Silverberg SJ. Primary Hyperparathyroidism. *Nat Rev Endocrinol* (2018) 14(2):115–25. doi: 10.1038/nrendo.2017.104
- Walker MD, Bilezikian JP. Primary Hyperparathyroidism: Recent Advances. *Curr Opin Rheumatol* (2018) 30(4):427–39. doi: 10.1097/BOR.0000000000000511
- Chiodini I, Cairolì E, Palmieri S, Pepe J, Walker MD. Non Classical Complications of Primary Hyperparathyroidism. *Best Pract Res Clin Endocrinol Metab* (2018) 32(6):805–20. doi: 10.1016/j.beem.2018.06.006
- Silverberg SJ. Non-Classical Target Organs in Primary Hyperparathyroidism. *J Bone Mineral Res: Off J Am Soc Bone Mineral Res* (2002) 17(Suppl 2):N117–25.
- Liu M, Sum M, Cong E, Colon I, Bucovsky M, Williams J, et al. Cognition and Cerebrovascular Function in Primary Hyperparathyroidism Before and After Parathyroidectomy. *J Endocrinol Invest* (2020) 43(3):369–79. doi: 10.1007/s40618-019-01128-0
- Ambrogini E, Cetani F, Cianferotti L, Vignali E, Banti C, Viceda G, et al. Surgery or Surveillance for Mild Asymptomatic Primary Hyperparathyroidism: A Prospective, Randomized Clinical Trial. *J Clin Endocrinol Metab* (2007) 92(8):3114–21. doi: 10.1210/jc.2007-0219
- Bollerslev J, Jansson S, Møllerup CL, Nordenström J, Lundgren E, Tørring O, et al. Medical Observation, Compared With Parathyroidectomy, for Asymptomatic Primary Hyperparathyroidism: A Prospective, Randomized Trial. *J Clin Endocrinol Metab* (2007) 92(5):1687–92.
- Amstrup AK, Rejnmark L, Mosekilde L. Patients With Surgically Cured Primary Hyperparathyroidism Have a Reduced Quality of Life Compared With Population-Based Healthy Sex-, Age-, and Season-Matched Controls. *Eur J Endocrinol* (2011) 165(5):753–60. doi: 10.1530/EJE-11-0301
- Kearns AE, Espiritu RP, Vickers Douglass K, Thapa P, Wermers RA. Clinical Characteristics and Depression Score Response After Parathyroidectomy in Primary Hyperparathyroidism. *Clin Endocrinol* (2019) 91(3):464–70. doi: 10.1111/cen.14045
- Silverberg SJ, Lewiecki EM, Mosekilde L, Peacock M, Rubin MR. Presentation of Asymptomatic Primary Hyperparathyroidism: Proceedings of the Third International Workshop. *J Clin Endocrinol Metab* (2009) 94(2):351–65. doi: 10.1210/jc.2008-1760
- Bilezikian JP, Khan AA, Potts JT. Guidelines for the Management of Asymptomatic Primary Hyperparathyroidism: Summary Statement From the Third International Workshop. *J Clin Endocrinol Metab* (2009) 94(2):335–9. doi: 10.1210/jc.2008-1763
- Keller J, Gomez R, Williams G, Lembke A, Lazzaroni L. HPA Axis in Major Depression: Cortisol, Clinical Symptomatology and Genetic Variation Predict Cognition. *Mol Psychiatry* (2017) 22(4):527–36. doi: 10.1038/mp.2016.120
- Gao C, Du Q, Li W, Deng R, Wang Q, Xu A, et al. Baicalin Modulates APPL2/ Glucocorticoid Receptor Signaling Cascade, Promotes Neurogenesis, and Attenuates Emotional and Olfactory Dysfunctions in Chronic Corticosterone-Induced Depression. *Mol Neurobiol* (2018) 55(12):9334–48. doi: 10.1007/s12035-018-1042-8
- Siopi E, Denizet M, Gabellec MM, de Chaumont F, Olivo-Marin JC, Guilloux JP, et al. Anxiety- and Depression-Like States Lead to Pronounced Olfactory Deficits and Impaired Adult Neurogenesis in Mice. *J Neurosci* (2016) 36(2):518–31. doi: 10.1523/JNEUROSCI.2817-15.2016
- Brummelte S, Galea LA. Chronic High Corticosterone Reduces Neurogenesis in the Dentate Gyrus of Adult Male and Female Rats. *Neuroscience* (2010) 168(3):680–90. doi: 10.1016/j.neuroscience.2010.04.023
- Cushing H. The Basophil Adenomas of the Pituitary Body and Their Clinical Manifestations (Pituitary Basophilism). *1932 Obes Res* (1994) 2(5):486–508. doi: 10.1002/j.1550-8528.1994.tb00097.x
- Kelly WF. Psychiatric Aspects of Cushing's Syndrome. *QJM: Monthly J Assoc Phys* (1996) 89(7):543–51. doi: 10.1093/qjmed/89.7.543
- Glatigny M, Moriceau S, Rivagorda M, Ramos-Brossier M, Nascimbeni AC, Lante F, et al. Autophagy Is Required for Memory Formation and Reverses Age-Related Memory Decline. *Curr Biol* (2019) 29(3):435–48.e8. doi: 10.1016/j.cub.2018.12.021
- Oury F, Khirimi L, Denny CA, Gardin A, Chamouni A, Goeden N, et al. Maternal and Offspring Pools of Osteocalcin Influence Brain Development and Functions. *Cell* (2013) 155(1):228–41. doi: 10.1016/j.cell.2013.08.042
- Guo XZ, Shan C, Hou YF, Zhu G, Tao B, Sun LH, et al. Osteocalcin Ameliorates Motor Dysfunction in a 6-Hydroxydopamine-Induced Parkinson's Disease Rat Model Through AKT/Gsk3 β Signaling. *Front Mol Neurosci* (2018) 11:343. doi: 10.3389/fnmol.2018.00343
- Sutton LP, Orlandi C, Song C, Oh WC, Muntean BS, Xie K, et al. Orphan Receptor GPR158 Controls Stress-Induced Depression. *Elife* (2018) 7:e33273. doi: 10.7554/eLife.33273
- Spielberger CD, Gorsuch RL, Lushene RE, Vagg PR. State-Trait Anxiety Inventory (STAI). *BiB* (1983) 2010:180. doi: 10.1037/t06496-000
- Steer RA, Rissmiller DJ, Beck AT. Use of the Beck Depression Inventory-II With Depressed Geriatric Inpatients. *Behav Res Ther* (2000) 38(3):311–8. doi: 10.1016/S0005-7967(99)00068-6
- Liao D, Valliant R. Condition Indexes and Variance Decompositions for Diagnosing Collinearity in Linear Model Analysis of Survey Data. *Surv Method* (2012) 38:189–202.
- Kim JH. Multicollinearity and Misleading Statistical Results. *Korean J Anesthesiol* (2019) 72(6):558–69. doi: 10.4097/kja.19087
- Puig J, Blasco G, Daunis-i-Estadella J, Moreno M, Molina X, Alberich-Bayarri A, et al. Lower Serum Osteocalcin Concentrations are Associated With Brain Microstructural Changes and Worse Cognitive Performance. *Clin Endocrinol (Oxf)* (2016) 84(5):756–63. doi: 10.1111/cen.12954
- Santos A, Granell E, Gómez-Ansón B, Crespo I, Pires P, Vives-Gilbert Y, et al. Depression and Anxiety Scores are Associated With Amygdala Volume in Cushing's Syndrome: Preliminary Study. *BioMed Res Int* (2017) 2017:2061935. doi: 10.1155/2017/2061935
- Rasia-Filho AA, Londero RG, Achaval M. Functional Activities of the Amygdala: An Overview. *J Psychiatry Neurosci: JPN* (2000) 25(1):14–23.
- Johnson LR, Farb C, Morrison JH, McEwen BS, LeDoux JE. Localization of Glucocorticoid Receptors at Postsynaptic Membranes in the Lateral Amygdala. *Neuroscience* (2005) 136(1):289–99. doi: 10.1016/j.neuroscience.2005.06.050
- Jiang H, Ren J, He NY, Liu C, Sun YH, Jian FF, et al. Volumetric Magnetic Resonance Imaging Analysis in Patients With Short-Term Remission of Cushing's Disease. *Clin Endocrinol* (2017) 87(4):367–74. doi: 10.1111/cen.13381
- Santos A, Resmini E, Crespo I, Pires P, Vives-Gilbert Y, Granell E, et al. Small Cerebellar Cortex Volume in Patients With Active Cushing's Syndrome. *Eur J Endocrinol* (2014) 171(4):461–9. doi: 10.1530/EJE-14-0371
- Amin SN, Hassan SS, Khashaba AS, Youakim MF, Latif NSA, Rashed LA, et al. Hippocampal and Cerebellar Changes in Acute Restraint Stress and the Impact of Pretreatment With Ceftriaxone. *Brain Sci* (2020) 10(4):193. doi: 10.3390/brainsci10040193
- Pendry P, Adam EK. Associations Between Parents' Marital Functioning, Maternal Parenting Quality, Maternal Emotion and Child Cortisol Levels. *Int J Behav Dev* (2007) 31(2):218–31. doi: 10.1177/0165025407074634
- Cohen S, Schwartz JE, Epel E, Kirschbaum C, Sidney S, Seeman T. Socioeconomic Status, Race, and Diurnal Cortisol Decline in the Coronary Artery Risk Development in Young Adults (CARDIA) Study. *Psychosom Med* (2006) 68(1):41–50. doi: 10.1097/01.psy.0000195967.51768.ea
- Tordjman S AG. Altered Circadian Patterns of Salivary Cortisol in Low-Functioning Children and Adolescents With Autism. *Psychoneuroendocrinology* (2014) 50:227–45. doi: 10.1016/j.psyneuen.2014.08.010
- Skowrońska-Józwiak E, Gałęcki E, Głowacka P, Wojtyła E, Biliński C, Lewiński P, et al. Bone Metabolism in Patients Treated for Depression. *Int J Environ Res Public Health* (2020) 17(13):4756. doi: 10.3390/ijerph17134756
- Bradburn S, McPhee JS, Bagley L, Sipila S, Stenroth L, Narici MV, et al. Association Between Osteocalcin and Cognitive Performance in Healthy Older Adults. *Age Ageing* (2016) 45(6):844–9. doi: 10.1093/ageing/afw137
- Choi JE, Park DM, Chun E, Choi JJ, Seo JH, Kim S, et al. Control of Stress-Induced Depressive Disorders by So-Ochim-Tang-Gamibang, A Korean Herbal Medicine. *J Ethnopharmacol* (2017) 196:141–50. doi: 10.1016/j.jep.2016.12.025

41. Espiritu RP, Kearns AE, Vickers KS, Grant C, Ryu E, Wermers RA, et al. Depression in Primary Hyperparathyroidism: Prevalence and Benefit of Surgery. *J Clin Endocrinol Metab* (2011) 96(11):E1737–45. doi: 10.1210/jc.2011-1486
42. Weber T, Eberle J, Messelhäuser U, Schiffmann L, Nies C, Schabram J, et al. Parathyroidectomy, Elevated Depression Scores, and Suicidal Ideation in Patients With Primary Hyperparathyroidism: Results of a Prospective Multicenter Study. *JAMA Surg* (2013) 148(2):109–15. doi: 10.1001/2013.jamasurg.316
43. Olgaard K, Lewin E, Bro S, Dagaard H, Egjford M, Pless V, et al. Enhancement of the Stimulatory Effect of Calcium on Aldosterone Secretion by Parathyroid Hormone. *Mineral Electrolyte Metab* (1994) 20(5):309–14.
44. Bargren AE, Repplinger D, Chen H, Sippel RS. Can Biochemical Abnormalities Predict Symptomatology in Patients With Primary Hyperparathyroidism? *J Am Coll Surgeons* (2011) 213(3):410–4. doi: 10.1016/j.jamcollsurg.2011.06.401
45. Low S, Ng TP, Lim CL, Ang SF, Moh A. Higher Ratio of Extracellular Water to Total Body Water Was Associated With Reduced Cognitive Function in

Type 2 Diabetes. *J Diabetes* (2021) 13(3):222–31. doi: 10.1111/1753-0407.13104

Conflict of Interest: The authors declare that the research was conducted in the absence of any commercial or financial relationships that could be construed as a potential conflict of interest.

Publisher's Note: All claims expressed in this article are solely those of the authors and do not necessarily represent those of their affiliated organizations, or those of the publisher, the editors and the reviewers. Any product that may be evaluated in this article, or claim that may be made by its manufacturer, is not guaranteed or endorsed by the publisher.

Copyright © 2021 Wang, He, Zhu, Tao, Zhao, Sun and Liu. This is an open-access article distributed under the terms of the Creative Commons Attribution License (CC BY). The use, distribution or reproduction in other forums is permitted, provided the original author(s) and the copyright owner(s) are credited and that the original publication in this journal is cited, in accordance with accepted academic practice. No use, distribution or reproduction is permitted which does not comply with these terms.



NLRP3 Inflammasome: A New Target for Prevention and Control of Osteoporosis?

Na Jiang^{1†}, Jinyang An^{1†}, Kuan Yang^{1†}, Jinjin Liu^{1,2}, Conghui Guan^{1,2}, Chengxu Ma² and Xulei Tang^{1,2*}

OPEN ACCESS

Edited by:

Lucas R Brun,
National University of
Rosario, Argentina

Reviewed by:

Juan Pablo de Rivero Vaccari,
University of Miami, United States
Divya Singh,
Central Drug Research
Institute (CSIR), India

*Correspondence:

Xulei Tang
xulei_tang@126.com

[†]These authors have contributed
equally to this work

Specialty section:

This article was submitted to
Bone Research,
a section of the journal
Frontiers in Endocrinology

Received: 03 August 2021

Accepted: 13 September 2021

Published: 27 September 2021

Citation:

Jiang N, An J, Yang K, Liu J,
Guan C, Ma C and Tang X (2021)
NLRP3 Inflammasome: A New
Target for Prevention and
Control of Osteoporosis?
Front. Endocrinol. 12:752546.
doi: 10.3389/fendo.2021.752546

¹ The First Clinical Medical College of Lanzhou University, Lanzhou, China, ² Department of Endocrinology, The First Hospital of Lanzhou University, Lanzhou, China

Osteoporosis is a systemic bone metabolism disease that often causes complications, such as fractures, and increases the risk of death. The nucleotide-binding oligomerization domain-like-receptor family pyrin domain-containing 3 (NLRP3) inflammasome is an intracellular multiprotein complex that regulates the maturation and secretion of Caspase-1 dependent proinflammatory cytokines interleukin (IL)-1 β and IL-18, mediates inflammation, and induces pyroptosis. The chronic inflammatory microenvironment induced by aging or estrogen deficiency activates the NLRP3 inflammasome, promotes inflammatory factor production, and enhances the inflammatory response. We summarize the related research and demonstrate that the NLRP3 inflammasome plays a vital role in the pathogenesis of osteoporosis by affecting the differentiation of osteoblasts and osteoclasts. IL-1 β and IL-18 can accelerate osteoclast differentiation by expanding inflammatory response, and can also inhibit the expression of osteogenic related proteins or transcription factors. *In vivo* and *in vitro* experiments showed that the overexpression of NLRP3 protein was closely related to aggravated bone resorption and osteogenesis deficiency. In addition, abnormal activation of NLRP3 inflammasome can not only produce inflammation, but also lead to pyroptosis and dysfunction of osteoblasts by upregulating the expression of Caspase-1 and gasdermin D (GSDMD). In conclusion, NLRP3 inflammasome overall not only accelerates bone resorption, but also inhibits bone formation, thus increasing the risk of osteoporosis. Thus, this review highlights the recent studies on the function of NLRP3 inflammasome in osteoporosis, provides information on new strategies for managing osteoporosis, and investigates the ideal therapeutic target to treat osteoporosis.

Keywords: NLRP3, inflammasome, osteoporosis, osteoclasts, osteoblasts

INTRODUCTION

Osteoporosis (OP) is a chronic disease characterized by changes in bone mass, bone microstructure, and fractures and is a causative factor of morbidity and death in senior adults (1). According to the National Health and Nutrition Examination Survey in 2010, more than 50% of seniors in the USA were affected by OP and low bone mass (2). Furthermore, severe medical and social issues caused by OP are accelerated with age (3).

Previous studies have suggested that estrogen is the main hormone regulator of bone metabolism. Estrogen deficiency can not only directly promote osteoclasts differentiation through estrogen receptors on osteoclasts, but also indirectly stimulate nuclear factor kappa- β ligand (RANKL) on osteoblasts, T cells and B cells to promote bone resorption (4). In addition, estrogen deficiency increases osteoblast apoptosis and inhibits osteoblast differentiation by increasing reactive oxygen species (ROS) and nuclear factor kappa-B (NF- κ B) pathway, causing a relative deficiency of bone formation (5, 6). As a result, the balance between osteoblasts and osteoclasts is broken while the rate of bone formation cannot keep up with the rate of bone resorption, leading to net bone loss. Therefore, the therapeutic effect of estrogen achieves in OP mainly through four effector cells such as osteoblasts, osteoclasts, osteocytes and T cells (7). Besides the effects of hormones on bone metabolism, chronic inflammation promotes bone loss and the onset of OP (8). The nucleotide-binding oligomerization domain-like-receptor family pyrin domain-containing 3 (NLRP3) inflammasome is an intracellular protein complex that mediates the systemic innate immune response and inflammation. The NLRP3 inflammasome mediates the activation of inflammatory caspase 1 (Caspase-1), interleukin (IL)-1 β , and IL-18, causing inflammation and inducing inflammatory cell death.

It has been demonstrated that the abnormal activation of the NLRP3 inflammasome is closely related to multiple metabolic diseases driven by aging and chronic inflammation, such as diabetes, obesity, and gout (9–12). Here, we briefly summarize recent studies on the mechanism of NLRP3 inflammasome in OP, provide information on new strategies for preventing and treating the disease, and investigate the ideal therapeutic target to treat osteoporosis.

CONCEPT AND STRUCTURE OF NLRP3 INFLAMMASOME

The maturation and activation of IL-1 β , a critical molecule involved in inflammation, was known to be mediated by Caspase-1; however, the underlying mechanism remained unclear until the discovery of the NLRP1 inflammasome that suggested the modulation of the process in monocytes (13). The NLRP3 inflammasome, a supramolecular complex concentrated in the cytoplasm, affects innate immunity and inflammation, responds to pathogen- and injury-related signals, and mediates the activity of Caspase-1 and IL-1 β (14). Additionally, various sensors are known to assemble into classic inflammasomes such as NLRP1, NLRP3, NLRC4, AIM2, and Pyrin (15).

The NLRP3 inflammasome is mainly composed of a signal sensor component (NLRP3) and an adaptor, apoptosis-associated speck-like protein containing a CARD (ASC). The ASC can recruit the proinflammatory caspase, Caspase-1 (16), or the non-classical caspases, Caspase-4 or Caspase-5 (17). In the inflammasome complex, Caspase-1 is composed of CARD and two subunits, p10 and p20, at the N-terminal. NLRP3 and ASC interact with their respective PYRIN domains (PYD), whereas clustered ASC and Caspase-1 interact with their respective caspase recruitment domains (CARD). The NLRP3 inflammasome acts as the molecular platform for Caspase-1 lysis and activation, and the two subunits form the activated Caspase-1 tetramer (18). The activated Caspase-1 processes the precursors IL-1 β and IL-18, resulting in the release of mature cytokines and the induction of the inflammatory response in the extracellular environment (**Figure 1**).

REGULATORY MECHANISM OF NLRP3 INFLAMMASOME

The recognition of activation signals by inflammasomes is the first step in inflammatory reactions. NLRP3 recognizes two types of extracellular stimulators, pathogen-associated molecular models (PAMPs), such as bacteria and viruses, and danger-associated molecular models (DAMPs), such as uric acid crystals, saturated

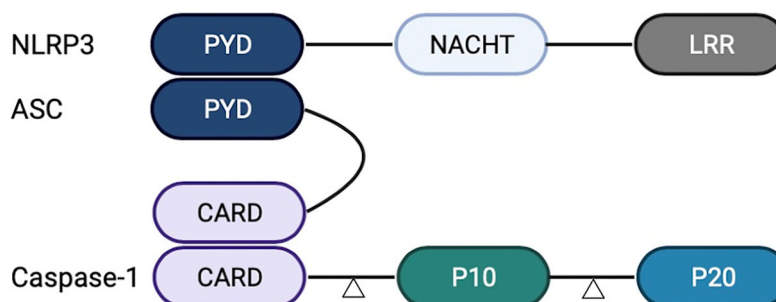


FIGURE 1 | Structure of nucleotide-binding oligomerization domain-like-receptor family pyrin domain-containing 3 (NLRP3) inflammasome. NLRP3 inflammasome comprises a leucine-rich repeat (LRR) domain, an N-terminal Pyrin domain (PYD), and a central adenosine triphosphatase (ATPase) domain known as NACHT. Caspase-1 comprises CARD and two subunits, p10 and p20. NLRP3 and ASC interact with their respective PYDs. ASC and Caspase-1 interact with their respective CARDS.

fatty acids, and cholesterol (19). Next, it induces uniform downstream host-derived cellular events, including K^+ efflux, Ca^{2+} efflux, ROS generation, and lysosomal damage (20). The activation of the NLRP3 inflammasome involves priming and activation. It is believed that the transcription of IL-1 β and NLRP3, mediated by NF- κ B, is the main event caused by the inflammasomes. In addition, post-translational modification of NLRP3, such as phosphorylation induced by JNK1, is a critical event during the initiation process (21). During inflammasome assembly, NLRP3 interacts with a NIMA-related enzyme (NEK7) through the NACHT domain to form large oligomers that form the basis of its activation (22). Finally, NLRP3 recruits Caspase-1 precursor (pro-Caspase-1) through ASC and promotes the processing of Caspase-1 and the subsequent maturation and secretion of the proinflammatory cytokines IL-1 β and IL-18, causing inflammation (23) (**Figure 2**).

NLRP3 INFLAMMASOME MEDIATED IL-1 β AND IL-18 IN OP

Reduced estrogen levels and aging promote low-grade inflammation in the body, and the generated proinflammatory cytokines stimulate OP by affecting the expression and transcription of osteogenic and osteoclastic factors (24, 25). The levels of many inflammatory factors, including IL-1, IL-6, and tumor necrosis factor (TNF)- α , increase

during the pathogenesis of OP (26). IL-1 β is one of the primary members of the IL-1 family (27) that plays an important role in bone loss following estrogen deficiency (28, 29). A previous study in early postmenopausal women after the discontinuation of estrogen therapy showed that bone resorption is reduced by approximately 50% in subjects randomly receiving anakinra, an IL-1 receptor blocker (30). IL-1 β stimulates the expression of Receptor activator of RANKL in osteoblasts or bone marrow mesenchymal stem cells as well as the generation of osteoclasts (25). Besides, IL-1 β binds its receptors on T lymphocytes, B lymphocytes, and macrophages, promotes the generation of RANKL, and binds to RANK on osteoclast precursor cells, thus facilitating the differentiation and activation of osteoclasts (31, 32). Therefore, IL-1 β is not only an effective bone resorption stimulator but also an effective osteogenic inhibitor. High doses of IL-1 β inhibit osteogenic differentiation by activating NF- κ B to inhibit the bone morphogenetic protein (BMP)/Smad signal transduction (33). IL-1 β decreases Runx2 activation and inhibits the osteoblastic differentiation by activating MAPK pathway (34) (**Figure 3**).

IL-18 and IL-1 β are closely related since they belong to the same structural family, have similar 3D structures, and their precursors remain inactive until they are cleaved by intracellular Caspase-1 (35). IL-18 promotes osteoclast differentiation through many pathways. Apart from the bone cells, T helper (Th) cells and various other immunocytes are also major factors participating in bone homeostasis (36). Th17 cells release the marker cytokine IL-17 to upregulate RANKL and promote bone resorption (37).

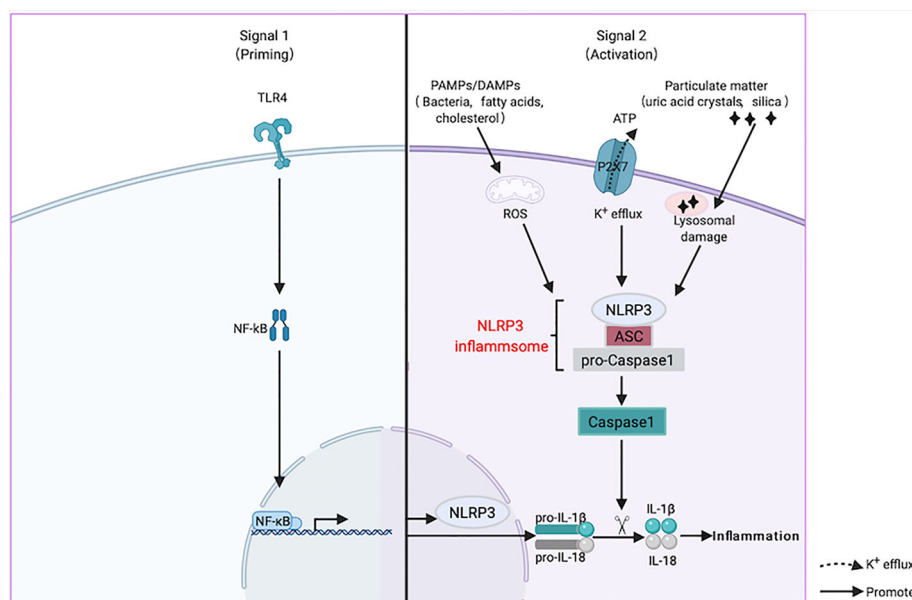


FIGURE 2 | Activation mechanism of nucleotide-binding oligomerization domain-like-receptor family pyrin domain-containing 3 (NLRP3) inflammasome. NLRP3 is activated by two signals when it senses the stimulation of aging or estrogen deficiency through toll like receptors (TLRs). The first priming process (Signal 1) is the expression of NLRP3 and inflammatory factors under the action of the NF- κ B transcription factor. Next, it induces uniform downstream host-derived cellular events, including K^+ efflux, Ca^{2+} efflux, reactive oxygen species (ROS) generation, and lysosomal damage. ASC is an adaptor molecule responsible for connecting NLRP3 and caspase-1 precursors, and then recruits the precursor caspase-1 into an activated form (Signal 2). Activated caspase-1 cleaves the precursors of IL-1 β and IL-18 into mature forms and causing inflammation.

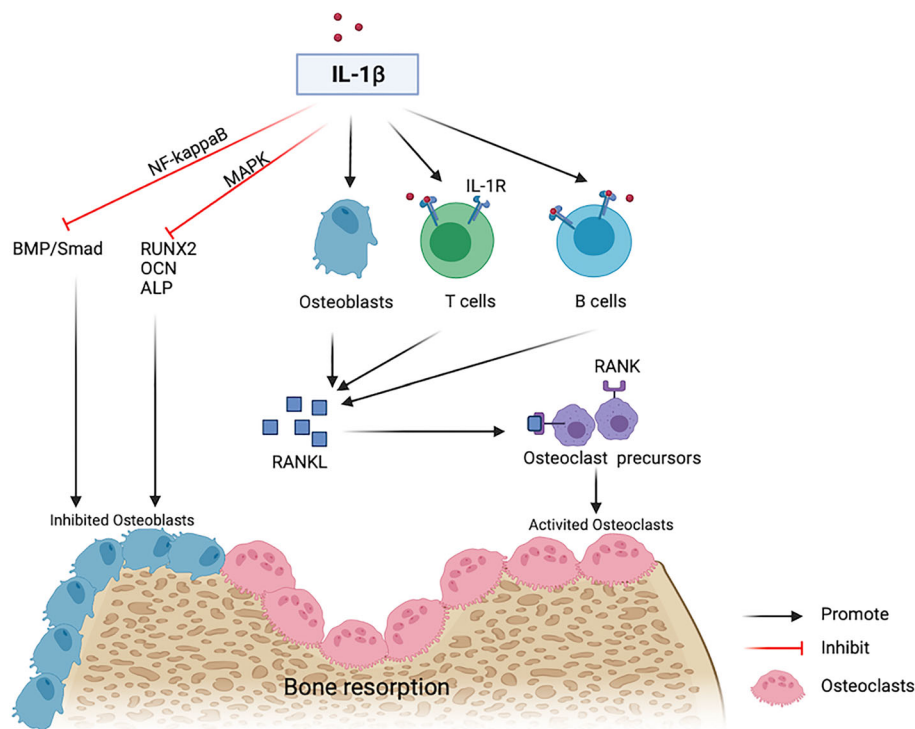


FIGURE 3 | IL-1beta contributes to bone resorption. IL-1 β inhibits osteogenic differentiation by inhibiting the BMP/Smad pathway and osteogenic markers including RUNX2, OCN and ALP. IL-1 β binds with IL-1R on T cells or B cells and induces the expression of RANKL on osteoblasts and then promotes activated osteoclasts via a RANKL-RANK independent mechanism.

Previous studies in ovariectomized (OVX) mice have suggested that increased IL-18 levels in peripheral monocytes stimulate Th17 cells to secrete IL-17, a process conducive to osteoclast differentiation. In addition, co-culture of osteoblasts with CD4⁺ T cells and CD11b⁺ macrophages isolated from OVX mice showed an upregulation of IL-18, activation of NLRP3 inflammasome-related molecules, and inhibition of osteoblasts manifested as reduced expression levels of Wnt-10b, Runt-related transcription factor 2 (Runx-2), and BMP-2 (38). Another *in vivo* study supported the hypothesis that IL-18 participates in the pathogenesis of OP. In OVX mice, the levels of IL-18 binding protein (IL-18BP, a natural specific IL-18 inhibitor) were declined, whereas IL-18BP supplementation markedly decreased the Th17/Treg ratio and proinflammatory cytokines, restoring the microstructure of bone trabeculae. These findings were confirmed in female patients with OP (38). In serum obtained from patients with Cushing's syndrome, IL-18 and osteocalcin (OCN) levels were negatively correlated (39). Therefore, IL-1 β and IL-18 participate in increased inflammation during OP.

NLRP3 INFLAMMASOME INDUCES PYROPTOSIS OF BONE CELLS IN OP

It has been reported that the NLRP3 inflammasome not only aggravates cellular inflammatory response through the Caspase-

1/IL-1 β /IL-18 activated pathway, but also forms pores on the cell membrane using gasdermin D (GSDMD) as the general substrate, digests the N-terminal domain of GSDMD to bind to the pore of the cell membrane, releases inflammatory mediators, and destructs osmotic pressure, inducing cell swelling, lysis, and death, known as pyroptosis (40). At high glucose concentrations, MC3T3-E1 osteoblasts and Caspase-1 in alveolar bone are activated. Enhanced IL-1 β activity increases the expression levels of GSDMD and reduces those of osteogenesis-related proteins, such as p-AKT and β -catenin, whereas Caspase-1 inhibitor can reverse this process (41). In a mouse osteomyelitis model, pyroptosis-related proteins were upregulated, whereas Ac-YVAD-CMK, a specific Caspase-1 inhibitor, not only inhibited the increases of Caspase-1 and GSDMD in mice induced by bacteria, but also helped to restore the osteogenic characteristics (42). Vx765, an inhibitor of Caspase-1, partially reduced bone resorption in apical periodontitis rats, although bone trabecular thickness increased and bone volume did not change significantly. *In vitro* experiments showed that ROS can induce osteoblast pyroptosis and lead to osteoblast dysfunction (43). Tao et al. (44) summarized the relationship between ROS and NLRP3 in OP, considering that ROS is an important component in the pathogenesis of OP, and speculated that it may be a trigger factor for pyroptosis in this pathological process. Therefore, we hypothesize that the NLRP3 inflammasome not only activates the downstream inflammatory factors to participate in OP

pathogenesis, but also induces pyroptosis and maintains or aggravates inflammation (Figure 4).

NLRP3 INFLAMMASOME PARTICIPATES IN OP PATHOGENESIS

During the growth and development of bones, the NLRP3 inflammasome and its associated proteins have positive regulatory effects. Compared with NLRP3^{+/+} mice, NLRP3^{-/-} mice have shorter stature, impaired long bone growth, and defective osteoblast differentiation and mineralization (45). ASC is an essential molecule in the osteoblast phenotype. Compared with osteoblasts obtained from wild-type mice, primary osteoblasts with ASC-source knockout have lower levels of osteogenic properties, and thus, tibial defect healing requires a longer period (46). However, over-activation of the NLRP3 inflammasome is related to osteopenia due to aging. A previous study found that NLRP3 is overexpressed in an aging mouse model, whereas its knockout increased the density of the bone cortex and trabecula (47). A humanized NLRP3 mouse strain created by replacing the mouse NLRP3 locus with the human allele associated with the disease developed progressive arthritis and OP, accompanied by granulocyte infiltration and increased IL-1 β levels, after attack by injury-related molecular model molecules (48). Recent studies

revealed that in an OVX mouse model, the NLRP3 inflammasome components are upregulated in the femoral bone; however, knockdown of NLRP3 notably enhanced the expression of Runx2 and OCN, which are responsible for osteogenic differentiation (49). Therefore, the NLRP3 inflammasome plays a dual role in bone metabolism, but its abnormal activation produces unfavorable effects in OP development (Table 1). The NLRP3 inflammasome and its components, IL-1 β and IL-18, jointly exert effects in OP, whereas the latter may be regulated by NLRP3 inflammasome to result in inflammatory bone injury.

NLRP3 Inflammasome Inhibits Osteogenesis

Bone mesenchymal stem cells (BMSCs) can differentiate into osteoblasts and adipocytes after stimulation by environmental factors (52). During the development of OP, BMSCs exhibit reduced osteogenic capacity and increased fat-forming capacity, resulting in reduced bone formation and increased bone marrow fat accumulation (53, 54). It has been confirmed that the NLRP3 inflammasome is involved in this process and may affect the differentiation of BMSCs via certain active molecules. The group III protein deacetylase, Sirtuin1 (SIRT1), has positive regulatory effects in inhibiting MSC fat formation and promoting bone formation (55). Lipopolysaccharide/palmitic acid (LPS/PA) was previously used to process *in vitro* MSCs by significantly

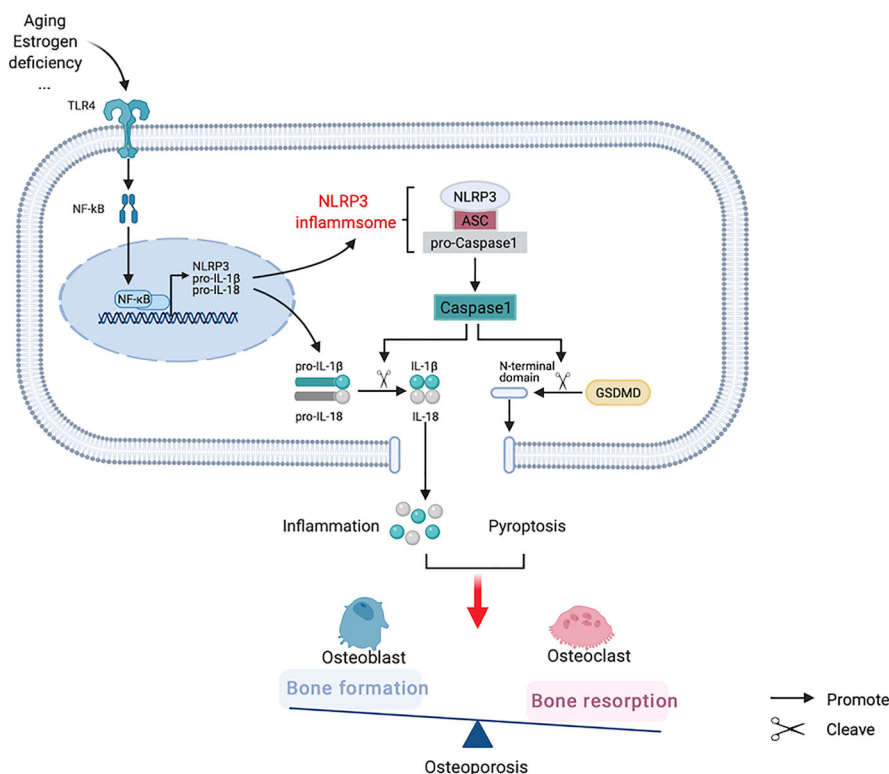


FIGURE 4 | Hypothesized participation of nucleotide-binding oligomerization domain-like-receptor family pyrin domain-containing 3 (NLRP3) inflammasome in the pathogenesis of osteoporosis.

TABLE 1 | The different effects of NLRP3 inflammasome on bone cells.

Effector cells	Effects	Crosstalk pathways	References
Osteoblasts	Decreased cell migration Inhibited the proliferation and differentiation of osteoblasts	ROS p-AKT and β -catenin	Liu SS et al. (43) Xu L et al. (49)
Osteoclasts	Enhanced bone-resorption capacity of osteoclasts, but inhibited their efferocytosis	ROS/MAPK/NF- κ B pathway	An Y et al. (50)
BMSCs	Inhibits osteogenic differentiation and promotes adipogenic differentiation	SIRT1	Wang L et al. (51)

increasing the expression of NLRP3 inflammasome in MSCs and reducing the expression levels of SIRT1; thus, the NLRP3 inflammasome inhibits osteogenic differentiation by inhibiting SIRT1 and promoting the differentiation of MSCs into adipocytes (51). One study showed that osteogenic differentiation is hampered by the NLRP3 inflammasome in MSCs isolated from the human cord blood and treated with LPS/ATP, probably through the inflammasome assembly, since the siRNA of ASC, the critical component of the targeted inflammasome assembly, can reverse the process (56). However, another study showed that the NLRP3 inflammasome does not promote adipogenic differentiation. Any discrepancies between the studies could be attributed to the different stimulants used.

The activated NLRP3 inflammasome contains multiple exogenous or endogenous substances, but none has been confirmed as the activating substances during bone metabolism. A previous study revealed that NLRP3 is expressed in osteoblasts, mediates cell death induced by bacteria, and participates in bone loss during the inflammatory process (57). In OVX mice, the femur protein and NLRP3 in the osteoblasts are highly expressed even when no direct bacterial infection is observed (49). Since various substances can activate the NLRP3 inflammasome during bone metabolism, it is necessary to investigate the mutual regulation mechanism between the metabolites and the NLRP3 inflammasome in OP due to aging or estrogen deficiency.

NLRP3 Inflammasome Promotes Bone Resorption

Previous *in vivo* experiments have indicated that the NLRP3 inflammasome accelerates bone resorption under multiple bone turnover states (i.e., estrogen deficiency and persistent parathyroid hormone exposure) and that NLRP3 knockout reduces bone loss in many high bone turnover models (58). Similarly, in osteoclasts exposed to high concentrations of glucose and the rat model of diabetic OP, the expression levels of NLRP3 inflammasome and its related proteins are increased, bone density is reduced, and osteoclast markers are increased. Besides, the overactivated NLRP3 inflammasome can be inhibited by exosomes originating from MSCs (59). It has been reported that the initiation step for NLRP3 inflammasome activation mainly depends on the NF- κ B pathway. NF- κ B is an inflammation regulation signal downstream of Toll-like receptor (TLR) and the classic inflammatory pathway of the immune response. Several studies have confirmed that the NF- κ B pathway has significant effects on the growth and maturation of osteoblasts and osteoclasts (6). At the molecular level, exposure to high glucose concentrations upregulated NLRP3 inflammasome expression and this is regulated by ROS/MAPKs/NF- κ B. NF- κ B inhibitors significantly reduce the expression level

of NLRP3 inflammasome and alleviate bone resorption (50). When bone marrow macrophages (BMMs), which are osteoclast precursors, are exposed to bone matrix particles, the NLRP3 inflammasome is activated, resulting in increased NF- κ B and MAPK phosphorylation (58). Therefore, the NLRP3 inflammasome and the classic inflammatory pathway mutually interfere and produce joint effects in osteoclast differentiation, which further confirms the critical role of NF- κ B in the initiation of the NLRP3 inflammasome.

POTENTIAL THERAPEUTIC TARGET OF NLRP3 INFLAMMASOME IN OP

Considering that the NLRP3 inflammasome has dual effects in OP pathogenesis, its regulation may be a novel ideal therapeutic target. Other anti-OP drugs, such as bisphosphonates, parathyroid hormone analogs, and RANKL inhibitors, can only either inhibit bone resorption or promote bone reconstruction to achieve therapeutic effects, and their long-term use has certain safety concerns (1). Previous studies have suggested that bisphosphonate, an antiresorptive agent, increases the secretion of NLRP3 dependent IL-1 β and induces osteonecrosis in diabetic mice (60). Therefore, combined treatment with an NLRP3 inhibitor might reduce the side effects of bisphosphonate, such as jaw necrosis. There are two categories of pharmacological inhibitors for targeting NLRP3 inflammasome: direct inhibitors that directly target NLRP3 protein and some others that are indirect inhibitors, which target constituents of the NLRP3 inflammasome such as Caspase-1, IL-1 β and IL-18. Some of the inhibitors that are related to osteoporosis has been reported (Table 2).

Anakinra, a targeted IL-1 β inhibitor, has been successfully applied to treat rheumatoid arthritis (68). A clinical study showed that it is also resistant to bone resorption in postmenopausal women (30). Auranofin, another drug used for the treatment of rheumatoid arthritis, significantly reduces bone loss in OVX mice by suppressing osteoclastogenesis induced by RANKL in BMMs and inhibiting IL-1 expression mediated by inflammasomes (67). The drugs, anakinra and auranofin, successfully regulate the cytokine components of the NLRP3 inflammasome to prevent osteoclast-related OP. Although the drugs alone cannot completely block the inflammation, they can be taken orally rather than through injection. Animal experiments have demonstrated that mouse IL-18BP has obvious anti-OP effects, but humanized IL-18BP needs to be further studied (38).

Novel drugs including natural or synthetic molecules that inhibit the maturation or release of IL-1 family cytokines (i.e., NLRP3 inflammasome or Caspase-1 inhibitor) are currently under

TABLE 2 | Inhibitors of NLRP3 inflammasome related to OP.

Targets	Agents	Benefits	Side effects or limitation	References
NLRP3	MCC950	Reduces age-related bone loss by inhibiting osteoclastogenesis	The effectiveness in bone formation remains to be confirmed	Zhang Y et al. (61)
	CY-09	Reverses osteogenic dysfunction	<i>In vitro</i> experiments only	Liu SS et al. (43)
		Reduced bone loss	Osteoarthritis modeling only and needs intra-articular injections	Li Z et al. (62)
	OLT1177	–	–	–
	Glyburide	Expedites diabetes-induced impaired fracture healing	The concentration of anti-inflammatory and anti-hyperglycemia is difficult to balance	Yang X et al. (63)
	Irisin	Reverses the expression of osteogenic markers and reduces the activation of osteoclasts	Studied in animal models of OP only	Kawahara Y et al. (64)
		Lowers inflammation and suppressed osteoblast apoptosis		Zhu X et al. (42)
Caspase-1	Melatonin	Promotes osteoblastogenesis through Wnt/ β -catenin pathway	The mechanism mediated through the inhibition of bone resorption is unclear	Xu L et al. (65)
	Dioscin	Inhibits the activation of NLRP3 inflammasome in mouse macrophages and promotes the osteogenesis of mouse pre-osteoblasts	Whether osteogenesis is promoted by inhibiting NLRP3 is unknown	Xu Lijun et al. (49)
	Ac-YVAD-CMK	Restores the osteogenic characteristics	Osteomyelitis model only	Yin Wei et al. (57)
	VX765	Reverses the inhibition of proliferation and differentiation osteoblast resulting from high glucose induced pyroptosis	The effect in bone resorption is unknown	Zhu X et al. (42)
		Partly decreases bone resorption		Yang L et al. (41)
IL-1 β	Anakinra	Reduces bone resorption	The effect of vx765 may be limited by dose and duration of the drug	Cheng R et al. (66)
IL-18	Auranofin	Inhibits osteoclastogenesis and can be orally available	Blocking cytokines alone cannot completely prevent the increase of bone resorption in estrogen deficiency. Combined blocking may be required	Charatcharoenwittaya N et al. (30)
	IL-18BP	Inhibits osteoclastogenesis and reduces bone loss.	More clinical trial data are needed	Kim H et al. (67)
			Humanized IL-18BP toward the treatment of OP remains to be investigated	Mansoori MN et al. (38)

development and expected to emerge as a new strategy for the treatment of OP, as confirmed by numerous *in vivo* and *in vitro* experiments. MCC950, an effective and specific inhibitor of the NLRP3 inflammasome, alleviates the inhibition of MG63 osteoblasts mediated by the NLRP3 inflammasome under oxidative stress (43). *In vivo* experiments have suggested that NLRP3 knockout and MCC950 supplementation significantly reduces age-related alveolar bone loss in elderly mice. In addition, MCC950 treatment results in higher bone mineral density and bone volume per tissue volume as well as the reduced formation of tartrate-resistant acid phosphatase (TRAP)-positive cells, delaying osteoclast differentiation (61). Other targeted NLRP3 inflammasome inhibitors, such as OLT1177 and CY-09, also exhibited good therapeutic properties (69). CY-09 reduced bone loss in osteoarthritis modeling. However, the route of administration is achieved by intra-articular injection in the knee (62). At present, the research on OLT1177 in OP has not been reported.

Glyburide, a drug in clinical use, also known as an NLRP3 inflammasome inhibitor, reversed the expression of osteogenic markers such as collagen I and Runx2 and reduced the abnormal activation of osteoclasts (42). However, in this study, the concentration of glyburide far exceeded the concentration of its application in hypoglycemia, which undoubtedly increased other side effects of the drug. In addition, glyburide accelerated the healing of diabetes induced fracture by inhibiting the production of inflammatory factors (63). In a rat model of periodontitis, glyburide suppressed the activation of Caspase-1 and IL-1 β , and oral glyburide significantly inhibited the number of osteoclasts in alveolar bone (64).

It has been found that many natural and endogenous or exogenous molecules exert anti-inflammatory effects by inhibiting NLRP3 inflammasome activation in OP. Ario et al. (70). have summarized the effect of melatonin, a widely used natural and endogenous molecule, on NLRP3 in a variety of different diseases. *In vivo* experiments have suggested that melatonin inhibits the activation of the NLRP3 inflammasome and improves the inhibition of osteogenic differentiation in OP through the Wnt pathway, which is related to osteogenic differentiation (49). Irisin, another natural molecule, suppressed osteoblast apoptosis and increased the content of ALP in postmenopausal OP rats through the inhibition of NLRP3 inflammasome (65). Dioscin, a plant product, can also inhibit the activation of NLRP3 inflammasome in mouse macrophages and promotes osteogenesis of mouse pre-osteoblasts (57). Therefore, exploring the endogenous and exogenous regulation mechanisms is helpful in improving the understanding of inflammasome activation in the body.

Many studies have focused on the post-transcriptional control of microRNAs (miRNA) based on NLRP3 (71). NLRP3-targeted miRNA is a successful therapeutic method for various diseases, including rheumatoid arthritis and cancer, but little is known about its effectiveness in the treatment of OP (72, 73).

SUMMARY AND OUTLOOK

The expression of NLRP3 inflammasome in bone cells affects osteoblast activation and osteoclast differentiation in OP. In addition, it maintains and aggravates the inflammation of

osteoblasts or osteoclasts in OP pathogenesis through its downstream inflammatory factors, IL-1 β and IL-18, and the induction of Caspase-1-dependent pyroptosis. The NLRP3 inflammasome is involved in bone metabolism by influencing various active molecules and other classic inflammatory pathways. It is obvious that reduced NLRP3 levels delay OP development, but the underlying mechanism involved needs further research. In order to achieve anti-inflammatory functions, the concentration of some drugs is increased, which also increases the possibility of side effects. Therefore, it is necessary to find more suitable drugs, such as MCC950, to inhibit the progress of OP. Basic and clinical studies that provide references for the prevention and treatment of various metabolic diseases are of the utmost necessity.

AUTHOR CONTRIBUTIONS

NJ, JA, and KY contributed equally to this paper. NJ drafted and prepared manuscript. JA, KY, and CM reviewed and edited the

manuscript. JL and CG extracted data and constructed figures with software. XT considered for ideas and overall structure of the article. All authors contributed to the article and approved the submitted version.

FUNDING

This study was supported by the National Natural Science Foundation of China under grant no. 81370970, and the Science and Technology Support Program of Gansu Province under grants no. 144FKCA075.

ACKNOWLEDGMENTS

We would like to thank Editage (www.editage.cn) for English language editing.

REFERENCES

- Compston JE, Mcclung MR, Leslie WD. Osteoporosis. *Lancet* (2019) 393 (10169):364–76. doi: 10.1016/S0140-6736(18)32112-3
- Wright NC, Looker AC, Saag KG, Curtis JR, Delzell ES, Randall S, et al. The Recent Prevalence of Osteoporosis and Low Bone Mass in the United States Based on Bone Mineral Density at the Femoral Neck or Lumbar Spine. *J Bone Miner Res* (2014) 29(11):2520–6. doi: 10.1002/jbmr.2269
- Harvey N, Dennison E, Cooper C. Osteoporosis: Impact on Health and Economics. *Nat Rev Rheumatol* (2010) 6(2):99–105. doi: 10.1038/nrrheum.2009.260
- Eghbali-Fatourehchi G, Khosla S, Sanyal A, Boyle WJ, Lacey DL, Riggs BL. Role of RANK Ligand in Mediating Increased Bone Resorption in Early Postmenopausal Women. *J Clin Invest* (2003) 111(8):1221–30. doi: 10.1172/JCI200317215
- Bai XC, Lu D, Bai J, Zheng H, Ke ZY, Li XM, et al. Oxidative Stress Inhibits Osteoblastic Differentiation of Bone Cells by ERK and NF-Kappa B. *Biochem Biophys Res Commun* (2004) 314(1):197–207. doi: 10.1016/j.bbrc.2003.12.073
- Novack DV. Role of NF-kappaB in the Skeleton. *Cell Res* (2011) 21(1):169–82. doi: 10.1038/cr.2010.159
- Khosla S, Oursler MJ, Monroe DG. Estrogen and the Skeleton. *Trends Endocrinol Metab* (2012) 23(11):576–81. doi: 10.1016/j.tem.2012.03.008
- Redlich K, Smolen JS. Inflammatory Bone Loss: Pathogenesis and Therapeutic Intervention. *Nat Rev Drug Discovery* (2012) 11(3):234–50. doi: 10.1038/nrd3669
- Rovira-Llopis S, Apostolova N, Banuls C, Muntane J, Rocha M, Victor VM. Mitochondria, the NLRP3 Inflammasome, and Sirtuins in Type 2 Diabetes: New Therapeutic Targets. *Antioxid Redox Signal* (2018) 29(8):749–91. doi: 10.1089/ars.2017.7313
- Mcallister MJ, Chemaly M, Eakin AJ, Gibson DS, McGilligan VE. NLRP3 as a Potentially Novel Biomarker for the Management of Osteoarthritis. *Osteoarthritis Cartilage* (2018) 26(5):612–9. doi: 10.1016/j.joca.2018.02.901
- Rheinheimer J, De Souza BM, Cardoso NS, Bauer AC, Crispim D. Current Role of the NLRP3 Inflammasome on Obesity and Insulin Resistance: A Systematic Review. *Metabol Clin Exp* (2017) 74:1–9. doi: 10.1016/j.metabol.2017.06.002
- Szekanecz Z, Szamosi S, Kovacs GE, Kocsis E, Benko S. The NLRP3 Inflammasome - Interleukin 1 Pathway as a Therapeutic Target in Gut. *Arch Biochem Biophys* (2019) 670:82–93. doi: 10.1016/j.abb.2019.01.031
- Martinson F, Burns K, Tschoep J. The Inflammasome: A Molecular Platform Triggering Activation of Inflammatory Caspases and Processing of ProIL-Beta. *Mol Cell* (2002) 10(2):417–26. doi: 10.1016/S1097-2765(02)00599-3
- Agostini L, Martinon F, Burns K, Hawkins PN, Tschoep J. NALP3 Forms an IL-1beta-Processing Inflammasome With Increased Activity in Muckle-Wells Autoinflammatory Disorder. *Immunity* (2004) 20(3):319–25. doi: 10.1016/S1074-7613(04)00046-9
- Place DE, Kanneganti TD. Recent Advances in Inflammasome Biology. *Curr Opin Immunol* (2018) 50:32–8. doi: 10.1016/j.coi.2017.10.011
- Abderrazak A, Syrovets T, Couchie D, El Hadri K, Friguet B, Simmet T, et al. NLRP3 Inflammasome: From a Danger Signal Sensor to a Regulatory Node of Oxidative Stress and Inflammatory Diseases. *Redox Biol* (2015) 4:296–307. doi: 10.1016/j.redox.2015.01.008
- Zheng D, Liwinski T, Elinav E. Inflammasome Activation and Regulation: Toward a Better Understanding of Complex Mechanisms. *Cell Discovery* (2020) 6:36. doi: 10.1038/s41421-020-0167-x
- Boucher D, Monteleone M, Coll RC, Chen KW, Ross CM, Teo JL, et al. Caspase-1 Self-Cleavage Is an Intrinsic Mechanism to Terminate Inflammasome Activity. *J Exp Med* (2018) 215(3):827–40. doi: 10.1084/jem.20172222
- Jiang D, Chen S, Sun R, Zhang X, Wang D. The NLRP3 Inflammasome: Role in Metabolic Disorders and Regulation by Metabolic Pathways. *Cancer Lett* (2018) 419:8–19. doi: 10.1016/j.canlet.2018.01.034
- He Y, Hara H, Nunez G. Mechanism and Regulation of NLRP3 Inflammasome Activation. *Trends Biochem Sci* (2016) 41(12):1012–21. doi: 10.1016/j.tibs.2016.09.002
- Song N, Liu ZS, Xue W, Bai ZF, Wang QY, Dai J, et al. NLRP3 Phosphorylation Is an Essential Priming Event for Inflammasome Activation. *Mol Cell* (2017) 68(1):1–13. doi: 10.1016/j.molcel.2017.08.017
- Sharif H, Wang L, Wang WL, Magupalli VG, Andreeva L, Qiao Q, et al. Structural Mechanism for NEK7-Licensed Activation of NLRP3 Inflammasome. *Nature* (2019) 570(7761):338–43. doi: 10.1038/s41586-019-1295-z
- Tschoep J, Schroder K. NLRP3 Inflammasome Activation: The Convergence of Multiple Signalling Pathways on ROS Production? *Nat Rev Immunol* (2010) 10(3):210–5. doi: 10.1038/nri2725
- Cline-Smith A, Axelbaum A, Shashkova E, Chakraborty M, Sanford J, Panesar P, et al. Ovariectomy Activates Chronic Low-Grade Inflammation Mediated by Memory T Cells, Which Promotes Osteoporosis in Mice. *J Bone Miner Res* (2020) 35(6):1174–87. doi: 10.1002/jbmr.3966
- Pietschmann P, Mechtcheriakova D, Meshcheryakova A, Foger-Samwald U, Ellinger I. Immunology of Osteoporosis: A Mini-Review. *Gerontology* (2016) 62(2):128–37. doi: 10.1159/000431091
- McLean RR. Proinflammatory Cytokines and Osteoporosis. *Curr Osteoporosis Rep* (2009) 7(4):134–9. doi: 10.1007/s11914-009-0023-2
- Dinarello C, Arend W, Sims J, Smith D, fcimb.2021.765039 H, O'Neill L, et al. IL-1 Family Nomenclature. *Nat Immunol* (2010) 11(11):973. doi: 10.1038/nri110-973
- Percegoni N, Ferreira AC, Rodrigues CF, Rosenthal D, Castelo Branco MT, Rumjanek VM, et al. Profile of Serum IL-1beta and IL-10 Shortly After Ovariectomy and Estradiol Replacement in Rats. *Horm Metab Res* (2009) 41 (1):50–4. doi: 10.1055/s-0028-1087173

29. Khosla S. Pathogenesis of Age-Related Bone Loss in Humans. *J Gerontol A Biol Sci Med Sci* (2013) 68(10):1226–35. doi: 10.1093/gerona/gls163
30. Charatcharoenwithaya N, Khosla S, Atkinson EJ, McCready LK, Riggs BL. Effect of Blockade of TNF-Alpha and Interleukin-1 Action on Bone Resorption in Early Postmenopausal Women. *J Bone Miner Res* (2007) 22(5):724–9. doi: 10.1359/jbmr.070207
31. Ruscitti P, Cipriani P, Carubbi F, Liakouli V, Zazzeroni F, Di Benedetto P, et al. The Role of IL-1beta in the Bone Loss During Rheumatic Diseases. *Mediators Inflamm* (2015) 2015:782382. doi: 10.1155/2015/782382
32. Nakamura I, Jimi E. Regulation of Osteoclast Differentiation and Function by Interleukin-1. *Vitam Horm* (2006) 74:357–70. doi: 10.1016/S0083-6729(06)74015-8
33. Mao CY, Wang YG, Zhang X, Zheng XY, Tang TT, Lu EY. Double-Edged-Sword Effect of IL-1beta on the Osteogenesis of Periodontal Ligament Stem Cells via Crosstalk Between the NF-Kappab, MAPK and BMP/Smad Signaling Pathways. *Cell Death Dis* (2016) 7:e2296. doi: 10.1038/cddis.2016.204
34. Huang RL, Yuan Y, Tu J, Zou GM, Li Q. Opposing TNF-Alpha/IL-1beta- and BMP-2-Activated MAPK Signaling Pathways Converge on Runx2 to Regulate BMP-2-Induced Osteoblastic Differentiation. *Cell Death Dis* (2014) 5:e1187. doi: 10.1038/cddis.2014.101
35. Ge Y, Huang M, Yao YM. Recent Advances in the Biology of IL-1 Family Cytokines and Their Potential Roles in Development of Sepsis. *Cytokine Growth F R* (2019) 45:24–34. doi: 10.1016/j.cytogr.2018.12.004
36. Srivastava RK, Dar HY, Mishra PK. Immunoporosis: Immunology of Osteoporosis-Role of T Cells. *Front Immunol* (2018) 9:657. doi: 10.3389/fimmu.2018.00657
37. Ke D, Fu X, Xue Y, Wu H, Zhang Y, Chen X, et al. IL-17A Regulates the Autophagic Activity of Osteoclast Precursors Through RANKL-JNK1 Signaling During Osteoclastogenesis *In Vitro*. *Biochem Biophys Res Commun* (2018) 497(3):890–6. doi: 10.1016/j.bbrc.2018.02.164
38. Mansoori MN, Shukla P, Kakaji M, Tyagi AM, Srivastava K, Shukla M, et al. IL-18BP Is Decreased in Osteoporotic Women: Prevents Inflammasome Mediated IL-18 Activation and Reduces Th17 Differentiation. *Sci Rep-Uk* (2016) 6:33680. doi: 10.1038/srep33680
39. Kristo C, Godang K, Ueland T, Lien E, Aukrust P, Froland S, et al. Raised Serum Levels of Interleukin-8 and Interleukin-18 in Relation to Bone Metabolism in Endogenous Cushing's Syndrome. *Eur J Endocrinol* (2002) 146(3):389–95. doi: 10.1530/eje.0.1460389
40. Shi JJ, Zhao Y, Wang K, Shi XY, Wang Y, Huang HW, et al. Cleavage of GSDMD by Inflammatory Caspases Determines Pyroptotic Cell Death. *Nature* (2015) 526(7575):660–5. doi: 10.1038/nature15514
41. Yang L, Liu J, Shan QS, Geng GN, Shao P. High Glucose Inhibits Proliferation and Differentiation of Osteoblast in Alveolar Bone by Inducing Pyroptosis. *Biochem Biophys Res Commun* (2020) 522(2):471–8. doi: 10.1016/j.bbrc.2019.11.080
42. Zhu X, Zhang K, Lu K, Shi T, Shen S, Chen X. Staphylococcus Aureus Inhibition of Pyroptosis Attenuates -Induced Bone Injury in Traumatic Osteomyelitis. *Ann Trans Med* (2019) 7(8):170. doi: 10.21037/atm.2019.03.40
43. Liu SS, Du J, Li DF, Yang PP, Kou YY, Li CS, et al. Oxidative Stress Induced Pyroptosis Leads to Osteogenic Dysfunction of MG63 Cells. *J Mol Histol* (2020) 51(3):221–32. doi: 10.1007/s10735-020-09874-9
44. Tao Z, Wang J, Wen K, Yao R, Da W, Zhou S, et al. Pyroptosis in Osteoblasts: A Novel Hypothesis Underlying the Pathogenesis of Osteoporosis. *Front Endocrinol (Lausanne)* (2020) 11:548812. doi: 10.3389/fendo.2020.548812
45. Detzen L, Cheat B, Besbes A, Hassan B, Marchi V, Baroukh B, et al. NLRP3 Is Involved in Long Bone Edification and the Maturation of Osteogenic Cells. *J Cell Physiol* (2021) 236(6):4455–69. doi: 10.1002/jcp.30162
46. Sartoretto S, Gemini-Piperni S, Da Silva R, Calasans M, Rucci N, Pires Dos Santos T, et al. Apoptosis-Associated Speck-Like Protein Containing a Caspase-1 Recruitment Domain (ASC) Contributes to Osteoblast Differentiation and Osteogenesis. *J Cell Physiol* (2019) 234(4):4140–53. doi: 10.1002/jcp.27226
47. Youm YH, Grant RW, McCabe LR, Albarado DC, Nguyen LKY, Ravussin A, et al. Canonical Nlrp3 Inflammasome Links Systemic Low-Grade Inflammation to Functional Decline in Aging. *Cell Metab* (2013) 18(4):519–32. doi: 10.1016/j.cmet.2013.09.010
48. Snouwaert J, Nguyen M, Repenning P, Dye R, Livingston E, Kovarova M, et al. An NLRP3 Mutation Causes Arthropathy and Osteoporosis in Humanized Mice. *Cell Rep* (2016) 17(11):3077–88. doi: 10.1016/j.celrep.2016.11.052
49. Xu L, Zhang L, Wang Z, Li C, Li S, Li L, et al. Melatonin Suppresses Estrogen Deficiency-Induced Osteoporosis and Promotes Osteoblastogenesis by Inactivating the NLRP3 Inflammasome. *Calcif Tissue Int* (2018) 103(4):400–10. doi: 10.1007/s00223-018-0428-y
50. An Y, Zhang H, Wang C, Jiao F, Xu H, Wang X, et al. Activation of ROS/ MAPKs/NF-Kappab/NLRP3 and Inhibition of Efferocytosis in Osteoclast-Mediated Diabetic Osteoporosis. *FASEB J* (2019) 33(11):12515–27. doi: 10.1096/fj.201802805RR
51. Wang L, Chen K, Wan X, Wang F, Guo Z, Mo Z. NLRP3 Inflammasome Activation in Mesenchymal Stem Cells Inhibits Osteogenic Differentiation and Enhances Adipogenic Differentiation. *Biochem Biophys Res Commun* (2017) 484(4):871–7. doi: 10.1016/j.bbrc.2017.02.007
52. Hu L, Yin C, Zhao F, Ali A, Ma J, Qian A. Mesenchymal Stem Cells: Cell Fate Decision to Osteoblast or Adipocyte and Application in Osteoporosis Treatment. *Int J Mol Sci* (2018) 19(2):360. doi: 10.3390/ijms19020360
53. Choi HK, Yuan H, Fang F, Wei X, Liu L, Li Q, et al. Tsc1 Regulates the Balance Between Osteoblast and Adipocyte Differentiation Through Autophagy/ Notch1/beta-Catenin Cascade. *J Bone Miner Res* (2018) 33(11):2021–34. doi: 10.1002/jbmr.3530
54. Li CJ, Cheng P, Liang MK, Chen YS, Lu Q, Wang JY, et al. MicroRNA-188 Regulates Age-Related Switch Between Osteoblast and Adipocyte Differentiation. *J Clin Invest* (2015) 125(4):1509–22. doi: 10.1172/JCI77716
55. Sun W, Qiao W, Zhou B, Hu Z, Yan Q, Wu J, et al. Overexpression of Sirt1 in Mesenchymal Stem Cells Protects Against Bone Loss in Mice by FOXO3a Deacetylation and Oxidative Stress Inhibition. *Metabol: Clin Exp* (2018) 88:61–71. doi: 10.1016/j.metabol.2018.06.006
56. Ahn JS, Seo Y, Oh SJ, Yang JW, Shin YY, Lee BC, et al. The Activation of NLRP3 Inflammasome Potentiates the Immunomodulatory Abilities of Mesenchymal Stem Cells in a Murine Colitis Model. *BMB Rep* (2020) 53(6):329–34. doi: 10.5483/BMBRep.2020.53.6.065
57. Yin W, Liu S, Dong M, Liu Q, Shi C, Bai H, et al. A New NLRP3 Inflammasome Inhibitor, Dioscin, Promotes Osteogenesis. *Small* (2020) 16(1):e1905977. doi: 10.1002/smll.201905977
58. Alippe Y, Wang C, Ricci B, Xiao J, Qu C, Zou W, et al. Bone Matrix Components Activate the NLRP3 Inflammasome and Promote Osteoclast Differentiation. *Sci Rep* (2017) 7(1):6630. doi: 10.1038/s41598-017-07014-0
59. Zhang L, Wang Q, Su H, Cheng J. Exosomes From Adipose Derived Mesenchymal Stem Cells Alleviate Diabetic Osteoporosis in Rats Through Suppressing NLRP3 Inflammasome Activation in Osteoclasts. *J Biosci Bioengineering* (2021) 131(6):671–8. doi: 10.1016/j.jbiosc.2021.02.007
60. Zhang Q, Yu W, Lee S, Xu Q, Naji A, Le A. Bisphosphonate Induces Osteonecrosis of the Jaw in Diabetic Mice via NLRP3/Caspase-1-Dependent IL-1 β Mechanism. *J Bone Mineral Res Off J Am Soc Bone Mineral Res* (2015) 30(12):2300–12. doi: 10.1002/jbmr.2577
61. Zang Y, Song JH, Oh SH, Kim JW, Lee MN, Piao X, et al. Targeting NLRP3 Inflammasome Reduces Age-Related Experimental Alveolar Bone Loss. *J Dent Res* (2020) 99(11):1287–95. doi: 10.1177/0022034520933533
62. Li Z, Huang Z, Zhang H, Lu J, Tian Y, Wei Y, et al. P2X7 Receptor Induces Pyroptotic Inflammation and Cartilage Degradation in Osteoarthritis via NF-Kappab/NLRP3 Crosstalk. *Oxid Med Cell Longev* (2021) 2021:8868361. doi: 10.1155/2021/8868361
63. Yang X, Qu C, Jia J, Zhan Y. NLRP3 Inflammasome Inhibitor Glyburide Expedites Diabetic-Induced Impaired Fracture Healing. *Immunobiology* (2019) 224(6):786–91. doi: 10.1016/j.imbio.2019.08.008
64. Kawahara Y, Kaneko T, Yoshinaga Y, Arita Y, Nakamura K, Koga C, et al. Effects of Sulfonylureas on Periodontopathic Bacteria-Induced Inflammation. *J Dental Res* (2020) 99(7):830–8. doi: 10.1177/0022034520913250
65. Xu L, Shen L, Yu X, Li P, Wang Q, Li C. Effects of Irisin on Osteoblast Apoptosis and Osteoporosis in Postmenopausal Osteoporosis Rats Through Upregulating Nrf2 and Inhibiting NLRP3 Inflammasome. *Exp Ther Med* (2020) 19(2):1084–90. doi: 10.3892/etm.2019.8313
66. Cheng R, Feng Y, Zhang R, Liu W, Lei L, Hu T, et al. The Extent of Pyroptosis Varies in Different Stages of Apical Periodontitis. *Biochim Biophys Acta Mol Basis Dis* (2018) 1864(1):226–37. doi: 10.1016/j.bbdis.2017.10.025
67. Kim HY, Kim KS, Kim MJ, Kim HS, Lee KY, Kang KW. Auranofin Inhibits RANKL-Induced Osteoclastogenesis by Suppressing Inhibitors of kappaB Kinase and Inflammasome-Mediated Interleukin-1beta Secretion. *Oxid Med Cell Longev* (2019) 2019:3503912. doi: 10.1155/2019/3503912
68. Kary S, Burmester G, Anakinra: The First Interleukin-1 Inhibitor in the Treatment of Rheumatoid Arthritis. *Int J Clin Pract* (2003) 57(3):231–4.

69. Yang Y, Wang H, Kouadir M, et al. Recent Advances in the Mechanisms of NLRP3 Inflammasome Activation and its Inhibitors. *Cell Death Dis* (2019) 10 (2):128. doi: 10.1038/s41419-019-1413-8
70. Arioiz BI, Tarakcioglu E, Olcum M, Genc S. The Role of Melatonin on NLRP3 Inflammasome Activation in Diseases. *Antioxid (Basel)* (2021) 10(7):1020. doi: 10.3390/antiox10071020
71. Tezcan G, Martynova EV, Gilazieva ZE, McIntyre A, Rizvanov AA, Khaiboullina SF. MicroRNA Post-Transcriptional Regulation of the NLRP3 Inflammasome in Immunopathologies. *Front Pharmacol* (2019) 10:451. doi: 10.3389/fphar.2019.00451
72. Xie Q, Wei M, Zhang B, Kang X, Liu D, Zheng W, et al. MicroRNA33 Regulates the NLRP3 Inflammasome Signaling Pathway in Macrophages. *Mol Med Rep* (2018) 17(2):3318–27. doi: 10.3892/mmr.2017.8224
73. Li S, Liang X, Ma L, Shen L, Li T, Zheng L, et al. MiR-22 Sustains NLRP3 Expression and Attenuates HPylori-Induced Gastric Carcinogenesis. *Oncogene* (2018) 37(7):884–96. doi: 10.1038/onc.2017.381

Conflict of Interest: The authors declare that the research was conducted in the absence of any commercial or financial relationships that could be construed as a potential conflict of interest.

Publisher's Note: All claims expressed in this article are solely those of the authors and do not necessarily represent those of their affiliated organizations, or those of the publisher, the editors and the reviewers. Any product that may be evaluated in this article, or claim that may be made by its manufacturer, is not guaranteed or endorsed by the publisher.

Copyright © 2021 Jiang, An, Yang, Liu, Guan, Ma and Tang. This is an open-access article distributed under the terms of the Creative Commons Attribution License (CC BY). The use, distribution or reproduction in other forums is permitted, provided the original author(s) and the copyright owner(s) are credited and that the original publication in this journal is cited, in accordance with accepted academic practice. No use, distribution or reproduction is permitted which does not comply with these terms.

Frontiers in Endocrinology

Explores the endocrine system to find new therapies for key health issues

The second most-cited endocrinology and metabolism journal, which advances our understanding of the endocrine system. It uncovers new therapies for prevalent health issues such as obesity, diabetes, reproduction, and aging.

Discover the latest Research Topics

[See more →](#)

Frontiers

Avenue du Tribunal-Fédéral 34
1005 Lausanne, Switzerland
frontiersin.org

Contact us

+41 (0)21 510 17 00
frontiersin.org/about/contact

